VAPOR PHASE PHOTOCHEMISTRY OF CYANOPYRIDINES AND PYRIDINE. DEUTERIUM LABELING STUDIES

by

Somchoke Laohhasurayotin

A Dissertation

Submitted to the Faculty

of the

WORCESTER POLYTECHNIC INSTITUTE

in partial fulfillment of the requirements for the

Degree of Doctor of Philosophy

in

Chemistry

by

_____

April, 2005

APPROVED:

Examining Committees

_____
Professor James W. Pavlik, Advisor

_____
Professor W. Grant McGimpsey

_____
Professor Venkat R. Thalladi

_____
Professor Richard P. Johnson
University of New Hampshire

ABSTRACT

The vapor phase photochemistry of the three isomeric cyanopyridines and the three methylpyridines was studied by irradiating their vapors at 254 nm. It was found that direct irradiation of any one cyanopyridine isomer resulted in the formation of the other two isomers of cyanopyridine or methylpyridines respectively. The reactivity of each isomer was found to be different. This was suggested to be based on the stability of their azaprefulvene intermediates formed during interconversion. The phototransposition of these molecules was suggested to result from 2,6-bonding, nitrogen migration around the five sides of cyclopentenyl ring followed by rearomatization. This mechanism was found to be consistent with the results of deuterium labeling studies of cyanopyridines These result suggest that cyanopyridines undergo phototransposition via the intermediacy of azaprefulvenes instead of Dewar-pyridine and azaprismane.

Thus, photochemical studies showed that the six trideuteriopyridine isomers constitute two separate photochemical triads. Each triad consists of three isomers that are photointerconverting upon irradiation at 254 nm in the vapor phase. Similary, it was found that the three isomeric tetradeuteriopyridine isomers also constitute a photochemical triad and are interconverting upon irradiation at 254 nm in the vapor phase. These phototranspositions are best explained by the cyclization, nitrogen migration, and rearomatization mechanism. These results are in contrast to the long-held belief that pyridine is photostable in the vapor phase. Instead, unlabeled pyridine undergoes a hidden phototransposition leading back to itself.

ACKNOWLEDGEMENT

I would like to express my gratitude to my advisor, Professor James W. Pavlik whose help, guidance, and encouragement helped me all the time during my Ph.D. research and writing of this dissertation. He showed me how to use time and effort efficiently, which is very important for my professional career in the future.

I am also grateful to Professor W. Grant McGimsey, Professsor Venkat R. Thalladi, and Professor Richard P. Johnson for the interest they have shown in this dissertation by accepting to be my Ph.D examination committee.

I would like to thank Dr. Naod Kebede, friend and colleague, who gave me bunches of his knowledge and advice. Special thanks to Professor Robert E. Connors for letting me use his vacuum rack for my photochemistry work.

All my thanks go also to my colleagues, Chuchawin Changtong, for his help in NMR and other instruments, as well as Vuthichai Ervithayasuporn, Jessica Martinez, Tharinee Vongnakorn for their chemistry techniques and the nice work atmosphere. Nantanit Wanichacheva, Hubert Nienaber and Ernesto Soto should not be forgotten because of several times of refreshment and research discussions. I also thanks to all people in Department of Chemistry and Biochemistry, WPI, for their helps and friendliness.

I would like to thank my father, mother, and my brother for their understanding and support during these years of study. Last thank go to Supara Tokunalai, for her endless support through my Ph.D study.

TABLE OF CONTENTS

ABSTRACT ..... **i**

ACKNOWLEDGEMENT ..... **ii**

TABLE OF CONTENTS ..... **iii**

LIST OF FIGURES ..... **xv**

LIST OF TABLES ..... **xxv**

CHAPTER I Introduction **1**

CHAPTER II Literature review **4**

2.1. Photochemistry of pyridine and its derivatives **4**

2.1.1. Spectroscopic properties of pyridine and methylpyridines 24

2.2. Photochemistry of cyanopyridines **32**

2.2.1. Spectroscopic properties of cyanopyridines 32

2.3. The triplet state of 4-cyanopyridine **39**

CHAPTER III Statement of purpose **40**

CHAPTER IV Results and discussion **43**

4.1. Photochemistry of cyanopyridines in the vapor phase **43**

4.1.1. Irradiation of 2-cyanopyridine (**36**) at 254 nm 43

4.1.2. Irradiation of 3-cyanopyridine (**37**) at 254 nm 48

4.1.3. Irradiation of 4-cyanopyridine (**38**) at 254 nm 53

4.1.4. Irradiation of 2-cyanopyridine (**36**) at ≥ 290 nm 58

4.1.5. Irradiation of 3-cyanopyridine (**37**) at ≥ 290 nm 59
4.1.6. Irradiation of 4-cyanopyridine (**38**) at ≥ 290 nm 61
4.1.7. Mechanistic discussion for cyanopyridines 64

4.2. Photochemistry of methylpyridines in vapor phase 75
4.2.1. Irradiation of 2-methylpyridine (**6**) 75
4.2.2. Irradiation of 3-methylpyridine (**7**) 81
4.2.3. Irradiation of 4-methylpyridine (**8**) 87
4.2.4. Mechanistic Discussion of methylpyridines 94

4.3. Deuterium labeling studies 105
4.3.1. Cyanopyridines 105
4.3.2. Proton-Deuterium exchange reaction with base catalyst 105
4.3.3. Synthesis of 4-cyanopyridine-2,6-d_2 (**38-2,6-d_2**) 109
4.3.4. Synthesis of 3-cyanopyridine-2,6-d_2 (**37-2,6-d_2**) 114
4.3.5. Synthesis of 2-cyanopyridine-4,6-d_2 (**36-4,6-d_2**) 118
4.3.6. Pyridines 127
4.3.7. Synthesis of dideuterio-2,6-pyridine (**1-2,6-d_2**) 129
4.3.8. Synthesis of 3,4,5-trideuteriopyridine (**1-3,4,5-d_3**) 133
4.3.9. Synthesis of 2,4,6-trideuteriopyridine (**1-2,4,6-d_3**) 136
4.3.10. Synthesis of 2,3,5,6-tetradeuteriopyridine (**1-2,3,5,6-d_4**) 142
4.3.11. Synthesis of 2,3,4,6-tetradeuteriopyridine (**1-2,3,4,6-d_4**) 149
4.3.12. Synthesis of 2,3,4,5-tetradeuteriopyridine (**1-2,3,4,5-d_4**) 155
4.3.13 Synthesis of 2,3,4-trideuteriopyridine (**1-2,3,4-d_3**), 2,4,5-trideuteriopyridine 160
(**1-2,4,5-d_3**), and 2,3,6-trideuteriopyridine (**1-2,3,6-d_3**) 160
4.3.14. Synthesis of 2,3,5-trideuteriopyridine (**1-2,3,5-d_3**) 170

4.4. Photochemistry of deuterated cyanopyridines 174
4.4.1. Irradiation of 2-Cyanopyridine-4,6-d_2 174
4.4.2. Irradiation of 3-cyanopyridine-2,6-d_2 180
4.5.3. Irradiation of 4-cyanopyridine-2,6-d_2 186

4.5. Photochemistry of deuterated pyridines 191
4.5.1. Irradiation of 2,6-dideuteriopyridine 191
4.5.2. Mechanistic discussion of deuterated pyridines 196
4.5.3. 2,6-Dideuteriopyridine 198

4.6. Photochemistry of trideuteriopyridines 203
4.6.1. Irradiation of 3,4,5-trideuteriopyridine (**1-3,4,5-d_3**) 203
4.6.2. Irradiation of 2,4,6-trideuteriopyridine (**1-2,4,6-d_3**) 207
4.6.3. Irradiation of 2,3,4-trideuteriopyridine (**1-2,3,4-d_3**) 210
4.6.4. Irradiation of 2,3,6-trideuteriopyridine (**1-2,3,6-d_3**) 213
4.6.5. Irradiation of 2,3,5-trideuteriopyridine (**1-2,3,5-d_3**) 217
4.6.6. Irradiation of 2,4,5-trideuteriopyridine (**1-2,4,5-d_3**) 220
4.6.7. Summary and mechanistic conclusion of trideuteriopyridines 223
4.6.8. Dewar-pyridine mechanism 227

4.7. Photochemistry of tetradeuteriopyridines 233
4.7.1. Irradiation of 2,3,5,6-tetradeuteriopyridine (**1-2,3,5,6-d_4**) 233
4.7.2. Irradiation of 2,3,4,6-tetradeuteriopyridine (**1-2,3,4,6-d_4**) 235
4.7.3. Irradiation of 2,3,4,5-tetradeuteriopyridine (**1-2,3,4,5-d_4**) 237
4.7.4. Summary and mechanistic conclusion of tetradeuteriopyridines 239
*4.7.5.1. 2,3,5,6-Tetradeuteriopyridine (**1-2,3,5,6-d_4**)* 240
*4.7.5.2. 2,3,4,6-Tetradeuteriopyridine (**1-2,3,4,6-d_4**)* 243
*4.7.5.3. 2,3,4,5-Tetradeuteriopyridine (**1-2,3,4,5-d_4**)* 249

CHAPTER V Experimental 263

5.1. General Procedures 263

5.2. Ultraviolet absorption 263

5.3. Methods of irradiation and analysis 264

5.4. GC analysis of photoproduct 264

5.5. Irradiation at 254 nm 265
5.5.1. 2-Cyanopyridine (**36**) 265
5.5.2. 3-Cyanopyridine (**37**) 266
5.5.3. 4-Cyanopyridine (**38**) 267
5.5.4. 2-Methylpyridine (**6**) 268
5.5.6. 3-Methylpyridine (**7**) 269
5.5.7. 4-Methylpyridine (**8**) 270

5.6. Irradiation at $\lambda \geq 290$ nm 271
5.6.1. 2-Cyanopyridine (**36**) 271
5.6.2. 3-Cyanopyridine (**37**) 271
5.6.3. 4-Cyanopyridine (**38**) 272

5.7. Deuterium labeling studies 273
5.7.1. 2-Cyanopyridine-4,6-d_2 (**36-4,6-d_2**) 273
5.7.2. 3-Cyanopyridine-2,6-d_2 (**37-2,6-d_2**) 273
5.7.3. 4-Cyanopyridine-2,6-d_2 (**38-2,6-d_2**) 274
5.7.4. 2,6-Dideuteriopyridine (**1-2,6-d_2**) 275
5.7.5. 3,4,5-Trideuteriopyridine (**1-3,4,5-d_3**) 275
5.7.6. 2,4,6-Trideuteriopyridine (**1-2,4,6-d_3**) 276
5.7.7. 2,3,6-Trideuteriopyridine (**1-2,3,6-d_3**) 276
5.7.8. 2,3,4-Trideuteriopyridine (**1-2,3,4-d_3**) 277
5.7.9. 2,3,5-Trideuteriopyridine (**1-2,3,5-d_3**) 277
5.7.10. 2,4,5-Trideuteriopyridine (**1-2,4,5-d_3**) 277
5.7.11. 2,3,4,5-Tetradeuteriopyridine (**1-2,3,4,5-d_4**) 278
5.7.12. 2,3,4,6-Tetradeuteriopyridine (**1-2,3,4,6-d_4**) 278
5.7.13. 2,3,5,6-Tetradeuteriopyridine (**1-2,3,5,6-d_4**) 279

5.8. Synthesis of 4-cyanopyridine-2,6-d_2 (36-2,6-d_2) 280
5.8.1. Preparation of isonicotinic acid N-oxide-2,6-d_2 (**54-2,6-d_2**) 280
5.8.2. Preparation of methyl isonicotinate N-oxide-2,6-d_2 (**58-2,6-d_2**) 280
5.8.3. Preparation of methyl isonicotinate-2,6-d_2 (**59-2,6-d_2**) 281

5.8.4. Preparation of isonicotinamide-2,6-d_2 (**60-2,6-d_2**) 281
5.8.5. Preparation of 4-cyanopyridine-2,6-d_2 (**38-2,6-d_2**)..... 282

5.9. Synthesis of 3-cyanopyridine-2,6-d_2 (37-2,6-d_2)..... 283
5.9.1. Preparation of nicotinic acid N-oxide -2,6-d_2 (**61-2,6-d_2**) 283
5.9.2. Preparation of methyl nicotinate N-oxide-2,6-d_2 (**62-2,6-d_2**)..... 283
5.9.3. Preparation of methyl nicotinate-2,6-d_2 (**63-2,6-d_2**) 284
5.9.4. Preparation of nicotinamide-2,6-d_2 (**64-2,6-d_2**) 284
5.9.5. Preparation of 3-cyanopyridine-2,6-d_2 (**37-2,6-d_2**)..... 285

5.10. Synthesis of 2-cyanopyridine-4,6-d_2 (36-2,6-d_2) 286
5.10.1. Preparation of picolinic acid-N-oxide-6-d (**75-6-d**) 286
5.10.2. Preparation of 4-nitropicolinic acid N-oxide-6-d (**71-6-d**)..... 286
5.10.3. Preparation of methyl 4-nitropicolinate N-oxide-6-d (**76-6-d**)..... 287
5.10.4. Preparation of methyl 4-chloropicolinate N-oxide-6-d (**77-6-d**)..... 287
5.10.5. Preparation of methyl 4-chloropicolinate-6-d (**78-6-d**) 288
5.10.6. Preparation of methyl picolinate-4,6-d_2 (**79-4,6-d_2**) 289
5.10.7. Preparation of picolinamide-4,6-d_2 (**80-4,6-d_2**) 290
5.10.8. Preparation of 2-cyanopyridine-4,6-d_2 (**36-4,6-d_2**)..... 291

5.11. Synthesis of 2,6-dideuteriopyridine (1-2,6-d_2) 292
5.11.1. Preparation of pyridine N-oxide-2,6-d_2 (**53-2,6-d_2**) 292
5.11.2. Preparation of 2,6-dideuteriopyridine (**1-2,6-d_2**) 292

5.12. Synthesis of 3,4,5-trideuteriopyridine (1-3,4,5-d_3) 293
5.12.1. Preparation of pyridine N-oxide-3,4,5-d_3 (**53-3,4,5-d_3**) 293
5.12.2. Preparation of 3,4,5-trideuteriopyridine (**1-3,4,5-d_3**)..... 293

5.13. Synthesis of 2,4,6-trideuteriopyridine (1-2,4,6-d_3) 295
5.13.1. Preparation of 4-nitropyridine N-oxide-2,6-d_2 (**81-2,6-d_2**)..... 295
5.13.2. Preparation of 4-chloropyridine N-oxide-2,6-d_2(**82-2,6-d_2**)..... 295
5.13.3. Preparation of 4-chloropyridine-2,6-d_2(**83-2,6-d_2**)..... 296
5.13.4. Preparation of 2,4,6-trideuteriopyridine (**1-2,4,6-d_3**)..... 296

5.14. Synthesis of 2,3,5,6-tetradeuteriopyridine (1-2,3,5,6-d_4) 298
5.14.1. Preparation of 3,5-dichloropyridine N-oxide (**85**) 298
5.14.2. Preparation of 3,5-dichloropyridine N-oxide-2,4,6-d_3 (**85-2,4,6-d_3**) 298
5.14.3. Preparation of 3,5-dichloropyridine-2,4,6-d_3 (**84-2,4,6-d_3**) 299
5.14.4. Preparation of 3,5-dichloropyridine-2,6-d_2 (**84-2,6-d_2**) 299
5.14.5. Preparation of 2,3,5,6-tetradeuteriopyridine (**1-2,3,5,6-d_4**) 300

5.15. Synthesis of 2,4,5,6-tetradeuteriopyridine (1-2,4,5,6-d_4) 301
5.15.1. Preparation of 3-chloropyridine N-oxide (**87**) 301
5.15.2. Preparation of 3-chloropyridine N-oxide-2,4,5,6-d_4 (**87-2,4,5,6-d_4**) 301
5.15.3. Preparation of 3-chloropyridine-2,4,5,6-d_4 (**86-2,4,5,6-d_4**) 302
5.15.4. Preparation of 2,3,4,6-tetradeuteriopyridine (**1-2,3,4,6-d_4**) 302

5.16. Synthesis of 2,3,4,5-tetradeuteriopyridine (1-2,3,4,5-d_4) 304
5.16.1. Preparation of pyridine N-oxide-d_5 (**53-2,3,4,5,6-d_5**) 304
5.16.2. Preparation of 2-chloropyridine-3,4,5,6-d_4 (**88-3,4,5,6-d_4**) 304
5.16.3. Preparation of 2,3,4,5-tetradeuteriopyridine (**1-2,3,4,5-d_4**) 305

5.17. Synthesis of 2,3,4-, 2,4,5-, and 2,3,6-trideuteriopyridine (1-2,3,4-d_3, ... 307

1-2,4,5-d_3, 1-2,3,6-d_3) 307
5.17.1. Preparation of 2,3-dichloropyridine (**91-4,5,6-d_3**), 2,5-dichloropyridine 307
(**92-3,4,6-d_3**), 3,4-dichloropyridine (**93-2,5,6-d_3**) 307
5.17.2. Preparation of 2,3,4-trideuteriopyridine (**1-2,3,4-d_3**) 308
5.17.3. Preparation of 2,4,5-trideuteriopyridine (**1-2,4,5-d_3**) 309
5.17.4. Preparation of 2,3,6-trideuteriopyridine (**1-2,3,6-d_3**) 310

5.18. Synthesis of 2,3,5-trideuteriopyridine (1-2,3,5-d_3) 311
5.18.1. Preparation of 4-nitropyridine N-oxide-2,3,5,6-d_4 (**81-2,3,5,6-d_4**) 311
5.18.2. Preparation of 4-chloropyridine N-oxide-2,3,5,6-d_4 (**82-2,3,5,6-d_4**) 311
5.18.3. Preparation of 2,4-dichloropyridine-3,5,6-d_3 (**94-3,5,6-d_3**) 312
5.18.4. Preparation of 2,3,5-trideuteriopyridine (**1-2,3,5-d_3**) 312

CHAPTER VI Conclusion 314

REFERENCES..... 317

APPENDIX..... 322

A. NMR spectra of synthetic compounds 323

B. Mass Spectra of synthetic compounds..... 358

C. UV spectra of cyanopyridines 369

D. UV spectra of methylpyridine vapors 372

LIST OF SCHEMES

Scheme 2.1 Irradiation of pyridine in butane 4

Scheme 2.2 Irradiation of pyridine in water or in $NaBH_4$ 5

Scheme 2.3 Irradiation of pyridine matrix isolated in argon at 8 K 6

Scheme 2.4 Irradiation of pyridine forms cyclobutadiene and HCN 7

Scheme 2.5 Photolytic ring cleavage of cyclobutadiene 7

Scheme 2.6 Photolysis of 2-methylpyridine 7

Scheme 2.7 2,5- and 3,6-Bridging for 2-methylpyridine 8

Scheme 2.8 1,4-Bridging for 2-methylpyridine 9

Scheme 2.9 Photolysis of pyridine in cyclohexane 11

Scheme 2.10 Photolysis of 2-methylpyridine in cyclohexane 11

Scheme 2.11 Photolysis of 4-methylpyridine in cyclohexane 12

Scheme 2.12 Photolysis of 2-methylpyridine vapor by Pascual's group 12

Scheme 2.13 Photolysis of 4-methylpyridine vapor by Pascual's group 12

Scheme 2.14 2,5- and 3,6-Bridging for 2,6-dimethylpyridine 14

Scheme 2.15 1,4-Bridging for 2,4-dimethylpyridine 15

Scheme 2.16 Photo-interconversion of dimethylpyridines 16

Scheme 2.17 Phototransposition mechanism in Triad 1 17

Scheme 2.18 Phototransposition mechanism in Triad 2 17

Scheme 2.19 Inter-triad reaction 18

Scheme 2.20 Formation of azaprefulvene 20

Scheme 2.21 Ultra-fast electron diffraction experiment 23

Scheme 2.22 Cyclization of ring-opened biradical 23

Scheme 3.1. Cyanopyridines and methylpyridines 40

Scheme 3.2 Dideuteriocyanopyridine 41

Scheme 3.3 Trideuteriopyridines 41

Scheme 3.4 Tetradeuteriopyridines 42

Scheme 4.1 Photolysis of 2-cyanopyridine (**36**) 43

Scheme 4.2 Photolysis of 3-cyanopyridine (**37**) 48

Scheme 4.3 Photolysis of 4-cyanopyridine (**38**) 53

Scheme 4.4 Photo-interconversion of cyanopyridines 64

Scheme 4.5 Phototransposition mechanism of cyanopyridines 65

Scheme 4.6 Radical stabilization of cyanopyridines 69

Scheme 4.7 Steric hindrance from substituents at C2 and C6 70

Scheme 4.8 Dewar-pyridine mechanism of 2-cyanopyridine 71

Scheme 4.9 Azaprismane mechanism: 3,6-bridging 72

Scheme 4.10 Azaprismane mechanism: 2,5-bridging 73

Scheme 4.11 Azaprismane mechanism: 1,4-bridging 74

Scheme 4.12 Photolysis of 2-methylpyridine (**6**) 75

Scheme 4.13 Photolysis of 3-methylpyridine (**7**) 81

Scheme 4.14 Photolysis of 4-methylpyridine (**8**) 87

Scheme 4.15 Photo-interconversion of methylpyridines 94

Scheme 4.16 Phototransposition mechanism of methylpyridines 95

Scheme 4.17 Radical stabilization of methylpyridines 100

Scheme 4.18 Steric hindrance from substituents at C2 and C6 101

Scheme 4.19 Dewar-pyridine mechanism of 2-methylpyridine 102

Scheme 4.20 Azaprismane mechanism: 3,6-bridging..... 103

Scheme 4.21 Azaprismane mechanism: 2,5-bridging..... 103

Scheme 4.22 Azaprismane mechanism: 1,4-bridging..... 104

Scheme 4.23 hydrolysis of cyano group in 4-cyanopyridine..... 106

Scheme 4.24 Proton abstraction by base for pyridine N-oxide 107

Scheme 4.25 Resonance stabilization..... 107

Scheme 4.26 Preparation of deuterium labeled isoniazid..... 108

Scheme 4.27 Synthesis of 4-cyanopyridine-2,6-d_2 (**38-2,6-d_2**)..... 109

Scheme 4.28 Synthesis of 3-cyanopyridine-2,6-d_2 (**37-2,6-d_2**)..... 114

Scheme 4.29 Proposed synthesis of 2-cyanopyridine-4,6-d_2 (**36-4,6-d_2**)..... 119

Scheme 4.30 Proposed synthesis of **36-4,6-d_2** from **71-6-d**..... 120

Scheme 4.31 Synthesis of 2-cyanopyridine-4,6-d_2 (**36-4,6-d_2**)..... 121

Scheme 4.32 Synthesis of 2,6-dideuteriopyridine (**1-2,6-d_2**)..... 129

Scheme 4.33 Synthesis of 3,4,5-trideuteriopyridine (**1-3,4,5-d_3**)..... 133

Scheme 4.34 Synthesis of 2,4,6-trideuteriopyridine (**1-2,4,6-d_3**)..... 136

Scheme 4.35 Proposed synthesis of 2,3,5,6-tetradeuteriopyridine (**1-2,3,5,6-d_4**)..... 142

Scheme 4.36 Proposed synthesis of 2,3,5,6-tetradeuteriopyridine (**1-2,3,5,6-d_4**)..... 143

Scheme 4.37 Synthesis of 2,3,5,6-tetradeuteriopyridine (**1-2,3,5,6-d_4**)..... 144

Scheme 4.38 Synthesis of 2,3,4,6-tetradeuteriopyridine (**1-2,3,4,6-d_4**)..... 149

Scheme 4.39 Proposed synthesis of 2,3,4,5-tetradeuteriopyridine (**1-2,3,4,5-d_4**)..... 155

Scheme 4.40 Synthesis of 2,3,4,5-tetradeuteriopyridine (**1-2,3,4,5-d_4**)..... 156

Scheme 4.41 Syntheses of 2,3,4-,2,4,5-, and 2,3,6-trideuteriopyridine..... 160

Scheme 4.42 Synthesis of 2,3,5-trideuteriopyridine (**1-2,3,5-d_3**) 170

Scheme 4.43 Photolysis of 2-cyanopyridine-4,6-d_2 (**36-2,6-d_2**) 177

Scheme 4.44 Phototransposition mechanism of 2-cyanopyridine-4,6-d_2 178

Scheme 4.45 Photolysis of 3-cyanopyridine-2,6-d_2 (**37-2,6-d_2**) 183

Scheme 4.46 Phototransposition mechanism of 3-cyanopyridine-2,6-d_2 184

Scheme 4.47 Photolysis of 4-cyanopyridine-2,6-d_2 (**38-2,6-d_2**) 188

Scheme 4.48 Phototransposition mechanism of 4-cyanopyridine-2,6-d_2 189

Scheme 4.49 Photolysis of 2,6-dideuteriopyridine (**1-2,6-d_2**) 196

Scheme 4.50 Phototransposition mechanism of 2,6-dideuteriopyridine (**1-2,6-d_2**) 199

Scheme 4.51 Dewar-pyridine mechanism of **1-2,6-d_2** 200

Scheme 4.52 Azaprismane mechanism of **DP-2,6-d_2** 201

Scheme 4.53 Photolysis of 3,4,5-trideuteriopyridine (**1-3,4,5-d_3**) 205

Scheme 4.54 Photolysis of 2,4,6-trideuteriopyridine (**1-2,4,6-d_3**) 209

Scheme 4.55 Photolysis of 2,3,4-trideuteriopyridine (**1-2,3,4-d_3**) 213

Scheme 4.56 Photolysis of 2,3,6-trideuteriopyridine (**1-2,3,6-d_3**) 217

Scheme 4.57 Photolysis of 2,3,5-trideuteriopyridine (**1-2,3,5-d_3**) 220

Scheme 4.58 Photolysis of 2,4,5-trideuteriopyridine (**1-2,4,5-d_3**) 222

Scheme 4.59 Photo-interconversion of trideuteriopyridines 223

Scheme 4.60 Phototransposition mechanism of trideuteriopyridines inTriad 1 224

Scheme 4.61 Phototransposition mechanism of trideuteriopyridines in Triad 2 226

Scheme 4.62 Dewar-pyridine mechanism of **1-3,4,5-d_3** 228

Scheme 4.63 Azaprismane mechanism of **DP-3,4,5-d_3** 229

Scheme 4.64 Dewar-pyridine mechanism of **1-2,4,6-d_3** 230

Scheme 4.65 Azaprismane mechanism of **DP-2,4,6-d_3** 231

Scheme 4.66 Different photoproducts from 2,6-bonding and azaprismane formation.. 232

Scheme 4.67 Photolysis of 2,3,5,6-tetradeuteriopyridine (**1-2,3,5,6-d_4**) 234

Scheme 4.68 Photolysis of 2,3,4,6-tetradeuteriopyridine (**1-2,3,4,6-d_4**) 236

Scheme 4.69 Photolysis of 2,3,4,5-tetradeuteriopyridine (**1-2,3,4,5-d_4**) 238

Scheme 4.70 Photolysis of 2,3,4,5-tetradeuteriopyridine (**1-2,3,4,5-d_4**) 238

Scheme 4.71 Photo-interconversion of tetradeuteriopyridines 239

Scheme 4.72 Dewar-pyridine mechanism of **1-2,3,5,6-d_4** 242

Scheme 4.73 Azaprismane mechanism of **DP-2,3,5,6-d_4** 243

Scheme 4.74 Phototransposition mechanism of **1-2,3,4,6-d_4** 244

Scheme 4.75 Dewar-pyridine mechanism of **1-2,3,4,6-d_4:** 2,5-bonding 246

Scheme 4.76 Dewar-pyridine mechanism of **1-2,3,4,6-d_4:** 3,6-bonding 247

Scheme 4.77 Azaprismane mechanism of **DP-2,3,4,6-d_4** 248

Scheme 4.78 Phototransposition mechanism of (**1-2,3,4,5-d_4**) 249

Scheme 4.79 Dewar-pyridine mechanism of **1-2,3,4,5-d_4:** 2,5-bonding 251

Scheme 4.80 Dewar-pyridine mechanism of **1-2,3,4,5-d_4:** 3,6-bonding 252

Scheme 4.81 Azaprismane mechanism of **DP-2,3,4,5-d_4** 253

LIST OF FIGURES

Figure 2.1 Potential energy surface representing photochemistry and photophysics of pyridine in solution phase 20

Figure 2.2 Energy level diagram of Pyridine 29

Figure 2.3 Energy level diagram of 2-methylpyridine 30

Figure 2.4 Energy level diagram of 3-methylpyridine 31

Figure 2.5 Energy level diagram of 2-Cyanopyridine 36

Figure 2.6 Energy level diagram of 3-Cyanopyridine 37

Figure 2.7 Energy level diagram of 4-Cyanopyridine 38

Figure 4.1 GC trace of 2-cynopyridine irradiated for 90 min 44

Figure 4.2 (a) ^{1}H-NMR of 2-cyanopyridine before irradiation 45

Figure 4.2 (b) ^{1}H-NMR of 2-cyanopyridine after 90 min of irradiation 45

Figure 4.3 Photoproduct ratio VS. irradiation time from irradiation of **36** 47

Figure 4.4 GC trace of 3-cyanopyridine at 254 nm irradiated for 360 minutes 49

Figure 4.5 (a) ^{1}H-NMR of 3-cyanopyridine before irradiation 50

Figure 4.5 (b) ^{1}H-NMR of 3-cyanopyridine after 360 min of irradiation 50

Figure 4.6 Photoproduct ratio VS Irradiation time from irradiation of **37** 52

Figure 4.7 GC trace of 4-cyanopyridine irradiated at 254 nm for 90 minutes 54

Figure 4.8 (a) ^{1}H-NMR of 4-cyanopyridine before irradiation 55

Figure 4.8 (b) ^{1}H-NMR of 4-cyanopyridine after 90 min of irradiation 55

Figure 4.9 Photoproduct ratio VS. Irradiation time from irradiation of **38** 56

Figure 4.10 GC trace of 2-cyanopyridine irradiated at $\geq$ 290 nm for 24 hours 59

Figure 4.11 GC trace of 3-cyanopyridine irradiated at ≥ 290 nm for 24 hours 60

Figure 4.12 GC trace of 4-cyanopyridine irradiated at > 290 nm for 24 hours 62

Figure 4.13 GC trace of photoproduct mixture from 2-methylpyridine after irradiation for 12 hours 76

Figure 4.14 Ratio of **7** / **8** from irradiation of 2-methylpyridine (**6**) 77

Figure 4.15 (a) ^{1}H-NMR of 2-methylpyridine before irradiation 78

Figure 4.15 (b) ^{1}H-NMR of 2-methylpyridine after 12 h of irradiation 78

Figure 4.16 (a) ^{13}C-NMR of 2-methylpyridine before irradiation 80

Figure 4.16 (b) ^{13}C-NMR of 2-methylpyridine after 12 h of irradiation 80

Figure 4.17 GC trace of photoproduct mixtures from 3-methylpyridine after irradiation for 12 hours 82

Figure 4.18 Ratio of **6** / **8** from irradiation of 3-methylpyridine (**7**) 83

Figure 4.19 (a) ^{1}H-NMR spectrum of 3-methylpyridine before irradiation 84

Figure 4.19 (b) ^{1}H-NMR spectrum of 3-methylpyridine after 12 h of irradiation 84

Figure 4.20 (a) ^{13}C-NMR spectrum of 3-methylpyridine before irradiation 86

Figure 4.20 (b) 13C-NMR spectrum of 3-methylpyridine after 12 h of irradiation 86

Figure 4.21 GC trace of photoproduct mixture from 4-methylpyridine after irradiation for 6 hours 88

Figure 4.22 Ratio of **7/6** from irradiation of 4-methylpyridine (**8**) 89

Figure 4.23 (a) ^{1}H-NMR spectrum of 4-methylpyridine before irradiaiton 91

Figure 4.23 (b) ^{1}H-NMR spectrum after 12 h of irradiation 91

Figure 4.24 (a) ^{13}C-NMR spectrum before irradiation 93

Figure 4.24 (b) ^{13}C-NMR spectrum after 12 h of irradiation 93

Figure 4.25 GC-MS of 4-cyanopyridine-2,6-d_2(**38-2,6-d_2**) 111

Figure 4.26 ^{1}H-NMR spectrum of 4-cyanopyridine-2,6-d_2 (**38-2,6-d_2**) 112

Figure 4.27 ^{13}C-NMR spectrum of 4-cynaopyridine-2,6-d_2 (**38-2,6-d_2**) 113

Figure 4.28 GC-MS of 3-cyanopyridine-2,6-d_2 (**37-2,6-d_2**) 115

Figure 4.29 ^{1}H-NMR spectrum of 3-cyanopyridine-2,6-d_2 (**37-2,6-d_2**) 116

Figure 4.30 ^{13}C-NMR spectrum of 3-cyanopyridine-2,6-d_2 (**37-2,6-d_2**) 117

Figure 4.31 GC-MS of methylpicolinate-4,6-d_2 (**79-4,6-d_2**) 122

Figure 4.32 ^{1}H-NMR spectrum of methylpicolinate-4,6-d_2 (**79-4,6-d_2**)..... 123

Figure 4.33 ^{13}C-NMR spectrum of methylpicolinate-4,6-d_2 (**79-4,6-d_2**)..... 123

Figure 4.34 GC-MS of 2-cyanopyridine-4,6-d_2 (**36-4,6-d_2**) 124

Figure 4.35 ^{1}H-NMR spectrum of 2-cyanopyridine-4,6-d_2 (**36-4,6-d_2**) 125

Figure 4.36 ^{13}C-NMR spectrum of 2-cyanopyridine-4,6-d_2 (**36-4,6-d_2**) 126

Figure 4.37 GC-MS of 2-cyanopyridine-4,6-d_2 130

Figure 4.38 ^{1}H-NMR of 2,6-dideuteriopyridine (**1-2,6-d_2**) 131

Figure 4.39 ^{13}C-NMR spectrum of 2,6-dideuteriopyridine (**1-2,6-d_2**)..... 131

Figure 4.40 GC-MS of 3,4,5-trideuteriopyridine (**1-3,4,5-d_3**) 133

Figure 4.41 ^{1}H-NMR spectrum of 3,4,5-trideuteriopyridine (**1-3,4,5-d_3**)..... 134

Figure 4.42 ^{13}C-NMR spectrum of 3,4,5-trideuteriopyridine (**1-3,4,5-d_3**)..... 135

Figure 4.43 GC and MS of 4-chloropyridine-2,6-d_2 (**83-2,6-d_2**)..... 137

Figure 4.44 ^{1}H-NMR spectrum of 4-chloropyridine-2,6-d_2 (**83-2,6-d_2**) 138

Figure 4.45 ^{13}C-NMR of 4-chloropyridine-2,6-d_2 (**83-2,6-d_2**)..... 138

Figure 4.46 GC-MS of 2,4,6-trideuteriopyridine (**1-2,4,6-d_3**) 139

Figure 4.47 ^{1}H-NMR spectrum of 2,4,6-trideuteriopyridine (**1-2,4,6-d_3**)..... 140

Figure 4.48 ^{13}C-NMR spectrum of 2,4,6-trideuteriopyridine (**1-2,4,6-d$_3$**) 141

Figure 4.49 GC-MS of 2,3,5,6-tetradeuteriopyridine (**1-2,3,5,6-d$_4$**) 146

Figure 4.50 ^{1}H-NMR spectrum of 2,3,5,6-tetradeuteriopyridine (**1-2,3,5,6-d$_4$**)..... 147

Figure 4.51 ^{13}C-NMR spectrum of 2,3,5,6-tetradeuteriopyridine (**1-2,3,5,6-d$_4$**)..... 148

Figure 4.52 GC-MS of 3-chloropyridine N-oxide-2,4,5,6-d$_4$ (**87-2,4,5,6-d$_4$**)..... 150

Figure 4.53 Expansion of ^{13}C-NMR spectrum of **87-2,4,5,6-d$_4$** shows 4 triplets..... 151

Figure 4.54 GC-MS of 2,3,4,6-tetradeuteriopyridine (**1-2,3,4,6-d$_4$**) 152

Figure 4.55 ^{1}H-NMR spectrum of 2,3,4,6-tetradeuteriopyridine (**1-2,3,4,6-d$_4$**)..... 153

Figure 4.56 ^{13}C-NMR spectrum of 2,3,4,6-tetradeuteriopyridine (**1-2,3,4,6-d$_4$**)..... 154

Figure 4.57 GC-MS of 2,3,4,5-tetradeuteriopyridine (**1-2,3,4,5-d$_4$**) 157

Figure 4.58 ^{1}H-NMR spectrum of 2,3,4,5-tetradeuteriopyridine (**1-2,3,4,5-d$_4$**)..... 158

Figure 4.59 ^{13}C-NMR spectrum of 2,3,4,5-tetradeuteriopyridine (**1-2,3,4,5-d$_4$**)..... 159

Figure 4.60 GC-MS of 2,3,4-trideuteriopyridine (**1-2,3,4-d$_3$**)..... 161

Figure 4.61 ^{1}H-NMR spectrum of 2,3,4-trideuteriopyridine (**1-2,3,4-d$_3$**) 162

Figure 4.62 ^{13}C-NMR spectrum of 2,3,4-trideuteriopyridine (**1-2,3,4-d$_3$**) 163

Figure 4.63 GC-MS of 2,4,5-trideuteriopyridine (**1-2,4,5-d$_3$**)..... 164

Figure 4.64 ^{1}H-NMR spectrum of 2,4,5-trideuteriopyridine (**1-2,4,5-d$_3$**) 165

Figure 4.65 ^{13}C-NMR spectrum of 2,4,5-trideuteriopyridine (**1-2,4,5-d$_3$**) 166

Figure 4.66 GC-MS of 2,3,6-trideuteriopyridine (**1-2,3,6-d$_3$**)..... 167

Figure 4.67 ^{1}H-NMR spectrum of 2,3,6-trideuteriopyridine (**1-2,3,6-d$_3$**) 168

Figure 4.68 ^{13}C-NMR spectrum of 2,3,6-trideuteriopyridine (**1-2,3,6-d$_3$**) 169

Figure 4.69 GC-MS of 2,3,5-trideuteriopyridine (**1-2,3,5-d$_3$**)..... 171

Figure 4.70 ^{1}H-NMR spectrum of 2,3,5-trideuteriopyridine (**1-2,3,5-d$_3$**) 172

Figure 4.71 ^{13}C-NMR spectrum of 2,3,5-trideuteriopyridine (**1-2,3,5-d_3**) 173

Figure 4.72 (a) ^{1}H-NMR spectrum of 2-cyanopyridine-4,6-d_2 before irradiation 175

Figure 4.72 (b) ^{1}H-NMR spectrum of 2-cyanopyridine-4,6-d_2 irradiated for 240 min.. 175

Figure 4.73 (a) ^{1}H-NMR spectrum of 3-cyanopyridine-2,6-d_2 before irradiation..... 181

Figure 4.73 (b) ^{1}H-NMR spectrum of 3-cyanopyridine-2,6-d_2 after irradiation for 360 min 181

Figure 4.74 (a) ^{1}H-NMR spectrum of 4-cyanopyridine-2,6-d_2 before irradiation..... 187

Figure 4.74 (b) ^{1}H-NMR spectrum of 4-cyanopyridine-2,6-d_2 after irradiation for 60 min 187

Figure 4.75 ^{1}H-NMR spectrum of 2,6-dideuteriopyridine before irradiation..... 191

Figure 4.76 ^{1}H-NMR spectrum of 2,6-dideuteriopyridine after 1 hour of irradiation... 192

Figure 4.77 ^{1}H-NMR spectrum of 2,6-dideuteriopyridine after 5 hours of irradiation . 193

Figure 4.78 Expansion of signal at δ 8.48 193

Figure 4.79 Expansion of proton position 3 and 5 after irradiated for 1, 5, and 10 h.... 194

Figure 4.80 ^{1}H-NMR spectrum of **1-3,4,5-d_3** before irradiation..... 203

Figure 4.81 ^{1}H-NMR spectrum of **1-3,4,5-d_3** after 24 hours irradiation..... 204

Figure 4.82 ^{1}H-NMR expansion of H5 from photoproducts 206

Figure 4.83 Scale expansion of H5 from 2,3,4-trideuteriopyridine (**1-2,3,4-d_3**)..... 206

Figure 4.84 ^{1}H-NMR spectrum of **1-2,4,6-d_3** before irradiation 208

Figure 4.85 ^{1}H-NMR spectrum of **1-2,4,6-d_3** after 11 hours irradiation 208

Figure 4.86 ^{1}H-NMR spectrum of **1-2,3,4-d_3** before irradiation 210

Figure 4.87 ^{1}H-NMR spectrum of **1-2,3,4-d_3** after 12 hours..... 211

Figure 4.88 Scale expansion of H6 after 12 hours of irradiation..... 212

Figure 4.89 ^{1}H-NMR spectrum of **1-2,3,6-d_3** before irradiation 214

Figure 4.90 ^{1}H-NMR spectrum of **1-2,3,6-d_3** before irradiation 214

Figure 4.91 Scale expansion of H2 and H6 215

Figure 4.92 Scale expansion of H5 after 12 hours of irradiation..... 216

Figure 4.93 ^{1}H-NMR spectrum of **1-2,3,5-d_3** before irradiation 218

Figure 4.94 ^{1}H-NMR spectrum of **1-2,3,5-d_3** after 12 hours of irradiation 218

Figure 4.95 ^{1}H-NMR spectrum of **1-2,4,5-d_3** before irradiation 221

Figure 4.96 ^{1}H-NMR spectrum of **1-2,4,5-d_3** after 12 hours of irradiation..... 221

Figure 4.97 ^{1}H-NMR spectrum of **1-2,3,5,6-d_4** before irradiation 233

Figure 4.98 ^{1}H-NMR spectrum of **1-2,3,5,6-d_4** after 12 hours irradiation 234

Figure 4.99 ^{1}H-NMR spectrum of **1-2,3,4,6-d_4** before irradiation 235

Figure 4.100 ^{1}H-NMR spectrum of **1-2,3,4,6-d_4** after 12 hours irradiation 236

Figure 4.101 ^{1}H-NMR spectrum of **1-2,3,4,5-d_4** before irradiation 237

Figure 4.102 ^{1}H-NMR spectrum of **1-2,3,4,5-d_4** after 12 hours irradiation 238

Figure 4.103 GC trace of 2-cyanopyridine before irradiation 255

Figure 4.104 GC trace of 2-cyanopyridine after irradiation for 4 hours..... 256

Figure 4.105 GC trace of 3-cyanopyridine before irradiation 257

Figure 4.106 GC trace of 3-cyanopyridine after irradiation for 4 hours..... 257

Figure 4.107 GC trace of 4-cyanopyridine before irradiation 258

Figure 4.108 GC trace of 4-cyanopyridine after irradiation for 4 hours..... 259

Figure 4.109 GC trace of 2-cyanopyridine in MCH before irradiation 260

Figure 4.110 GC trace of 2-cyanopyridine in MCH after 30 minutes of irradiation 260

Figure 4.111 GC trace of 3-cyanopyridine in MCH before irradiation 261

Figure 4.112 GC trace of 3-cyanopyridine in MCH after 30 minutes of irradiation 261

Figure 4.113 GC trace of 4-cyanopyridine in MCH before irradiation 262

Figure 4.114 GC trace of 4-cyanopyridine in MCH after 30 minutes of irradiation 262

Figure A.1 ^{1}H-NMR spectrum of picolinic acid N-oxide-6-d 323

Figure A.2 ^{13}C-NMR spectrum of picolinic acid N-oxide-6-d 324

Figure A.3 ^{1}H-NMR spectrum of 4-nitropicolinic acid N-oxide-6-d 325

Figure A.4 ^{13}C-NMR spectrum of 4-nitropicolinic acid N-oxide-6-d 325

Figure A.5 ^{1}H-NMR spectrum of methyl 4-nitropicolinate N-oxide-6-d 326

Figure A.6 ^{13}C-NMR spectrum of methyl 4-nitropicolinate N-oxide-6-d 326

Figure A.7 ^{1}H-NMR spectrum of methyl 4-chloropicolinate N-oxide-6-d 327

Figure A.8 ^{13}C-NMR spectrum of methyl 4-chloropicolinate N-oxide-6-d 327

Figure A.9 ^{1}H-NMR spectrum of methyl 4-chloropicolinate-6-d 328

Figure A.10 ^{1}H-NMR spectrum of methyl 4-chloropicolinate-6-d 328

Figure A.11 ^{1}H-NMR spectrum of methyl picolinate-4,6-d_2 329

Figure A.12 ^{13}C-NMR spectrum of methyl picolinate-4,6-d_2 329

Figure A.13 ^{1}H-NMR spectrum of picolinamide-4,6-d_2 330

Figure A.14 ^{13}C-NMR spectrum of picolinamide-4,6-d_2 330

Figure A.15 ^{1}H-NMR spectrum of nicotinic acid N-oxide-2,6-d_2 331

Figure A.16 ^{13}C-NMR spectrum of nicotinic acid N-oxide-2,6-d_2 331

Figure A.17 ^{1}H-NMR spectrum of methyl nicotinate N-oxide-2,6-d_2 332

Figure A.18 ^{13}C-NMR spectrum of methyl nicotinate N-oxide-2,6-d_2 332

Figure A.19 ^{1}H-NMR spectrum of methyl nicotinate-2,6-d_2 333

Figure A.20 ^{13}C-NMR spectrum of methyl nicotinate-2,6-d_2 333

Figure A.21 ^{1}H-NMR spectrum of nicotinamide-2,6-d_2 334

Figure A.22 ^{13}C-NMR spectrum of nicotinamide-2,6-d_2 334

Figure A.23 ^{1}H-NMR spectrum of isonicotinic acid N-oxide-2,6-d_2 335

Figure A.24 ^{13}C-NMR spectrum of isonicotinic acid N-oxide-2,6-d_2 335

Figure A.25 ^{1}H-NMR spectrum of methyl isonicotinate N-oxide-2,6-d_2 336

Figure A.26 ^{13}C-NMR spectrum of methyl isonicotinate N-oxide-2,6-d_2 336

Figure A.27 ^{1}H-NMR spectrum of methyl isonicotinate-2,6-d_2 337

Figure A.28 ^{13}C-NMR spectrum of methyl isonicotinate-2,6-d_2 337

Figure A.29 ^{1}H-NMR spectrum of pyridine N-oxide-2,6-d_2 338

Figure A.30 ^{13}C-NMR spectrum of pyridine N-oxide-2,6-d_2 338

Figure A.31 ^{1}H-NMR spectrum of pyridine N-oxide-3,4,5-d_3 339

Figure A.32 ^{13}C-NMR spectrum of pyridine N-oxide-3,4,5-d_3 339

Figure A.33 ^{1}H-NMR spectrum of 4-nitropyridine N-oxide-2,6-d_2 340

Figure A.34 ^{13}C-NMR spectrum of 4-nitropyridine N-oxide-2,6-d_2 340

Figure A.35 ^{1}H-NMR spectrum of 4-chloropyridine N-oxide-2,6-d_2 341

Figure A.36 ^{13}C-NMR spectrum of 4-chloropyridine N-oxide-2,6-d_2 341

Figure A.37 ^{1}H-NMR spectrum of 4-chloropyridine-2,6-d_2 342

Figure A.38 ^{13}C-NMR spectrum of 4-chloropyridine-2,6-d_2 342

Figure A.39 ^{1}H-NMR spectrum of 3,5-dichloropyridine N-oxide 343

Figure A.40 ^{13}C-NMR spectrum of 3,5-dichloropyridine N-oxide 343

Figure A.41 ^{13}C-NMR spectrum of 3,5-dichloropyridine N-oxide-2,4,6-d_3 344

Figure A.42 ^{13}C-NMR spectrum of 3,5-dichloropyridine-2,4,6-d_3 345

Figure A.43 ^{1}H-NMR spectrum of 3,5-dichloropyridine-2,6-d_2 346

Figure A.44 ^{13}C-NMR spectrum of 3,5-dichloropyridine-2,6-d_2 346

Figure A.45 ^{13}C-NMR spectrum of pyridine N-oxide-d_5 347

Figure A.46 ^{13}C-NMR spectrum of 3-chloropyridine N-oxide-2,4,5,6-d_4 348

Figure A.47 ^{13}C-NMR spectrum of 3-chloropyridine-2,4,5,6-d_4 349

Figure A.48 ^{13}C-NMR spectrum of 2-chloropyridine-3,4,5,6-d_4 350

Figure A.49 ^{13}C-NMR spectrum of 2,5-dichloropyridine-3,4,6-d_3 351

Figure A.50 ^{13}C-NMR spectrum of 2,3-dichloropyridine-4,5,6-d_3 352

Figure A.51 ^{13}C-NMR spectrum of 3,5-dichloropyridine-2,4,6-d_3 353

Figure A.52 ^{13}C-NMR spectrum of 3,4-dichloropyridine-2,5,6-d_3 354

Figure A.53 ^{13}C-NMR spectrum of 2,4-dichloropyridine-3,5,6-d_3 355

Figure A.54 ^{13}C-NMR spectrum of 4-nitropyridine N-oxide-2,3,5,6-d_4 356

Figure A.55 ^{13}C-NMR spectrum of 4-chloropyridine N-oxide-2,3,5,6-d_4 357

Figure B.1 MS of methyl 4-chloropicolinate N-oxide-6-d 358

Figure B.2 MS of methyl 4-chloropicolinate-6-d 358

Figure B.3 MS of picolinamide-4,6-d_2 359

Figure B.4 MS of nicotinamide-2,6-d_2 359

Figure B.5 MS of Isonicotinamide-2,6-d_2 360

Figure B.6 MS of methyl isonicotinate N-oxide-2,6-d_2 360

Figure B.7 MS of pyridine N-oxide-2,6-d_2 361

Figure B.8 MS of 4-nitropyridine N-oxide-2,6-d_2 361

Figure B.9 MS of 4-chloropyridine N-oxide-2,6-d_2 362

Figure B.10 MS of 4-chloropyridine-2,6-d_2 362

Figure B.11 MS of 3,5-dichloropyridine N-oxide 363

Figure B.12 MS of 3,5-dichloropyridine N-oxide-2,4,6-d_3 363

Figure B.13 MS of 3,5-dichloropyridine-2,4,6-d_3 364

Figure B.14 MS of 3,5-dichloropyridine-2,6-d_2 364

Figure B.15 MS of 3-Chloropyridine-2,4,5,6-d_4 365

Figure B.16 MS of 2-Chloropyridine-3,4,5,6-d_4 365

Figure B.17 MS of 2,5-dichloropyridine-3,4,6-d_3 366

Figure B.18 MS of 2,3-dichloropyridine-4,5,6-d_3 366

Figure B.19 MS of 3,4-dichloropyridine-2,5,6-d_3 367

Figure B.20 MS of 2,4-dichloropyridine-3,5,6-d_3 367

Figure B.21 MS of 4-nitropyridine N-oxide-2,3,5,6-d_4 368

Figure B.22 MS of 4-chloropyridine N-oxide-2,3,5,6-d_4 368

Figure C.1 Absorption spectrum of 2-cyanopyridine in 1:1 ethanol/methanol 369

Figure C.2 Absorption spectrum of 3-cyanopyridine in 1:1 ethanol/methanol 370

Figure C.3 Absorption spectrum of 4-cyanopyridine in 1:1 ethanol/methanol 371

Figure D.1 Absorption spectrum of 2-methylpyridine vapor 372

Figure D.2 Absorption spectrum of 3-methylpyridine vapor 372

Figure D.3 Absorption spectrum of 4-methylpyridine vapor 374

LIST OF TABLES

Table 2.1 Experimental data from Caplain and Lablache-Combier work 13

Table 2.2 Experimental energetic data of pyridine vapor and derivatives 24

Table 2.3 Fluorescence and Intersystem crossing quantum yields 26

Table 2.4 Phosphorescence maxima energy, lifetime, and quantum yield 27

Table 2.5 Experimental spectral and energetic data for cyanopyridines 33

Table 2.6 Singlet and Triplet energy levels from phosphorescence excitation spectra at 77K .. 34

Table 2.7 Triplet energies from Phosphorescence band origins, phosphorescence lifetimes, quantum yields..... 35

Table 4.1 Experimental details for photolysis of 2-cyanopyridine (**36**) 46

Table 4.2 Experimental details for photolysis of 3-cyanopyridine (**37**) 51

Table 4.3 Experimental details for photolysis of 4-cyanopyridien (**38**) 56

Table 4.4 Experimental details for photolysis of **36** at ≥ 290 nm 58

Table 4.5 Experimental details for photolysis of **37** at ≥ 290 nm 60

Table 4.6 Experimental details for photolysis of **38** at ≥ 290 nm 61

Table 4.7 GC data of photoproduct mixture from irradiation of 2-methylpyridine (**6**)... 76

Table 4.8 Experimental details for irradiation of 3-methylpyridine (**7**) 82

Table 4.9 GC data of photoproduct mixture from irradiation of 4-methylpyridine (**8**)... 88

Table 4.10 The substituent effects on stability of allylic radicals..... 98

Table 4.11 Experimental details for photolysis of 2-cyanopyridine-4,6-d_2..... 174

Table 4.12 Experimental details for photolysis of 3-cyanopyridine-2,6-d_2..... 180

Table 4.13 Experimental details for photolysis of 4-cyanopyridine-2,6-d_2..... 186

Table 5.1 Irradiation of 2-cyanopyridine (**36**) at 254 nm 265

Table 5.2 Irradiation of 3-cyanopyridine (**37**) at 254 nm 266

Table 5.3 Irradiation of 4-cyanopyridine (**38**) at 254 nm 267

Table 5.4 Irradiation of 2-methylpyridine (**6**) at 254 nm 268

Table 5.5 Irradiation of 3-methylpyridine (**7**) at 254 nm 269

Table 5.6 Irradiation of 4-methylpyridine (**8**) at 254 nm 270

Table 5.7 Irradiation of 2-cyanopyridine (**36**) at $\lambda \geq 290$ nm 271

Table 5.8 Irradiation of 3-cyanopyridine (**37**) at $\lambda \geq 290$ nm 272

Table 5.9 Irradiation of 4-cyanopyridine (**38**) at $\lambda \geq 290$ nm 272

Table 5.10 Irradiation of 2-cyanopyidine-4,6-d_2 (**36-4,6-d_2**) 273

Table 5.11 Irradiation of 3-cyanopyridine-2,6-d_2 (**37-2,6-d_2**) 274

Table 5.12 Irradiation of 4-cyanopyridine-2,6-d_2 (**38-2,6-d_2**) 275

CHAPTER I

Introduction

The photochemical isomerization of heterocyclic ring compounds which contain a C-N double bond have received considerable attention for many decades.[1] Surprisingly, their photochemical and photophysical properties have not been clearly understood. Although there have been many accounts of this area of photochemistry, very little is known about the photochemistry of these compounds.

For many years the light-induced isomerization of simple benzenoid compounds into phototransposition intermediates such as benzvalene, Dewar benzene, prismane, and fulvene derivatives have been reported.[2]

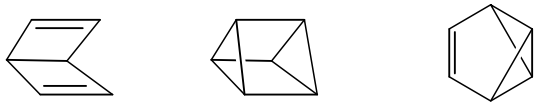

Dewar-benzene prismane benzvalene

The photochemistry of pyridine and its derivatives have also been of much interest because they exhibit many distinct and interesting features. Like benzene, it is known that after pyridine and its derivatives are irradiated by UV light, they undergoes valence bond isomerization to yield non-planar isomers such as Dewar-pyridine, azabenzvalene, and azaprismane, which have been suggested to be the intermediates in the photochemical transformation.[3]

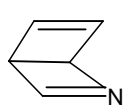

Dewar-pyridine

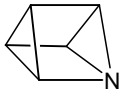

azaprismane

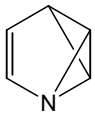

azabenzvalene

However, a study of photochemical and photophysical properties of the six isomeric dimethylpyridines, in our laboratory revealed that these dimethylpyridines undergo phototransposition upon irradiation in the vapor phase at 254 nm. It was discovered that the non-planar isomer, azaprefulvene, formed by 2,6-bridging is the major intermediate in the phototransposition mechanism. Nevertheless, Dewar-Pyridine intermediates were also observed in the interconversion between 2,3-dimethylpyridine and 2,5-dimethylpyridine upon irradiation in the condensed phase at -30 ^{o}C.

Recently, the vapor phase photochemistry of the three isomers of cyanopyridine has been studied in our laboratory. The photochemical and photophysical properties of the three isomers were previously reported by Sarkar and co-workers.[4] To understand the phototransposition mechanism of cyanopyridines, the vapor phase photochemistry of all three cyanopyridine isomers were carried out. Furthermore, to simplify the ^{1}H-NMR data of photoproducts, the photochemistry of deuterium-labeled cyanopyridines has been studied. The results from both experiments have been compared to explain the behavior of pyridine and its derivatives at the excited state level.

The photochemistry of deuterium labeled pyridines is also a major part of this thesis. The study of deuterium labeled pyridine allows observation of phototransposition reactions which would not be observed in the absence of suitable labels.

The following chapter will provide a review of the photochemical and photophysical information of pyridine, methylpyridines, and cyanopyridines that were reported in the literature. Theoretical studies of some pyridine derivatives are also reviewed.

CHAPTER II

Literature review

2.1. Photochemistry of pyridine and its derivatives

The photochemistry of pyridine (**1**) under various conditions has been studied extensively for many decades. In 1970, Wilzbach and Rausch[5] discovered that irradiation of pyridine (**1**) at 254 nm in butane solution at -15 ^{o}C for 45 minutes lead to the formation of Dewar-pyridine (**2**), as confirmed by ^{1}H-NMR spectrum. This NMR spectrum

Scheme 2.1 Irradiation of pyridine in butane

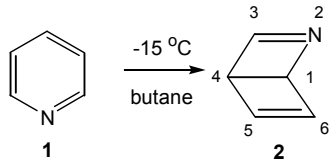

recorded at -25 ^{o}C gave proton signals at δ 4.03, 5.22, 6.51, and 6.54 which correspond to the protons at position 4, 1, 6, and 5, respectively, of Dewar-pyridine. The first two were assigned to the bridgehead protons and the latter two were assigned to the vinyl protons. At more elevated temperatures the valence isomer **2** reverted back to pyridine (**1**). In acetonitrile solution, the half-life of Dewar-pyridine (**2**) was found to be 36 minutes at 0 ^{o}C and 2 minutes at room temperature. These results show that in butane or acetonitrile solvent the only reaction of the photochemically generated Dewar-pyridine (**2**) is its reversion back to pyridine (**1**). It should be noted that the half-life of Dewar-pyridine (**2**)

is much shorter than the half-life of synthetic Dewar-benzene, which was reported to be ~2 days at room temperature in a solution of pyridine.[6]

These workers also showed that if pyridine is irradiated in water or in aqueous sodium borohydride, then Dewar-pyridine is trapped by reaction with water or by reduction of the imine double bond. The hydration step was proposed to take place on the Dewar-pyridine **2** by addition of water across the imine double bond. The unstable hydrated Dewar-pyridine **4** was then proposed to undergo ring opening to yield the δ-aminopentadienal (**5**). This mechanism is shown in Scheme 2.2. In the presence of sodium borohydride, reduction of the double bond occurs to yield the stable bicyclic compound **3**. Isolation of **3** is excellent evidence for the intermediacy of Dewar-pyridine (**2**).

Scheme 2.2 Irradiation of pyridine in water or in $NaBH_4$

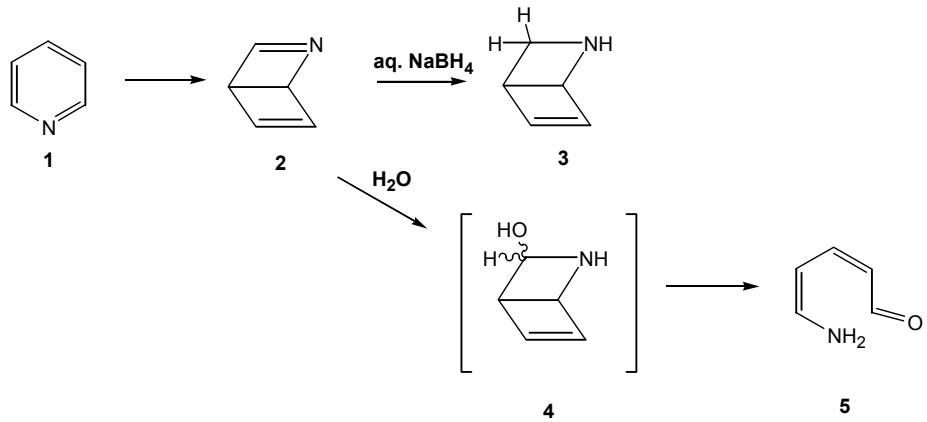

Linnell and Noyes discovered that irradiation of pyridine in the vapor phase at 253.7 nm led to little decomposition.[7] This result is consistent with the work of Mathias

and Heicklen who observed little or no decomposition when pyridine was irradiated at 254 nm.[8] In addition, there was no gaseous photoproduct observed upon irradiation at 265 or 248 nm. Interestingly, irradiation at shorter wavelength (228.8 and 213.9 nm) converted pyridine to acetylene and acrylonitrile.

A qualitative study using flash photolysis by Roquitte[9] identified the products of pyridine irradiation to be acetylene and hydrogen cyanide.[10] Identically, irradiation of pyridine matrix isolated in argon at 8K gave rise to hydrogen cyanide and cyclobutadiene as secondary products.[11]

Scheme 2.3 Irradiation of pyridine matrix isolated in argon at 8 K

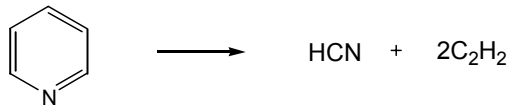

1

It was assumed that these products arise from photofragmentation of initially formed Dewar-Pyridine (**2**), as shown in scheme 2.4, followed by ring opening to form cyclobutadiene and hydrogen cyanide. Cyclobutadiene subsequently undergoes reverse 2+2 cycloaddition to form two molecules of acetylene (Scheme 2.5).

Scheme 2.4 Irradiation of pyridine forms cyclobutadiene and HCN

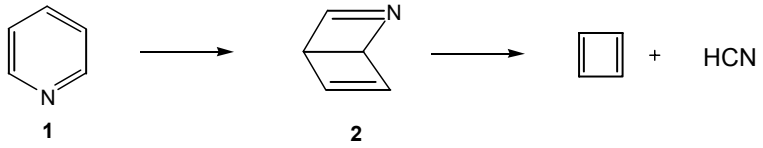

1 **2**

Scheme 2.5 Photolytic ring cleavage of cyclobutadiene

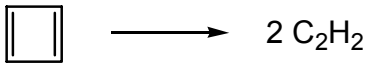

The vapor phase photochemistry of 2-methylpyridine (**6**) was studied by Roebke.[12] The irradiation of 2-methylpyridine (**6**) vapor at 238-266 nm resulted in the formation of 3-methyl and 4-methylpyridine in a 10:1 ratio.

Scheme 2.6 Photolysis of 2-methylpyridine

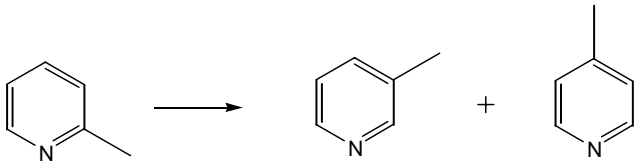

6 **7** **8**

According to Roebke, a mechanism involving an azaprismane intermediate formed from Dewar-pyridine was suggested as a reasonable reaction pathway for the observed rearrangements. Roebke speculated that the mechanism involving an azabenzvalene would not allow the photoisomerization of 2-methylpyridine (**6**) to 3- and 4-methylpyridine (**7** and **8**).

If this speculation is true, the conversion of 2-methylpyridine (**6**) to 3-methylpyridine (**7**) and 4-methylpyridine (**8**) via an azaprismane mechanism requires the formation of Dewar-pyridine. This mechanism was discussed in Kebede's thesis.[13] Two possible azaprismane structures can result from the formation of Dewar-pyridine either by 2,5- or 3,6-bridging that will yield Dewar pyridine **9** and **11**, respectively.

Scheme 2.7 2,5- and 3,6-Bridging for 2-methylpyridine

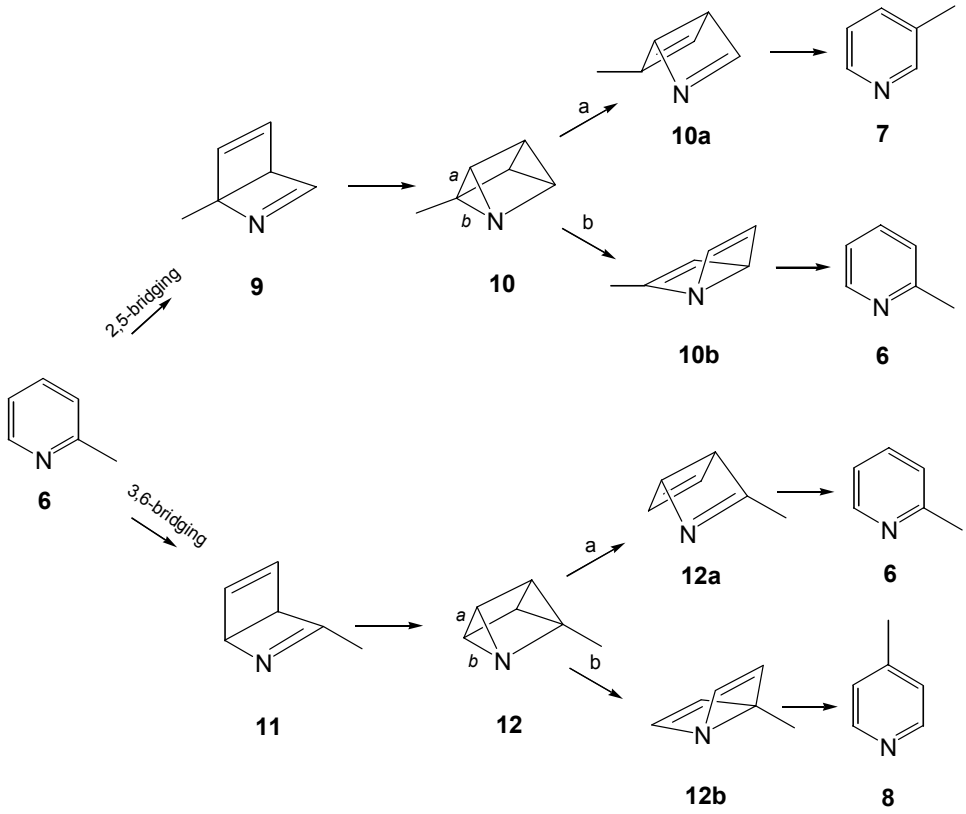

Subsequent [2+2] cycloaddition reaction of **9** and **11** would give azaprismane **10** and **12**. The azaprismane **10** can then undergo ring-opening by three distinct bond cleavages that will result in the formation of isomeric Dewar-pyridines **9**, **10a**, **10b**.

Rearomatization of the Dewar-pyridines **10a** and **10b** therefore formed the starting material, 2-methylpyridine (**6**), and 3-methylpyridine (**7**), one of the photoproducts.

The second possible Dewar-pyridine **11**, formed from 3,6-bridging, will yield the azaprismane **12** by a [2+2] cycloaddition reaction. Ring opening reactions in this case also results in three possible Dewar-pyridines **11**, **12a**, and **12b**. Rearomatization of these Dewar-pyridines will yield the starting material and 4-methylpyridine (**8**), the other observed photoproduct.

Moreover, 1,4-bridging in 2-methylpyridine (**6**) can result in the formation of a third Dewar-pyridine **13** which can undergo [2+2] cycloaddition to give azaprismane **14**. When **14** rearranges by the three possible ring opening and rearomatization processes, the products formed from **14a** and **14b** are the starting material, 2-methylpyridine (**6**) and one of the observed photoisomerization products 3-methylpyridine (**7**).

Scheme 2.8 1,4-Bridging for 2-methylpyridine

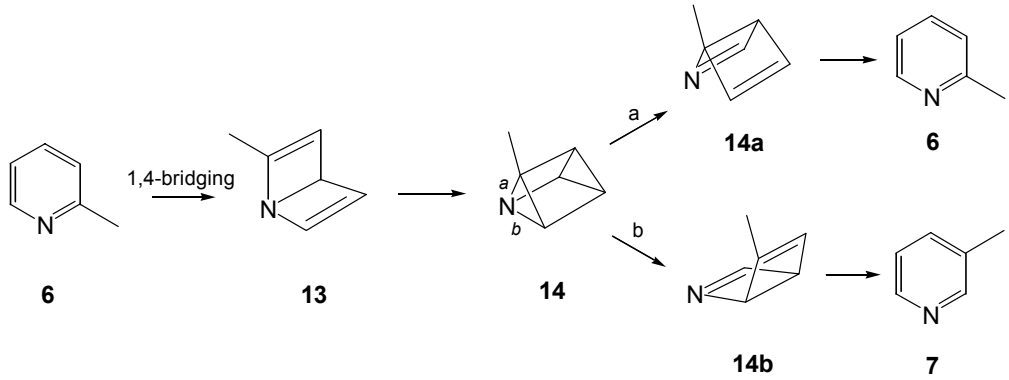

If all of these suggested reactions occur in a statistical basis, 3-methylpyridine and 4-methylpyridine should be formed in a ratio of 2: 1. This statistically expected ratio is very different from the observed ratio of 10: 1. Thus, if the suggested mechanistic pathway is correct, a number of very arbitrary assumptions regarding the selectivity of bond formation and bond opening would be required. It is difficult to see how these arbitrary decisions would be justified.

In contrast to Roebke's report, Caplain and Lablache-Combier[14] reported that irradiation of 2-methylpyridine vapor resulted in the formation of 4-methylpyridine as the only photoproduct. This product was reported by Roebke to be the minor product and that 3-methylpyridine was the major product. If Caplain and Lablache-Combier could observe the minor product, it is difficult to understand why they were unable to detect the major product.

Caplain and coworkers[15] reported evidence that supports the involvement of radical intermediates by irradiating pyridine and its 2- and 4-methyl derivatives in cyclohexane. According to these workers, irradiation of pyridine in cyclohexane solution led to the formation of 2-cyclohexylpyridine (**15**) and 4-cyclohexylpyridine (**16**) as shown in Scheme 2.9.

Scheme 2.9 Photolysis of pyridine in cyclohexane

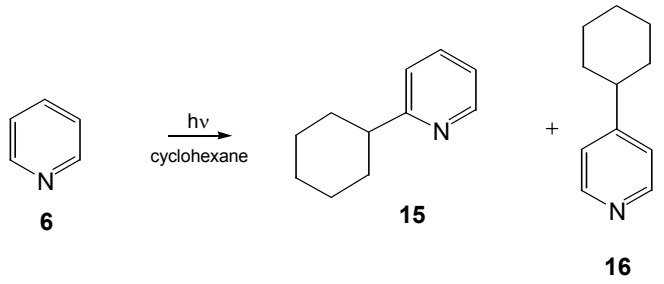

In addition, irradiation of 2-methylpyridine in cyclohexane produced 6- and 4-cyclohexyl-2-methylpyridine (**17** and **18**), bis-cyclohexane (**19**) and methylcyclohexane (**20**), as shown in Scheme 2.10, in a ratio of 10:10:20:1.

Scheme 2.10 Photolysis of 2-methylpyridine in cyclohexane

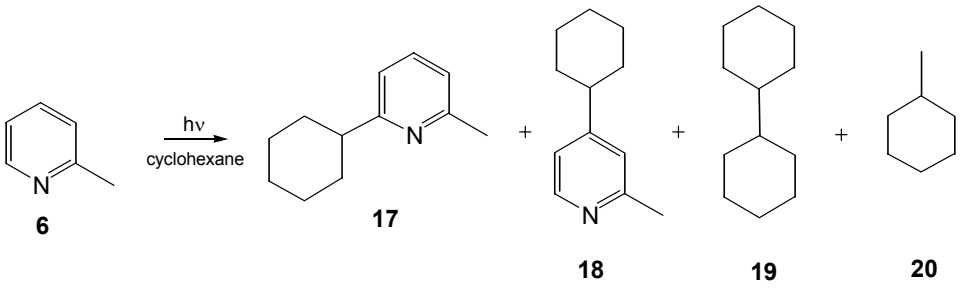

In the case of 4-methylpyridine (**8**), it was reported to undergo photoisomerization to 2-methylpyridine (**6**) and to photosubstitution with cyclohexane at C4 and C6 to yield **17** and **18** (Scheme 2.11).

Scheme 2.11 Photolysis of 4-methylpyridine in cyclohexane

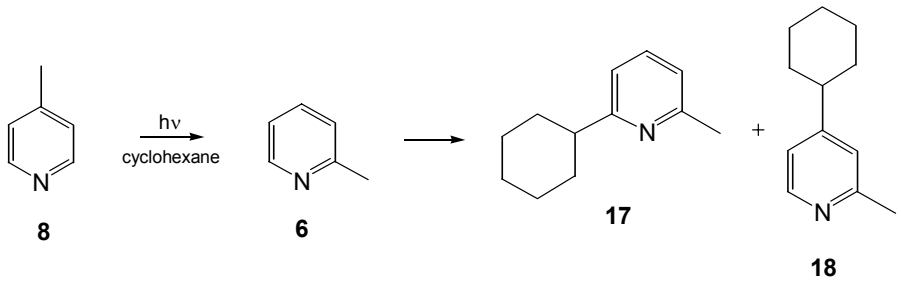

Pascual[16] reported the vapor phase photolysis of 2- and 4-methylpyridine (**6** and **8**) with a mercury lamp for 72 hours. It was observed that **6** yielded **8**, 2,4-dimethylpyridine (**21**), and a large amount of polymer as shown in Scheme 2.12.

Scheme 2.12 Photolysis of 2-methylpyridine vapor by Pascual's group

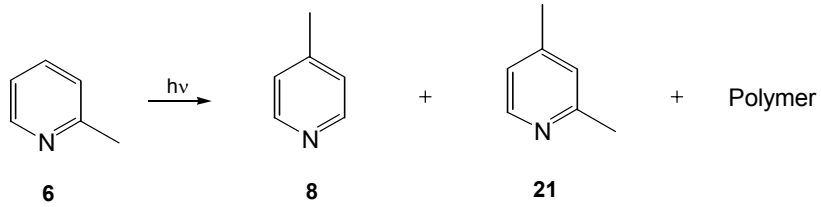

Interestingly, it was found that irradiation of **8** yielded **6**, pyridine (**1**), and a small amount of polymer. There was, however, no dimethylpyridine product that could be observed.

Scheme 2.13 Photolysis of 4-methylpyridine vapor by Pascual's group

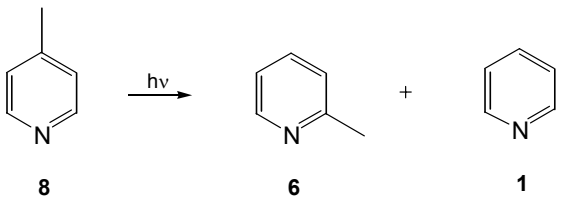

Hence, Pascual suggested that the product **1** and **21** may result from reactions that proceed via radical type methylation-demethylation.

The vapor phase photochemistry of 2,4-, 2,3-, 2,5-, 2,6-, 3,4-, and 3,5-dimethylpyridines (**21-26**) was also studied by Caplain and Lablache-Combier.[14] Table 2.1 shows the experimental results from irradiation of dimethylpyridines reported by Caplain and Lablache-Combier.

Table 2.1 Experimental data from Caplain and Lablache-Combier work

Dimethylpyridine	Photoproducts
2,3-	2,5-, 3,4-
2,4-	2,6-
2,5-	2,3-, 3,4-
2,6-	2,4-
3,4-	2,3-, 2,5-
3,5-	None

Caplain and Lablache-Combier explained these reactions by the Dewar-pyridine azaprismane mechanism also suggested by Roebke. Their explanations, however, leave substantial unanswered mechanistic questions. For example, according to Caplain and Lablache-Combier, irradiation of 2,6-dimethylpyridine (**24**) results in the formation of 2,4-dimethylpyridine (**21**). The conversion to **21** requires that the reactant first undergoes 2,5- or 3,6-bridging to form Dewar-pyridine 27 as shown in Scheme 2.14.

Scheme 2.14 2,5- and 3,6-Bridging for 2,6-dimethylpyridine

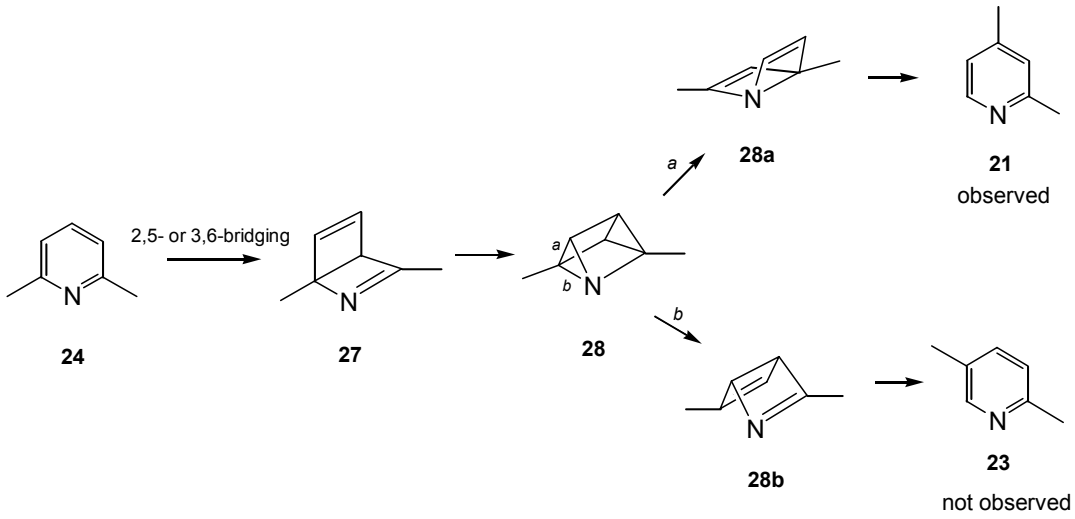

The subsequent azaprismane **28** undergoes regiospecific opening via cleavage by path *a*, but not path *b* which would result in the formation of 2,5-dimethylpyridine (**23**). Caplain and Lablache-Combier could not explain the reason why this transformation undergoes only by path *a*.

Alternatively, shown in Scheme 2.15 the conversion of 2,3-dimethylpyridine (**22**) to a mixture of 2,5-dimethylpyridine (**23**) and 3,4-dimethylpyridine (**25**) requires initial N-C4 bonding (1,4- but not 2,5- or 3,6-bonding), followed by cleavage of azaprismane (**30**) via both *a* and *b* pathways.

Scheme 2.15 1,4-Bridging for 2,4-dimethylpyridine

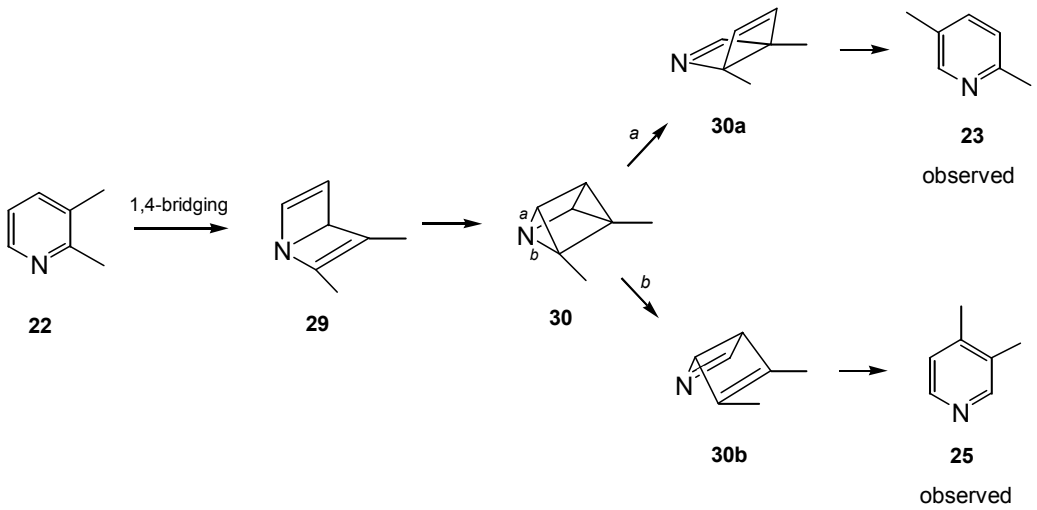

These examples illustrate the arbitrary selectivity that must be imposed upon the possible modes of formation of the initially formed Dewar-pyridines as well as on the rearomatization of the subsequently formed azaprismanes.[13]

Work on photochemistry of dimethylpyridines was reinvestigated by Pavlik and colleagues.[17] It was discovered that dimethylpyridines undergo phototransposition upon irradiation in the vapor phase at 254 nm to yield different products than those reported by Caplain and Lablache-Combier. It was found that the six dimethylpyridines (**21-26**) could be divided into two triads as shown in Scheme 2.16.

Scheme 2.16 Photo-interconversion of dimethylpyridines

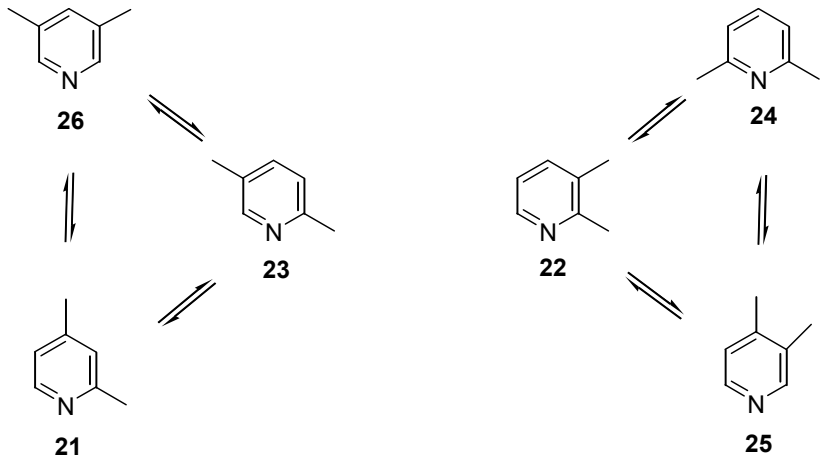

The interconversions within each triad were suggested to occur via a mechanism involving 2,6-bonding followed by nitrogen migration and rearomatization as shown in Scheme 2.17 and 2.18.

Scheme 2.17 Phototransposition mechanism in triad 1

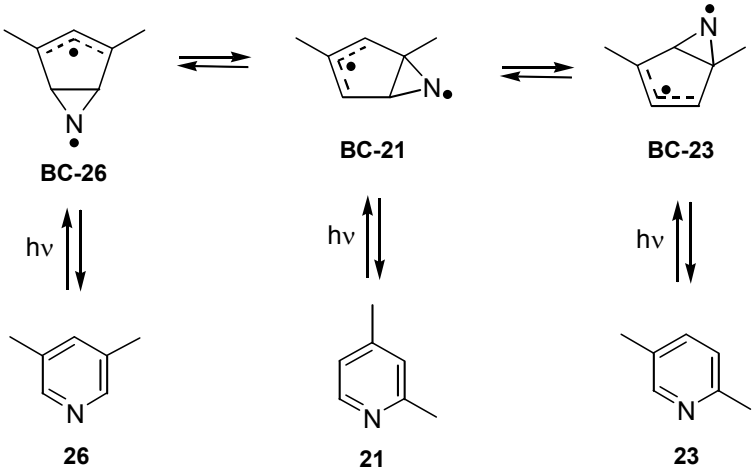

Scheme 2.18 Phototransposition mechanism in triad 2

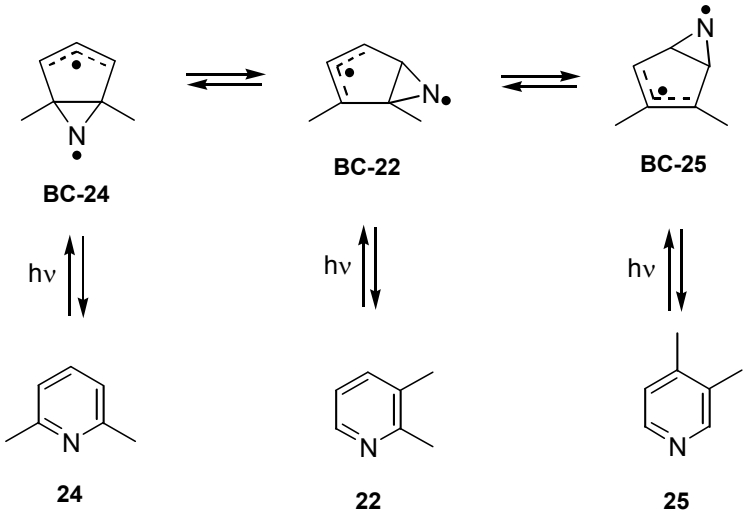

In addition to the reactions within each triad, 2,5-dimethylpyridine(**23**), a member of triad 1, was observed to interconvert with 2,3-dimethylpyridine (**22**), a member of triad 2. These inter-triad reactions were suggested to occur via interconverting Dewar pyridine intermediates as shown in Scheme 2.19.

Scheme 2.19 Inter-triad reaction

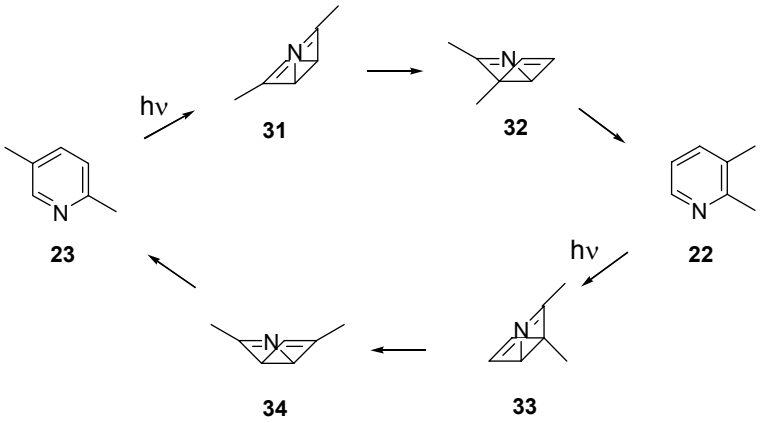

The intra-triad interconversions occur upon irradiation of the dimethylpyridine with light of 254 nm. These reactions are quenched by adding nitrogen (15-20 Torr) to the reaction mixture and do not occur when the dimethylpyridines are irradiated with light of wavelength greater than 290 nm.

When the dimethylpyridines absorb light of λ = 254 nm the molecules undergo a π,π^* transition leading to the formation of vibrationally excited $S_2(\pi,\pi^*)_{vib}$ molecules. It should be noted here that if pyridine was excited into the relaxed vibrationally excited $S_2(\pi,\pi^*)_0$ state, the formation of azaprefulvene would not take place since the carbon

atoms at ring position 2 and 6 are still far apart. The structure of pyridine molecule, however, would transform in a way that C2 and C6 come close resulting in 2,6-bonding when it absorbs energy into a vibrationally excited state. In the presence of nitrogen gas in the reaction mixture, this excess vibrational energy can be transferred from the dimethylpyridine $S_2(\pi,\pi^*)_{vib}$ to nitrogen leaving the dimethylpyridine molecules in the vibrationally relaxed $S_2(\pi,\pi^*)_0$ state. Since the addition of nitrogen was observed to quench the intra-triad interconversions, it was concluded that the intra-triad reactions occur from the vibrationally excited $S_2(\pi,\pi^*)_{vib}$ molecules and that the vibrationally relaxed $S_2(\pi,\pi^*)$molecules are less reactive in the 2,6-bonding mechanism.

The inter-triad interconversions of 2,3-dimethylpyridine (**22**) and 2,5-dimethylpyridine (**23**) were enhanced by the addition of N_2 gas to the reaction mixture, were observed upon irradiation with light of $\lambda > 290$ nm, and took place in the condensed phase at low temperature (-30^oC). These observations indicate that the inter-triad reactions occur from a state of lower energy than the S_2 (π,π^*) state. This could be the S_1 (n,π^*) or a T_1 state.

The phototransposition of dimethylpyridines was suggested to occur *via* 2,6-bonding cyclization resulting in a non-planar structure, azaprefulvene (**BC-1**). This intermediate (scheme 2.20) will allows nitrogen to migrate around the five sides of cyclopentenyl ring followed by rearomatization to form the isomeric products.

Scheme 2.20 Formation of azaprefulvene

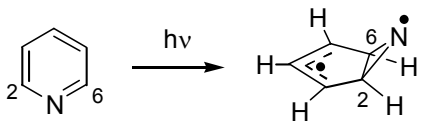

1 **BC-1**

An azaprefulvene intermediate was also suggested by Chachisvillis and Zewail[18] to result from deactivation of the $S_2(\pi,\pi^*)$ state of pyridine. These workers investigated the deactivation pathway for excited pyridine in solution phase using the technique of femtosecond transient spectroscopy. In this work pyridine in acetonitrile solvent was excited with a femtosecond pulse of 266 nm. This resulted in the population of vibrationally excited $S_1(n,\pi^*)_{vib}$ and $S_2(\pi,\pi^*)_{vib}$ molecules.

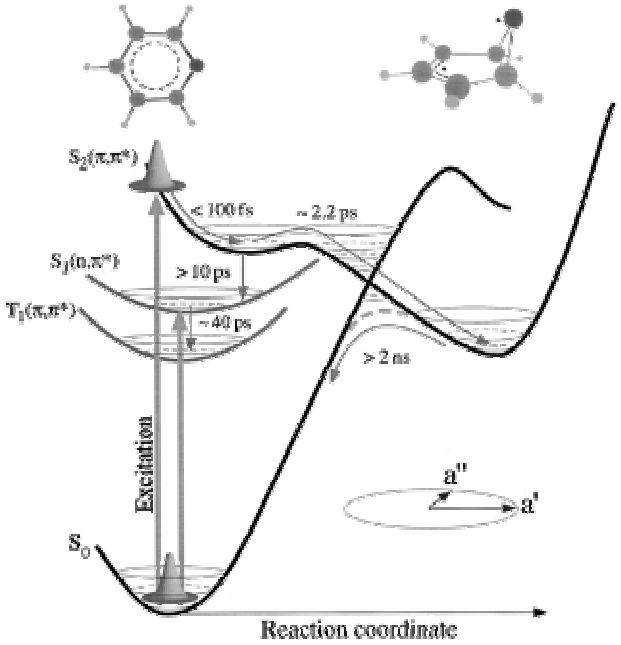

Figure 2.1 Potential energy surface representing photochemistry and photophysics of pyridine in solution phase[18]

The vibrationally excited $S_2(\pi,\pi^*)_{vib}$ molecule was observed to relax to its equilibrium geometry in less than 100 fs. Two pathways were detected for this vibrationally relaxed $S_2(\pi,\pi^*)$ molecule. First, this $S_2(\pi,\pi^*)$ molecule was observed to undergo internal conversion to the $S_1(n,\pi^*)$ state in a time greater than 10 ps. Second, the $S_2(\pi,\pi^*)$ pyridine molecule rapidly (~2.2 ps) isomerizes to the azaprefulvene species by passing over a low energy barrier and through a conical intersection. Theoretical calculation also have previously suggested that the $S_2(\pi,\pi^*)$ pyridine would isomerize to the azaprefulvene molecule. This azaprefulvene species is the same species that we suggest as the key intermediate in the cyclization-heteroatom migration mechanism. According to Chachivisllis and Zewail this azaprefulvene can pass over a barrier and revert to the ground state of pyridine in greater than 2 ns.

Zewail and co-workers also studied the deactivation dynamics of excited pyridine in the gas phase.[19] In these experiments, pyridine vapor was excited with femtosecond light pulses of 277 nm. Although this is sufficient energy to populate the $S_1(n,\pi^*)$ singlet state (0-0 = 287.6 nm) it cannot bring about excitation to the $S_2(\pi,\pi^*)$ singlet which has a 0-0 origin at 260.7 nm. Furthermore, although the $S_1(n,\pi^*)$ singlet is populated with excess vibrational energy, it is about 300 cm^{-1} below the onset of channel three activity. After this excitation, time-resolved mass spectroscopy showed a decay component of 400 fs which describes the initial motion of pyridine on the pyridine potential surface. These experiments also revealed components of 3.5 ps and 15 ps which were assigned to Dewar-pyridine and azabenzvalene respectively. Presummably, an azaprefulvene species is on the reaction coordinate leading to the azabenzvalene.

It is interesting to note that for pyridine-d_5, the decay time for the d_5-Dewar isomer increased from 3.5 ps to 5.1 ps but remained nearly the same, ~16 ps, for the d_5-azabenzvalene isomer. According to these workers, the difference in the effect of deuteration is due to the differences in the motion of the nuclei during the formation of the transition states leading to the two valence isomers. During the formation of the Dewar-pyridine all five deuterium atoms are involved in bending motions while during azabenzvalene formation C-C twisting is localized and only two deuterium atoms participate. Thus, perdeuteration effects Dewar-pyridine formation to a greater extent than it effects azabenzvalene formation.

Zewail and Colleagues[20] have also studied the deactivation pathways for excited pyridine in the vapor phase using ultra-fast electron diffraction. In these experiments, a femtosecond light pulse of 267 nm was used to excite pyridine vapor into the $S_1(n,\pi^*)$ state with excess vibrational energy of approximately 2700 cm^{-1}, well above the 1600 cm^{-1} threshold for channel three behavior. Sequentially delayed ultra-short electron pulses were then used to probe the resulting structural changes. Interestingly, the results of this experiment were not consistent with either direct $S_1 \rightarrow (S_0)_{vib}$ internal conversion to a vibrationally excited ground state pyridine molecules or $S_1 \rightarrow S_0$ internal conversion by way of an azabenzvalene intermediate. Instead, the results indicated that the primary

Scheme 2.21 Ultra-fast electron diffraction experiment

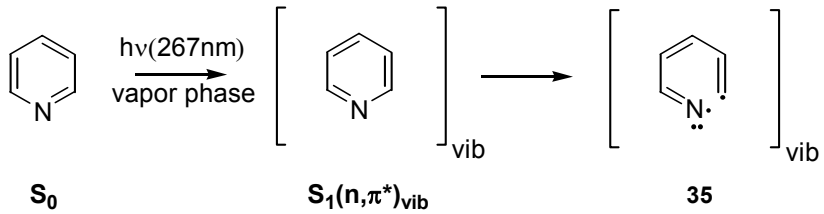

product from the vibrationally excited $S_1(n,\pi^*)_{vib}$ pyridine molecule is a vibrationally excited ring-opened biradical (**35**) formed by cleavage of the C-N bond.

No suggestions have been given for the role that such a ring-opened species might have in pyridine photochemistry. It is possible that the initially formed vibrationally excited biradical could undergo rapid vibrational relaxation followed, by recyclization to a ground state pyridine molecule. This ring opening-ring closure pathway would therefore be an energy wasting process. It is also interesting to speculate that this ring-opened biradical could cyclize as shown in Scheme 2.22 and lead to the azaprefulvene

Scheme 2.22 Cyclization of ring-opened biradical

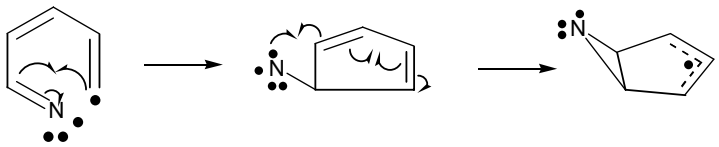

intermediate. No experimental evidence exists for this pathway and it must therefore only be considered as a possibility.

2.1.1. Spectroscopic properties of pyridine and methylpyridines

The spectroscopic behavior of pyridine (**1**) and isomeric methylpyridines (**6** and **7**) was studied by Yamasaki and coworkers.[21] The positions of the 0-0 bands of $S_1 \rightarrow S_0$ absorption for pyridine, pyridine-d_5, 2-methylpyridine (**6**), and 3-methylpyridine (**7**) in the gas phase are shown in Table 2.2.

Table 2.2 Experimental energetic data of pyridine vapor and derivatives

	$S_0 \rightarrow S_1\ (n,\pi^*)_{0-0}$	$S_0 \rightarrow S_2\ (\pi,\pi^*)_{0-0}$
	nm (kcalmol^{-1})	nm (kcalmol^{-1})
Pyridine-h_5	288 (99.3)	261 (110.0)
Pyridine-d_5	286 (100.0)	259 (110.4)
2-MP (**6**)	288 (99.3)	266 (107.5)
3-MP (**7**)	288 (99.3)	268 (106.7)
2,6-DMP (**22**)	285 (100.3)	271 (105.5)

The $S_1(n, \pi^*)_{0-0}$ state of pyridine (**1**) and its methylpyridines (**6-8**) lie above their ground states at the same energy level of 99.3 kcal mol^{-1}. The 0-0 point level of pyridine-d_5 is about 0.7 kcalmol^{-1} higher than that of pyridine-h_5. The $S_2(\pi,\pi^*)$ states of pyridine and the methylpyridines were located from the 0-0 bands to lie approximately 107 kcal mol^{-1} above their ground states.

The methyl-substitution on pyridine gives rise to a significant red shift of the $S_0 \rightarrow S_2$ transition but the substitution has only a slight effect on the $S_0 \rightarrow S_1$ transition. This therefore results in a decrease in the energy gap between S_1 and S_2 states.

Fluorescence properties and non-radiative processes of pyridine, pyridine-d_5 and methylpyridines were also reported. These workers observed that pyridine is only very weakly fluorescent with a fluorescence quantum yield of only 10^{-4} after excitation into the 0-0 band of the $S_0 \rightarrow S_1(n,\pi^*)$ transition. Interestingly, the quantum yield of fluorescence decreases by a factor of 100 to 10^{-6} when the molecule is excited at the $S_0 \rightarrow S_2$ origin. This decrease in the quantum yield of fluorescence with increasing energy of excitation has also been observed for benzene. Thus, the fluorescence quantum yield of benzene has been reported to be only 0.57 as great at an excitation energy of 248 nm as when benzene is excited at 254 nm.[22] This decrease in the fluorescence is quite dramatic. Thus, the quantum yield for benzene fluorescence has been reported to be 0.18 at 253 nm, 0.10 at 248 nm, and 0 at 242 nm.[23]

This decrease in fluorescence has been taken to indicate that an efficient non-radiative pathway for benzene or pyridine becomes available at vibrational energy levels above the 0-0 origin. This new non-radiative pathway has been termed channel three. The onset for channel three in benzene has been reported to occur at ~3000 cm^{-1} above the S_1 origin while for pyridine the onset occurs at ~1600 cm^{-1} above the S_1 origin.[24] This non-radiative pathway has been viewed to lead to a meta-bonded ground state prevalene diradical which can revert to the aromatic reactant or cyclize to a benzvalene isomer. In

the case of pyridine,[25] this channel three pathway has been shown to result in cleavage of the aromatic ring.[20,26]

The inherent S_1 lifetimes of pyridine (**1**) and methylpyridines (**6** and **7**) were estimated to be 0.02-0.03 ns from the fluorescence quantum yields and the radiative rate constants derived from the oscillator strengths.[27,28] The fluorescence quantum yields (ϕ_F) for excitation at 0-0 band of the $S_0 \rightarrow S_1$ and $S_0 \rightarrow S_2$ absorption were given in Table 2.3.

Table 2.3 Fluorescence and Intersystem crossing quantum yields

	$S_0 \rightarrow S_1$ $(n,\pi^*)_{0\text{-}0}$		$S_0 \rightarrow S_2$ $(\pi,\pi^*)_{0\text{-}0}$	
	$\phi_{F\ (x10^{-5})}$	ϕ_{ISC}	$\phi_{F(x10^{-5})}$	ϕ_{ISC}
Pyridine-h_5	5.9	0.5	0. 27	0.02
Pyridine-d_5	6.0		0.46	
2-MP	3.5	0.6	0.44	0.08
3-MP	5.4		0.30	
2,6-DMP	2.5		2.6	

The ϕ_F decreases significantly as the excitation energy is changed from the value corresponding to the $S_0 \rightarrow S_1$ transition ($\sim 3.5\text{-}5.9 \times 10^{-5}$) to the one corresponding to the $S_0 \rightarrow S_2$. Furthermore, the changes in ϕ_F of all compounds were found to be independent on increasing the pressure or adding the foreign gas.

The intersystem crossing yields (ϕ_{ISC}) of the compounds were also determined. The ϕ_{ISC} after $S_0 \rightarrow S_1$ excitation is greater than ϕ_{ISC} after $S_0 \rightarrow S_2$ excitation. The maximum value of ϕ_{ISC} from $S_1(n,\pi^*)$ state is 0.5 at a total pressure of 15 Torr. The intersystem crossing yield of 2-methylpyridine (**6**) vapor reported by Roebke shows values of 0.21, 0.12, 0.08, 0.03 for excitation at 280, 275, 266, and 248 nm, respectively.

The phosphorescence properties of pyridine (**1**) and its methyl pyridines (**6** and **8**) were studied by Suzuki and coworkers.[29] In this work, excitation of all sample vapors was carried out at the 0-0 band of $S_0 \rightarrow S_1$ absorption except for 2,6-lutidine (**24**) which does not have a well-resolved 0-0 band. It was observed that the phosphorescence spectra of all compounds remain unchanged in shape and position under the excitation wavelength and the vapor pressure factors. The phosphorescence characteristics of pyridine and its methyl derivatives in the vapor phase were shown in Table 2.4.

Table 2.4 Phosphorescence maxima energy, lifetime, and quantum yield

	λ^p_{max} nm (kcal mol^{-1})	τ_p (μs)	ϕ_p
Pyridine	450 (63.6)	0. 27	4.4×10^{-7}
2-MP	420 (68.1)	0.44	2.4×10^{-7}
3-MP	430 (66.8)	0.30	-
2,6-DMP	415 (69.0)	2.6	2.0×10^{-7}

The phosphorescence spectra have onsets near 350 nm (81.7 kcal mol^{-1}) for all compounds, but the intensity maximum blue shifts upon increasing the number of methyl groups in the ring. This 0-0 transition energy was consistent with the value of 84.8 kcal mol^{-1} from the $S_0 \rightarrow T$ absorption spectrum of pyridine vapor reported by Japar and Ramsay.[30] The phosphorescence maxima wavelength, λ^p_{max}, of pyridine is 450 nm, while the maxima for other compounds are shifted to the blue. It should be noted that the excitation spectra of all compounds agree well with their absorption spectra.

Furthermore, the phosphorescence lifetimes and quantum yields have also been reported. The phosphorescence lifetimes of pyridine and methylpyridines are of the order of 1 μs which is considered as a short lifetime. The phosphorescence quantum yield is also anomously low, on the order of 10^{-7}. These behaviors of pyridine and methylpyridines result from the strong vibronic coupling between the lowest triplet state, $T_1(\pi,\pi^*)$ and the second lowest triplet state $T_2(n, \pi^*)$ which gives rise to a pseudo-Jahn-Teller interaction. This interaction causes distortion of the potential surface of T_1, resulting in the extremely weak phosphorescence of pyridine.[31,32]

The energies and configurations of the various states of each pyridine and dimethylpyridines are summarized in Figure 2.2, 2.3, and 2.4.

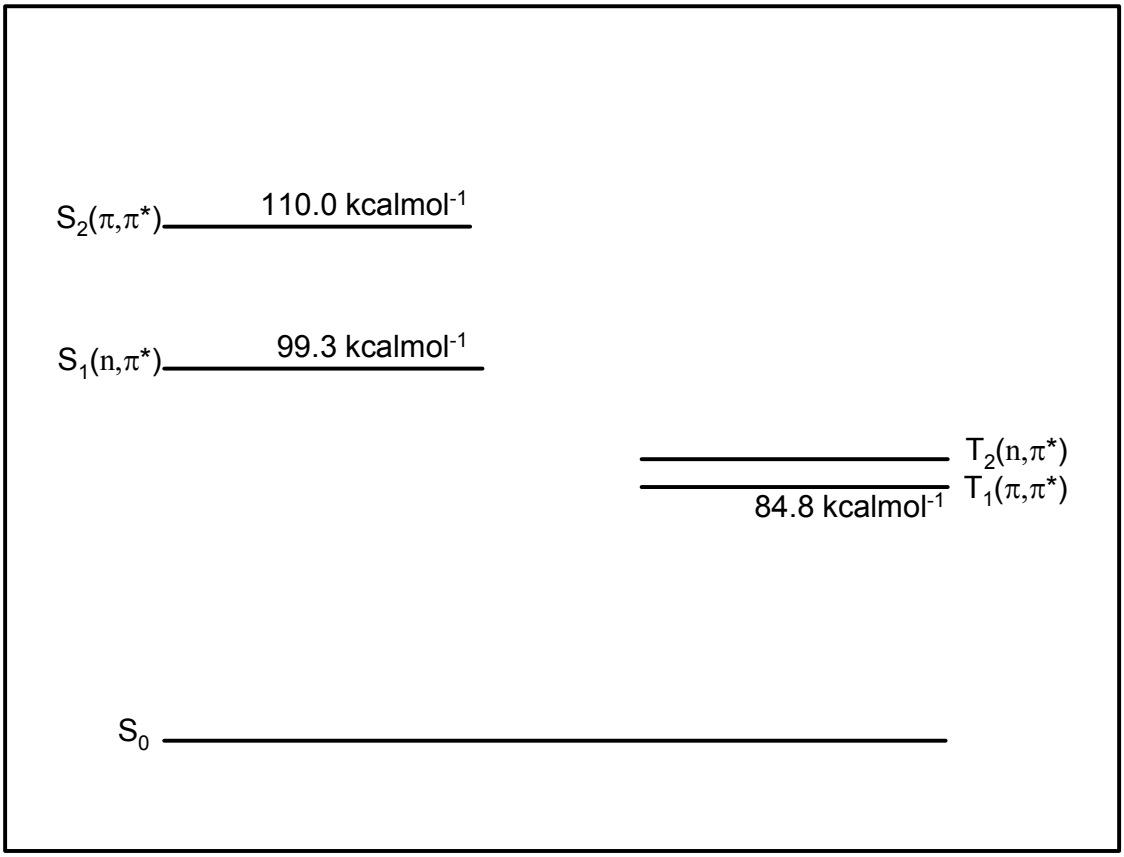

Figure 2.2. Energy level diagram of pyridine

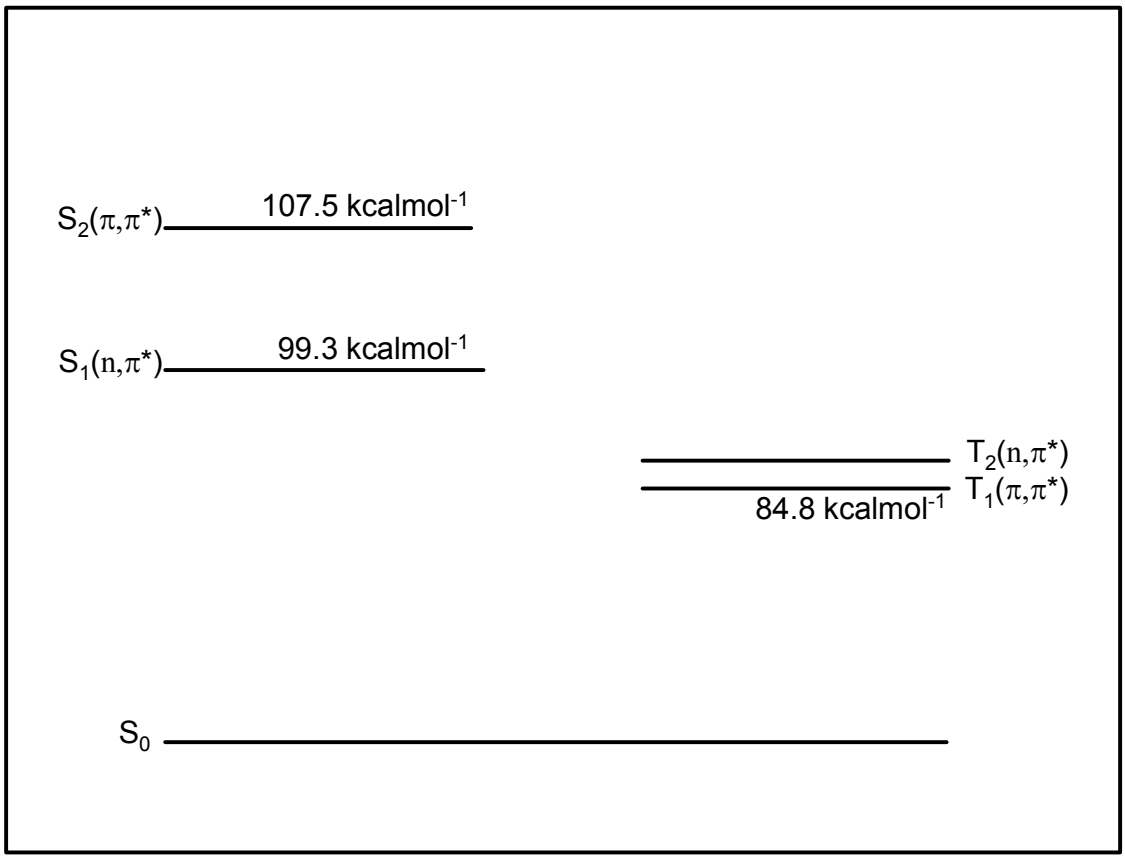

Figure 2.3 Energy level diagram of 2-methylpyridine

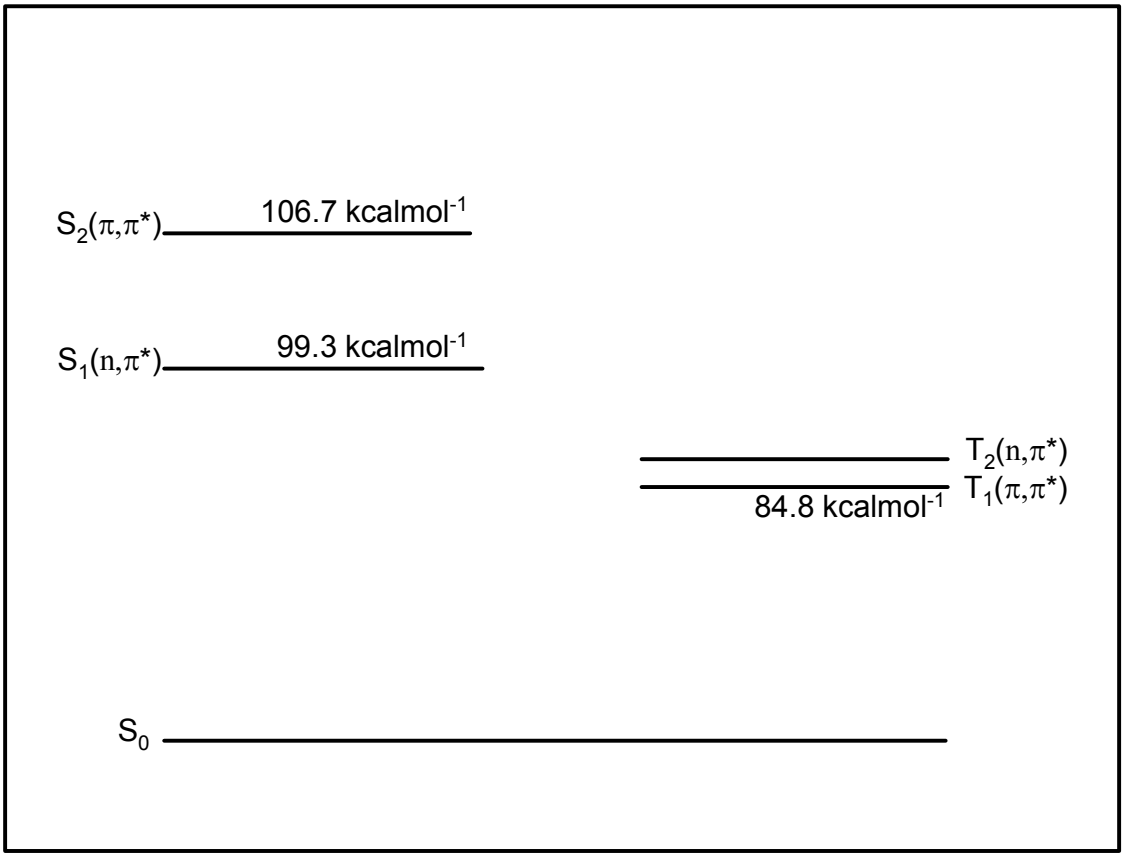

Figure 2.4 Energy level diagram of 3-methylpyridine

2.2. Photochemistry of cyanopyridines

Although the photochemistry of cyanopyridine vapors (**36-38**) has been experimentally studied in many works, their molecular rearrangement after irradiation

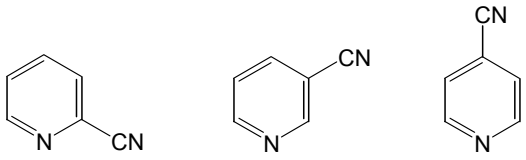

36 **37** **38**

has never been discussed. The photoproducts from irradiation of cyanopyridines are not yet known even though the effect of the cyano group which is considered to be a strong withdrawing group that is attached to the pyridine ring is interesting. In this thesis, the phototransposition mechanism by irradiating cyanopyridines with certain energies will be studied. The following is the spectroscopic properties of isomeric cyanopyridines which were obtained by spectroscopic study in various systems.

2.2.1. Spectroscopic properties of cyanopyridines

Sarkar and coworkers[4] have studied the absorption and luminescence behavior of isomeric cyanopyridines. The $S_2(\pi,\pi^*)$ states of the cyanopyridines (**36-38**) were located from the 0,0 bands in the vapor phase absorption spectra and, as shown in Table 2.5, lie approximately 105 kcalmol^{-1} above their ground states. In addition, the $S_0 \rightarrow S_1$ (n,π^*) vapor phase spectrum of 4-cyanopyridine (**38**) was also observed with an origin at 335 nm. Such $n \rightarrow \pi^*$ bands have also been detected in the spectra of hydrocarbon solutions

of 3-cyanopyridine and 4-cyanopyridine (**38**) at high concentrations (~10^{-2}M) but not in the spectrum of 2-cyanopyridine.

Table 2.5 Experimental spectral and energetic data for cyanopyridines

	$S_0 \rightarrow S_2$ $(\pi,\pi^*)_{0\text{-}0}$ nm(kcalmol^{-1})	
Compound	Vapor	Ethanol
2-CNP	268 (106.7)	271 (105.5)
3-CNP	269 (106.3)	271 (105.5)
4-CNP	277 (103.3)	282 (101.4)

Although these cyanopyridines were found to be non-fluorescent, the phosphorescence excitation spectra in rigid polar media at 77 K reveal $S_0 \rightarrow S_1$ and $S_0 \rightarrow S_2$ excitation bands and two relatively weak $S_0 \rightarrow T$ excitation bands. The lower energy $S_0 \rightarrow T$ band which is very close to and overlaps with the phosphorescence emission band origin was independent of solvent polarity and was thus identified as the $S_0 \rightarrow T_1$ (π,π^*) transition whereas the sensitivity of the higher energy band (a few hundred wave numbers higher) to solvent polarity confirmed that this band is due to the $S_0 \rightarrow T_1(n,\pi^*)$ transition. The singlet and triplet energy levels of the cyanopyridine isomers determined from the phosphorescence excitation spectra at 77 K are shown in Table 2.6.

Table 2.6 Singlet and Triplet energy levels from phosphorescence excitation spectra at 77K

(a) Singlet Energies

	$(\pi,\pi^*)_{0,0}$ nm(kcal mol^{-1})		$(n,\pi^*)_{0,0}$ nm(kcal mol^{-1})	
Compound	Ethanol	MCH	Ethanol	MCH
2-CNP	273 (105.8)	287 (99.6)	344 (83.0)	360 (79.4)
3-CNP	274 (104.4)	273 (105.8)	338 (84.6)	341 (83.9)
4-CNP	285 (100.4)	318 (89.9)	333 (85.9)	354 (80.8)

These $S_2(\pi,\pi^*)$ energies determined from the phosphorescence excitation spectra in ethanol shown in Table 2.6(a) agree well with the values given in Table 2.5 which were determined from absorption spectra in the vapor phase or in ethanol solvent. In addition, the energy for the $S_1(n,\pi^*)$ state at 333 nm (85.9 kcal mol^{-1}) for 4-cyanopyridine determined from the phosphorescence excitation spectrum, is very close to the value of 335 nm (85.4 kcal mol^{-1}) determined from the vapor phase absorption spectrum. Surprisingly, there is less agreement between the values in Table 2.5 and the data determined from the phosphorescence excitation spectra at 77 K in MCH solvent.

(b) Triplet Energies

	$^3(n,\pi^*)_{0,0}$ nm(kcal mol^{-1})		$^3(\pi,\pi^*)_{0,0}$ nm(kcal mol^{-1})	
Compound	Ethanol	MCH	Ethanol	MCH
2-CNP	358 (79.9)	386 (74.1)	370 (77.3)	398 (71.9)
3-CNP	355 (80.6)	366 (78.1)	369 (77.5)	371 (77.1)
4-CNP	347 (82.4)	372 (76.9)	354 (80.8)	379 (75.5)

From the values shown above, all three cyanopyridines have two low-lying triplet states which are separated by only several kcal mol^{-1}. In all three cases the lowest lying triplet state was identified as the π,π^* state.

Furthermore, the energies of the lowest-lying triplet states were also determined from the phosphorescence band origins. These data, phosphorescence lifetimes (τ_p), and quantum yields (ϕ_p) have also been reported. These data are shown in Table 2.7.

Table 2.7 Triplet energies from Phosphorescence band origins, phosphorescence lifetimes, quantum yields

	Phosphorescence band origins nm ($kcalmol^{-1}$)		τ_p(sec)		ϕ_p(77 K)	
	Ethanol	MCH	Ethanol	MCH	Ethanol	MCH
2-CNP	375 (76.3)	401 (71.3)	2.0	0.8	0.32	0.10
3-CNP	369 (77.5)	334 (77.1)	2.0	1.8	0.48	0.30
4-CNP	358 (79.9)	383 (74.7)	0.6	0.4	0.69	0.25

The triplet energies determined from the onset of phosphorescence in ethanol matrix at 77K are in good agreement with the energies of the $^3(\pi,\pi^*)$ states determined from the phosphorescence spectra in ethanol which are shown in Table 2.6(b). The phosphorescence lifetimes, which range from 0.6 to 2.0 seconds, are typical of the lifetimes of $^3(\pi,\pi^*)$ states.

The intersystem crossing yields of these cyanopyridines were also determined in glassy hydrocarbon matrices. The triplet yields were estimated from the efficiency of these molecules in sensitizing the biacetyl phosphorescence. The measured values were 0.8 ± 0.05 for 2-cyanopyridine and 3-cyanopyridine and 0.85 ± 0.05 for 4-cyanopyridine. Under this condition the triplet yields are very high.

The energies and configurations of the various states of each cyanopyridine are summarized in Figure 2.5, 2.6, and 2.7.

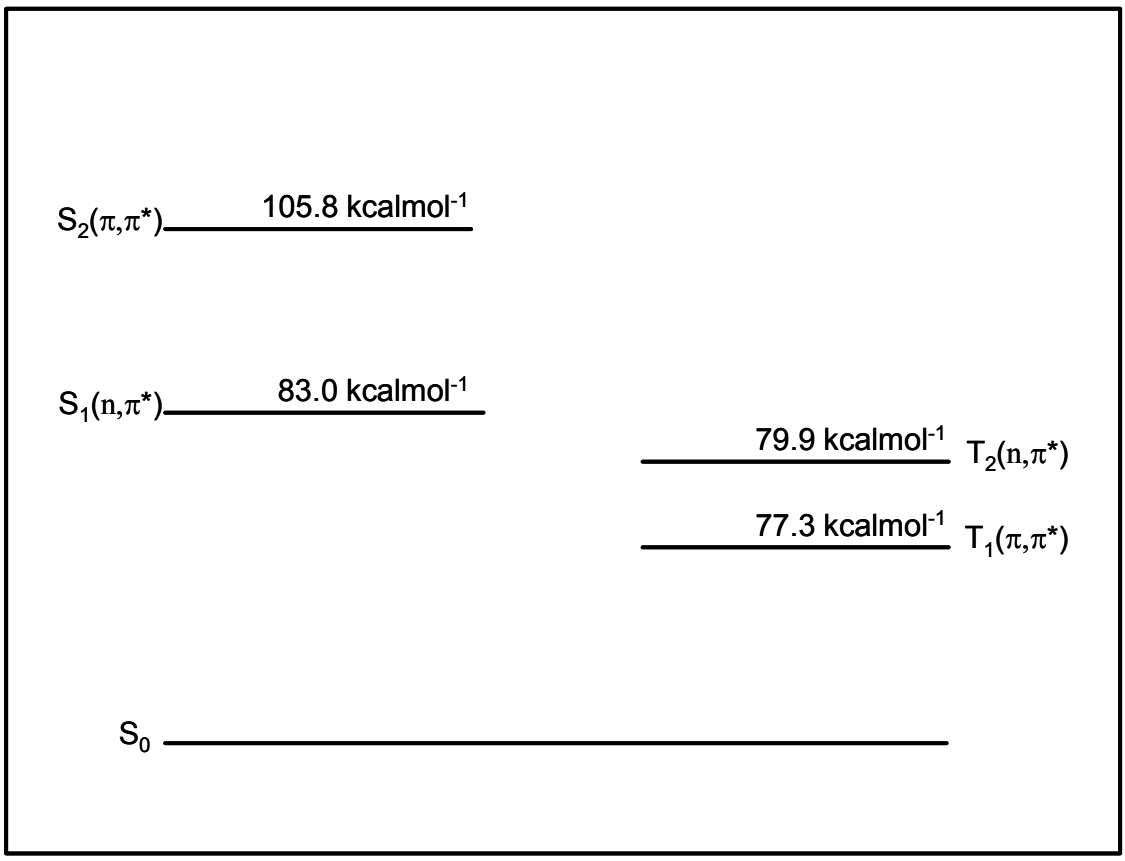

Figure 2.5 Energy level diagram of 2-Cyanopyridine

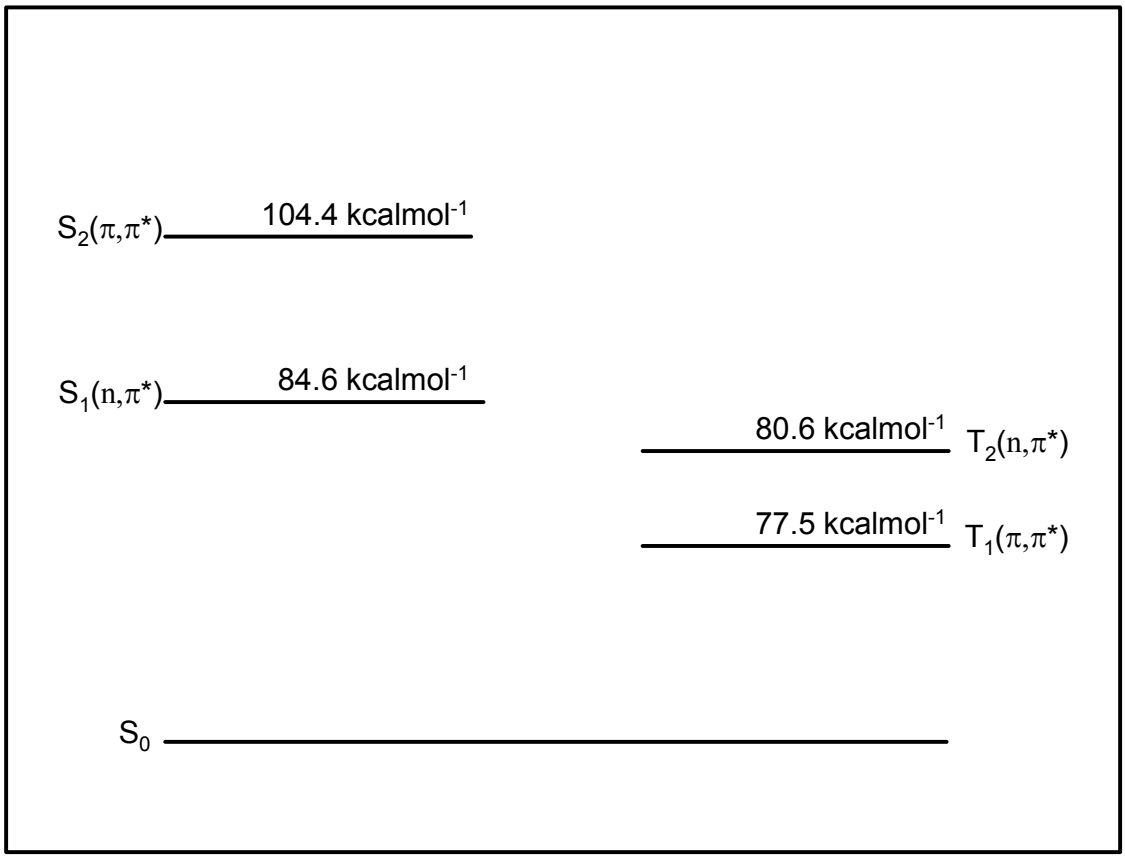

Figure 2.6 Energy level diagram of 3-Cyanopyridine

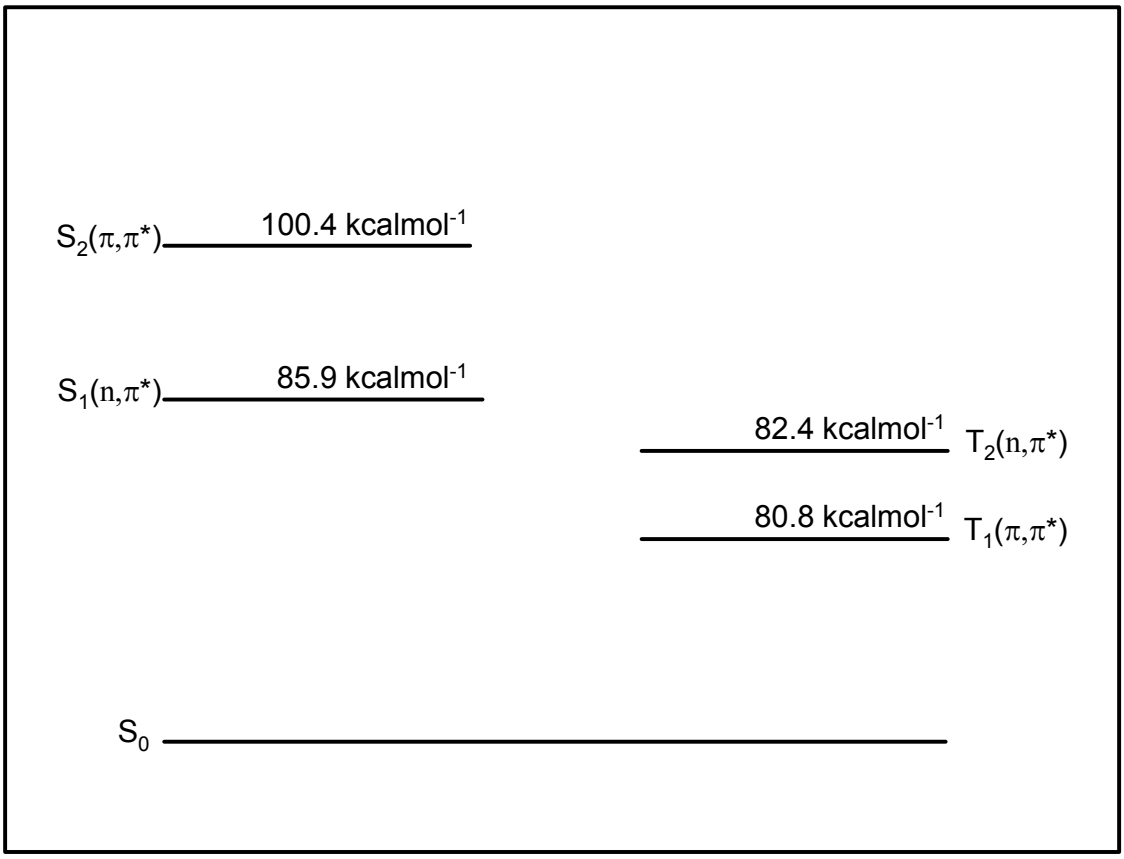

Figure 2.7 Energy level diagram of 4-Cyanopyridine

2.3. The triplet state of 4-cyanopyridine

Akiyama, Yamauchi, and Hirota[33] studied the lowest triplet (T_1) state of 4-cyanopyridine by time-resolved EPR, phosphorescence, and ab initio calculations. It has been known earlier that the phosphorescence lifetime of 4-cyanopyridine is very short.[34] The configuration character, however, is not clear whether it is $^3n\pi^*$ or $^3\pi\pi^*$. The contradiction among many research groups still remain for decades.[35,36,37.]

Unlike other pyridine derivatives, 4-cyanopyridine (**38**) has the ability to give a moderate phosphorescence signal which makes it possible in the study of T_1 state both with EPR and phosphorescence method.

The solvent effect studied in EPR method was found to be independent on the character of the T_1 state both in nonpolar and polar solvent. This is different from the long understanding that the azaaromatics and aromatic carbonyls with nearby $^3n\pi^*$ and $^3\pi\pi^*$ can be tremendously affected by solvents. The temperature effect on the triplet state was also found to be small. This was suggested to result from a strong vibronic coupling that produces a distorted T_1 state with a very large separation between T_1 and T_2.

With phosphorescence results, the T_1 state of 4-cyanopyridine was suggested to be of mixed $n\pi^*$ and $\pi\pi^*$ character. Ab initio calculations predict a strong vibronic coupling between $n\pi^*$ and $\pi\pi^*$ states which leads to geometric distortion of the T_1 state. This explains the low phosphorescence that was generally observed in pyridine analogs.

CHAPTER III

Statement of purpose

In this thesis, the photochemical and photophysical properties of pyridine derivatives has been studied. Previous work in our laboratory provided evidence that dimethylpyridines undergo phototransposition upon irradiation in the vapor phase via 2,6-bonding-nitrogen migration mechanism and rearomatization instead of the mechanism involving an azaprismane intermediate suggested by Caplain and Lablache-Combier.[14] The purpose of this thesis is to determine if the 2,6-bonding-nitrogen migration mechanism is general to other pyridine derivatives and to the parent pyridine molecule.

To determine this the vapor phase photochemistry of 2-,3-, and 4-methylpyridine (**6**-**8**) and 2-, 3-, and 4-cyanopyridine (**36**-**38**) (Scheme 3.1) has been studied.

Scheme 3.1. Cyanopyridines and methylpyridines

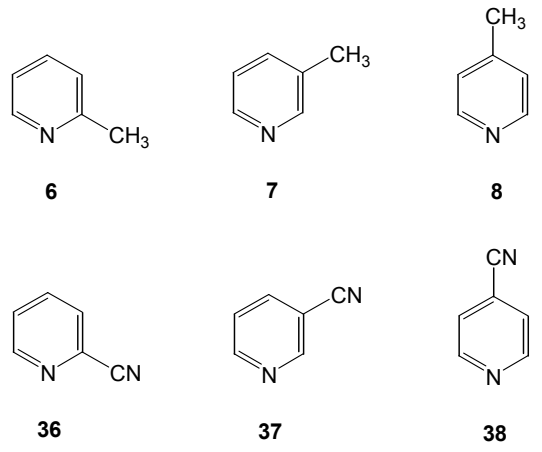

In order to more completely monitor the phototransposition reactions, the dideuteratedcyanopyridines **36-4,6-d_2**, **37-2,6-d_2**, and **38-2,6-d_2** shown in Scheme 3.2 will be synthesized and their photochemistry in the vapor phase studied.

Scheme 3.2 Dideuteriocyanopyridine

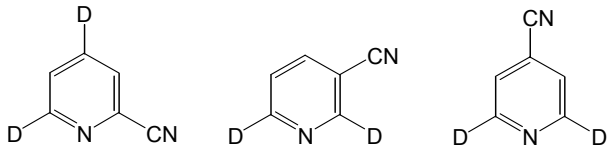

In order to study these photoreactions in the parent pyridine molecule, extensive deuterium labeling will be employed. The six possible trideuteriopyridines shown in Scheme 3.3, which are analogous in their substitution patterns to the dimethylpyridines, will be synthesized and their vapor phase photochemistry studied.

Scheme 3.3 Trideuteriopyridines

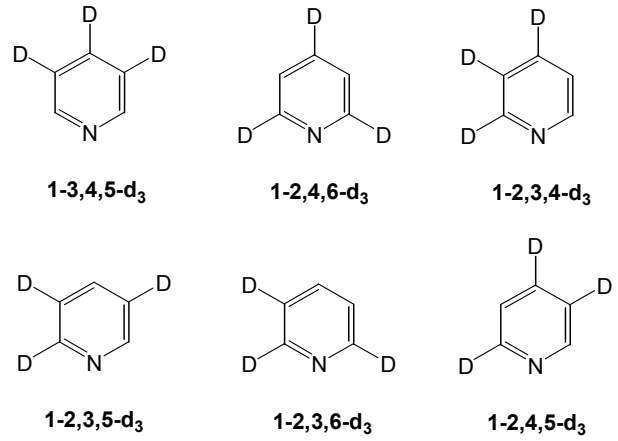

These reactions will be monitored by ^{1}H-NMR spectroscopy which will allow the transposition of the two protons in each molecule to be followed. In addition, the three possible isomeric tetradeuteriopyridines shown in Scheme 3.4 will also be synthesized and their vapor phase photochemistry studied.

Scheme 3.4 Tetradeuteriopyridines

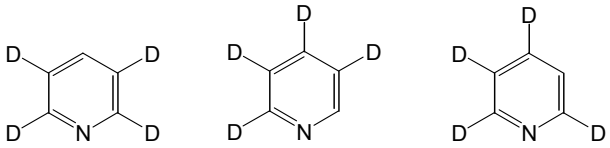

CHAPTER IV

Results and discussion

4.1. Photochemistry of cyanopyridines in the vapor phase

The photochemistry of cyanopyridines **36**-**38** was studied by irradiating the vapor (0.3-0.4 Torr) in a 3 liter quartz reaction vessel at 254 nm or at wavelengths greater than 290 nm. The 0-0 origin of **36**, **37**, and **38** are 268, 269, and 277 nm respectively.

4.1.1. Irradiation of 2-cyanopyridine (36) at 254 nm

2-Cyanopyridine (**36**) vapor (0.3-0.4 Torr) was irradiated at 254 nm with four low-pressure mercury lamps in a Rayonet reactor for 15, 30, 60, 75, or 90 minutes. GC analysis of the resulting product mixtures showed that irradiation resulted in the consumption of various amounts of the reactant (retention time 12 minutes) and the formation of 3-cyanopyridine (**37**), and 4-cyanopyridine (**38**) (retention time 7 and 6 minutes, respectively).

Scheme 4.1 Photolysis of 2-cyanopyridine (**36**)

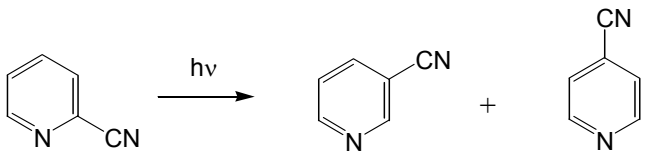

36 **37** **38**

Figure 4.1 shows the GC trace observed after 90 minutes of irradiation to illustrate a typical GC analysis.

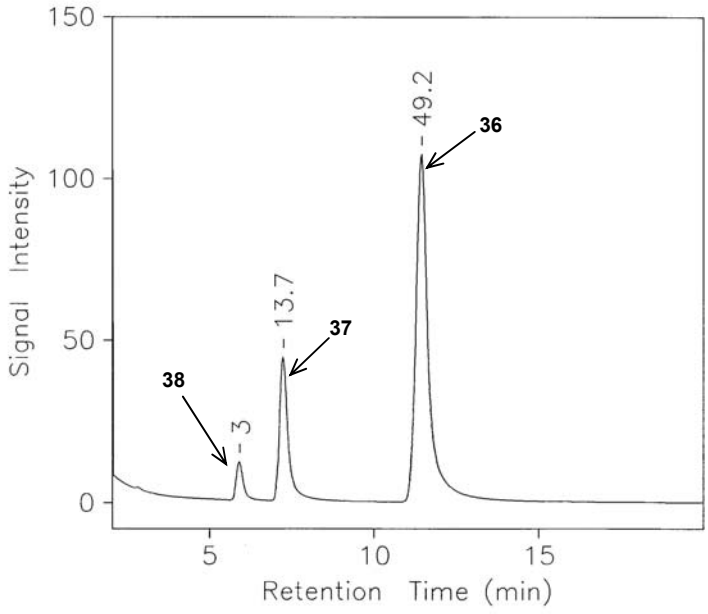

Figure 4.1 GC trace of 2-cyanopyridine irradiated for 90 minutes

After each irradiation the resulting product mixture was also analyzed by 400 MHz ^{1}H-NMR in acetone-d_6 solvent. Figure 4.2a and 4.2b shows the ^{1}H NMR spectra of 2-cyanopyridine (**36**) before and after irradiation at 254 nm for 90 minutes. Before irradiation, the ^{1}H-NMR spectrum in Figure 4.2a shows the signals of **38** only at δ 7.63(H5), 7.80 (H3), 8.08 (H4) and 8.63 (H6). After irradiation, the ^{1}H-NMR spectrum in Figure 4.2b also shows signals for 4-cyanopyridine (**38**) at δ 7.63(H3, H5) and at δ 8.73 (H2, H6) and also signals for 3-cyanopyridine (**37**) at δ 7.43 (H5), 8.12 (H4) and

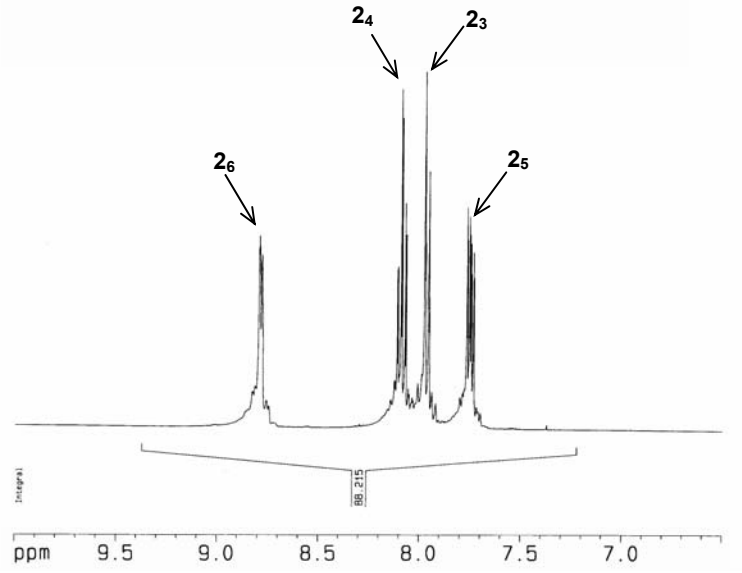

(a)

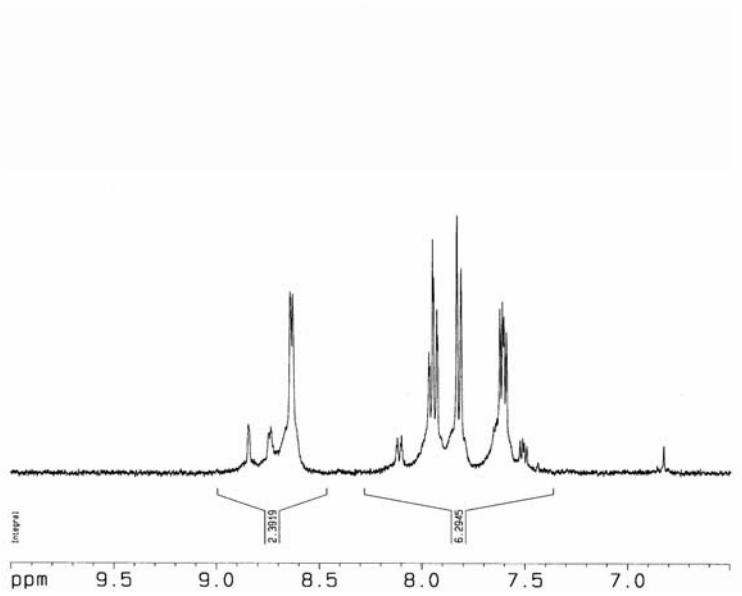

Figure 4.2 (a) ^{1}H-NMR spectrum of 2-cyanopyridine before irradiation

(b) ^{1}H-NMR spectrum of 2-cyanopyridine after 90 min of irradiation

8.87 (H2). The H6 signal of **37** is overlapped with the signal for the H3 and H5 of **38** at δ 8.87 and thus it cannot be observed.

Table 4.1 shows the data obtained for the irradiation of 2-cyanopyridine (**36**) at 254 nm with 4 lamps at the various irradiation times.

Table 4.1 Experimental details for photolysis of 2-cyanopyridine (**36**)

Exp no.	Irradiation time (min)	Sample weight (mg)	Recovered weight (mg)	2-CNP consumption (%)	3-CNP formation (%)	4-CNP formation (%)
1	15	13	5	4.9	3.6	1.29
2	60	20	7	22.7	18.4	4.31
3	75	18	9	27.0	22.4	4.64
4	90	17	8	35.3	29.4	5.92

The ratio of **37** to **38** as a function of irradiation time is shown in Figure 4.3. Over the range of 15-90 minutes of irradiation the ratio increased linearly from 2.8-5.0.

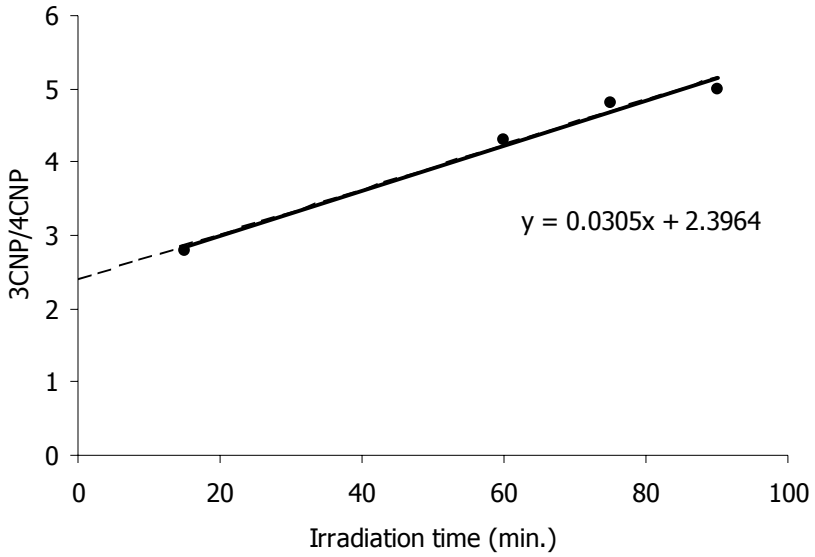

Figure 4.3 Photoproduct ratio VS. irradiation time from irradiation of **36**

Assuming that this plot can be extrapolated to zero minutes of irradiation time leading to a ratio of 2.40:1, the obtained ratio of photoproduct **37** and **38** suggests that both photoproducts must have been formed at early irradiation. This shows that irradiation of **36** directly results in the formation of **37** and **38**. Thus, these two new isomers are primary photoproducts of **36**. It should be noted here that irradiation of **36** for less than 15 minutes could not give a detectable amount of photoproduct. In addition, since the ratio of **37**:**38** increases with irradiation time, it appears that once formed, **38** phototransposes to **37** faster than **37** is transposed. Subsequent experiments have confirmed that **38** is substantially more photoreactive than the **37** isomer.

4.1.2. Irradiation of 3-cyanopyridine (37) at 254 nm

3-Cyanopyridine (**37**) vapor (0.3-0.4 Torr) was irradiated at 254 nm with four low-pressure mercury lamps in a Rayonet reactor for 60, 120, 240, and 360 minutes. GC analysis of the resulting product mixtures showed that irradiation resulted in the consumption of 3-cyanopyridine (**37**) (retention time 7 minutes) and the formation of 2-cyanopyridine (**36**) (12 minutes) and 4-cyanopyridine (**38**) (6 minutes).

Scheme 4.2 Photolysis of 3-cyanopyridine (**37**)

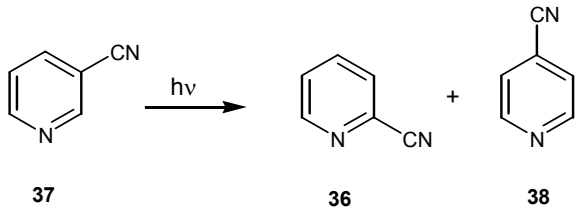

The GC trace of **37** shown in Figure 4.4 was observed after 360 minutes of irradiation indicates the typical formation of **36** and **38** isomers. The long irradiation time required shows that the reactivity of 3-cyanopyridine (**37**) is much less than that of 2-cyanopyridine (**36**). Even after prolonged irradiation, only a small amount of 3-cyanopyridine (**37**) was converted to **36** and **38**.

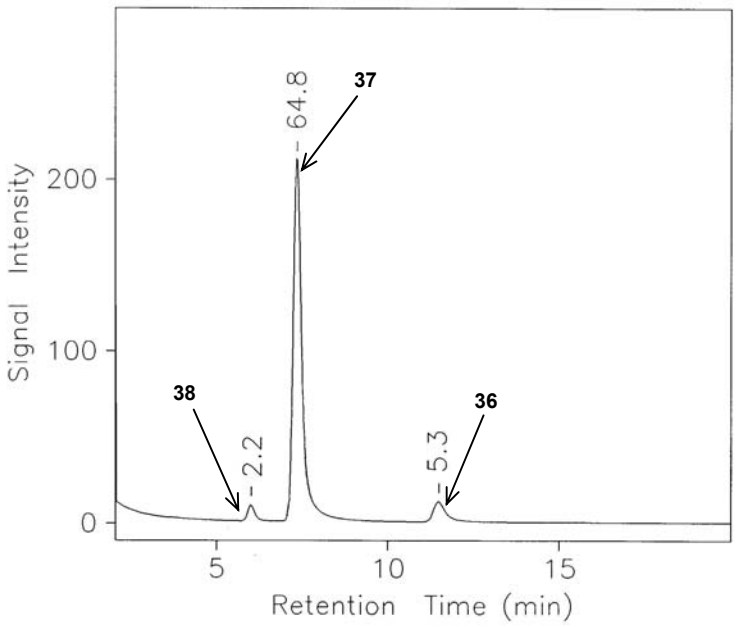

Figure 4.4 GC trace of 3-cyanopyridine at 254 nm irradiated for 360 minutes

After each irradiation the resulting product mixture was also analyzed by ^{1}H-NMR in acetone-d_6 solvent. Figure 4.5a shows the ^{1}H-NMR spectrum of 3-cyanopyridine (**37**) before irradiation. The proton signals of **37** are located at δ 7.65 (H5), 8.26 (H4), 8.89 (H6), and 9.00 (H2). After irradiation for 360 minutes, the ^{1}H-NMR spectrum in Figure 4.5b shows the proton signals of products **36** and **38**. The proton signals at δ 7.60(H5), 7.81 (H3), 7.94 (H4), and 8.62 (H6) are due to the formation of 2-cyanopyridine (**36**) and the proton signals at δ 7.65 (H3,5) and 8.73 (H2,6) are due to the formation of 4-cyanopyridine (**38**). Again, the signal due to the H2 and H6 of 4-cyanopyridine (**38**) is overlapped with the signal due to the H6 of 3-cyanopyridine (**37**). Thus, these protons cannot be distinguished.

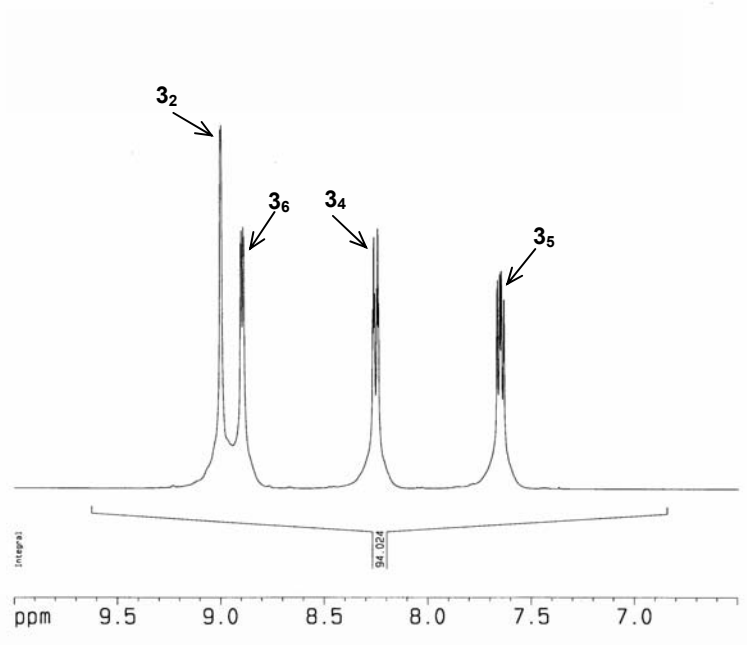

(a)

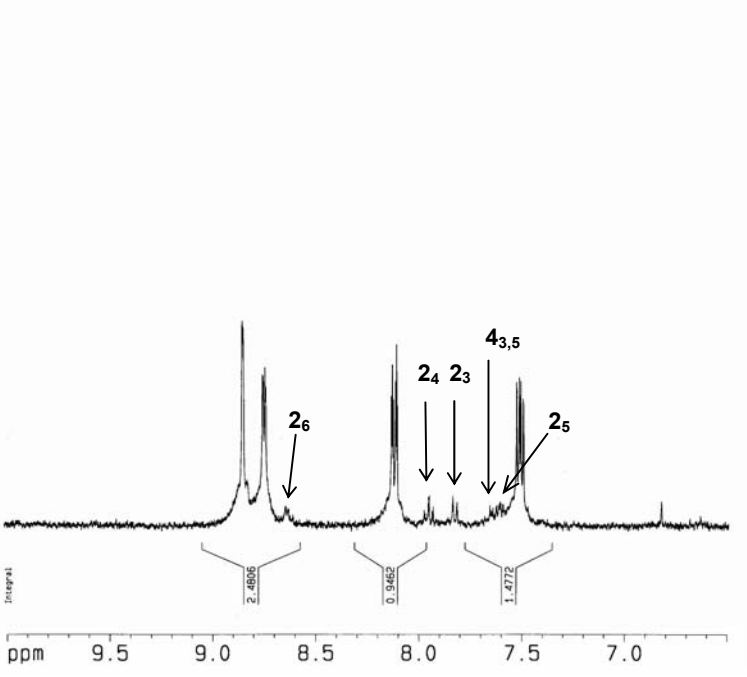

(b)

Figure 4.5 (a) ^{1}H-NMR spectrum of 3-cyanopyridine before irradiation
(b) ^{1}H-NMR spectrum of 3-cyanopyridine after 360 min of irradiation

Table 4.2 shows the data obtained for the irradiation time of 60, 120, 240, and 360 minutes.

Table 4.2 Experimental details for photolysis of 3-cyanopyridine (**37**)

Exp no.	Irradiation time (min)	Sample weight (mg)	Recovered weight (mg)	3-CNP consumption (%)	4-CNP formation (%)	2-CNP formation (%)
5	60	11	8	3.0	1.58	1.46
6	120	9	7	4.5	2.08	2.45
7	240	9	4	8.9	3.80	5.06
8	360	13	8	7.5	2.89	4.64

In addition, the ratio of **36** and **38** as a function of irradiation time shown in Figure 4.6 shows that over the range of 60-360 minutes of irradiation, the ratio increases linearly from 0.9 to 1.6. This indicates that during this period, 2-cyanopyridine (**36**) is more formed than 4-cyanopyridine (**38**).

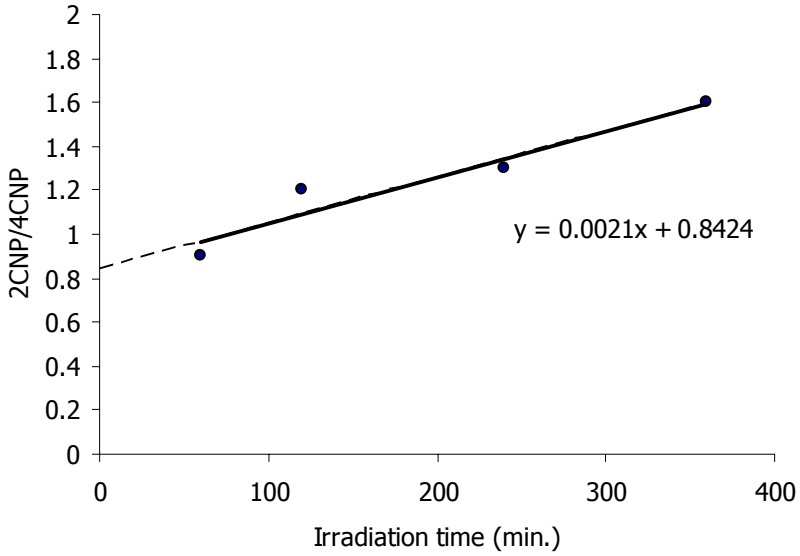

Figure 4.6 Photoproduct ratio VS Irradiation time from irradiation of **37**

Extrapolation to zero minutes of irradiation gives a ratio of 0.84:1. This value indicates that both **36** and **38** are formed at early irradiation time and therefore they are primary products. Since the ratio of **36**:**38** increases at longer irradiation time, it appears that once formed, **38** is consumed in a second photoreaction faster than **36**.

4.1.3. Irradiation of 4-cyanopyridine (38) at 254 nm

4-Cyanopyridine (**38**) vapor (0.3-0.4 Torr) was irradiated at 254 nm with four low pressure mercury lamps in a Rayonet reactor for a variety of irradiation times of 23, 45, 70, and 90 minutes. GC analysis of the resulting product mixtures showed that irradiation resulted in the consumption of reactant (retention time 6 minutes) and the formation of 3-cyanopyridine (**37**) (7 minutes), and 4-cyanopyridine (**38**) (12 minutes).

Scheme 4.3 Photolysis of 4-cyanopyridine (**38**)

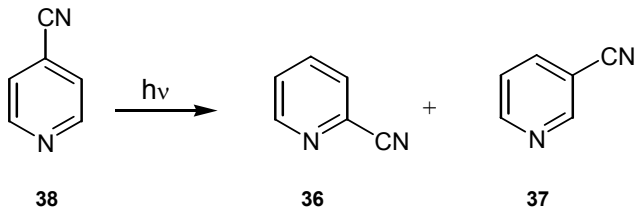

38 **36** **37**

The GC result observed from 90 minutes of irradiation shown in Figure 4.7 indicates that **38** is consumed and **37** and **36** are formed. However, the yields of **36** and **37** from **38** are quite different. 3-Cyanopyridine (**37**) which appears to be the most photostable isomer is formed in a much higher yield than the yield of 2-cyanopyridine (**36**).

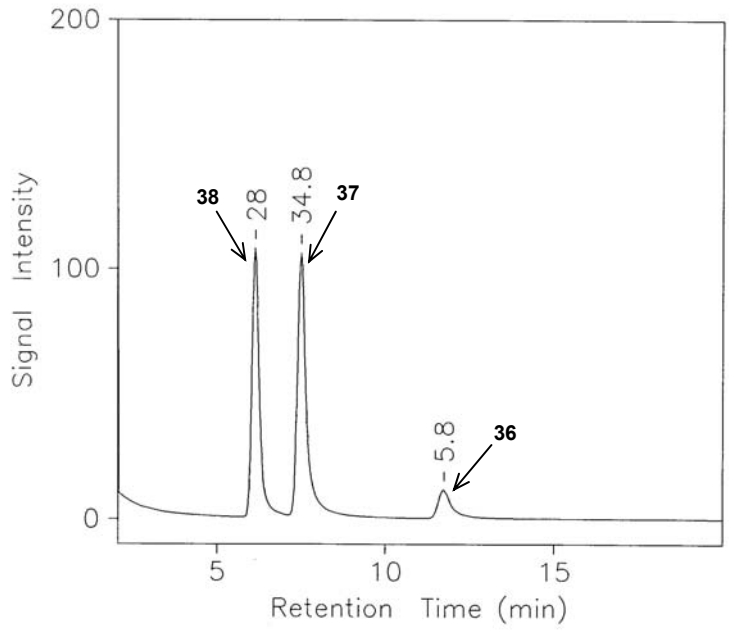

Figure 4.7 GC trace of 4-cyanopyridine irradiated at 254 nm for 90 minutes

After each irradiation the residue was analyzed in acetone-d_6 by ^{1}H-NMR spectroscopy. Figure 4.8a and 4.8b shows the ^{1}H-NMR spectra of 4-cyanopyridine (**38**) before and after irradiation at 254 nm for 90 minutes. Before irradiation, the ^{1}H-NMR spectrum shown in Figure 4.8a shows the proton signals of **38** only at δ 7.80(H3,5) and 8.85(H2,6). After irradiation for 90 minutes, the ^{1}H-NMR spectrum shown in Figure 4.8b reveals that the proton signals of product **36** and **37** were observed. The proton signals at δ 7.75 (H5), 7.96(H3), 8.10(H4), and 8.80(H6) are due to the formation of 2-cyanopyridine (**36**). The proton signals at δ 7.65(H5), 8.27(H4), 8.89 (H6), and 9.02 (H2) are due to the formation of 3-cyanopyridine.

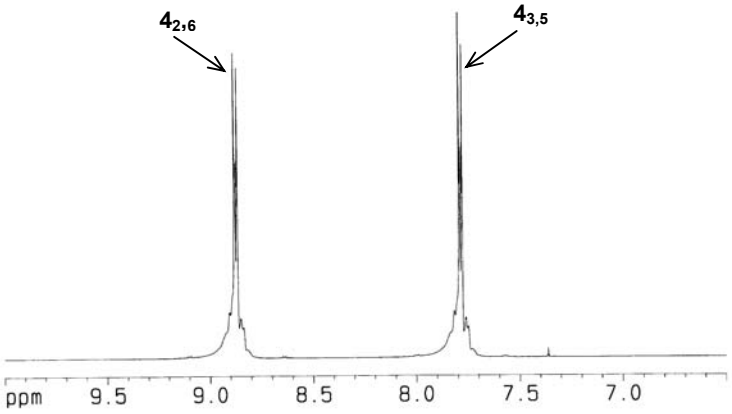

(a)

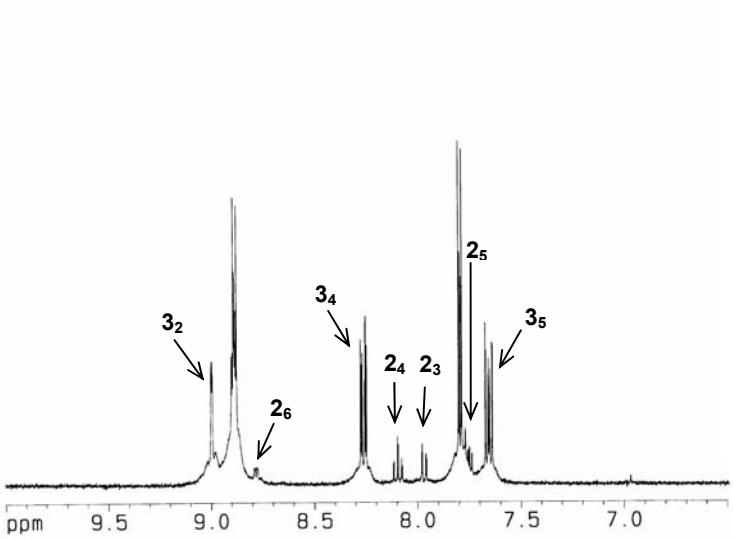

(b)

Figure 4.8 (a) ^{1}H-NMR spectrum of 4-cyanopyridine before irradiation
(b) ^{1}H-NMR spectrum of 4-cyanopyridine after 90 min of irradiation

The proton at position 6 of 3-cyanopyridine (**37**) also gives the signal that overlaps with the proton at position 2 and 6 of 4-cyanopyridine (**38**) as previously mentioned.

Table 4.3 Experimental details for photolysis of 4-cyanopyridine (**38**)

Exp no.	Irradiation time (min)	Sample weight (mg)	Recovered weight (mg)	4-CNP consumption (%)	3-CNP formation (%)	2-CNP formation (%)
9	23	15	10	26.6	24.5	2.13
10	45	11	10	39.7	36.8	2.91
11	70	13	10	47.0	43.5	3.50
12	90	16	15	59.8	54.3	5.55

Figure 4.9 shows the ratio of 3-cyanopyridine (**37**) to 2-cyanopyridine (**36**) as a function of irradiation time.

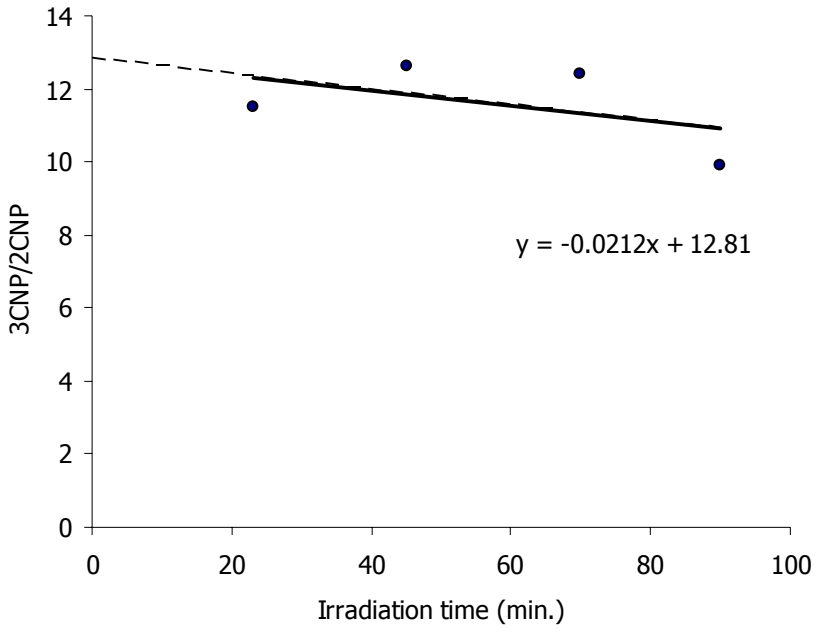

Figure 4.9 Photoproduct ratio VS. Irradiation time from irradiation of **38**

Although there is more scatter in this data, the ratio still remains constant at about 13:1. This means that **37** and **36** are the primary products. However, **37** is the major product.

It should be noted again that the photochemical reactivity of cyanopyridine isomers (**36-38**) are not similar. This can be observed from the GC results shown in Figure 4.1, 4.4, and 4.7 together with result data shown in Table 4.1, 4.2, and 4.3, which exhibit that after irradiation, their time of the formation of photoproducts are different. 4-Cyanopyridine (**38**) seems to be the most reactive because it forms both photoproducts, **36** and **37** in significant amounts within the time range from 23 to 90 min. The 59.8 % comsumption of **38** and 54.3 % formation of **37** shows that 4-cyanopyridine (**38**) is the most reactive isomer. 2-Cyanopyridine (**36**) was also found to be more reactive than 3-cyanopyridine (**37**) because it forms significant amounts of photoproducts within time range from 15 to 90 minutes which is in the same reaction time of 4-cyanopyridine (**38**). However, it is less reactive than **38** since only about 35% was consumed after 90 min. of irradiation. In contrast to **38** and **36**, 3-cyanopyridine (**37**) was observed to be only 7.5% consumed even after 360 minutes of irradiation time. The difference in reactivity among the cyanopyridine isomers is expected to result from the stability of their intermediates, which are formed in the excited state. The mechanistic scheme and cause of this reactive difference will be discussed in a later section.

4.1.4. Irradiation of 2-cyanopyridine (36) at ≥ 290 nm

2-Cyanopyridine (**36**) vapor (0.3-0.4 Torr) was also irradiated at wavelength ≥ 290 nm using the pyrex filtered light from 16 lamps that emit a broad band of light with a maximum at 300 nm. This irradiation wavelength precludes $S_0 \rightarrow S_2$ (π,π^*) excitation [($S_2(\pi,\pi^*)_{0,0}$ = 268 nm)] but allows direct excitation to the $S_1(n,\pi^*)$ state [($S_1(n,\pi^*)_{0,0}$ = 344 nm)] and population of the T_1 state via intersystem crossing.

The data in Table 4.4 shows that after 24 hours of irradiation, 18.3% of the reactant 2-cyanopyridine (**36**) was consumed but that the yields of 3-cyanopyridine (**37)** and 4-cyanopyridine (**38)** were only 9.6 % and 8.7 % respectively. By comparison with the data in Table 4.1, after irradiation at 254 nm until 22.7 % of **36** was consumed, the yields of **37** and **38** were 18.4 and 4.3 % respectively. Thus, irradiation with light ≥ 290 nm leads to decreased yields of the phototranposition products and to a different ratio of their yields. This indicates that phototransposition is less effective from the $S_1(n,\pi^*)$ singlet or from the lowest triplet state of 2-cyanopyridine (**36**).

Table 4.4 Experimental details for photolysis of **36** at ≥ 290 nm

Exp no.	Sample weight (mg)	Recovered weight (mg)	Irradiation time (hours)	2-CNP consumption (%)	3-CNP formation (%)	4-CNP formation (%)
13	7	7	24	18.3	9.6	8.7

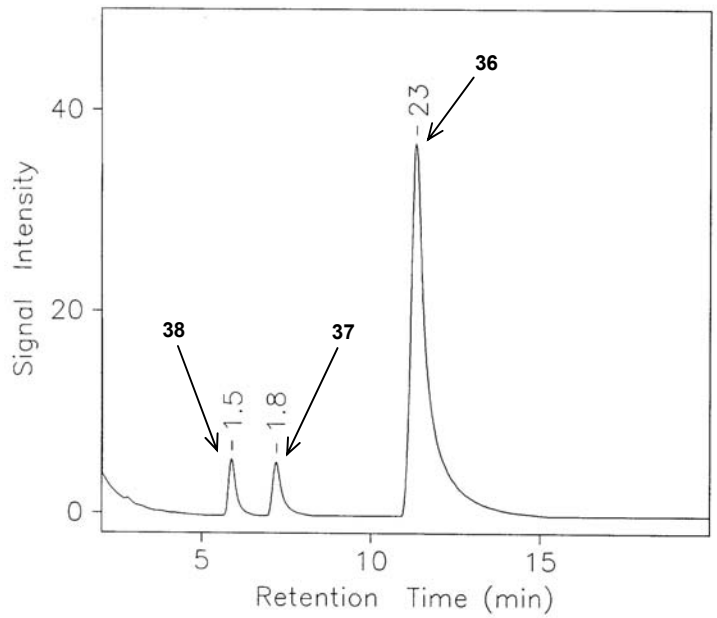

Figure 4.10 GC trace of 2-cyanopyridine irradiated at ≥ 290 nm for 24 hours

4.1.5. Irradiation of 3-cyanopyridine (37) at ≥ 290 nm

3-Cyanopyridine (**37**) vapor (0.3-0.4 Torr) was also irradiated by wavelengths at ≥ 290 nm using pyrex filtered light from 16 lamps which emit a broad band of light with a maximum at 300nm. This irradiation wavelength precludes $S_0 \rightarrow S_2(\pi,\pi^*)$ excitation [$(S_2(\pi,\pi^*)_{0,0}$ = 269 nm)] but allows direct excitation to the $S_1(n,\pi^*)$ state [$(S_1(n,\pi^*)_{0,0}$ = 338 nm)] and population of the T_1 state via intersystem crossing.

The data in Table 4.5 shows that after 24 hours of irradiation, 4.1 % of the reactant 3-cyanopyridine was consumed while the yield of 2-cyanopyridine (**36**) and 4-

cyanopyridine (**38**) were observed to be 3.1 % and 1.0 % respectively. The data in Table 4.2, however, shows that after 4 hours of irradiation at 254 nm, when a comparable amount of **37** was consumed, the yields of **36** and **38** were 3.2 % and 0.8 % respectively. Thus, changing the excitation wavelength from 254 nm to ≥ 290 nm results in decreased yields of the phototransposition products and a different ratio of **36** to **37** and again suggests that phototransposition is less effective from the $S_1(n, \pi^*)$ singlet or from the lowest triplet state of 3-cyanopyridine (**37**).

Table 4.5 Experimental details for photolysis of **37** at ≥ 290 nm

Exp no.	Sample weight (mg)	Recovered weight (mg)	Irradiation time (hours)	3-CNP consumption (%)	4-CNP formation (%)	2-CNP formation (%)
14	10	8	24	4.1	1.0	3.1

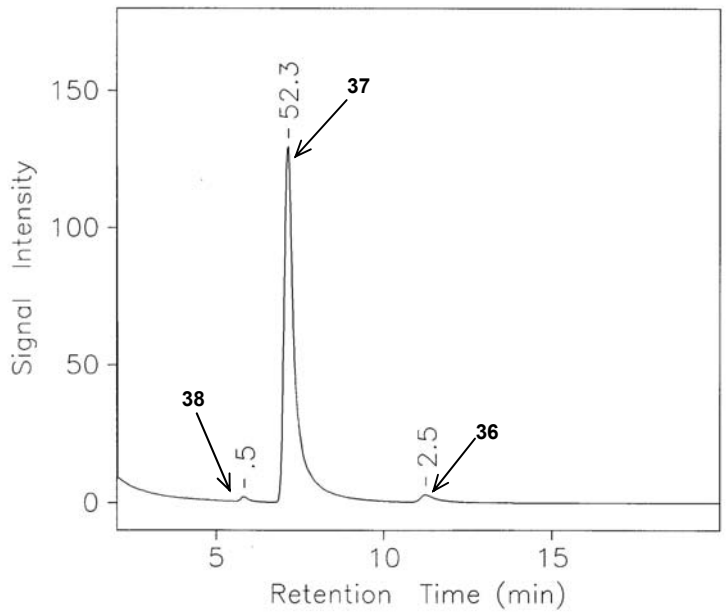

Figure 4.11 GC trace of 3-cyanopyridine irradiated at ≥ 290 nm for 24 hours

The GC data from ≥290-nm irradiation shown in Figure 4.11 is analogous to that from 254 nm irradiation. The GC peak of **37** is also high in intensity comparing to signals of **36** and **38** indicating that 3-cyanopyridine (**37**) is very stable in both wavelength excitations.

4.1.6. Irradiation of 4-cyanopyridine (38) at ≥ 290 nm

4-cyanopyridine (**38**) vapor was irradiated at ≥ 290 nm using the pyrex filtered light from 16 lamps that emit a broad band of light with a maximum at 300 nm. The data in Table 4.6 obtained by irradiation of 4-cyanopyridine at ≥ 290 nm for 24 hours shows that 4-cyanopyridine (**38**) phototransposed to only one product, 3-cyanopyridine (**37**). After 1.9 % consumption of **38**, the yield of **37** is only 1.9 %. 2-Cyanopyridine (**36**) was not observed as a product in this experiment. This result indicates that 4-cyanopyridine (**38**) reactivity at the absorption of ≥ 290 nm energy is much less than that from the irradiation at 254 nm.

Table 4.6 Experimental details for photolysis of **38** at ≥ 290 nm

Exp no.	Sample weight (mg)	Recovered weight (mg)	Irradiation time (hours)	4-CNP consumption (%)	3-CNP formation (%)	2-CNP formation (%)
15	8	6	24	1.9	1.9	0.0

Figure 4.12 shows the GC trace of 4-cyanopyridine (**38**) after irradiation at $\lambda \geq$ 290 nm. The 2-cyanopyridine (**36**) peak is not observed indicating that it is probably not formed or its intensity cannot be detected by GC analysis.

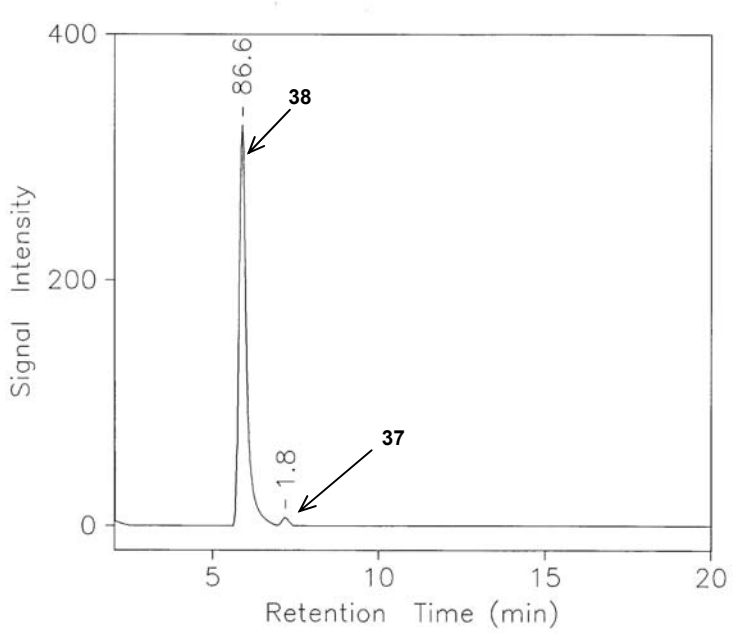

Figure 4.12 GC trace of 4-cyanopyridine irradiated at > 290 nm for 24 hours

The result from this experiment gave some interesting information that should be pointed out. The formation of 3-cyanopyridine (**37**) from irradiation of 4-cyanopyridine (**38**) indicates that 3-cyanopyridine (**37**) is formed faster than 2-cyanopyridine (**36**). This results in the formation of only one product, **37**, after 24 h of irradiation. It seems to be consistent with the previous experiments for irradiation at 254 nm of cyanopyridines that **37** is more stable than the other isomers (**36** and **38**) and it is usually formed first. However, when this result shown in Figure 4.12 is considered together with the result

from the experiment of 3-cyanopyridine (**37**) shown in Figure 4.11, it gives an interesting result. The GC trace from irradiation of 3-cyanopyridine (**37**) at ≥ 290 nm shows that the photoproducts **36** and **38** are formed after 24 h of irradiation. At the same irradiation time, **38** is found to form only one photoproduct. This means that **37** is more reactive than **38** by excitation at ≥ 290 nm. This comment agrees well with the calculated percent consumption shown in Table 4.5 and 4.6. It is about 4.1% of 3-cyanopyridine (**37**) that was consumed whilst only 1.9 % of 4-cyanopyridine (**38**) was consumed for the same irradiation period. Furthermore, the GC result in Figure 4.10 shows that 2-cyanopyridine (**36**) is more reactive than any other cyanopyridine isomers. It exhibits the percent consumption at 18.3 %. Hence, it can be concluded that 2-cyanopyridine (**36**) is the most reactive and 4-cyanopyridine is the most unreactive upon irradiation at ≥ 290 nm.

4.1.7. Mechanistic discussion for cyanopyridines

The experimental results from vapor phase photochemistry of isomeric cyanopyridine (**38**-**40**) show that irradiation of any one isomer results in the formation of the other two as shown in Scheme 4.4.

Scheme 4.4 Photo-interconversion of cyanopyridines

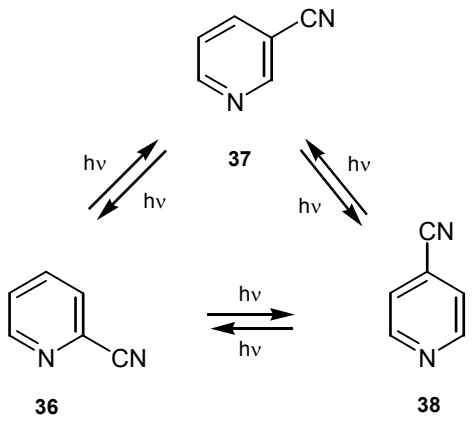

These interconversions are consistent with a mechanism involving 2,6-bridging, nitrogen migration around five sides of cyclopentenyl ring, and rearomatization as shown in Scheme 4.5.

Scheme 4.5 Phototransposition mechanism of cyanopyridines

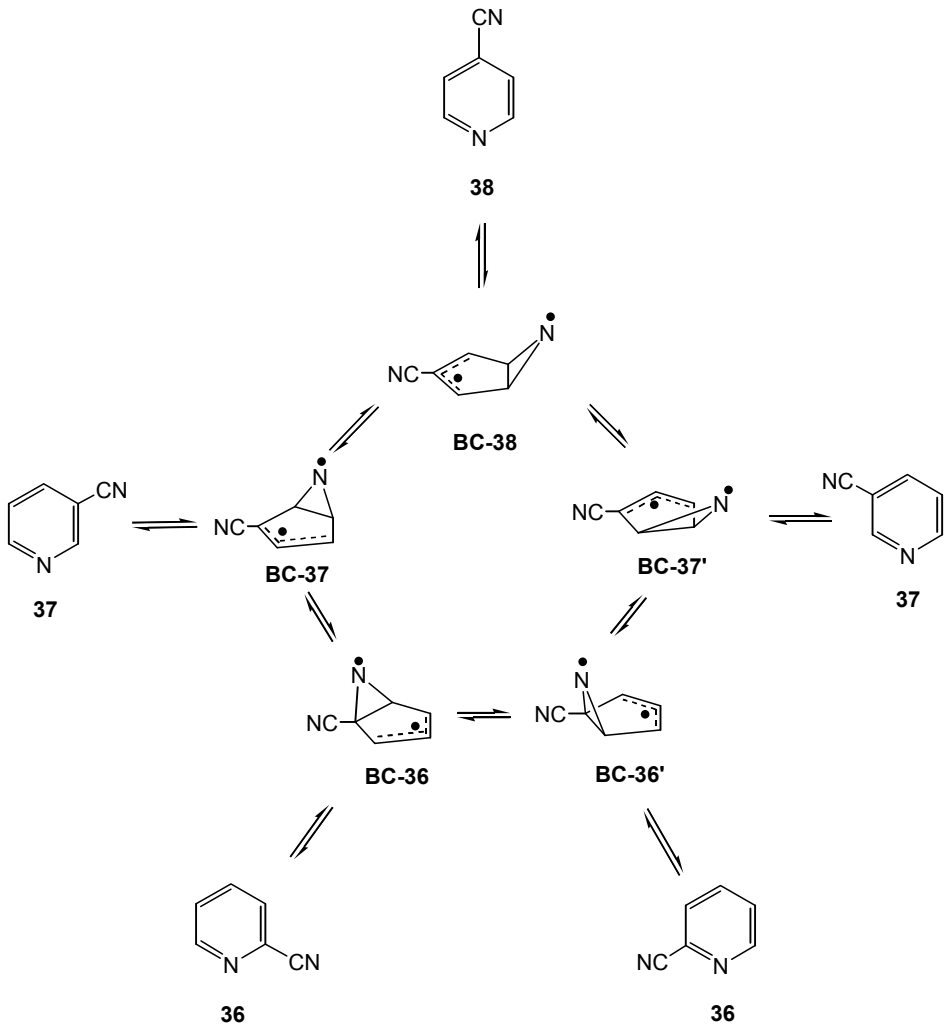

Cyanopyridines **36-38** are expected to interconvert by this mechanism. Cyclization between positions 2 and 6 of any one of the cyanopyridine **36-38** results in the formation of a bicyclic azaprefulvene intermediate. Nitrogen migration around the five sides of the cyclopentenyl ring, followed by rearomatization, results in the formation of the other two cyanopyridines. For example, excitation of 4-cyanopyridine (**38**) will convert **38** to azaprefulvene **BC-38**. Nitrogen migration of this intermediate can be

clockwise or counterclockwise. Counterclockwise nitrogen migration would result in the formation of **BC-37** which rearomatizes to 3-cyanopyridine (**37**). The second nitrogen migration converts **BC-37** to **BC-36** and this intermediate will rearomatize to 2-cyanopyridine (**36**). The clockwise nitrogen migration of **BC-40** also results in the formation of **BC-37',** which rearomatize to 3-cyanopyridine (**37**), one of the photoproduct. The second nitrogen migration from **BC-37'** results in the formation of **BC-36'** and will aromatize to **36**. Thus, these photoproducts are consistent with the suggested mechanism.

Since the photoproduct **36** from **BC-36** and **BC-36'** are identical, at this level of labeling, they cannot be distinguished. Similarly, the photoproduct **37** resulting from **BC-37** and **BC-37'** are also undistinguishable.

It should be pointed out that the experimental results indicate that **38** is very reactive when it was excited at 254 nm. This reactivity is consistent with the mechanistic diagram shown in Scheme 4.5. It is likely that **BC-37** is more stable than **BC-38**. Thus the conversion from **BC-38** to **BC-37** can compete effectively with the conversion from **BC-38** to **38**. This is the reason why 4-cyanopyridine (**38**) is reactive and 3-cyanopyridine (**37**) is unreactive. Moreover, the mechanism suggests that photolysis of **38** would result in the formation of **36** and **37** in a ratio of 1:1. The data shown in Table 4.3, however, shows that after 90 minutes of irradiation, the yield of **37** was found to be ~ 10 times greater than **36**. This result is not consistent with the statistical ratio suggested in Scheme 4.5. The reason for this observation can be explained in term of the stability

of intermediate **BC-37**(**37'**). The cyclopentenyl radical **BC-37** (**37'**) is stabilized by delocalization of the odd electron with the cyano group located at the end of the allyl system. This stabilization is not possible in **BC-36** (**36'**) since the cyano group is at the bridgehead and not conjugated with the allyl system. Thus, conversion of the more stable **BC-37** (**37'**) to the less stable **BC-36** (**36'**) would be expected to be slower than the rearomatization of **BC-37** (**BC-37'**) to **37**.

Irradiation of 3-cyanopyridine (**37**) would result in the formation of **BC-37**. Nitrogen migration in the counterclockwise direction would result in the formation of **BC-38** which is the precursor of **38**, one of the photoproduct. The second nitrogen migration would form **BC-37'** which upon rearomatization would result in the formation of starting material, **37**. The other photoproduct, **36**, would result from nitrogen migration from **BC-37** in the opposite direction. In this case, the intermediate **BC-36** and **BC-36'** would result from the first and second nitrogen migration, respectively. This intermediate would rearomatize to **36**, the second photoproduct. On a statistical basis this mechanism shows that irradiation of **37** will form **36** and **38** in a ratio of 2:1. Quantitative analysis from irradiation of 3-cyanopyridine (**37**) shows that after 360 minutes of irradiation the ratio of **36**:**38** is close to 2:1, which is consistent with the mechanistic interpretation. It should be noted that at short irradiation times, the photoproduct ratio was found to be less than 1. This indicates that the photolysis of **37** has not reached a photo-equilibrium point. Therefore, the ratio of photoproduct formed is different from the statistically expected ratio.

Irradiation of 2-cyanopyridine (**36**) would result in the formation of **BC-36.** Nitrogen migration in the clockwise direction would result in the formation of **BC-37** which rearomatizes to the photoproduct, **37**. The second nitrogen migration would form **BC-38** which rearomatizes to another photoproduct, **38**. In the opposite direction, **BC-36** undergoes nitrogen migration to form **BC-38'** which would rearomatize back to the starting material, **36**. The second nitrogen migration would result in the formation of **BC-37'** which would rearomatize to **37**. From the mechanism, the ratio of photoproduct **37** to **38** should be 2:1. However, because of the resonance stabilization of **BC-37** (**37'**), this ratio would be expected to be experimentally higher than 2:1. Quantitative analysis shows that irradiation for 15 minutes of 2-cyanopyridine (**36**) forms **37** and **38** in a ratio of 2.5:1. However, after prolonged irradiation time to 90 minutes, the ratio increases to be about 5:1. This is due to the greater stability of **BC-37** (**37'**) as previously discussed.

The photochemical reactivity of cyanopyridines (**36-38**) described above is found to be consistent with the substituent-site influence on stability of allylic radicals obtained from theoretical calculation by Lehd and Jensen.[38] Using AUMP2 method, the radical stabilization energies of electron withdrawing CN group at position 1 and 2 of the allyl radical were calculated as 9.9 and 3.0. These values can be applied to the allylic system in azaprefulvene structures **BC-36**, **BC-37**, and **BC-38**. **BC-37** has the cyano group at the end of the allyl system and should be the most stable. **BC-38**, however, has the cyano substituent at position 2 of the allyl system and should be less stable. These interpretations are consistent with the experimental results showing that 3-cyanopyridine

(**39**) is much less reactive than 4-cyanopyridine (**38**). Scheme 4.6 shows the bicyclic radicals resulting from photolysis of **36**, **37**, and **38**.

Scheme 4.6 Radical stabilization of cyanopyridines

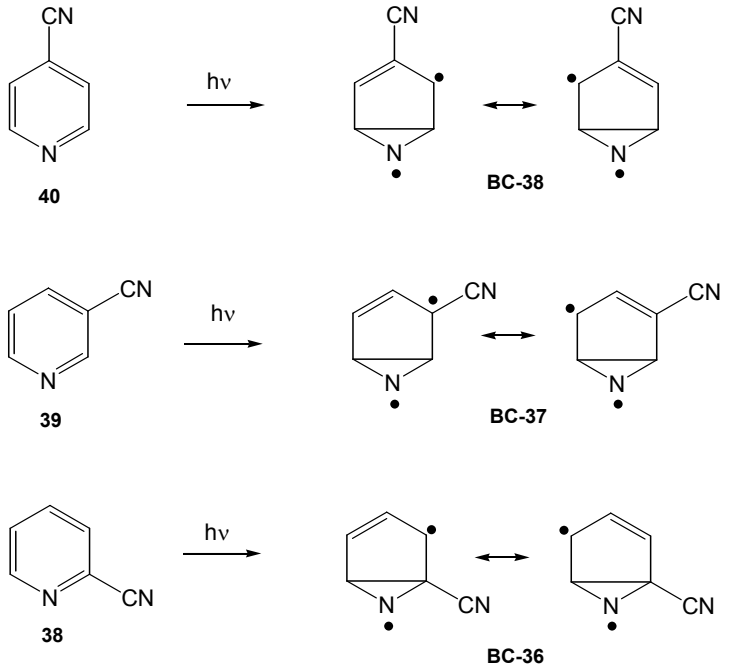

With the relative radical stabilization energy of 9.0, **BC-37** is expected to be the most stable intermediate due to the resonance delocalization of the allylic system which is extended into the CN group. In the case of **BC-38,** its stability is expected to be less than the stability of **BC-37** because it does not have resonance stabilization with CN. This is consistent with the relative stabilization energy of 3.0 in **BC-38**. Thus, **38** is more reactive than **37**.

In a similar way, **BC-36** does not have resonance stabilization due to the CN group. Therefore, **BC-36** should be less stabilized than **BC-37** and **BC-38** because the

CN group is not located at position 1 or position 2 in allylic system. 2-Cyanopyridine (**36**) should be the most reactive species.

However, there are some other factors in **BC-36** structure that should be considered. **BC-36** is an azaprefulvene that contains the CN group at ring position 2. It should be noted that the substituents at C2 and C6 can sterically inhibit the formation of azaprefulvene. Scheme 4.7 shows the azaprefulvene structure with R groups on C2 and C6.

Scheme 4.7 Steric hindrance from substituents at C2 and C6

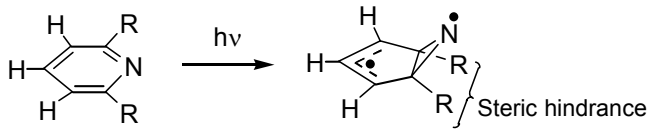

The R groups attached to C2 and C6 come closure together as 2,6-bridging occurs, inhibiting the formation of azaprefulvene. The larger the R groups, the greater the inhibition to its reactivity. In this case, steric hindrance from CN group inhibits the reaction. This causes **BC-36** to be less reactive than **BC-38** which does not contain any CN group at ring position 2 and 6. In addition, the **BC-36** intermediate also would undergo energy wasting process by one nitrogen migration to itself (Scheme 4.5). These result in the less reactive 2-cyanopyridine (**36**) than 4-cyanopyridine (**38**). Therefore, the reactivity of cyanopyridines should be in order of **38**>**36**>**37**, which is consistent with the experimental results.

Moreover, to ensure that the Dewar-pyridine and azaprismane mechanisms are not involved in the photo-reaction of cyanopyridine, these mechanistic pathways are examined. Scheme 4.8 shows that, irradiation of 2-cyanopyridine (**36**) would either form

Scheme 4.8 Dewar-pyridine mechanism of 2-cyanopyridine

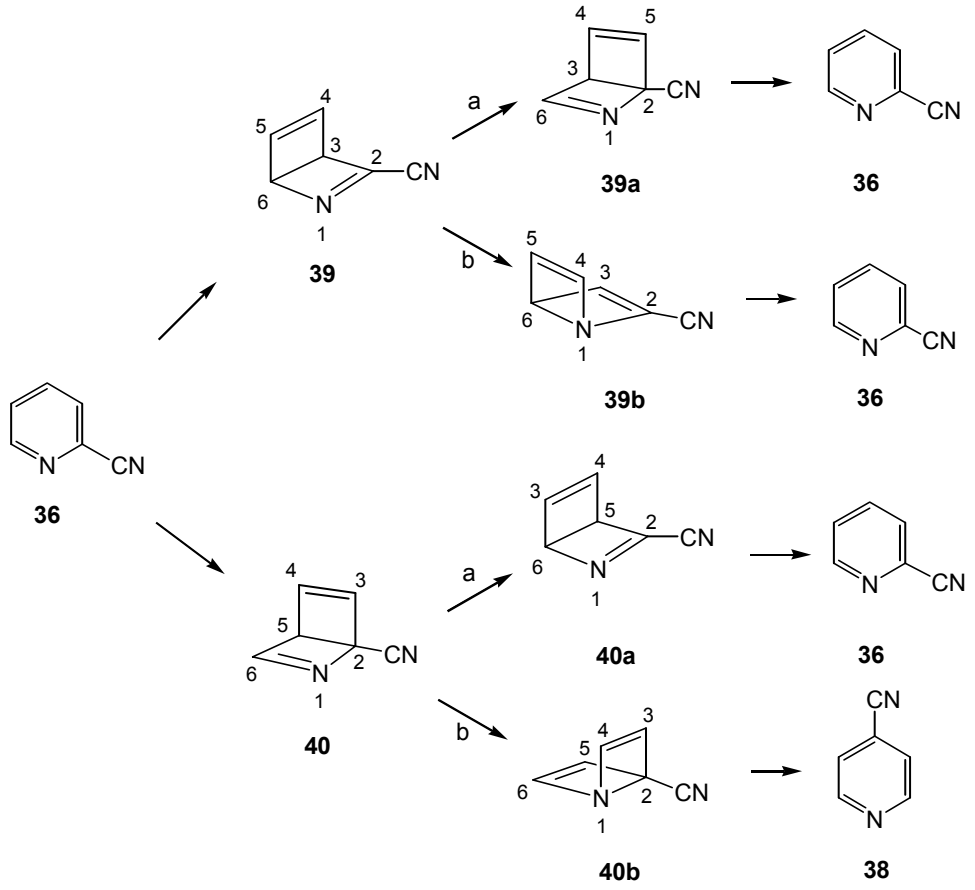

Dewar-pyridine **39** (3,6-bridging) or **40** (2,5-bridging). From Dewar-pyridine **39**, it would undergo bond cleavage between C5 and C6 and bond linkage between C2 and C5 to form Dewar-pyridine **39a** which will rearrange to the starting material, **36**. In the other pathway, **39** would undergo bond cleavage between C3 and C4 and bond linkage between C4 and N1 to form Dewar-pyridine **39b**, which would also rearrange to the starting

material, **36**. The Dewar-pyridine **40** would undergo bond cleavage between C2 and C3 followed by bond linkage between C3 and C6 to form **40a**. This structure will also rearrange back to cyanopyridine **36**, the starting material. Interestingly, the bond cleavage between C4 and C5 of **40** and bond forming between N1 and C4 would result in the formation of **40b**. This species will rearrange to 4-cyanopyridine (**38**). This mechanistic examination clearly shows that rearrangement of 2-cyanopyridine (**36**) by the Dewar-pyridine mechanism would lead to only photoproduct **38** but not **37** that was also observed in ^{1}H-NMR spectrum. This indicates that the phototransposition of 2-cyanopyridine (**36**) does not occur via the Dewar-pyridine pathway.

Another possible mechanism is also examined. The azaprismane-intermediate mechanism is shown in Scheme 4.9.

Scheme 4.9 Azaprismane mechanism: 3,6-bridging

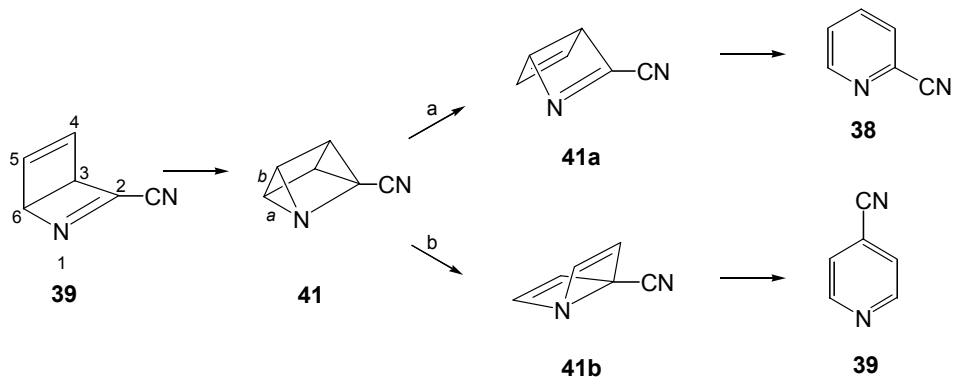

Dewar-pyridine **39** (3,6-bridging) would undergo [2+2] cycloaddition between C5 and N1 as well as C4 and C2 to form azaprismane structure **41**. Three distinct bond cleavages of **41** would result in the formation of **39**, **41a**, and **41b**. In this case, only **41b** would rearrange to form 4-cyanopyridine **38**.

Dewar-pyridine **40** (2,5-bridging) can also undergo [2+2] cycloaddition as shown in Scheme 4.10 between C3 and N1 as well as C4 and C6 to form azaprismane **42**. Three distinct cleavages of **42** would result in **40**, **42a**, and **42b**. In the case of **45a**, it will rearomatize back to the starting material, **38**. The **42b** structure will rearomatize to 3-cyanopyridine (**37**).

Scheme 4.10 Azaprismane mechanism: 2,5-bridging

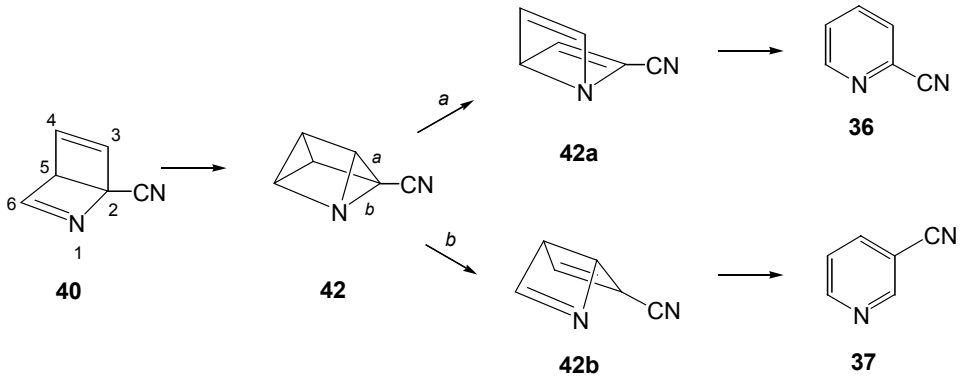

Furthermore, the other azaprismane structure of 2-cyanopyridine (**36**) can result from the 1,4-bridging between C4 and nitrogen atom to form Dewar-pyridine **43** as shown in Scheme 4.11.

Scheme 4.11 Azaprismane mechanism: 1,4-bridging

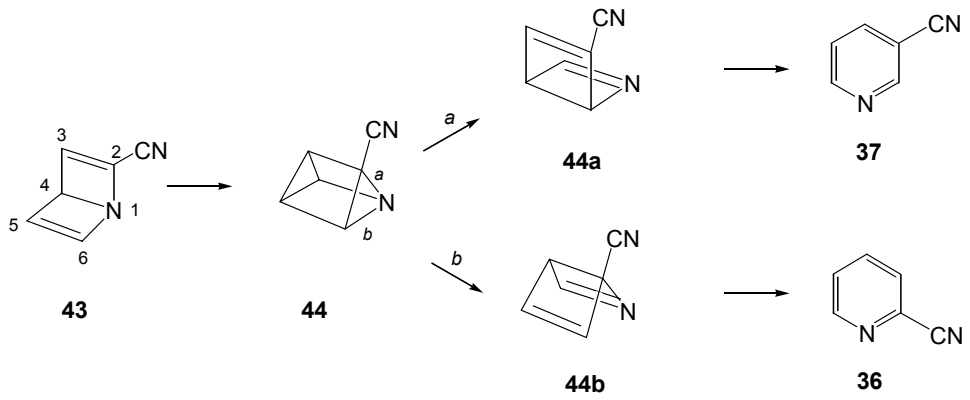

[2+2] cycloaddtion of **43** result in the formation of azaprismane **44** which would undergo bond cleavage either by *a* or *b* pathway. The resulting Dewar-pyridine structure **44a** would rearrange to **37** and **44b** would rearrange back to the starting material, **36**. From all these mechanistic possibilities, the statistical ratio of photoproducts **37** and **38** is found to be 2:1. This value is consistent with the quantitative analysis showing that the ratio is greater than 2:1 since the short irradiation time and it increased constantly for the range from 15-90 minutes. However, it indicates that 2-cyanopyridine (**36**) should be very unreactive even though the experimental photoproduct ratio indicates that 3-cyanopyridine (**37**) is the least reactive isomer. If the arbitrary selectivity regarding to the bond formation or cleavage in transposition pathway may be present, it is difficult to explain how these decisions occur.

4.2. Photochemistry of methylpyridines in vapor phase

The photochemistry of methylpyridines (**6-8**) was studied by irradiating the vapors (2.5-3.5 Torr) in a 3-L quartz reaction vessel at 254 nm.

4.2.1. Irradiation of 2-methylpyridine (6)

2-Methylpyridine (**6**) vapor (2.5-3.5 Torr) was irradiated at 254 nm with 15 low-pressure mercury lamps in a Rayonet reactor for 3, 6, and 12 hours. GC analysis of the resulting product mixtures showed that irradiation of 2-methylpyridine (**6**) at retention time 19 minutes resulted in the formation of pyridine (**1**) at 15 minutes, 3-methylpyridine (**7**) at 30 minutes, and 4-methylpyridine (**8**) at 31 minutes. In addition, one unknown compound was also formed which may be formed from the methyl-demethylation process. The structures of these photoproducts are shown in scheme 4.12.

Scheme 4.12 Photolysis of 2-methylpyridine (**6**)

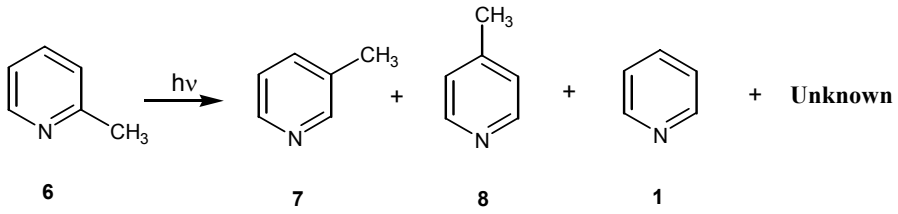

Figure 4.13 shows the GC trace of the resulting mixture of photoproducts after 12 hours of irradiation. It clearly shows all components shown in Scheme 4.12.

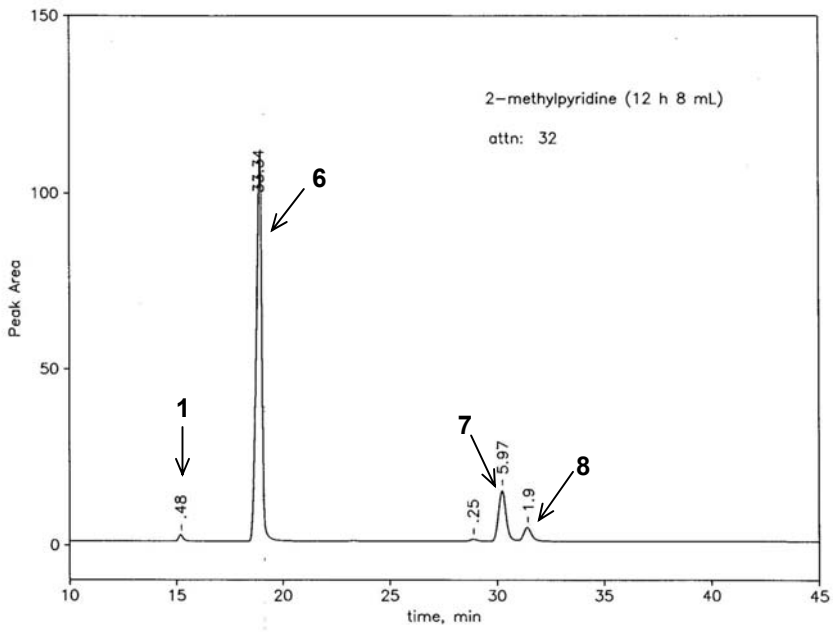

Figure 4.13 GC trace of photoproduct mixture from 2-methylpyridine after irradiation for 12 hours

In each experiment, the photoproduct mixture was analyzed by GC. The quantitative data of all photoisomerization products are given in Table 4.7. It should be noted that pyridine (**1**) was also formed from the methylation-demethylation reaction and thus is excluded from this discussion.

Table 4.7 GC data of photoproduct mixture from irradiation of 2-methylpyridine (**6**)

Exp no.	Irradiation time (min)	Sample weight (mg)	Recovered weight (mg)	2-MP consumption (%)	3-MP formation (%)	4-MP formation (%)
16	3	75.1	48.7	5	3.41	0.62
17	6	72.6	42.5	9.9	6.60	1.85
18	12	50.3	29.8	19.5	13.2	4.39

In Table 4.7, it is observed that **6** was consumed upon irradiation and then **7** was formed as the major product and **8** as the minor product. After 12 hours of irradiation, the yield of **7** is greater than the yield of **8** in a ratio of 3:1. Figure 4.14 shows a plot of product ratio VS irradiation time.

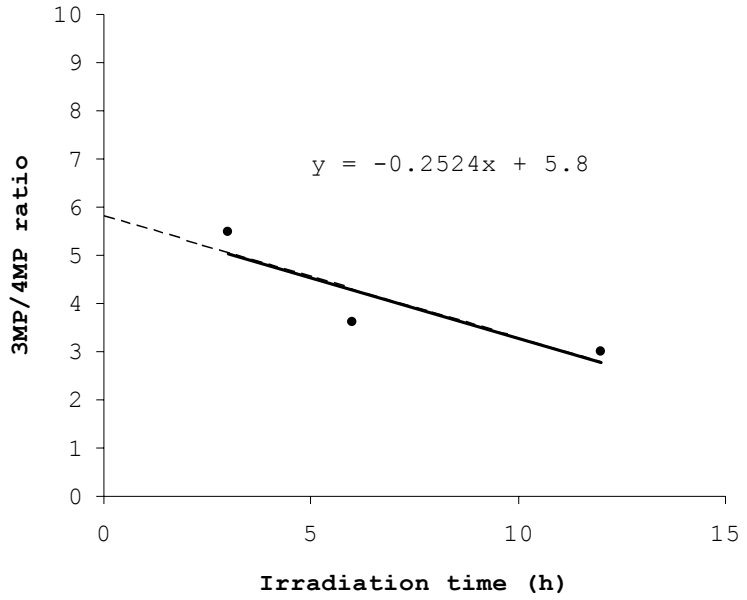

Figure 4.14 Ratio of 7 / 8 from irradiation of 2-methylpyridine (**6**)

The ratios of **7** to **8** decrease upon irradiation time. This means that once formed 3-methylpyridine (**7**) undergoes phototransposition more rapidly than 4-methylpyridine (**8**). Extraporation to zero minute of irradiation gave the ratio of 5.8:1 indicating that both **7** and **8** have been formed directly from **6** at early irradiation time. Hence, **7** and **8** are primary photoproducts. After irradiation, the product mixtures were analyzed by ^{1}H-NMR in $CDCl_3$. Figure 4.15a and 4.15b show the ^{1}H-NMR spectra before and after irradiation, respectively.

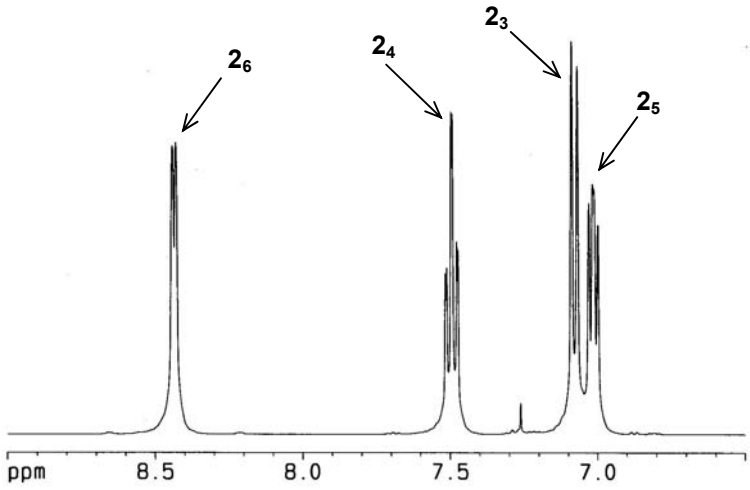

(a)

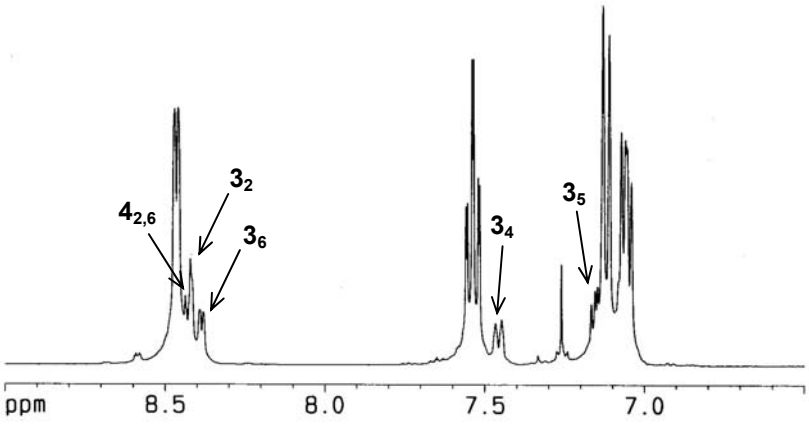

(b)

Figure 4.15 (a) ^{1}H-NMR spectrum of 2-methylpyridine before irradiation
(b) ^{1}H-NMR spectrum of 2-methylpyridine after 12 hours of irradiation

In Figure 4.15a, the signal due to the H6 proton of **6** appears as a doublet at δ 8.36 (J = 4.6 Hz) because it is coupling with the adjacent H5 proton. The H4 signal is observed at δ 7.41. A doublet signal due to H3 absorbs at δ 7.00 (J = 7.8 Hz) and a distorted triplet due to H5 absorbs at δ 6.93. After irradiation, the ^{1}H-NMR spectrum shown in Figure 4.15b shows the proton signals of the photoproducts, 3-methylpyridine (**7**), and 4-methylpyridine (**8**). The singlet that absorbs at δ 8.42 is due to the H2 proton of **7**. The doublet that absorbs at δ 8.38 (J = 4.1 Hz) is due to the H6 of **7**. A doublet due to proton 4 of 3-methylpyridine (**7**) is observed at δ 7.45 (J = 7.6 Hz). A complicate signal due to the H5 of 7 is observed at δ 7.15.

In addition, A singlet signal observed at δ 8.42 is due to the H2,6 proton of 4-methylpyridine (**8**). The signal due to the H3,5 protons of **8** are obscured by the H5 signal of 2-methylpyridine (**7**).

The photoproduct mixture from irradiation of 2-methylpyridine (**6**) was also analyzed by ^{13}C-NMR. Figure 4.16a and 4.16b show the ^{13}C-NMR spectra of 2-methylpyridine (**6**) before and after irradiation. In Figure 4.16a, the carbon signals due to C2, C6, C4, C3, and C5 are observed at δ 158.6, 149.4, 136.5, 123.5, and 120.9, respectively. After irradiation, the new signals due to photoproducts are observed. As shown in Figure 4.16b, the C2, C6, C4, C3, and C5 signals due to **7** are observed at δ 150.6, 147.3, 136.8, 133.5, and 123.5, respectively. The C2,6 and C3,5 due to **8** are observed at δ 149.9 and 125.0, respectively. It should be noted that the C4 of 4-methylpyridine could not be observed in ^{13}C-NMR spectrum because of low intensity.

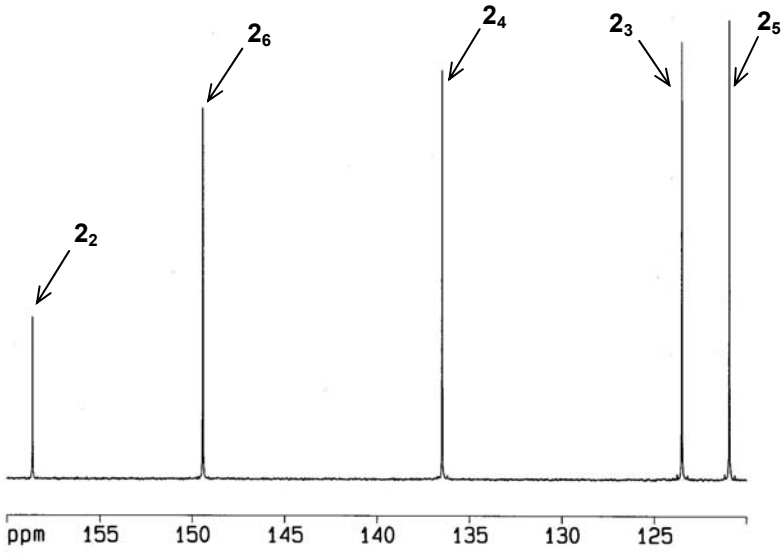

(a)

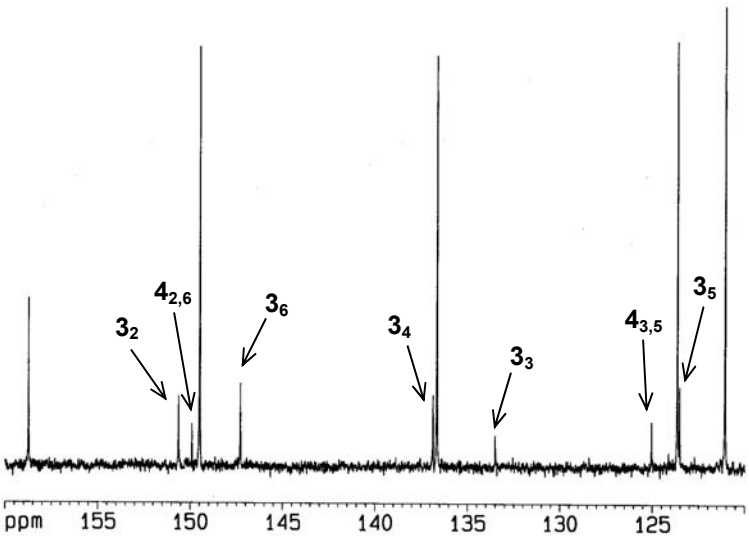

(b)

Figure 4.16 (a) ^{13}C-NMR spectrum of 2-methylpyridine before irradiation
(b) ^{13}C-NMR spectrum of 2-methylpyridine after 12 hours of irradiation

From these results, it can be concluded that irradiation of **6** results in the formation of **7** and **8**. Thus, it is consistent with the mechanism involving 2,6-bridging, nitrogen migration, and rearomatization.

4.2.2. Irradiation of 3-methylpyridine (7)

3-Methylpyridine (**7**) vapor (2.5-3.5 Torr) was irradiated at 254 nm with 15 low-pressure mercury lamps in a Rayonet reactor for 3, 6, and 12 hours. GC analysis of the resulting photoproducts showed that irradiation of 3-methylpyridine (**7**) at retention time 30 minutes resulted in the formation of pyridine (**1**) at 15 minutes, 2-methylpyridine (**6**) at 19 minutes, and 4-methylpyridine (**8**) at 32 minutes as shown in Scheme 4.13.

Scheme 4.13 Photolysis of 3-methylpyridine (**7**)

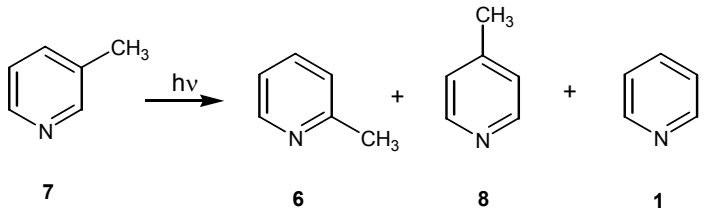

Figure 4.17 shows the GC analysis result of 3-methylpyridine (**7**) after 6 hours of irradiation. Pyridine (**1**) which was suggested to be the product from methyl-demethylation reaction is also observed.

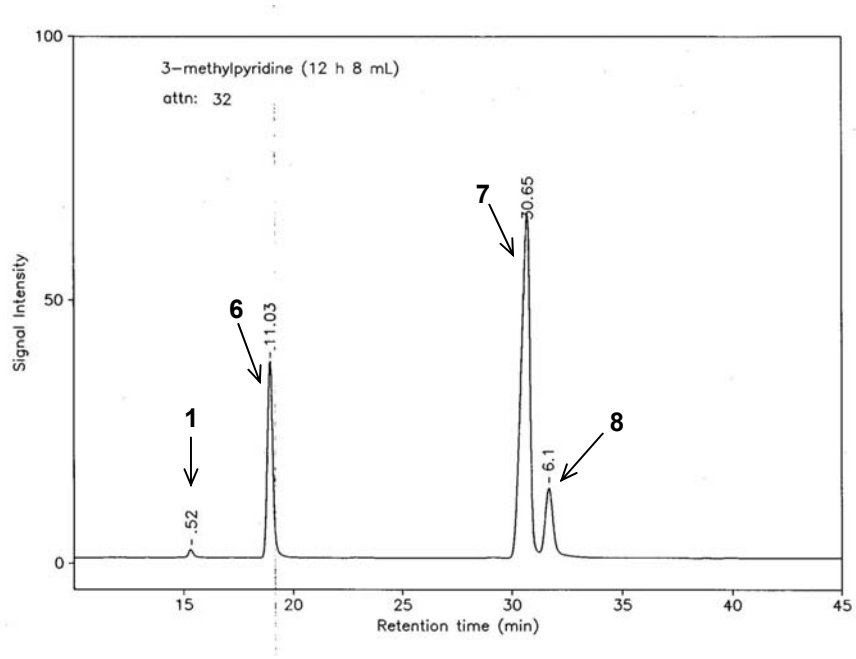

Figure 4.17 GC trace of photoproduct mixtures from 3-methylpyridine after irradiation for 12 hours

In separate experiments, the photoproduct mixtures from irradiation for 3 and 12 hours were also analyzed. The data from all these experiments are given in Table 4.8.

Table 4.8 Experimental details for irradiation of 3-methylpyridine (**7**)

Exp no.	Irradiation time (min)	Sample weight (mg)	Recovered weight (mg)	3-MP consumption (%)	2-MP formation (%)	4-MP formation (%)
19	3	72.4	28.4	16.5	10.5	5.7
20	6	72.8	38.5	27.3	17.2	9.5
21	12	77.3	36.5	38.3	24.2	14.4

The formation of 2-methylpyridine (**6**) and 4-methylpyridine (**8**) are in a ratio of 2:1 after the first three hours of irradiation.

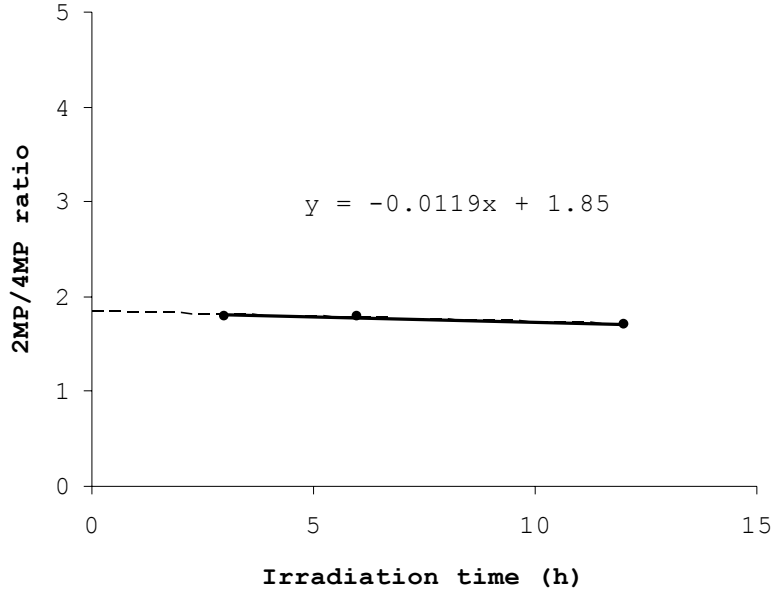

Figure 4.18 Ratio of 6 / 8 from irradiation of 3-methylpyridine (**7**)

The plot shows that the ratio of **6**/**8** is constant upon irradiation from 3 hours to 12 hours. Extrapolation back to zero irradiation shows the ratio of **6** to **8** as 1.85 indicating that both products are primary products and they are formed at the very short time.

Figure 4.19a and 4.19b show the ^{1}H-NMR spectra of 3-methylpyridine before and after 12 hours of irradiation. In Figure 4.19a, a singlet due to the H2 proton is observed at δ 8.39. The doublet due to H6 proton is observed at δ 8.36 (J = 4.7 Hz). The last signal is a distorted triplet due to the H5 proton which is observed at δ 7.12.

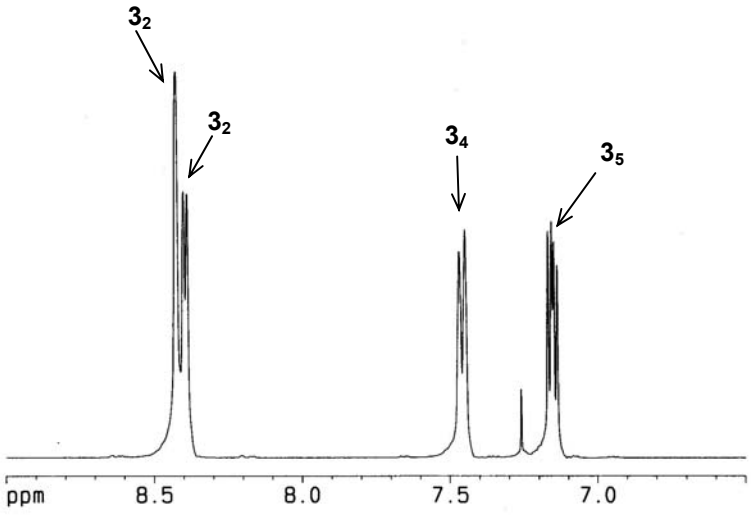

(a)

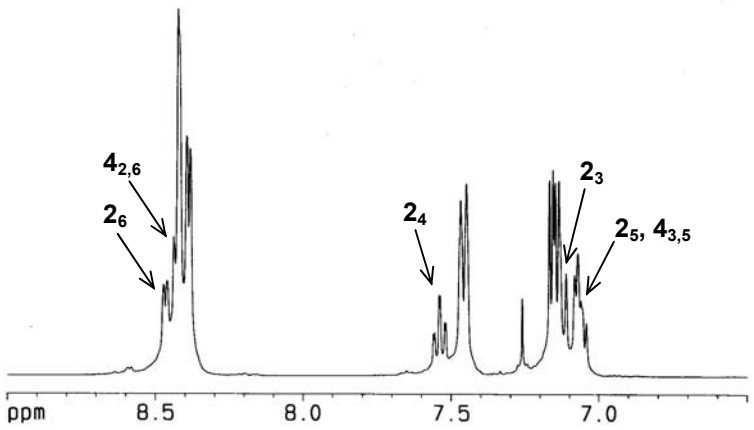

(b)

Figure 4.19 (a) ^{1}H-NMR spectrum of 3-methylpyridine before irradiation
(b) ^{1}H-NMR spectrum of 3-methylpyridine after 12 hours of irradiation

After irradiation, the ^{1}H-NMR spectrum in Figure 4.19b exhibits a doublet signal due to the H6 proton of 2-methylpyridine (**6**) at δ 8.46 (J = 4.7 Hz). The H4 proton is observed at δ 7.54 as a triplet of doublet. A doublet of H3 in **6** is overlapping with the H5 of the reactant at δ 7.11. This signal looks like a singlet because of this coincidence. The H5 signal of **6** is also overlapping but with the signal of another photoproduct 4-methylpyridine (**8**). This signal appears in a region between δ 7.04-7.08 with the H3,5 signal of **8**. The signal due to H2,6 of **8** is overlapping with the H2 of the reactant **7** at δ 8.44.

The ^{13}C-NMR spectra were also recorded. Shown in Figure 4.20a, the carbon spectrum shows the C2, C6, C4, C3, and C5 at δ 150.6, 147.3, 136.8, 133.4, and 123.5, respectively. After irradiation, Figure 4.20b shows that the photoproducts have been formed. The new signals that absorb at δ 158.7, 149.5, 136.6, 123.6, and 121.1 are due to the C2, C6, C4, C3, and C5 of 2-methylpyridine (**6**), respectively. In addition, the signals due to the C2,6 and C3,5 of 4-methylpyridine (8) are observed at δ 149.9 and 125.0, respectively. The small singlet appearing at δ 147.4 is due to the C4 carbon of **8**.

Hence, irradiation of 3-methylpyridine (**7**) results in the formation of 2-methylpyridine (**6**) and 4-methylpyridine (**8**) which is consistent with the mechanism involving electrocyclic ring closure 2,6-bonding reaction, nitrogen migration, and rearomatization.

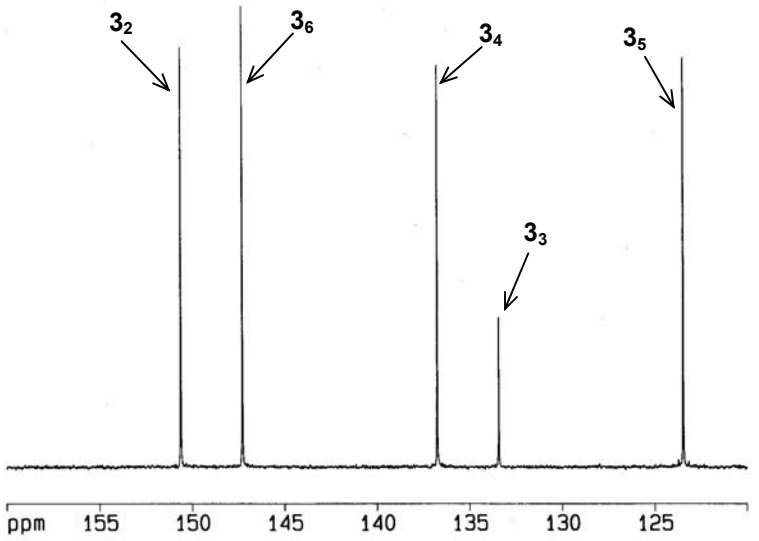

(a)

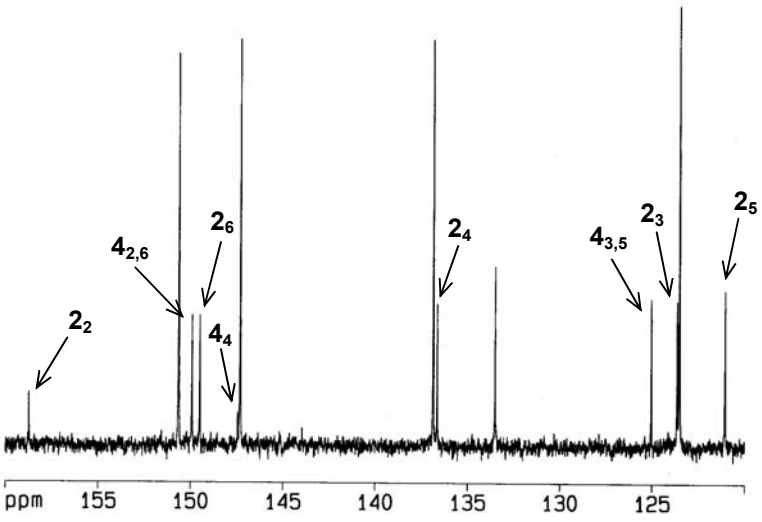

(b)

Figure 4.20 (a) ^{13}C-NMR spectrum of 3-methylpyridine before irradiation
(b) ^{13}C-NMR spectrum of 3-methylpyridine after 12 hours of irradiation

4.2.3. Irradiation of 4-methylpyridine (8)

4-Methylpyridine (**8**) vapor (2.7-3.7 Torr) was irradiated at 254 nm with 15 low-pressure mercury lamps in a Rayonet reactor for 3, 6, and 12 hours. GC analysis of the resulting photoproducts showed that irradiation of 4-methylpyridine (**8**) which was observed as a peak at retention time 32 minutes resulted in the formation of pyridine (**1**) at 15 minutes, 2,6-dimethylpyridine (**22**) at 24 minuites, 2-methylpyridine (**6**) at 19 minutes, and 3-methylpyridine (**7**) at 30 minutes as shown in Scheme 4.14.

Scheme 4.14 Photolysis of 4-methylpyridine (**8**)

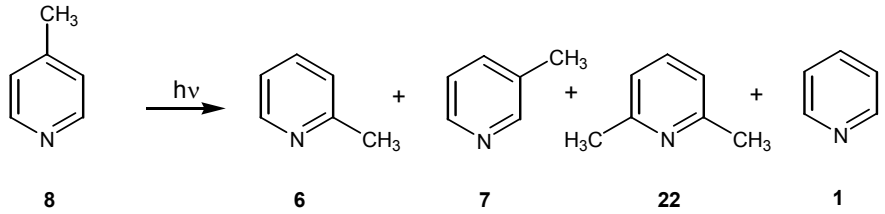

GC analysis shown in Figure 4.21 shows that irradiation of 4-methylpyridine (**8**) resulted in the formation of 2-methylpyridine (**6**) at retention time 19 minutes, 3-methylpyridine (**7**) at 30 minutes, pyridine (**1**) at 15 minutes, and 2,6-dimethylpyridine (**22**) at 24 minutes.

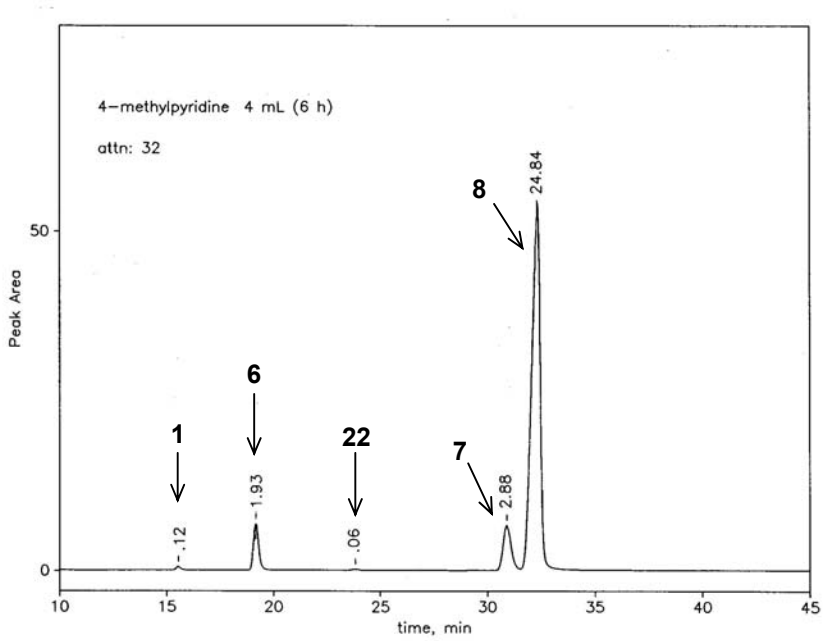

Figure 4.21 GC trace of photoproduct mixture from 4-methylpyridine after irradiation for 6 hours

In Table 4.9, the quantitative analysis for each separated experiment shows that 2-methylpyridine (**6**) is formed in greater yield than 3-methylpyridine (**7**). For example, after 12 hours of irradiation, 20.5% of **8** was consumed at and **6** and **7** were formed in yield of 8.7% and 11.4%, respectively.

Table 4.9 GC data of photoproduct mixture from irradiation of 4-methylpyridine (**8**)

Exp no.	Irradiation time (min)	Sample weight (mg)	Recovered weight (mg)	4-MP consumption (%)	2-MP formation (%)	3-MP formation (%)
22	3	29.4	20.6	11.7	4.4	6.7
23	6	77.1	29.1	16.6	6.7	9.3
24	12	70.1	20.6	20.5	8.7	11.4

The ratio of **7**/**6** is plotted as a function of irradiation time and it is shown in Figure 4.22.

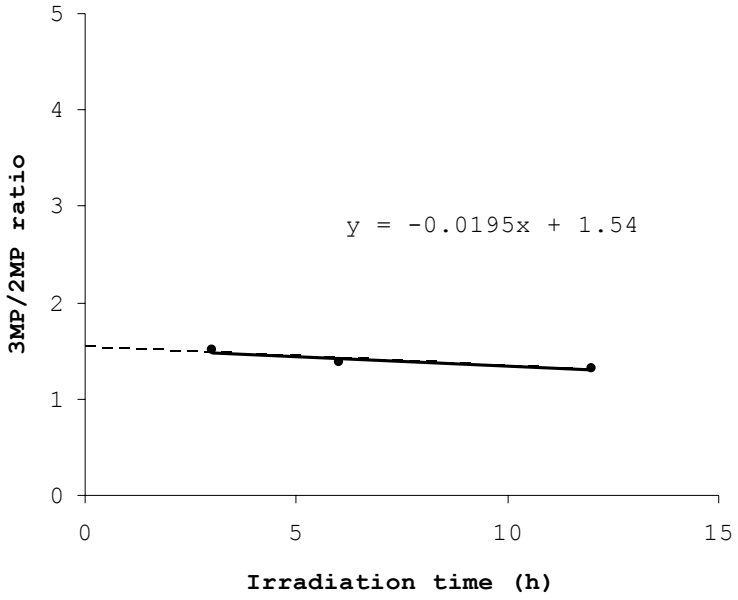

Figure 4.22 Ratio of **7**/**6** from irradiation of 4-methylpyridine (**8**)

Extrapolation back to zero irradiation leads to the **7**/**6** ratio of 1.54:1. This indicates that both photoproducts are formed at very short irradiation time and they are primary products.

Furthermore, the photoproduct mixture of **8** was analyzed by NMR. The ^{1}H-NMR spectra recorded in $CDCl_3$ shown in Figure 4.23a and 4.23b exhibit the proton signals of reactant before irradiation and photoproduct after irradiation for 12 hours. In Figure 4.23a, the doublet signal due to protons at ring position 2 and 6 is observed at δ

8.38 (J= 4.3 Hz) whilst the doublet signal due to protons at ring position 3 and 5 is observed at δ 7.01 (J = 4.4 Hz).

After irradiation, the ^{1}H-NMR spectrum in Figure 4.23b shows the same signals of reactant and weak signals of photoproducts. The small signal as a doublet at δ 8.39 (J = 4.8 Hz) is due to the H6 of 3-methylpyridine (**7**). In addition, the doublet signal absorbing at δ 7.46 (J = 7.8 Hz) is due to the H4 proton of **7**. The signal that absorbs at δ 7.16 also represents the H5 of 3-methylpyridine (**7**). However, the H2 signal of **7** is overlapping with the H2,6 signal of the reactant.

Furthermore, the triplet of doublet signal due to the H4 of 2-methylpyridine (**6**) are observed at δ 7.55. However, the signals due to the H6 of **6** is overlapping with the H2,6 signal of the reactant **8**. The H5 signal of **6** is also overlapping with the intense signal due to H3,5 signal of **8**.

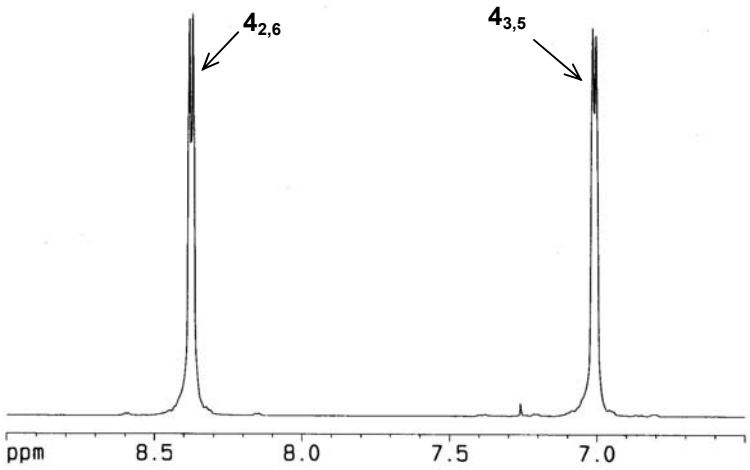

(a)

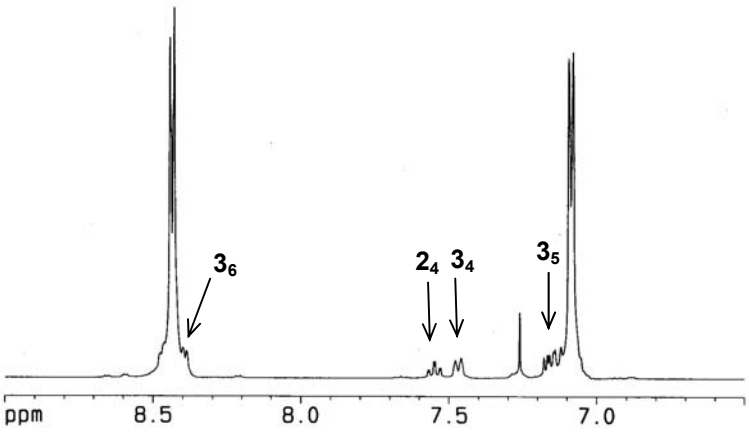

(b)

Figure 4.23 (a) ^{1}H-NMR spectrum of 4-methylpyridine before irradiation
(b) ^{1}H-NMR spectrum of 4-methylpyridine after 12 hours of irradiation

In addition, the ^{13}C-NMR spectra of 4-methylpyridine before and after irradiation were also recorded. In Figure 4.24a the carbon signal due to C2,6 and C3,5 are observed as intense peaks at δ 149.6 and 124.6, respectively. The quarternary C4 carbon is observed as a small peak at δ 147.0.

Figure 4.24b shows the ^{13}C-NMR spectrum of photoproducts after irradiation. The intense peaks of the reactant carbon signal are still observed. However, photoproducts are also clearly observed. The signal at δ 150.6, 147.3, 136.9, 133.3, and 123.5 are due to the C2, C6, C4, C3, and C5 of 3-methylpyridine (**7**), respectively. The signals at δ 149.5, 136.6, 123.6, and 121.1 are due to the C6, C4, C3, and C5 of 2-methylpyridine (**6**), respectively. It should be noted that because of the very low intensity, the quarternary C2 of 2-methylpyridine could not be observed in this ^{13}C-NMR spectrum.

According to these results, the phototransposition of **8** to **6** and **7** is consistent with the suggested mechanism involving 2,6-bonding, nitrogen migration, and rearomatization.

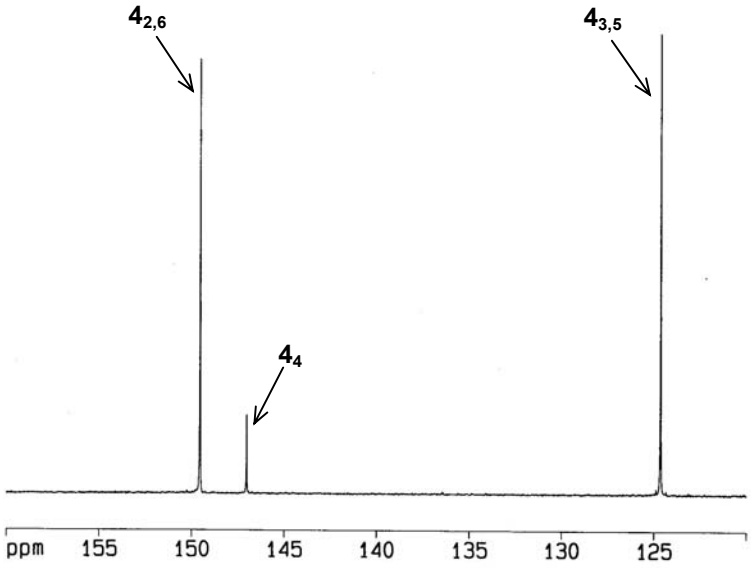

(a)

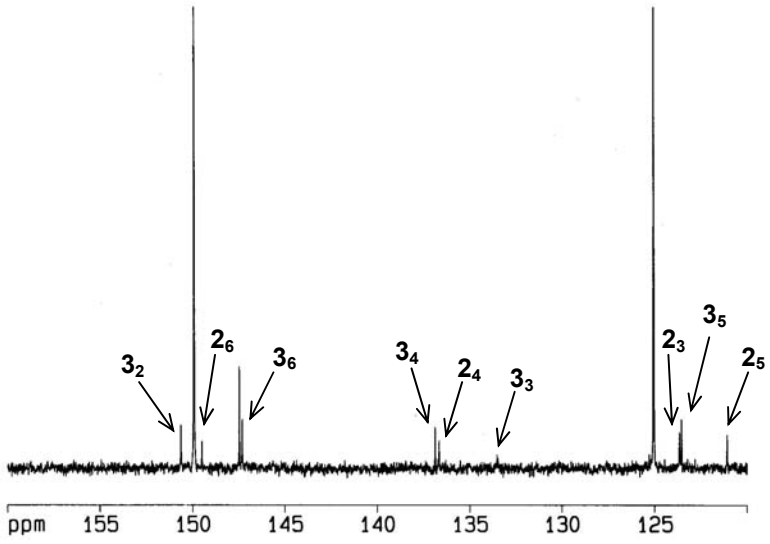

(b)

Figure 4.24 (a) ^{13}C-NMR spectrum of 4-methylpyridine before irradiation
(b) ^{13}C-NMR spectrum of 4-methylpyridine after 12 hours of irradiation

4.2.4. Mechanistic Discussion of methylpyridines

The experimental results from the photochemistry of isomeric methylpyridine vapors (**6-8**) show that irradiation of any one isomer results in the formation of the other two as shown in Scheme 4.15.

Scheme 4.15 Photo-interconversion of methylpyridines

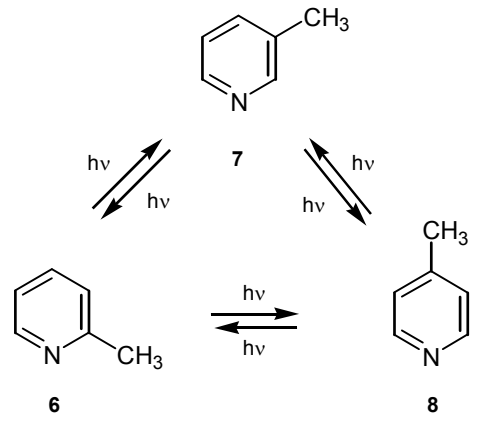

The interconversions are found to be consistent with the mechanism involving cyclization-2,6-bonding followed by nitrogen migration around five sides of cyclopentenyl ring. Finally, rearomatization gives the other two isomers.

The mechanism shown in Scheme 4.16 shows that irradiation of any one isomer would result in the formation of an azaprefulvene intermediate which allows nitrogen to migrate from one side to the other side in both directions.

Scheme 4.16 Phototransposition mechanism of methylpyridines

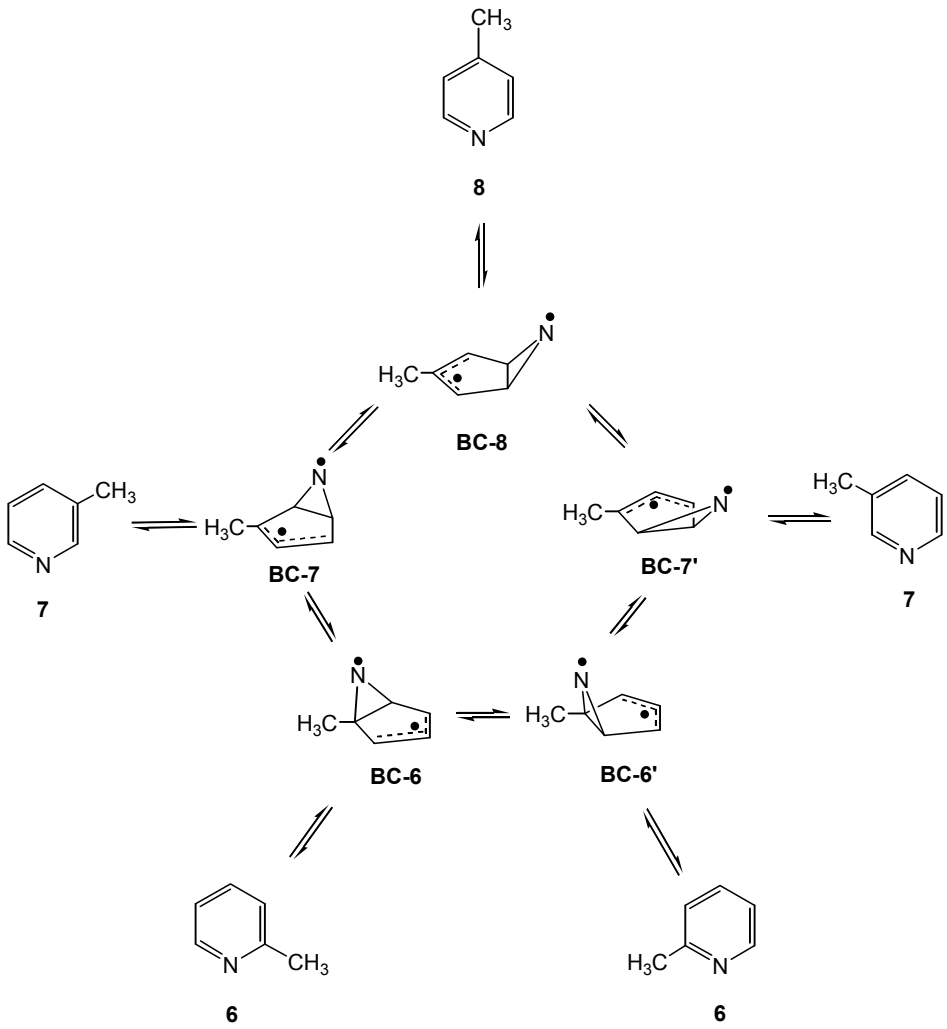

Irradiation of 4-methylpyridine (**8**) would result in the formation of **BC-8**. This species can undergo nitrogen migration in both directions. Nitrogen migration in the counterclockwise direction leads to **BC-7** followed by rearomatization to 3-methylpyridine (**7**). The second migration along the same direction gives **BC-6** which would rearomatize to 2-methylpyridine (**6**), another photoproduct. The nitrogen migration from **BC-8** in clockwise direction results in the formation **BC-7'** and **7** after

rearomatization. The second nitrogen migration results in the formation of **BC-6'** which is followed by rearomatization to form **6**. Hence, the photoproducts formed from irradiation of 4-methylpyridine (**8**) are expected to be in a ratio of 1:1. Quantitative analysis shows that the photolysis of **8** at very short irradiation time leads to the photoproduct ratio of **7** and **6** as 1.5:1 (Figure 4.21). This ratio, however, tends to decrease upon longer irradiation time and eventually it becomes close to 1. This indicates that at short irradiation times the photolysis has not reached the equilibrium state but finally it would come close to the 1:1 ratio of **7**:**6** when all compounds are in equilibrium. It can be seen that this suggested mechanism is consistent with the experimental result.

In addition, since the photoproducts **6** from rearomatization of **BC-6 and BC-6'** are identical, without an appropriated labeling they are undistinguishable. Similarly, the photoproducts **7** from rearomatization of **BC-7** and **BC-7'** are identical. These pathways could not be distinguished at this time.

Irradiation of 3-methylpyridine (**7**) would result in the formation of **BC-7**. Nitrogen migration in the counterclockwise direction leads to **BC-6** which is followed by rearomatization to form **6**. The second nitrogen migration would result in the formation of **BC-6'** which would also undergo rearomatization to **6**. In the clockwise direction, **BC-7** also undergo nitrogen migration to form **BC-8** which rearomatizes to **8**. In addition, the second nitrogen migration would result in the formation of **BC-7'** which rearomatizes back to **7**.

A similar process also occurs in the vapor phase photochemistry of 2-methylpyridine (**6**). Excitation of 2-methylpyridine (**6**) would result in the formation of **BC-6**. Nitrogen migration in the counterclockwise direction leads to the formation of **BC-6'** which undergoes rearomatization to form **6**, the starting material. The second nitrogen migration would result in the formation of **BC-7'** which would rearomatize to **7**. The nitrogen migration in the clockwise direction of **BC-6** leads to **BC-7** followed by rearomatization to yield **7**. The second nitrogen migration would result in the formation of **BC-8**, a precursor of **8**.

These overall mechanistic interpretations for methylpyridine isomers (**6-8**) are consistent with the 2,6-bonding-nitrogen migration and rearomatization. The photoproducts that were predicted by this mechanism have been successfully observed in the ^{1}H-NMR and ^{13}C-NMR spectra.

Furthermore, the relative reactivity of methylpyridine isomers (**6-8**) are consistent with the suggested mechanism. According to the experimental data shown in Table 4.7-4.9, the percent consumptions of methylpyridines **6**, **7**, and **8** after 12 hours of irradiation are 19.5, 38.3, and 20.5, respectively. This indicates that the methylpyridine photoreactivity in an order of isomer **7** > **8** > **6**. This reactivity difference can be explained by the stability of intermediates. Unlike cyanopyridines, azaprefulvene intermediates from methylpyridines (**6-8**) are not resonance stabilized with the methyl group. The stabilities resulting from radical stabilization in azaprefulvene structures **BC-6**, **BC-7**, and **BC-8** may not be considerably different. In allylic radical system, the

AUMP2 calculation by Lehd and Jensen[38] showed that the difference in radical stabilization energies upon substitutent site (1- or 2-position) due to the electron-withdrawing CN group is much greater than the difference due to the electron-donating CH_3 group.[39] Table 4.10 shows the substituent effects on stability of allylic radicals from theoretical calculation of radical stabilization energies.

Table 4.10 The substituent effects on stability of allylic radicals

Substituent	1-position 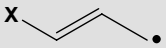	2-position 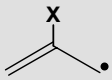
CH_3	5.6	4.3
CN	9.9	3.0

Based on the consumption of the reactant as a function of irradiation time, it was observed that 2-methylpyridine (**6**) is the least reactive isomer. Inspection of Scheme 4.16 shows why this is the case. Thus, electrocyclic ring closure of **6** leads to **BC-6**. One nitrogen migration from **BC-6** leads either to **BC-7**, the precursor of 3-methylpyridine (**7**), or to **BC-6'** which leads to reactant. Thus, the pathway **6→BC-6→BC-6'→6** is an energy wasting pathway and would reduce the apparent reactivity of **6**. In contrast to the analogous pathways originating from **7** or **8**, all lead to product formation and not back to the reactant.

According to Scheme 4.16, after electrocyclic ring closure of **7**, one nitrogen migration leads either to the formation of 2-methylpyridine (**6**) or 4-methylpyridine (**8**) whereas the second nitrogen migration leads to 2-methylpyridine (**6**) and back to 3-

methylpyridine (**7**). Thus, one nitrogen migration in either direction leads to product and neither is energy wasting. Thus, 3-methylpyridine (**7**) is predicted to be more reactive than 2-methylpyridine (**6**) and this was observed. Also, Scheme 4.16 predicts that **6** and **8** should be formed from **7** in a ratio of 2:1. This is very close to the observed ratio of ~1.8.

In case of 4-methylpyridine (**8**), the first nitrogen migration from **BC-8** results in the formation of **BC-7** and **BC-7'**. Both lead to the same methylpyridine isomer, **7**. Therefore, **8** phototransposes to **7** only in the first nitrogen walk and **6** is formed as a result of second nitrogen migration. It was found that the ratio of **6** to **7** increases upon irradiation time. This is due to the fact that once formed, **7** phototransposes to **6** faster than the reverse reaction takes place. Thus, as the irradiation time increases the concentration of **6** increases faster than the concentration of **7** and hence the **6**:**7** ratio increases.

Scheme 4.17 shows the stabilized and non-stabilized forms of azaprefulvene intermediates **BC6, BC-7**, and **BC**-8 at an extremely short time-scale according to the radical stabilization.

Scheme 4.17 Radical stabilization of methylpyridines

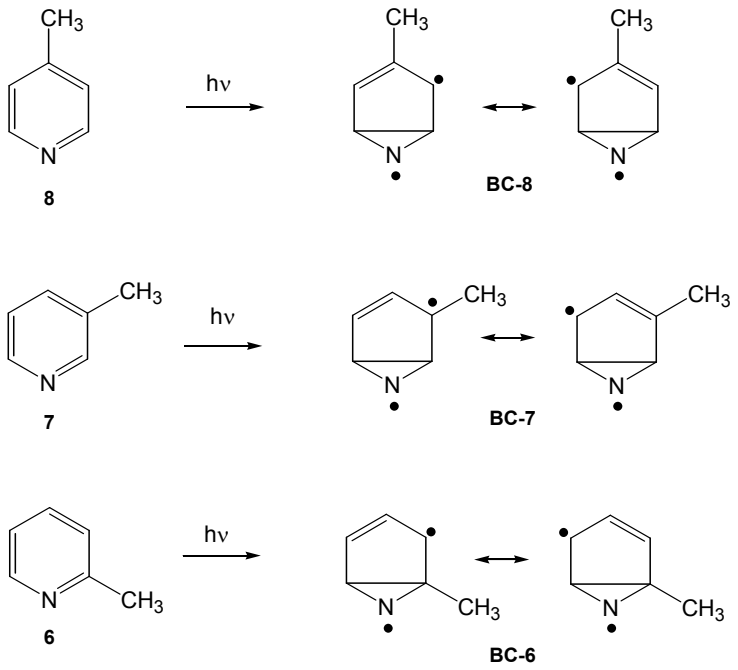

The radical stabilization energies of **BC-8** and **BC-7** are not expected to be much different. The radical stabilization energy shown in Table 4.10 supports this conclusion. In the case of 2-methylpyridine (**6**), however, there are two factors that should be considered. **BC-6** undergoes energy wasting process by one nitrogen migration to itself (Scheme 4.16). This process causes 2-methylpyridine (**6**) less reactive than the other two isomers. Furthermore, it should be noted that substituents at C2 and C6 might sterically inhibit reaction. Scheme 4.18 shows the azaprefulvene structure with R groups on C2 and C6.

Scheme 4.18 Steric hindrance from substituents at C2 and C6

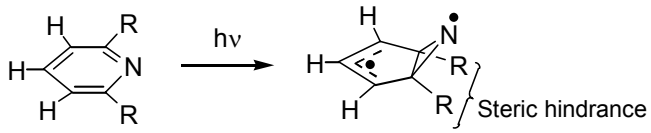

The R groups attached to the C2 and C6 come closer together as 2,6-bridging occurs. This inhibits the formation of azaprefulvene. The larger the R groups, the greater the inhibition to its reactivity. Thus, if both substituents are H atoms, the inhibition is at minimum. This structure would be the most reactive. This is contrast to the case of **BC-7** and **BC-8**, which do not contain the methyl group at C2 or C6. Therefore, **BC-7** and **BC-8** has minimum steric hindrance, thus they would be more reactive than **BC-6**. If one H atom and one methyl groups are present, it would be slightly more inhibited, which means that this structure is slightly less reactive. This prediction was exactly observed in the photochemistry of deuterated pyridine and methylpyridine vapors. Deuterated pyridine was photolyzed by 4 low-pressure mercury lamps whilst methylpyridines had to be photolyzed by 15 lamps in order to detect photoproducts.

The mechanisms involving Dewar-pyridine and azaprismane intermediates have also been examined. Scheme 4.19 shows the phototransposition mechanism of 2-methylpyridine (**6**) via Dewar-pyridine intermediate.

Scheme 4.19 Dewar-pyridine mechanism of 2-methylpyridine

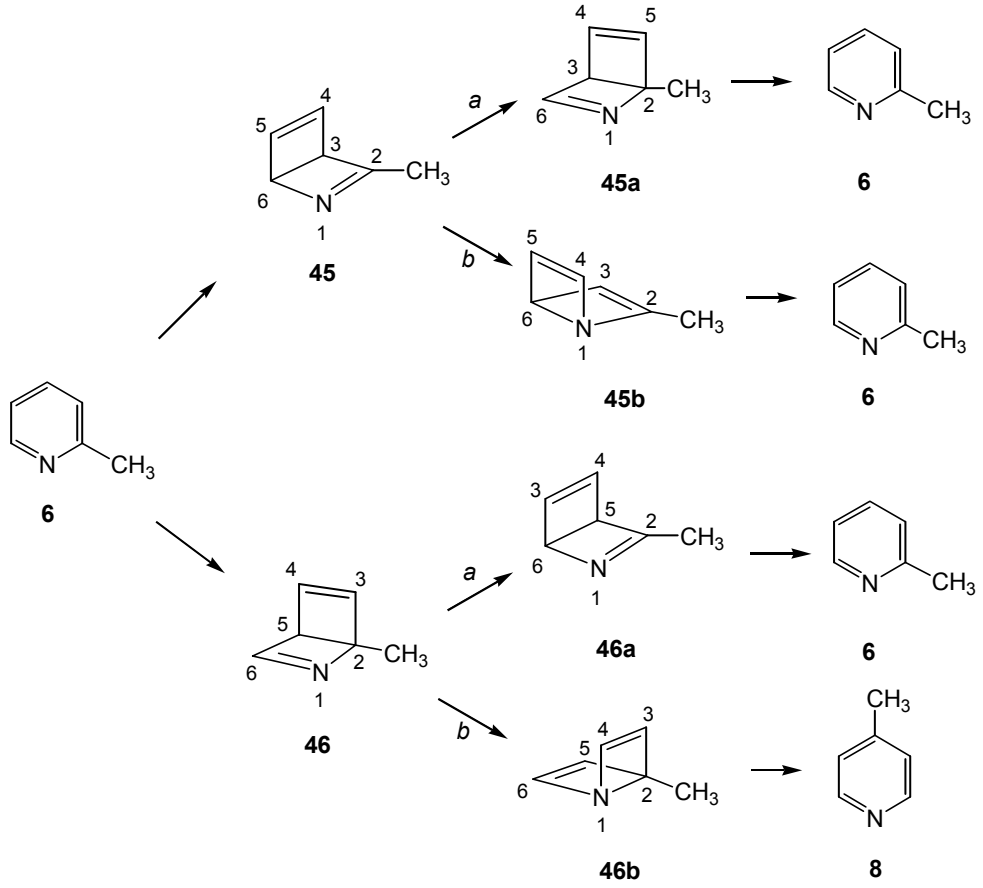

As shown in this Scheme, the only predicted photoproduct is 4-methylpyridine (**8**). This obviously shows that this mechanism is not consistent with the experimental results. Since 3-methylpyridine (**7**) is not predicted as a product, it indicates that the phototransposition pathway via Dewar-pyridine can be ruled out.

The mechanism involving azaprismane intermediate was also considered. Scheme 4.20 shows the mechanism for 2-methylpyridine (**6**) reacting by this mechanism.

Scheme 4.20 Azaprismane mechanism: 3,6-bridging

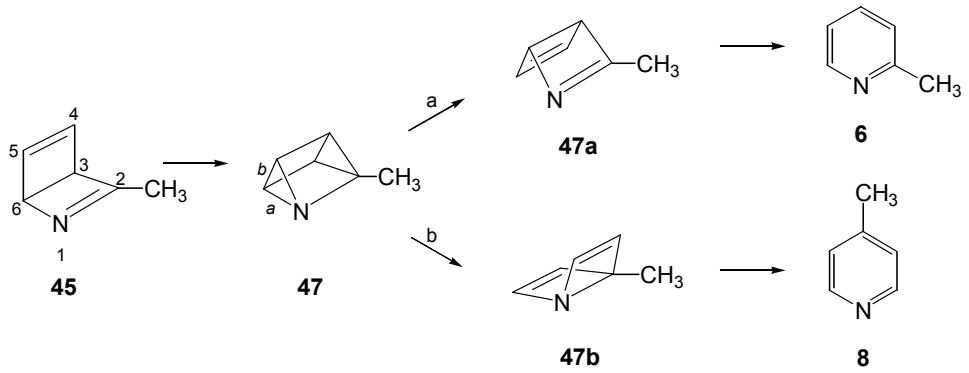

The Dewar-pyridine **45** which would result from 3,6-bridging undergoes [2+2] cycloaddition to form azaprismane **47**. This species would undergo bond cleavage resulting in the formation of **45**, **47a**, or **47 b**. The Dewar-pyridine **47a** would rearrange back to **6**, the starting material. The Dewar-pyridine **47b** would rearrange to **8**, only photoproduct.

Scheme 4.21 shows the azaprismane mechanism resulting from the 2,5-bridged Dewar-pyridine, **46**. The only photoproduct in this Scheme is **7**.

Scheme 4.21 Azaprismane mechanism: 2,5-bridging

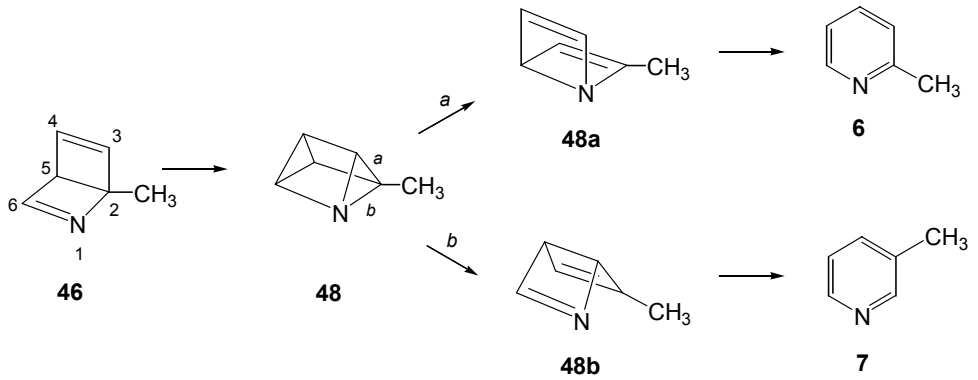

Furthermore, one other azaprismane can result from **6** by 1,4-bridging between C4 and the nitrogen atom as shown in Scheme 4.22. Cleavage of this azaprismane would result in the formation of 3-methylpyridine **7** or back to **6**, the reactant.

Scheme 4.22 Azaprismane mechanism: 1,4-bridging

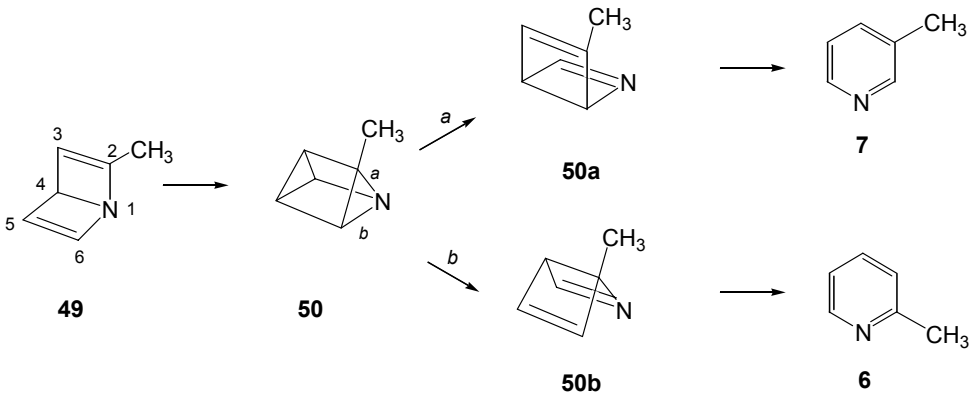

If the reaction occurs by all possible azaprismane pathways the mechanism predicts that 2-methylpyridine (**6**) would phototranspose to 3-methylpyridine (**7**) and 4-methylpyridine (**8**) in a ratio of 2:1. This is not consistent with the experimental results.

4.3. Deuterium labeling studies

4.3.1. Cyanopyridines

In order to simplify the ^{1}H-NMR spectra of the cyanopyridines to allow the transposition of selected ring protons to be monitored, a study of the synthesis and photochemistry of 2-cyanopyridine-4,6-d_2, (**36-4,6-d_2**), 3-cyanopyridine-2,6-d_2 (**37-2,6-d_2**), and 4-cyanopyridine-2,6-d_2 (**38-2,6-d_2**) was undertaken.

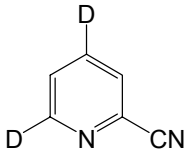

36-4,6-d_2

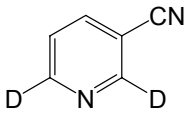

37-2,6-d_2

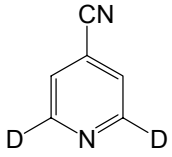

38-2,6-d_2

4.3.2. Proton-Deuterium exchange reaction with base catalyst

Previous work in this lab showed that heating dimethylpyridines in D_2O containing K_2CO_3 at 180 ^oC for 5.5 days led to H-D exchange at ring positions 2 and 6 when these positions were unsubstituted and at methyl groups located at ring positions 2, 4, and 6, exclusively.[40]

The procedure described above was also used for the H-D exchange at ring position 2 and 6 to form 4-cyanopyridine-2,6-d_2 (**38-2,6-d_2**) from 4-cyanopyridine (**38**).

However, it was found that after heating in aqueous base solution, the cyano group at position 4 was also hydrolyzed. This led to the formation of a complex mixture of the nitrile with the corresponding amide and carboxylate.

Scheme 4.23 hydrolysis of cyano group in 4-cyanopyridine

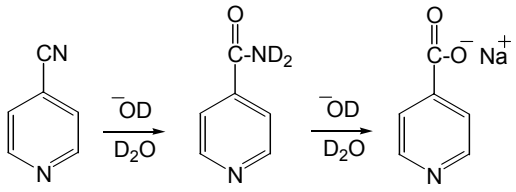

38 **51** **52**

In fact, the H-D exchange reaction in pyridine derivatives has already been reported by Kawazoe and co-workers[41]. The use of strong bases, such as Na_2CO_3, Na_2CO_3, or Na^+OD^- in deuterium oxide as catalyst at an ambient temperature was found successful in preparation of pyridine N-oxide-2,6-d_2 or pyridine N-oxide-d_5. This method is convenient and it usually gives a high percent of deuterium exchange.

The mechanism for this reaction has been considered in several ways. The mechanistic discussion reported by Zoltewicz and Kauffman[42] suggested that the H-D exchange reaction should involve proton abstraction by base to give an intermediate carbanion as shown in Scheme 4.24.

Scheme 4.24 Proton abstraction by base for pyridine N-oxide

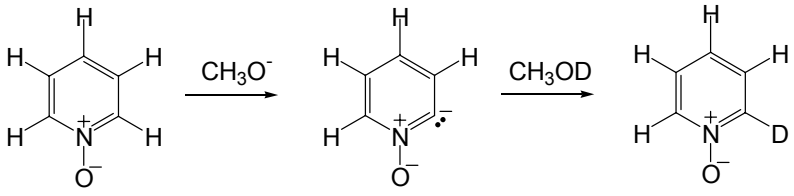

53 **53a** **53-1-d**

The carbanion at the ortho position generated from pyridine N-oxide can be looked upon as being stabilized by resonance with the nucleophilic carbene structure **53b**.[43]

Scheme 4.25 Resonance stabilization

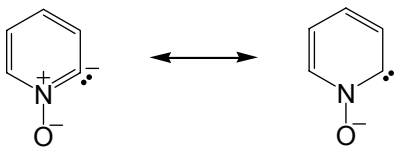

53a **53b**

The authors also studied the reactivity order of hydrogen-deuterium exchange in heteroaromatic systems. The reactivity of dedeuteration at the various ring position of pyridine N-oxide-d_5 in CH_3ONa/CH_3OH has been reported to be in the order 2,6 >> 3,5 > 4. The 2,6 position is readily exchanged at temperatures as low as 75 ^oC.

Substituted pyridine N-oxides can also undergo H-D exchange by base catalysis (Na_2CO_3 or NaOD). The H-D exchange is possible for methyl derivatives of pyridine N-oxide and even benzyl substituted pyridine N-oxides.[44]

Accordingly, Matsuki and coworkers[45] reported that the preparation of deuterium-labeled isoniazid (**57-2,6-d_2**) started with isonicotinic acid N-oxide.

Scheme 4.26 Preparation of deuterium labeled isoniazid

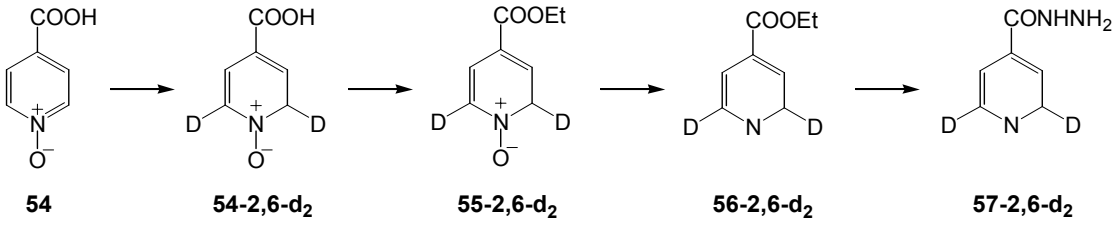

This base-catalyzed hydrogen exchange in D_2O solution provided the deuterium-labeled compound **57-2,6-d_2** in a high yield.

The procedure developed by Matsuki for the preparation of deuterated isoniazid was found to be useful in the synthesis of some deuterated cyanopyridines.

4.3.3. Synthesis of 4-cyanopyridine-2,6-d_2 (38-2,6-d_2)

The synthetic route to 4-cyanopyridine-2,6-d_2 (**38-2,6-d_2**) starting from isonicotinic acid N-oxide (**54**) is shown in Scheme 4.27. The synthetic procedures have been adapted from methods in the literatures.[45,46]

Scheme 4.27 Synthesis of 4-cyanopyridine-2,6-d_2 (**38-2,6-d_2**)

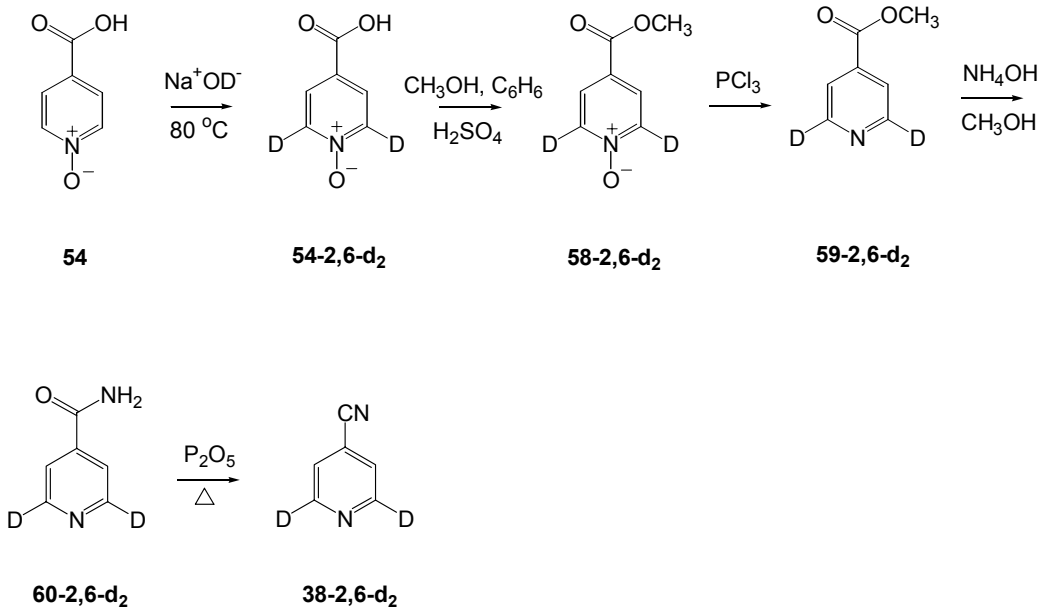

54 **54-2,6-d_2** **58-2,6-d_2** **59-2,6-d_2**

60-2,6-d_2 **38-2,6-d_2**

Isonicotinic acid N-oxide (**54**) is commercially available. Although the multi-step synthesis to obtain amide **54-2,6-d_2** has already been reported in the literature, some published experimental procedures did not give good results in our laboratory. Thus, all synthetic procedures were reinvestigated and modified. Isonicotinic acid N-oxide-2,6-d_2 (**54-2,6-d_2**) was prepared in a good yield (95.5%) by two successive base-catalysed H-D exchanges. The methylester **58-2,6-d_2** was prepared in a moderate yield (40.7%) using

sulfuric acid as catalyst in methanol instead of using saturated-HCl methanol as in the literature.[46] In this reaction benzene was used to increase the esterification yield by azeotropic distillation to remove water as it is formed. This methylester N-oxide **58-2,6-d_2** was then reduced using PCl_3 to give methylester **59-2,6-d_2** in a high yield (72.2%). In the next step, it was found that even though amide **60-2,6-d_2** was easily formed by reacting **59-2,6-d_2** with concentrated aqueous ammonia, it would not crystallize out from the aqueous solution.

The crude amide **60-2,6-d_2** obtained by concentration in vacuum was therefore directly used for the next step to synthesize cyanopyridine **38-2,6-d_2**. To obtain 4-cyanopyridine-2,6-d_2 (**38-2,6-d_2**), many attempts were tried. The reaction of nicotinamide with benzenesulfonyl chloride in the presence of pyridine to form nicotinonitrile has been reported.[47] However, the yield of 4-cyanopyridine (**38**) using this method was found to be very low and that the compound was difficult to separate from the reactants.

Finally, the dehydration was successful by heating **60-2,6-d_2** and phosphorous pentoxide in the absence of a solvent.[48] The reaction was carried out in a Kugelrohr apparatus and the cyanopyridine **38-2,6-d_2** was isolated by sublimation from the reaction mixture. Although the dideuteriocyanopyridine **38-2,6-d_2** obtained in this manner was contaminated by the starting material, the pure cyanopyridine **38-2,6-d_2** was obtained by sublimation.

The mass spectrum of **38-2,6-d_2**, shown in Figure 4.25 exhibits a molecular ion at m/z = 106, consistent with the exchange of two hydrogen atoms with deuterium. The fragmentation of 78 (68.4%, -DCN) was observed.

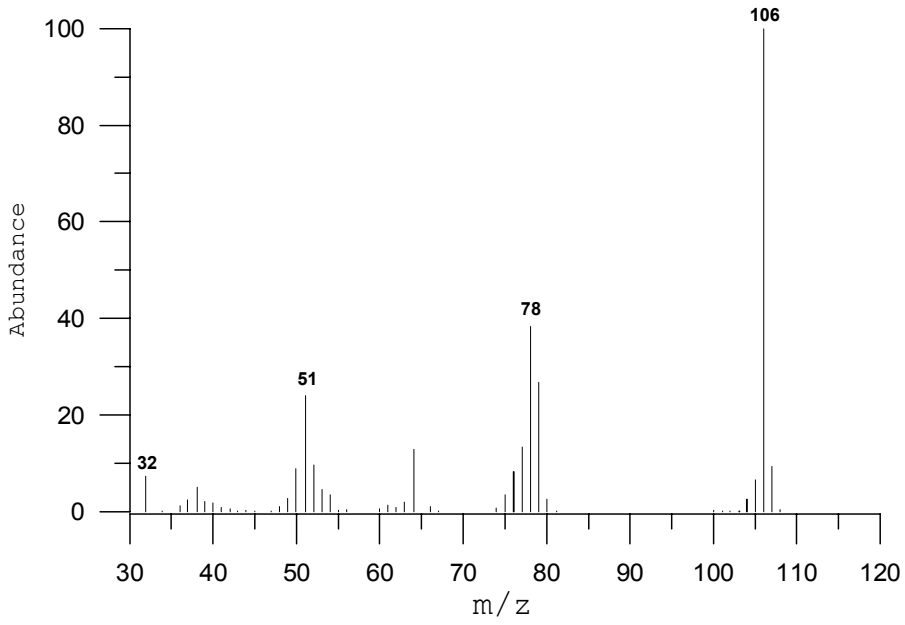

Figure 4.25 GC-MS of 4-cyanopyridine-2,6-d_2 (**38-2,6-d_2**)

Figure 4.26 shows the ^{1}H-NMR spectrum of **38-2,6-d$_2$** which was recorded and compared to the ^{1}H-NMR spectrum of authentic 4-cyanopyridine (**38**). The singlet signal at δ 7.56 is due to the proton at positions 3 and 5 of the pyridine ring. It also exhibits a very small signal at δ 8.87 which was assigned to the residual protons at positions 2 and 6.

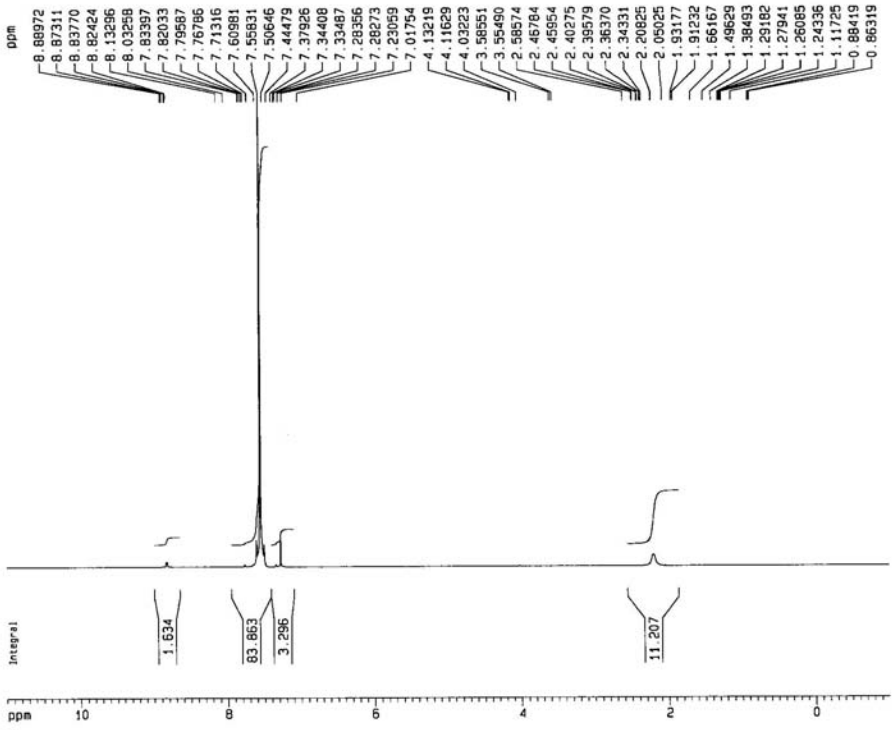

Figure 4.26 ^{1}H-NMR spectrum of 4-cyanopyridine-2,6-d$_2$ (**38-2,6-d$_2$**)

In addition, the ^{13}C-NMR spectrum shown in Figure 4.27 is consistent with the structure of **38-2,6-d$_2$**. This spectrum exhibits singlets at δ 125.6 and 120.9 for the carbon atoms at ring positions 3/5, and 4 and at δ 116.8 for the cyano carbon while the signal due to the C2 and C6 carbons is observed at δ 150.8 as a triplet (J = 28.2 Hz) due to coupling with the attached deuterium atoms. This confirms that deuteration has occurred regiospecifically at ring positions 2 and 6.

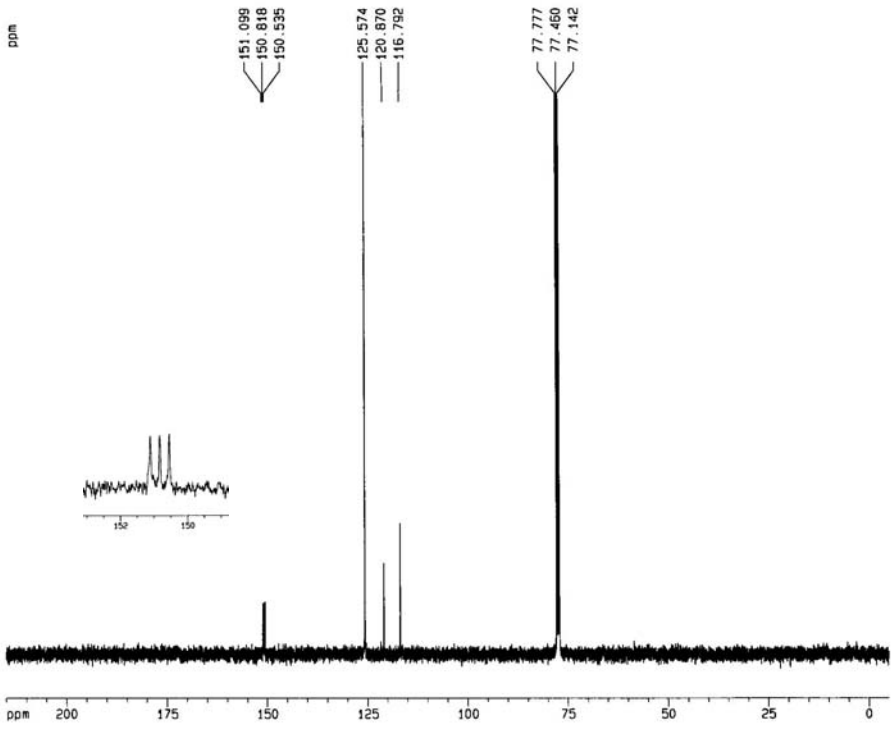

Figure 4.27 ^{13}C-NMR spectrum of 4-cyanopyridine-2,6-d$_2$ (**38-2,6-d$_2$**)

4.3.4. Synthesis of 3-cyanopyridine-2,6-d$_2$ (37-2,6-d$_2$)

The synthetic route to 3-cyanopyridine-2,6-d$_2$ (**37-2,6-d$_2$**) starting from nicotinic acid N-oxide (**61**) is shown in Scheme 4.28.

Scheme 4.28 Synthesis of 3-cyanopyridine-2,6-d$_2$ (**37-2,6-d$_2$**)

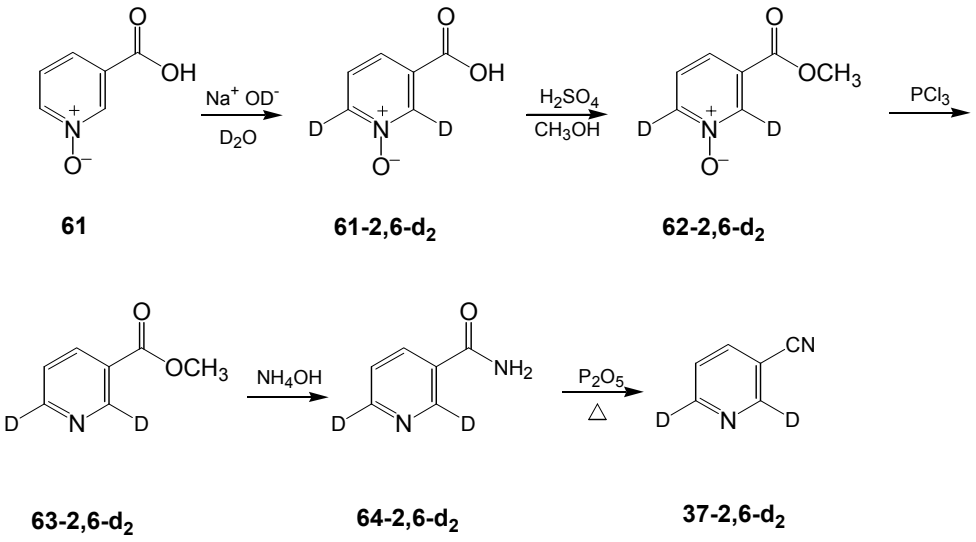

Nicotinic acid N-oxide **61**, which is commercially available, was transformed to nicotinic acid N-oxide **61-2,6-d$_2$** by two successive base-catalyzed H-D exchange reactions. Esterification followed by N-oxide reduction led to the methylester **62-2,6-d$_2$** in a good yield (85.7%). It was then converted to amide **64-2,6-d$_2$** by reaction with concentrated aqueous ammonia.

Although the direct conversion of nicotinamide to 3-cyanopyridine is described by Vogel[49], reaction with P_2O_5 in the Kugelrohr asparatus was found to be superior.

Dehydration of the amide by heating with P_2O_5 until in the Kugelrohr apparatus up to 190 ^oC provided 2,6-dideuterio-3-cyanopyridine (**37-2,6-d_2**), which was further purified by sublimation.

The mass spectrum of **37-2,6-d_2** shows a molecular ion at m/z = 106, which is consistent with a dideuterated product. The first fragmentation to 78 (48%) is due to the loss of DCN (28) which is consistent with the molecular structure of pyridine.

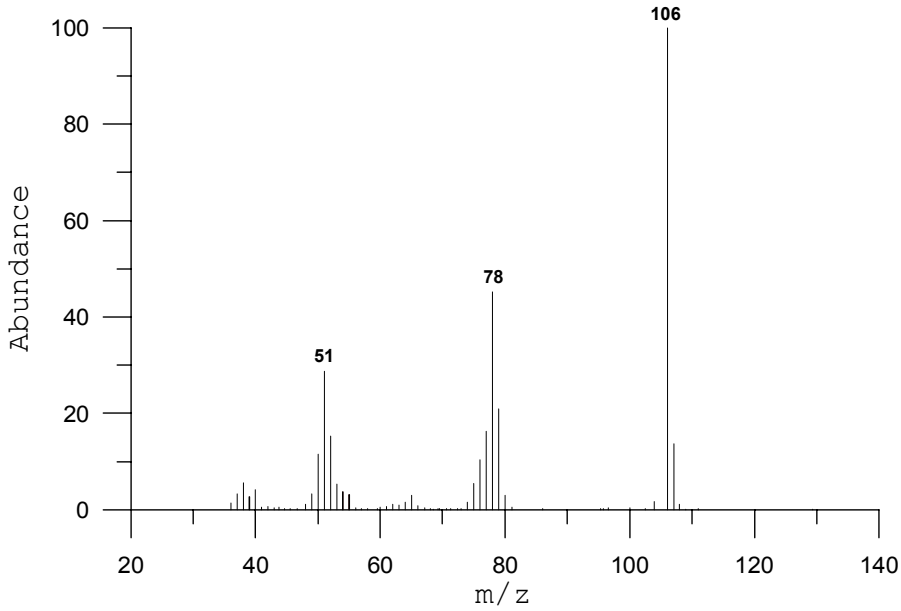

Figure 4.28 GC-MS of 3-cyanopyridine-2,6-d_2 (**37-2,6-d_2**)

As expected for the assigned structure, the ^{1}H-NMR spectrum of 3-cyanopyridine-2,6-d_2 (**37-2,6-d_2**) shown in Figure 4.29 exhibits two doublets at δ 7.91 (J = 7.9 Hz) and 7.39 (J = 7.9 Hz) where H4 and H5 are expected to absorb. In addition, very small signals are visible at δ 8.84 and 8.76 due to the small amount of residual

hydrogen at ring positions 2 and 6. This is consistent with deuteration at ring positions 2 and 6. This was further confirmed by the ^{13}C-NMR spectrum shown in Figure 4.30. Thus, the signals for the C2 and C6 carbons are shown as two overlapping triplets at δ 153.0 (J =27.3 Hz) and 152.5 (J =27.7 Hz) due to their coupling with the deuterium atoms on those carbons. The remaining signals due to C4, C5, C3, and CN all appear as singlets at δ 139.7, 123.9, 116.9, and 110.4, respectively.

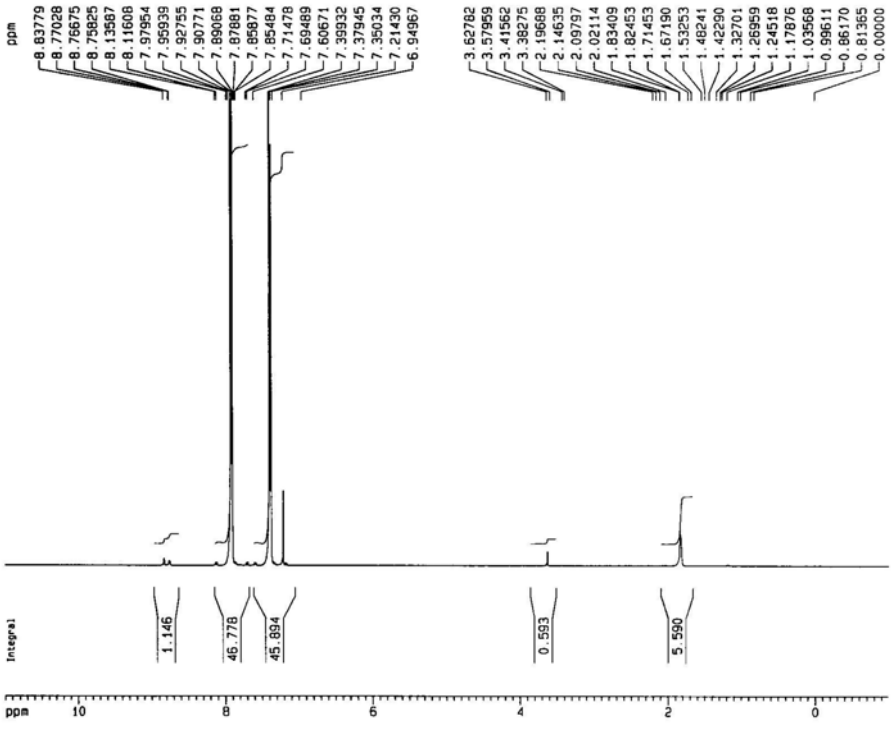

Figure 4.29 ^{1}H-NMR spectrum of 3-cyanopyridine-2,6-d_2 (**37-2,6-d_2**)

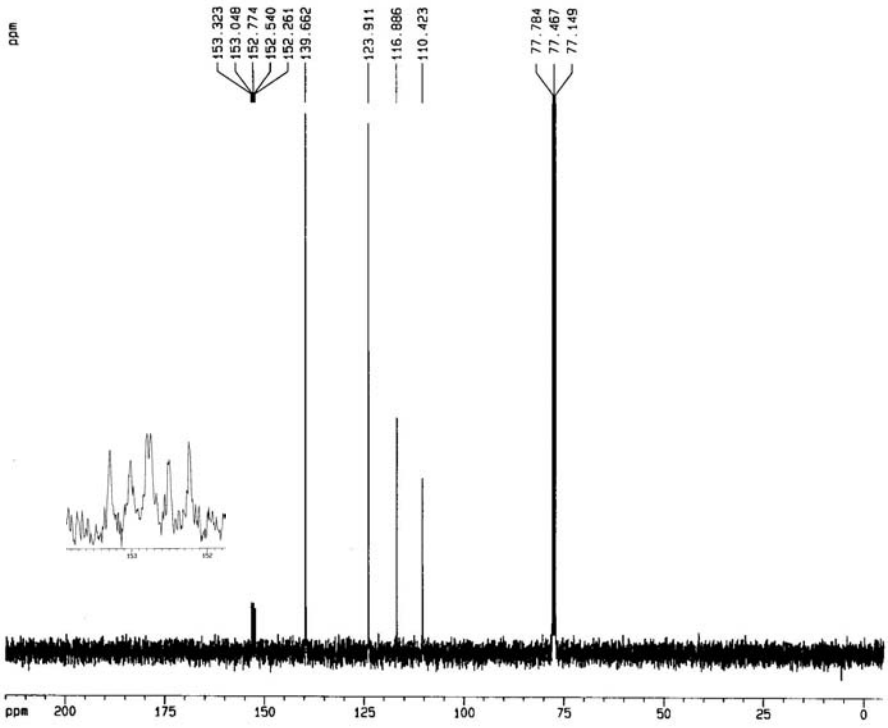

Figure 4.30 ^{13}C-NMR spectrum of 3-cyanopyridine-2,6-d_2 (**37-2,6-d_2**)

4.3.5. Synthesis of 2-cyanopyridine-4,6-d_2 (36-4,6-d_2)

The synthesis of 2-cyanopyridine-4,6-d_2 (**36-4,6-d_2**) was started from commercially available picolinic acid N-oxide (**65**). The synthetic route to **36-4,6-d_2** was much different from the procedures for **38-2,6-d_2** and **36-2,6-d_2**. The previous procedure could not be used to prepare a dideuterated 2-cyanopyridine because this compound has only one open position α to nitrogen which undergoes direct base-catalyzed H-D exchange. The photoreaction of a monodeuterated 2-cyanopyridine (**36-6-d**) could not give the sufficient information to explain the photochemical mechanism of 2-cyanopyridine.

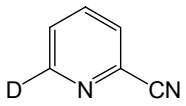

36-6-d

The synthesis of **36-4,6-d_2** was attempted in several ways. First, the synthesis was started with 2-picoline N-oxide (**65**). Scheme 4.29 shows the synthetic route starting from 2-picoline N-oxide (**65**). Whereas the deuterium labeling on positions 3, 4, and 5 is not favorable under mild conditions, the use of high temperature and pressure as well as a strong base leads to exchange at all ring position with no selectivity. Generally, a specific H-D exchange of one of these three protons would not be successful using this high temperature method.

The specific substitution on ring position 4 was found possible by some methods. The nitration at the γ–position of the pyridine ring can be accomplished by gently refluxing pyridine N-oxide in fuming HNO_3 in conc. H_2SO_4.

Scheme 4.29 Proposed synthesis of 2-cyanopyridine-4,6-d_2 (**36-4,6-d_2**)

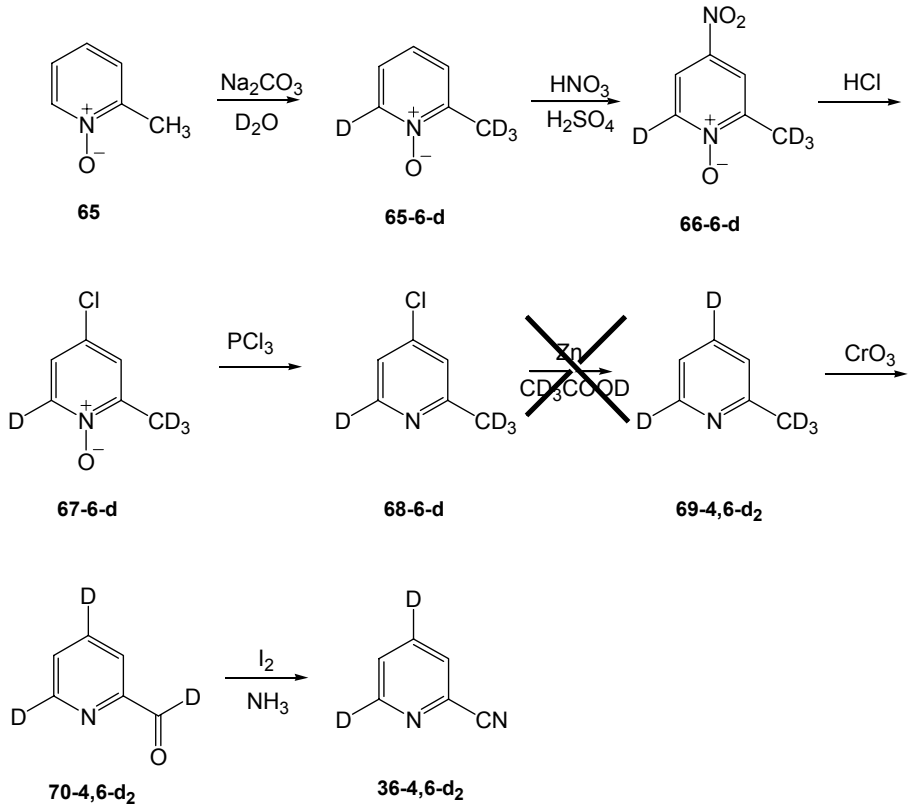

According to the literature reported by Ochiai,[50] the nitration of pyridine N-oxide (**53**) at the γ-position is a consequence of the polar effect of the N-oxide function on the pyridine nucleus. The γ-position is much activated by tautomeric effect of the N-oxide group.

In this synthetic route, the preparations of **65-6-d** and **66-6-d** were carried out successfully and they were obtained in good yields. The nitration reaction at ring position 4 of the pyridine ring was very effective. However, the reaction of **66-6-d** with conc.HCl gave **67-6-d** in poor yield and the conversion of 4-chloro **68-6-d** to 4-deuterio **69-4,6-d_2** was found to be difficult using Zn/CD_3COOD despite the fact that dehalogenation using Zn/CH_3COOH has been used successfully in other heterocyclic compounds.[51] White gel by-products due to Zn salts hindered extraction of the product by dichloromethane. Furthermore, the oxidation of **69-4,6-d_2** in the following step from methylpyridine **69-4,6-d_2** to aldehyde **70-4,6-d_2** was expected to be difficult even though its transformation to the final product **36-4,6-d_2** should be simple by adapting the technique using iodine in ammonia which was reported by Talukda and co-worker.[52]

The synthesis of cyanopyridine **36-4,6-d_2** was also attempted using the approach shown in scheme 4.30. According to this approach 4-nitro-2-picolinic acid N-oxide-6-d (**71-6-d**) was converted to the 4-chloro derivative **72-6-d** by refluxing in conc. HCl. Reduction of **72-6-d** with PCl_3 gave **73-6-d**. However, the reaction of $PdCl_2$ with

Scheme 4.30 Proposed synthesis of **36-4,6-d_2** from **71-6-d**

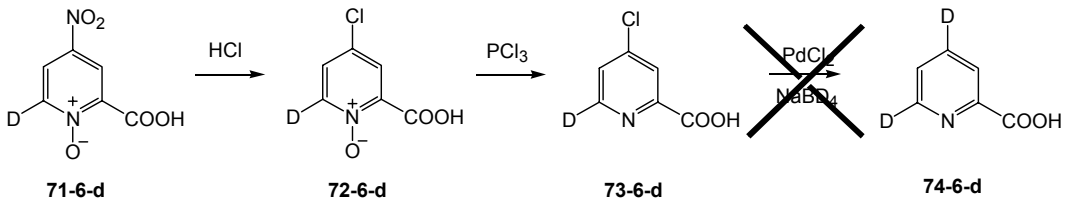

4-chloropicolinic acid **73-6-d** was not successful even though this reagent has been used to reduce aryl halides in the presence of sodium borodeuteride. Bosin and Co-Worker

reported that the use of $PdCl_2$ and sodium borodeuteride could lead to the dehalodeuteriolysis at ring position 2, 3 or 4 in 2-,3-, or 4-chlorobenzoic acid at 20 ^oC.[53] However, compound **73-6-d** was clearly not converted to **74-6-d** by this reaction.

The deuterium labeling at position 4 was successful from the synthetic route shown in Scheme 4.31. Picolinic acid N-oxide (**75**) was subjected to H-D exchange reaction followed by nitration at carbon position 4. This nitration of picolinic acid

Scheme 4.31 Synthesis of 2-cyanopyridine-4,6-d_2 (**36-4,6-d_2**)

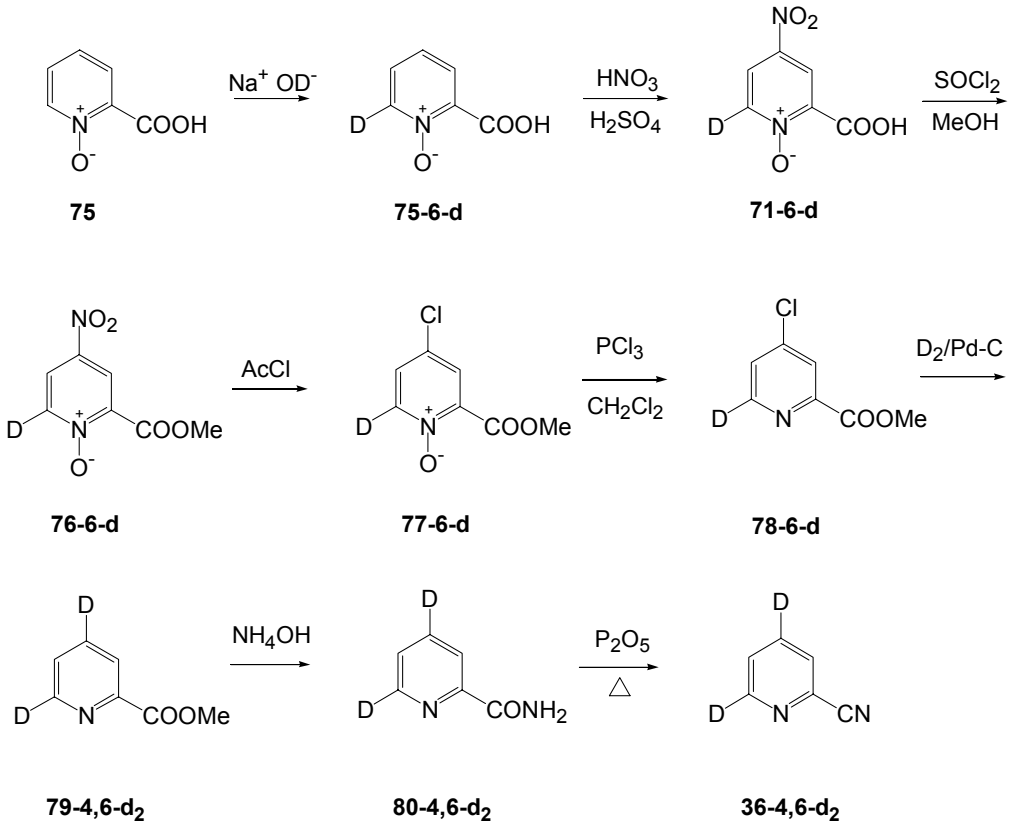

N-oxide was published by Proffet and Steinke.[54] They also reported that **71** could be esterified using $SOCl_2$ in methanol to make methyl 4-nitro-picolinate N-oxide (**76**). The

reason for this conversion is that the chlorination of the ester is easier than chlorination of the acid. Chlorination of **76-6-d** was made possible by using acetyl chloride. The resulting 4-chloro **77-6-d** was changed to **78-6-d** by reduction with PCl_3 to remove the N-oxide. Several deuteriolysis experiments had been attempted by using reagents, such as Zn/CD_3COOD, Zn/ND_4Cl, and $PdCl_2/NaBD_4$, but the reaction was eventually successful using 10% Pd-C and D_2 gas. This procedure was a modification of the procedure reported by Azzam and co-worker.[55] Their preparation of a pyrazinone product by hydrogenolysis was successful by using 10% Pd-C in hydrogen atmosphere at room temperature. The deuteriolysis was carried out in our laboratory by using $NaBD_4$ and D_2SO_4 in D_2O to generate D_2. The reaction succeeded and the deuterium-labeled methylester (**79-4,6-d_2**) was confirmed by GC-MS and NMR data shown in Figure 4.31-4.33.

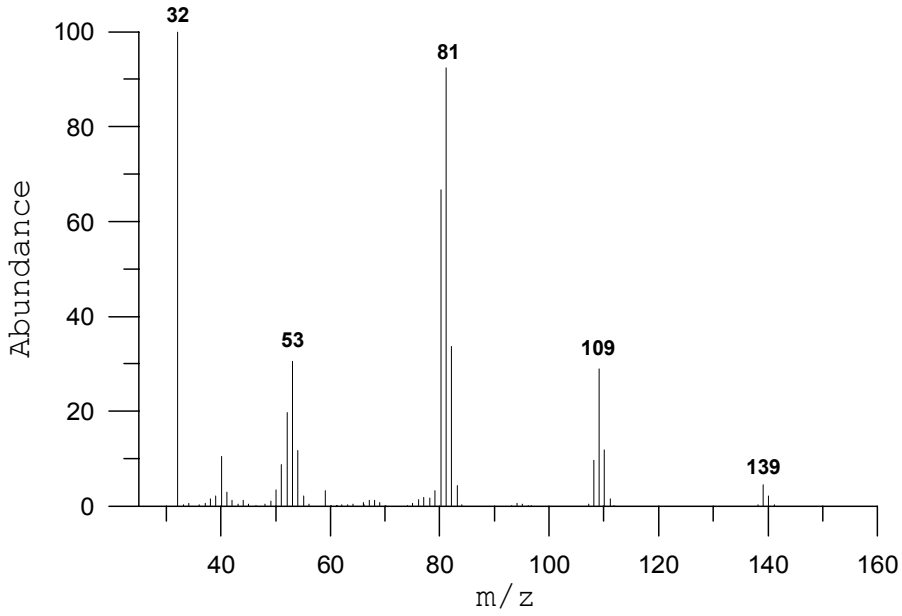

Figure 4.31 GC-MS spectrum of methylpicolinate-4,6-d_2 (**79-4,6-d_2**)

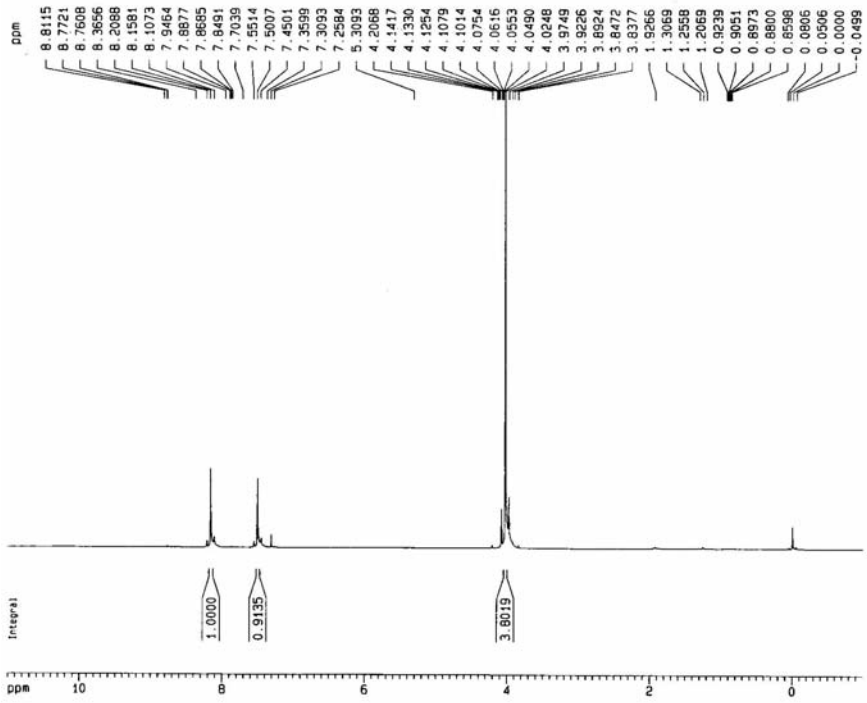

Figure 4.32 ^{1}H-NMR spectrum of methylpicolinate-4,6-d_2 (**79-4,6-d_2**)

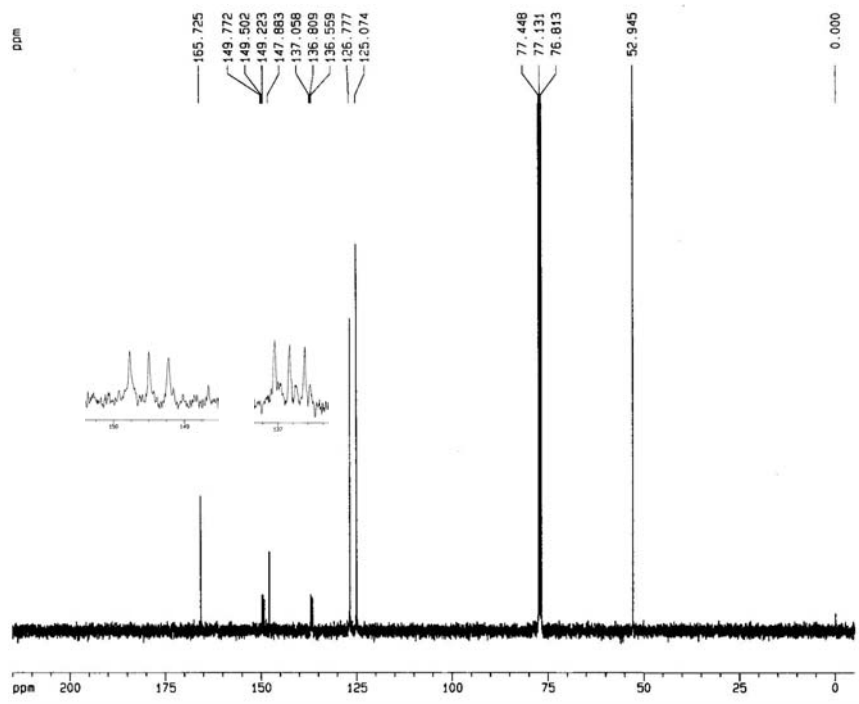

Figure 4.33 ^{13}C-NMR spectrum of methylpicolinate-4,6-d_2 (**79-4,6-d_2**)

Methylester **79-4,6-d_2** was converted to amide **80-4,6-d_2** by using concentrated aqueous ammonia. The preparation of cyanopyridine **36-4,6-d_2** from reaction with phosphorous pentoxide was in a low yield but sufficient for photochemical study.

The mass spectrum of 2-cyanopyridine-4,6-d_2, shown in Figure 4.34, exhibits a molecular ion at m/z=106 which is consistent with the molecular weight 106 of **36-4,6-d_2**.

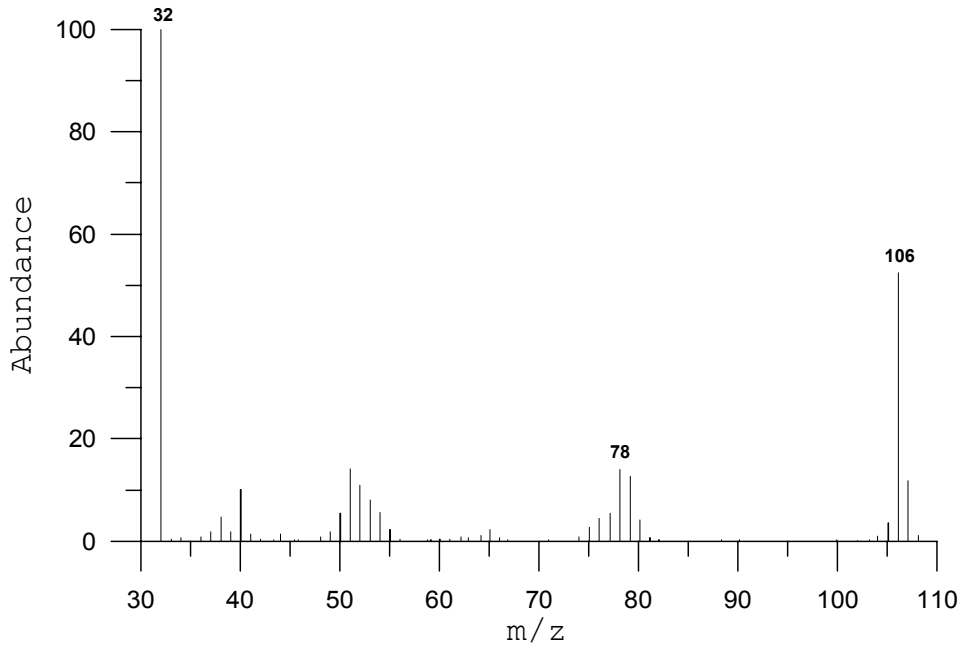

Figure 4.34 GC-MS of 2-cyanopyridine-4,6-d_2 (**36-4,6-d_2**)

Figure 4.35 shows the ^{1}H-NMR spectrum of 2-cyanopyridine-4,6-d_2. The H3 and H5 singlet signals are observed at δ 7.66 and 7.50 respectively while the H4 at δ 8.10 and H6 at 8.66 are labeled with deuterium.

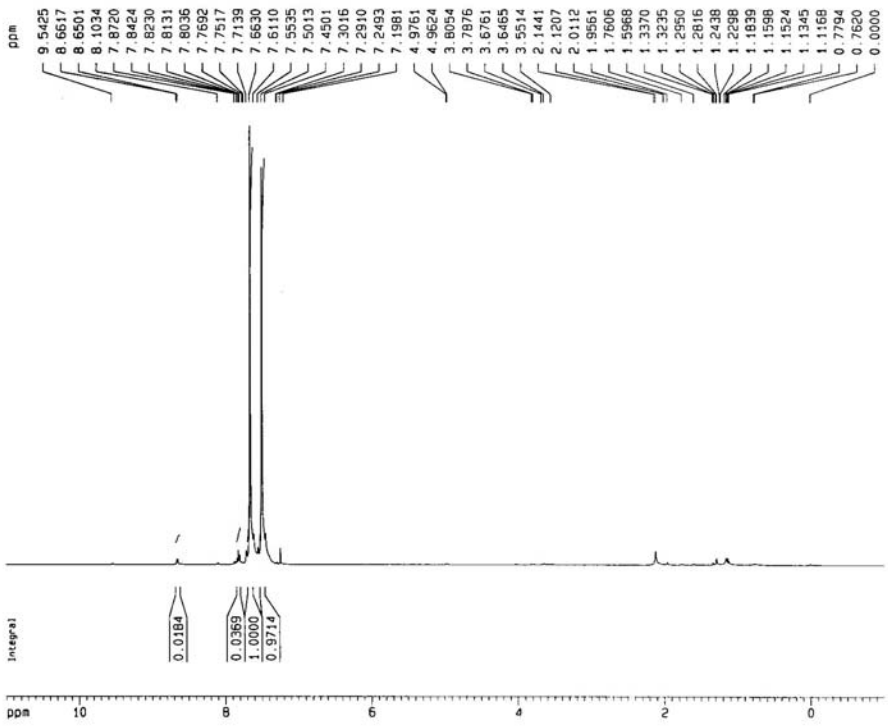

Figure 4.35 ^{1}H-NMR spectrum of 2-cyanopyridine-4,6-d_2 (**36-4,6-d_2**)

The ^{13}C-NMR spectrum recorded in $CDCl_3$ confirmed the deuterium labeling by showing two triplets of carbon position 4 and 6 as δ 152.1 (J = 28.0 Hz) and 138.2 (J = 25.6 Hz). The singlets due to C2, C3, C5, and CN are observed at δ 135.0, 129.9, 128.2, and 118.5, respectively.

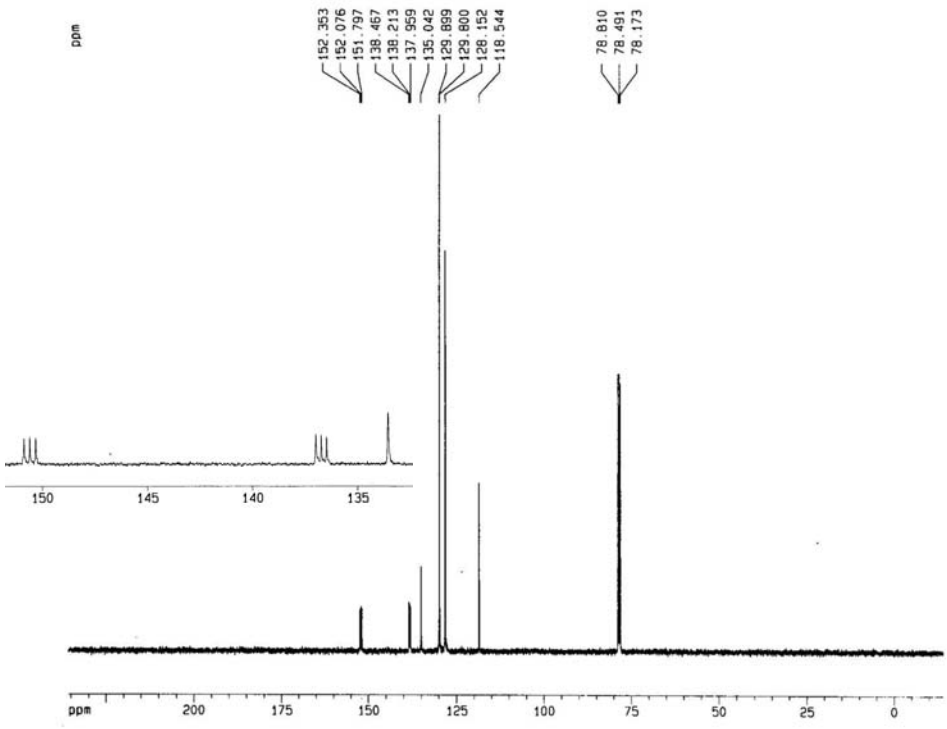

Figure 4.36 ^{13}C-NMR spectrum of 2-cyanopyridine-4,6-d_2 (**36-4,6-d_2**)

4.3.6. Pyridines

In order to simplify the ^{1}H-NMR spectra and to allow specific ring positions to be followed during the phototransposition reaction, A series of deuterium-labeled pyridines have been synthesized. These compounds include 2,6-dideuteriopyridine (**1-2,6-d_2**), 3,4,5-trideuteriopyridine **(1-3,4,5-d_3),** 2,4,6-trideuteriopyridine **(1-2,4,6-d_3)**, 2,3,4-trideuteriopyridine (**1-2,3,4-d_3**), 2,3,6-trideuteriopyridine (**1-2,3,6-d_3**), 2,3,5-trideuteriopyridine (**1-2,3,5-d_3**), 2,4,5-trideuteriopyridine (**1-2,4,5-d_3**) 2,3,5,6-tetradeuteriopyridine **(1-2,3,5,6-d_4),** 2,3,4,6-tetradeuteriopyridine (**1-2,3,4,6-d_4**), and 2,3,4,5-tetradeuteriopyridine (**1-2,3,4,5-d_4**).

Scheme 4.32 All synthetic deuterium-labeled compounds

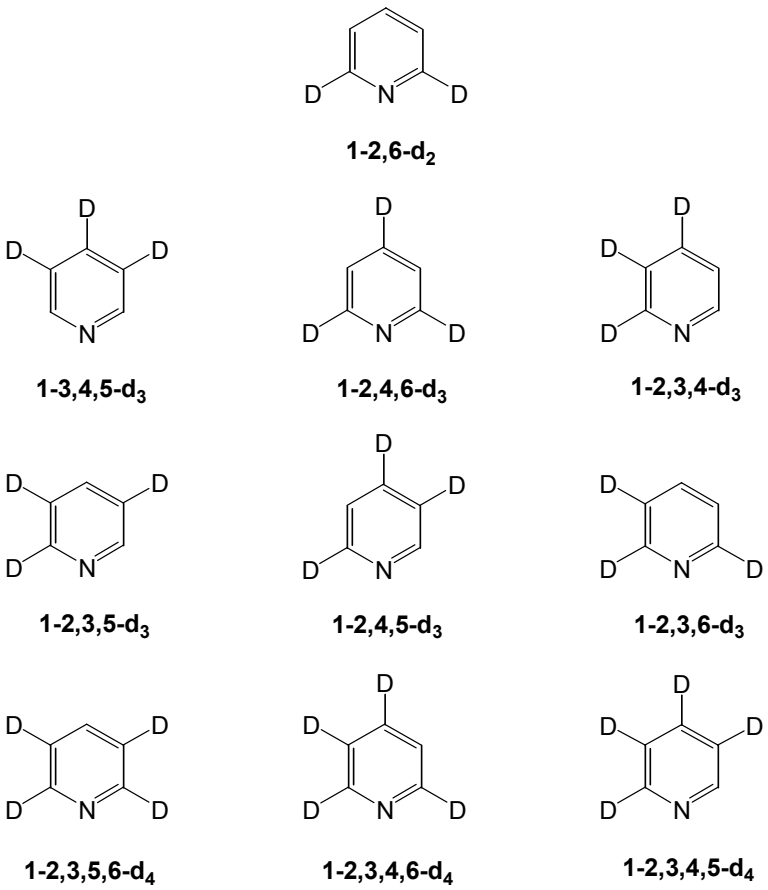

A variety of starting materials, such as pyridine N-oxide (**53**), pyridine N-oxide-d_5 (**53-d_5**) or 3,5-dichloropyridine (**84**), which are commercially available, were used for synthesizing the deuterated pyridines shown above.

4.3.7. Synthesis of dideuterio-2,6-pyridine (1-2,6-d_2)

The synthesis of 2,6-dideuteriopyridine (**1-2,6-d_2**) was started by allowing pyridine N-oxide (**53**) to undergo base catalyzed H-D exchange at ring positions 2 and 6 to yield **53-2,6-d_2**. Reduction of **53-2,6-d_2**, by reaction with PCl_3, gave 2,6-dideuteriopyridine (**1-2,6-d_2**) as shown in Scheme 4.33.

Scheme 4.33 Synthesis of 2,6-dideuteriopyridine (**1-2,6-d_2**)

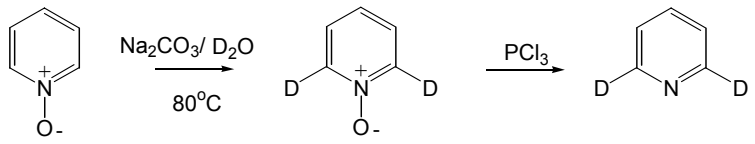

53 **53-2,6-d_2** **1-2,6-d_2**

The mass spectrum of the product from this reaction shown in Figure 4.37 exhibits a molecular ion at m/z = 81 which is consistent with the exchange of two hydrogen atoms for deuterium. Major fragmentation signals at 53 and 54 are consistent with loss of DCN and HCN respectively from the molecular ion. Loss of both DCN and HCN is consistent with the finding that scrambling of the ring atoms occurs before fragmentation.[56]

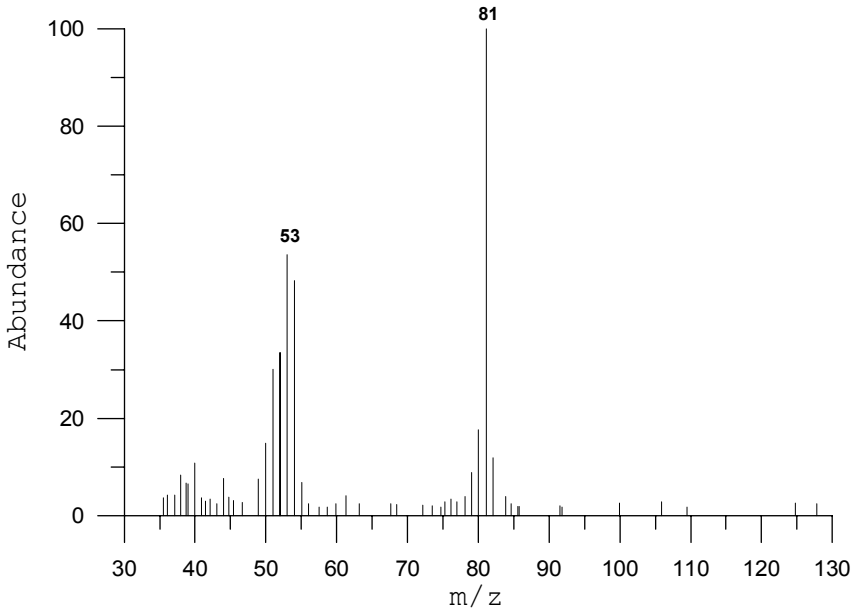

Figure 4.37 GC-MS of 2,6-dideuteriopyridine (**1-2,6-d_2**)

The ^{1}H-NMR spectrum of **1-2,6-d_2**, shown in Figure 4.38, shows signals at δ 7.71 due to the H4 proton and at δ 7.21 for the equivalent protons at ring positions 3 and 5. In addition, a very small signal is observed downfield at δ 8.60 due to residual protons at ring positions 2 and 6. Integration indicates that the protons at these ring positions are 97% exchanged.

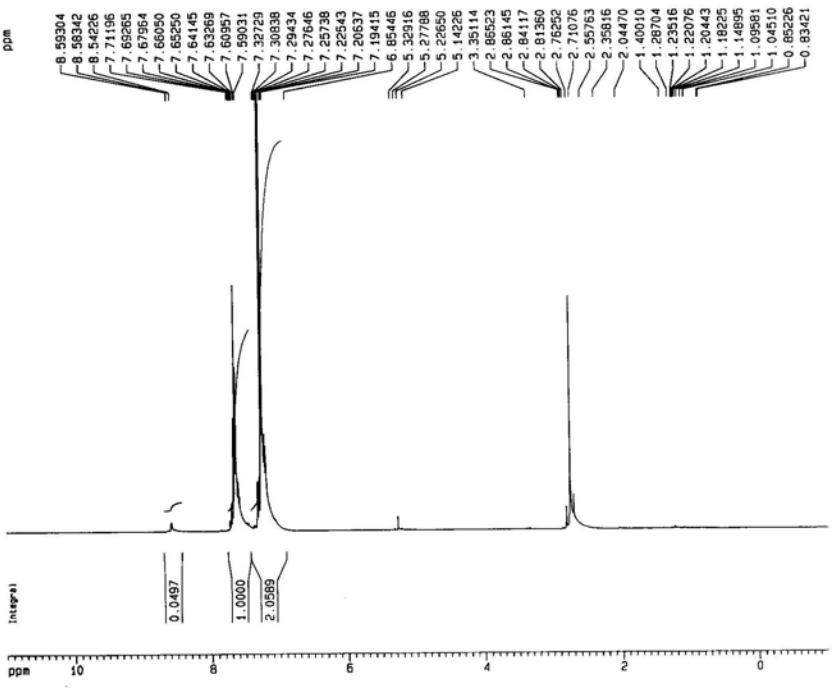

Figure 4.38 ^{1}H-NMR of 2,6-dideuteriopyridine (**1-2,6-d$_2$**)

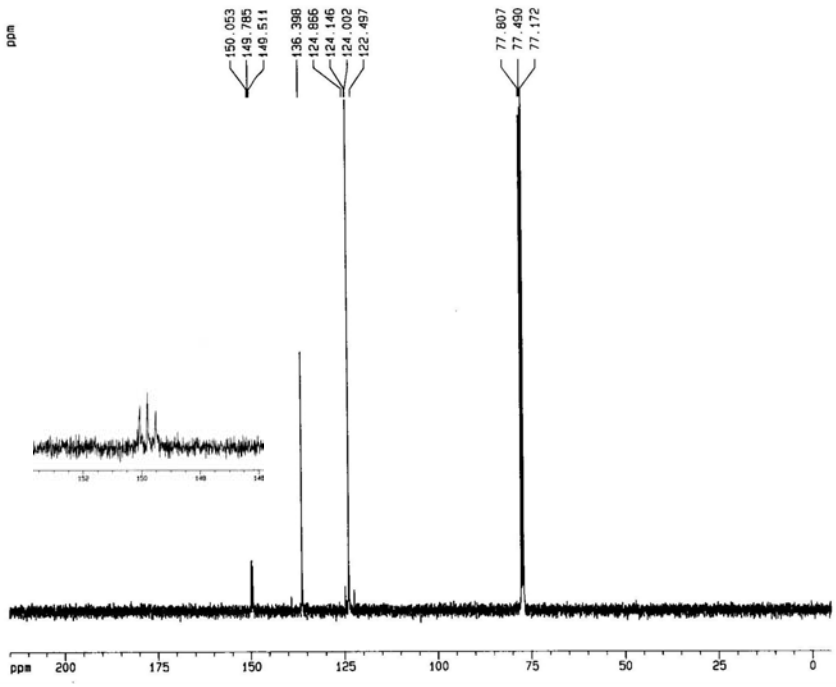

Figure 4.39 ^{13}C-NMR spectrum of 2,6-dideuteriopyridine (**1-2,6-d$_2$**)

The ^{13}C-NMR spectrum of **1-2,6-d$_2$** is shown in Figure 4.39. As expected for this structure, the spectrum exhibits singlets at δ 124.1 for C3 and C5 and at δ 136.4 for the C4 carbon and a triplet (J = 27.3 Hz) at δ 149.8 for the two equivalent carbons at ring positions 2 and 6 which are coupled with deuterium atoms. A scale expansion of the triplet region of the spectrum is shown in Figure 4.39. This confirms that the deuterium atoms are located at C2 and C6 of the pyridine ring.

4.3.8. Synthesis of 3,4,5-trideuteriopyridine (1-3,4,5-d_3)

3,4,5-Trideuteriopyridine (**1-3,4,5-d_3**) was synthesized from perdeuteriopyridine N-oxide (**53-2,3,4,5,6-d_5**) as shown in Scheme 4.34 by base catalyzed exchange of the deuterium atoms at position 2 and 6 for hydrogen followed by reduction of the N-oxide (**53-3,4,5-d_3**) by treatment with PCl_3.

Scheme 4.34 Synthesis of 3,4,5-trideuteriopyridine (**1-3,4,5-d_3**)

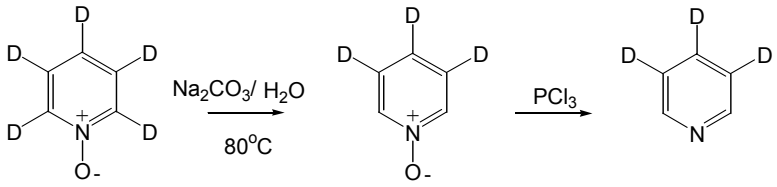

53-2,3,4,5,6-d_5 **53-3,4,5-d_3** **1-3,4,5-d_3**

The mass spectrum of the product from this reaction shown in Figure 4.40 exhibits a molecular ion at m/z = 82 which is consistent with a trideuterated pyridine.

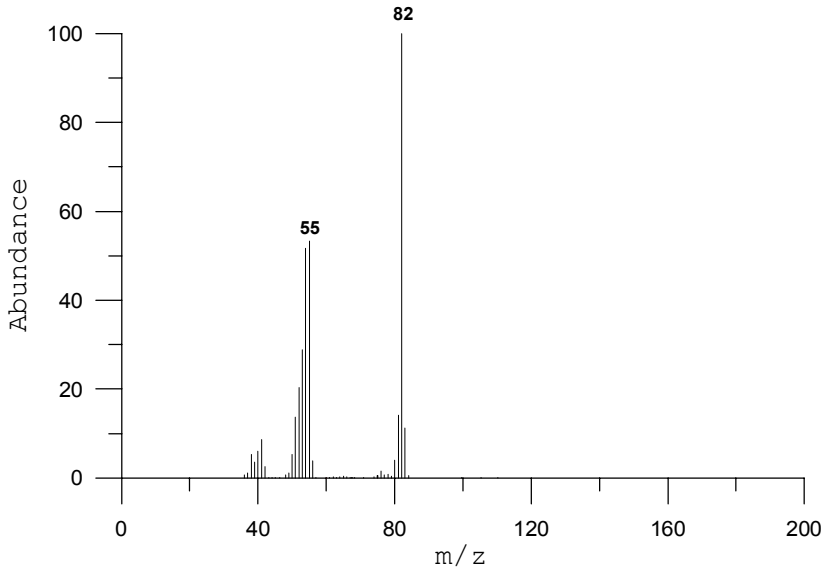

Figure 4.40 GC-MS of 3,4,5-trideuteriopyridine (**1-3,4,5-d_3**)

The ^{1}H-NMR spectrum shown in Figure 4.41 exhibits an intense signal at δ 8.48, where the H2 and H6 protons of pyridine are known to absorb, and only very small signals where the H3, H4, and H5 protons are expected. This confirms that the deuterium atoms at ring positions 2 and 6 have been exchanged for hydrogen.

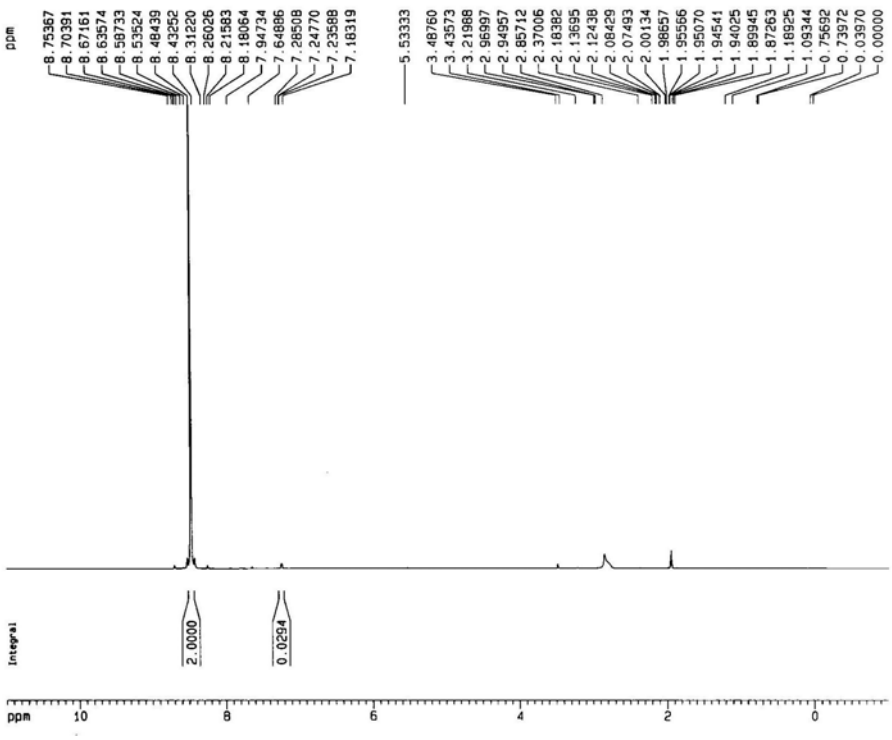

Figure 4.41 ^{1}H-NMR spectrum of 3,4,5-trideuteriopyridine (**1-3,4,5-d_3**)

The ^{13}C-NMR spectrum shown in Figure 4.42 is also consistent with this conclusion. Thus, the spectrum shows signals for C3 and C5, C4 and C6 at δ 125.3, 137.2, and 151.7 respectively. As required, the signals for C3 and C5 and for C4 appear as triplets (J = 25.3 and 24.9 Hz) indicating that these carbons are coupling with the attached deuterium atoms while the signal for the C2 and C6 carbons appears as a sharp singlet.

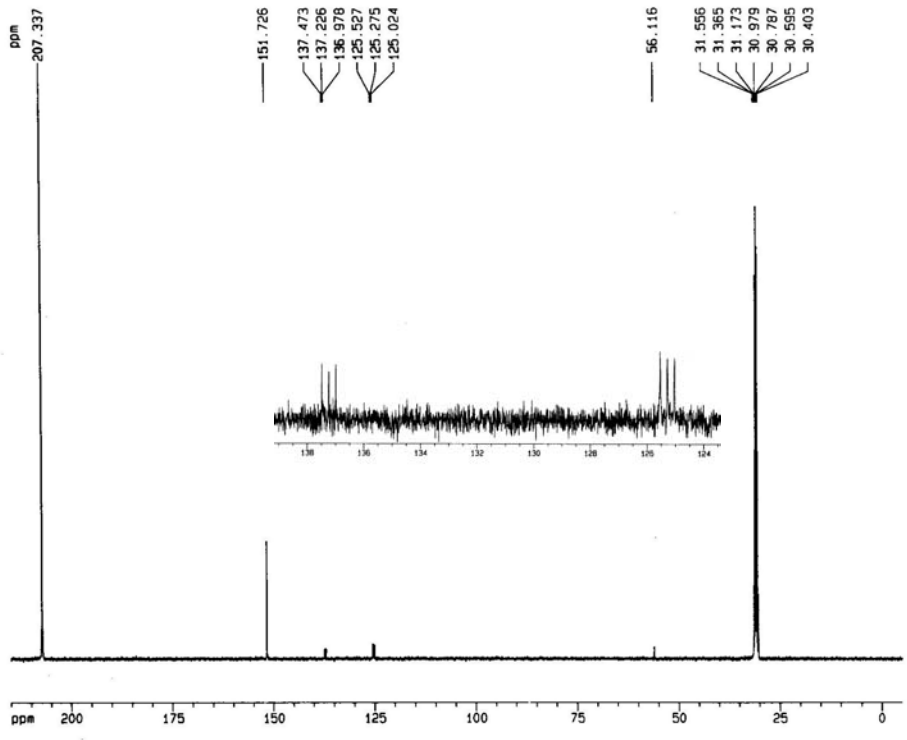

Figure 4.42 ^{13}C-NMR spectrum of 3,4,5-trideuteriopyridine (**1-3,4,5-d$_3$**)

4.3.9. Synthesis of 2,4,6-trideuteriopyridine (1-2,4,6-d_3)

2,4,6-Trideuteriopyridine (**1-2,4,6-d_3**) was synthesized from pyridine N-oxide (**37**). The synthetic route to the final product is shown in Scheme 4.35. The deuterium labeling at position 2 and 6 was carried out by base catalyzed H-D exchange reaction and the deuterium labeling at position 4 was accomplished by deuteiumolysis.

Scheme 4.35 Synthesis of 2,4,6-trideuteriopyridine (**1-2,4,6-d_3**)

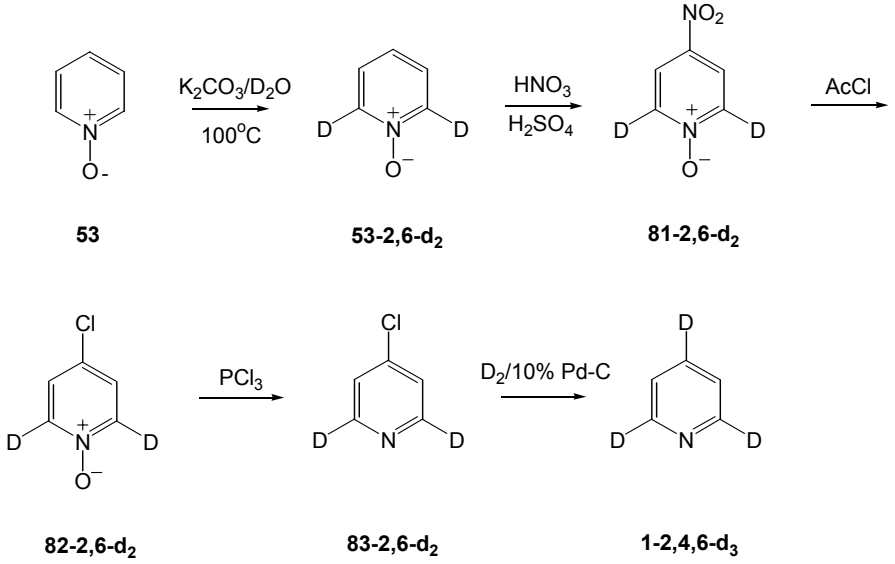

Nitration of pyridine N-oxide-2,6-d_2 (**53-2,6-d_2**) gave 4-nitropyridine N-oxide-2,6-d_2 (**81-2,6-d_2**) in a good yield by treating **53-2,6-d_2** with a mixture of nitric acid and sulfuric acids according to the method reported by Ochiai.[49] Warming **81-2,6-d_2** with acetyl chloride gave 4-chloropyridine N-oxide-2,6-d_2 (**82-2,6-d_2**) as the product which was confirmed by the ^{1}H-NMR spectrum, which was consistent with the spectrum reported by Sojka.[57] 4-Chloropyridine-2,6-d_2 (**83-2,6-d_2**) was obtained by reduction with

PCl_3 and purified by Kugelrohr distillation to give a colorless liquid. The GC-MS, ^{1}H-NMR, and ^{13}C-NMR of pure **83-2,6-d$_2$** are shown in Figure 4.43, 4.44, and 4.45.

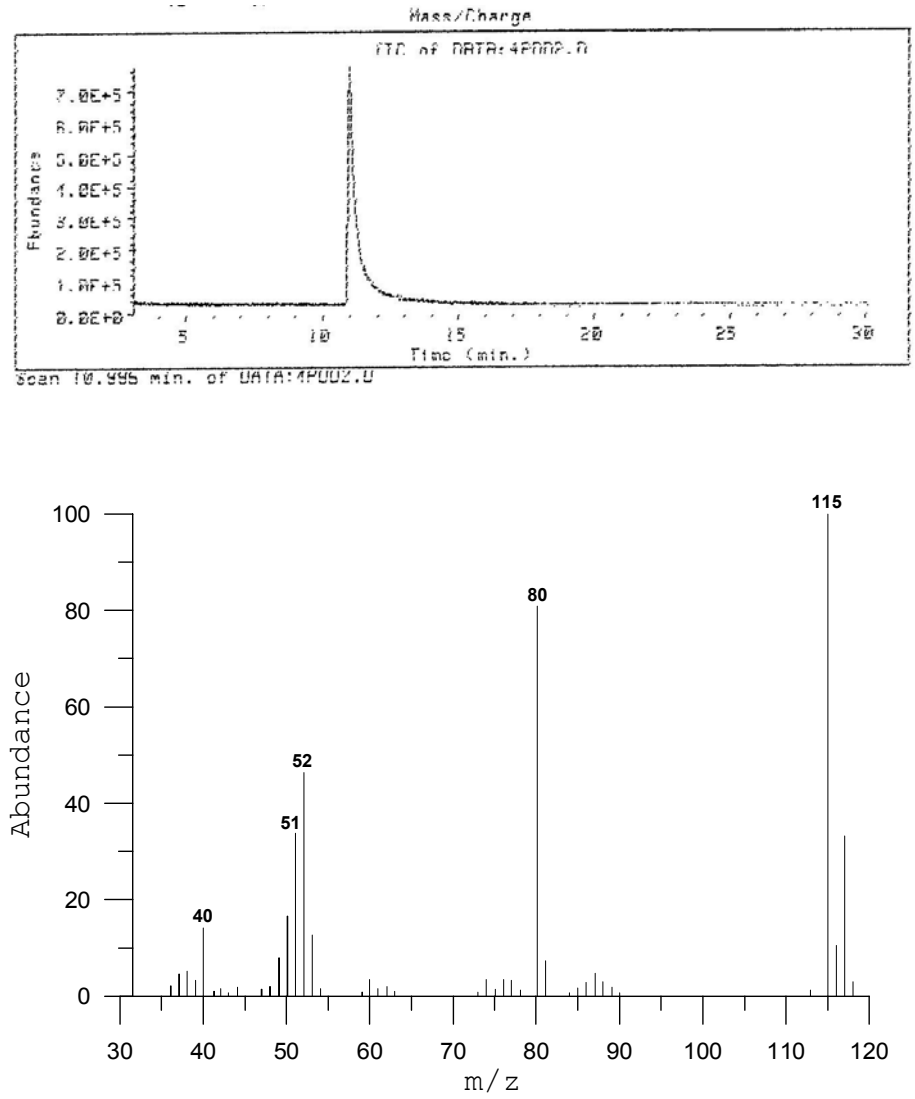

Figure 4.43 GC and MS of 4-chloropyridine-2,6-d$_2$ (**83-2,6-d$_2$**)

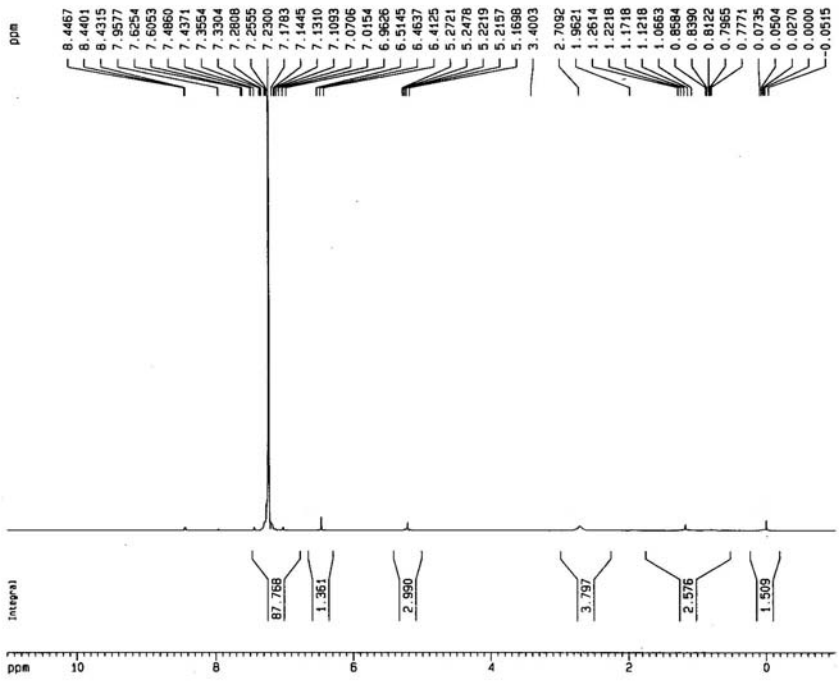

Figure 4.44 ^{1}H-NMR spectrum of 4-chloropyridine-2,6-d_2 (**83-2,6-d_2**)

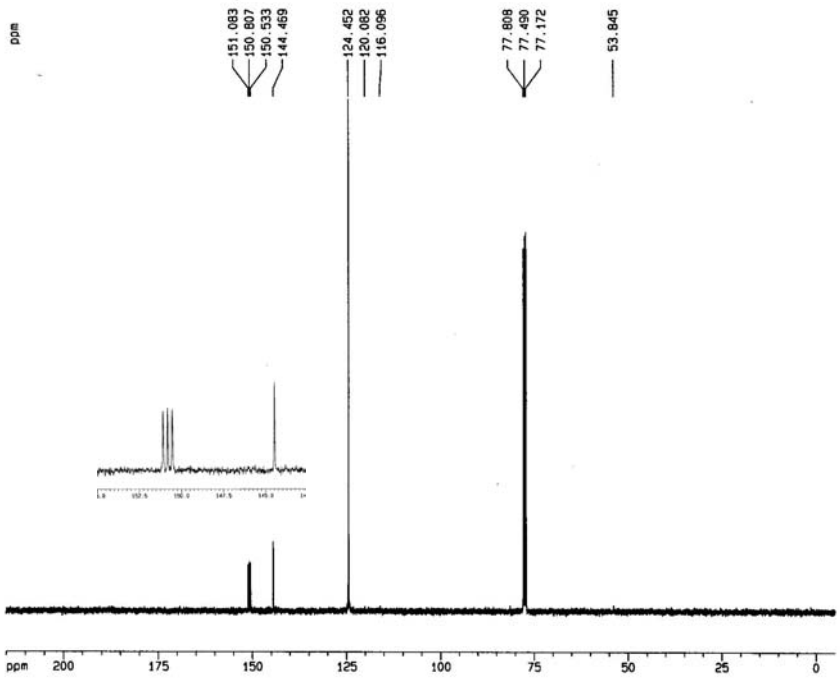

Figure 4.45 ^{13}C-NMR spectrum of 4-chloropyridine-2,6-d_2 (**83-2,6-d_2**)

The chloro group in **83-2,6-d_2** was then exchanged for deuterium by treating **83-2,6-d_2** with palladium on charcoal in a deuterium atmosphere according to the method of Azzam[55]. 2,4,6-Trideuteriopyridine (**1-2,4,6-d_3**) was obtained as a colorless liquid which was further purified by Kugelrohr distillation.

The mass spectrum of this product is shown in Figure 4.46. The molecular ion at m/z = 82 consistent with a trideuteriopyridine (**1-2,4,6-d_3**). The observation of DCN

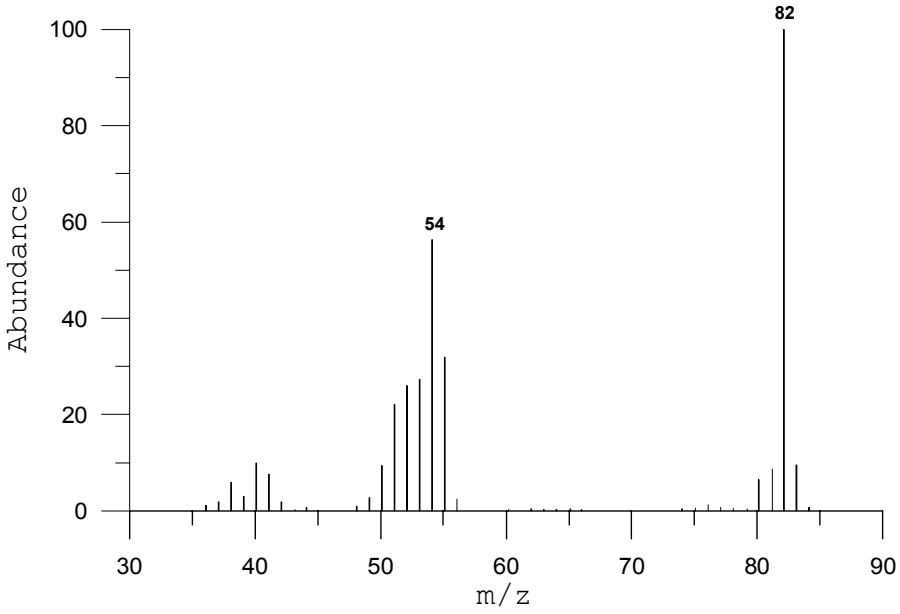

Figure 4.46 GC-MS of 2,4,6-trideuteriopyridine (**1-2,4,6-d_3**)

fragment by m/z = 54 confirms that deuterium has been labeled on α position of the pyridine ring. However, the observation of molecular ion 55 indicates that the loss of HCN due to H-D interchange is occurred before fragmentation.

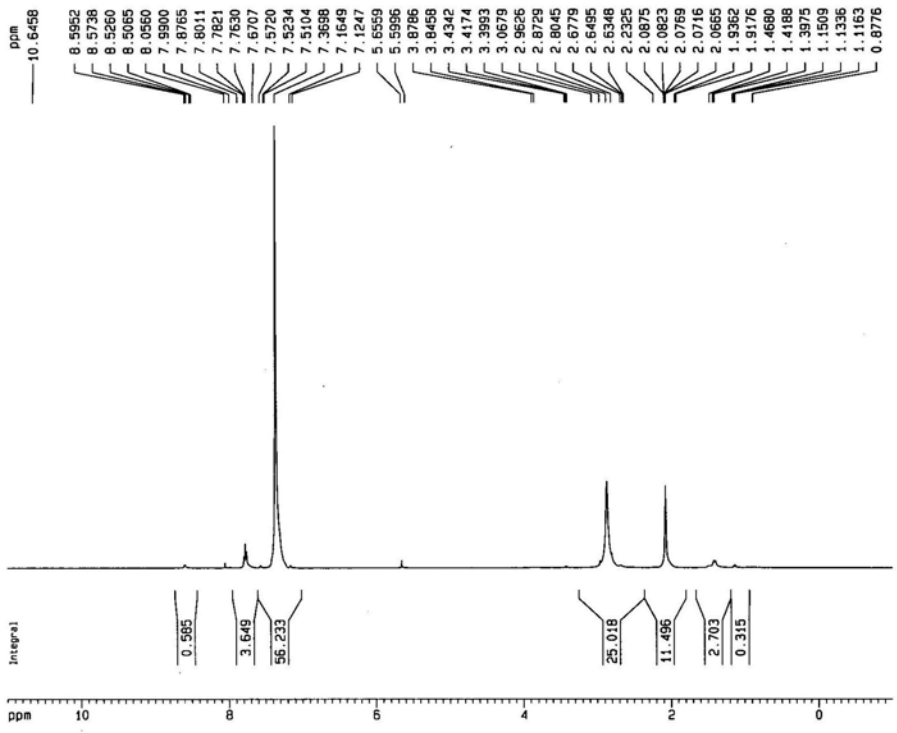

Figure 4.47 ^{1}H-NMR spectrum of 2,4,6-trideuteriopyridine (**1-2,4,6-d$_3$**)

The ^{1}H-NMR spectrum, shown in Figure 4.47, exhibits a singlet for H3 and H5 as an intense signal at δ 7.37. Two very small signals are observed at δ 8.60 and 7.77 due to residual protons at H2,6 and H4 confirms that protons at these positions have been mainly exchanged by deuterium.

In addition, the ^{13}C-NMR spectrum, shown in Figure 4.48, exhibits triplet signals which are due to C-2 and C-6 at δ 150.7 (J = 26.7 Hz) and C-4 at 137.0 (J = 28.0 Hz), respectively. The carbon signal due to C3 and C5 was observed at δ 124.7 as an intense singlet. This result clearly confirms the structure of 2,4,6-trideuteriopyridine (**1-2,4,6-d$_3$**).

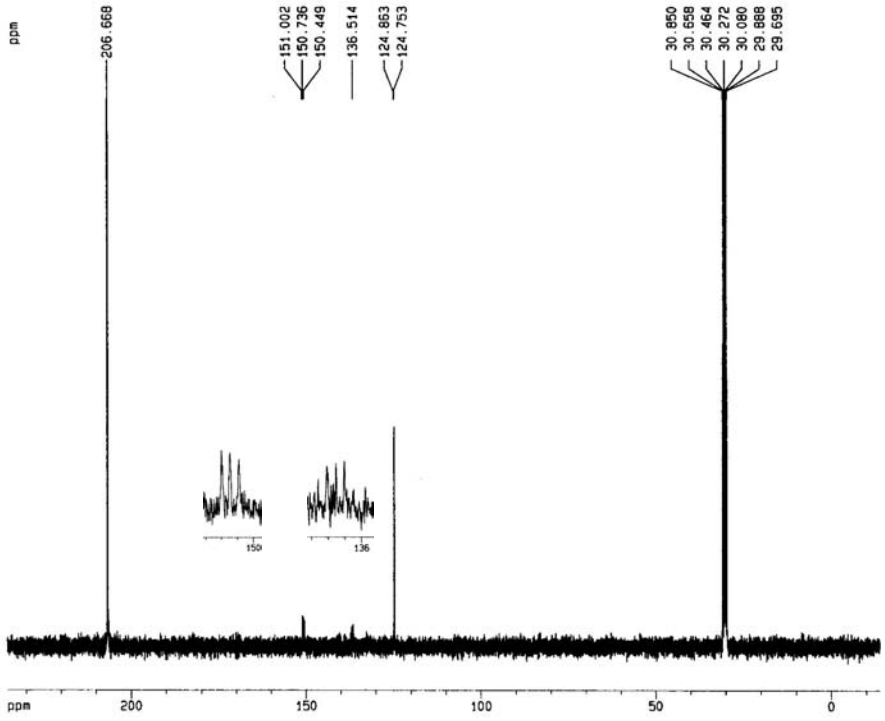

Figure 4.48 ^{13}C-NMR spectrum of 2,4,6-trideuteriopyridine (**1-2,4,6-d_3**)

4.3.10. Synthesis of 2,3,5,6-tetradeuteriopyridine (1-2,3,5,6-d_4)

The synthesis of 2,3,5,6-tetradeuteriopyridine (**1-2,3,5,6-d_4**) was first envisioned from 3,5-dichloropyridine (**84**) by the series of reactions shown in Scheme 4.36.

Scheme 4.36 Proposed synthesis of 2,3,5,6-tetradeuteriopyridine (**1-2,3,5,6-d_4**)

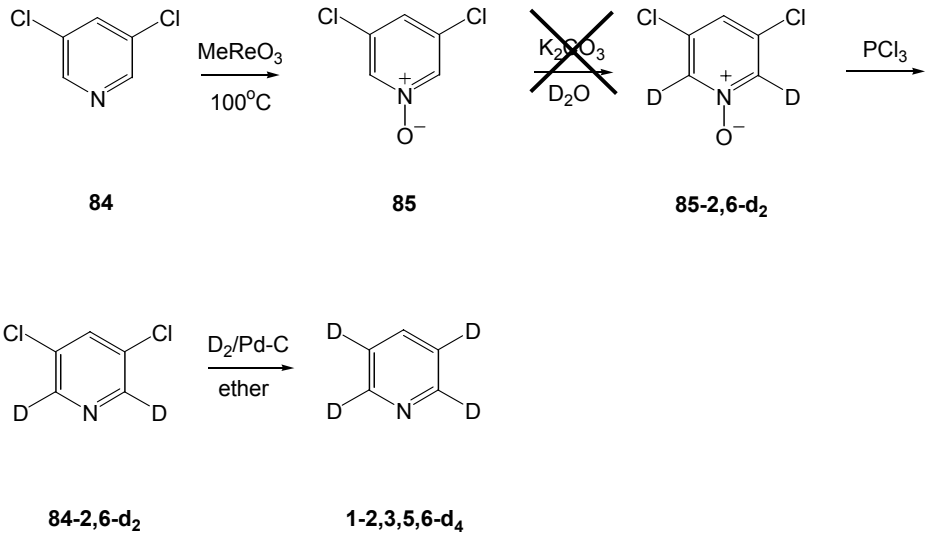

According to this approach, 3,5-dichloropyridine (**84**) was first oxidized by treatment with methyltrioxorhenium ($MeReO_3$) according to the method of Copéret[58] to provide 3,5-dichloropyridine N-oxide (**85**). Treatment of N-oxide **85** with K_2CO_3/D_2O, in an attempt to synthesize 2,6-dideuterio-3,5-dichloropyridine N-oxide (**85-2,6-d_2**), led however to 2,4,6-trideuterio-3,5-dichloropyridine (**85-2,4,6-d_3**). This result is consistent with the report by Zoltewicz and Kauffman[42] that chlorine substitution at position 3

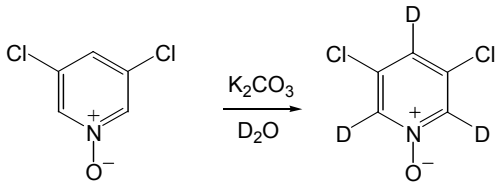

85 **85-2,4,6-d_3**

and 5 increases the reactivity of pyridine N-oxide toward H-D exchange. The increased reactivity of **85** to the H-D exchange reaction was the major concern. To avoid this problem, it was decided to exchange the chlorine atoms on positions 3 and 5 for deuterium before the H-D exchange of the protons at ring position 2 and 6. The synthesis shown in Scheme 4.37 was then suggested.

Scheme 4.37 Proposed synthesis of 2,3,5,6-tetradeuteriopyridine (**1-2,3,5,6-d_4**)

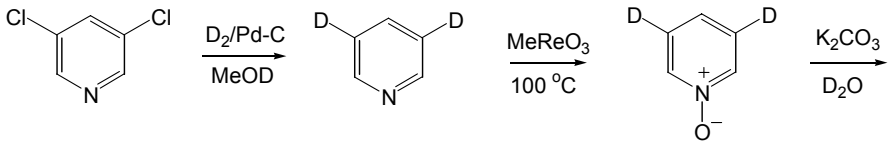

84 **1-3,5-d_2** **53-3,5-d_2**

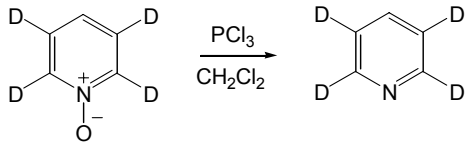

53-2,3,5,6-d_4 **1-2,3,5,6-d_4**

The synthetic method in Scheme 4.37 seems to be simple. However, it was difficult to obtain the products from each step. The high volatility of 3,5-dideuteriopyridine (**1-3,5-d_2**) was a serious problem which made it impossible to obtain

enough of this compound to continue the synthesis. Also, the water solubility of N-oxides **53-3,5-d_2** and **53-2,3,5,6-d_4** made it difficult to extract these products from the aqueous reaction mixture. Therefore, because of the low yields, this approach could not be utilized.

A new approach was designed using the starting material **84**. According to this method, compound **84** was converted directly to the N-oxide **85** which is not very soluble in the aqueous phase. Furthermore, none of the intermediates shown in Scheme 4.38, were found to be very soluble. This low solubility in water allowed high yield to be obtained by extraction with organic solvents.

Scheme 4.38 Synthesis of 2,3,5,6-tetradeuteriopyridine (**1-2,3,5,6-d_4**)

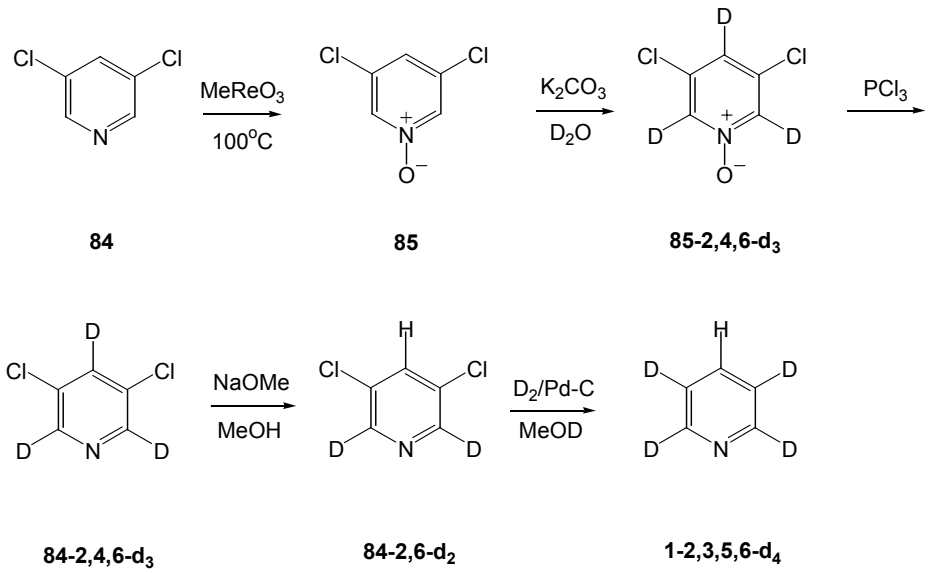

The new approach, shown in Scheme 4.38, makes use of the fact that while 3,5-dichloropyridine N-oxide (**42**) undergoes H-D exchange at ring positions 2,4 and 6,[59] 3,5-dichloropyridine is known to undergo exchange more rapidly at position 4 then at positions 2 and 6.[60] Thus, once N-oxide **85** is allowed to undergo exchange at positions 2, 4, and 6, the deuterium at position 4 in the reduced pyridine **84-2,4,6-d_3** is re-exchanged with hydrogen to form **84-2,6-d_2**. This approach was superior to attempting to limit the H-D exchange in N-oxide **85** to ring positions 2 and 6 as described by Zoltewics and Kauffman.[59] In our laboratory this approach always led to the trideuterated N-oxide (**85-2,4,6-d_3**).

In the last step, the synthesis of **1-2,3,5,6-d_4** gave interesting results. The dehalodeuteriumolysis was not successful in some solvents. Using ether or dichloromethane as the solvent led to a low reaction rate and therefore gave 50 % return of starting material even though large amounts of Pd-carbon were used. The reaction in dichloromethane or ether for 6 hours gave incomplete deuteriumolysis while the reaction in methanol-d solvent gave complete conversion within 4 hours. Unfortunately, because of the volatility of pyridine, recovery of **1-2,3,5,6-d_4** from methanol solvent was not an easy task. To purify this compound from methanol, the pyridine had to be converted to the pyridinium salt by treating with conc. HCl. Once the methanol was removed by evaporation, the residue was neutralized with base and extracted with a volatile solvent, such as dichloromethane or ethyl ether. The solvent-free **1-2,3,5,6-d_4** was then obtained after purifying by fractional distillation followed by Kugelrohr distillation.

The mass spectrum of the product from this reaction shown in Figure 4.49 exhibits the molecular ion m/z = 83, which is consistent with a tetradeuterated pyridine.

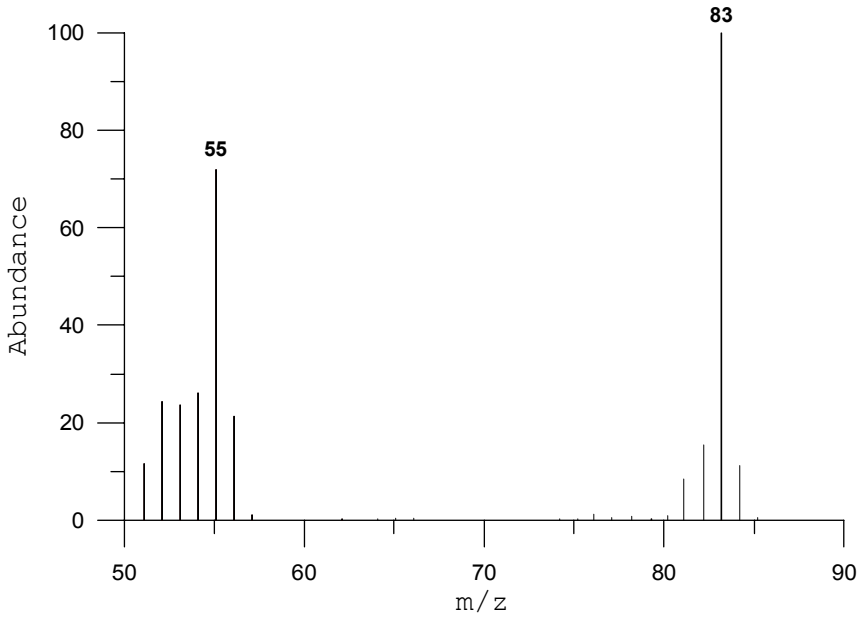

Figure 4.49 GC-MS of 2,3,5,6-tetradeuteriopyridine (**1-2,3,5,6-d_4**)

The ^{1}H-NMR spectrum shown in Figure 4.50 exhibits an intense singlet at δ 7.75, where the H4 proton is known to absorb, and small signals where the H2,6 and H3,5 protons are expected. This confirms that the protons at ring position 2,3,5, and 6 have been exchanged with deuterium.

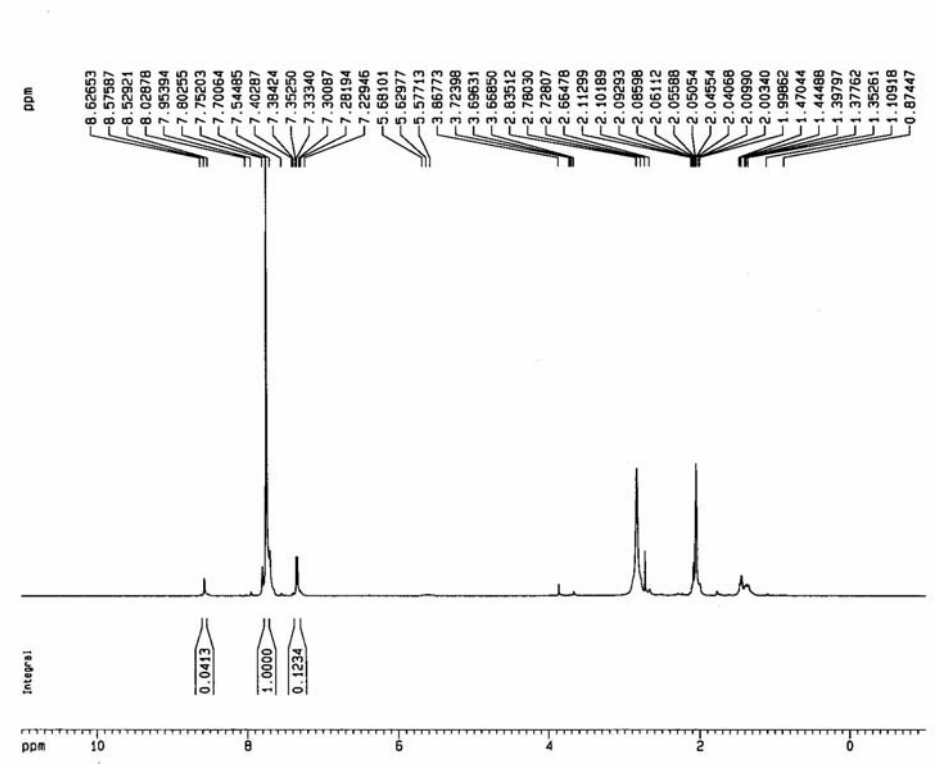

Figure 4.50 ^{1}H-NMR spectrum of 2,3,5,6-tetradeuteriopyridine (**1-2,3,5,6-d$_4$**)

In addition to the ^{1}H-NMR, the ^{13}C-NMR shown in Figure 4.51 was also recorded. As required, the signals due to C-2,6 at δ 150.3 and C-3,5 at δ 124.2 appear as triplets (J = 27.9 Hz and J = 25.5 Hz respectively) indicating that they are coupling with the attached deuterium atoms. The signal for the C-4 carbon observed at δ 136.5, however, appears as an intense singlet. This ^{13}C-NMR is consistent with the deuterium labeling at ring positions 2, 3, 5, and 6.

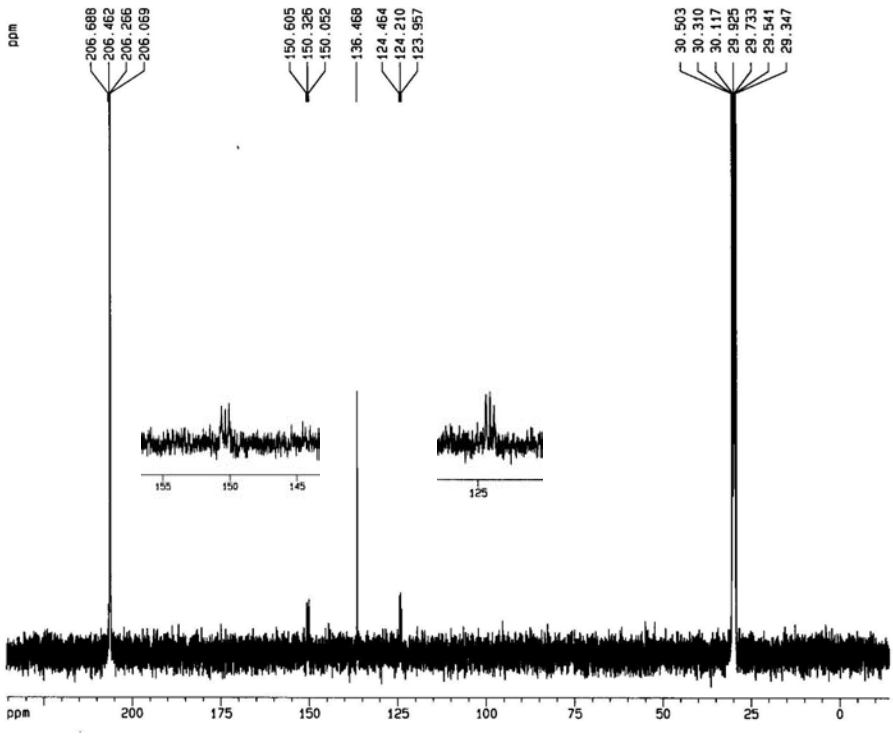

Figure 4.51 ^{13}C-NMR spectrum of 2,3,5,6-tetradeuteriopyridine (**1-2,3,5,6-d$_4$**)

4.3.11. Synthesis of 2,3,4,6-tetradeuteriopyridine (1-2,3,4,6-d_4)

2,3,4,6-Tetradeuteriopyridine (**1-2,3,4,6-d_4**) was synthesized by first oxidizing 3-chloropyridine (**86**) to 3-chloropyridine N-oxide **87**. To accomplish this, the **86** was converted to **87** by reacting with glacial acetic acid and 37% hydrogen peroxide. Oxidation formed the N-oxide **44** as a pure liquid confirmed by ^{1}H-NMR spectrum.

Scheme 4.39 Synthesis of 2,3,4,6-tetradeuteriopyridine (**1-2,3,4,6-d_4**)

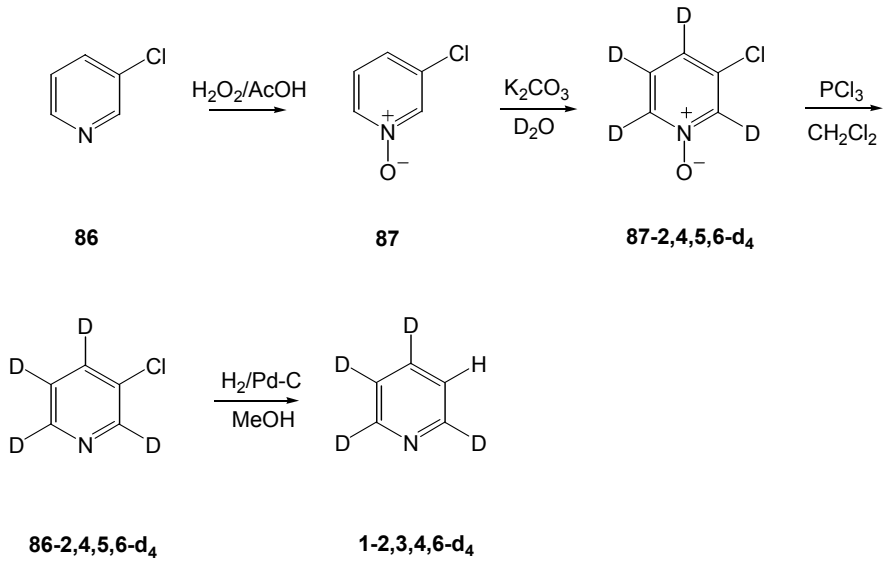

3-Chloropyridine N-oxide-2,4,5,6-d_4 (**87-2,4,5,6-d_4**) was then synthesized by base-catalyzed H-D exchange reaction at 190 ^{o}C in an autoclave. The result from this reaction is different from the results reported by Zoltewicz.[60] According to his work, H-D exchange of 3-chloropyridine N-oxide in CH_3ONa/CH_3OH was observed in order of position 2 → 6 → 4. The H-D exchange at position 5 was not observed owing to the

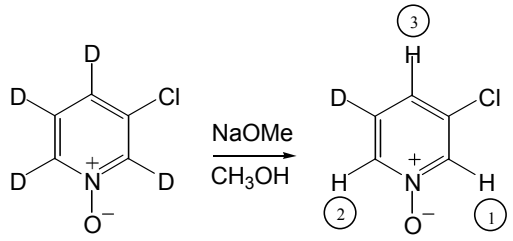

incursion of methoxydechlorination at reaction temperatures higher than 80 ^{o}C. However, our H-D exchange reaction gave a different result. The mass spectrum shown in Figure 4.52 exhibits a molecular ion with m/z = 133 which is consistent with the molar mass of a tetradeuterated structure. However, the 10% abundance of the trideuterated structure was also observed as m/z =132. It should be noted that the mass spectum also shows that Cl atom and isotope abundance (M+2) are still present in the molecule.

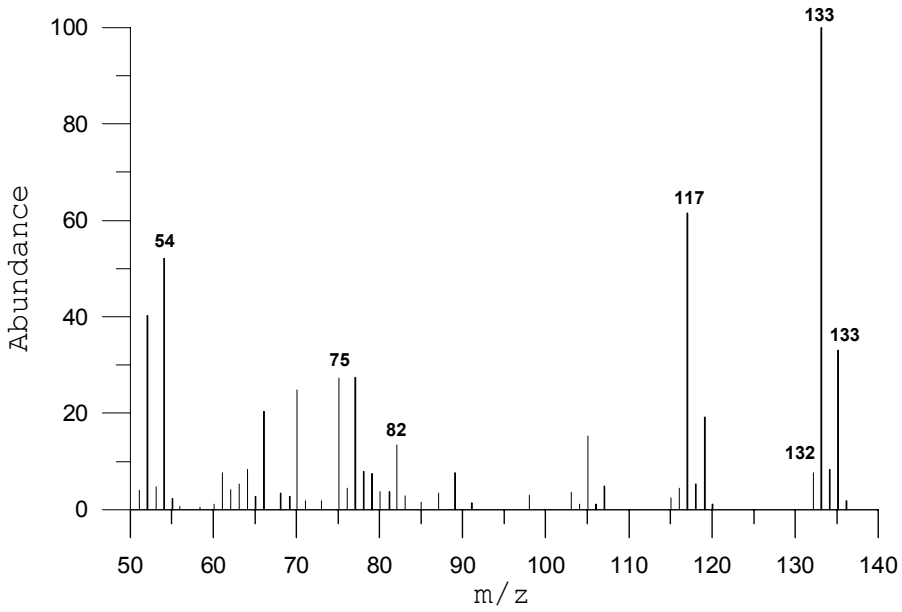

Figure 4.52 GC-MS of 3-chloropyridine N-oxide-2,4,5,6-d_4 (**87-2,4,5,6-d_4**)

The NMR result showed that no deuteroxydechlorination was taken place. Instead, the H-D reaction carried out at 190 ^{o}C in an autoclave gave deuteration at all 4 proton positions (2, 4, 5, and 6). This was confirmed by the ^{13}C-NMR spectrum shown in Figure 4.53. The ^{13}C spectrum exhibits four triplets due to C2, C6, C4, and C5 at δ 139.0 (J = 30.2 Hz), 137.9 (J = 28.9 Hz), 126.1 (J = 26.9 Hz), and 125.8 (J = 25.8 Hz) respectively and a singlet at δ 133.6 due to the C3 carbon. This confirms that H-D exchange has occurred at each of these ring positions but not at the C3 position.

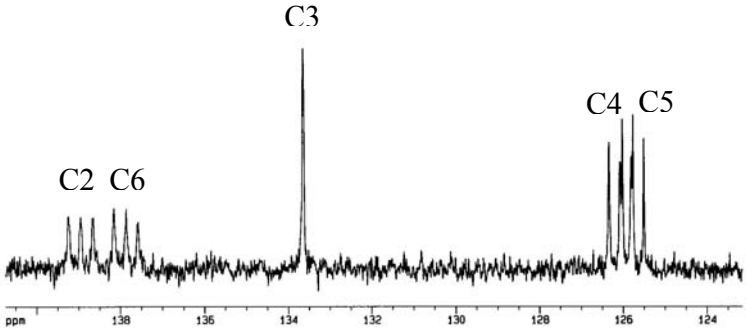

Figure 4.53 Expansion of ^{13}C-NMR spectrum of **87-2,4,5,6-d$_4$** shows 4 triplets

Moreover, two successive H-D exchange reactions were applied to obtain the highest deuterium content in **87-2,4,5,6-d$_4$**.

Reduction to remove the N-oxide was achieved by using PCl_3 to give 3-chloropyridine-2,4,5,6-d$_4$ (**86-2,4,5,6-d$_4$**) as a pure liquid. This compound was then subjected to the dehalohydrogenolysis at position 3 using 10% Pd-C and methanol in a hydrogen atmostphere. Because of the high volatility of pyridine, the resulting solution

was made acid to convert pyridine to the pyridinium salt and methanol was then removed by evaporation. The product tetradeuteriopyridine **1-2,3,4,6-d_4** was obtained after purification by fractional distillation followed by Kugelrohr distillation.

The mass spectrum of **1-2,3,4,6-d_4** shown in Figure 4.54 shows a molecular ion at m/z = 83 confirming that the compound is a tetradeuterated pyridine. The ion at m/z 82 indicates that about 10% of a trideuterated pyridine is also present.

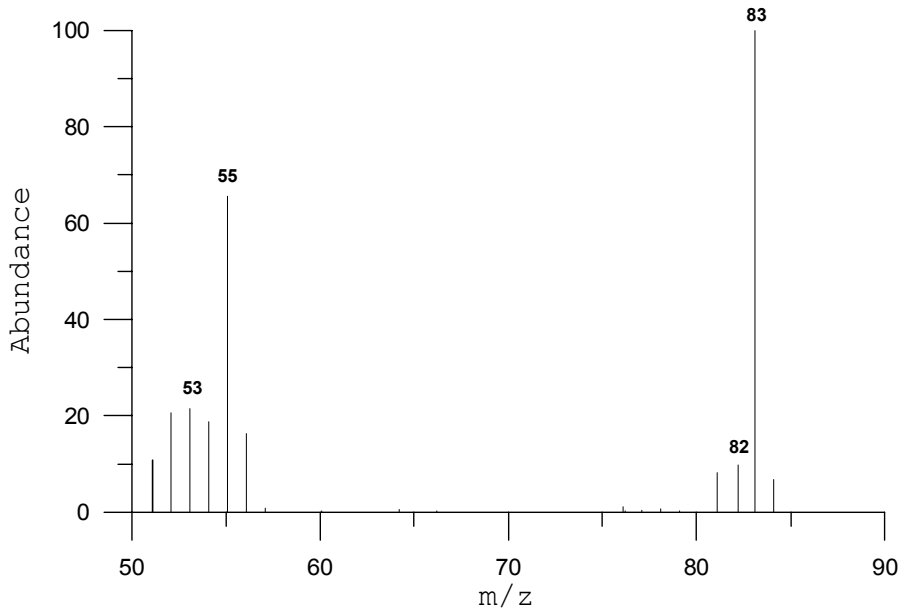

Figure 4.54 GC-MS of 2,3,4,6-tetradeuteriopyridine (**1-2,3,4,6-d_4**)

The ^{1}H-NMR spectrum recorded in acetone-d_6 is shown in Figure 4.55. As expected, the spectrum exhibits an intense singlet observed at δ 7.36 where the H5 proton of pyridine absorbs. Residual protons at positions 2 and 6 and at position 4 are observed as very small signals at δ 8.59 and 7.78, respectively.

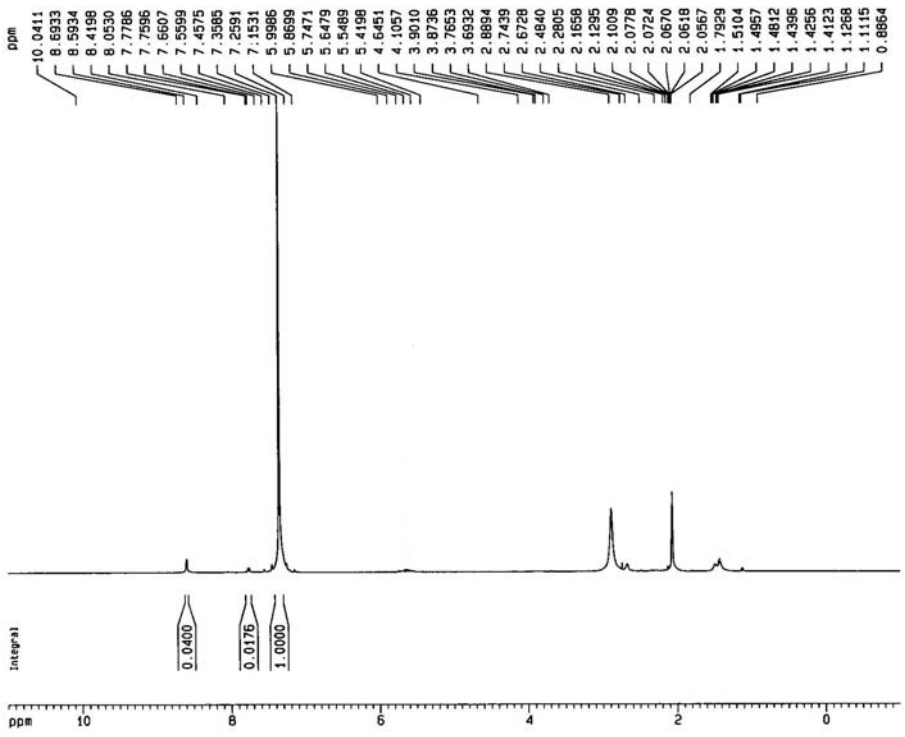

Figure 4.55 ^{1}H-NMR spectrum of 2,3,4,6-tetradeuteriopyridine (**1-2,3,4,6-d_4**)

The ^{13}C-NMR spectrum shown in Figure 4.56, shows the three triplet signals for C2 and 6, C4, and C5 at δ 152.1 (J = 30.4 Hz), 138.0 (J = 24.9 Hz) and 125.8 (J = 25.8 Hz), respectively, indicating that these carbons are labeled with deuterium atoms.

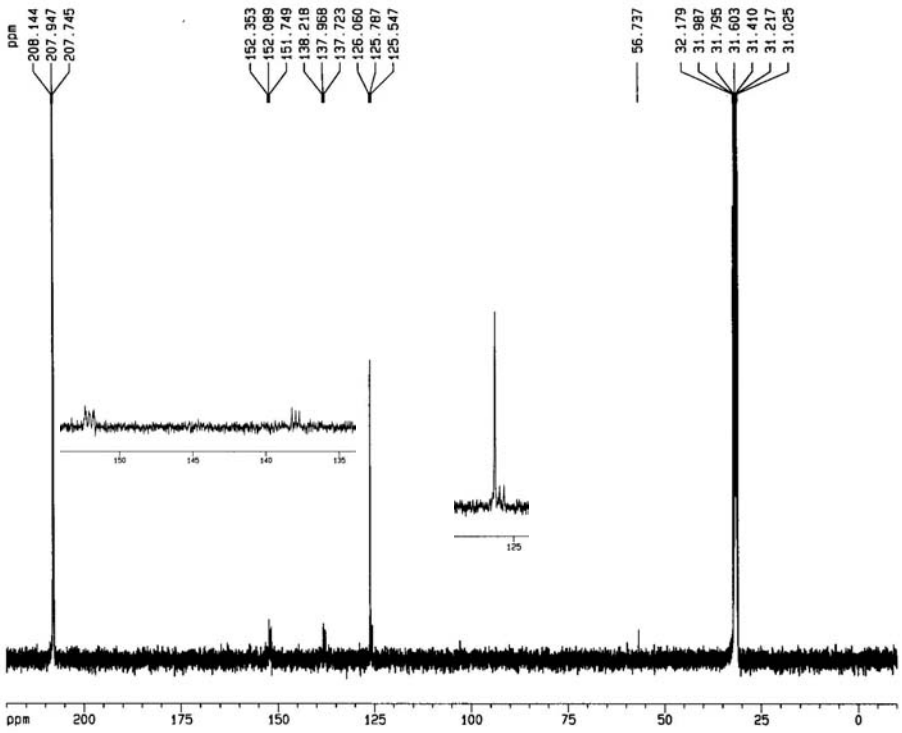

Figure 4.56 ^{13}C-NMR spectrum of 2,3,4,6-tetradeuteriopyridine (**1-2,3,4,6-d$_4$**)

4.3.12. Synthesis of 2,3,4,5-tetradeuteriopyridine (1-2,3,4,5-d_4)

In this experiment 2-chloropyridine (**88**) was first used as a starting material (Scheme 4.40) in an attempt to synthesize 2,3,4,5-tetradeuteriopyridine (**1-2,3,4,5-d_4**) by a procedure analogous to the procedure used for the synthesis of 2,4,5,6-tetradeuteriopyridine (**1-2,4,5,6-d_4**), shown in scheme 4.39, from 3-chloropyridine (**86**).

Scheme 4.40 Proposed synthesis of 2,3,4,5-tetradeuteriopyridine (**1-2,3,4,5-d_4**)

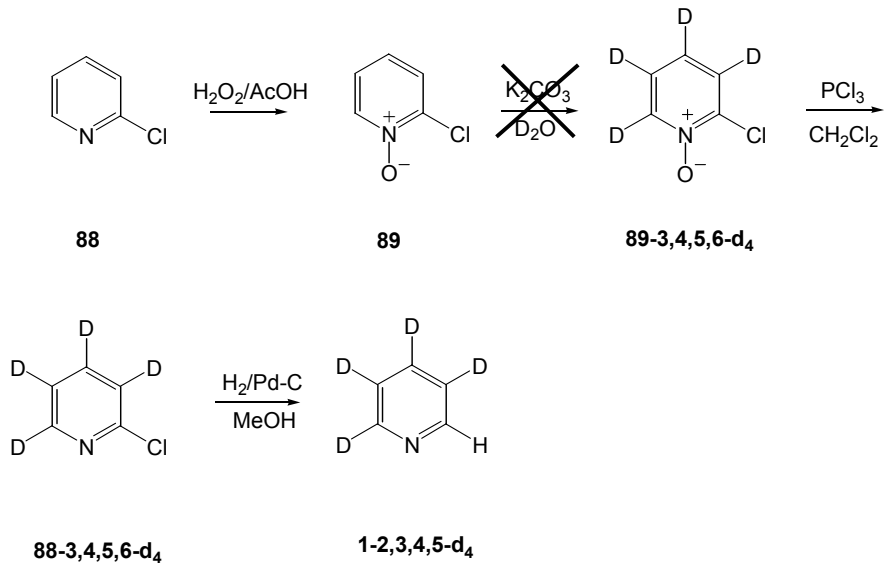

Unfortunately, it was found that 2-chloropyridine (**88**) does not react in the same way that 3-chloropyridine (**86**) reacted under these same conditions. Oxidation of **88** with glacial acetic acid and hydrogen peroxide does not lead to the complete formation of 2-chloropyridine N-oxide (**89**). Even after prolonged reaction time, a large amount of the starting material still remained. Nevertheless, the 2-chloropyridine N-oxide (**89**) was isolated via column chromatography and allowed to react with K_2CO_3/D_2O in an

autoclave. However, this reaction did not give 2-chloropyridine N-oxide-3,4,5,6-d_4 (**89-3,4,5,6-d_4**). The cause of this unsuccessful reaction can be due to nucleophilic displacement of the chlorine atom in 2-chloropyridine N-oxide (**89**).[62] Therefore, this gave a product different from the desired perdeuterated 2-chloropyridine N-oxide. The synthesis of **1-2,3,4,5-d_4** was thus redesigned. One approach is shown in scheme 4.41 which led to the successful synthesis of **1-2,3,4,5-d_4**.

Scheme 4.41 Synthesis of 2,3,4,5-tetradeuteriopyridine (**1-2,3,4,5-d_4**)

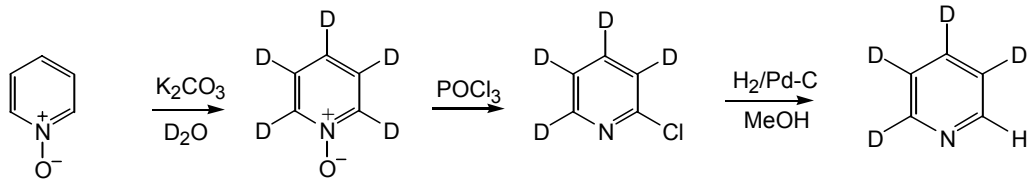

Pyridine N-oxide-d_5 (**53-2,3,4,5,6-d_5**), prepared by the base catalyzed H-D exchange of pyridine N-oxide (**53**), was allowed to react with phosphorous oxychloride at 120 ^oC. This resulted in the formation of perdeuterio 2-chloropyridine (**88-3,4,5,6-d_4**) and perdeuterio 4-chloropyridine (**90-2,3,5,6-d_4**) in a ratio of 7:3.[62] Pure 2-chloropyridine-3,4,5,6-d_4 (**88-3,4,5,6-d_4**) was obtained after purification by column chromatography. The dechlorohydrogenolysis of this compound resulted in the formation of 2,3,4,5-tetradeuteriopyridine (**1-2,3,4,5-d_4**), which was confirmed by GC-MS and NMR spectra.

The mass spectrum of the product form this reaction shown in Figure 4.57 exhibits a molecular ion at m/z = 83, which is consistent with a tetradeuterated pyridine. In addition, the ion at m/z = 82 indicates that a trideuteratedpyridine is present in approximately 10%. Major fragmentation signals at 55 and 56 are consistent with loss of DCN and HCN respectively from the molecular ion. This suggests that the scrambling of the ring atoms occur before fragmentation.[56]

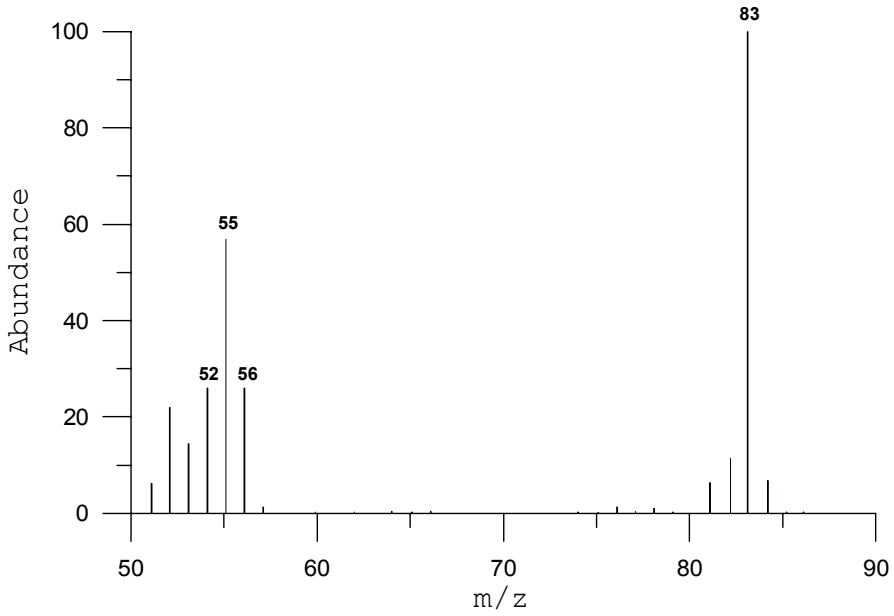

Figure 4.57 GC-MS of 2,3,4,5-tetradeuteriopyridine (**1-2,3,4,5-d_4**)

The ^{1}H-NMR spectrum, shown in Figure 4.58, exhibits a signal at δ 8.60 where the H2 proton of pyridine absorbs. The residual protons due to H4 and H3 or H5 are observed as very small signals at δ 7.77 and 7.36, respectively. Integration of these signals indicates that the protons at these ring positions are 95% exchanged.

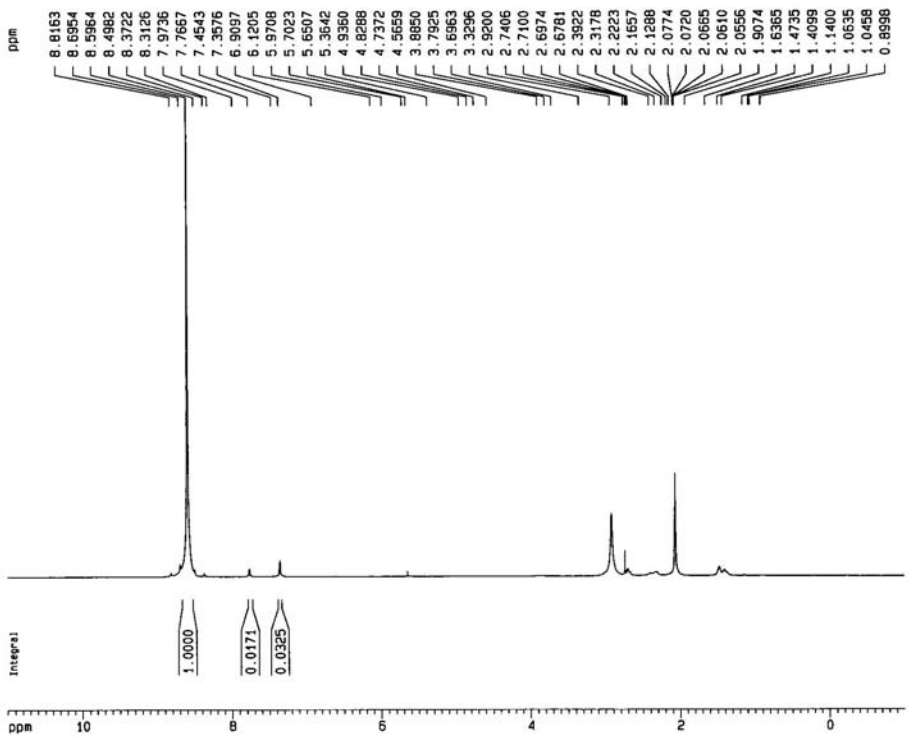

Figure 4.58 ^{1}H-NMR spectrum of 2,3,4,5-tetradeuteriopyridine (**1-2,3,4,5-d$_4$**)

The ^{13}C-NMR spectrum, shown in Figure 4.59, also supports this conclusion. Therefore, the spectrum shows signals for C3, C4, C5, and C6, as triplets at δ 122.1, 134.1, 122.0, and 148.3, respectively (J = 25.2, 24.6, 25.5, 27.2 Hz) indicating that these carbons are coupling with the attached deuterium atoms. The signal for the C2 carbon at δ 148.6 appears as a sharp singlet.

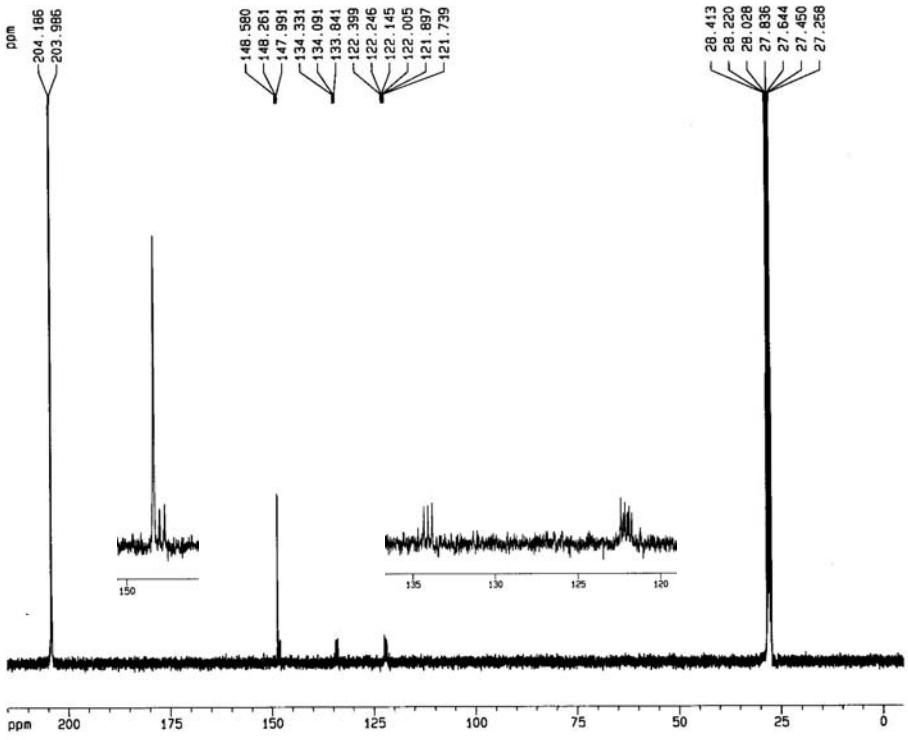

Figure 4.59 ^{13}C-NMR spectrum of 2,3,4,5-tetradeuteriopyridine (**1-2,3,4,5-d$_4$**)

4.3.13 Synthesis of 2,3,4-trideuteriopyridine (1-2,3,4-d_3), 2,4,5-trideuteriopyridine (1-2,4,5-d_3), and 2,3,6-trideuteriopyridine (1-2,3,6-d_3)

The syntheses of 2,3,4-trideuteriopyridine (**1-2,3,4-d_3**), 2,4,5-trideuteriopyridine (**1-2,4,5-d_3**), and 2,3,6-trideuteriopyridine (**1-2,3,6-d_3**) were started from commercially available 3-chloropyridine (**86**). According to Yamanaka and colleagues, reaction of 3-substituted pyridine N-oxide with phosphoryl chloride ($POCl_3$) results in the formation of site-selective products.[62] In our case, reaction of 3-chloropyridine N-oxide **87-2,4,5,6-d_4** with $POCl_3$ is expected to form 2,3-dichloropyridine (**91-4,5,6-d_3**), 2,5-dichloropyridine (**92-3,4,5-d_3**), and 3,4-dichloropyridine (**93-2,5,6-d_3**) in a ratio of 47: 38: 15. These compounds can be the precursors for the preparation of **1-2,3,4-d_3**, **1-2,4,5-d_3**, and **1-2,3,6-d_3**, respectively by hydrogenolysis reaction in the presence of H_2 and Pd-C. Scheme 4.41 shows the synthetic route for the target products, **1-2,3,4-d_3**, **1-2,4,5-d_3**, and **1-2,3,6-d_3**.

Scheme 4.42 Syntheses of 2,3,4-,2,4,5-, and 2,3,6-trideuteriopyridine

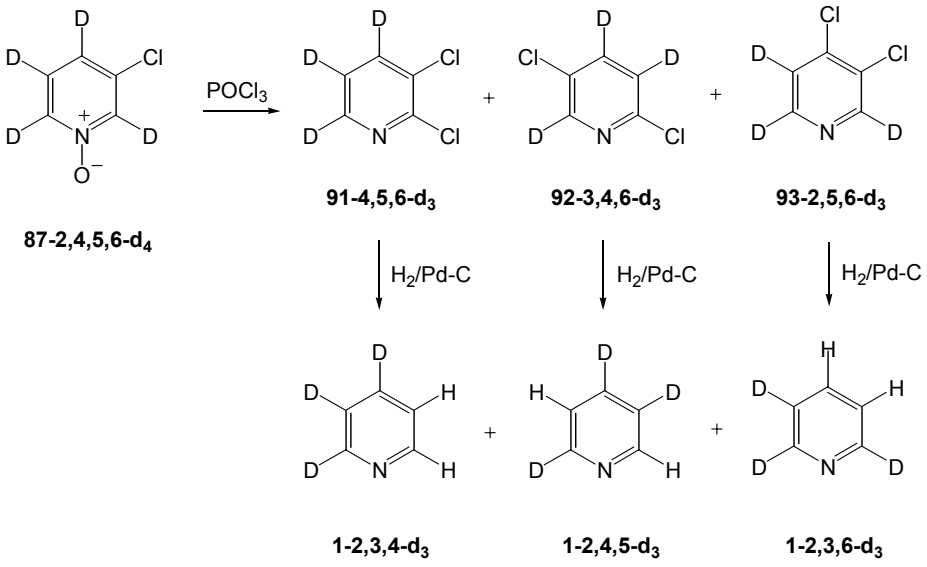

87-2,4,5,6-d_4 → **91-4,5,6-d_3** + **92-3,4,6-d_3** + **93-2,5,6-d_3**

91-4,5,6-d_3 → **1-2,3,4-d_3**

92-3,4,6-d_3 → **1-2,4,5-d_3**

93-2,5,6-d_3 → **1-2,3,6-d_3**

Perdeuterio 3-chloropyridine N-oxide **87-2,4,5,6-d$_4$** was prepared from **86** as previously described in the synthesis of **1-2,3,4,6-d$_4$**. After **87-2,4,5,6-d$_4$** was allowed to react with $POCl_3$ at 80-90 ^oC, the resulting mixture was purified by column chromatography. All components were isolated using 90:10 dichloromethane/hexane as a solvent system. Each compound was converted to the final product by dechlorohydrogenolysis in the presence of H_2 and Pd-C. All products were confirmed by GC-MS and NMR.

The mass spectrum of **1-2,3,4-d$_3$** shown in Figure 4.60 exhibits a molecular ion at m/z = 82, which is consistent with a trideuterated product.

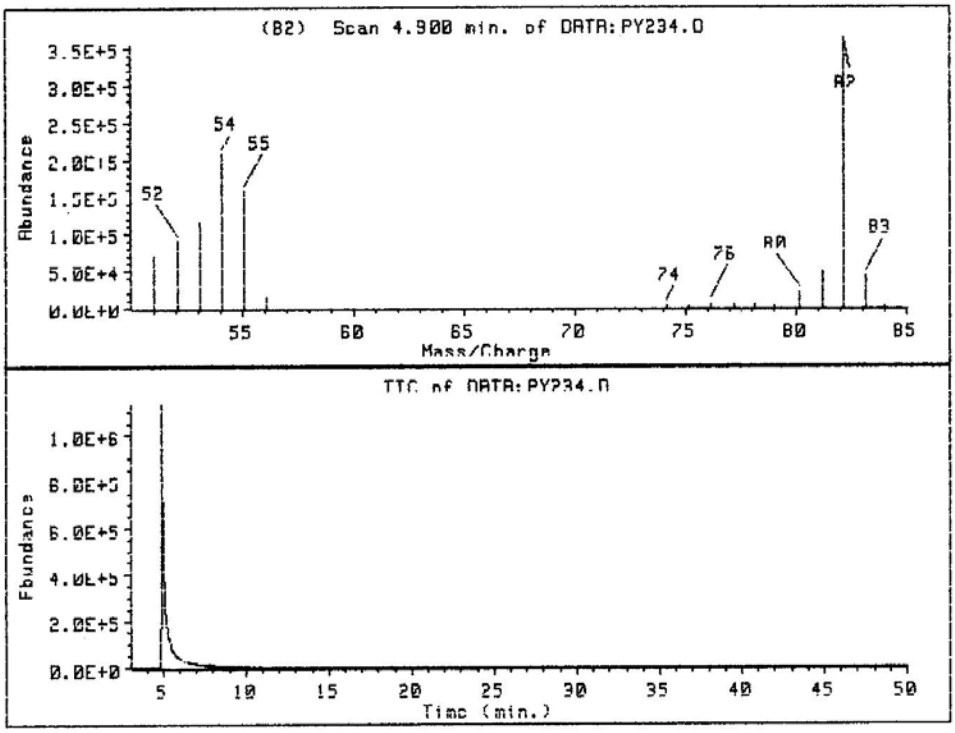

Figure 4.60 GC-MS of 2,3,4-trideuteriopyridine (**1-2,3,4-d$_3$**)

Figure 4.61 shows the ^{1}H-NMR spectrum of **1-2,3,4-d$_3$** recorded in acetone-d$_6$. The doublet signals due to H6 and H5 are observed at δ 8.58 (J = 4.8 Hz) and 7.34 (J = 4.8 Hz). The H4 proton at δ 7.75 is labeled with deuterium, it was not observed. This NMR result is consistent with the structure of 2,3,4-trideuteriopyridine.

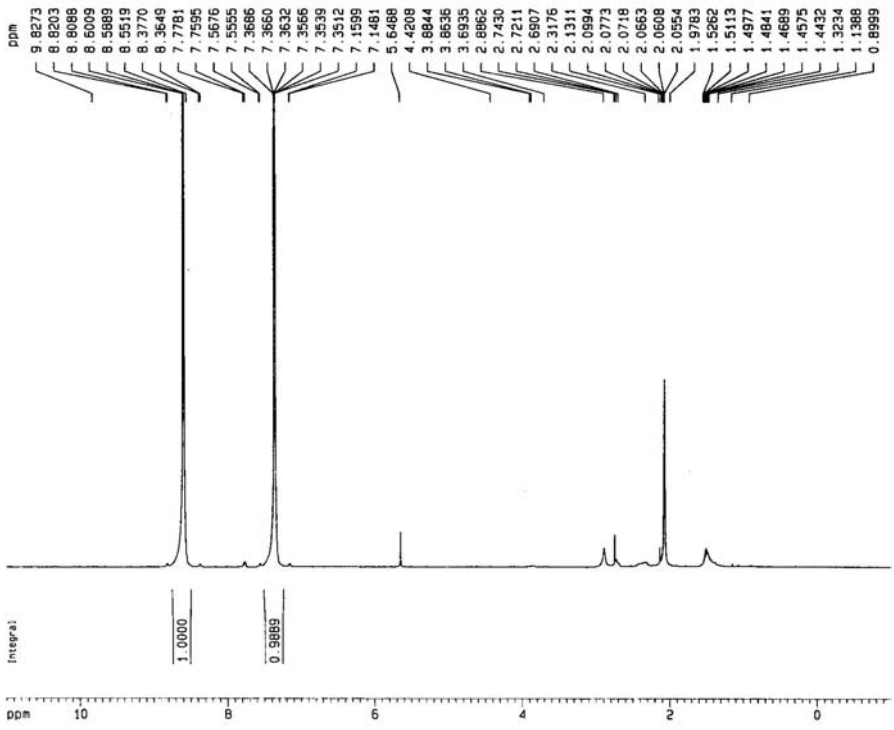

Figure 4.61 ^{1}H-NMR spectrum of 2,3,4-trideuteriopyridine (**1-2,3,4-d$_3$**)

This product is also confirmed by the ^{13}C-NMR spectrum shown in Figure 4.62. The singlet signals due to C6 and C5 are observed at δ 150.6 and 124.4 whereas the triplet signals due to C2, C4, and C3 are observed at δ 150.2 (J = 27.2 Hz), 136.2 (J = 25.3 Hz), and 124.0 (J = 25.6 Hz). The scale expansion of each triplet is also shown in Figure 4.62.

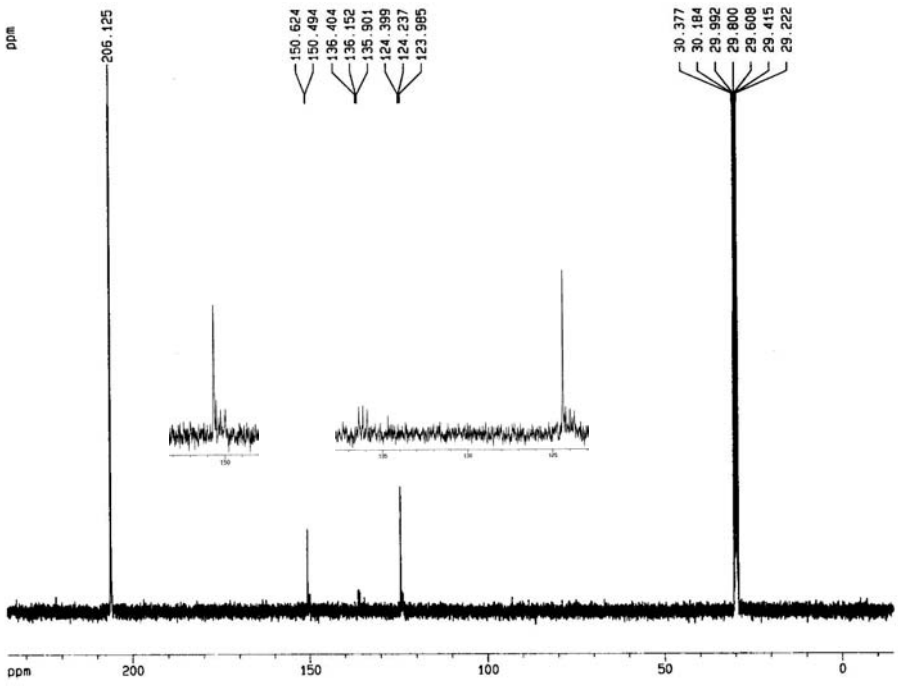

Figure 4.62 ^{13}C-NMR spectrum of 2,3,4-trideuteriopyridine (**1-2,3,4-d$_3$**)

The mass spectrum of 2,4,5-trideuteriopyridine (**1-2,4,5-d_3**) is shown in Figure 4.63. The molecular ion at m/z 82 is observed in the spectrum confirming the trideuteriopyridine compound. Fragmentation of DCN and HCN gave molecular ion at m/z 54 and 55, respectively.

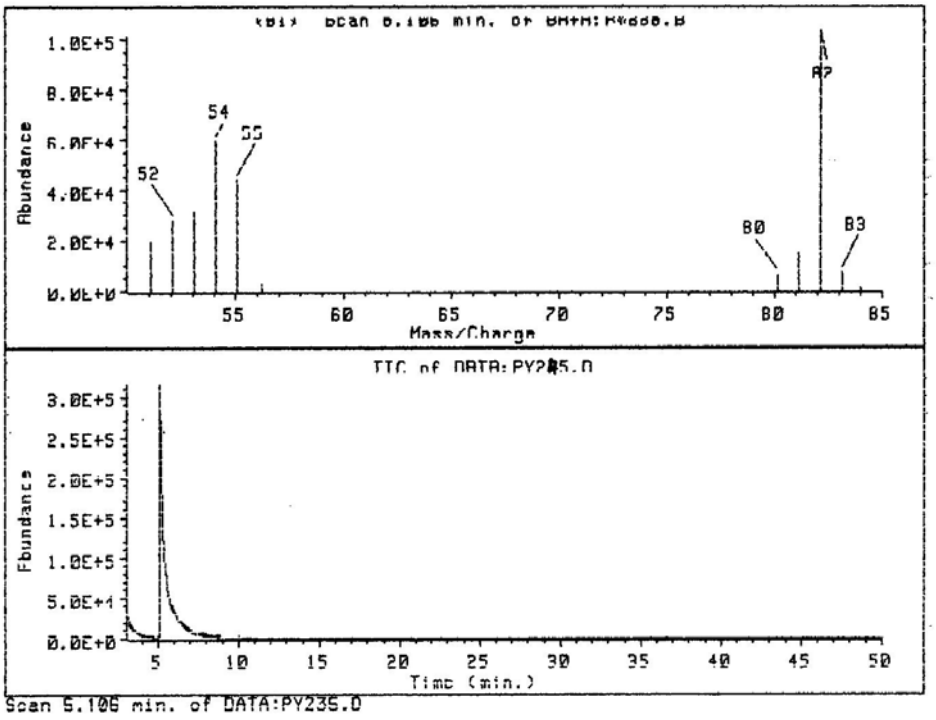

Figure 4.63 GC-MS of 2,4,5-trideuteriopyridine (**1-2,4,5-d_3**)

In addition, the ^{1}H-NMR spectrum of **1-2,4,5-d$_3$** is also recorded in acetone-d$_6$. The singlet signal due to H6 and H3 are observed at δ 8.60 and 7.36. The H4 proton is not observed because of deuterium labeling. These results agree well with the structure of **1-2,4,5-d$_3$**.

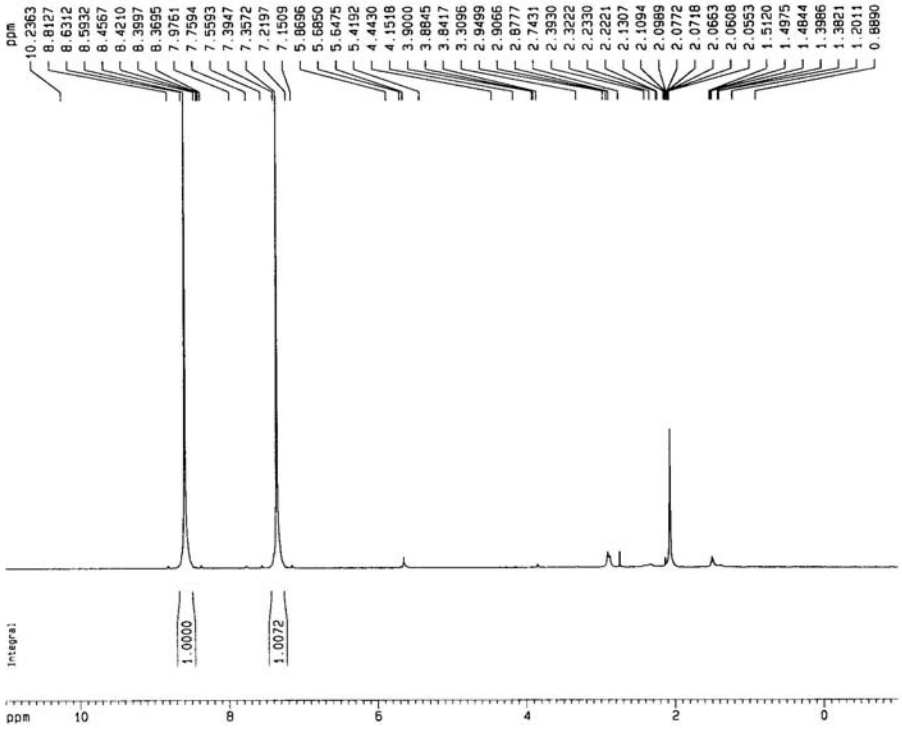

Figure 4.64 ^{1}H-NMR spectrum of 2,4,5-trideuteriopyridine (**1-2,4,5-d$_3$**)

The ^{13}C-NMR spectrum of 2,4,5-trideuteriopyridine (**1-2,4,5-d$_3$**) is shown in Figure 4.65. It exhibits the carbon signals due to C3 and C6 as intense singlets at δ 150.6 and 124.2. The C2, C4, and C5 carbon, which are labeled with deuterium, are observed as small triplets at δ 150.3 (J = 26.9 Hz), 136.2 (J = 25.3 Hz), 124.1 (J = 25.0 Hz), respectively.

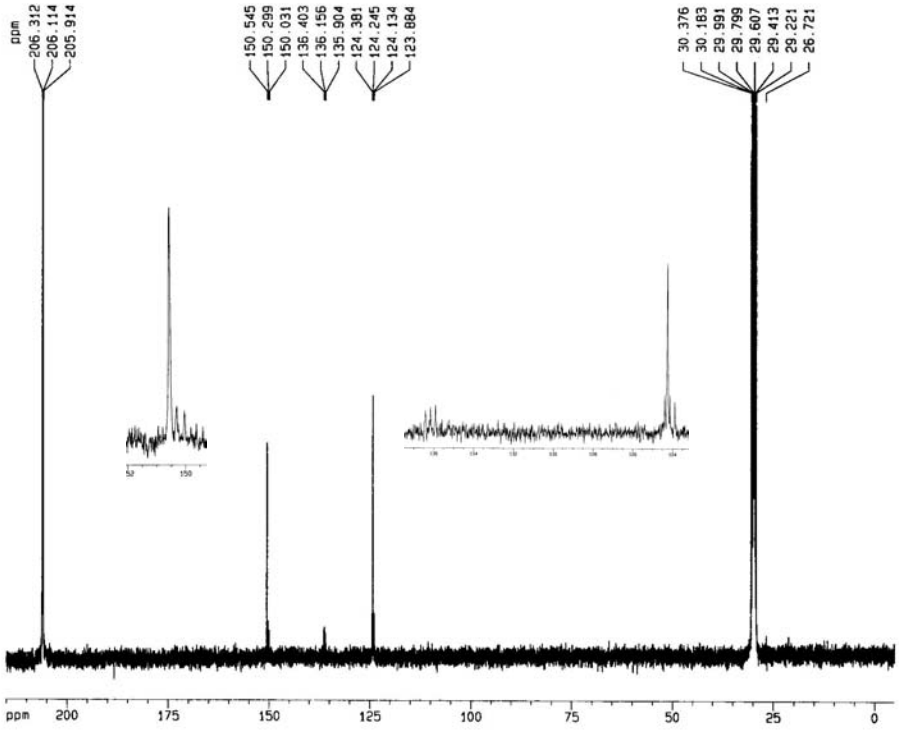

Figure 4.65 ^{13}C-NMR spectrum of 2,4,5-trideuteriopyridine (**1-2,4,5-d$_3$**)

Futhermore, the GC-MS spectrum of 2,3,6-trideuteriopyridine (**1-2,3,6-d_3**) are shown in Figure 4.66, exhibiting the molecular ion at m/z 82. Fragmentation of DCN or HCN leads to m/z 54 or 55 respectively. This confirms the structure of a trideuteriopyridine.

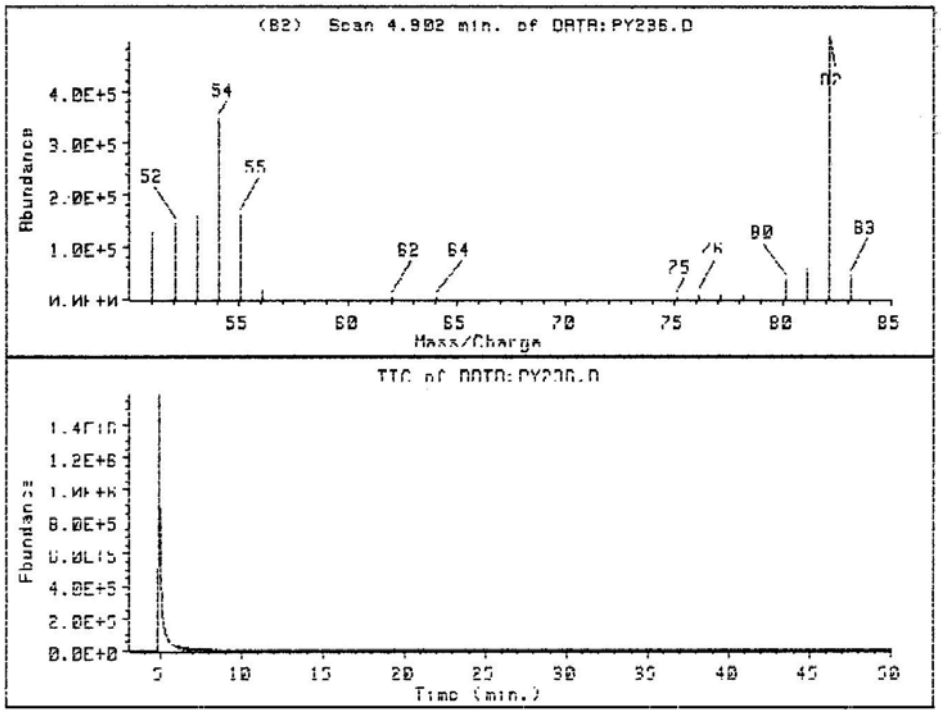

Figure 4.66 GC-MS of 2,3,6-trideuteriopyridine (**1-2,3,6-d_3**)

Figure 4.67 shows the ^{1}H-NMR spectrum of 2,3,6-trideuteriopyridine (**1-2,3,6-d$_3$**). As expected for the assigned structure, the doublet due to the H4 and H5 protons are observed at δ 7.76 (*J* = 7.6 Hz) and 7.34 (J = 7.6 Hz). In addition, the residual protons H2 and H6 are observed as a singlet at δ 8.57.

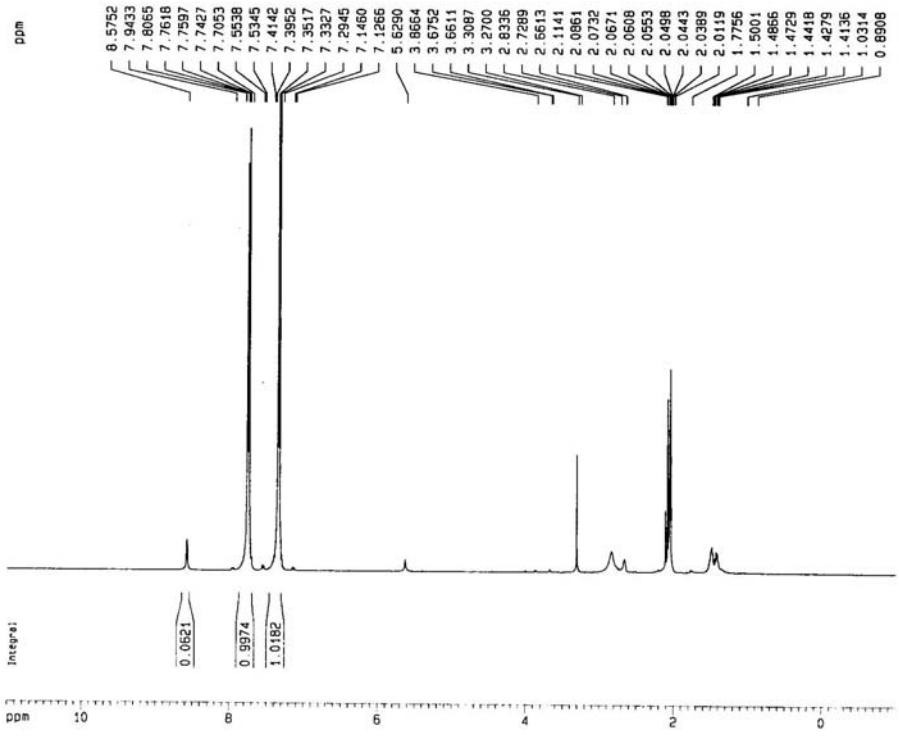

Figure 4.67 ^{1}H-NMR spectrum of 2,3,6-trideuteriopyridine (**1-2,3,6-d$_3$**)

The structure of **1-2,3,6-d_3** is confirmed by ^{13}C-NMR spectrum shown in Figure 4.68. This spectrum exhibits a triplet signal at δ 150.3, which is due to the C2 and C6 carbon coupling with deuteriums. Another triplet can be observed at δ 124.1 which is due to C3 coupling with deuterium. This signal is overlapping with an intense singlet of C5 at δ 124.3. A singlet of C4 can be observed in this spectrum at δ 136.4.

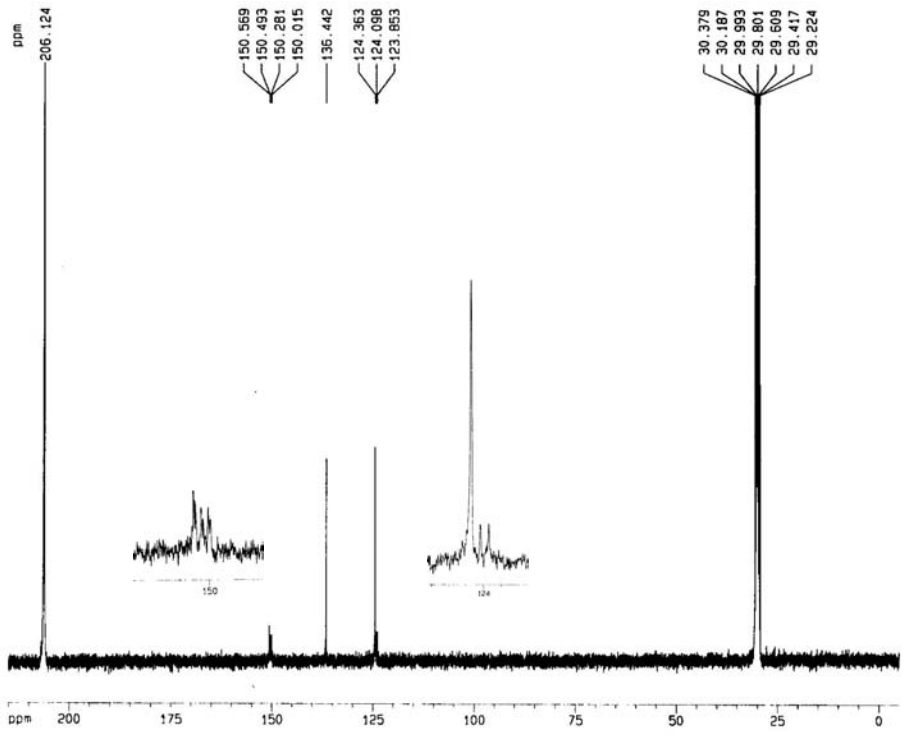

Figure 4.68 ^{13}C-NMR spectrum of 2,3,6-trideuteriopyridine (**1-2,3,6-d_3**)

4.3.14. Synthesis of 2,3,5-trideuteriopyridine (1-2,3,5-d_3)

2,3,5-Trideuteriopyridine (**1-2,3,5-d_3**) was synthesized from pyridine N-oxide (**53**) by the multistep synthesis shown in Scheme 4.43.

Scheme 4.43 Synthesis of 2,3,5-trideuteriopyridine (**1-2,3,5-d_3**)

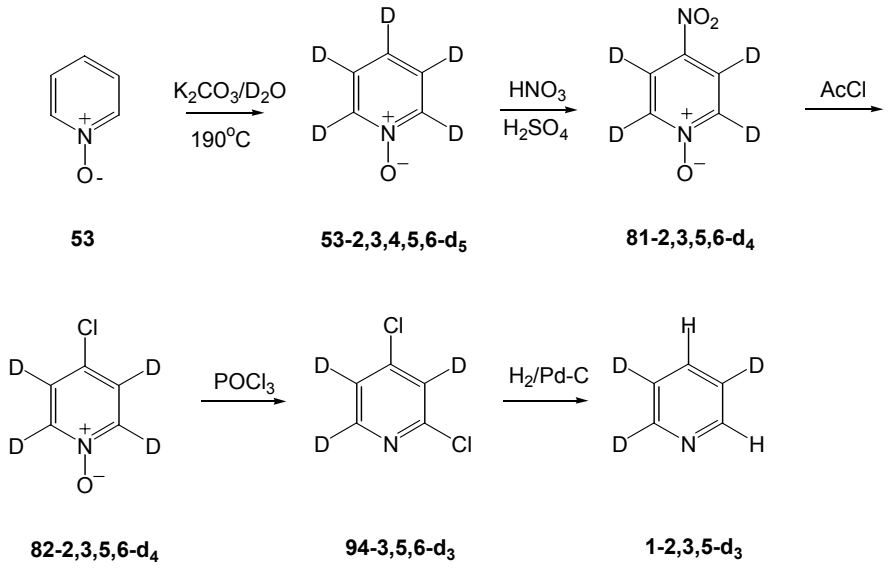

Pyridine N-oxide (**53**) was subjected to three consecutive H-D exchange reaction to obtain perdeuterated pyridine N-oxide (**53-2,3,4,5,6-d_5**) which was then nitrated to give 4-nitropyridine N-oxide-2,3,5,6-d_4 (**81-2,3,5,6-d_4**). This compound was reacted with acetylchloride to form 4-chloropyridine N-oxide-2,3,5,6-d_4 (**82-2,3,5,6-d_4**). All these steps generally gave reaction products in a high yield. Reaction of **82-2,3,5,6-d_4** with $POCl_3$, however, would form two dichloropyridine products. The major product is 2,4-dichloropyridine-3,5,6-d_3 (**94-3,5,6-d_3**) which was obtained in 47% yield. The minor product is 3,4-dichloropyridine-2,5,6-d_3 (**93-2,5,6-d_3**) which was obtained only in a trace

amount. Column chromatography was used to isolate **94-3,5,6-d_3** which was then reacted with H_2 in the presence of Pd-Charcoal to form a hydrogenolysis product, 2,3,5-trideuteriopyridine (**1-2,3,5-d_3**). This compound was analyzed by GC-MS and NMR spectroscopy.

The mass spectrum shown in Figure 4.69 exhibits the molecular ion at m/z 82 which is consistent with the molecular weight of desired product, **1-2,3,5-d_3**. This fragmentation of DCN or HCN gave molecular ion at m/z 54 and 55, respectively.

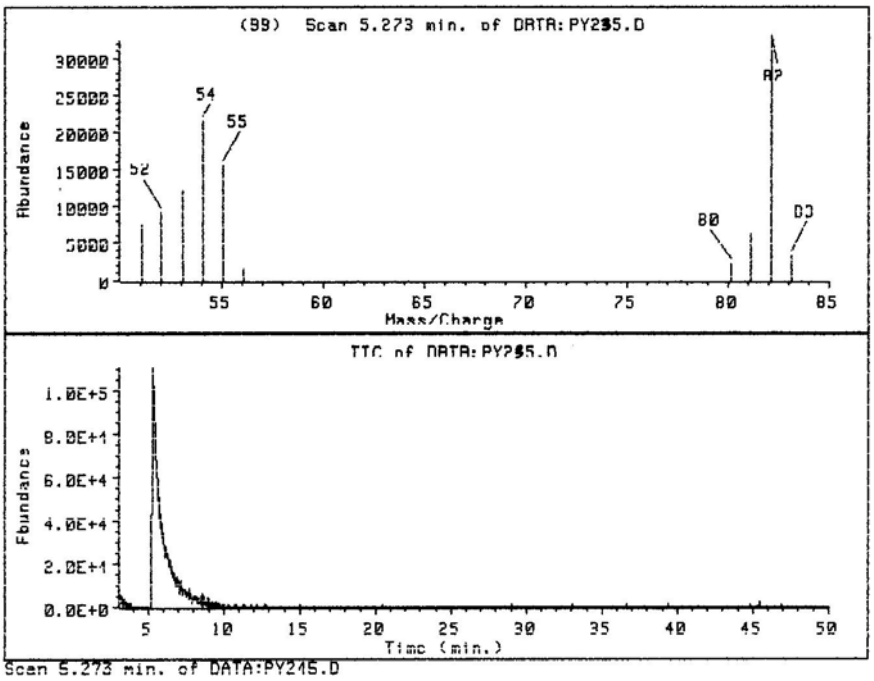

Figure 4.69 GC-MS of 2,3,5-trideuteriopyridine (**1-2,3,5-d_3**)

The ^{1}H-NMR spectrum shown in Figure 4.70 exhibits two singlets due to H4 and H6 at δ 7.75 and 8.58, respectively whereas the H3 and H5 at δ 7.35 are labeled with deuterium atoms.

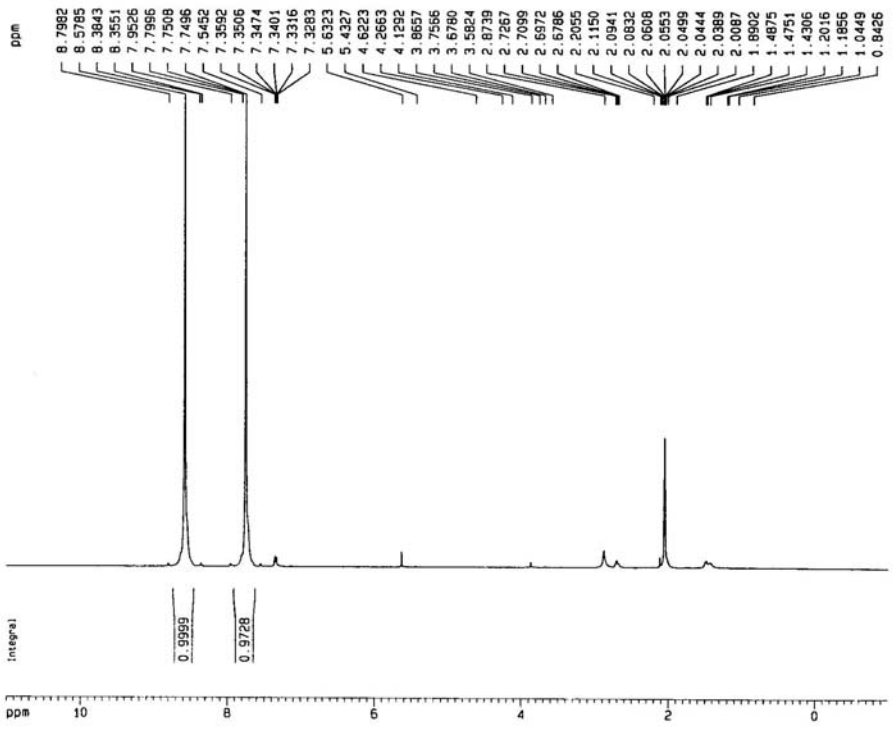

Figure 4.70 ^{1}H-NMR spectrum of 2,3,5-trideuteriopyridine (**1-2,3,5-d_3**)

Figure 4.71 shows the ^{13}C-NMR spectrum of 2,3,5-trideuteriopyridine (**1-2,3,5-d_3**). The singlets due to C6 and C4 are observed at δ 150.5 and 136.3, respectively. The triplet signals absorbing at δ 150.2 (J = 31.3 Hz) and 124.2 (J = 24.6 Hz) are due to the C2 and C5 carbon atoms. This confirms the structure of **1-2,3,5-d_3**.

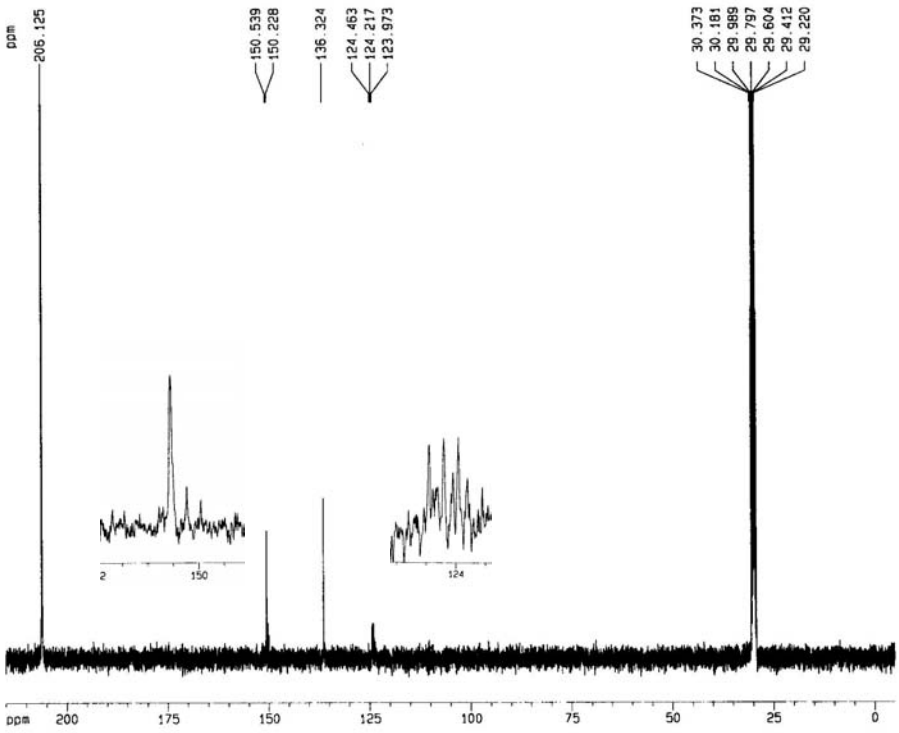

Figure 4.71 ^{13}C-NMR spectrum of 2,3,5-trideuteriopyridine (**1-2,3,5-d_3**)

4.4. Photochemistry of deuterated cyanopyridines

4.4.1. Irradiation of 2-Cyanopyridine-4,6-d_2

Irradiation of 2-cyanopyridine-4,6-d_2 (**36-4,6-d_2**) vapor (0.3-0.4 Torr) at 254 nm resulted in the formation of 3-cyanopyridine-2,5-d_2 (**37-2,5-d_2**), 3-cyanopyridine-4,6-d_2(**37-4,6-d_2**), 2-cyanopyridine-3,5-d_2(**36-3,5-d_2**), and 4-cyanopyridine-2,5-d_2(**38-2,5-d_2**). Table 4.11 shows the data from 4 hours of irradiation time.

Table 4.11 Experimental details for photolysis of 2-cyanopyridine-4,6-d_2

Exp no.	Irradiation time (min.)	Sample weight (mg)	Recovered weight (mg)	2-CNP consumption (%)	3-CNP formation (%)	4-CNP formation (%)
25	240	17	10	39.2	35.0	4.3

The ^{1}H-NMR spectra of 2-cyanopyridine-4,6-d_2 (**36-4,6-d_2**) recorded in acetone-d_6 before and after 240 minutes of irradiation are shown in Figure 4.72a and 4.72b, respectively. In Figure 4.72a, the H3 and H5 protons are observed as intense singlets at δ 7.95 and at δ 7.72, respectively. The residual proton due to H4 and H6 are observed as very tiny signals (0.04 %) at δ 8.10 and 8.79, respectively. After 240 minutes of irradiation, the ^{1}H-NMR spectrum shown in Figure 4.72b shows that four major singlets and several minor singlets have appeared after irradiation. The major signals at δ 7.63, 8.65, 8.89, and 8.99 can be assigned to the H5, H4, H2, and H6, respectively, of 3-cyanopyridine (**37**). Since each dideuterio-3-cyanopyridine photoproduct can have only two hydrogens, this indicates that two dideuterio-3-cyanopyridine isomers have been formed.

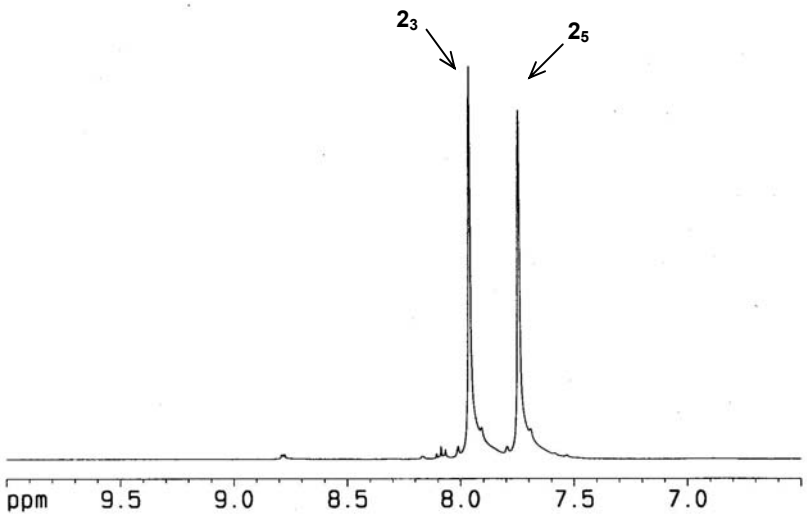

(a)

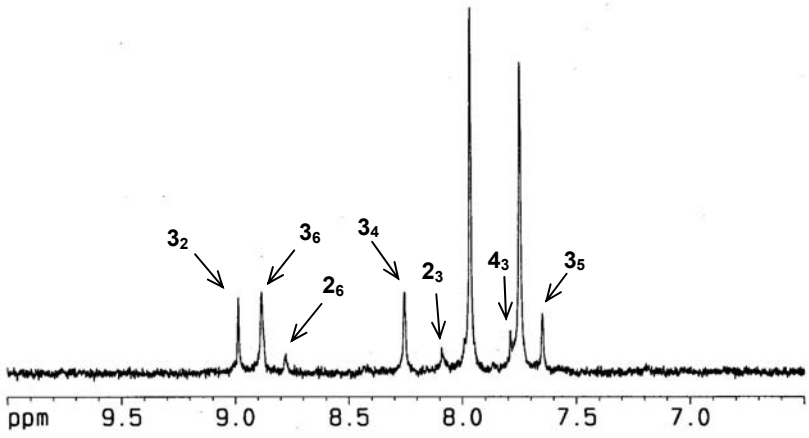

(b)

Figure 4.72 (a) ^{1}H-NMR spectrum of 2-cyanopyridine-4,6-d_2 before irradiation
(b) ^{1}H-NMR spectrum of 2-cyanopyridine-4,6-d_2 irradiated for 240 min.

Furthermore, since all four of these signals are singlets neither product can have hydrogens on adjacent carbons. Therefore, the two photoproducts must be 3-cyanopyridine-2,5-d_2 (**37-2,5-d_2**) and 3-cyanopyridine-4,6-d_2 (**37-4,6-d_2**). In addition to the proton signals of 3-cyanopyridine (**37**), small singlets at δ 8.10 and 8.87 are also observed where the H4 and H6 protons of 2-cyanopyridine (**36**) absorb. This indicates that a minor photoproduct is 2-cyanopyridine-3,5-d_2(**36-3,5-d_2**). A small singlet at δ 7.79 that is close to the intense peak of H5 proton of **36** is also observed. This signal is due to 4-cyanopyridine-2,5-d_2 (**38-2,5-d_2**) which is the last photoproduct from this particular irradiation. This NMR result shows that 3-cyanopyridine (**37**) is the major product formed from irradiation of 2-cyanopyridine (**36**). This is consistent with the quantitative GC analysis which showed a ratio of 8:1.

Therefore, excitation of 2-cyanopyridine-4,6-d_2 (**36-4,6-d_2**) results in the formation of 3-cyanopyridine-2,5-d_2 (**37-2,5-d_2**), 3-cyanopyridine-4,6-d_2(**37-4,6-d_2**), 2-cyanopyridine-3,5-d_2(**36-3,5-d_2**), and 4-cyanopyridine-2,5-d_2 (**38-2,5-d_2**) as shown in Scheme 4.44.

Scheme 4.44 Photolysis of 2-cyanopyridine-4,6-d_2 (**36-2,6-d_2**)

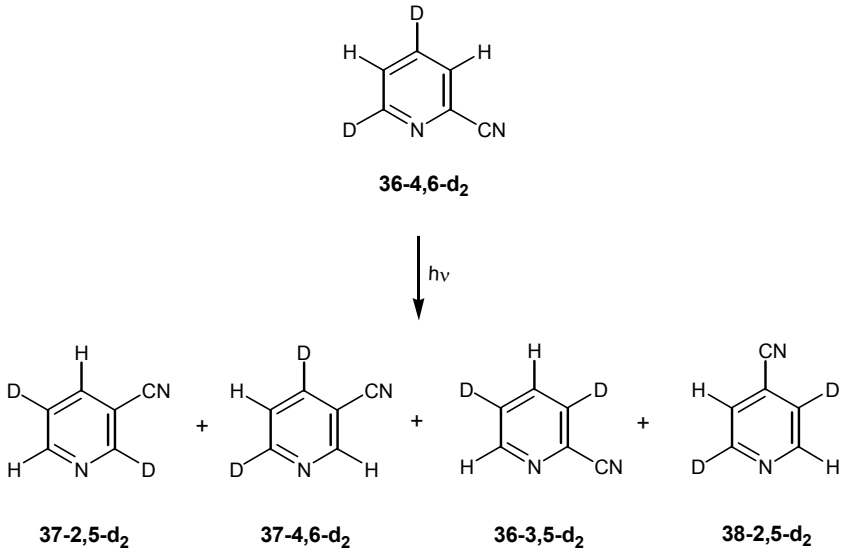

Scheme 4.45 shows the phototransposition mechanism of 2-cyanopyridine-4,6-d_2 (**36-4,6-d_2**).

Scheme 4.45 Phototransposition mechanism of 2-cyanopyridine-4,6-d_2

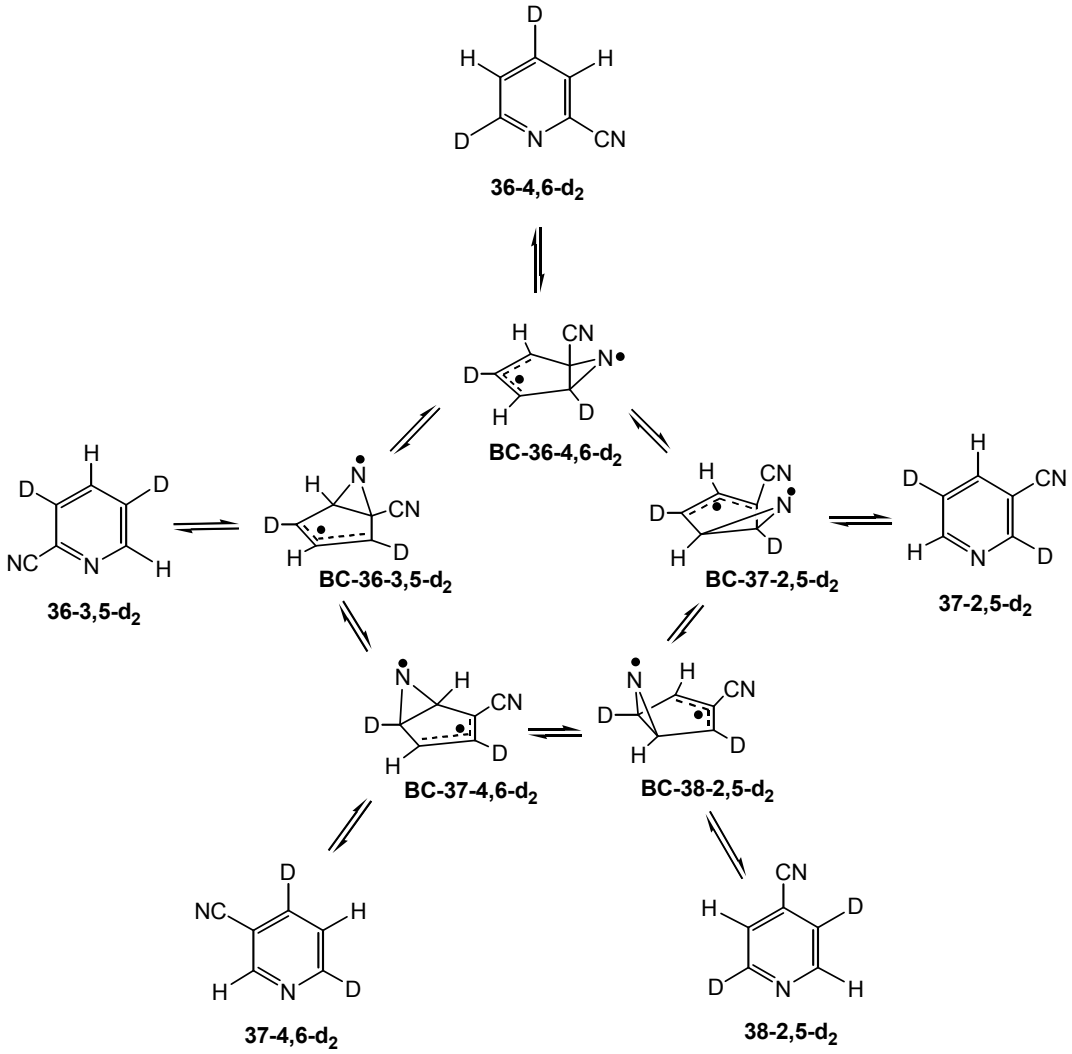

These NMR results are consistent with the mechanism shown in Scheme 4.45 which involves cyclization-2,6-bonding and nitrogen migration around five sides of cyclopentenyl ring. Excitation of **36-4,6-d_2** would result in the formation of an

azaprefulvene, **BC-36-4,6-d_2**, which undergoes nitrogen migration to form another azaprefulvene, **BC-36-3,5-d_2**. This species would rearomatize to **36-3,5-d_2** which is one minor photoproduct. Alternatively, **BC-36-3,5-d_2** would be expected to undergo rapid nitrogen migration to **BC-37-4,6-d_2**, the more stable bicyclic species. Since nitrogen migration of **BC-37-4,6-d_2** is expected to be slow, rearomatization to **37-4,6-d_2**, one of the major products, is expected to be a major reaction pathway.

Furthermore, nitrogen migration in the opposite direction from **BC-36-4,6-d_2** results in the formation of **BC-37-2,5-d_2**,which would rearrange to **37-2,5-d_2** as a major product, or undergo a second nitrogen migration to **BC-38-2,5-d_2**, the precursor of **38-2,5-d_2**, a minor product.

4.4.2. Irradiation of 3-cyanopyridine-2,6-d_2

Irradiation of 3-cyanopyridine-2,6-d_2 vapor (**37-2,6-d_2**) (0.3-0.4 Torr) at 254 nm resulted in the formation of 3-cyanopyridine-4,5-d_2 (**37-4,5-d_2**), 2-cyanopyridine-5,6-d_2 (**36-5,6-d_2**), 2-cyanopyridine-3,4-d_2 (**36-3,4-d_2**), and 4-cyanopyridine-5,6-d_2 (**38-5,6-d_2**). Table 4.12 shows the data obtained for the radiation times of 360 minutes.

Table 4.12 Experimental details for photolysis of 3-cyanopyridine-2,6-d_2

Exp no.	Irradiation time (min.)	Sample weight (mg)	Recovered weight (mg)	3-CNP consumption (%)	2-CNP formation (%)	4-CNP formation (%)
26	360	22	13	8.2	3.0	5.2

Figure 4.73a and 4.73b show the ^{1}H-NMR spectra recorded in acetone-d_6 of 3-cyanopyridine-2,6-d_2 (**37-2,6-d_2**) before irradiation and after irradiation for 360 minutes, respectively. In Figure 4.73a, the H_4 proton is observed as a doublet at δ 8.09 and the H_5 proton is observed as a doublet at δ 7.48. The residual protons at ring positions 2 and 6 are observed as very small signals (0.01%) at 8.72 and 8.82, respectively. After 360 minutes of irradiation the ^{1}H NMR spectrum shown in Figure 4.73b reveals the formation of three sets of signals. The major signals formed at δ 8.63 and 8.74 are in the region where H2 and H6 of pyridine are known to absorb. These chemical shifts are not, however, due to H2 and H6 protons of either 2-cyanopyridine (**36**) or 4-cyanopyridine (**38**). Interestingly, these signals are due to H2 and H6 of 3-cyanopyridine (**37**). This shows that the major product from irradiation of 3-cyanopyridine-2,6-d_2 (**37-2,6-d_2**) is 3-cyanopyridine-4,5-d_2 (**37-4,5-d_2**). Since this phototransposition would not be observed in

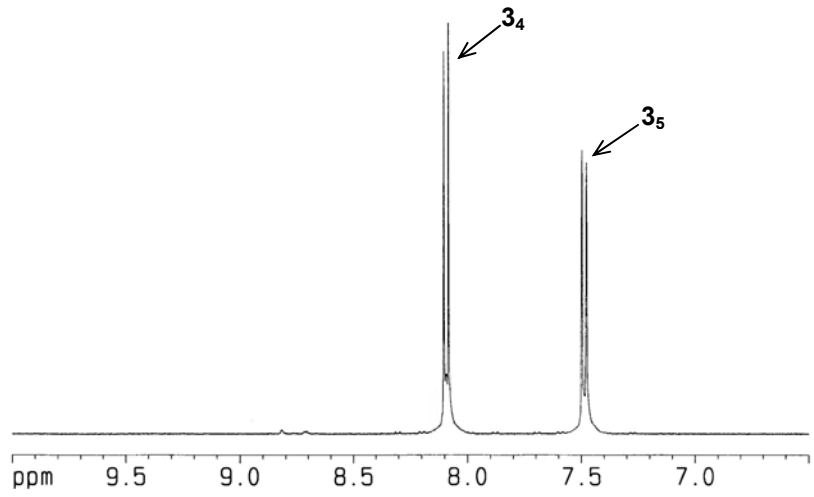

(a)

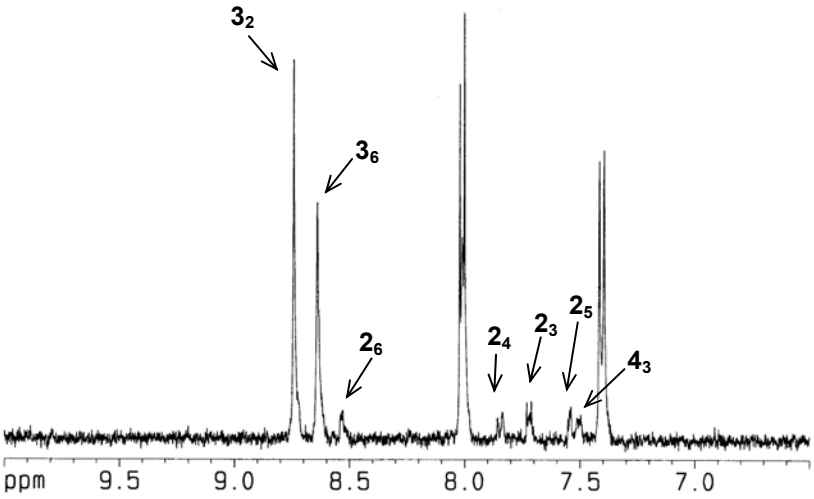

(b)

Figure 4.73 (a) ^{1}H-NMR spectrum of 3-cyanopyridine-2,6-d_2 before irradiation
(b) ^{1}H-NMR spectrum of 3-cyanopyridine-2,6-d_2 after irradiation for 360 minutes

the absence of a suitable label, this explains why undeuterated 3-cyanopyridine (**39**) appears to be so photochemically unreactive. This is because it phototransposes to itself.

In addition, a minor series of proton signals at δ 7.55, 7.72, 7.74, and 8.53 have the same chemical shift values as the H5, H3, H4, and H6 protons of 2-cyanopyridine (**36**). Because a particular dideuterio-2-cyanopyridine can exhibit signals for only two hydrogens, these four signals indicate that two different dideuterio-2-cyanopyridines, 2-cyanopyridine-3,4-d_2 (**36-3,4-d_2**) and 2-cyanopyridine-5,6-d_2 (**36-5,6-d_2**) have been formed. Furthermore, the small signal at δ 7.50 has the same chemical shift as the H3 of 4-cyanopyridine. Since this signal appears as a doublet, this product must also have a proton at ring position 2. This indicates that this minor product is 4-cyanopyridine-5,6-d_2 (**38-5,6-d_2**).

These results show that **37-2,6-d_2** phototransposes to **37-4,5-d_2** as the major product, and also to **36-3,4-d_2**, **36-5,6-d_2**, and **38-5,6-d_2** as minor products. The heights of proton signals from minor products are almost the same corresponding to the GC data showing that the minor products are formed in equal quantities.

Scheme 4.46 Photolysis of 3-cyanopyridine-2,6-d_2 (**37-2,6-d_2**)

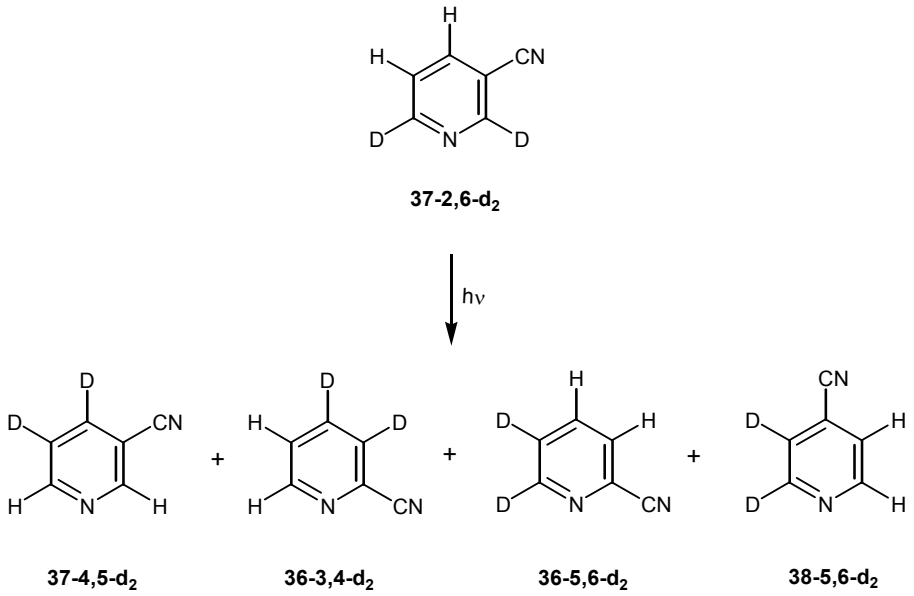

Scheme 4.47 shows the phototransposition mechanism after excitation of **37-2,6-d_2**.

Scheme 4.47 Phototransposition mechanism of 3-cyanopyridine-2,6-d_2

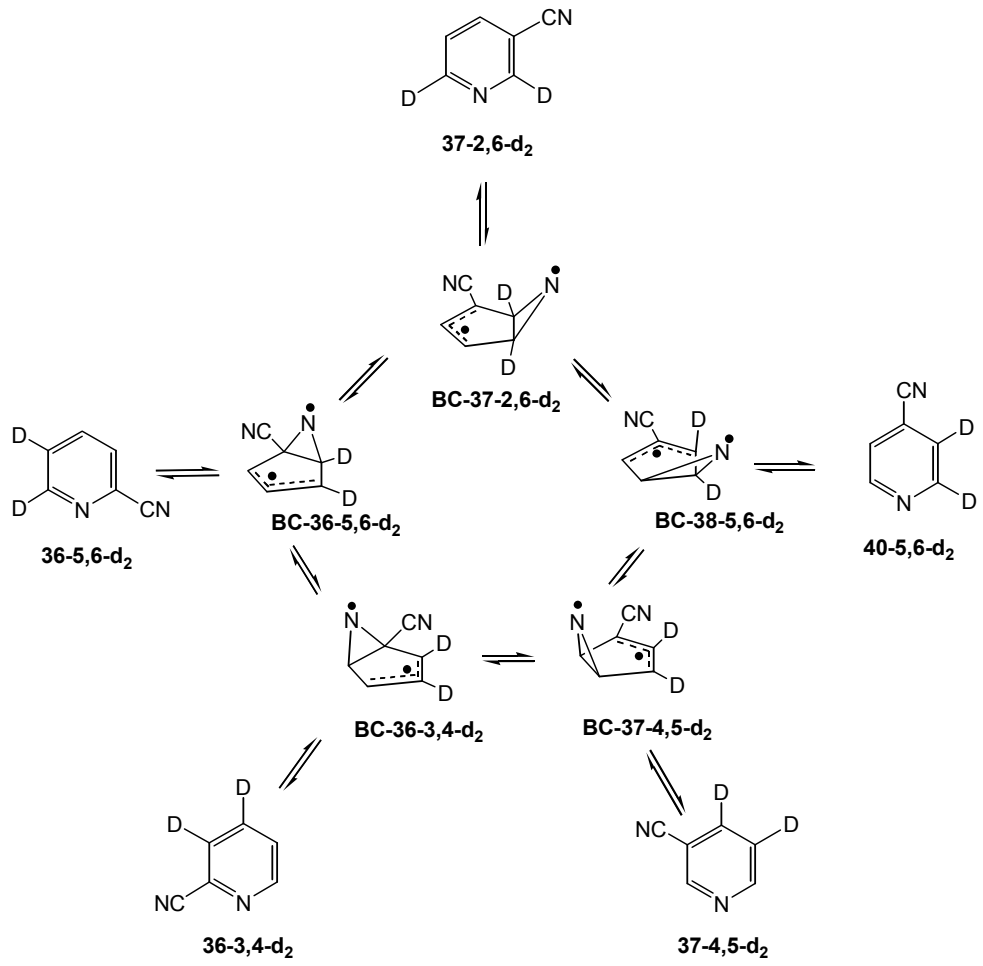

The experimental results are consistent with the mechanism shown in Scheme 4.47 which involves cyclization and nitrogen migration around all five sides of the cyclopentenyl ring. After excitation, **37-2,6-d_2** undergoes electrocyclic ring closer resulting in the formation of azaprefulvene **BC-37-2,6-d_2**, which either reverts back to

37-2,6-d_2 or undergoes sigmatropic nitrogen migration to form azaprefulvene **BC-36-5,6-d_2**. This intermediate can either rearomatize to **36-5,6-d_2**, a minor product, or azaprefulvene **BC-36-5,6-d_2** can undergo a second nitrogen migration to azaprefulvene **BC-36-3,4-d_2**, which can rearomatize resulting in the formation of a second minor product **36-3,4-d_2**. The major reaction pathway for **BC-36-3,4-d_2**, however, is expected to be the rearrangement to the more stable species **BC-37-4,5-d_2**. Since rearrangement of **BC-37-4,5-d_2** to the less stable azaprefulvenes **BC-36-3,4-d_2** or **BC-38-5,6-d_2** is expected to be slow, the major reaction pathway is rearomatization to the major product **37-4,5-d_2**.

In addition, the initially formed azaprefulvene **BC-37-2,6-d_2** can undergo nitrogen migration in the opposite direction to yield **BC-38-5,6-d_2**, the precursor of the minor product **40-5,6-d_2**, or more rapidly isomerize to **37-2,6-d_2** via **BC-37-4,5-d_2**. Thus, excitation of 3-cyanopyridine-2,6-d_2 (**37-2,6-d_2**) leads to the formation of 2-cyanopyridine-5,6-d_2 (**36-5,6-d_2**), 2-cyanopyridine-3,4-d_2 (**36-3,4-d_2**), 4-cyanopyridine-5,6-d_2 (**38-5,6-d_2**) as minor products and 3-cyanopyridine-4,5-d_2 (**37-4,5-d_2**) as a major product.

Note that in this mechanism compound **37-4,5-d_2** is the major product because it is formed from the most stabilized azaprefulvene **BC-37-4,5-d_2** which is stabilized by resonance interaction with the cyano group when it is at the end of the allyl system.

4.5.3. Irradiation of 4-cyanopyridine-2,6-d_2

Irradiation of 4-cyanopyridine-2,6-d_2 (**38-2,6-d_2**) vapor (0.3-0.4 Torr) at 254 nm resulted in the formation of 3-cyanopyridine-5,6-d_2 (**37-5,6-d_2**) and 2-cyanopyridine-4,5-d_2 (**36-4,5-d_2**). Table 4.13 shows the data obtained for the irradiation times of 30 and 60 minutes.

Table 4.13 Experimental details for photolysis of 4-cyanopyridine-2,6-d_2

Exp no.	Irradiation time (min)	Sample weight (mg)	Recovered weight (mg)	4-CNP consumption (%)	3-CNP formation (%)	2-CNP formation (%)
27	30	16	8	49.4	45.3	4.1
28	60	16	7	66.3	61.0	5.3

Figure 4.74a and 4.74b show the ^{1}H-NMR spectra recorded in acetone-d_6 of 4-cyanopyridine-2,6-d_2, **38-2,6-d_2**, before irradiation and after irradiation for 60 minutes, respectively. In Figure 4.74a, the identical H3 and H5 protons are observed as a singlet at δ 7.79 while the residual protons at positions 2 and 6 are observed as a very small signal (0.01%) at δ 8.9. After 60 minutes of irradiation the ^{1}H-NMR spectrum shown in Figure 4.74b reveals the formation of two sets of signals. The major signals at δ 9.00 and 8.27 have the same chemical shift values as the H2 and H4 protons of 3-cyanopyridine. This indicates that the major phototransposition product is 3-cyanopyridine-5,6-d_2 (**37-5,6-d_2**). The minor set of signals at δ 8.78 and 7.96 have the same chemical shift values as the H6 and H3 protons of 2-cyanopyridine (**38**) indicating that the minor phototransposition product is 2-cyanopyridine-4,5-d_2 (**36-4,5-d_2**).

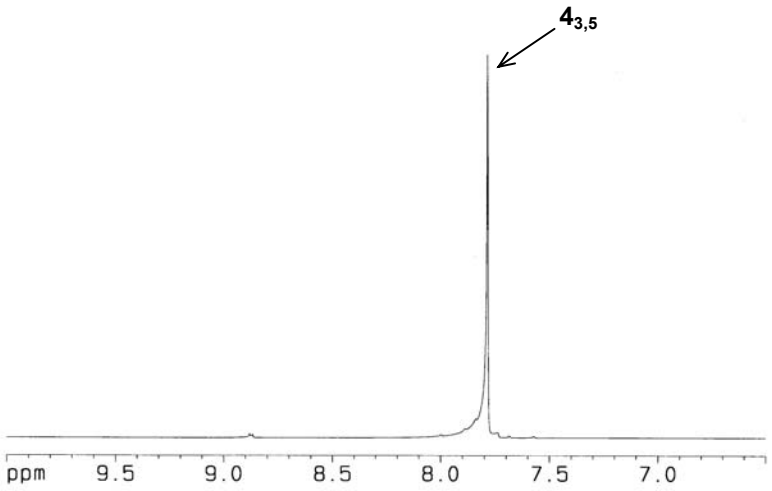

(a)

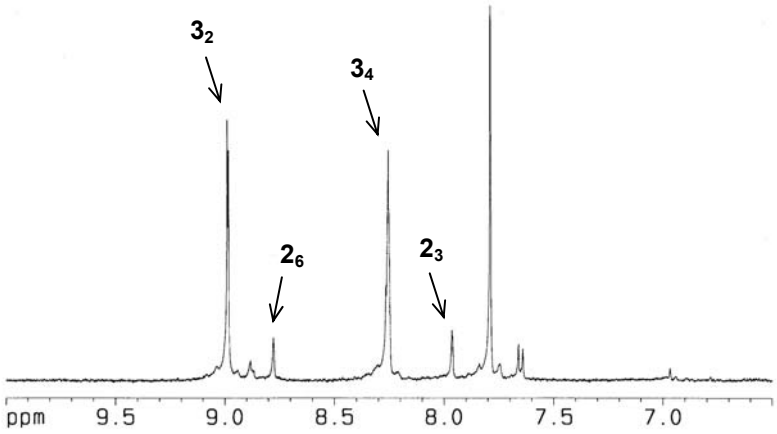

(b)

Figure 4.74 (a) ^{1}H-NMR spectrum of 4-cyanopyridine-2,6-d_2 before irradiation (b) ^{1}H-NMR spectrum of 4-cyanopyridine-2,6-d_2 after irradiation for 60 min

These results show that 4-cyanopyridine-2,6-d_2 (**38-2,6-d_2**) has phototransposed to 3-cyanopyridine-5,6-d_2 (**37-5,6-d_2**) and 2-cyanopyridine-4,5-d_2 (**36-4,5-d_2**).

Scheme 4.48 Photolysis of 4-cyanopyridine-2,6-d_2 (**38-2,6-d_2**)

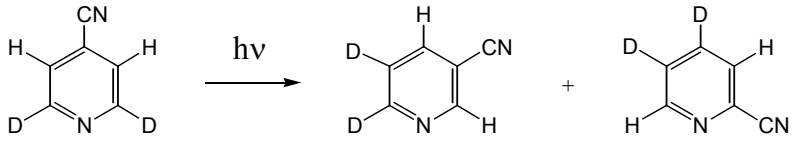

38-2,6-d_2 **37-5,6-d_2** **36-3,6-d_2**

Based on the relative heights of the major and minor ^{1}H-NMR signals, which is a very qualitative measure, the ratio of the yields of **37-5,6-d_2** to **36-4,5-d_2** is 5:1. Scheme 4.49 shows the phototransposition mechanism of 4-cyanopyridine-2,6-d_2.

Scheme 4.49 Phototransposition mechanism of 4-cyanopyridine-2,6-d_2

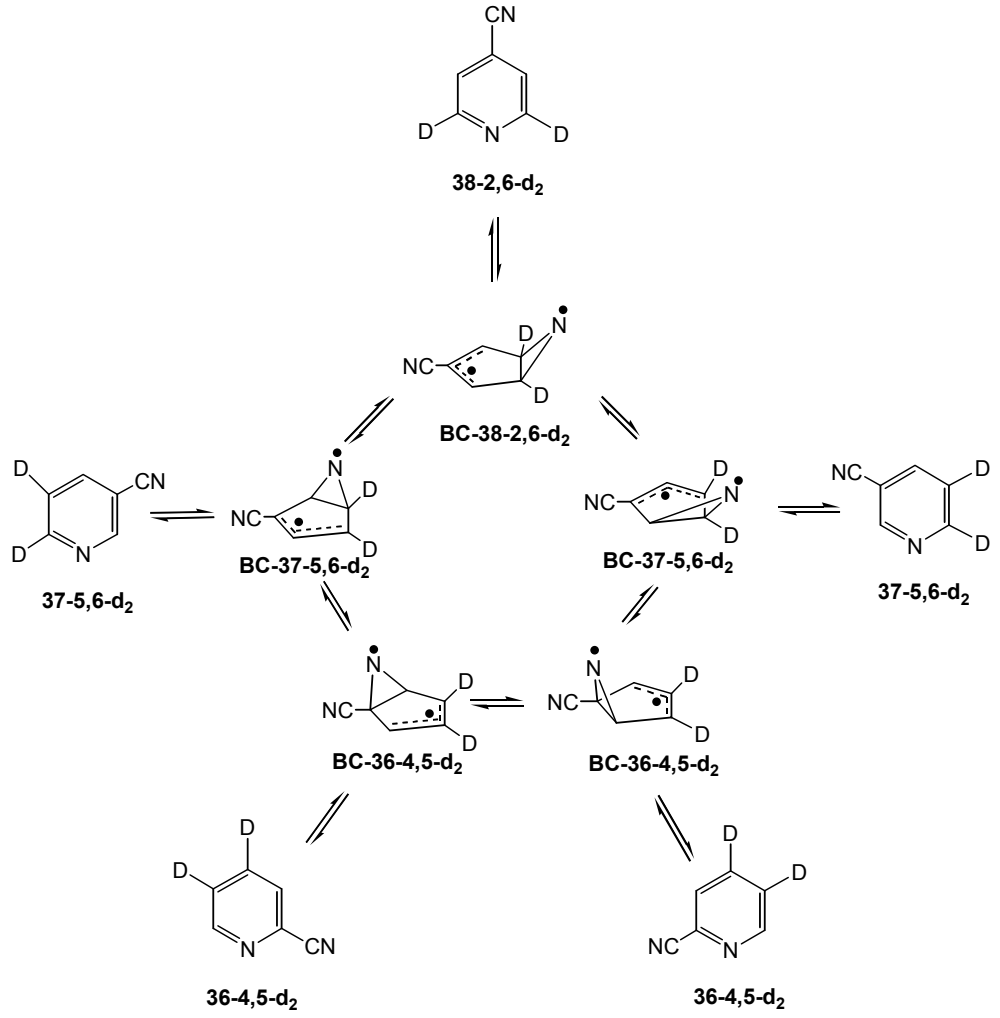

The NMR results are consistent with the mechanism shown in Scheme 4.49 involving 2,6-bonding, nitrogen migration around five sides of cyclopentenyl ring, and rearomatization. As expected, **38-2,6-d_2** undergoes cyclization between carbon position 2 and 6 resulting in the formation of **BC-38-2,6-d_2**. This intermediate can revert back to **38-2,6-d_2** or undergo nitrogen migration in either clockwise or counterclockwise directions. In the counterclockwise direction, **BC-38-2,6-d_2** would isomerize to

azaprefulvene **BC-37-5,6-d_2** which mainly rearomatizes to **37-5,6-d_2** as major product. A small portion of **BC-37-5,6-d_2**, however, can undergo a second migration of nitrogen, resulting in the formation of **BC-36-4,5-d_2**. Rearomatization of this intermediate would result in the formation of **36-4,5-d_2**, the observed minor product. This process can also occur in the opposite direction (clockwise from **BC-38-2,6-d_2**). Interestingly, from this scheme the formation of photoproducts is estimated to be in a ratio of 1:1. This inconsistency with the experimental result can be explained in term of the resonance stabilization of **BC-37-5,6-d_2**. It is stabilized by the cyano group and thus **37-5,6-d_2** is formed in higher yield than **36-4,5-d_2**. In addition, **36-4,5-d_2** is produced from the second nitrogen walk. Although **36-4,5-d_2** is also a primary product but its intermediate, **BC-36-4,5-d_2**, is scantly formed from the first nitrogen-migration intermediate.

4.5. Photochemistry of deuterated pyridines

In an attempt to simplify the ^{1}H-NMR spectrum of pyridine in order to monitor the phototransposition reactions, a number of deuterated pyridine compounds were synthesized and their photochemistry studied.

4.5.1. Irradiation of 2,6-dideuteriopyridine

The ^{1}H-NMR spectrum of 2,6-dideuteriopyridine (**1-2,6-d$_2$**) before irradiation shown in Figure 4.75 exhibits the expected triplet for the H4 proton at δ 7.6 (J = 7.6 Hz) and a doublet upfield at δ 7.2 (J = 7.6 Hz) for the two identical protons at ring positions 3 and 5. A very small signal is also visible at δ 8.55 due to residual protons at ring positions 2 and 6.

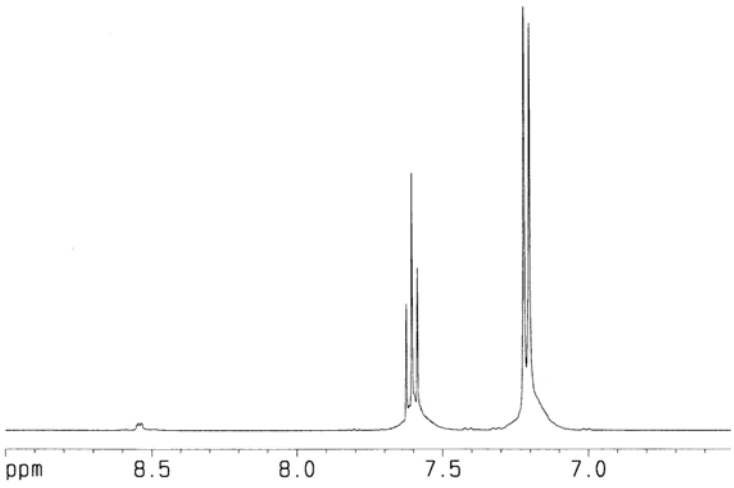

Figure 4.75 ^{1}H-NMR spectrum of 2,6-dideuteriopyridine before irradiation

The 2,6-dideuteriopyridine vapor was irradiated at 254 nm with four low pressure mercury lamps in a Rayonet photochemical reactor for 1, 5, and, 10 hours and the

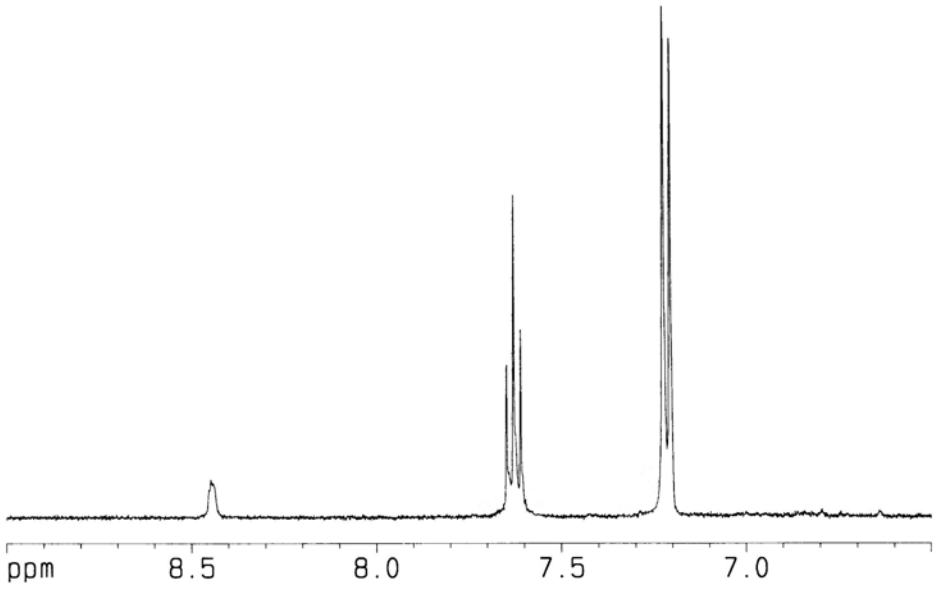

Figure 4.76 ^{1}H NMR spectrum of 2,6-dideuteriopyridine after 1 hour irradiation

progression of the reaction was monitored by ^{1}H-NMR spectroscopy. After irradiation for one hour the ^{1}H-NMR spectrum in Figure 4.76 shows that a new signal has appeared at δ 8.45 where H2 and H6 of pyridine are known to absorb. Figure 4.77 shows that the ^{1}H-NMR spectral changes are more pronounced after 5 hours of irradiation. The scale expansion shown in Figure 4.78 shows that the signal in the δ 8.45 region consists of a broad singlet at δ 8.48 (this signal may be two closely spaced singlets) overlapped by a doublet at δ 8.48 (J = 4.4 Hz). This suggests that a photoproduct has been formed in which H2 appears as a singlet, and thus a deuterium atom is located at position 3, and H6

appears as a doublet, and thus a hydrogen atom is located at position 3. This indicates that the photoproduct is 3,4-dideuteriopyridine (**1-3,4-d_2**).

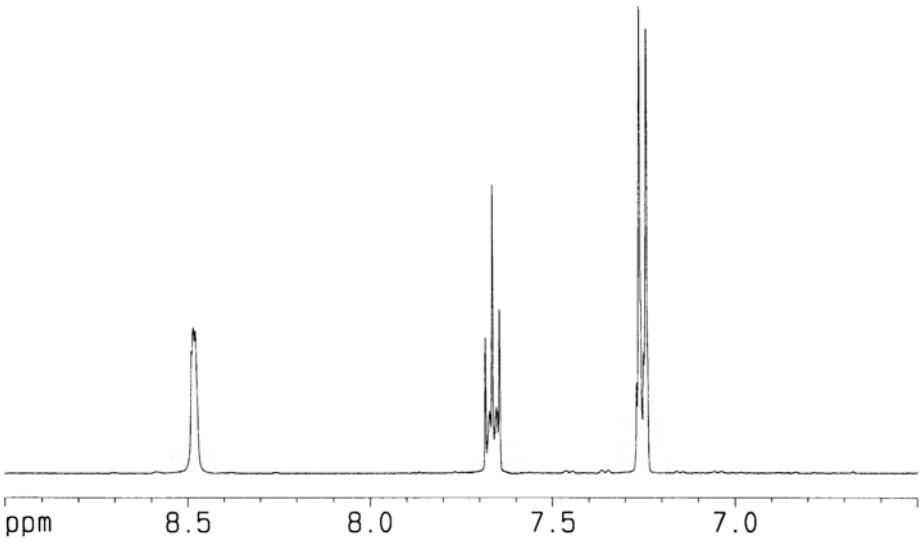

Figure 4.77 ^{1}H NMR spectrum of 2,6-dideuteriopyridine after 5 hours irradiation

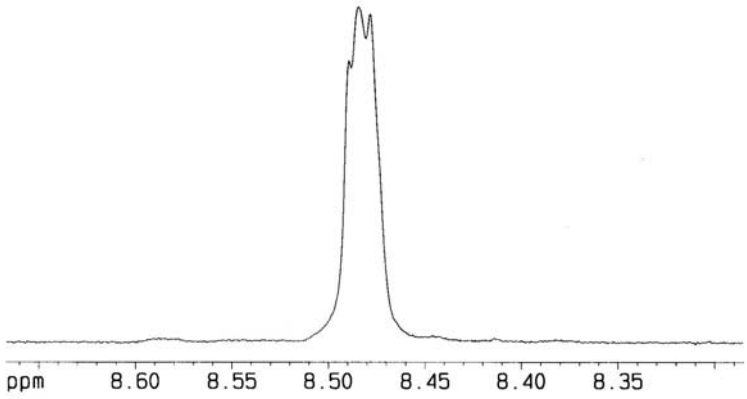

Figure 4.78 Expansion of signal at δ 8.48

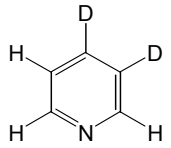

1-3,4-d_2

In addition to the singlet and doublet for the H2 and H6 protons, this compound also requires a doublet for the H5 proton in the δ 7.25 region of the spectrum which should exhibit a coupling constant of ~4.5 Hz since it is coupling with the H6 proton in **1-3,4-d_2**.

Examination of the scale-expansions of that spectral region recorded after 1, 5, and 10 hours of irradiation as shown in Figure 4.79 shows the appearance of four new signals at δ 7.261, 7.249, 7.242, and 7.233 which are apparently due to two new doublets. Considering the requirement that the coupling constant be ~ 4.5 Hz, the two new signals at δ 7.261 and 7.249 have been assigned to the H5 proton in **1-3,4-d_2**. This proton thus appears as a doublet (J = 4.8 Hz) at δ 7.255.

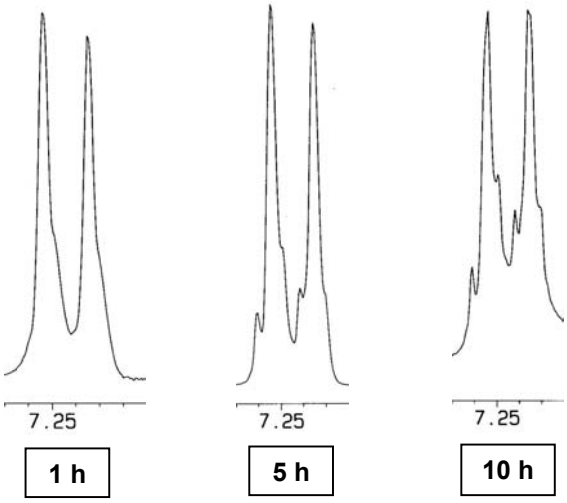

Figure 4.79 Expansion of proton position 3 and 5 after irradiated for 1, 5, and 10 h

In addition to the signals due to the formation of **1-3,4-d_2**, examination of the δ 7.6-7.7 region of the spectrum where the H4 proton of pyridine is known to absorb shows the appearance of a doublet at δ 7.66 (J = 7.6 Hz) overlapping with the triplet due to H4 proton of the reactant. This indicates that an additional product has been formed that has a proton at H4 which is adjacent to only one other hydrogen at C3 or C5. The coupling constant of 7.6 Hz is consistent with this. This suggests that the second product is either 2,3-dideuteriopyridine (**1-2,3-d_2**) or 2,5-dideuteriopyridine (**1-2,5-d_2**).

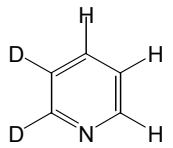

1-2,3-d_2

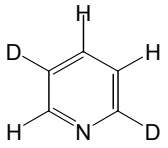

1-2,5-d_2

Further examination of the δ 7.25 region of the spectrum reveals that a second doublet has been formed at δ 7.236 (J = 4.8 Hz) indicating the presence of a second H3 or H5 proton coupling with a proton at H2 and H6. This suggests that the second photoproduct is **1-2,3-d_2**.

In summary, the best interpretation of the ^{1}H-NMR spectroscopic data indicates that 2,6-dideuteriopyridine (**1-2,6-d_2**) has undergone phototransposition to a mixture of 2,3-dideuteriopyridine (**1-2,3-d_2**) and 3,4-dideuteriopyridine (**1-3,4-d_2**) as shown in Scheme 4.50.

Scheme 4.50 Photolysis of 2,6-dideuteriopyridine (**1-2,6-d_2**)

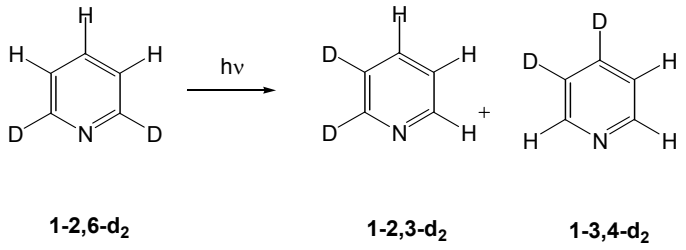

1-2,6-d_2 **1-2,3-d_2** **1-3,4-d_2**

4.5.2. Mechanistic discussion of deuterated pyridines

The experimental results described earlier have shown that the isomerization products observed from irradiation of pyridine result from the insertion of a nitrogen atom between two carbons of carbon skeleton of the pyridine ring.

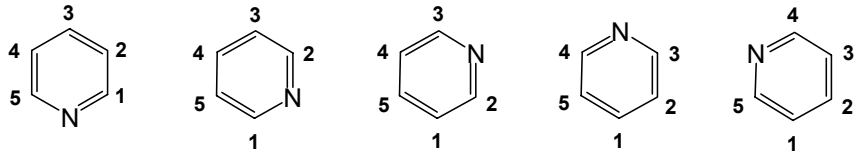

The mechanism that will allow this selective nitrogen insertion involves 2,6-bonding followed by nitrogen migration around the five sides of cyclopentenyl ring and rearomatization to the new pyridine isomers.[63] Cyclization-heteroatom migration mechanisms have been employed to explain the phototransposition of 5- and 6-membered heteroaromatic compounds, such as cyanotoluenes and lutidines. [17,64]

The bonding between carbon at position 2 and 6 of pyridine results in the formation of non-planar azabicyclohexenyl species as a diradical called azaprefulvene.

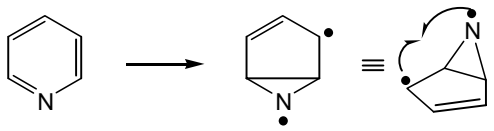

azaprefulvene

Nitrogen migration around the five sides of the cyclopentenyl ring leads to the interconversion of the bicyclic intermediates, which after rearomatization it results in the formation of pyridine isomers. This nitrogen migration could occur via the intermediacy of an azabenzvalene valence isomer but there is no evidence of its involvement in the present case.

The photochemistry of pyridine vapor was studied by several research groups.[7,8] Interestingly, there was no photoproduct upon irradiation of pyridine vapor that could be identified and thus it was suggested to be non-reactive. With deuterium labeling study developed in our laboratory, the photochemistry of pyridine vapor was reinvestigated. Irradiation of deuterium-labeled pyridine could lead to the formation of deuterium-labeled pyridine isomers different from the original pyridine compound. In this way, it could be observed that pyridine vapor is indeed not non-reactive but that it undergoes phototransposition to itself. Our work in the deuterium-labeled pyridine is successful in defining two significant points. First, it reveals that pyridine vapor is reactive and it undergoes phototransposition when it is irradiated. Second, it phototransposes via the azaprefulvene intermediate, supporting the Cyclization-heteroatom migration mechanism.

4.5.3. 2,6-Dideuteriopyridine

Irradiation of 2,6-dideuteriopyridine (**1-2,6-d_2**) in the vapor phase at 254 nm yielded 2,3-dideuteriopyridine(**1-2,3-d_2**) and 3,4-dideuteriopyridine (**1-3,4-d_2**) which were identified by the ^{1}H-NMR spectrum shown in Figure 4.75 and 4.77. The observation of **1-2,3-d_2** and **1-3,4-d_2** are consistent with the proposed mechanism. Shown in Scheme 4.51, the interconversion of **1-2,6-d_2**, **1-2,3-d_2** and **1-3,4-d_2** can be rationalized by the 2,6-bridging-cyclization to form bicyclic intermediate **BC-2,6-d_2**. One nitrogen migration in a clockwise direction leads to the formation of another bicyclic isomer, **BC-2,3-d_2**, which can rearomatize to form **1-2,3-d_2** or undergo a second nitrogen migration to form **BC-3,4-d_2** which would rearomatize to **1-3,4-d_2**. **BC-2,6-d_2** can undergo one nitrogen migration in a counter clockwise direction resulting in the formation of **BC-2,3-d_2'**, which could rearomatize to **1-2,3-d_2** pyridine or undergo a second nitrogen migration and then rearomatization to **1-3,4-d_2**. All photoproducts that were observed in the ^{1}H-NMR spectrum therefore confirmed the suggested mechanism.

Scheme 4.51 Phototransposition mechanism of 2,6-dideuteriopyridine (**1-2,6-d$_2$**)

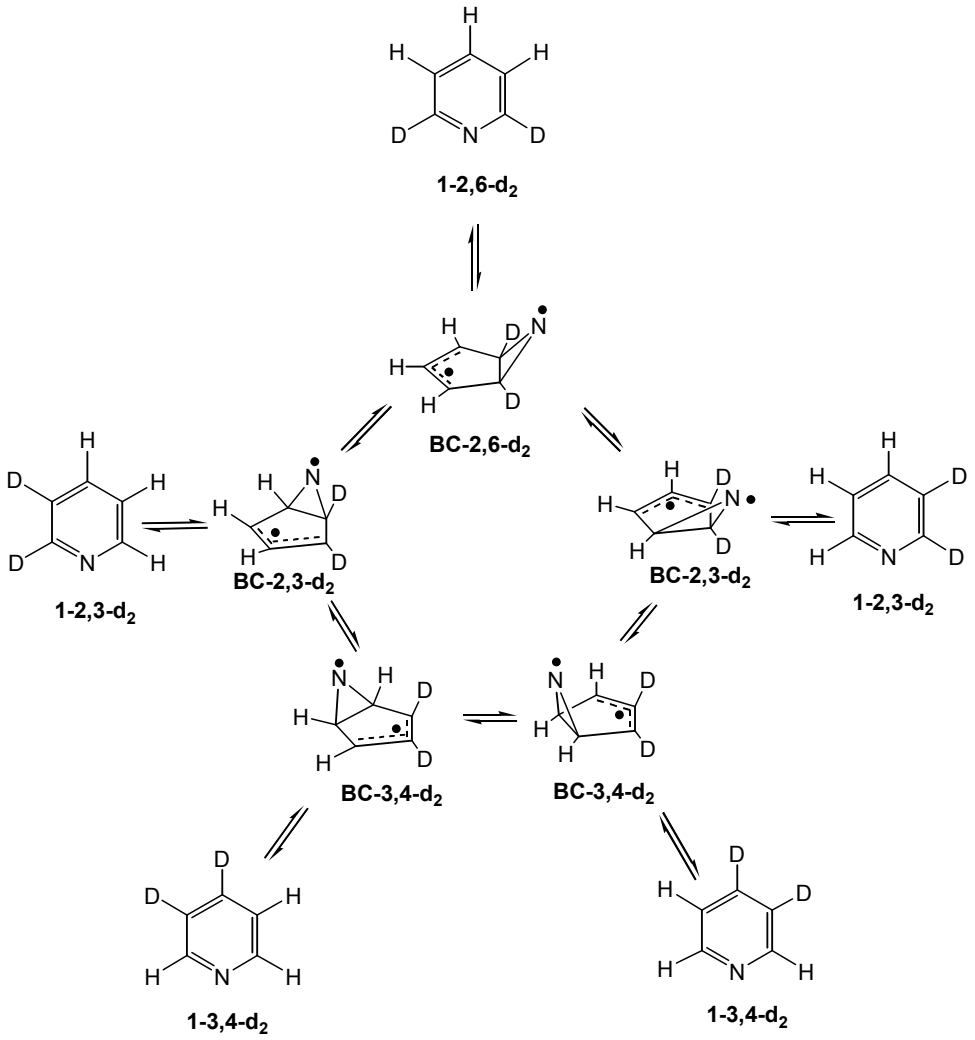

In addition to the 2,6-briging cyclization-nitrogen migration mechanism shown in Scheme 4.51, mechanisms involving rearranging Dewar-pyridine and azaprismanes should also be considered.

The phototransposition mechanism via the Dewar-pyridine sigmatropic shift mechanism is shown in Scheme 4.52. The 2,5- and 3,6- bridging of **1-2,6-d$_2$** yields the same Dewar-pyridine, **DP-2,6-d$_2$**.

Scheme 4.52 Dewar-pyridine mechanism of **1-2,6-d$_2$**

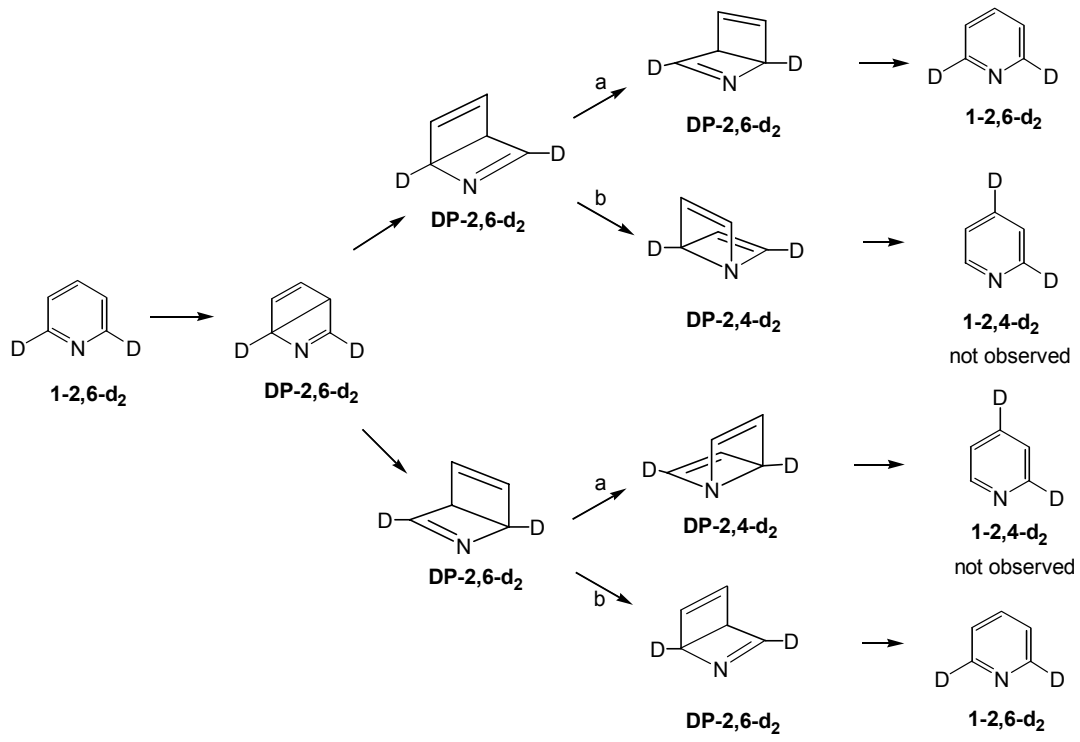

Scheme 4.52 shows that sigmatropic nitrogen migration of **DP-2,6-d$_2$** would result in the formation of **DP-2,6-d$_2$** itself or a new Dewar-pyridine structure, **DP-2,4-d$_2$**. Rearomatization of this species would lead to 2,4-dideuteriopyridine (**1-2,4-d$_2$**) which is not one of the products observed in the ^{1}H-NMR spectrum shown in Figure 4.77. This indicated that in this reaction the Dewar-pyridine mechanism is not in operation.

The phototransposition of **1-2,6-d$_2$** via the formation of azaprismane was also examined. Scheme 4.53 shows that [2+2] cycloaddition of **DP-2,6-d$_2$** would result in the formation of azaprismane (**96**). The ring cleavage of **96** can either result back to the Dewar structure of **1-2,6-d$_2$** or in the formation of two Dewar-pyridine intermediates **96a** and **96b**. Rearomatization of these species results in the formation of 2,4-dideuteriopyridine (**1-2,4-d$_2$**) and 2,5-dideuteriopyridine (**1-2,5-d$_2$**).

Scheme 4.53 Azaprismane mechanism of **DP-2,6-d$_2$**

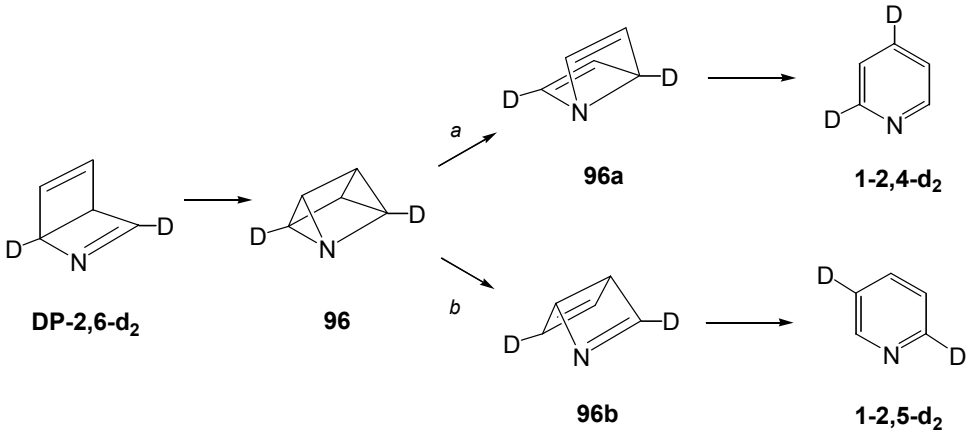

The photoproducts predicted by this mechanism should be carefully considered. Although the structure of **1-2,4-d$_2$** is not consistent with the ^{1}H-NMR spectrum obtained for the photoproducts, the predicted product **1-2,5-d$_2$** would be consistent with the observed ^{1}H-NMR spectrum. Thus, **1-2,5-d$_2$** would be expected to exhibit a doublet due to the H4 proton and H3 and H6 would be expected to appear as a doublet in the H3 region and a singlet in the H2,6 region of the spectrum. Thus, the ^{1}H-NMR spectrum might be interpreted to suggest that **1-2,5-d$_2$** has been formed. If the azaprismane mechanism is in operation it seems strange that it is selective to yield **1-2,5-d$_2$** but not **1-**

2,4-d_2. Since the latter product is not observed, it does not seem likely that the photoreaction has followed the azaprismane mechanism.

4.6. Photochemistry of trideuteriopyridines

4.6.1. Irradiation of 3,4,5-trideuteriopyridine (1-3,4,5-d_3)

Irradiation of the 3,4,5-trideuteriopyridine (**1-3,4,5-d_3**) vapor was carried out at 254 nm with four low-pressure mercury lamps in a Rayonet photochemical reactor for 12 and 24 hours. After each of irradiation, the photoproduct was analyzed by ^{1}H-NMR in acetone-d_6. Figure 4.80 and 4.81 show the ^{1}H-NMR spectra of 3,4,5-trideuteriopyridine (**1-3,4,5-d_3**) before and after irradiation at 254 nm for 24 hours.

Figure 4.80 shows that the ^{1}H-NMR spectrum of 3,4,5-trideuteriopyridine (**1-3,4,5-d_3**) before irradiation exhibits only a singlet at δ 8.60 due to the equivalent H2 and H6 protons. A small signal which is barely observed at δ 7.35 is due to the residual protons H3 and H5.

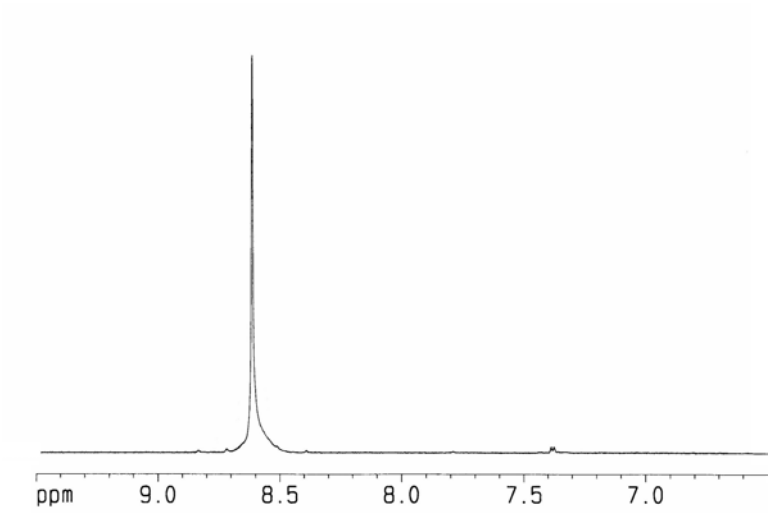

Figure 4.80 ^{1}H-NMR spectrum of **1-3,4,5-d_3** before irradiation

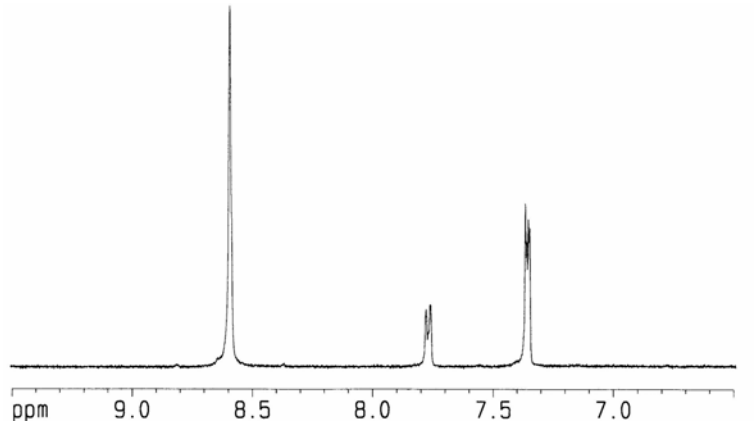

Figure 4.81 ^{1}H NMR spectrum of **1-3,4,5-d$_3$** after 24 hours irradiation

After irradiation, the spectrum in Figure 4.81 shows that a new signal has appeared as a doublet at δ 7.75 (J = 6.63 Hz), where H4 of pyridine absorbs, and a multiplet at δ 7.35 due to H3 and H5 protons. This result is consistent with the formation of new pyridines which contain H4, H3, and H5 protons. In addition, since the H4 proton is observed as a doublet, there is one adjacent proton coupling with it. The H3 and H5 proton signal consists of two overlapping doublets which indicate that in both cases the H3 and H5 protons are also coupling with only one adjacent proton. This interpretation leads to the conclusion that the product is a mixture of 2,3,4-trideuteriopyridine (**1-2,3,4-d$_3$**) and 2,3,6-trideuteriopyridine (**1-2,3,6-d$_3$**). The structures of these new photoproducts are shown in Scheme 4.54.

Scheme 4.54 Photolysis of 3,4,5-trideuteriopyridine (**1-3,4,5-d$_3$**)

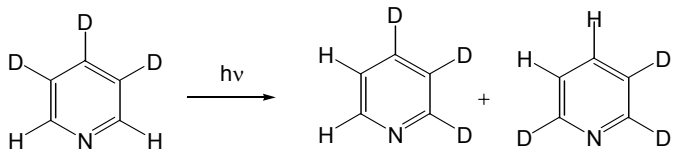

1-3,4,5-d$_3$ **1-2,3,4-d$_3$** **1-2,3,6-d$_3$**

The H6 proton of **1-2,3,4-d$_3$** is obscured by the signal for the H2,6 protons of the reactant and the H5 proton appears as a doublet (J ~ 4.8 Hz) in the H3-H5 region. The second photoproduct, 2,3,6-trideuteriopyridine (**1-2,3,6-d$_3$**), exhibits the doublet for the H4 proton which is observed in the H4 region and a doublet (J = 7.0 Hz) for the H5 proton which is overlapping with the H5 doublet from **1-2,3,4-d$_3$**. As expected for an equimolar mixture of **1-2,3,4-d$_3$** and **1-2,3,6-d$_3$**, the signals for the H5 and H4 protons are observed in Figure 4.81 as an integrated ratio of approximately 2:1.

Figure 4.82 shows an expansion of the region showing the overlapping doublets for the H5 proton for the two products. This signal is expected to consist of two overlapping doublets with essentially the same chemical shifts but with coupling constants of approximately 4.8 Hz ($J_{5,6}$) and approximately 7.0 Hz ($J_{4,5}$). Thus, the signal was expected to appear as four lines as simulated below.

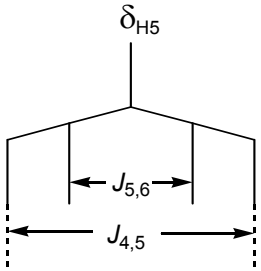

Figure 4.82, however, shows that the signal shows additional coupling and is therefore more complicated. It was suspected that this additional coupling may be due to H-D coupling.

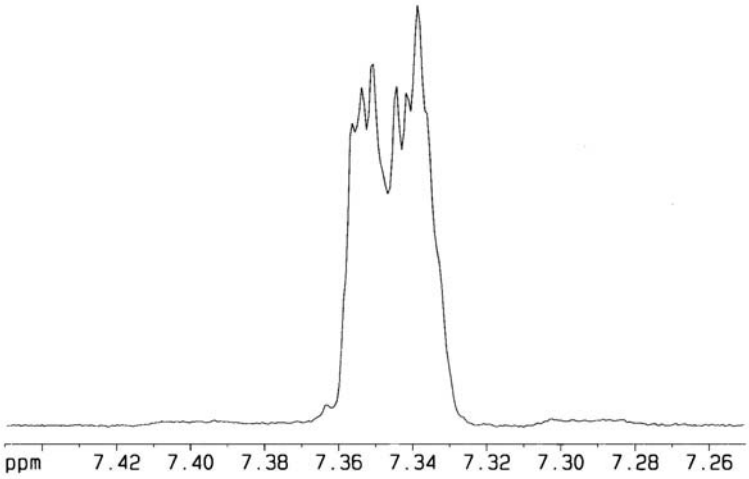

Figure 4.82 ^{1}H-NMR expansion of H5 from photoproducts

In order to explore this, one of the photoproducts, 2,3,4-trideuteriopyridine (**1-2,3,4-d_3**) was synthesized and its ^{1}H-NMR spectrum was studied. The scale expansion of the signal due to the H5 proton is shown in Figure 4.83.

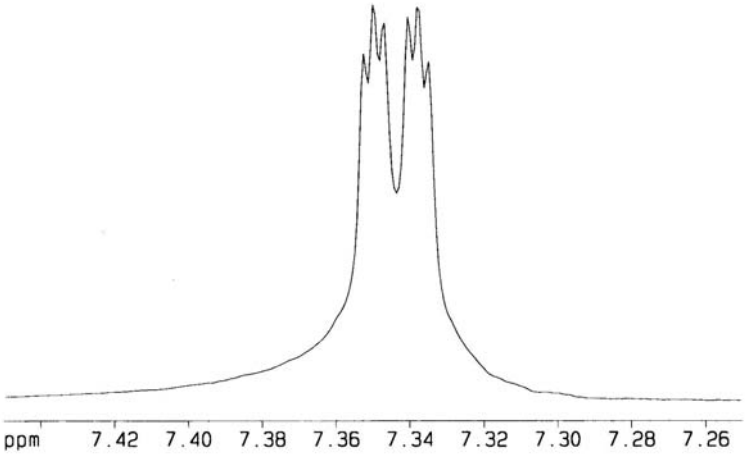

Figure 4.83 Scale expansion of H5 from 2,3,4-trideuteriopyridine (**1-2,3,4-d_3**)

Since this proton is coupling with the H6 proton, in the absence of additional coupling, this signal would be expected to appear as a doublet with a coupling constant of 4.8 Hz. Figure 4.83 shows, however, that the signal appears as a doublet of triplets with coupling constants of 1.0 Hz and 4.8 Hz. This is consistent with the H5 proton coupling with the H6 proton (J = 4.8 Hz) and with the deuterium (J = 1.0 Hz) at ring position 4. The signal due to the photoproduct shown in Figure 4.82 also shows this additional H-D coupling.

4.6.2. Irradiation of 2,4,6-trideuteriopyridine (1-2,4,6-d_3)

Irradiation of the 2,4,6-trideuteriopyridine (**1-2,4,6-d_3**) vapor (2-4 Torr) was carried out at 254 nm with four low pressure mercury lamps in the Rayonet photochemical reactor for 5 and 11 hours. The ^{1}H-NMR spectra of **1-2,4,6-d_3** recorded in acetone-d_6 before and after irradiation are shown in Figure 4.84 and 4.85, respectively.

In Figure 4.84, the ^{1}H-NMR spectrum shows a singlet signal due to the H3 and H5 protons at δ 7.37 which confirms the deuterium exchange at the other ring positions. In addition, a small triplet signal due to the residual H4 proton is observed at δ 7.78 and a tiny signal due to the residual H2,6 protons is observed at δ 8.60.

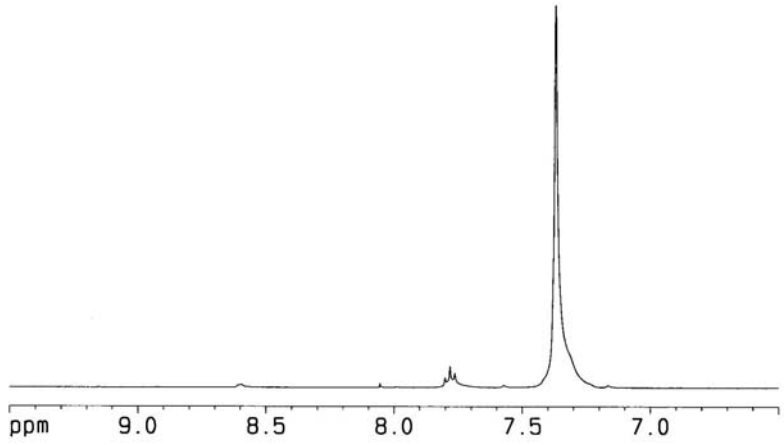

Figure 4.84 ^{1}H-NMR spectrum of **1-2,4,6-d$_3$** before irradiation

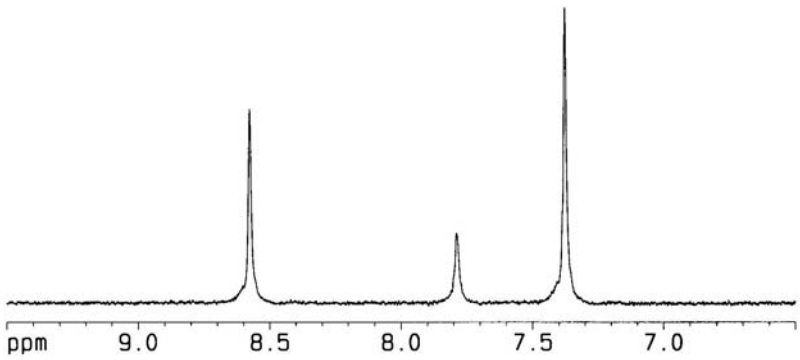

Figure 4.85 ^{1}H-NMR spectrum of **1-2,4,6-d$_3$** after 11 hours irradiation

The ^{1}H-NMR spectrum after irradiation of **1-2,4,6-d$_3$** for 11 h, shown in Figure 4.85, exhibits new singlets at δ 8.58, where H2 and H6 protons are known to absorb, and

at δ 7.79, where the H4 proton of pyridine is known to absorb, in an integrated ratio of 2: 1.

According to these new signals, one of the photoproducts must have a proton at ring position 4 with deuterium atoms at ring position 3 and 5. The third deuterium atom must be at ring position 2 while the second hydrogen must be at ring position 6. Thus, one of the photoproducts must be 2,3,5-trideuteriopyridine, **1-2,3,5-d_3**.

The second photoproduct must have one proton at ring position 6. According to the spectrum, the second proton cannot be at ring positions 2, 4, or 5. This proton therefore must be at ring position 3 and the product must be 2,4,5-trideuteriopyridine, **1-2,4,5-d_3**.

Scheme 4.55 Photolysis of 2,4,6-trideuteriopyridine (**1-2,4,6-d_3**)

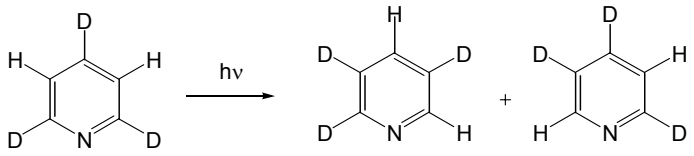

1-2,4,6-d_3 **1-2,3,5-d_3** **1-2,4,5-d_3**

These ^{1}H-NMR results thus show that 2,4,6-trideuteriopyridine (**1-2,4,6-d_3**) undergoes phototransposition to a mixture of 2,3,5-trideuteriopyridine, **1-2,3,5-d_3**, and 2,4,5-trideuteriopyridine, **1-2,4,5-d_3**.

4.6.3. Irradiation of 2,3,4-trideuteriopyridine (1-2,3,4-d_3)

2,3,4-Trideuteriopyridine (**1-2,3,4-d_3**) vapor was irradiated at 254 nm with four low pressure mercury lamps in the Rayonet photochemical reactor for 12 hours. The ^{1}H-NMR spectrum of **1-2,3,4-d_3** before irradiation shown in Figure 4.86 exhibits two doublets due to the H6 and H5 protons at δ 8.59 and 7.34. As previously shown in Figure 4.83, scale-expansion of the signal at δ 7.34 shows that the signal can be resolved into a doublet of triplets due to coupling of H5 with H6 and with the deuterium atom at position 4.

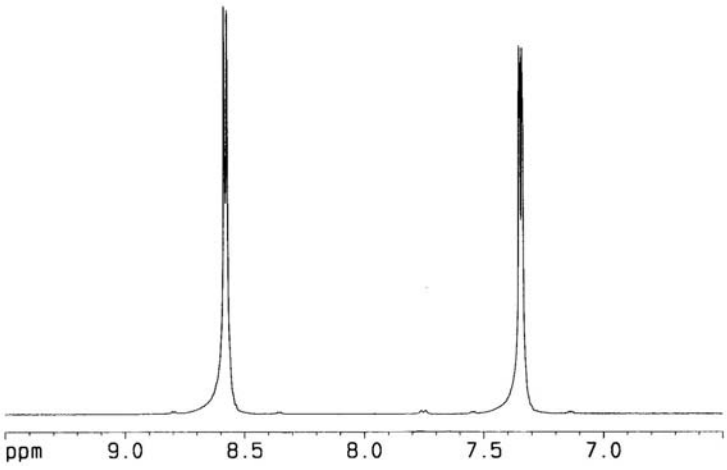

Figure 4.86 ^{1}H-NMR spectrum of **1-2,3,4-d_3** before irradiation

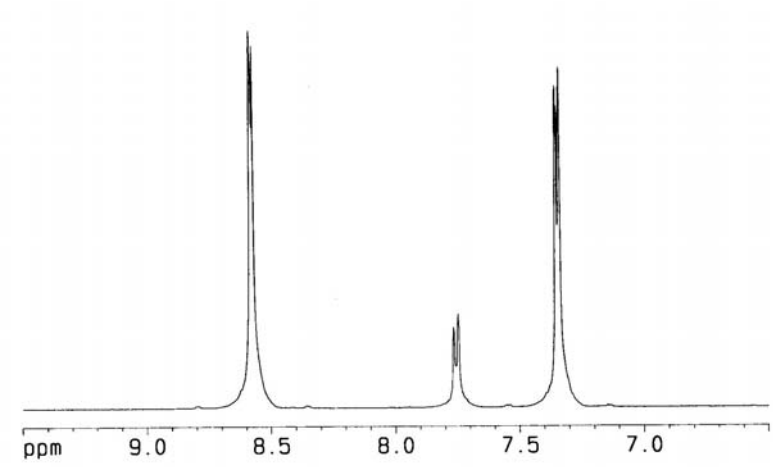

Figure 4.87 ^{1}H-NMR spectrum of **1-2,3,4-d$_3$** after 12 hours

Figure 4.87 shows that after 12 hours of irradiation a doublet signal appears in the ^{1}H-NMR spectrum at δ 7.76 (J = 7.57 Hz) due to the formation of a product with protons at ring positions 4 and 3(5). This photoproduct must be **1-2,3,6-d$_3$**.

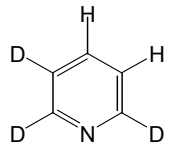

1-2,3,6-d$_3$

A scale expansion of the signal at δ 8.59 shown in Figure 4.88 shows that after irradiation a singlet is now superimposed on the doublet due to the H6 proton of the reactant.

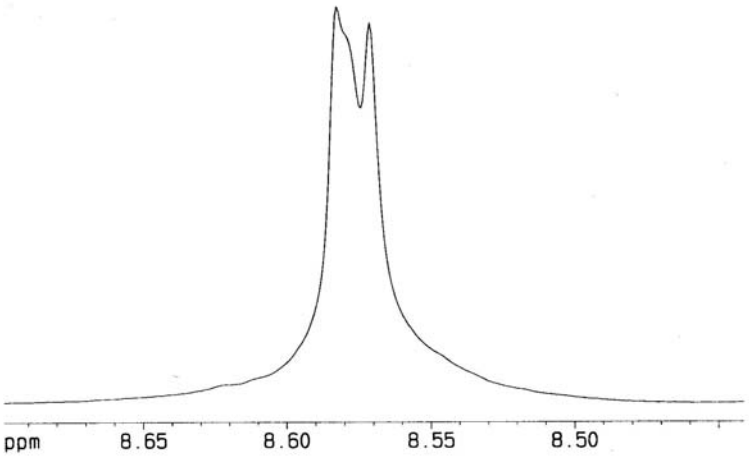

Figure 4.88 Scale expansion of H6 after 12 hours of irradiation

Since no other new signals are apparent in the ^{1}H-NMR spectrum, this new singlet must be due to a photoproduct with two protons at H2 and H6 and the new product must be **1-3,4,5-d_3**.

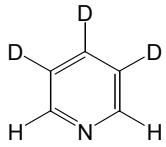

1-3,4,5-d_3

Interestingly, the ^{1}H-NMR spectrum of this same mixture of compounds, i.e., **1-2,3,4-d_3** and **1-3,4,5-d_3**, was also observed as the product mixture formed from irradiation of **1-2,3,6-d_3**. A scale expansion of the H2(H6) signal in that case is shown in Figure 4.91. The slightly different appearance of the two signals is due to the different ratios of the compounds in the two samples. In Figure 4.91, **1-2,3,4-d_3** and **1-3,4,5-d_3** were both photoproducts. In Figure 4.88, **1-2,3,4-d_3** is unconsumed reactant while **1-3,4,5-d_3** is a photoproduct.

This shows that **1-2,3,4-d$_3$** has undergone phototransposition to yield a mixture of **1-2,3,6-d$_3$** and **1-3,4,5-d$_3$**.

Scheme 4.56 Photolysis of 2,3,4-trideuteriopyridine (**1-2,3,4-d$_3$**)

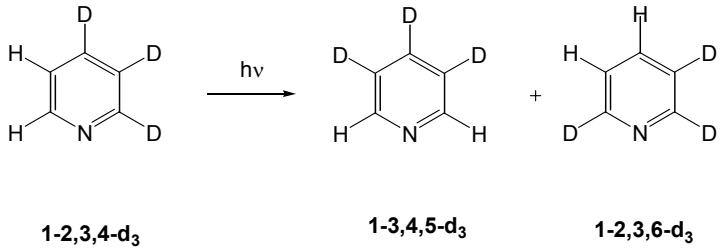

1-2,3,4-d$_3$ **1-3,4,5-d$_3$** **1-2,3,6-d$_3$**

4.6.4. Irradiation of 2,3,6-trideuteriopyridine (1-2,3,6-d$_3$)

The photolysis of 2,3,6-trideuteriopyridine (**1-2,3,6-d$_3$**) was carried out by irradiating its vapor in Rayonet reactor with four 254nm lamps for 12 hours. Figure 4.89 and 4.90 show the ^{1}H-NMR spectra in acetone-d$_6$ of **1-2,3,6-d$_3$** before and after irradiation for 12 hours.

Before irradiation, the ^{1}H-NMR spectrum shown in Figure 4.89 exhibits two doublets due to the H4 and H5 protons of **1-2,3,4-d$_3$**. These signals are observed at δ 7.76 (J = 7.6 Hz) and 7.34 (J = 7.6 Hz), respectively. The residual protons at ring positions 2 and 6 are also observed as a small singlet at δ 8.60.

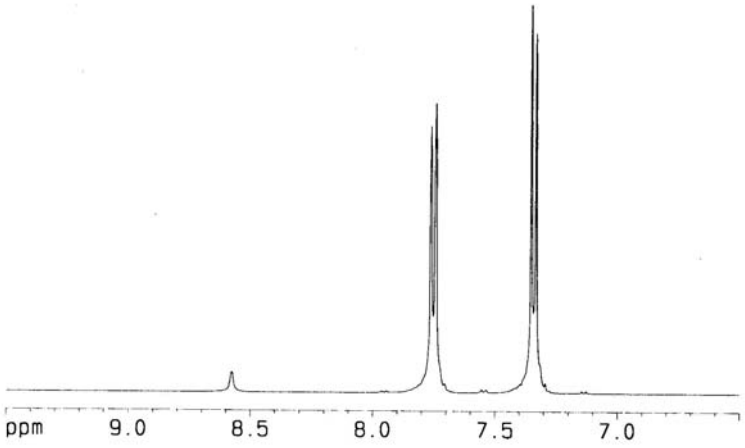

Figure 4.89 ^{1}H-NMR spectrum of **1-2,3,6-d$_3$** before irradiation

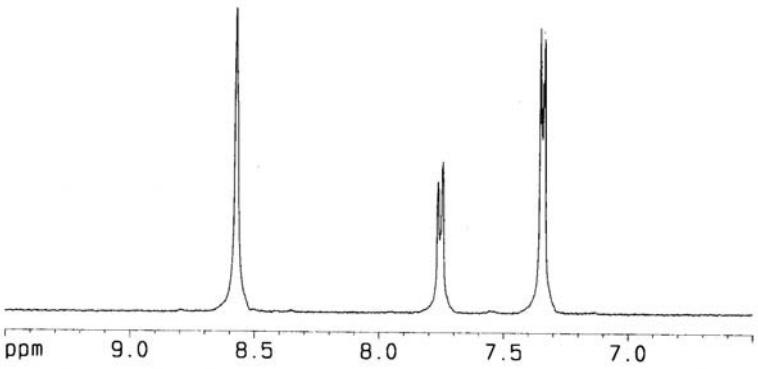

Figure 4.90 ^{1}H-NMR spectrum of **1-2,3,6-d$_3$** before irradiation

Figure 4.90 shows that after 12 hours of irradiation, an intense signal appears in the ^{1}H-NMR spectrum at δ 8.58. Because of its intensity, this signal must be due to more than one proton. A scale expansion of this signal is shown in Figure 4.91 which reveals

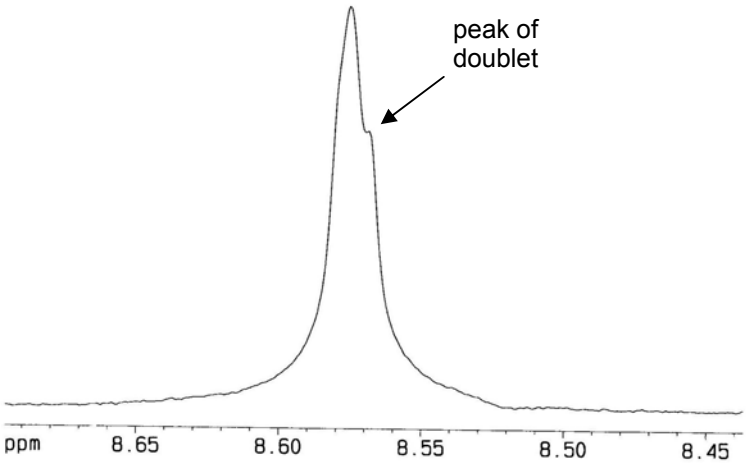

Figure 4.91 Scale expansion of H2 and H6

that the signal can be resolved into a doublet overlapping with a singlet. Thus, the photoproducts must have the partial structures A and B shown below.

A **B**

Furthermore, since each product must have three deuterium atoms, the partial structure B must be due to 2,3,4-trideuteriopridine (**1-2,3,4-d$_3$**)

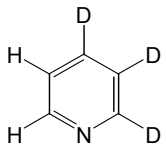

1-2,3,4-d$_3$

A scale expansion of the signal at δ 7.45 is shown in Figure 4.92 which reveals that the signal can be resolved into two overlapping doublets. One of these doublets with J = 7.1 Hz is due to the unconverted reactant **1-2,3,6-d$_3$** in which H5 is coupling with a proton at C6. This is consistent with the product **1-2,3,4-d$_3$**.

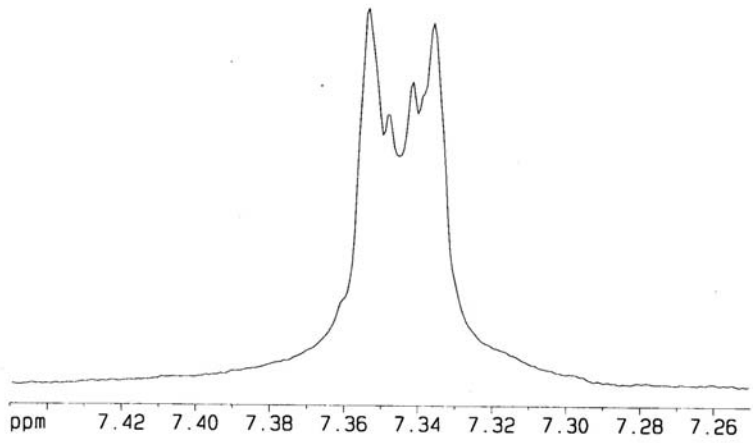

Figure 4.92 Scale expansion of H5 after 12 hours of irradiation

Based on partial structure A, two structures are possible for the second product. These are **1-3,4,5-d$_3$** and **1-2,4,5-d$_3$** shown below.

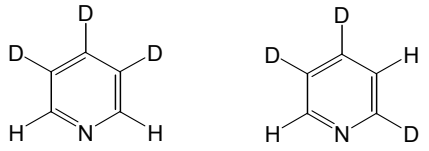

1-3,4,5-d$_3$ **1-2,4,5-d$_3$**

It is important to note that no evidence for the formation of a singlet can be seen in the scale expansion shown in Figure 4.92. Since the formation of **1-2,4,5-d$_3$** would demand the appearance of a singlet at this chemical shift, **1-2,4,5-d$_3$** is not formed in this reaction. The second product must be **1-3,4,5-d$_3$**.

These results show that **1-2,3,6-d_3** has undergone phototransposition to yield a mixture of **1-2,3,4-d_3** and **1-3,4,5-d_3**.

Scheme 4.57 Photolysis of 2,3,6-trideuteriopyridine (**1-2,3,6-d_3**)

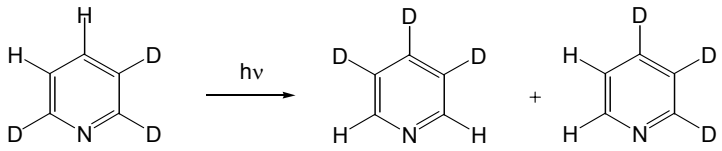

1-2,3,6-d_3 **1-3,4,5-d_3** **1-2,3,4-d_3**

4.6.5. Irradiation of 2,3,5-trideuteriopyridine (1-2,3,5-d_3)

2,3,5-Trideuteriopyridine (**1-2,3,5-d_3**) vapor was irradiated by four 254 nm lamps for 12 hours. Figure 4.93 and 4.94 show the ^{1}H-NMR spectra in acetone-d_6 of **1-2,3,5-d_3** before and after irradiation for 12 hours.

In Figure 4.93, two intense singlets due to the H4 and H6 protons of **1-2,3,5-d_3** are observed at δ 7.75 and 8.60, respectively. A very small signal due to the residual H3 proton is also observed at δ 7.36.

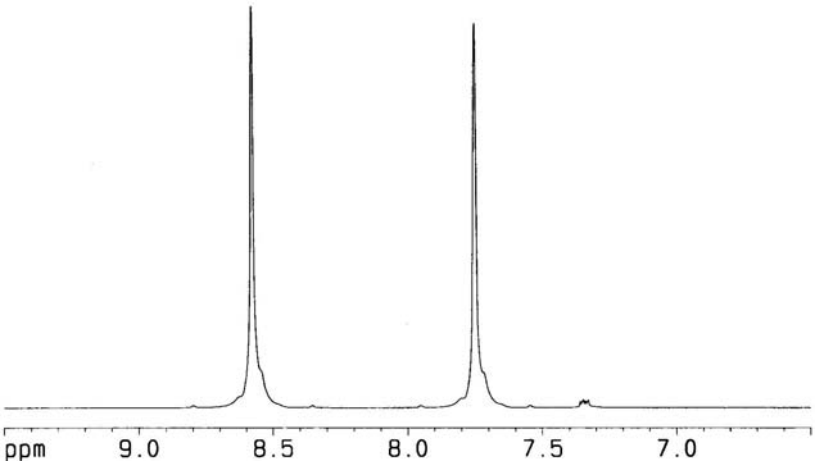

Figure 4.93 ^{1}H-NMR spectrum of **1-2,3,5-d$_3$** before irradiation

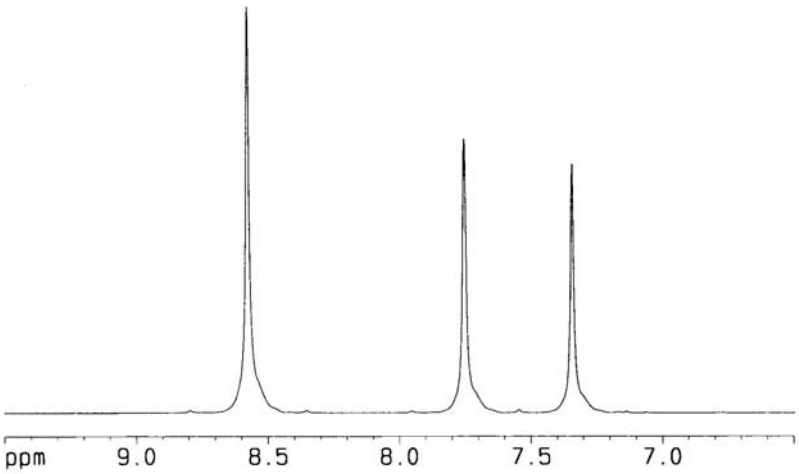

Figure 4.94 ^{1}H-NMR spectrum of **1-2,3,5-d$_3$** after 12 hours of irradiation

The ^{1}H-NMR spectrum shown in Figure 4.94 shows that irradiation is accompanied by the formation of a new singlet at δ 7.34 where H3 and H5 protons of pyridine are known to absorb. Furthermore, the intensity of this signal shows that it is due to more than one proton. Considering the relative decrease in the intensity of the H4 signal at δ 7.75 due to the consumption of the reactant and the relative increase in the signal at δ 7.34, this new signal must be due to the formation of products with three protons at the H3/H5 ring positions. Since all of these protons appear as singlets, this indicates the partial structures C and D.

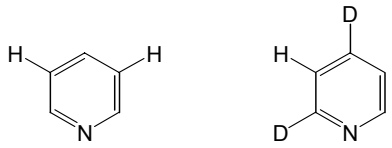

C **D**

Since each structure must also have three deuterium atoms and since the two structures must be different, the two photoproducts must be **1-2,4,6-d$_3$** and **1-2,4,5-d$_3$**. The increase

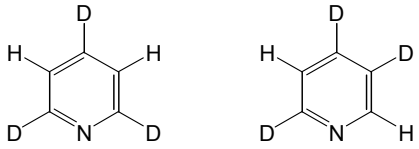

1-2,4,6-d$_3$ **1-2,4,5-d$_3$**

in the intensity of the signal at δ 8.6 in Figure 4.94 is also consistent with the formation of a product, i.e, **1-2,4,5-d$_3$**, which has a proton at ring position 6.

These results shows that **1-2,3,5-d$_3$** has undergone phototransposition to yield a mixture of **1-2,4,6-d$_3$** and **1-2,4,5-d$_3$** (Scheme 4.58).

Scheme 4.58 Photolysis of 2,3,5-trideuteriopyridine (**1-2,3,5-d$_3$**)

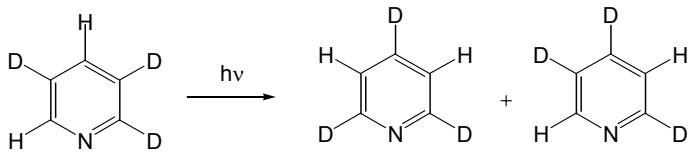

1-2,3,5-d$_3$ **1-2,4,6-d$_3$** **1-2,4,5-d$_3$**

4.6.6. Irradiation of 2,4,5-trideuteriopyridine (1-2,4,5-d$_3$)

The ^{1}H-NMR spectrum of **1-2,4,5-d$_3$** before irradiation shown in Figure 4.95 exhibits singlets due to the H6 and H3 protons at δ 8.59 and 7.36 respectively. The ^{1}H-NMR spectrum in Figure 4.96 shows that irradiation is accompanied by the formation of a new singlet at δ 7.75 due to the formation of a product with a proton at ring position 4. Since this signal is a singlet and since the product must have three deuterium atoms, the product must be **1-2,3,5-d$_3$**.

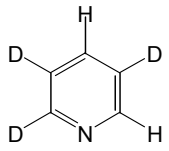

1-2,3,5-d$_3$

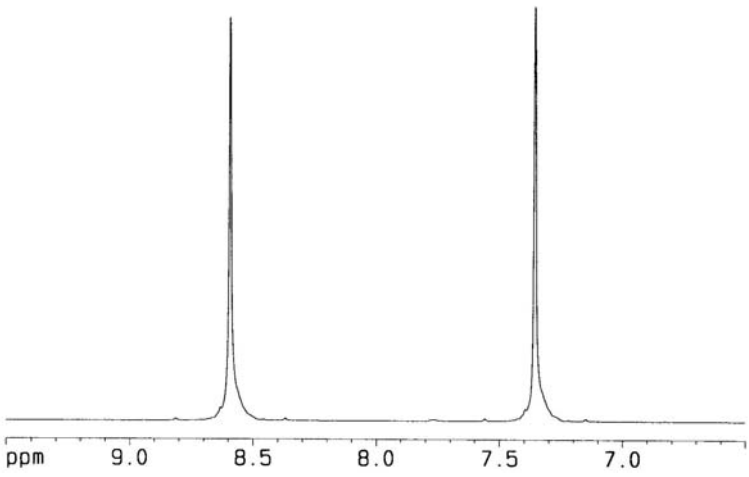

Figure 4.95 ^{1}H-NMR spectrum of **1-2,4,5-d$_3$** before irradiation

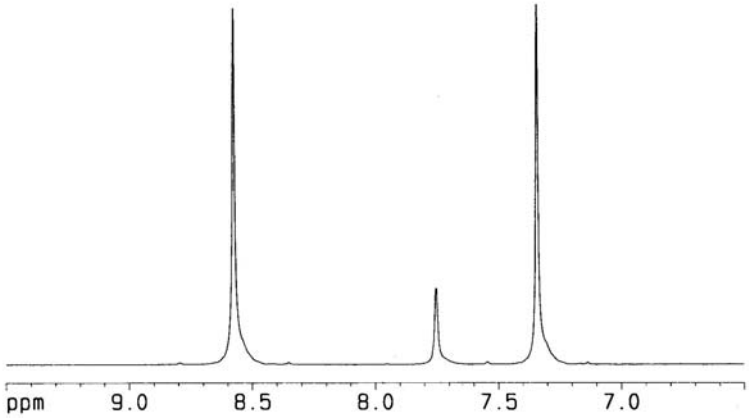

Figure 4.96 ^{1}H-NMR spectrum of **1-2,4,5-d$_3$** after 12 hours of irradiation

The second product must have protons at ring positions 3(5) and/or 2(6) which all appear as singlets in the ^{1}H-NMR spectrum. Excluding the reactant, **1-2,4,5-d$_3$** of the six trideuterated pyridines, only **1-2,4,6-d$_3$** and **1-3,4,5-d$_3$** are possible structures.

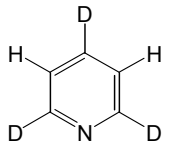

1-2,4,6-d_3

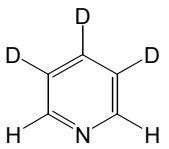

1-3,4,5-d_3

As seen in Figure 4.96, the intensities of the signals at δ 7.35 due to H3(H5) and δ 8.60 due to H2(H6) remain essentially equal after irradiation. On this basis, structure **1-3,4,5-d_3** can be eliminated as a possible product since the formation of **1-2,3,5-d_3** and **1-3,4,5-d_3** would require that the intensity of the signal at δ 8.60 due to H2(H6) would be much larger than the intensity of the signal at δ 7.35 due to H3(H5). Accordingly, the second product must be **1-2,4,6-d_3**. Thus, whereas the formation of **1-2,3,5-d_3** would result in an increase in the intensity of the signal at δ 8.60 due to the H6 proton, the formation of **1-2,4,6-d_3** would result in an increase in the intensity of the signal at δ 7.35 due to the protons at ring positions 3 and 5. Since the intensities of the signals remain identical, it appears that the relative yields of **1-2,3,5-d_3** and **1-2,4,6-d_3** is 2:1.

These results show that **1-2,4,5-d_3** has undergone phototransposition resulting in a mixture of **1-2,3,5-d_3** and **1-2,4,6-d_3** as shown in Scheme 4.59.

Scheme 4.59 Photolysis of 2,4,5-trideuteriopyridine (**1-2,4,5-d_3**)

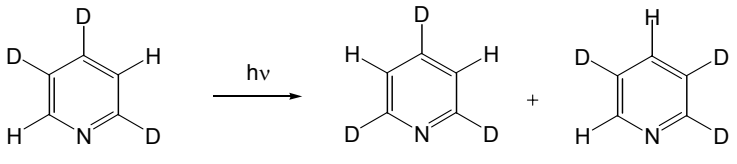

1-2,4,5-d_3 **1-2,4,6-d_3** **1-2,3,5-d_3**

4.6.7. Summary and mechanistic conclusion of trideuteriopyridines

These photochemical studies show that each of the six trideuteriopyridine undergoes phototransposition to yield two isomeric trideuteriopyridines. Based on the observed phototransposition products, the six trideuteriopyridines can be divided into two triads of three compounds each which photochemically interconvert. Triad 1 consists of

Scheme 4.60 Photo-interconversion of trideuteriopyridines

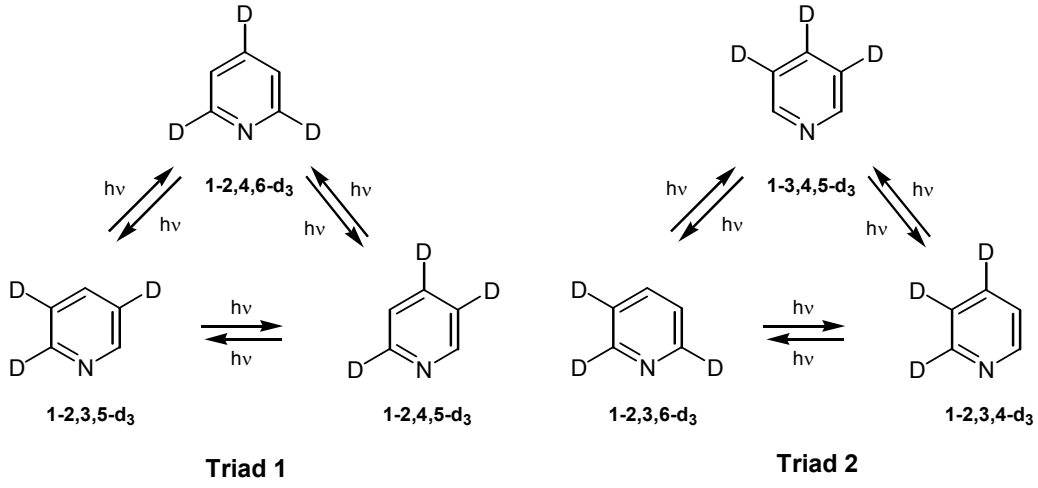

1-2,4,5-d$_3$, **1-2,3,5-d$_3$**, and **1-2,4,6-d$_3$** which interconvert upon irradiation at 254 nm in the vapor phase whereas Triad 2 consists of **1-2,3,4-d$_3$**, **1-2,3,6-d$_3$**, and **1-3,4,5-d$_3$** which are also interconverting upon irradiation at 254 nm in the vapor phase. These results are almost identical to the results of the photochemical reactions of the six isomeric dimethylpyridines. In that case, the six isomers could also be divided in two triads of three photochemically interconverting compounds. Although in the case of the dimethylpyridines a leakage between the two triads was observed, in the case of the

trideuteriopyridines, no interconversion of any member of triad 1 with any member of triad 2 was detected.

Two photochemically interconverting triads in ^{1}H-NMR spectra, the photoproducts in each Triad are consistent with the proposed mechanism involving cyclization-2,6-bridging, nitrogen migration and rearomatization. Scheme 4.61 shows the phototransposition mechanism of the trideuteriopyridine members in Triad 1.

Scheme 4.61 Phototransposition mechanism of trideuteriopyridines in Triad 1

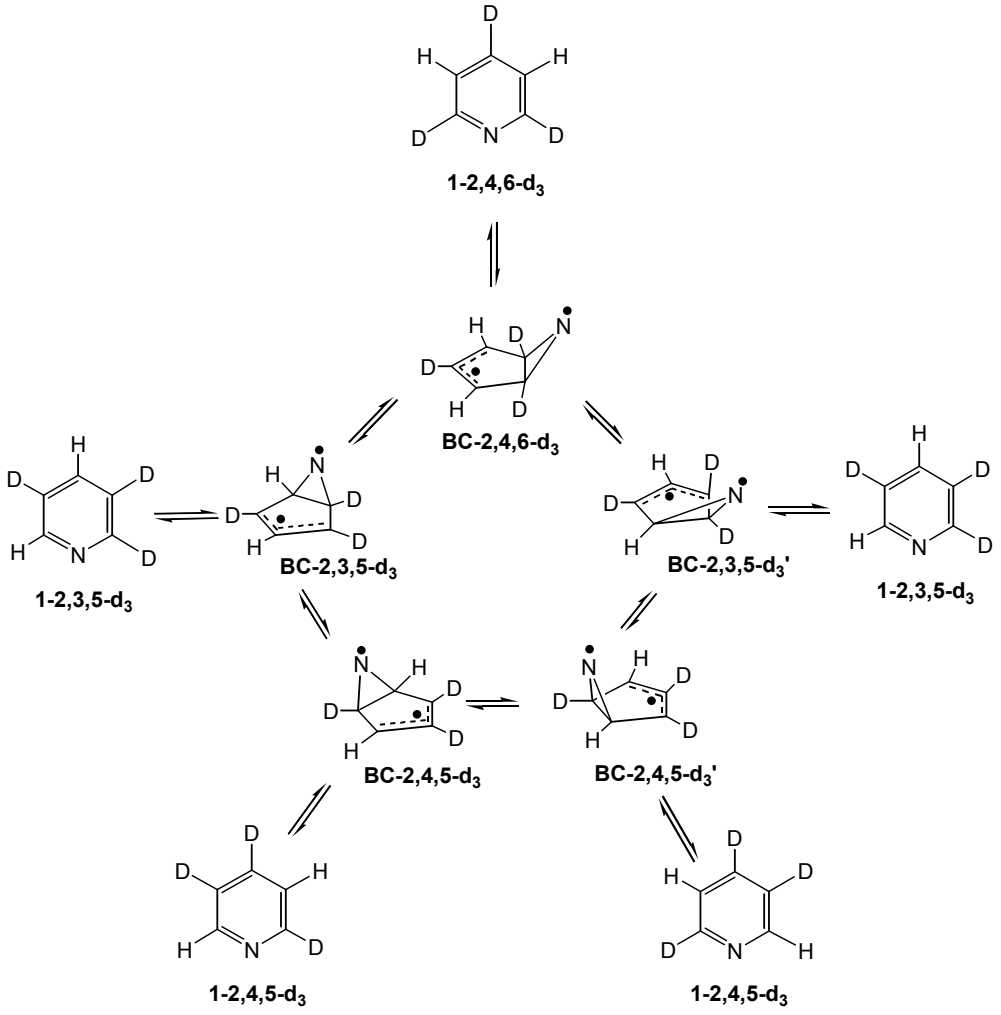

As expected, irradiation of any isomer in Triad 1 results in the formation of the other two isomers. For example, **1-2,4,6-d_3** undergoes cyclization between carbon position 2 and 6 resulting in the formation of **BC-2,4,6-d_3**. This intermediate can revert back to **1-2,4,6-d_3** or undergo nitrogen migration in either clockwise or counterclockwise directions. In one of this two directions, **BC-2,4,6-d_3** would isomerize to azaprefulvene **BC-2,3,5-d_3** (**BC-2,3,5-d_3'**) which would either rearomatize to **1-2,3,5-d_3**, a member of Triad 1, or undergo a second nitrogen migration, resulting in the formation of **BC-2,4,5-d_3** (**BC-2,4,5-d_3**'). This intermediate would also either rearomatize to **1-2,4,5-d_3,** the other member of Triad 1, or continue nitrogen migration to **BC-2,4,5-d_3'**(**BC-2,4,5-d_3**) which is an energy wasting process. The formation of photoproducts in this triad based on the above mechanistic scheme is estimated to be 2:2:1 for **1-2,3,5-d_3**, **1-2,4,5-d_3**, and **1-2,4,6-d_3**, respectively.

The similar mechanism is also consistent with the photochemistry of the members in Triad 2. Scheme 4.62 shows the phototransposition mechanism of trideuteriopyridines in Triad 2.

Scheme 4.62 Phototransposition mechanism of trideuteriopyridines in Triad 2

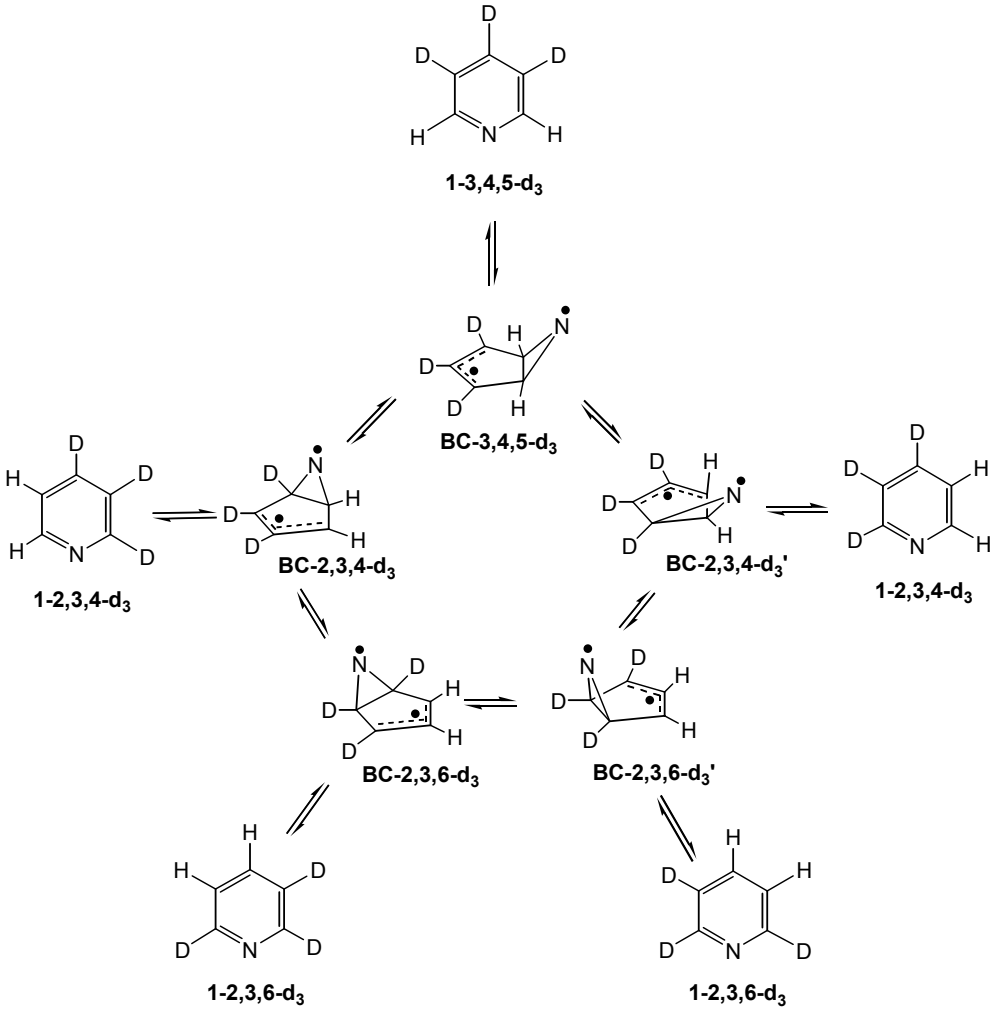

Again, irradiation of any one isomer in Triad 2 results in the formation of the other two isomers. For example, **1-3,4,5-d$_3$** would undergo 2,6-bonding resulting in the formation of **BC-3,4,5-d$_3$**. Nitrogen migration in the counterclockwise direction would result in the formation of **BC-2,3,4-d$_3$**, which would rearomatize to **1-2,3,4-d$_3$**, a second member of Triad 2. However, **BC-2,3,4-d$_3$** can undergo a nitrogen migration to **BC-2,3,6-d$_3$,** which is followed by rearomatization to form **1-2,3,6-d$_3$**, another member of

Triad 2. Nitrogen migration in the clockwise direction of **BC-3,4,5-d_3** undergoes nitrogen migration to yield **BC-2,3,4-d_3**' followed by rearomatization to yield **1-2,3,4-d_3**. Second nitrogen migration from **BC-2,3,4-d_3**' results in the formation of **BC-2,3,6-d_3'** followed by rearomatization to **1-2,3,6-d_3**.

The statistical ratio of photoproduct **1-2,3,6-d_3, 1-2,3,4-d_3**, and **1-3,4,5-d_3,** is 2:1:1.

4.6.8. Dewar-pyridine mechanism

The phototransposition of **1-3,4,5-d_3** via interconverting Dewar-pyridine was also considered. The formation of Dewar-pyridine **DP-3,4,5-d_3** results from 2,5- and 3,6-bonding reaction. Scheme 4.63 shows the phototransposition mechanism involving this Dewar-pyridine intermediate.

Scheme 4.63 Dewar-pyridine mechanism of **1-3,4,5-d$_3$**

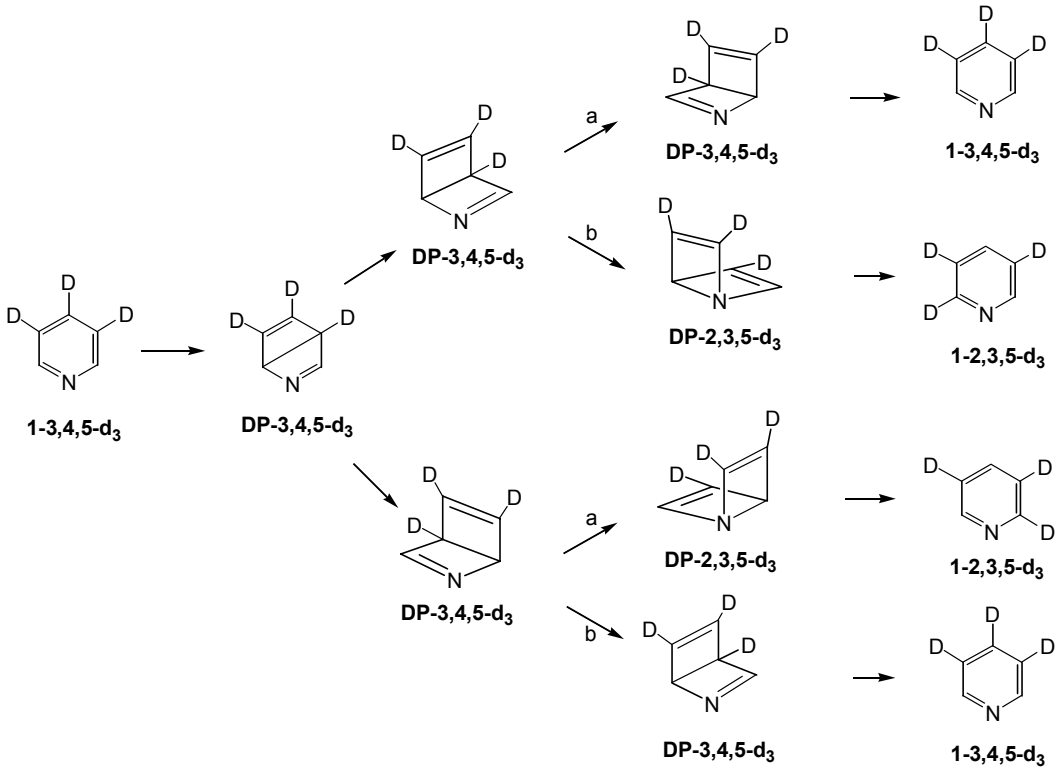

This mechanism suggests that **1-2,3,5-d$_3$** would be the only photoproduct. This is not consistent with the ^{1}H-NMR results which shows the presence of signals due to H3,5 from the new product. In addition, the H4 proton in **1-2,3,5-d$_3$** would give a singlet signal but the experimental result exhibits H4 as a doublet. Therefore, the phototransposition of **1-3,4,5-d$_3$** does not occur by this pathway.

In the mechanism involving an azaprismane intermediate shown in Scheme 4.64, the Dewar-pyridine **DP-3,4,5-d$_3$** would undergo [2+2] cycloaddition to yield an azaprismane **97**. This intermediate would undergo ring cleavage to yield **1-3,4,5-d$_3$**, **97a**

and **97b**. Rearrangement of **97a** and **97b** would result in the formation of **1-2,4,5-d$_3$** and **1-2,3,5-d$_3$**.

Scheme 4.64 Azaprismane mechanism of **DP-3,4,5-d$_3$**

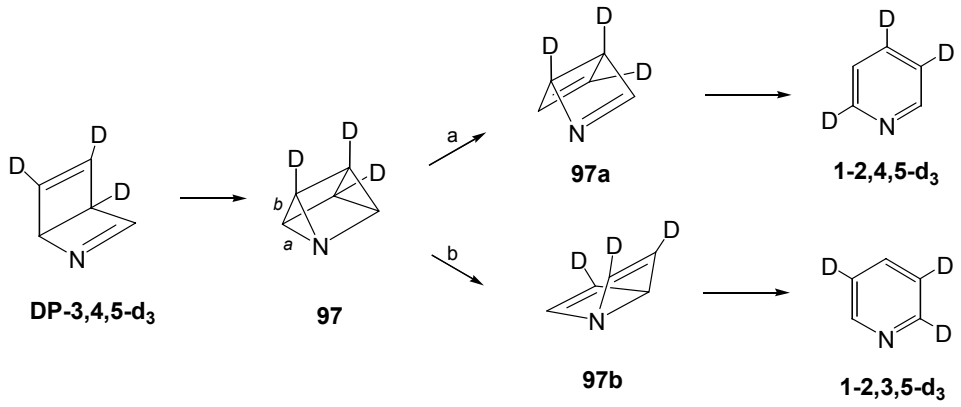

These photoproducts, however, are not consistent with the proton signals observed in ^{1}H-NMR spectrum. Neither structure would exhibit the observed doublet signals in the NMR spectra. Thus, phototransposition involving the azaprismane mechanism is not in operation.

Scheme 4.65 shows the products expected from the interconverting Dewar-pyridine mechanism for **1-2,4,6-d$_3$**. Because of the symmetry of **1-2,4,6-d$_3$**, C2-C5 and C3-C6 bonding leads to the same Dewar-pyridine, **DP-2,4,6-d$_3$**. Scheme 4.65 shows that all possible sigmatropic migrations result in the formation of the same Dewar-pyridine, **DP-2,4,6-d$_3$**.

Scheme 4.65 Dewar-pyridine mechanism of **1-2,4,6-d$_3$**

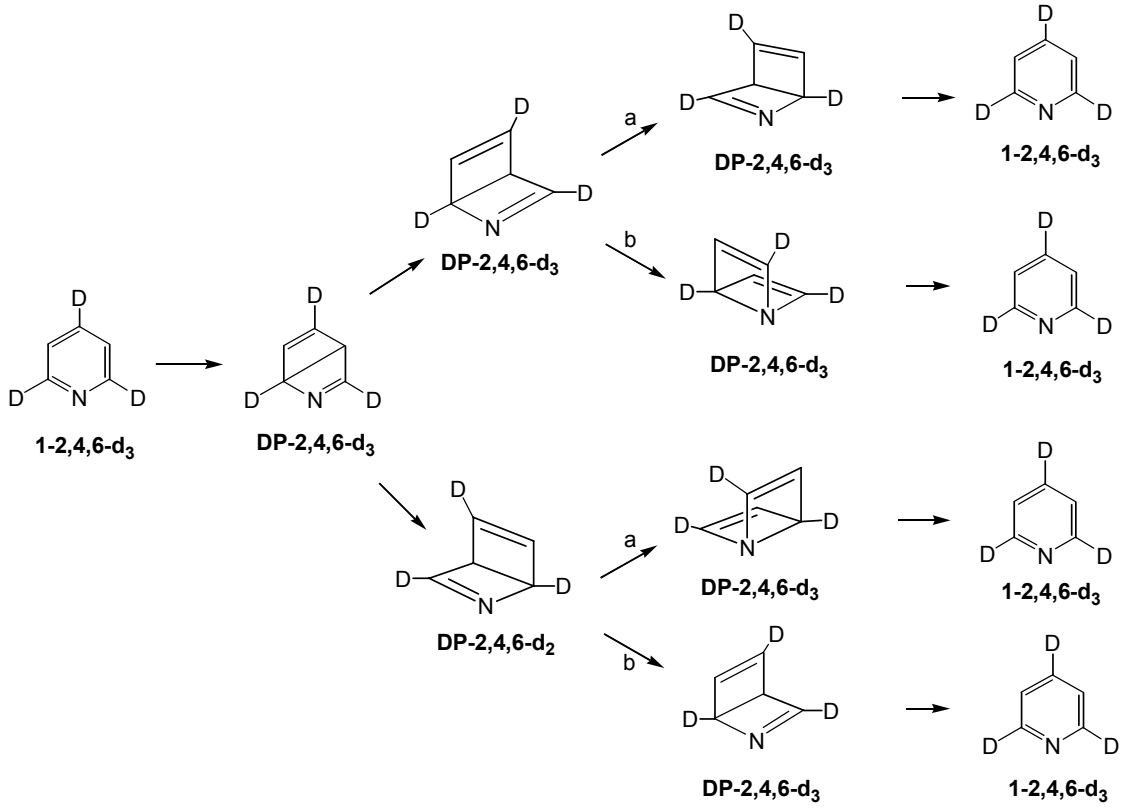

Rearomatization of all of these leads back to 2,4,6-trideuteriopyridine (**1-2,4,6-d$_3$**). Thus, if this mechanism is operating it cannot be detected by product formation.

Scheme 4.66 shows the products expected if the initially formed Dewar-pyridine undergoes a [2+2] cycloaddition reaction to form azaprismane **98**. In addition to

Scheme 4.66 Azaprismane mechanism of **DP-2,4,6-d$_3$**

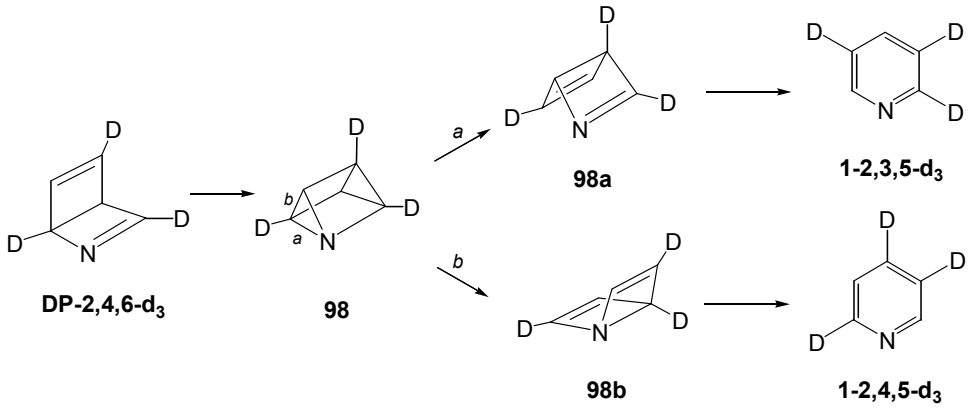

reverting back to the reactant **1-2,4,6-d$_3$**, **77** can undergo ring opening via path *a* or path *b* to give Dewar-pyridines **98a** or **98b** and, after rearomatization, 2,3,5-trideuteriopyridine (**1-2,3,5-d$_3$**) and 2,4,5-trideuteriopyridine (**1-2,4,5-d$_3$**). These are the same products that were experimentally observed and the same products that are predicted by the electrocyclic ring closure-heteroatom migration mechanism. Thus, in the case of 2,4,6-trideuteriopyridine (**1-2,4,6-d$_3$**) it is not possible to distinguish between the elctrocyclic ring closure-heteroatom migration mechanism and the azaprismane mechanism on the basis of product formation.

As was previously discussed, in the case of 3,4,5-trideuteriopyridine (**1-3,4,5-d$_3$**), these pathways lead to different products as shown below.

Scheme 4.67 Different photoproducts from 2,6-bonding and azaprismane formation

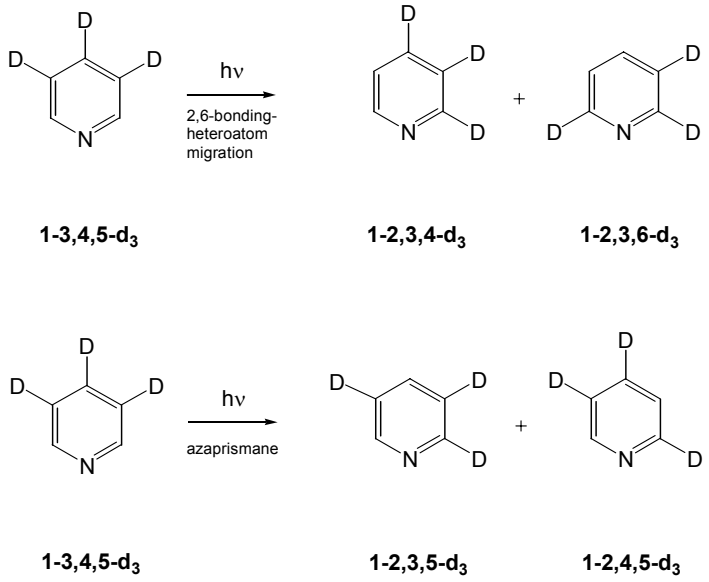

Thus, since irradiation of **1-3,4,5-d$_3$** led to the formation of 2,3,4-trideuteriopyridine (**1-2,3,4-d$_3$**) and 2,3,6-trideuteriopyridine (**1-2,3,6-d$_3$**), the reaction must have occurred by the 2,6-bonding-heteroatom migration mechanism. By analogy, it is suggested that 2,4,6-trideuteriopyridine(**1-2,4,6-d$_3$**) also phototransposes via this pathway.

4.7. Photochemistry of tetradeuteriopyridines

4.7.1. Irradiation of 2,3,5,6-tetradeuteriopyridine (1-2,3,5,6-d_4)

Irradiation of 2,3,5,6-tetradeuteriopyridine (**1-2,3,5,6-d_4**) vapor (2-4 Torrs) was carried out at 254 nm with the same procedure that was previously described. Analysis of the photoproduct mixture after 3, 6, and 12 hours of irradiation was carried out by ^{1}H-NMR spectroscopy. Figure 4.97 and 4.98 shows the ^{1}H-NMR spectra in acetone-d_6 of **1-2,3,5,6-d_4** before and after irradiation for 12 hours.

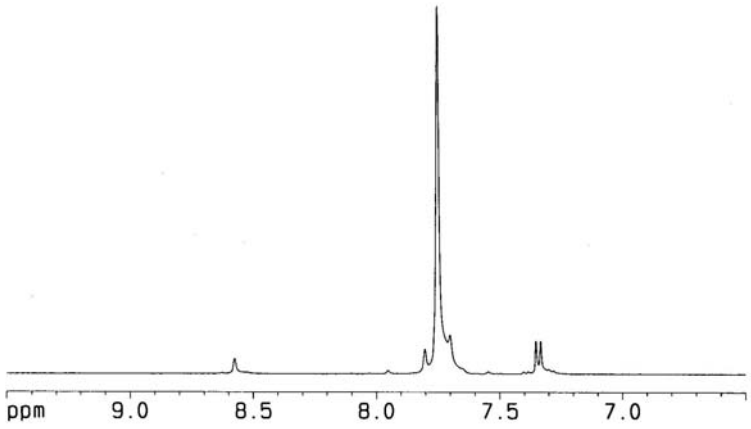

Figure 4.97 ^{1}H-NMR spectrum of **1-2,3,5,6-d_4** before irradiation

In addition to the singlet at δ 7.75 due to **1-2,3,5,6-d_4**, after irradiation, the ^{1}H-NMR spectrum shown in Figure 4.98 exhibits new singlets at δ 7.34, where the H3/5 proton absorbs and a new singlet at δ 8.58 where the H2/6 proton absorbs. These new signals are formed in an integrated ratio of 1:1.

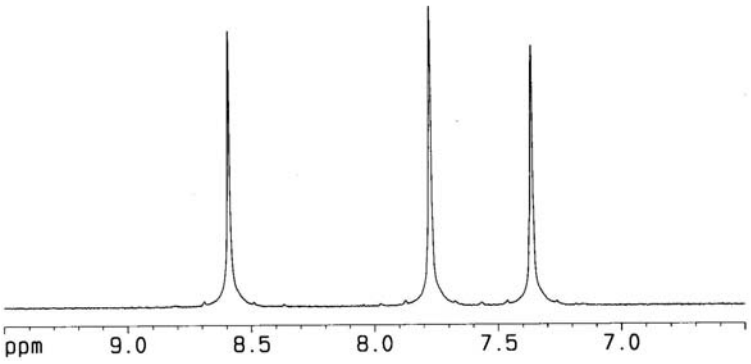

Figure 4.98 ^{1}H-NMR spectrum of **1-2,3,5,6-d$_4$** after 12 hours irradiation

Since each new photoproduct can have only one ring proton, these spectral results show that the products are 2,3,4,5-tetradeteriopyridine, **1-2,3,4,5-d$_4$**, and 2,3,4,6-tetradeuteriopyridine, **1-2,3,4,6-d$_4$**.

Scheme 4.68 Photolysis of 2,3,5,6-tetradeuteriopyridine (**1-2,3,5,6-d$_4$**)

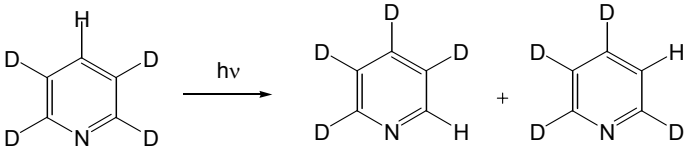

1-2,3,5,6-d$_4$ **1-2,3,4,5-d$_4$** **1-2,4,5,6-d$_4$**

4.7.2. Irradiation of 2,3,4,6-tetradeuteriopyridine (1-2,3,4,6-d_4)

The 2,3,4,6-tetradeuteriopyridine (**1-2,3,4,6-d_4**) vapor (2-4 Torrs) was irradiated at 254 nm with four low-mercury lamps in the Rayonet reactor for 3, 6, and 12 hours. After each irradiation the resulting photoproduct was analyzed by ^{1}H-NMR in acetone-d_6. Figure 4.99 and 4.100 shows the ^{1}H-NMR spectra of **1-2,3,4,6-d_4** before and after irradiation for 12 h.

The ^{1}H-NMR spectrum in Figure 4.99 shows only one singlet observed at δ 7.36 which is due to the H5 proton in **1-2,3,4,6-d_4**. However, two tiny signals at δ 8.59 and 7.77 due to the residual H2,6 (96%) and H4 (98%) protons, respectively, are also observed.

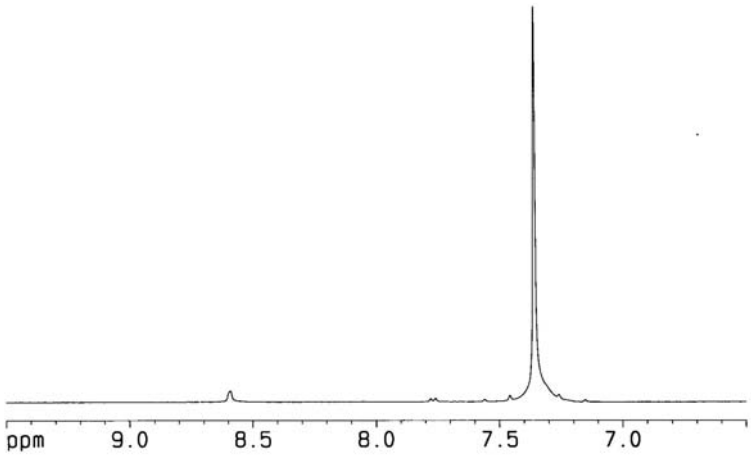

Figure 4.99 ^{1}H-NMR spectrum of **1-2,3,4,6-d_4** before irradiation

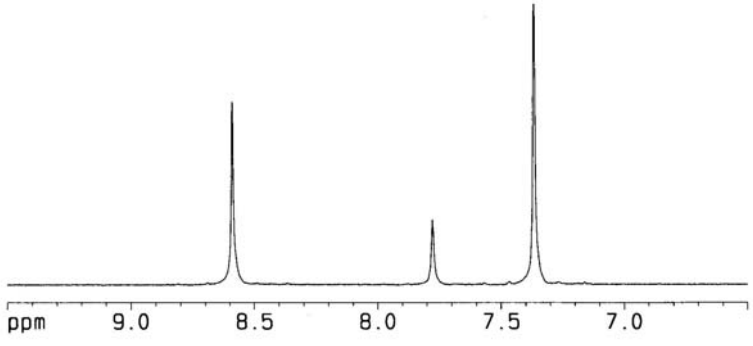

Figure 4.100 ^{1}H-NMR spectrum of **1-2,3,4,6-d$_4$** after 12 hours irradiation

After 12 hours of irradiation, in addition to the signal at δ 7.36 due to **1-2,3,5,6-d$_4$**, the ^{1}H-NMR spectrum shown in Figure 4.100 exhibits two new singlet signals observed at δ 8.58 and 7.79 in a ratio of 2:1. The most downfield signal is due to a proton at the H2,6 ring position and the singlet at δ 7.79 is due to a proton at ring position 4. The presence of singlets at ring positions 2 and 4 indicate that the products are 2,3,4,5-tetradeuteriopyridine (**1-2,3,4,5-d$_4$**) and 2,3,5,6-tetradeuteriopyridine (**1-2,3,5,6-d$_4$**) as shown in Scheme 4.69.

Scheme 4.69 Photolysis of 2,3,4,6-tetradeuteriopyridine (**1-2,3,4,6-d$_4$**)

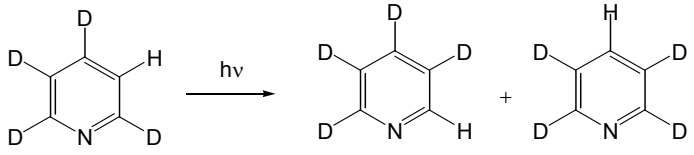

1-2,3,4,6-d$_4$ **1-2,3,4,5-d$_4$** **1-2,3,5,6-d$_4$**

4.7.3. Irradiation of 2,3,4,5-tetradeuteriopyridine (1-2,3,4,5-d_4)

2,3,4,5-Tetradeuteriopyridine (**1-2,3,4,5-d_4**) vapor was irradiated at 254 nm with fours low pressure mercury lamps in the Rayonet photochemical reactor for 3, 6, and 12 hours. After each irradiation, the product mixture was dissolved in acetone-d_6 and analyzed by ^{1}H-NMR. Figure 4.101 and Figure 4.102 show the ^{1}H-NMR spectra of **1-2,3,4,5-d_4** before and after irradiation for 12 hours.

In Figure 4.101, the ^{1}H-NMR spectrum exhibits only one singlet at δ 8.60 which is due to the H2 proton. Small signals at δ 7.77 and 7.36 due to the residual protons at ring position 4 and 3,5, respectively. After irradiation for 12 hours, in addition to the

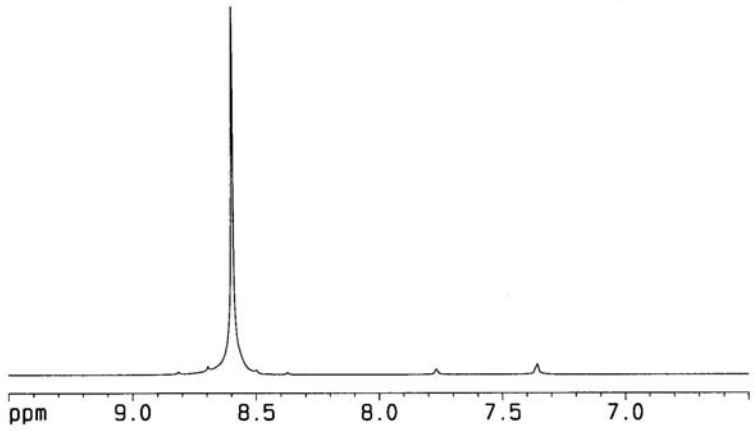

Figure 4.101 ^{1}H-NMR spectrum of **1-2,3,4,5-d_4** before irradiation

singlet at δ 8.60 due to the reactant, the ^{1}H-NMR spectrum shown in Figure 4.102 exhibits two singlets at 7.78 due to a proton at ringposition 4 and 7.36 due to a proton at H3,5 in a ratio of 1:2.

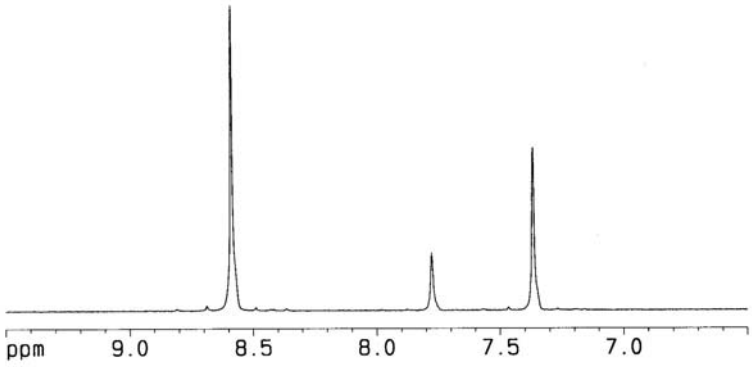

Figure 4.102 ^{1}H-NMR spectrum of **1-2,3,4,5-d$_4$** after 12 hours irradiation

These new peaks show that **1-2,3,4,5-d$_4$** has undergone phototransposition resulting in the formation of 2,3,5,6-tetradeuteriopyridine (**1-2,3,5,6-d$_4$**) and 2,4,5,6-tetradeuteriopyridine (**1-2,3,4,6-d$_4$**) as shown in Scheme 4.70.

Scheme 4.70 Photolysis of 2,3,4,5-tetradeuteriopyridine (**1-2,3,4,5-d$_4$**)

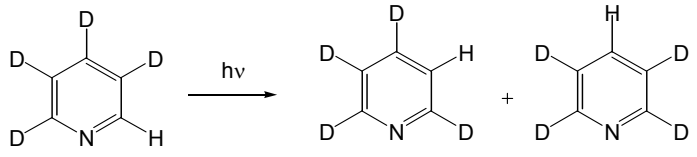

1-2,3,4,5-d$_4$ **1-2,3,4,6-d$_4$** **1-2,3,5,6-d$_4$**

4.7.4. Summary and mechanistic conclusion of tetradeuteriopyridines

The experimental results from the photochemistry tetradeuteriopyridines show that each tetradeuterio isomer undergo phototransposition to yield two isomeric tetradeuteriopyridines. Scheme 4.71 shows the photo-interconversion of tetradeuteriopyridines.

Scheme 4.71 Photo-interconversion of tetradeuteriopyridines

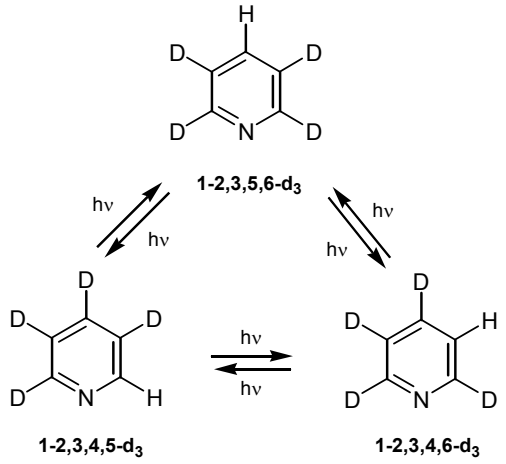

These interconversion are found to be consistent with the mechanism involving cyclization by 2,6-bridging followed by nitrogen migration. Finally rearomatization gives the other two isomers.

4.7.5.1. 2,3,5,6-Tetradeuteriopyridine (1-2,3,5,6-d_4)

Irradiation of 2,3,5,6-tetradeuteriopyridine (**1-2,3,5,6-d_4**) results in the formation of 2,3,4,6-tetradeuteriopyridine (**1-2,3,4,6-d_4**) and 2,3,4,5-tetradeuteriopyridine (**1-2,3,4,5-d_4**). The ^{1}H-NMR spectrum shown in Figure 4.98 shows that two new singlets are observed at δ 7.86 and 7.35 where the H2,6 and H3,5 of pyridine absorb in a ratio of 1:1. This result is consistent with the photoproducts predicted from the phototransposition mechanism involving 2,6-bridging, nitrogen migration, and rearomatization. The mechanistic scheme of this reaction is shown in Scheme 4.72.

Scheme 4.72 Phototransposition mechanism of **1-2,3,5,6-d$_4$**

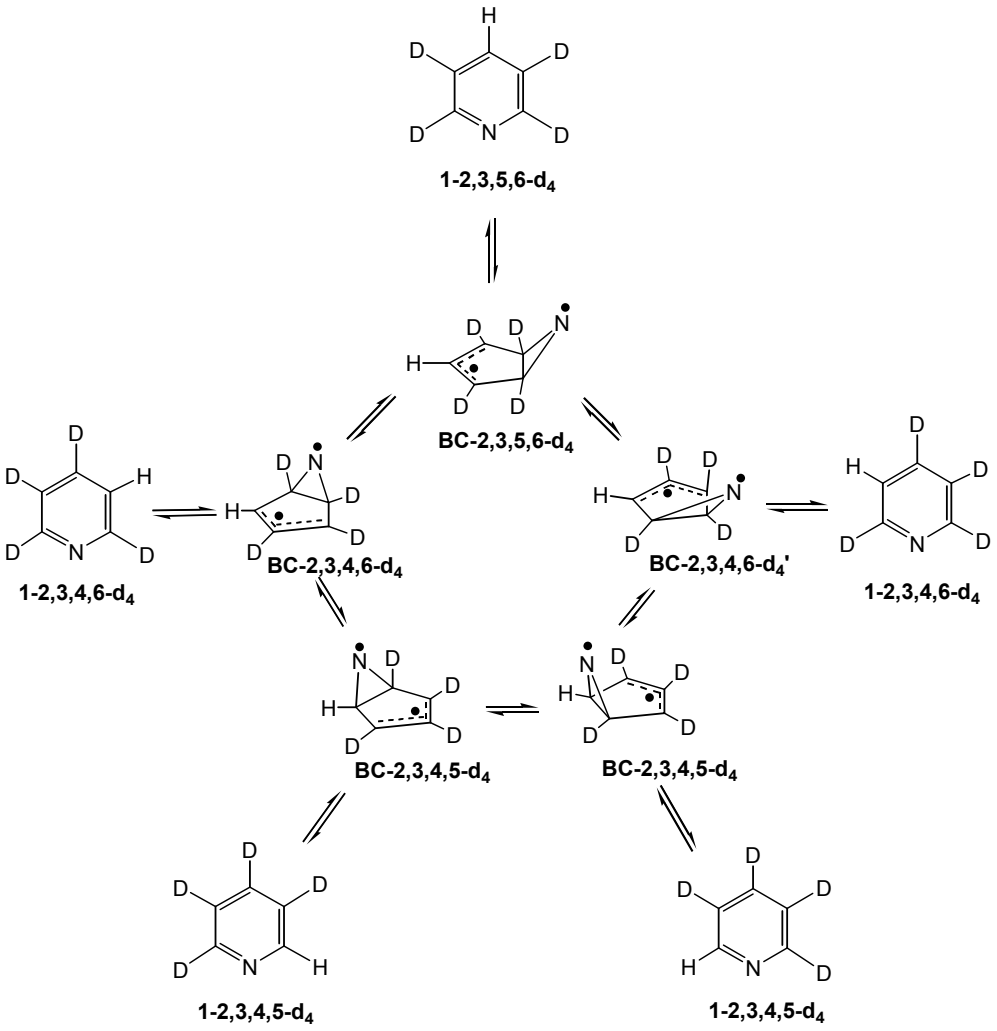

Once **1-2,3,5,6-d$_4$** absorbs light, it undergoes 2,6-bonding cyclization to form an azaprefulvene intermediate, **BC-2,3,5,6-d$_4$**. This bicyclic species can undergo nitrogen migration in both directions to give **BC-2,3,4,6-d$_4$** and **BC-2,3,4,6-d$_4$'**. Rearomatization of this intermediate results in the formation of one of the observed photoproduct, 2,3,4,6-tetradeuteriopyridine (**1-2,3,4,6-d$_4$**). The second nitrogen migration, however, form **BC-**

2,3,4,6-d$_4$ (**BC-2,3,4,6-d$_4$'**) will result in the formation of another bicyclic species, **BC-2,3,4,5-d$_4$** (**BC-2,3,4,5-d$_4$'**). Again, these structures will rearrange to form the second photoproduct, 2,3,4,5-tetradeuteriopyridine (**1-2,3,4,5-d$_4$**).

Scheme 4.73 shows that the Dewar-pyridine sigmatropic shift mechanism also

Scheme 4.73 Dewar-pyridine mechanism of **1-2,3,5,6-d$_4$**

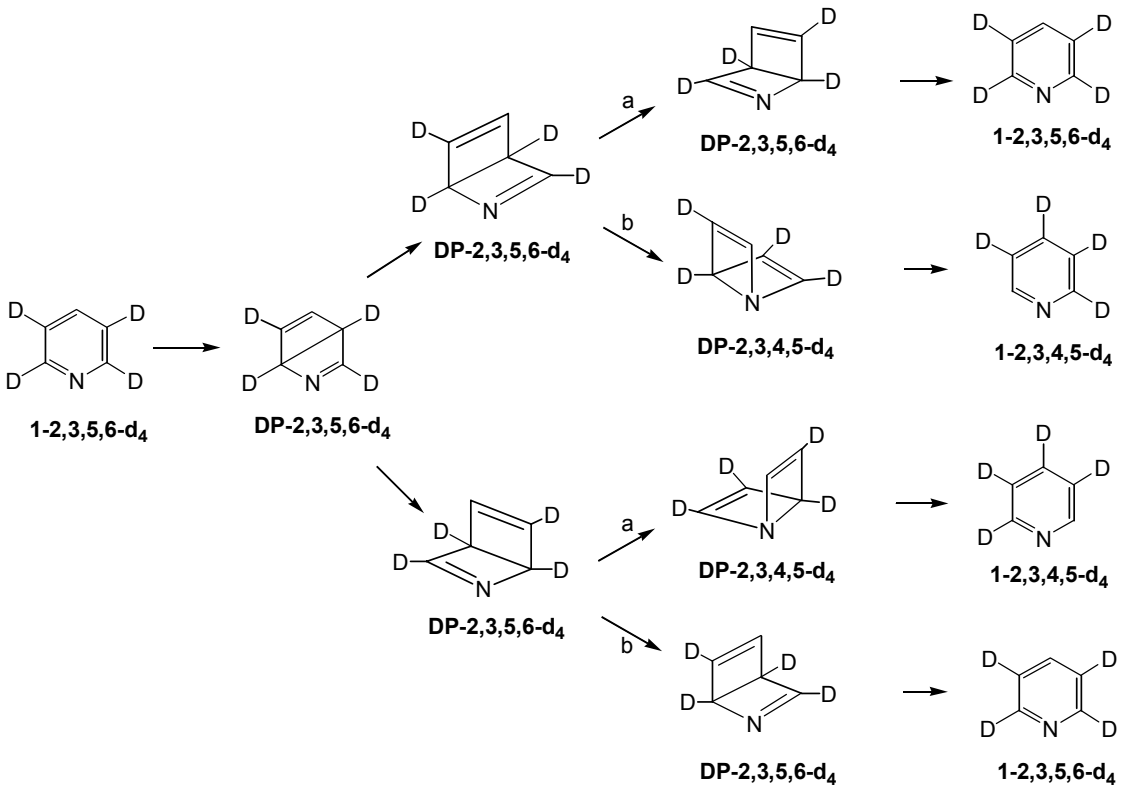

predicts the formation of 2,3,4,5-tetradeuteriopyridine (**1-2,3,4,5-d$_4$**) and 2,3,4,6-tetradeuteriopyridine (**1-2,3,4,6-d$_4$**). On a purely statistical basis the products would be formed in a 2:1 ratio respectively. This is in contrast to the electrocyclic ring closure-

heteroatom migration mechanim which predicts that the ratio of these products should be 1:1. Thus, the experimentally observed ratio of 1:1 is more consistent with the electrocyclic ring closure-heteroatom migration mechanism.

Scheme 4.74 shows that 2,3,5,6-tetradeuteratiopyridine (**1-2,3,5,6-d$_4$**) is converted to 2,3,4,6-tetradeuteriopyridine (**1-2,3,4,6-d$_4$**) as the only product by the azaprismane mechanism. This is clearly not consistent with the experimental observations.

Scheme 4.74 Azaprismane mechanism of **DP-2,3,5,6-d$_4$**

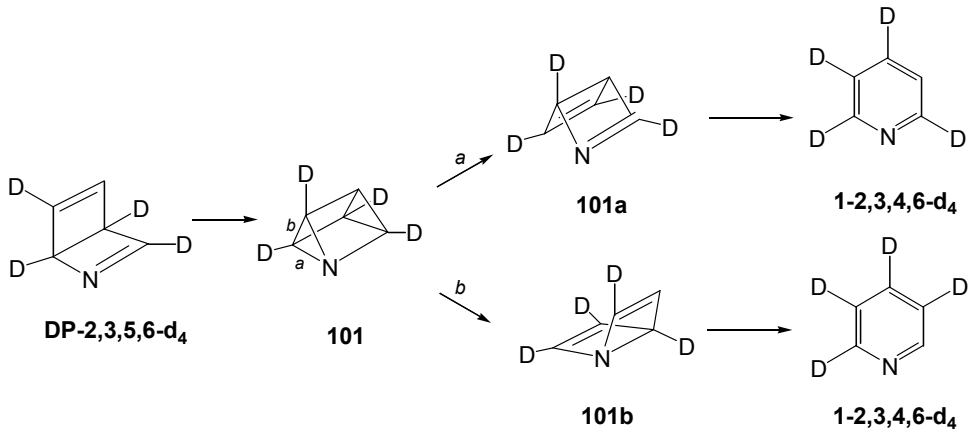

4.7.5.2. 2,3,4,6-Tetradeuteriopyridine (1-2,3,4,6-d$_4$)

Irradiation of 2,3,4,6-tetradeuteriopyridine (**1-2,3,4,6-d$_4$**) yielded 2,3,5,6-tetradeuterio-pyridine (**1-2,3,5,6-d$_4$**) and 2,3,4,5-tetradeuteriopyridine (**1-2,3,4,5-d$_4$**) in a ratio of 1:2. The ^{1}H-NMR spectrum of photoproducts shown in Figure 4.100 shows that

the proton signals observed at δ 7.79 and 8.60 where the H4 and H2,6 of pyridine absorb are due to the two new photoproducts. The interconversion among **1-2,3,4,6-d$_4$**, **1-2,3,5,6-d$_4$**, and **1-2,3,4,5-d$_4$** is suggested to occur via the azaprefulvene intermediate which is formed from the mechanism involving 2,6-bridging, nitrogen migration, and rearomatization as shown in Scheme 4.75.

Scheme 4.75 Phototransposition mechanism of **1-2,3,4,6-d$_4$**

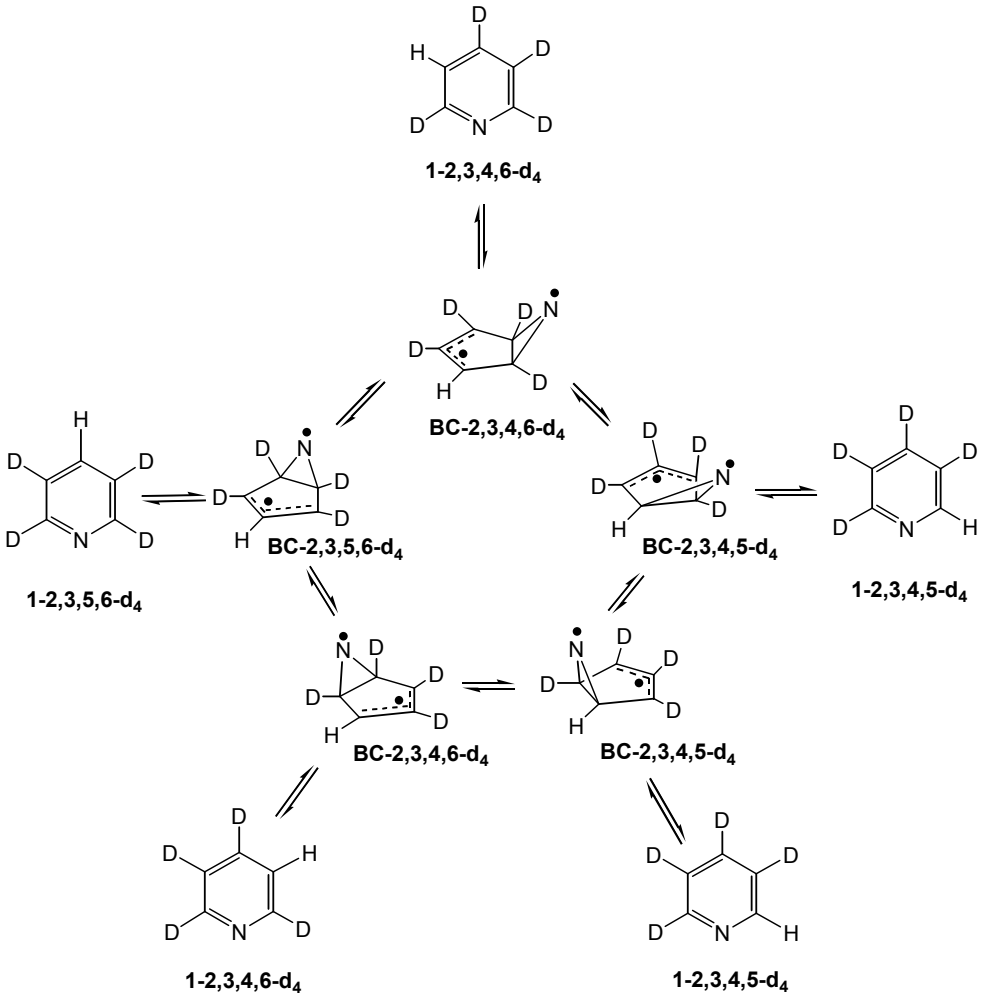

Excitation of **1-2,3,4,6-d_4** results in the formation of a bicyclic intermediate, **BC-2,3,4,6-d_4** by 2,6-bonding between C-2 and C-6. Once formed, this species undergoes nitrogen migration in both directions resulting in new azaprefulvene intermediate. Clockwise direction leads to the formation of **BC-2,3,4,5-d_4** which subsequently rearomatize to **1-2,3,4,5-d_4**. The second migration from this species leads to the formation of **BC-2,3,4,5-d_4'** which will undergo rearomatization to **1-2,3,4,5-d_4**, identical structure to the photoproduct from the first nitrogen migration. In the counterclockwise direction, **BC-2,3,4,6-d_4** undergo first nitrogen migration to form **BC-2,3,5,6-d_4** which leads to the formation of **1-2,3,5,6-d_4** after rearomatization. The second nitrogen migration would result in the formation of **BC-2,3,4,6-d_4'** followed by rearomatization to **1-2,3,4,6-d_4**, the starting material. The experimental observation evidences that the product ratio is 2:1 for **1-2,3,4,5-d_4** to **1-2,3,5,6-d_4** which is consistent with the statistical ratio from Scheme 4.75.

In addition to the electrocyclic ring closure-nitrogen migration mechanism shown in Scheme 4.75, the mechanism involving Dewar-Pyridine intermediates mechanism shown in Scheme 4.76 and 4.77 has also been examined. Unlike the deuterated pyridines that were previously described, the different Dewar pyridine intermediates can be formed from **1-2,3,4,6-d_4** by 2,5-, or 3,6-bonding of the pyridine ring followed by C and N sigmatropic shifts. This would result in two different mechanistic pathways originating from different intermediates.

Scheme 4.76 shows the Dewar pyridine mechanism formed from 2,5-bonding which results in the formation of **DP-2,3,4,6-d$_4$**. Rearomatization of all possible Dewar-pyridines leads back to 2,3,4,6-tetradeuteriopyridine (**1-2,3,4,6-d$_4$**).

Scheme 4.76 Dewar-pyridine mechanism of **1-2,3,4,6-d$_4$**: 2,5-bonding

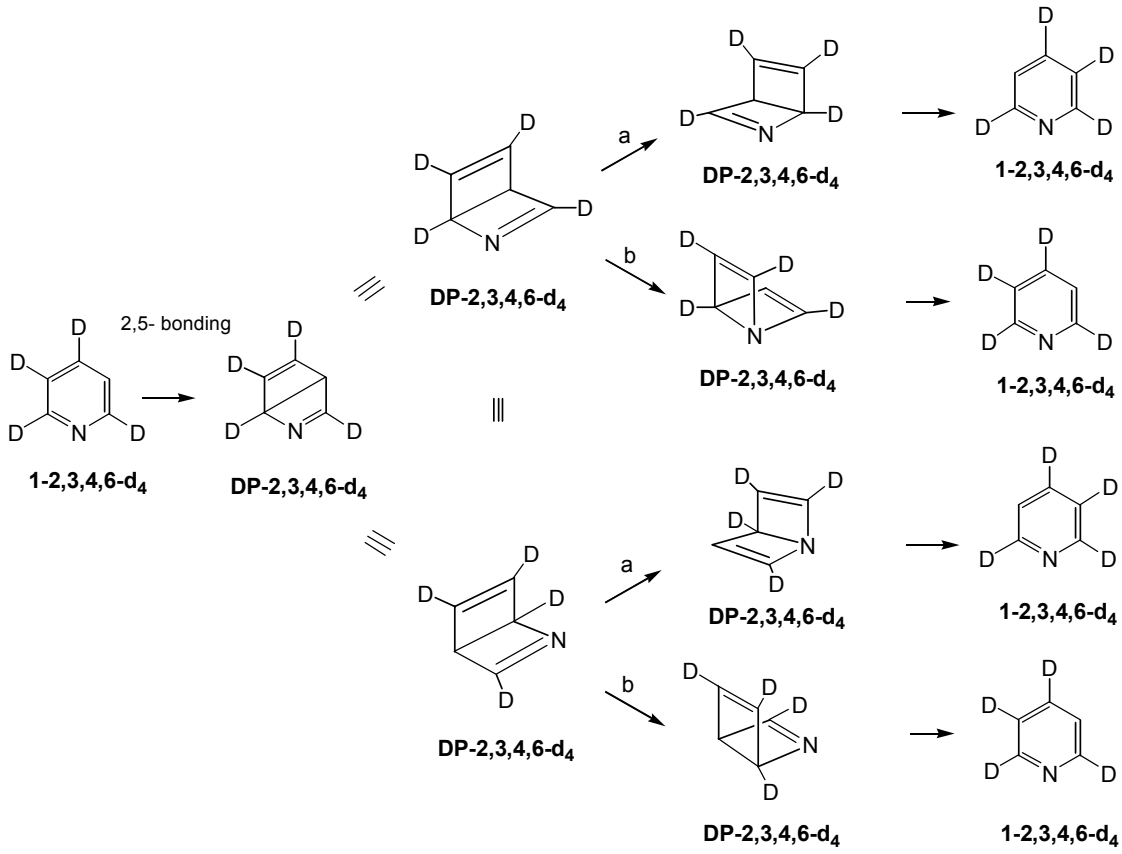

Scheme 4.77 shows the Dewar-pyridine mechanism originating from 3,6-bonding. The resulting Dewar-pyridine is **DP-2,3,4,6-d$_2$** which undergoes nitrogen rearrangement to **DP-2,3,4,6-d$_4$** itself. Thus, all possible Dewar-pyridine leads to the starting material.

Scheme 4.77 Dewar-pyridine mechanism of **1-2,3,4,6-d$_4$**: 3,6-bonding

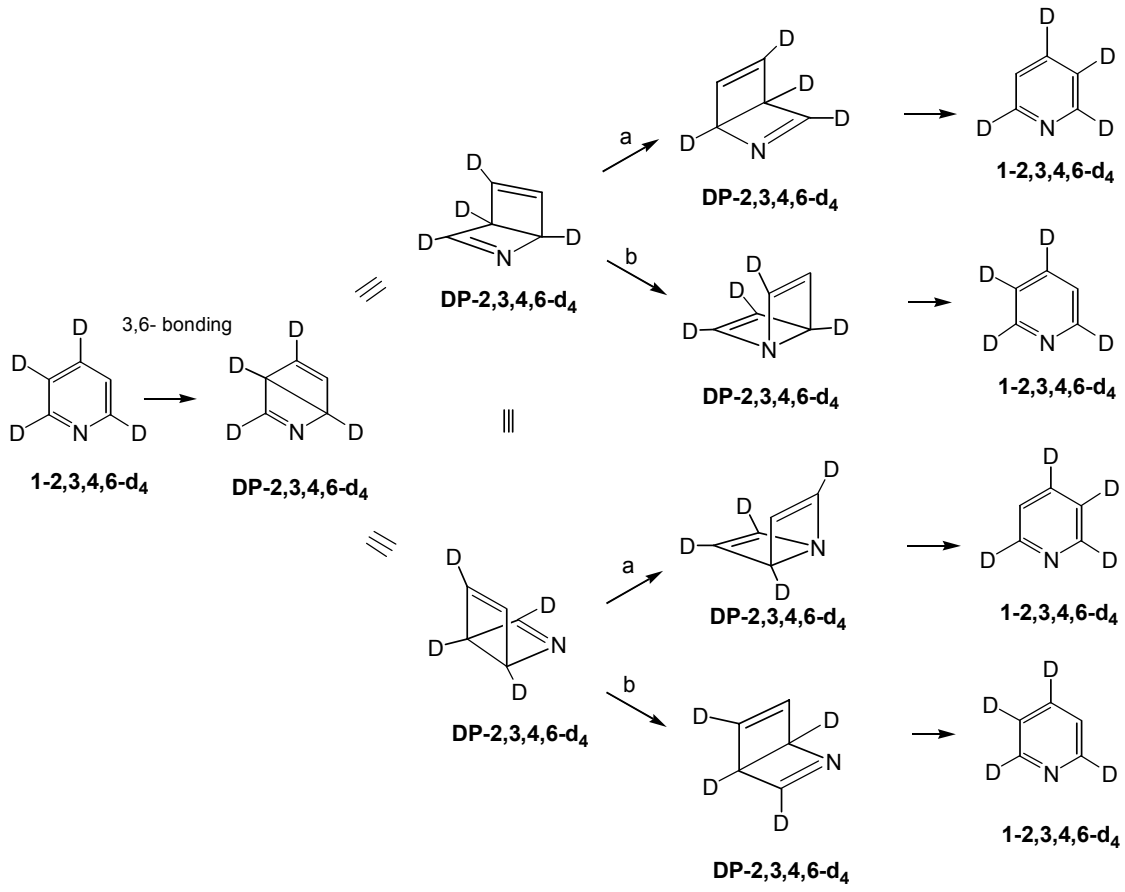

This shows that if Dewar-pyridine mechanism is operating it cannot be detected.

In addition, the [2+2] cycloaddition of Dewar-Pyridine **DP-2,3,4,6-d$_4$** from 2,5- and 3,6-bonding can form azaprismane structures shown in Scheme 4.78.

Scheme 4.78 Azaprismane mechanism of **DP-2,3,4,6-d$_4$**

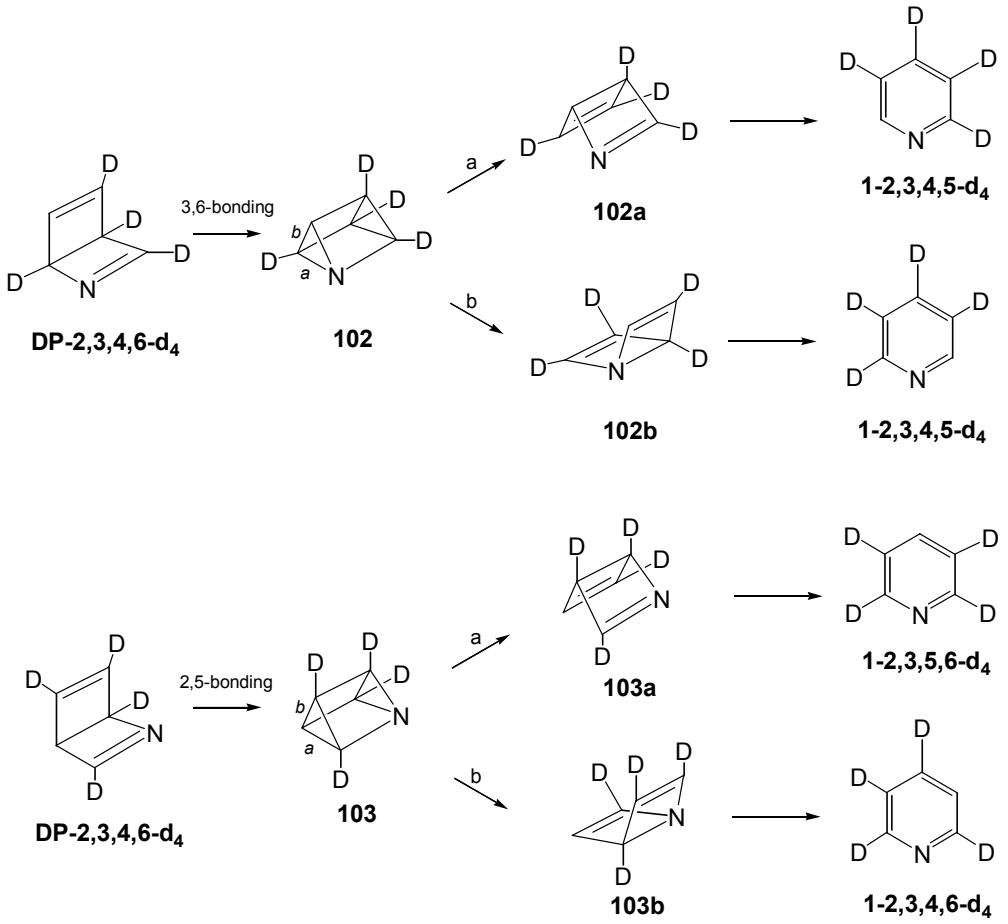

The azaprismane mechanism shows that irradiation of **1-2,3,4,6-d$_4$** would result in the formation of **1-2,3,4,5-d$_4$** and **1-2,3,5,6-d$_4$** in a statistical ratio of 2:1 identical to electrocyclic ring closure-heteroatom migration.

4.7.5.3. 2,3,4,5-Tetradeuteriopyridine (1-2,3,4,5-d$_4$)

Irradiation of **1-2,3,4,5-d$_4$** was found to result in the formation of **1-2,3,4,6-d$_4$** and **1-2,3,5,6-d$_4$**. Scheme 4.79 shows that excitation of **1-2,3,4,5-d$_4$** results in the formation

Scheme 4.79 Phototransposition mechanism of (**1-2,3,4,5-d$_4$**)

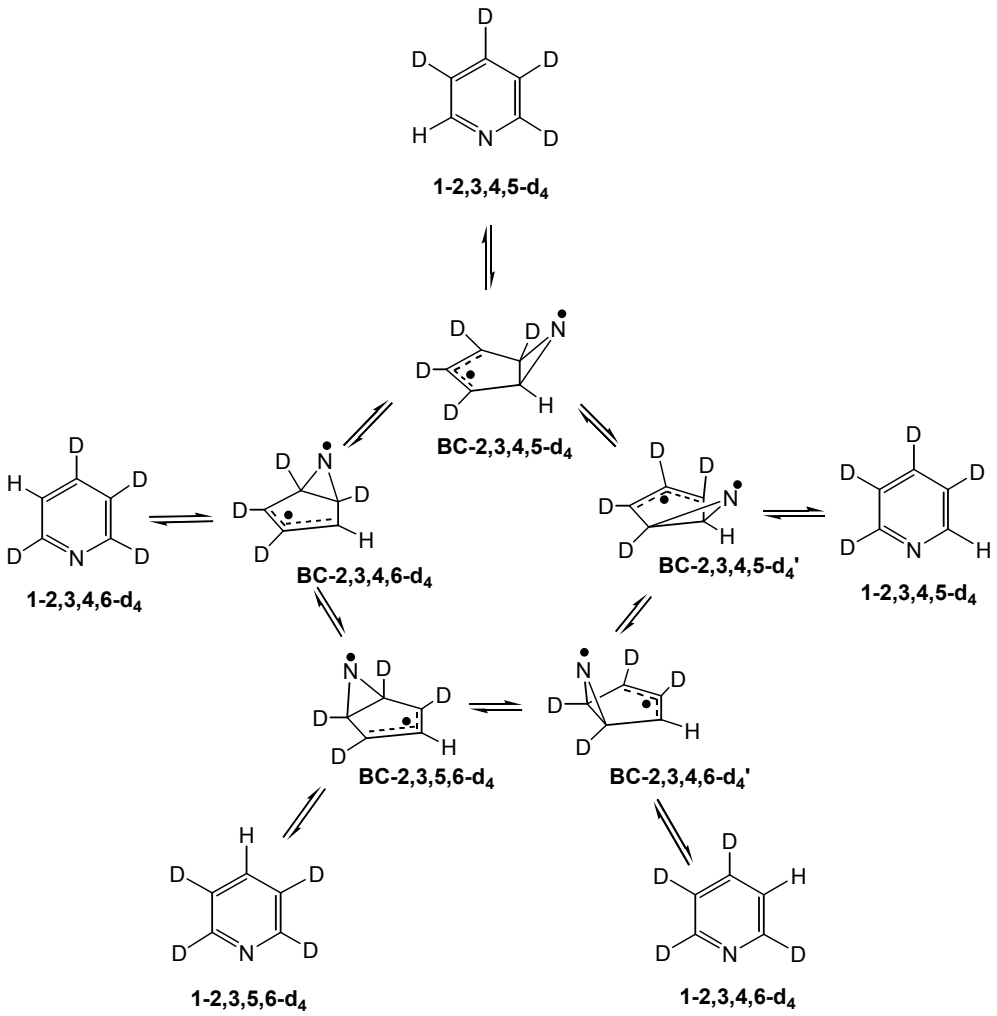

of azaprefulvene **BC-2,3,4,5-d$_4$**. These intermediate undergoes nitrogen migration around five sides of the cyclopentenyl ring. One nitrogen migration in

counterclockwise direction result in the formation of **BC-2,3,4,6-d_4** which is allowed to rearomatize to **1-2,3,4,6-d_4**, one of the photoproduct. The second nitrogen migration subsequently forms **BC-2,3,5,6-d_4** followed by aromatization to **1-2,3,5,6-d_4** as another photoproduct. The nitrogen migration in the clockwise direction of **BC-2,3,4,5-d_4** results in the formation of **BC-2,3,4,5-d_4'**. This azaprefulvene structure leads back to the starting material after rearomatization. The second nitrogen migration of **BC-2,3,4,5-d_4'** results in the formation of **BC-2,3,4,6-d_4'** which then undergo rearomatization to **1-2,3,4,6-d_4**. These results are consistent with the ^{1}H-NMR spectrum shown in Figure 4.102. The two new singlets observed at δ 7.36 and 7.79 represent the H3,5 and H4 of two new pyridine isomers. The integrated ratio of H3,5 to H4 of 2:1 in NMR result also confirms this mechanistic scheme.

The mechanism involving Dewar-Pyridine intermediate has also been examined. The Dewar-Pyridines that result from 2,5- or 3,6-bonding as shown in Schemes 4.80 and 4.81.

Scheme 4.80 Dewar-pyridine mechanism of **1-2,3,4,5-d$_4$**: 2,5-bonding

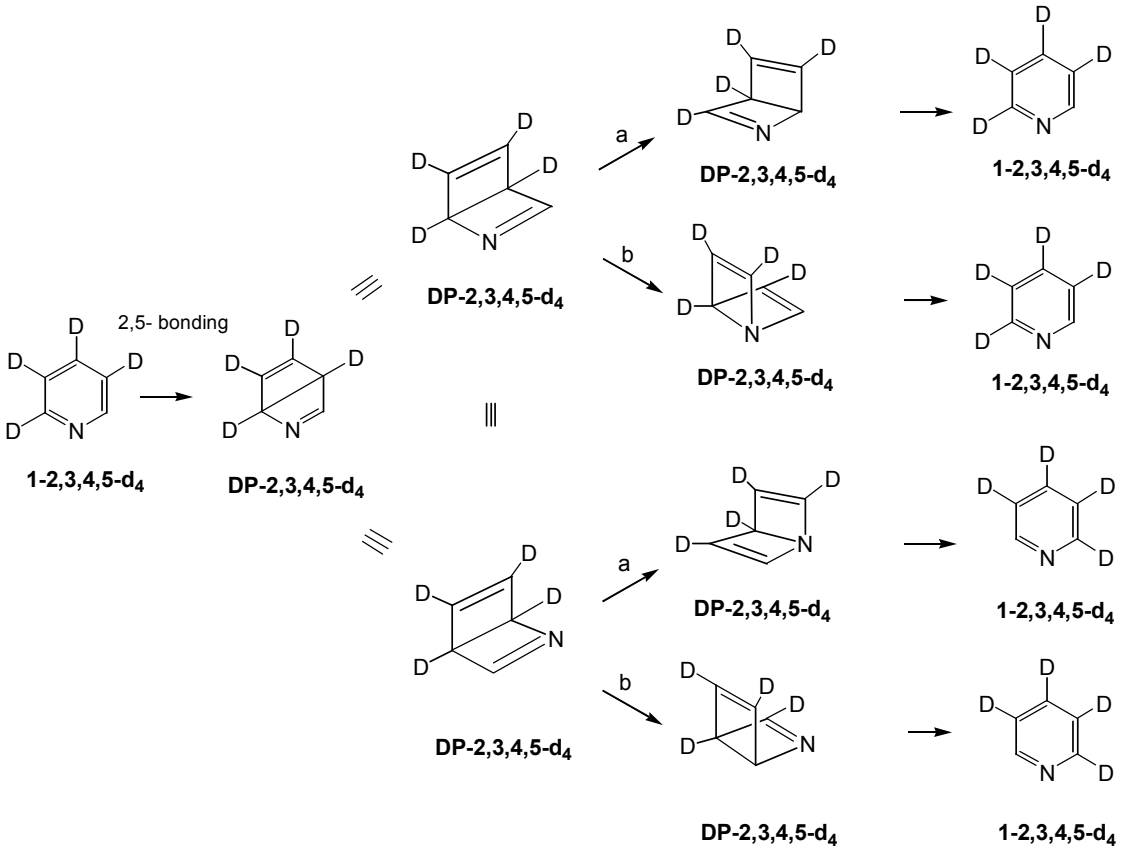

The rearrangement of all possible Dewar-pyridines in Scheme 4.80 leads back to the starting material **1-2,3,4,5-d$_4$**. This means that if this mechanism exists, it cannot be detected. However, the ^{1}H-NMR result shown in Figure 4.102 indicates that there are indeed new photoproducts formed from irradiation of **1-2,3,4,5-d$_4$**.

Scheme 4.81 Dewar-pyridine mechanism of **1-2,3,4,5-d$_4$**: 3,6-bonding

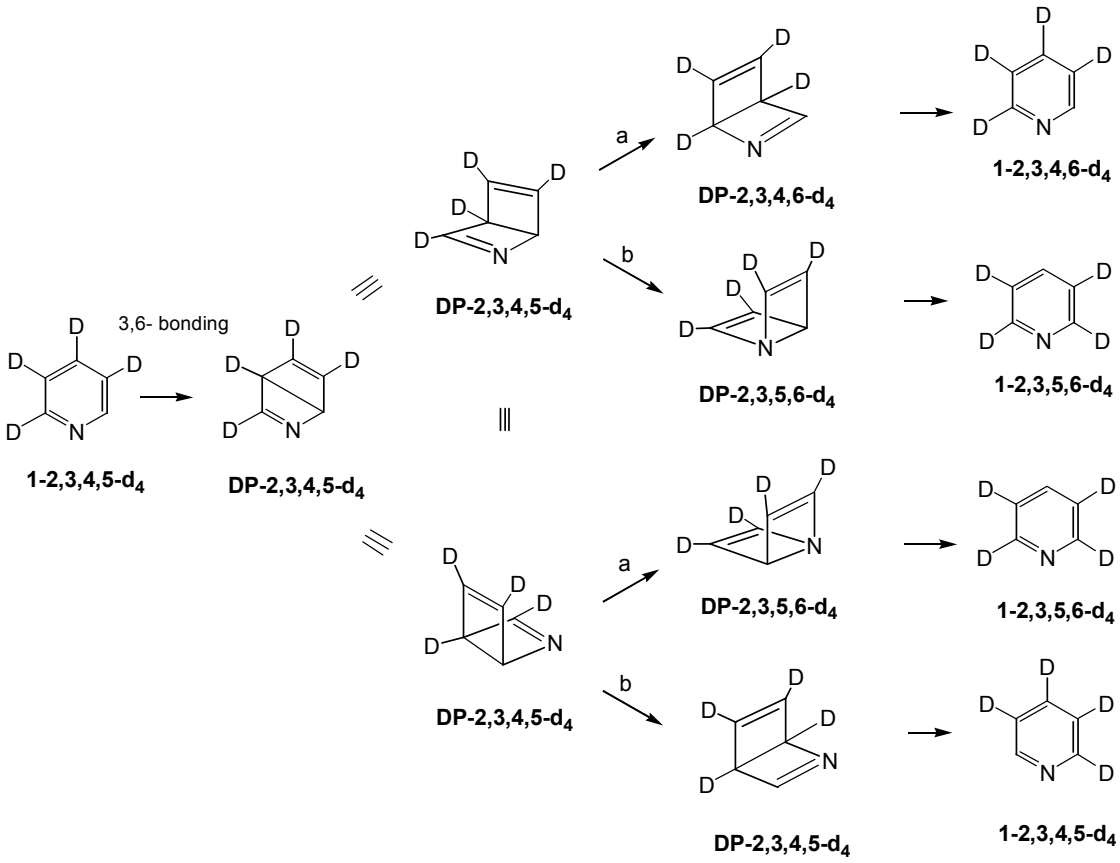

Scheme 4.81 shows that the rearrangement of **DP-2,3,4,5-d$_4$** from 3,6-bridging leads to the formation of **1-2,3,4,5-d$_4$**, the starting material, and **1-2,3,5,6-d$_4$** as only photoproduct. This is not consistent with the experimental results which shows that **1-2,3,4,5-d$_4$** is photochemically converted to **1-2,3,4,5-d$_4$** and **1-2,3,5,6-d$_4$**. Therefore, the Dewar-pyridine mechanism does not take place in the photochemistry of **1-2,3,4,5-d$_4$**.

In addition to the Dewar-pyridine, the azaprismane possibility was also examined. Scheme 4.82 shows the [2+2] cycloaddition of **DP-2,3,4,5-d$_4$** resulting from 2,5-bonding and 3,6-bonding followed by rearranging to photoproducts.

Scheme 4.82 Azaprismane mechanism of **DP-2,3,4,5-d$_4$**

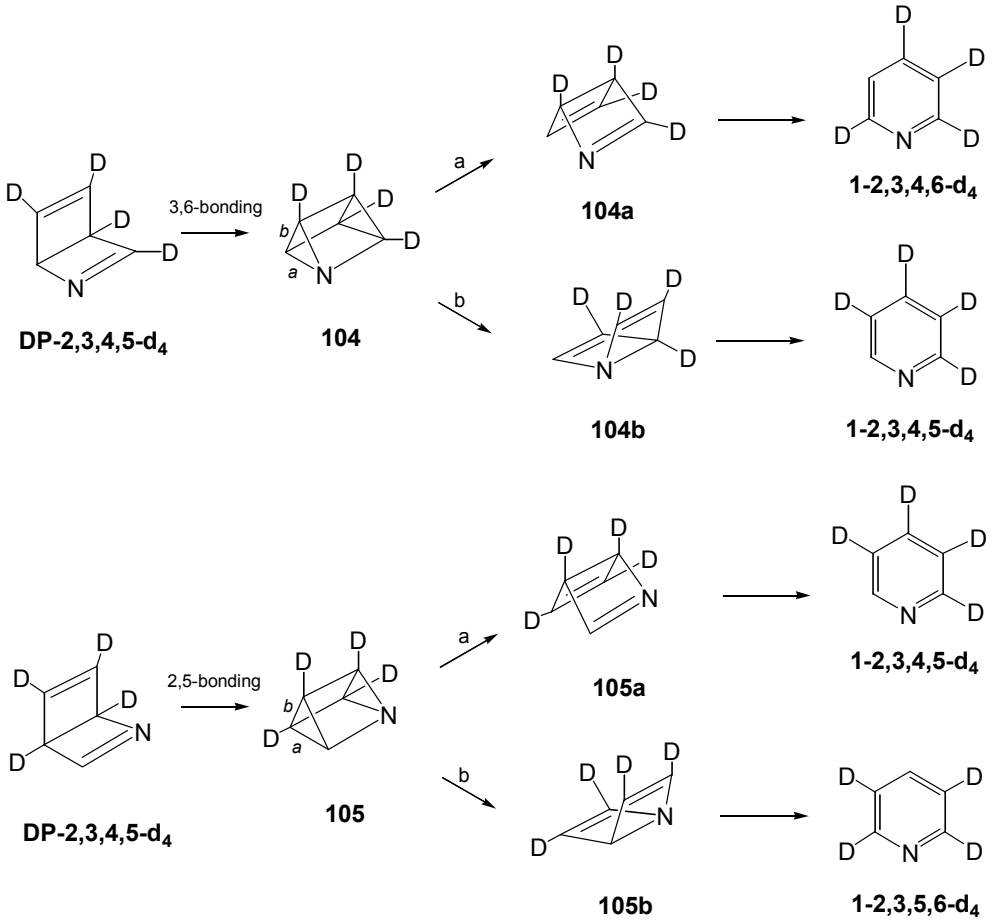

Although this mechanism would result in the formation of the other two isomers of pyridine **1-2,3,4,5-d$_4$**, the ratio of **1-2,3,4,6-d$_4$** and **1-2,3,5,6-d$_4$** is 1:1. This is not consistent with the experimental result suggesting that the ratio is 2:1. Therefore, the phototransposition of **1-2,3,4,5-d$_4$** does not occur via this pathway.

This discussion shows that mechanism involving interconverting Dewar-pyridines or azaprismanes predict the correct photoproducts in some cases but not in others. Of the pathways considered, the mechanistic pathway that consistenly predicts the correct products is the cyclization-nitrogen migration mechanism.

4.8. Photochemistry of cyanopyridines in solution phase

4.8.1. Irradiation of cyanopyridines in the solution phase

A $2x10^{-2}$ M solution of 2-cyanopyridine (**36**), 3-cyanopyridine (**37**), or 4-cyanopyridine (**38**) in acetonitrile was irradiated with 16 low-pressure mercury lamps at 254 nm. Figure 4.103 shows the GC trace of 2-cyanopyridine before irradiation.

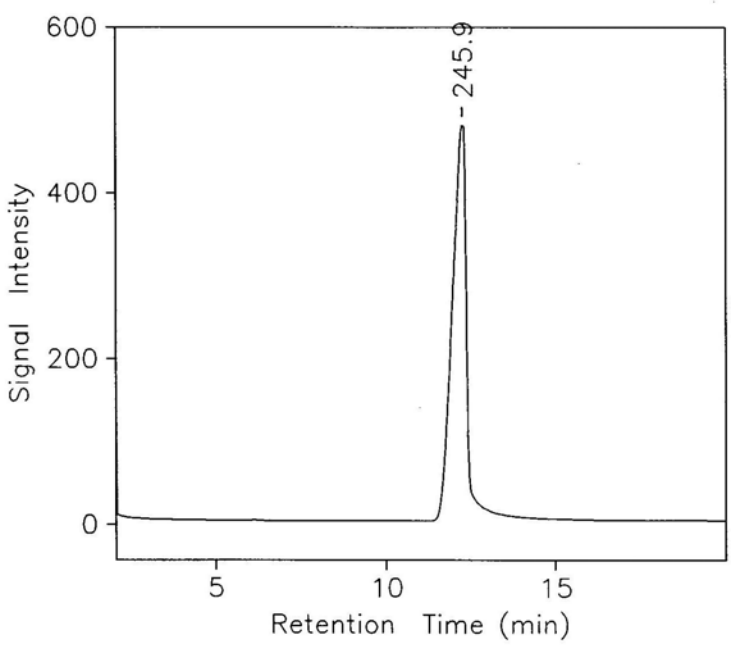

Figure 4.103 GC trace of 2-cyanopyridine before irradiation

The GC analysis shows one intense signal for 2-cyanopyridine (**36**) observed at a retention time of 12 min with a peak area of 245.9.

Figure 4.104 shows the GC trace for this solution of 2-cyanopyridine after irradiation for 4 hours.

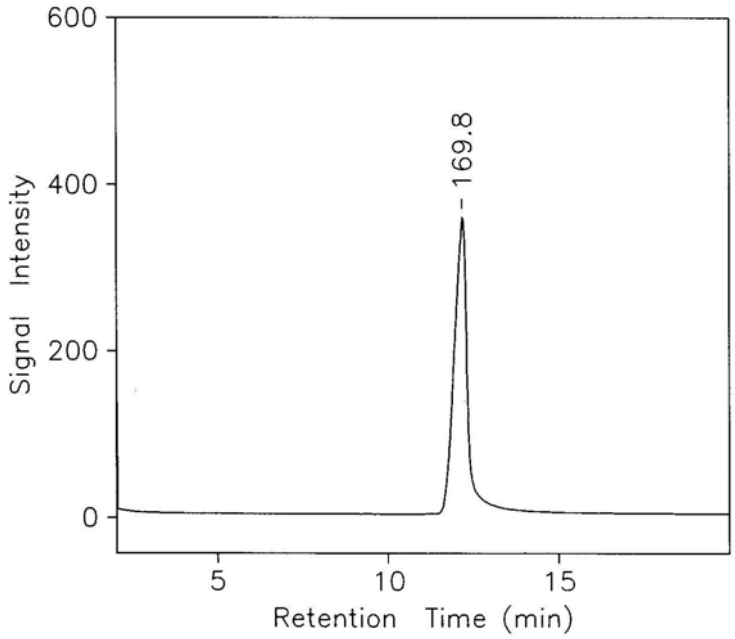

Figure 4.104 GC trace of 2-cyanopyridine after irradiation for 4 hours

After irradiation, GC analysis shows that approximately 30% of 2-cyanopyridine (**36**) was consumed. However, this analysis shows that there was no GC-volatile photoproduct formed from this irradiation.

In a different experiment, a 3-cyanopyridine (**37**) solution was irradiated for 2 and 4 hours. Figure 4.105 shows the GC trace of 3-cyanopyridine (**37**) before irradiation exhibiting an intense signal of **37** at 7 min. retention time.

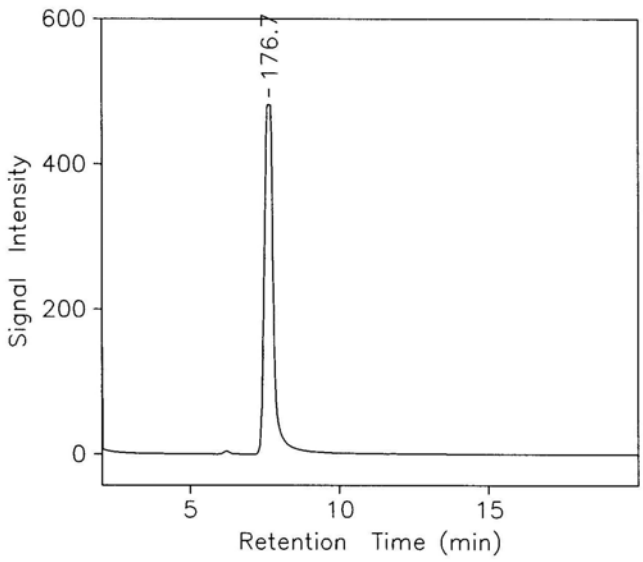

Figure 4.105 GC trace of 3-cyanopyridine before irradiation

After irradiation, the GC-trace in Figure 4.106 shows that after 4 hours of irradiation, 13% of 3-cyanopyridine was consumed but no GC-volatile photoproduct could be detected.

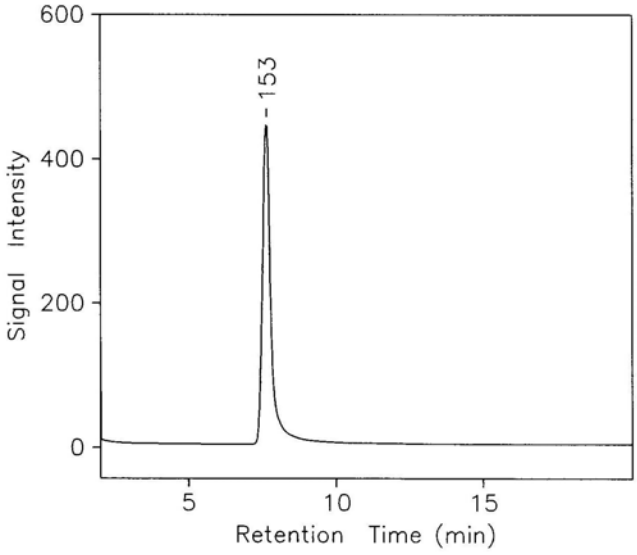

Figure 4.106 GC trace of 3-cyanopyridine after irradiation for 4 hours

The GC trace shown in Figure 4.107 shows the GC-trace of the 4-cyanopyridine solution (**38**) before irradiation.

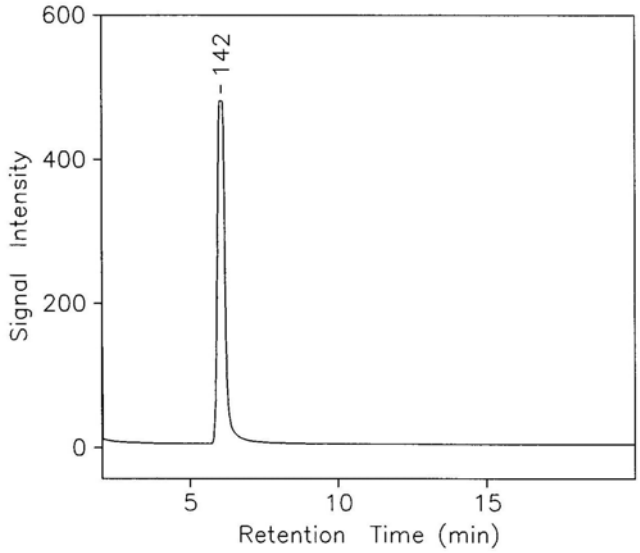

Figure 4.107 GC trace of 4-cyanopyridine before irradiation

After irradiation for 4 hours, GC analysis shown in Figure 4.108 shows that approximately 90% of 4-cyanopyridine (**40**) was consumed without the formation of any GC-volatile products.

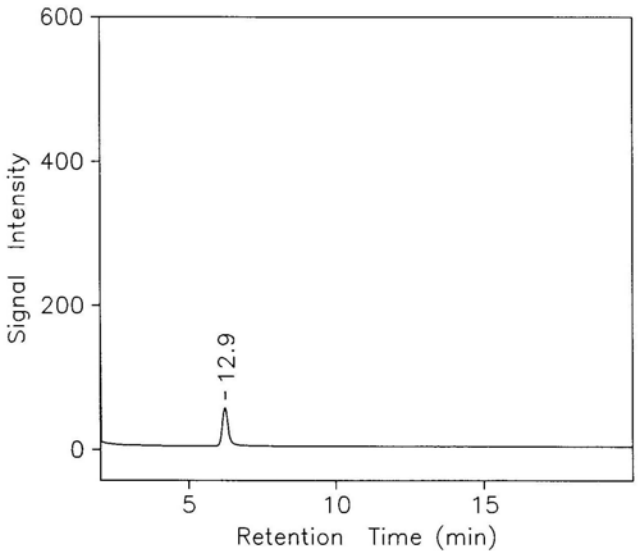

Figure 4.108 GC trace of 4-cyanopyridine after irradiation for 4 hours

These experiments show that irradiation of 2-, 3-, or 4-cyanopyridine in acetonitrile solution does not lead to the formation of any GC-volatile products. Thus, phototransposition does not occur in the solution phase.

The analogous results for the photochemistry of cyanopyridines **36-38** were also observed in non-polar solvent. In a different experiment, 2, 3, or 4-cyanopyridine ($2x10^{-2}$ M) solution in methylcyclohexane was photochemically studied. Irradiation of cyanopyridine solutions were carried out in a Rayonet reactor at 254 nm (13 lamps) for 30 minutes. After irradiation, the solution color turned yellow. The GC analysis shows that all reactants were consumed but no isomerized products could be observed. In other word, irradiation of one cyanopyridine isomer did not result in the formation of the other two isomers that was observed in the gas phase photolysis. Figure 4.109 shows the GC trace of 2-cyanopyridine before irradiation. Only peak of 2-cyanopyridine at 13 minutes

is observed. After irradiation, the relative area of this peak was 12% decreased without the formation of any new product.

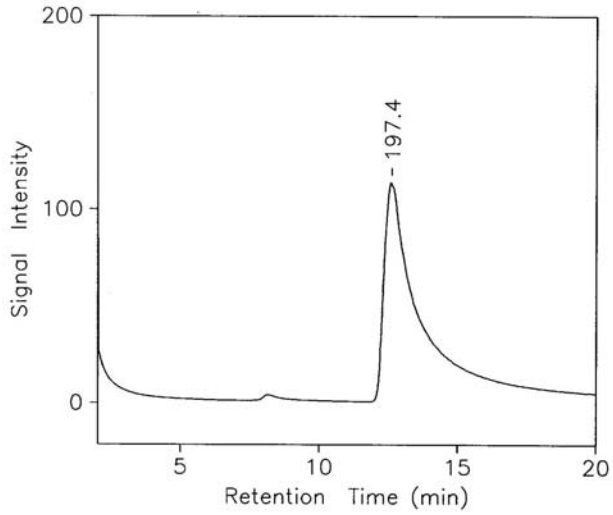

Figure 4.109 GC trace of 2-cyanopyridine in MCH before irradiation

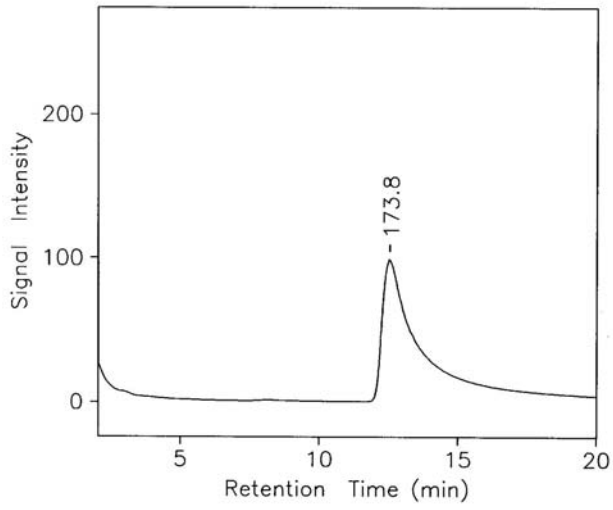

Figure 4.110 GC trace of 2-cyanopyridine in MCH after 30 minutes of irradiation

In the photolysis of 3-cyanopyridine (**37**), no any photoproduct could be observed after irradiation. This shows that irradiation of **37** in non-polar solvent also did not give the isomer of 3-cyanopyridine and the reactant was consumed only 6.02%. Figure 4.111 shows the GC trace of **37** before irradiation and Figure 4.112 shows the GC trace of **37** after irradiation.

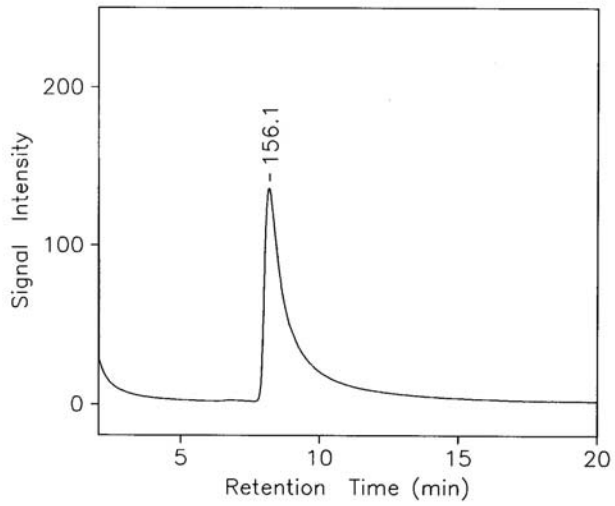

Figure 4.111 GC trace of 3-cyanopyridine in MCH before irradiation

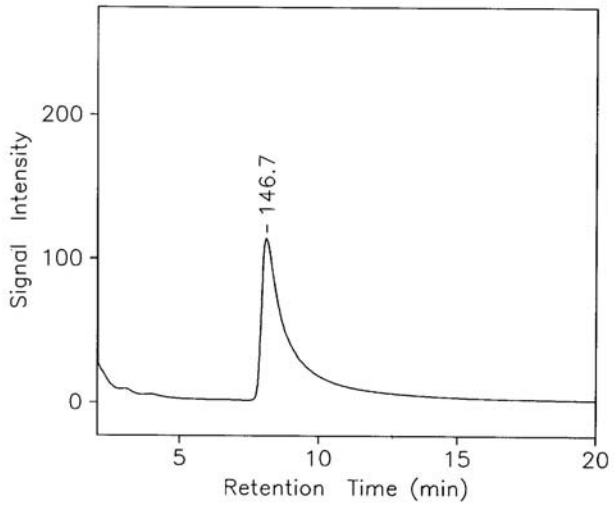

Figure 4.112 GC trace of 3-cyanopyridine in MCH after 30 minutes of irradiation

The photolysis of 4-cyanopyridine (**38**) also shows the similar result. The decrease in relative peak area from 160.6 to 92.2 (57%) shows that 4-cyanopyridine was consumed without the formation of any GC-volatile product. Figure 4.113 shows the GC trace of 4-cyanopyridine (**38**) before irradiation. After irradiation, the GC trace still shows the peak of the reactant in a less extent.

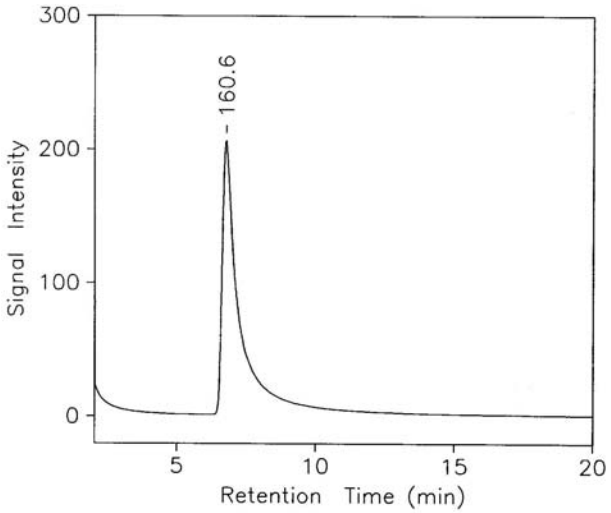

Figure 4.113 GC trace of 4-cyanopyridine in MCH before irradiation

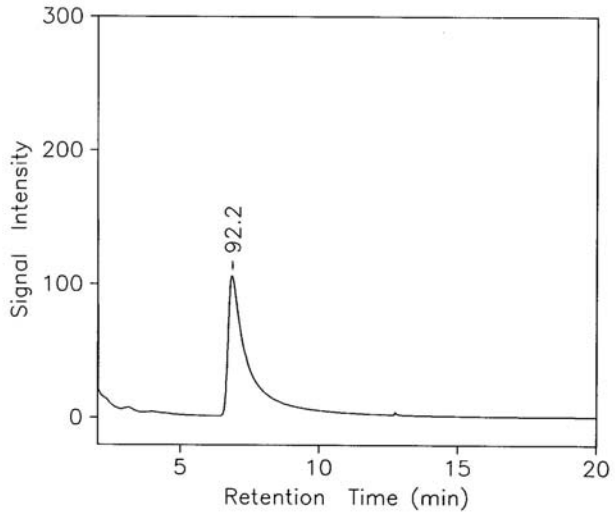

Figure 4.114 GC trace of 4-cyanopyridine in MCH after 30 minutes of irradiation

CHAPTER V

Experimental

5.1. General Procedures

2-Cyanopyridine, 3-cyanopyridine, 4-cyanopyridine, 2-methylpyridine, 3-methylpyridine, and 4-methylpyridine were purchased from Aldrich Chemical Company. All of these compounds were distilled before use. The ^{1}H NMR and ^{13}C NMR spectra were recorded at 400 MHz on a Bruker FT-NMR system. ^{1}H and ^{13}C chemical shifts were measured relative to internal $(CH_3)_2CO$ or $CDCl_3$. GLC was performed on a PE-9000 FID instrument equipped with 15 m x 3 μm methyl 50 % phenylsilicon phase capillary column. Mass spectra were recorded with an HP 5970B mass selective detector interfaced to an HP 5880 capillary gas chromatograph. Ultraviolet absorption spectra were performed on a Hitachi U-2000 and Shimadzsu UV-2100U spectrometers. Luminescence spectra were recorded on a PE-LS 50 spectrometer. Flash column chromatography was carried out on silica gel, 45-60 μm average particle size. Preparative-layer chromatography was carried out on 20 x 20 cm glass plates coated with 2 mm of silica gel 60 $F_{254+366\ nm}$ (EM Science).

5.2. Ultraviolet absorption

Absorption spectra of cyanopyridines (**36-38**) were recorded by placing $8x10^{-5}$ M-solution in 1:1 ethanol/methanol or acetonitrile in a cuvette, which was always capped

during analysis. The range of UV absorption wavelength is between 220-350 nm. The λ_{max} of 2-cyanopyridine (**36**) is 264 nm; 3-cyanopyridine (**37**) is 264 nm; 4-cyanopyridine (**38**) is 282 nm.

5.3. Methods of irradiation and analysis

Irradiation of cyanopyridine, methylpyridine, deuterated cyanopyridine, deuterated pyridine vapors were carried out in a Rayonet reactor equipped with 4 or 15 low-pressure mercury arc lamps. The materials were introduced into a 3-L quartz reactor as a gas at the reduced pressure. Prior to introduction of the materials into the reactor, the dissolved gas was removed by two freeze-thaw cycles using an acetone-dry ice bath.

5.4. GC analysis of photoproduct

The quantitative analysis of photoproduct was calculated from GC area results. Because of material losses during filling the reaction vessel and during recovery after irradiation, the percent consumption of starting material and percent formation of photoproducts were not obtained accurately. The relative values of the peak area in the GC results were therefore used to calculate the percent formation of products. To ensure that the peak areas of compounds are accurate, each peak area is multiplied by its detector response value calculated from 1mg-injection peak area of each substance. The percent formations of products are assumed to obtain from the percent starting material consumed.

It should be noted that the loss of starting materials during analysis are uncertain and unavoidable in each experiment.

5.5. Irradiation at 254 nm

5.5.1. 2-Cyanopyridine (36)

The vapor of 2-cyanopyridine (**36**) (0.3 Torr) was obtained from 100 mg of the sample in a 3-L quartz reactor at 24 ^{o}C. This was then irradiated in a Rayonet reactor equipped with 4-low mercury arc lamps for 15, 60, 75, and 90 minutes. After irradiation, the resulting material was recovered by pumping it out through a trap cooled in an acetone-dry ice bath. The resulting product was dissolved in 2 mL of ether. The GC analysis was obtained by injecting this solution through capillary column at oven temp of 100 ^{o}C. The GC traces showed the consumption of **36** and the formation of **37** and **38** with retention times of 12, 7, and 6 minutes, respectively. Table 5.1 shows photolysis conditions and quantitative results.

Table 5.1 Irradiation of 2-cyanopyridine (**36**) at 254 nm

Exp no.	Irradiation time (min)	Sample weight (mg)	Recovered weight (mg)	2-CNP consumption (%)	3-CNP formation (%)	4-CNP formation (%)
1	15	13	5	4.9	3.6	1.29
2	60	20	7	22.7	18.4	4.31
3	75	18	9	27.0	22.4	4.64
4	90	17	8	35.3	29.4	5.92

After GC-analysis, the ether solvent was removed by purging with nitrogen. The resulting crude was dissolved in acetone-d_6 and analyzed by ^{1}H-NMR.

5.5.2. 3-Cyanopyridine (37)

The vapor of 3-cyanopyridine (**37**) (0.3 Torr) was obtained from 100 mg of the sample in a 3-L quartz reactor at 25 ^{o}C. This was then irradiated in a Rayonet reactor equipped with 4-low mercury arc lamps for 60, 120, 240, and 360 minutes. After irradiation, the resulting material was recovered by pumping it out through a trap cooled in an acetone-dry ice bath. The resulting product was dissolved in 2 mL of ether. The GC analysis was obtained by injecting this solution through capillary column at oven temp of 100 ^{o}C. The GC traces showed the consumption of **37** and the formation of **36** and **38** with retention times of 7, 12, and 6 minutes, respectively. Table 5.2 shows photolysis conditions and quantitative results.

Table 5.2 Irradiation of 3-cyanopyridine (**37**) at 254 nm

Exp no.	Irradiation time (min)	Sample weight (mg)	Recovered weight (mg)	3-CNP consumption (%)	4-CNP formation (%)	2-CNP formation (%)
5	60	11	8	3.0	1.58	1.46
6	120	9	7	4.5	2.08	2.45
7	240	9	4	8.9	3.80	5.06
8	360	13	8	7.5	2.89	4.64

After GC analysis, the sample in the ether solution was concentrated by purging with nitrogen. Aceton-d_6 was added and the solution was analyzed by ^{1}H-NMR.

5.5.3. 4-Cyanopyridine (38)

4-Cyanopyridine vapor (**38**) (0.3 Torr) was obtained from 100 mg of the sample in a 3-L quartz reactor at 24 ^{o}C. This was then irradiated in a Rayonet reactor equipped with 4-low mercury arc lamps for 23, 45, 70, and 90 minutes. After irradiation, the resulting material was recovered by pumping it out through a trap cooled in an acetone-dry ice bath. The resulting product was dissolved in 2 mL of ether. The GC analysis was obtained by injecting this solution through a capillary column at an oven temperature of 100 ^{o}C. The GC traces showed the consumption of **38** and the formation of **37** and **36** with retention times of 6, 7, and 12 minutes, respectively. Table 5.3 shows photolysis conditions and quantitative results.

Table 5.3 Irradiation of 4-cyanopyridine (**38**) at 254 nm

Exp no.	Irradiation time (min)	Sample weight (mg)	Recovered weight (mg)	4-CNP consumption (%)	3-CNP formation (%)	2-CNP formation (%)
9	23	15	10	26.6	24.5	2.13
10	45	11	10	39.7	36.8	2.91
11	70	13	10	47.0	43.5	3.50
12	90	16	15	59.8	54.3	5.55

After GC analysis, the ether solvent was removed and acetone-d_6 was added. The resulting solution was analyzed by ^{1}H-NMR spectroscopy.

5.5.4. 2-Methylpyridine (6)

The vapor of 2-methylpyridine (**6**) (2.7 Torr) was obtained by vaporizing the sample (72 mg) into the 3-L quartz reactor at 25 ^{o}C. It was irradiated in the Rayonet reactor at 254 nm using 15 low-pressure mercury arc lamps for 3, 6, and 12 hours. After irradiation, the material was recovered by pumping it out through a trap cooled in acetone-dry ice. This was then dissolved in 1 mL $CDCl_3$ and analyzed by ^{1}H-NMR and ^{13}C-NMR. The GC analysis was obtained by diluted this solution to 8 mL and injecting an aliquot into the capillary column at oven temp of 55 ^{o}C. The GC trace showed the consumption of 2-methylpyridine (**6**) at retention time 19 minutes and formation of 3-methylpyridine (**7**) at 31 minutes and 4-methylpyridine (**8**) at 32 minutes as phototransposition products. It also shows pyridine at 15 minutes and an unknown compound at 29 minutes as methyl-demethylation products. Table 5.4 shows photolysis conditions and quantitative results.

Table 5.4 Irradiation of 2-methylpyridine (**6**) at 254 nm

Exp no.	Irradiation time (min)	Sample weight (mg)	Recovered weight (mg)	2-MP consumption (%)	3-MP formation (%)	4-MP formation (%)
16	3	75.1	48.7	5	3.41	0.62
17	6	72.6	42.5	9.9	6.60	1.85
18	12	50.3	29.8	19.5	13.2	4.39

5.5.6. 3-Methylpyridine (7)

The vapor of 3-methylpyridine (**7**) (2.5 Torr) was obtained by vaporizing 100 mg of the sample into the 3-L quartz reactor at 25 ^{o}C. This was then irradiated in the Rayonet reactor at 254 nm using 15 low-pressure mercury arc lamps for 3, 6, and 12 hours. After irradiation, the material was recovered by pumping it out through a trap cooled in an acetone-dry ice bath. The material was dissolved in 1 mL $CDCl_3$ and analyzed by ^{1}H-NMR and ^{13}C-NMR. This solution was diluted to 8 mL and then it was analyzed by GC at an oven temperature of 55 ^{o}C. The GC traces showed the consumption of 3-methylpyridine (**7**) at retention time 31 minutes and the formation of 2-methylpyridine (**6**) at 19 minutes and 4-methylpyridine (**8**) at 32 minutes as phototranspositon products. It also showed the formation of pyridine (**1**) at 15 minutes as a demethylation product. No methylation product was observed. Table 5.5 shows photolysis conditions and quantitative results.

Table 5.5 Irradiation of 3-methylpyridine (**7**) at 254 nm

Exp no.	Irradiation time (min)	Sample weight (mg)	Recovered weight (mg)	3-MP consumption (%)	2-MP formation (%)	4-MP formation (%)
19	3	72.4	28.4	16.5	10.5	5.7
20	6	72.8	38.5	27.3	17.2	9.5
21	12	77.3	36.5	38.3	24.2	14.4

5.5.7. 4-Methylpyridine (8)

The vapor of 4-methylpyridine (**8**) (2.7 Torr) was obtained by vaporizing 100 mg of the sample into the 3-L quartz reactor at 25 ^{o}C. This was then irradiated in the Rayonet reactor at 254 nm using 15 low-pressure mercury arc lamps for 3, 6, and 12 hours. After irradiation, the material was recovered by pumping it out through a trap cooled in an acetone-dry ice bath. The material was dissolved in 1 mL $CDCl_3$ and analyzed by ^{1}H-NMR and ^{13}C-NMR. This solution was diluted to 8 mL and then analyzed by GC at oven temperature of 55 ^{o}C. The GC traces showed the consumption of 4-methylpyridine (**8**) at a retention time of 32 minutes and the formation of 3-methylpyridine (**7**) at 31 minutes and 4-methylpyridine (**8**) at 19 minutes as phototranspositon products. It also showed the formation of pyridine (**1**) at 15 minutes as a demethylation product, and 2,6-dimethylpyridine at 24 minutes as a methylation product. Table 5.6 shows photolysis conditions and quantitative results.

Table 5.6 Irradiation of 4-methylpyridine (**8**) at 254 nm

Exp no.	Irradiation time (min)	Sample weight (mg)	Recovered weight (mg)	4-MP consumption (%)	2-MP formation (%)	3-MP formation (%)
22	3	29.4	20.6	11.7	4.4	6.7
23	6	77.1	29.1	16.6	6.7	9.3
24	12	70.1	20.6	20.5	8.7	11.4

5.6. Irradiation at $\lambda \geq 290$ nm

5.6.1. 2-Cyanopyridine (36)

The vapor of 2-cyanopyridine (**36**) (0.3 Torr) was obtained from 100 mg of the sample in a 3-L quartz reactor. This was then irradiated through a pyrex filter in the Rayonet reactor using sixteen 300 nm lamps for 24 hours. After irradiation, the material was recovered by pumping it out through a trap cooled in an acetone-dry ice bath. The material was dissolved in 2 mL ether. The resulting solution was analyzed by GC. Table 5.7 shows photolysis conditions and quantitative analysis.

Table 5.7 Irradiation of 2-cyanopyridine (**36**) at $\lambda \geq 290$ nm.

Exp no.	Sample weight (mg)	Recovered weight (mg)	Irradiation time (hours)	2-CNP consumption (%)	3-CNP formation (%)	4-CNP formation (%)
13	7	7	24	18.3	9.6	8.7

5.6.2. 3-Cyanopyridine (37)

The vapor of 3-cyanopyridine (**37**) (0.3 Torr) was obtained from 100 mg of the sample in a 3-L quartz reactor. This was then irradiated through a pyrex filter in the Rayonet reactor using sixteen 300 nm lamps for 24 hours. After irradiation, the material was recovered by pumping it out through a trap cooled in an acetone-dry ice bath. The

material was dissolved in 2 mL ether. The resulting solution was analyzed by GC. Table 5.8 shows photolysis conditions and quantitative analysis.

Table 5.8 Irradiation of 3-cyanopyridine (**37**) at $\lambda \geq 290$ nm

Exp no.	Sample weight (mg)	Recovered weight (mg)	Irradiation time (hours)	3-CNP consumption (%)	4-CNP formation (%)	2-CNP formation (%)
14	10	8	24	4.1	1.0	3.1

5.6.3. 4-Cyanopyridine (38)

The vapor of 4-cyanopyridine (**38**) (0.4 Torr) was obtained from 100 mg of the sample in a 3-L quartz reactor. This was then irradiated through a pyrex filter in the Rayonet reactor using sixteen 300 nm lamps for 24 hours. After irradiation, the material was recovered by pumping it out through a trap cooled in an acetone-dry ice bath. The material was dissolved in 2 mL ether. The resulting solution was analyzed by GC. Table 5.9 shows photolysis conditions and quantitative analysis.

Table 5.9 Irradiation of 4-cyanopyridine (**38**) at $\lambda \geq 290$ nm

Exp no.	Sample weight (mg)	Recovered weight (mg)	Irradiation time (hours)	4-CNP consumption (%)	3-CNP formation (%)	2-CNP formation (%)
15	8	6	24	1.9	1.9	0.0

5.7. Deuterium labeling studies

5.7.1. 2-Cyanopyridine-4,6-d_2 (36-4,6-d_2)

The vapor of 2-cyanopyridine-4,6-d_2 (**36-4,6-d_2**) (0.4 Torr) was obtained from 20 mg of the sample in a 3-L quartz reactor. This was then irradiated in a Rayonet reactor equipped with 4-low mercury arc lamps. After irradiation, the material was recovered by pumping it out through a trap cooled in an acetone-dry ice bath. The material was dissolved in 2 mL ether. The resulting solution was analyzed by GC. Table 5.10 shows photolysis conditions and quantitative analysis.

Table 5.10 Irradiation of 2-cyanopyidine-4,6-d_2 (**36-4,6-d_2**)

Exp no.	Irradiation time (min.)	Sample weight (mg)	Recovered weight (mg)	2-CNP consumption (%)	3-CNP formation (%)	4-CNP formation (%)
25	240	17	10	39.2	35.0	4.3

The ethereal solution was concentrated to remove solvent and the residue was analyzed by ^{1}H-NMR in acetone-d_6.

5.7.2. 3-Cyanopyridine-2,6-d_2 (37-2,6-d_2)

The vapor of 3-cyanopyridine-2,6-d_2 (**37-2,6-d_2**) (0.4 Torr) was obtained from 25 mg of the sample in a 3-L quartz reactor. This was then irradiated in a Rayonet reactor equipped with 4-low mercury arc lamps. After irradiation, the material was recovered by

pumping it out through a trap cooled in an acetone-dry ice bath. The material was dissolved in 2 mL ether. The resulting solution was analyzed by GC. Table 5.11 shows photolysis conditions and quantitative analysis.

Table 5.11 Irradiation of 3-cyanopyridine-2,6-d_2 (**37-2,6-d_2**)

Exp no.	Irradiation time (min.)	Sample weight (mg)	Recovered weight (mg)	3-CNP consumption (%)	2-CNP formation (%)	4-CNP formation (%)
26	360	22	13	8.2	3.0	5.2

The ethereal solution was concentrated to remove the solvent and the residue was analyzed by ^{1}H-NMR in acetone-d_6.

5.7.3. 4-Cyanopyridine-2,6-d_2 (38-2,6-d_2)

The vapor of 4-cyanopyridine-2,6-d_2 (**38-4,6-d_2**) (0.4 Torr) was obtained from 30 mg of the sample in a 3-L quartz reactor. This was then irradiated in a Rayonet reactor equipped with 4-low mercury arc lamps. After irradiation, the material was recovered by pumping it out through a trap cooled in an acetone-dry ice bath. The material was dissolved in 2 mL ether. The resulting solution was analyzed by GC. Table 5.12 shows photolysis conditions and quantitative analysis.

Table 5.12 Irradiation of 4-cyanopyridine-2,6-d_2 (**38-2,6-d_2**)

Exp no.	Irradiation time (min)	Sample weight (mg)	Recovered weight (mg)	4-CNP consumption (%)	3-CNP formation (%)	2-CNP formation (%)
27	30	16	8	49.4	45.3	4.1
28	60	16	7	66.3	61.0	5.3

The ethereal solution was concentrated to remove the solvent and the residue was analyzed by ^{1}H-NMR in acetone-d_6.

5.7.4. 2,6-Dideuteriopyridine (1-2,6-d_2)

The vapor of 2,6-dideuteriopyridine (**1-2,6-d_2**) (1.5 Torr) was obtained from 20 mg of the sample in a 3-L quartz reactor at 24 ^{o}C. This was then irradiated in a Rayonet reactor equipped with 4-low mercury arc lamps for 1, 3, 4, 6 and 10 hours. After irradiation, the resulting material was recovered (6 mg) by pumping it out through a trap cooled in an acetone-dry ice bath. The resulting product was dissolved in acetone-d_6. The resulting solution was analyzed by ^{1}H-NMR.

5.7.5. 3,4,5-Trideuteriopyridine (1-3,4,5-d_3)

The vapor of 3,4,5-dideuteriopyridine (**1-3,4,5-d_3**) (1.5 Torr) was obtained from 20 mg of the sample in a 3-L quartz reactor at 25 ^{o}C. This was then irradiated in a Rayonet reactor equipped with 4-low mercury arc lamps for 6 and 12 hours. After irradiation, the resulting material was recovered (3 mg) by pumping it out through a trap

cooled in an acetone-dry ice bath. The resulting product was dissolved in acetone-d_6. The resulting solution was analyzed by ^{1}H-NMR.

5.7.6. 2,4,6-Trideuteriopyridine (1-2,4,6-d_3)

The vapor of 2,4,6-trideuteriopyridine (**1-2,4,6-d_3**) (1.5 Torr) was obtained from 20 mg of the sample in a 3-L quartz reactor at 24 ^{o}C. This was then irradiated in a Rayonet reactor equipped with 4-low mercury arc lamps for 6 and 12 hours. After irradiation, the resulting material was recovered (5 mg) by pumping it out through a trap cooled in an acetone-dry ice bath. The resulting product was dissolved in acetone-d_6. The resulting solution was analyzed by ^{1}H-NMR.

5.7.7. 2,3,6-Trideuteriopyridine (1-2,3,6-d_3)

The vapor of 2,3,6-trideuteriopyridine (**1-2,3,6-d_3**) (1.0 Torr) was obtained from 14 mg of the sample in a 3-L quartz reactor at 24 ^{o}C. This was then irradiated in a Rayonet reactor equipped with 4-low mercury arc lamps for 12 hours. After irradiation, the resulting material was recovered (10 mg) by pumping it out through a trap cooled in an acetone-dry ice bath. The resulting product was dissolved in acetone-d_6. The resulting solution was analyzed by ^{1}H-NMR.

5.7.8. 2,3,4-Trideuteriopyridine (1-2,3,4-d_3)

The vapor of 2,3,4-trideuteriopyridine (**1-2,3,4-d_3**) (1.5 Torr) was obtained from 20 mg of the sample in a 3-L quartz reactor at 25 ^{o}C. This was then irradiated in a Rayonet reactor equipped with 4-low mercury arc lamps for 12 hours. After irradiation, the resulting material was recovered (19 mg) by pumping it out through a trap cooled in an acetone-dry ice bath. The resulting product was dissolved in acetone-d_6. The resulting solution was analyzed by ^{1}H-NMR.

5.7.9. 2,3,5-Trideuteriopyridine (1-2,3,5-d_3)

The vapor of 2,3,5-trideuteriopyridine (**1-2,3,5-d_3**) (1.5 Torr) was obtained from 20 mg of the sample in a 3-L quartz reactor at 25 ^{o}C. This was then irradiated in a Rayonet reactor equipped with 4-low mercury arc lamps for 12 hours. After irradiation, the resulting material was recovered (19 mg) by pumping it out through a trap cooled in an acetone-dry ice bath. The resulting product was dissolved in acetone-d_6. The resulting solution was analyzed by ^{1}H-NMR.

5.7.10. 2,4,5-Trideuteriopyridine (1-2,4,5-d_3)

The vapor of 2,4,5-trideuteriopyridine (**1-2,4,5-d_3**) (1.5 Torr) was obtained from 25 mg of the sample in a 3-L quartz reactor at 25 ^{o}C. This was then irradiated in a Rayonet reactor equipped with 4-low mercury arc lamps for 12 hours. After irradiation,

the resulting material was recovered (21 mg) by pumping it out through a trap cooled in an acetone-dry ice bath. The resulting product was dissolved in acetone-d_6. The resulting solution was analyzed by ^{1}H-NMR.

5.7.11. 2,3,4,5-Tetradeuteriopyridine (1-2,3,4,5-d_4)

The vapor of 2,3,4,5-tetradeuteriopyridine (**1-2,3,4,5-d_4**) (1.7 Torr) was obtained from 20 mg of the sample in a 3-L quartz reactor at 25 ^{o}C. This was then irradiated in a Rayonet reactor equipped with 4-low mercury arc lamps for 3, 6 and 12 hours. After irradiation, the resulting material was recovered (10 mg) by pumping it out through a trap cooled in an acetone-dry ice bath. The resulting product was dissolved in acetone-d_6. The resulting solution was analyzed by ^{1}H-NMR.

5.7.12. 2,3,4,6-Tetradeuteriopyridine (1-2,3,4,6-d_4)

The vapor of 2,3,4,6-tetradeuteriopyridine (**1-2,3,4,6-d_4**) (1.5 Torr) was obtained from 20 mg of the sample in a 3-L quartz reactor at 25 ^{o}C. This was then irradiated in a Rayonet reactor equipped with 4-low mercury arc lamps for 3, 6 and 12 hours. After irradiation, the resulting material was recovered (7 mg) by pumping it out through a trap cooled in an acetone-dry ice bath. The resulting product was dissolved in acetone-d_6. The resulting solution was analyzed by ^{1}H-NMR.

5.7.13. 2,3,5,6-Tetradeuteriopyridine (1-2,3,5,6-d_4)

The vapor of 2,3,5,6-tetradeuteriopyridine (**1-2,3,5,6-d_4**) (1.5 Torr) was obtained from 25 mg of the sample in a 3-L quartz reactor at 20 ^{o}C. This was then irradiated in a Rayonet reactor equipped with 4-low mercury arc lamps for 3, 6 and 12 hours. After irradiation, the resulting material was recovered (8 mg) by pumping it out through a trap cooled in an acetone-dry ice bath. The resulting product was dissolved in acetone-d_6. The resulting solution was analyzed by ^{1}H-NMR.

5.8. Synthesis of 4-cyanopyridine-2,6-d_2 (36-2,6-d_2)

5.8.1. Preparation of isonicotinic acid N-oxide-2,6-d_2 (54-2,6-d_2)

Isonicotinic acid N-oxide (**54**) (3.0 g, 21.6 mmole) was dissolved in a solution of Na^+OD^- prepared from sodium metal (0.71 g, 31.0 mmole) dissolved in deuterium oxide (10 mL). The mixture was heated at 80 ^oC for 4 h. The resulting solution was acidified to pH=1 by addition of conc. HCl. The resulting white precipitate (~2.95 g) was collected by suction filtration to give partially deuterated isonicotinic acid N-oxide. The white solid was subjected to a second hydrogen-deuterium exchange in Na^+OD^-/D_2O as above. Acidification as above gave isonicotinic acid N-oxide-2,6-d_2 (**54-2,6-d_2**) as a white precipitate: m.p. 267-270 ^oC; yield 2.9 g (20.6 mmole, 95.5 %); ^{1}H-NMR(D_2O) δ 7.69 (s, 2H); ^{13}C-NMR (D_2O) δ 170.6 (CO), 139.6 (C-4), 139.0 (t: C-2,C-6; J = 29.0 Hz), 127.0 (C-3, C-5); ^{13}C-Dept135 δ 170.6(0), 139.6(0), 139.0 (0), 127.0 (+).

5.8.2. Preparation of methyl isonicotinate N-oxide-2,6-d_2 (58-2,6-d_2)

Isonicotinic acid-2,6-d_2 N-oxide (**54-2,6-d_2**) (2.9 g, 20.6 mmole) was dissolved in a mixture of benzene (10 mL), methanol (10 mL), and conc.H_2SO_4 (2 mL). This solution was refluxed for 2 h and then the azeotropic mixture was slowly distilled. The residue was poured on ice (10 g) and made basic to pH 8 with 10% aqueous Na_2CO_3. The solution was extracted with dichloromethane (5x20 mL) and the extract was dried (Na_2SO_4). Evaporation at room temperature gave methyl isonicotinate N-oxide-2,6-d_2 (**58-2,6-d_2**) as a white precipitate: mp 118-120 ^oC; yield 1.3 g (8.4 mmole, 40.7 %; ^{1}H-

NMR ($CDCl_3$) δ 7.79 (s, 2H), 3.88 (s, 3H); ^{13}C-NMR($CDCl_3$) δ 164.2 (CO), 139.6 (t: C-2,C-6; J = 29.0 Hz), 126.8 (C-4) 126.7 (C-3,C-5), 53.2 (CH_3); ^{13}C-Dept135 δ 164.2(0), 139.6(0), 126.8(0), 126.7(+), 53.2(+); MS m/z (%) 155 (29), 139 (89).

5.8.3. Preparation of methyl isonicotinate-2,6-d_2 (59-2,6-d_2)

Methyl isonicotinate N-oxide-2,6-d_2 (**58-2,6-d_2**) (1.4 g, 9.0 mmole) was dissolved in dichloromethane (60 mL). The solution was added dropwise to PCl_3(1.2 mL) at 0 ^{0}C. The mixture was then refluxed for 1 hour and mixed with ice water (30 g) and then made basic with 10 N NaOH. The basic solution was extracted with dichloromethane (5x20 mL) and dried (Na_2SO_4). Evaporation gave methyl isonicotinate-2,6-d_2 (**59-2,6-d_2**) as a brown-oily liquid: yield 0.9 g (6.5 mmole, 72.2 %); ^{1}H-NMR($CDCl_3$) δ 7.73 (s, 2H), 3.86 (s, 3H); ^{13}C-NMR($CDCl_3$) δ 165.7 (CO), 150.3(t: C-2, C-6; J = 27.6 Hz), 137.7 (C-4), 123.1 (C-3, C-5), 53.0 (CH_3); ^{13}C-Dept135 δ 165.7(0), 150.3(0), 137.7(0), 123.0(+), 53.0(+); MS m/z (%) 139 (100), 108 (90).

5.8.4. Preparation of isonicotinamide-2,6-d_2 (60-2,6-d_2)

Methyl isonicotinate-2,6-d_2 (**59-2,6-d_2**) (0.97 g, 6.5 mmole) was dissolved in a small amount of methanol (3 mL). This solution was then added dropwise to concentrated aqueous ammonia (10 mL). The resulting cloudy solution was made clear by adding methanol (~80 mL). After 5 h at room temperature, the solution was cooled in the freezer overnight. The solution was evaporated, giving isonicotinamide-2,6-d_2 (**60-**

2,6-d_2) as a white precipitate: mp 149-150 ^oC; yield 0.64 g (5.2 mmole, 80 %); ^1H-NMR(D_2O) δ 7.53 (s, 2H); ^{13}C-NMR(D_2O) δ 170.6 (CO), 148.9 (t: C-2, C-6; J = 27.9 Hz), 142.1 (C-4), 122.1 (C-3, C-5); ^{13}C-Dept135 δ 170.6 (0), 148.9(0), 142.1(0), 122.1(+); MS m/z (%) 124 (100), 108 (41).

5.8.5. Preparation of 4-cyanopyridine-2,6-d_2 (38-2,6-d_2)

Isonicotinamide-2,6-d_2 (**60-2,6-d_2**) (0.23 g, 1.9 mmole) was heated with phosphorous pentoxide (0.54 g, 1.9 mmole) in a round bottom flask at 160-180 ^oC for 3 h (Kugelrohr). The mixture was neutralized with 10% aqueous Na_2CO_3 and extracted with dichloromethane (5x20 mL). The organic layer was dried (Na_2SO_4) and evaporated. The solid residue (0.15 g) was sublimed (70 ^oC, water aspirator) to give 4-cyanopyridine-2,6-d_2 (**38-2,6-d_2**) as white crystal; mp 70-72 ^oC; yield 0.07 g (0.6 mmole, 31.6 %); ^1H-NMR ($CDCl_3$) δ 7.47 (s, 2H); ^{13}C-NMR ($CDCl_3$) δ 151.5 (t: C-2, C-6; J = 28.1 Hz), 125.6 (C-3, C-5), 120.8 (C-4), 116.8 (CN); ^{13}C-Dept135 δ 151.5(0), 125.6(+), 120.8(0), 116.8(0); MS m/z (%) 106 (100), 78 (42).

5.9. Synthesis of 3-cyanopyridine-2,6-d_2 (37-2,6-d_2)

5.9.1. Preparation of nicotinic acid N-oxide -2,6-d_2 (61-2,6-d_2)

Nicotinic acid N-oxide (**61**) (2.0 g, 14.4 mmole) was dissolved in a solution prepared from sodium (0.41 g, 18 mmole) dissolved in deuterium oxide (20 mL). The solution was heated at 80 ^oC for 5 h. The resulting solution was acidified to pH=2 by conc. HCl at 0 ^oC. The white precipitate of partially deuterated nicotinic acid N-oxide (~1.9 g) was subjected to a second hydrogen-deuterium exchange as described above. Acidification as above gave a white precipitate of nicotinic acid N-oxide-2,6-d_2 (**61-2,6-d_2**): m.p. 260 ^oC ; yield 1.9 g (13.5 mmole, 93.6 %); ^{1}H-NMR(D_2O) δ 7.91(d, 1H, *J* = 8.0 Hz), 7.44 (d, 1H, *J* = 8.0 Hz); ^{13}C-NMR (D_2O) δ 168.2 (CO), 144.0 (t: C-2; *J* = 28.4 Hz), 141.9 (t: C-6; *J* = 26.1 Hz), 135.1 (C-4), 133.8 (CN), 129.3 (C-5); ^{13}C-Dept135 δ 168.2 (0), 144.0 (0), 141.9 (0), 135.1 (0), 133.1(+), 127.4 (+).

5.9.2. Preparation of methyl nicotinate N-oxide-2,6-d_2 (62-2,6-d_2)

Nicotinic acid-2,6-d_2 N-oxide (**61-2,6-d_2**) (1.9 g, 13.5 mmole)was dissolved in a mixture of benzene (20 mL), methanol (20 mL), and conc. H_2SO_4 (2 mL). This solution was refluxed for 2 hours and slowly distilled in order to remove the azeotrope of bezene and water. The viscous residue was poured on ice (10 g) and made basic to pH 8 with 10% aqueous Na_2CO_3. The aqueous solution was extracted with dichloromethane (5x20 mL) and the organic layer was dried (Na_2SO_4). Evaporation at room temperature gave

methyl nicotinate N-oxide-2,6-d_2 as a brown precipitate. This product was recrystallized twice from dichloromethane/hexane system to give methyl nicotinate N-oxide-2,6-d_2 (**62-2,6-d_2**): m.p. 46-48 ^oC; yield 1.2 g (7.7 mmole, 57.3 %); ^{1}H-NMR($CDCl_3$) δ 7.81(d, 1H, *J* = 8.0 Hz), 7.41 (d, 1H, *J* = 8.0 Hz); ^{13}C-NMR ($CDCl_3$) δ 163.5 (CO), 142.5 (t: C-2; *J* = 28.4 Hz), 140.1(t: C-6; *J* = 29.1 Hz), 132.2(C-3), 126.9 (C-4), 126.2 (C-5), 53.8 (CH_3); ^{13}C-Dept 135 δ 163.5(0), 142.5(0), 140.1(0), 132.2(0), 126.9(+), 126.2(+) 53.4(+).

5.9.3. Preparation of methyl nicotinate-2,6-d_2 (63-2,6-d_2)

Methyl nicotinate N-oxide-2,6-d_2 (**62-2,6-d_2**) (1.2 g, 7.7 mmole) was dissolved in dichloromethane (60 mL). The solution was added dropwise to PCl_3 (1.0 mL) at 0 ^oC. The mixture was refluxed for 1 h and poured on ice water (30 g). The mixture was made basic with 10 N NaOH. The basic solution was extracted with dichloromethane (5x20 mL) and dried (Na_2SO_4). Evaporation gave methyl nicotinate-2,6-d_2(**63-2,6-d_2**) as reddish-viscous liquid: 0.92 g (6.6 mmole, 85.7%); ^{1}H-NMR ($CDCl_3$) δ 8.98 (d, 1H *J* = 8.1 Hz), 8.17 (d, 1H *J* = 8.1 Hz), 4.01 (s, 3H); ^{13}C-NMR($CDCl_3$) δ 162.1 (CO), 146.3 (C-4), 144.6 (t: C-2; *J* = 29.1 Hz), 142.3 (t: C-6; *J* = 29.5 Hz), 130.2 (C-3), 127.8 (C-5), 54.2 (CH_3); ^{13}C-Dept 135 δ 162.1(0), 146.3(+), 144.6(0), 142.3(0), 130.2(0), 127.8(+), 54.2(+).

5.9.4. Preparation of nicotinamide-2,6-d_2 (64-2,6-d_2)

Methyl nicotinate-2,6-d_2 (**63-2,6-d_2**) (0.76 g, 5.4 mmole) was dissolved in cold conc. aqueous ammonia (2 mL) at 0 ^oC. The flask was capped and shaken occasionally.

Additional ammonia was added (1mL) every hour to saturate the solution. The flask was allowed to stand at room temperature for 5 h, shaking occasionally and then stored in the refrigerator for 4 days. The solvent was evaporated and the light brown precipitate of nicotinamide-2,6-d_2 (**64-2,6-d_2**) was obtained; yield 0.42 g (3.4 mmole, 63.0 %); m.p. 110 ^oC ^{1}H-NMR(D_2O) δ 7.97 (d, 1H, *J* = 8.0 Hz), 7.32 (d, 1H, *J* = 8.0 Hz); ^{13}C-NMR(D_2O) δ 170.9(CO), 151.9 (t: C-2; *J* = 27.1 Hz), 147.5 (t: C-6; *J* = 27.0 Hz), 136.7(C-4), 129.4(C-3), 124.3(C-5); ^{13}C-Dept 135 δ 170.9(0), 151.9(0), 147.5(0), 136.7(+), 129.4(0), 124.3(+); MS m/z (%) 124 (100), 108 (55).

5.9.5. Preparation of 3-cyanopyridine-2,6-d_2 (37-2,6-d_2)

Nicotinamide-2,6-d_2 (**64-2,6-d_2**) (0.42 g, 3.4 mmole) was mixed with P_2O_5 (1.0 g, 1.0 mmole) and heated gradually to 160-180 ^oC in the Kugelrohr apparatus. The reaction was allowed to occur for 3 h and the product was sublimed out of the mixture at reduced pressure (water aspirator) and trapped with dry ice. The snow white crystals of 3-cyanopyridine-2,6-d_2 (**37-2,6-d_2**): m.p. 48-50 ^oC; yield 0.10 g (0.9 mmole, 26.5%); ^{1}H-NMR ($CDCl_3$) δ 7.91 (d, 1H, *J* = 7.9 Hz), 7.39 (d, 1H, *J* = 7.9 Hz); ^{13}C-NMR ($CDCl_3$) δ 153.0 (t: C-6; *J* = 27.3 Hz), 152.5 (t: C-2; *J* = 27.7 Hz), 139.7 (C-4), 124.0 (C-5), 116.9 (CN), 110.4 (C-3); ^{13}C-Dept 135 δ 153.0(0), 152.5 (0), 139.7(+), 124.0(+), 116.9(0), 110.4 (0); MS m/z (%) 106(100), 78(45).

5.10. Synthesis of 2-cyanopyridine-4,6-d_2 (36-2,6-d_2)

5.10.1. Preparation of picolinic acid-N-oxide-6-d (75-6-d)

Picolinic acid N-oxide (**75**) (2.05 g, 14.7 mmole) was dissolved in Na^+OD^- prepared freshly by dissolving sodium (0.41 g) in to D_2O (20 mL). This solution was heated at reflux in an oil bath at 80 ^oC for 5 h. The resulting solution was acidified at 0 ^oC with conc. HCl until pH=2. The white precipitate (~2.00 g) was collected by suction filtration to obtain partially deuterated picolinic acid N-oxide. The white precipitate was subjected to a second hydrogen-deuterium exchange in Na^+OD^-/D_2O as above. Acidification as above gave white precipitate of picolinic acid N-oxide-6-d (**75-6-d**); m.p.162 ^oC; yield 1.96 g (14.0 mmol, 95.2%) ^{1}H-NMR (D_2O) 7.53 (m, 1H) 7.34 (m, 2H); ^{13}C-NMR (D_2O) δ 168.0 (CO), 147.7 (C-2), 139.0 (C-6: t; J = 28.6 Hz), 132.6 (C-4), 126.2 (C-3), 124.0 (C-5); ^{13}C Dept-135 δ 168.0(0), 147.7(0), 139.0(0), 132.6 (+), 126.2 (+), 124.0 (+).

5.10.2. Preparation of 4-nitropicolinic acid N-oxide-6-d (71-6-d)

Picolinic acid N-oxide-6-d (**75-6-d**) (1.92 g, 13.7 mmole) was dissolved in fuming HNO_3 (3.3 mL) and conc. H_2SO_4 (12 mL) in a 25 mL two-neck pear shape flask equipped with a thermometer. This reaction flask was then heated in an oil bath until the solution refluxed and the temperature reached to 120-127 ^oC for 1 h. The resulting mixture was diluted with water (72 mL). A brown gas was evolved and a light yellow crystal was formed. This aqueous solution was stored in the freezer overnight which

gave light yellow crystals of 4-nitropicolinic acid N-oxide-6-d (**71-6-d**): m.p.148 ^{o}C; yield 1.14 g (6.2 mmole, 45.2%). ^{1}H-NMR (DMSO-d_6) δ 8.52 (s, 1H), 8.35 (s, 1H); ^{13}C-NMR (DMSO-d_6) δ 165.0 (CO) , 154.9 (C-2), 152.4 (t: C-6; J = 28.4 Hz) , 151.3 (C-4) , 119.7 (C-3), 117.4 (C-5); ^{13}C Dept-135 δ 165.0 (0), 154.9 (0), 152.4 (0), 151.3 (0), 119.7 (+), 117.4 (+).

5.10.3. Preparation of methyl 4-nitropicolinate N-oxide-6-d (76-6-d)

4-nitropicolinic acid N-oxide-6-d (**71-6-d**) (0.19 g, 1.0 mmole) was placed in a 10 mL round bottom flask and warmed in a water bath at 50 ^{o}C. To this solid was added thionyl chloride (0.18 mL). While stirring and refluxing, methanol (5 mL) was added to the mixture and a condenser was equipped. At 62 ^{o}C the solid dissolved and the solution was allowed to reflux for 1 h. The reaction flask was cooled to room temperature to give yellow crystals of methyl 4-nitropicolinate N-oxide-6-d (**76-6-d**): m.p. 136 ^{o}C; yield 0.11 g (0.6 mmole, 60 %); ^{1}H-NMR ($CDCl_3$) δ 8.56 (s, 1H), 8.17 (s, 1H), 4.03 (s, 3H); ^{13}C-NMR ($CDCl_3$) δ 160.3 (CO), 142.4 (t: C-6; J = 28.8 Hz), 142.1 (C-2), 141.5 (C-4), 122.8 (C-3), 122.0 (C-5), 54.2 (CH_3); ^{13}C Dept-135 δ 160.3 (0), 142.4 (0), 142.1 (0), 141.5 (0), 122.8 (+), 122.0 (+), 54.2 (+).

5.10.4. Preparation of methyl 4-chloropicolinate N-oxide-6-d (77-6-d)

Methyl 4-nitropicolinate N-oxide-6-d (**76-6-d**) (0.81 g, 4.1 mmole) was placed in a 10 mL round bottom flask and warmed in water bath at 40 ^{o}C. Acetyl chloride (4.1 mL)

was then added dropwise which led to the evolution of a gas. After gas evolution ceased, the resulting solution was cooled to room temperature and concentrated by evaporation until dryness (0.85 g). This crude was purified by column chromatography using dichloromethane and methanol (90:10) as solvent. The major product was isolated and recrystallized from dichloromethane/hexane to give white crystals of methyl 4-chloropicolinate N-oxide-6-d (**77-6-d**). m.p. 112 ^{o}C; yield 0.65 g (3.4 mmole, 82.9%); ^{1}H-NMR ($CDCl_3$) δ 7.56 (s, 1H), 7.33 (s, 1H), 3.99 (s, 3H); ^{13}C-NMR($CDCl_3$) δ 161.2 (CO), 142.3 (C-2), 141.8 (t: C-6; *J* = 29.1 Hz), 131.4 (C-4), 128.1 (C-3), 127.5 (C-5), 54.0 (CH_3); ^{13}C Dept-135 δ 161.2 (0), 142.3 (0), 141.8 (0), 131.4 (0), 128.1 (+), 127.5 (+), 54.0 (+). MS m/z (%) 188(3.81), 114 (100).

5.10.5. Preparation of methyl 4-chloropicolinate-6-d (78-6-d)

Methyl 4-chloropicolinate N-oxide-6-d (**77-6-d**) (0.42 g, 2.2 mmole) was dissolved in dichloromethane (20 mL). This solution was added dropwise into PCl_3 (0.9 mL) at 0 ^{o}C (ice bath) while stirring. The solution was refluxed for 1 h. The resulting solution was poured onto ice (20 g) and made basic with 10N NaOH solution until pH=8. The aqueous solution was extracted with dichloromethane (5x20 mL). The organic phase was combined, dried (Na_2SO_4) and the solvent was removed by evaporation to give methyl 4-chloropicolinate-6-d (**78-6-d**) as a yellow liquid: yield 0.34 g (1.9 mmole, 87%). ^{1}H-NMR ($CDCl_3$) δ 8.20 (s, 1H), 7.67 (s, 1H), 3.99 (s, 3H); ^{13}C-NMR ($CDCl_3$) δ 163.6 (CO), 149.4 (t: C-6; *J* = 28.2 Hz), 148.2 (C-2), 147.6 (C-4), 128.3 (C-3), 126.7 (C-5),

54.0 (CH_3); ^{13}C-Dept 135 δ 163.6 (0), 149.4 (0), 148.2 (0), 147.6 (0), 128.3 (+), 126.7 (+), 54.0 (+); MS m/z (%) 172.5 (3), 142 (27), 114 (100).

5.10.6. Preparation of methyl picolinate-4,6-d_2 (79-4,6-d_2)

a.) Methyl 4-chloropicolinate-6-d **(78-6-d)** (0.20 g, 1.2 mmole) was dissolved in MeOD (15 mL) and placed in a Büchner flask containing K_2CO_3 (0.16 g), Pd-C (0.03 g), and a magnetic bar. This flask was sealed with a septum and equipped with a balloon at the side arm. A side-arm test tube containing $NaBD_4$ (0.10 g, 2.4 mmole) was sealed with a septum and the side-arm was connected to the Büchner flask via a syringe needle passed through the septum of the Büchner flask. The entire system was purged with nitrogen for 10 minutes. A solution of D_2O (2.0 mL) containing D_2SO_4 (5 drops) was then added through the septum to the $NaBD_4$ in the side-arm test tube. The D_2 generated filled the system and caused the balloon to expand. The reaction mixture in the Büchner flask was stirred in the D_2 atmosphere for 4 h.

The resulting solution was checked by TLC (only one spot was observed). The Pd-C was filtered and the filtrate was evaporated. This residue was diluted with 60-70 mL CH_2Cl_2 and washed with water twice. The organic layer was dried (Na_2SO_4) and the solvent was evaporated to give a colorless liquid of methyl picolinate-4,6-d_2 (**79-4,6-d_2**): yield 0.14 g (1 mmole, 83.3%); ^{1}H-NMR ($CDCl_3$) δ 8.16(s, 1H), 7.50 (s, 1H), 4.02(s, 3H); ^{13}C-NMR ($CDCl_3$) δ 165.7(CO), 149.5 (t: C-6; J = 27.6 Hz), 147.9 (C-2), 136.8 (t: C-4; J = 25.1 Hz), 126.8 (C-3), 125.1 (C-5), 52.9 (CH_3); ^{13}C-Dept 135 δ 165.7

(0), 149.5 (0), 147.9 (0), 136.8 (0), 126.8 (+), 125.1 (+), 52.9 (+); MS m/z (%) 139 (4.54), 81(92.4).

b) Methyl 4-chloropicolinate-6-d (**78-6-d**) (0.25 g, 1.4 mmole) was dissolved in MeOH (15 mL) and placed in a Büchner flask containing K_2CO_3 (0.30 g), Pd-C (0.05 g), and magnetic bar. This flask was sealed with septum and equipped with a balloon as in the above procedure but in order to generate the D_2 gas, Na (0.5 g) and D_2O (2 mL) were used. The reaction mixture was stirred in the D_2 atmosphere for 4 h.

The resulting solution was filtered to remove Pd-carbon. The solution was evaporated. Dichloromethane (60 mL) was added and the solution was washed twice with water. The solvent was removed by evaporation to give liquid residue of methyl picolinate-4,6-d_2 (**79-4,6-d_2**): yield 0.13 g (0.9 mmole, 64.3%).

5.10.7. Preparation of picolinamide-4,6-d_2 (80-4,6-d_2)

Methyl picolinate-4,6-d_2 (**79-4,6-d_2**) (1.04 g, 7.5 mmole) was dissolved in cold concentrated aqueous ammonia (~20 mL). Another portion (5 mL) of aqueous ammonia was added to saturate the solution. The reaction flask was shaken occasionally and stored in the freezer overnight. The solvent was removed by evaporation to give a white precipitate of picolinamide-4,6-d_2 (**80-4,6-d_2**): m.p. 122 ^{o}C; yield 0.61 g (4.9 mmole, 65.3%); ^{1}H-NMR($CDCl_3$) δ 8.22 (s, 1H), 7.90(broad, 1H), 7.46(s, 1H), 6.18(broad, 1H); ^{13}C-NMR ($CDCl_3$) δ 167.4 (CO), 149.9 (C-2), 148.4(t: C-6; J = 25.2 Hz) 137.7 (t:

C-4; J = 20.1 Hz), 126.6(C-3), 122.7(C-5); ^{13}C-Dept 135 δ 167.4 (0), 149.9 (C-2), 148.4 (0), 137.7 (0), 126.6 (+), 122.7 (+); MS m/z (%) 124 (38), 81 (100).

5.10.8. Preparation of 2-cyanopyridine-4,6-d_2 (36-4,6-d_2)

Picolinamide-4,6-d_2 (**80-4,6-d_2**) (0.20 g, 1.6 mmole) was mixed with P_2O_5 (0.7 g) in a 25 mL-round bottom flask. The reaction was carried out in the Kugelrohr apparatus at high temperature (oven: 120-190 ^{o}C) and reduced pressure (0.1 Torr). Once the temperature was higher than 190 ^{o}C for 15 minutes, the reaction was stopped. The 2-cyanopyridine-4,6-d_2 (**36-4,6-d_2**)was collected as white solid in a glass bulb. Purification by column or TLC chromatography (DCM/EtOAc (1:1)) gave 2-cyanopyridine-4,6-d_2 (**36-4,6-d_2**) as a colorless liquid: yield 0.07 g (0.7 mmole, 41.3%); ^{1}H NMR ($CDCl_3$) δ 7.66 (s, 1H), and 7.50(s, 1H); ^{13}C-NMR ($CDCl_3$) δ 152.2 (t: C-6; J = 28.0 Hz), 138.2 (t: C-4; J = 25.6 Hz), 135.0 (C-2), 129.9(C-3), 128.1(C-5), 118.5(CN); ^{13}C-Dept 135 δ 152.2 (0), 138.2(0), 135.0 (0), 129.9 (+), 128.1 (0), 118.5 (0). MS m/z(%) 106 (52), 32 (100).

5.11. Synthesis of 2,6-dideuteriopyridine (1-2,6-d_2)

5.11.1. Preparation of pyridine N-oxide-2,6-d_2 (53-2,6-d_2)

Pyridine N-oxide (**53**) (2.00 g, 21 mmole) was dissolved in D_2O (20 mL). To the solution Na_2CO_3 (3.0 g) was added. This solution was refluxed for 12 h and then extracted with dichloromethane (10 x 20 mL). The dichloromethane layer was dried (Na_2SO_4) and the solvent was removed to give liquid residue. Drying in the desiccators gave 2,6-dideuteriopyridine N-oxide (**53-2,6-d_2**) as a white solid of: 1.65 g (17 mmole, 81.0 %); ^{1}H- NMR(D_2O) δ 7.41(m, 1H), 7.22(m, 2H); ^{13}C-NMR (D_2O) δ 138.9 (t: C-2,C-6; J = 28.3 Hz), 132.9 (C-4), 127.5 (C-3,C-5); ^{13}C-Dept135 (D_2O) δ 138.9(0), 132.9(+), 127.5(+); MS m/z (%) 98 (64), 97 (100), 82 (73), 81 (100).

5.11.2. Preparation of 2,6-dideuteriopyridine (1-2,6-d_2)

Pyridine N-oxide-2,6-d_2 (**53-2,6-d_2**) (0.42 g, 4.3 mmole) was dissolved in dichloro-methane (30 mL). The solution was added dropwise into PCl_3 (1.2 mL) at 0 ^{o}C. The mixture was refluxed for 2 h. The reaction mixture was poured onto ice (15 g) and basified with 10 N NaOH solution and extracted with dichloromethane (5x10 mL). The organic layer was dried (Na_2SO_4). Evaporation off the solvent gave dideuterio-2,6-pyridine (**1-2,6-d_2**) as colorless liquid which was further purified by distillation (Kugelrohr: 95 ^{o}C; water aspirator): yield 0.18 g (2.2 mmole, 51.1%); ^{1}H-NMR($CDCl_3$) δ 7.64 (m, 1H), 7.28 (m, 2H); ^{13}C-NMR ($CDCl_3$) δ 149.8 (t: C-2,C-6; J = 27.3 Hz),

136.4(C-4), 124.1 (C-3,C-5); 13C-Dept ($CDCl_3$) δ 149.8(0), 136.4(+), 124.0 (+); MS m/z (%) 81(100), 53 (53).

5.12. Synthesis of 3,4,5-trideuteriopyridine (1-3,4,5-d_3)

5.12.1. Preparation of pyridine N-oxide-3,4,5-d_3 (53-3,4,5-d_3)

Pyridine-d_5 N-oxide (**53-2,3,4,5,6-d_3**) (0.96 g, 9.6 mmole) was dissolved in 10% Na_2CO_3 solution and refluxed for 12 h. The resulting solution was extracted with dichloromethane (5x10 mL). The organic layer was dried (Na_2SO_4) and the solvent was removed by evaporation, obtaining pyridine N-oxide-3,4,5-d_3(**53-3,4,5-d_3**) as a liquid residue that was stored in desiccators until solidified: yield 0.48 g (4.9 mmole, 51.0 %); ^{1}H NMR(D_2O) δ 8.18 (s, 2H); ^{13}C-NMR (D_2O) 139.2 (C-2,C-6), 132.5 (t: C-4; J = 26.0 Hz), 127.3 (t: C-3,C-5; J = 25.9 Hz).

5.12.2. Preparation of 3,4,5-trideuteriopyridine (1-3,4,5-d_3)

3,4,5-Trideuteriopyridine N-oxide (**53-3,4,5-d_3**) (0.48, 4.9 mmole) was dissolved in dichloro-methane (40 mL). The solution was added dropwise into PCl_3 (1.0 mL) at 0^{o}C. The solution flask was equipped with a condenser and refluxed for 1 h. The resulting mixture was poured on ice (20 g) and made basic with 10N NaOH solution. The aqueous phase was extracted with dichloromethane (3x10 mL). This layer was dried

(Na_2SO_4) and the solvent was evaporated to obtain liquid residue. This crude was purified by distillation (Kugelrohr: 95°C. water aspirator) to give 3,4,5-trideuteriopyridine (**1-3,4,5-d_3**) as a colorless liquid: yield 0.18 g (2.2 mmole, 44.9%); ^{1}H-NMR ($(CD_3)_2CO$) δ 8.44 (s, 2H); ^{13}C-NMR ($(CD_3)_2CO$) δ 151.7(C-2,C-6), 137.2 (t: C-4; J = 24.9 Hz), 125.3 (t: C-3,C-5; J = 25.3 Hz); ^{13}C-Dept 135 ($(CD_3)_2CO$) δ 151.7 (+), 137.2 (0), 125.3 (0); MS m/z (%) 82 (100), 55 (90).

5.13. Synthesis of 2,4,6-trideuteriopyridine (1-2,4,6-d_3)

5.13.1. Preparation of 4-nitropyridine N-oxide-2,6-d_2 (81-2,6-d_2)

Pyridine N-oxide-2,6-d_2 (**53-2,6-d_2**) (1.80 g, 18 mmole) was dissolved in conc. H_2SO_4 (4 mL) and fuming HNO_3 (2 mL). This mixture was heated in an oil bath until reflux at 130 ^oC for 5 h. The resulting solution was poured onto ice (20 g) and neutralized by Na_2CO_3 solution. Extraction with dichloromethane (5x20 mL) gave separated organic phase which subsequently dried by Na_2SO_4. Evaporation off the solvent gave bright yellow precipitate, which was recrystallized in acetone to give 4-nitropyridine N-oxide-2,6-d_2 (**81-2,6-d_2**) as a lustrous yellow crystal: yield 1.58 g (11 mmole, 61.1%).; ^{1}H-NMR($CDCl_3$) δ 8.14 (s, 2H); ^{13}C-NMR ($CDCl_3$) δ 142.2 (C-4), 139.9 (t: C-2, C-6; J = 29.0 Hz), 120.8 (C-3, C-5); ^{13}C-Dept 135 ($CDCl_3$) δ 142.2(0), 139.9 (0), 120.8 (+); MS m/z (%) 142 (34), 126 (78).

5.13.2. Preparation of 4-chloropyridine N-oxide-2,6-d_2(82-2,6-d_2)

4-Nitropyridine N-oxide-2,6-d_2 (**81-2,6-d_2**) (1.00 g, 7.0 mmole) was warmed at 50 ^oC in water bath. After acetyl chloride (5.0 mL) was added, the mixture was refluxed until obtaining the yellow solid (30 minutes). The resulting solid was cooled in ice bath and the cold water was added. Once the vigorous reaction stopped, the resulting solution was made basic with 10% Na_2CO_3 solution and extracted with dichloromethane (7x20 mL). The organic layer was dried (Na_2SO_4) and the solvent was removed by evaporation to give 4-chloropyridine N-oxide-2,6-d_2 (**82-2,6-d_2**) as white pure solid: yield 0.75 g (5.7

mmole, 81%); ^{1}H-NMR($CDCl_3$) δ 7.21 (s, 2H); ^{13}C-NMR ($CDCl_3$) 140.2 (t: C-2,C-6; J = 28.5 Hz), 132.3 (C-4), 126.7 (C-3, C-5); ^{13}C-Dept 135 ($CDCl_3$) 140.2 (0), 132.3 (0), 126.7 (+); MS m/z (%) 131 (26), 115 (100).

5.13.3. Preparation of 4-chloropyridine-2,6-d_2(83-2,6-d_2)

4-Chloropyridine N-oxide-2,6-d_2 (**82-2,6-d_2**) (0.83 g, 6.3 mmole) was dissolved in ice-cold dichloromethane (15 mL). At 0 ^{o}C, to the solution PCl_3 (0.8 mL) was added and the mixture was refluxed in water bath at 70-80 ^{o}C for 1 h. The resulting mixture was then poured onto ice water and made strong basic with Na_2CO_3 solution. The aqueous phase was extracted with dichloromethane (7x20 mL). The emulsion of two phase was a common problem but finally the organic layer was dried (Na_2SO_4) and the solvent was removed by evaporation without heating. The cloudy liquid was obtained and it was purified by Kugelrohr distillation at reduced pressure (1 Torr) to give 4-chloropyridine-2,6-d_2 (**83-2,6-d_2**) as colorless liquid: yield 0.40 g (3.0 mmole, 47.6%): ^{1}H-NMR($CDCl_3$) δ 7.23 (s, 2H); ^{13}C-NMR($CDCl_3$) δ 150.8 (t: C-2,C-6; J = 30.8 Hz), 144.5 (C-4), 123.4(C-3, C-5); ^{13}C-Dept 135($CDCl_3$) δ 150.8(0), 144.5(0), 123.4(+). MS m/z(%) 117.0(33.2), 115(100), 80(81).

5.13.4. Preparation of 2,4,6-trideuteriopyridine (1-2,4,6-d_3)

4-Chloropyridine-2,6-d_2 (**83-2,6-d_2**) (0.12 g, 1.1 mmole) was dissolved in ethyl ether (20 mL) and placed in a 50 mL Büchner flask containing 10% Pd-C (0.07 g),

K_2CO_3 (0.3 g), and a magnetic bar. This flask was sealed with a balloon and a septum. In order to generate D_2, sodium (0.6 g) was placed in another Büchner flask sealed with a septum. The second flask was connected via a syringe needle pass through the septum of the first Büchner flask. This sealed system was purged with Argon for 10 minutes. The D_2O (4 mL) was syringed through the septum of the sodium flask to obtain D_2 which was brought to the reaction flask via syringe needle. The dechlorodeuteriolysis was allowed to proceed for 4 hours. The resulting mixture was filtered to remove black powder of Pd-C. The filtrate was concentrated by evaporation. The liquid residue was purified by Kugelrohr distillation (100 ^oC, water aspirator) to give 2,4,6-trideuteriopyridine (**1-2,4,6-d_3**) as colorless liquid: yield 42 mg (0.51 mmole, 46.8%); ^{1}H-NMR($CDCl_3$) δ 7.08 (s, 2H); ^{13}C-NMR ($CDCl_3$) δ 149.8 (t: C-2, C-6; J = 27.1 Hz), 136.1 (t: C-4; J = 25.1 Hz), 123.9 (C-3, C-5); ^{13}C-Dept135 ($CDCl_3$) δ 149.8 (0), 136.1 (0), 123.9 (+); MS m/z (%) 82 (100), 54 (56).

5.14. Synthesis of 2,3,5,6-tetradeuteriopyridine (1-2,3,5,6-d_4)

5.14.1. Preparation of 3,5-dichloropyridine N-oxide (85)

3,5-Dichloropyridine (**84**) (14.8 g, 100 mmole) was mixed with methyltrioxo-rhenium (VII) (50 mg, 0.2 mmole) in dichloromethane (40 mL). To this mixture 30% aqueous H_2O_2 (17 mL) was added and then it was stirred for 17 hours. The biphasic mixture was added with MnO_2 (25 mg) and the stirring was continued until oxygen evolution stopped (~1 h). The aqueous phase was separated and extracted with dichloromethane (3x20 mL). The combined organic layers were dried over Na_2SO_4 and the solvent was removed by evaporation to give white solid. The starting material was isolated by column chromatography (EtOAc/DCM 1:1) and the pure 3,5-dichloropyridine N-oxide (**85**) was obtained as a white solid: yield 11.5 g (70 mmole, 70 %); ^{1}H-NMR ($CDCl_3$) δ 8.15 (s, 2H), 7.27(s, 1H); ^{13}C-NMR ($CDCl_3$) δ 137.8 (C-2, C-6), 133.7(C-3, C-5), 126.5 (C-4); ^{13}C Dept-135 ($CDCl_3$) 137.8 (+), 133.7 (0), 126.5(+); MS m/z (%) 165 (67), 163 (100), 147 (54).

5.14.2. Preparation of 3,5-dichloropyridine N-oxide-2,4,6-d_3 (85-2,4,6-d_3)

3,5-Dichloropyridine N-oxide (**85**) (1.0 g, 6.1 mmole) and K_2CO_3 (1.0 g) was dissolved in D2O (10 mL). The solution was heated at 110 ^{o}C in an oil bath. The resulting solution was let cooled to room temperature. 3,5-dichloropyridine N-oxide-2,4,6-d_3 (**51**) was formed as a white needle crystal. The crystals were collected by filtration and dried at room temperature. The filtrate was extracted with dichloromethane

(3x10 mL). The organic phase was dried (Na_2SO_4) and the solvent was removed by evaporation to give 3,5-dichloropyridine N-oxide-2,4,6-d_3 (**85-2,4,6-d_3**) as a small white crystal. All white products were combined: yield 0.84 g (5 mmole, 82%); ^{13}C-NMR($CDCl_3$) δ 137.6 (t: C-2, C-6; J = 29.6 Hz), 133.5 (C-3, C-5), 126.4 (t: C-4; J = 27.2 Hz); MS m/z (%) 168 (47), 166 (74), 152 (68), 150 (100), 115 (62).

5.14.3. Preparation of 3,5-dichloropyridine-2,4,6-d_3 (84-2,4,6-d_3)

3,5-Dichloropyridine N-oxide-2,4,6-d_3 (**85-2,4,6-d_3**) (0.83 g, 5 mmole) was dissolved in cold dichloromethane (30 mL). To the solution was added PCl_3 (0.64 mL) and then heated at 80 ^{o}C for 2 h. in an oil bath. The resulting solution was poured onto ice (15 g). The aqueous phase was made basic with 10% K_2CO_3 solution, extracted with dichloromethane. The organic phase was dried over anhydrous Na_2SO_4. Evaporation off the solvent gave 3,5-dichloropyridine-2,4,6-d_3 (**84-2,4,6-d_3**) as a white precipitate: yield 0.69 g (4.6 mmole, 92 %); ^{13}C-NMR($CDCl_3$) δ 146.7 (t: C-2, C-6; J = 29.1 Hz), 135.8 (t: C-4; J = 26.5 Hz), 132.4 (C-3, C-5); MS m/z(%) 162 (64), 150 (100), 117 (17), 115(53).

5.14.4. Preparation of 3,5-dichloropyridine-2,6-d_2 (84-2,6-d_2)

3,5-Dichloropyridine-2,4,6-d_3 (**84-2,4,6-d_3**) (0.59 g, 3.9 mmole) was stirred in 1.6 M NaOMe/MeOH (17 mL) solution for 24 h in a water bath controlled at room temperature. The resulting solution was concentrated by evaporation. The liquid residue was added with water (10 mL) and extracted with dichloromethane (5x10 mL). The

organic layer was dried (Na_2SO_4) and the solvent was removed by evaporation to give 3,5-dichloropyridine-2,6-d_2 (**84-2,6-d_2**) as a white crystal: yield 0.33g (2.2 mmole, 56 %); ^{1}H-NMR($CDCl_3$) δ 7.71 (s, 1H); ^{13}C-NMR($CDCl_3$) δ 146.8 (t: C-2, C-6; J = 29.3 Hz), 136.0 (C-4), 132.5 (C-3, C-5); ^{13}C-Dept 135 ($CDCl_3$) δ 146.8 (0), 136.0 (+), 132.5 (0); MS m/z (%) 151 (63), 149 (100), 114 (58).

5.14.5. Preparation of 2,3,5,6-tetradeuteriopyridine (1-2,3,5,6-d_4)

3,5-Dichloropyridine-2,6-d_2 (**84-2,6-d_2**)(0.3 g, 2 mmole), 10% Pd-C (0.3 g), and K_2CO_3 (0.6 g) was dissolved in methanol-d (10 mL) and placed in a Buchner flask sealed with balloon and septum. In another flask, Na (0.8 g) was placed. This system was purged with Argon for 15 min. The deuteriolysis was introduced by adding of 5 mL D_2O into the sodium flask in order to form D_2. The reaction was allowed to proceed for 4 h and the resulting mixture was filtered to remove Pd-C. The filtrate was made acid with conc. HCl (2 mL) and methanol was evaporated, leaving wet white precipitate which was basified with K_2CO_3 solution. The aqueous solution was extracted with dichloromethane (5x20 mL). The organic phase was dried (Na_2SO_4) and the solvent was removed by fractional distillation. The liquid residue was further purified by Kugelrohr distillation (100 ^{o}C, water aspirator) to give colorless liquid of 2,3,5,6-tetradeuteriopyridine (**1-2,3,5,6-d_4**): yield 79 mg (1.0 mmole, 50%); ^{1}H-NMR(($CD_3)_2CO$) δ 7.75 (s, 1H); ^{13}C-NMR ($(CD_3)_2CO$) δ 150.3 (t: C-2, C-6; *J* = 27.9 Hz), 136.5 (C-4), 124.2 (t: C-3, C-5; *J* = 25.5 Hz). 13C-Dept 135 (($(CD_3)_2CO$) δ 150.3(0), 136.8(+), 124.2(0); MS m/z (%) 83(100), 55(72).

5.15. Synthesis of 2,4,5,6-tetradeuteriopyridine (1-2,4,5,6-d_4)

5.15.1. Preparation of 3-chloropyridine N-oxide (87)

3-Chloropyridine (**86**) (2 g, 17.6 mmole), glacial acetic acid (10.8 mL), and hydrogen peroxide (3.6 mL) were heated at 80 ^{o}C for 10 h. The conversion was monitored by TLC (dichloromethane/ EtOAc 1:1). The resulting solution was concentrated and the acid was removed as much as possible. The liquid residue was made basic with K_2CO_3 granules and it was then shaken with chloroform. The precipitate and K_2CO_3 were filtered and the filtrate was dried (Na_2SO_4). The solvent was removed by evaporation to give 3-chloropyridine N-oxide (**87**) as a light yellow solid: yield 1.69 g (13.0 mmole, 73.9%); m.p. 54 ^{o}C; ^{1}H-NMR ($CDCl_3$) δ 8.22 (s, 1H), 8.10 (d, 1H), 7.23 (m, 2H); ^{13}C-NMR($CDCl_3$) δ 139.2 (C-2), 138.2 (C-6), 133.8 (C-3), 126.9 (C-5), 126.3(C-4); ^{13}C-Dept135 ($CDCl_3$) δ 139.2 (+), 138.2 (+), 133.8 (0), 126.9 (+), 126.3 (+); MS m/z (%) 131 (27), 129 (100), 115 (33), 113 (95).

5.15.2. Preparation of 3-chloropyridine N-oxide-2,4,5,6-d_4 (87-2,4,5,6-d_4)

3-Chloropyridine N-oxide (**87**) (1.69, 13.0 mmole) and K_2CO_3 (1.0 g) was dissolved in D_2O (10 mL). This solution was placed in the glass liner inserted in a metal bomb. The bomb was heated in an oven at 190 ^{o}C for 5 h. The resulting solution analyzed by NMR and concentrated to remove D_2O. The residue was subjected to the second H-D exchange reaction at the same reaction temperature for 3 h. The resulting solution was extracted with dichloromethane (5x20 mL). The organic phase was dried

(Na_2SO_4) and the solvent was removed by evaporation to give 3-chloropyridine N-oxide-2,4,5,6-d_4 (**87-2,4,5,6-d_4**) as yellow solid: yield 0.8 g (6.0 mmole, 46%); m.p. 52-54 ^oC; ^{13}C-NMR($CDCl_3$) δ 138.9 (t: C-2; *J* = 30.2 Hz), 137.9 (t: C-6; *J* = 28.9 Hz), 133.6 (C-3), 126.1 (t: C-5; *J* = 26.9 Hz) , 125.8 (t: C-4; *J* = 25.8 Hz); MS m/z (%) 135 (33), 133 (100), 119 (19), 117 (61).

5.15.3. Preparation of 3-chloropyridine-2,4,5,6-d_4 (86-2,4,5,6-d_4)

3-Chloropyridine N-oxide-2,4,5,6-d_4 (**87-2,4,5,6-d_4**) (0.76 g, 5.7 mmole) was dissolved in cold dichloromethane (30 mL). To this solution PCl_3 (0.82 mL) was added. The mixture was refluxed at 70 ^oC with oil bath for 2 h. The resulting solution was poured onto ice and it was basified with 10% K_2CO_3 solution. The aqueous phase was extracted with dichloromethane, which was dried over anhydrous Na_2SO_4. The solvent was removed at reduced pressure to give 3-chloropyridine-2,4,5,6-d_4 (**86-2,4,5,6-d_4**) as light yellow liquid: yield 0.60 g (5.1 mmole, 89.5%); ^{13}C-NMR ($CDCl_3$) δ 148.8 (C-2, *J*= 28.0 Hz), 147.7 (C-6, *J*= 28.7 Hz), 136.0 (C-4, *J*= 26.1 Hz), 132.4 (C-3), 124.3 (C-5, *J*= 25.8 Hz); MS m/z(%) 113(32.9), 117 (100), 82(66.3).

5.15.4. Preparation of 2,3,4,6-tetradeuteriopyridine (1-2,3,4,6-d_4)

3-Chloropyridine-2,4,5,6-d_4 (**86-2,4,5,6-d_4**) (0.3 g, 2.6 mmole) was dissolved in methanol (10 mL) containing 10% Pd-C (0.08 g) and K_2CO_3 (0.6 g). The mixture was placed in a balloon-sealed Büchner flask. In another Büchner flask containing $NaBH_4$

(0.2 g), the syringe needle was connected to the reaction flask. This system was purged with Argon for 15 min. The dehalohydrogenation was initiated by adding H_2SO_4 (5 drops) diluted in water (3 mL). The reaction was allowed to proceed for 4 h. The Pd-C was filtered off and the filtrate was acidified with conc.HCl (2 mL). The methanol was removed by evaporation and the residue was made basic by 10% K_2CO_3 solution and extracted with dichloromethane (3x15 mL). This layer was dried and fractional distilled to concentrate the product which was further purified by Kugelrohr distillation (100 ^oC, water aspirator) to give 2,3,4,6-tetradeuteriopyridine (**1-2,3,4,6-d_4**) as colorless liquid: yield 68 mg (0.82 mmole, 32%); ^{1}H-NMR($CDCl_3$) δ 7.36 (s, 1H); ^{13}C-NMR ($(CD_3)_2CO$) δ 152.1 (C-2, *J* = 30.4 Hz), 138.0 (C-4, *J* = 24.9 Hz), 125.8 (C-5, *J* = 25.8 Hz); MS m/z(%) 83 (100), 55 (65.5).

5.16. Synthesis of 2,3,4,5-tetradeuteriopyridine (1-2,3,4,5-d_4)

5.16.1. Preparation of pyridine N-oxide-d_5 (53-2,3,4,5,6-d_5)

Pyridine N-oxide (**53**) (2.0 g, 21 mmole) and K_2CO_3 (2.0 g) were dissolved in D_2O (20 mL). The solution was placed in a bomb and heated at 190 ^oC for 5 h. The resulting solution was concentrated to remove solvent. The liquid residue was subjected to the second H-D exchange reaction by adding 10 mL of D_2O and heated at the same temperature for 5 h. The resulting solution was extracted with chloroform (6x20 mL). The organic layer was dried (Na_2SO_4) and the solvent was removed by evaporation. The rest of solvent in the residue was purged with nitrogen. Pyridine N-oxide-d_5 (**53-2,3,4,5,6-d_5**) was obtained as a highly hygroscopic white solid: yield 2.0 g (20 mmole, 95%); m.p. 50 ^oC; ^{13}C-NMR ($CDCl_3$) δ 139.4 (t: C-6; *J* = 28.5 Hz), 126.1 (t: C-4; J = 25.6 Hz), 125.9 (t: C-3, C-5; J = 26.3) ; MS m/z(%) 100 (100), 84 (81).

5.16.2. Preparation of 2-chloropyridine-3,4,5,6-d_4 (88-3,4,5,6-d_4)

Pyridine N-oxide-d_5 (**53-2,3,4,5,6-d_5**) (1.33 g, 13 mmole) was added with phosphorous oxychloride (11 mL) and this mixture was heated until reflux at 120 ^oC in an oil bath for 3 h. The resulting mixture was concentrated by evaporation to remove $POCl_3$ as much as possible. The viscous residue was compleltely dissolved in ice water and made strongly basic with aqueous ammonia to give a reddish solution. Extraction with dichloromethane (5x 20 mL) gave organic layer which was dried over anhydrous Na_2SO_4. The solvent was removed by evaporation to give a red liquid. Purification of

this crude via column chromatography (dichloromethane) gave 2-chloropyridine-3,4,5,6-d_4 (**88-3,4,5,6-d_4**) as a colorless liquid: yield 0.44 g (3.7 mmole, 28 %); ^{13}C-NMR ($CDCl_3$) δ 151.5(C-2), 149.4 (t: C-6; *J* = 28.1 Hz), 138.2(t: C-4; *J* = 25.2 Hz), 124.1 (t: C-3; *J* = 26.6 Hz), 121.7 (t: C-5; *J* = 25.4 Hz); MS m/z (%) 119 (25), 117 (79), 116 (7), 82(100).

5.16.3. Preparation of 2,3,4,5-tetradeuteriopyridine (1-2,3,4,5-d_4)

2-Chloropyridine-3,4,5,6-d_4 (**88-3,4,5,6-d_4**) (0.44, 3.7 mmole) was dissolved in MeOH (10 mL) and placed in a Büchner flask containing K_2CO_3 (0.6 g), Pd-C (0.1 g), and a magnetic bar. This flask was sealed with a septum and equipped with a balloon at the side arm. A side-arm test tube containing $NaBH_4$ (0.2 g) was sealed with a septum and the side-arm was connected to the Büchner flask via a syringe needle passed through the septum of the Büchner flask. The entire system was purged with nitrogen for 10 minutes. A solution of H_2O (3.0 mL) containing H_2SO_4 (5 drops) was then added through the septum to the $NaBH_4$ in the side-arm test tube. The H_2 generated filled the system and caused the balloon to expand. The reaction mixture in the Büchner flask was stirred in the H_2 atmosphere for 4 h. The resulting mixture was filtered to remove Pd-C. The black solid of Pd was washed with methanol and the filtrates were combined. This solution was acidified with conc. HCl and the solvent was removed by evaporation. The residue was made basic with K_2CO_3 solution and the aqueous was extracted with dichloromethane (3 x 10 mL). The organic layer was dried (Na_2SO_4) and the solvent was removed by fractional distillation. The residue was further purified by Kugelrohr distillation at reduced pressure (water aspirator) and the pure 2,3,4,5-

tetradeuteriopyridine (**1-2,3,4,5-d_4**) was obtained in a glass bulb cooling with dry ice as a colorless liquid: yield 0.10 g (1.2 mmole, 32.4%); ^{1}H-NMR ($(CD_3)_2CO$) δ 8.60 (s, 1H); ^{13}C-NMR ($(CD_3)_2CO$) δ 148.6 (C-2), 148.3 (t: C-6; J = 27.2 Hz), 134.1 (t: C-4; J = 24.6 Hz), 122.1 (t: C-3; J = 25.2 Hz), 122.0 (t: C-5; J = 25.5 Hz); ^{13}C-Dept135 ($(CD_3)_2CO$) δ 148.6(+), 148.3(0), 134.1(0), 122.1(0), 122.0(0); MS m/z (%) 83(100), 82(11), 55(57).

5.17. Synthesis of 2,3,4-, 2,4,5-, and 2,3,6-trideuteriopyridine (1-2,3,4-d_3, 1-2,4,5-d_3, 1-2,3,6-d_3)

5.17.1. Preparation of 2,3-dichloropyridine (91-4,5,6-d_3), 2,5-dichloropyridine (92-3,4,6-d_3), 3,4-dichloropyridine (93-2,5,6-d_3)

3-Chloropyridine N-oxide-2,4,5,6-d_4 (**87-2,4,5,6-d_4**) (2.20 g, 16.5 mmole) was mixed with phosphorousoxychloride (16.5 mL) in a round bottom flask. This solution was heated until reflux at 120 ^{o}C for 2 hours. The resulting solution was concentrated by evaporation to give brown liquid which was added with ice (10 g) and made basic with 10% K_2CO_3 solution. It was then extracted with dichloromethane (10 x 20 mL) and dried with anhydrous Na_2SO_4. Evaporation of this crude gave a brown liquid residue (1.90 g). Column chromatography using 10% Hexane in dichloromethane as eluent was used to isolate all four components. The solvent of each collected fraction was removed by evaporation. The first fraction was obtained as a white solid of 2,5-dichloropyridine-3,4,6-d_3 (**92-3,4,6-d_3**): yield 0.34 g (2.3 mmole, 13.7%); ^{13}C-NMR ($CDCl_3$) δ 149.7 (C-2), 148.5 (t: C-6; J = 28.8 Hz), 138.5 (t: C-4; J = 26.1 Hz), 131.1 (C-5), 125.2 (t: C-3; J = 26.4 Hz); MS m/z (%) 154 (10), 152 (54), 150 (100), 117 (25), 115 (79).

Fraction two was obtained as a white solid of 2,3-dichloropyridine-4,5,6-d_3 (**91-4,5,6-d_3**): yield 0.62 g (4.1 mmole, 25 %); ^{13}C-NMR ($CDCl_3$) δ 149.6 (C-2), 147.3 (t: C-6; J = 28.1 Hz), 138.8 (t: C-4; J = 25.9 Hz), 131.0 (C-3), 123.1 (t: C-5; J = 25.5 Hz); MS m/z (%) 154 (11), 152 (59), 150 (96), 117 (31) 115 (100).

Fraction three was obtained as a white crystal of 3,5-dichloropyridine-2,4,6-d_3 (**95-2,4,6-d_3**): yield 0.07 g (0.5 mmole, 2.8 %); ^{13}C-NMR ($CDCl_3$) δ 146.8 (t: C-2,C-6; *J* = 29.2 Hz), 135.7 (t: C-4; *J* = 26.3 Hz), 132.4 (C-3,C-5); MS m/z (%) 154 (10), 152 (66), 150 (100), 117 (19), 115 (61).

Fraction four was obtained as a yellowish liquid of 3,4-dichloropyridine-2,5,6-d_3 (**93-2,5,6-d_3**): yield 0.20 g (1.3 mmole, 8%); ^{13}C-NMR ($CDCl_3$) δ 150.4 (t: C-2; *J* = 29.2 Hz), 148.2 (t: C-6; J = 28.0 Hz), 142.3 (C-4), 131.1(C-3), 125.2 (t: C-5; *J* = 26.5 Hz); MS m/z (%) 150(10), 152 (64), 150 (100), 117 (20), 115 (67).

5.17.2. Preparation of 2,3,4-trideuteriopyridine (1-2,3,4-d_3)

2,3-Dichloropyridine-4,5,6-d_3 (**91-4,5,6-d_3**) (0.37 g, 2.5 mmole) was added to the mixture of Pd-C (0.2 g), K_2CO_3 (0.6 g), and methanol (15 mL). The mixture was sealed in a Büchner flask equipped with a magnetic bar and balloon and purged with nitrogen for 15 minutes. The H_2 gas generated from $NaBH_4$ (0.2 g), H_2SO_4 (5 drops), and deionized water (3 mL) was added through a syringe to the solution. After 4 hours of stirring at room temperature, the resulting mixture was filtered to get rid off the Pd-C. The black precipitate of Pd-C was washed well with methanol. The filtrate was acidified with conc.HCl to form deuterated pyridinium salts. The methanol solvent was removed by evaporation to give wet solid. After basified with 10% K_2CO_3, the solution was extracted with dichloromethane, giving organic layer which was then dried over anhydrous Na_2SO_4. The solvent was removed by fractional distillation. The resulting

residue was purified by Kugelrohr distillation to give 2,3,4-trideuteriopyridine (**1-2,3,4-d_3**) as a colorless liquid: yield 0.11 g (1.3 mmole, 52%); ^{1}H-NMR ($(CD_3)_2CO$) δ 8.59 (d, 1H; *J* = 4.8 Hz), 7.34 (dt, 1H, *J* = 4.8 Hz); ^{13}C-NMR ($(CD_3)_2CO$) δ 150.6 (C-6), 150.2 (t: C-2; *J* = 26.8 Hz), 136.2 (t: C-4; *J* = 25.3 Hz); 124.4 (C-5), 124.0 (t: C-3; *J* = 25.4 Hz); MS m/z (%) 82 (100), 55 (45), 54 (59).

5.17.3. Preparation of 2,4,5-trideuteriopyridine (1-2,4,5-d_3)

2,5-Dichloropyridine-3,4,6-d_3 (**92-3,4,6-d_3**) (0.41 g, 2.7 mmole) was added to the mixture of Pd-C (0.2 g), K_2CO_3 (0.6 g), and methanol (15 mL). The mixture was sealed in a Büchner flask equipped with a magnetic bar and balloon and purged with nitrogen for 15 minutes. The H_2 gas generated from $NaBH_4$ (0.2 g), H_2SO_4 (5 drops), and deionized water (3 mL) was added through a syringe to the solution. After 4 hours of stirring at room temperature, the resulting mixture was filtered to get rid off the Pd-C. The black precipitate of Pd-C was washed well with methanol. The filtrate was acidified with conc.HCl to form deuterated pyridinium salts. The methanol solvent was removed by evaporation to give wet solid. After basified with 10% K_2CO_3, the solution was extracted with dichloromethane, giving organic layer which was then dried over anhydrous Na_2SO_4. The solvent was removed by fractional distillation. The resulting residue was purified by Kugelrohr distillation to give 2,4,5-trideuteriopyridine(**1-2,4,5-d_3**) as a colorless liquid: yield 0.12 g (1.5 mmole, 55.5 %); ^{1}H-NMR ($(CD_3)_2CO$) δ 8.59 (s, 1H), 7.36 (s, 1H); ^{13}C-NMR ($(CD_3)_2CO$) δ 150.6 (C-6), 150.3 (t: C2; *J* = 26.9 Hz), 136.2

(t: C4; J = 25.3 Hz); 124.2 (C3), 124.1 (t: C5; J = 25.0 Hz); MS m/z (%) 82 (100), 55 (43), 54 (59).

5.17.4. Preparation of 2,3,6-trideuteriopyridine (1-2,3,6-d_3)

3,4-Dichloropyridine-2,5,6-d_3 (**93-2,5,6-d_3**) (0.27 g, 1.8 mmole) was added to the mixture of Pd-C (0.2 g), K_2CO_3 (0.6 g), and methanol (15 mL). The mixture was sealed in a Büchner flask equipped with a magnetic bar and balloon and purged with nitrogen for 15 minutes. The H_2 gas generated from $NaBH_4$ (0.2 g), H_2SO_4 (5 drops), and deionized water (3 mL) was added through a syringe to the solution. After 4 hours of stirring at room temperature, the resulting mixture was filtered to get rid off the Pd-C. The black precipitate of Pd-C was washed well with methanol. The filtrate was acidified with conc.HCl to form deuterated pyridinium salts. The methanol solvent was removed by evaporation to give wet solid. After basified with 10% K_2CO_3, the solution was extracted with dichloromethane, giving organic layer which was then dried over anhydrous Na_2SO_4. The solvent was removed by fractional distillation. The resulting residue was purified by Kugelrohr distillation to give 2,3,6-trideuteriopyridine (**1-2,3,6-d_3**) as a colorless liquid: yield 0.08 g (1.0 mmole, 54.2 %); ^{1}H-NMR ($(CD_3)_2CO$) δ 8.59 (d, 1H; J = 7.6 Hz), 7.36 (d, 1H; J = 7.6 Hz); ^{13}C-NMR ($(CD_3)_2CO$) δ 150.3 (t: C-2, C-6; J = 27.8 Hz), 136.4 (C-4); 124.4 (C-5), 124.1 (t: C-3; J = 25.6 Hz); MS m/z (%) 82 (100), 55 (33), 54 (70).

5.18. Synthesis of 2,3,5-trideuteriopyridine (1-2,3,5-d_3)

5.18.1. Preparation of 4-nitropyridine N-oxide-2,3,5,6-d_4 (81-2,3,5,6-d_4)

Pyridine N-oxide-d_5 (**53-2,3,4,5,6-d_5**) (2.74 g, 27.4 mmole) prepared from H-D exchange reaction of pyridine N-oxide (**53**) with K_2CO_3/D_2O solution was mixed with conc. H_2SO_4 (10.0 mL) and fuming HNO_3 (5.0 mL). This mixture was heated until reflux at 130 ^oC for 5 hours. The resulting solution was poured on ice and made basic with Na_2CO_3 solution. The precipitate was filtered and all combined filtrate was extracted with dichloromethane (8x 20 mL). The organic layer was dried over anhydrous Na2SO4 and the solvent was evaporated to give 4-nitropyridine N-oxide-2,3,5,6-d_4 (**81-2,3,5,6-d_4**) as a yellow crystal. This was further purified by recrystallization in acetone: yield 2.47 g (17.1 mmole, 62.4%); ^{13}C-NMR ($CDCl_3$) δ 142.7 (C-4), 140.5 (t: C-2, C-6; J = 29.8 Hz), 121.2 (t: C-3, C-5; J = 26.7 Hz); MS m/z (%) 144 (53), 128 (40), 114 (43).

5.18.2. Preparation of 4-chloropyridine N-oxide-2,3,5,6-d_4 (82-2,3,5,6-d_4)

4-Nitropyridine N-oxide-2,3,5,6-d_4 (**81-2,3,5,6-d_4**) (2.12 g, 14.7 mmole) was warmed at 50 ^oC in water bath. After acetyl chloride (11.0 mL) was added, the mixture was refluxed until obtaining the white solid (30 minutes). The acid residue was removed by vacuum. The white solid residue was cooled in ice bath and added with ice. The aqueous solution was made basic with 10% Na_2CO_3 solution and extracted with dichloromethane (8x20 mL). The organic layer was dried (Na_2SO_4) and the solvent was removed by evaporation to give 4-chloropyridine N-oxide-2,3,5,6-d_4 (**82-2,3,5,6-d_4**) as a

white solid. This crude was purified by recrystallization in acetone: yield 1.84 g (13.7 mmole, 93.2 %); ^{13}C-NMR ($CDCl_3$) δ 140.1 (t: C-2,C-6; J = 28.8 Hz), 132.0 (C-4), 126.7 (t: C-3, C-5; J = 26.2 Hz); MS m/z (%) 135 (30), 133 (100), 117 (64), 82 (59).

5.18.3. Preparation of 2,4-dichloropyridine-3,5,6-d_3 (94-3,5,6-d_3)

4-Chloropyridine N-oxide-d_4 (**82-2,3,5,6-d_4**) (1.7 g, 12.7 mmole) was mixed with $POCl_3$ (13 mL) in a round bottom flask. This mixture was heated until reflux in an oil bath at 110 ^{o}C for 2 hours. The resulting solution was concentrated to remove excess $POCl_3$ by evaporator. The yellow crude was added with ice (3 g), basified with K_2CO_3 solution, extracted with dichloromethane (8 x 20 mL). The organic layer was dried (Na_2SO_4) and the solvent was removed by evaporation to give a red mixture. Preparative chromatography (9:1 DCM/Hexane) was used to isolate the major product as a colorless liquid of 2,4-dichloropyridine-3,5,6-d_3 (**94-3,5,6-d_3**) after removal of solvent: yield 0.90 g (6.0 mmole, 47.2 %); ^{13}C-NMR($CDCl_3$) δ 152.6 (C-6), 150.2 (t: C-2; J = 28.2 Hz), 146.1(C-4), 124.6(t: C-3; J = 26.8 Hz), 123.0(t: C-5; J = 26.2 Hz); MS m/z (%) 154 (8), 152 (59), 150 (91), 117 (33), 115 (100), 78 (41).

5.18.4. Preparation of 2,3,5-trideuteriopyridine (1-2,3,5-d_3)

2,4-Dichloropyridine-3,5,6-d_3 (**94-3,5,6-d_3**) (0.40 g, 2.6 mmole) was added to the mixture of Pd-C (0.2 g), K_2CO_3 (0.6 g), and methanol (15 mL). The mixture was sealed in a Büchner flask equipped with a magnetic bar and balloon and purged with nitrogen

for 15 minutes. The H_2 gas generated from $NaBH_4$ (0.2 g), H_2SO_4 (5 drops), and water (3 mL) was added through a syringe to the solution. After 4 hours of stirring at room temperature, the resulting mixture was filtered to remove Pd-C. This precipitate was washed well with methanol. The filtrate portions were combined and acidified with conc.HCl. Methanol was removed by evaporation to give wet solid which was made basic with K_2CO_3 solution. Extraction with dichloromethane gave organic layer which was dried over anhydrous Na_2SO_4. The solvent was removed by fractional distillation. The resulting residue was purified by Kugelrohr distillation to give 2,3,5-trideuteriopyridine (**1-2,3,5-d_3**) as a colorless liquid: yield 0.16 g (2.1 mmole, 77%); ^{1}H-NMR ($(CD_3)_2CO$) δ 8.60 (s, 1H), 7.75 (s, 1H); ^{13}C-NMR ($(CD_3)_2CO$) δ 150.5 (C-6), 150.2 (t: C-2; J = 27.6 Hz), 136.3 (C-4), 124.2 (t: C-3; *J* = 24.6 Hz), 123.8 (t: C-5; *J* = 24.9 Hz); MS m/z (%) 82(100), 55(48), 54 (66).

CHAPTER VI

Conclusion

Photolysis of cyanopyridines (**36-38**) vapors at 254 nm resulted phototransposition. Irradiation of any cyanopyridine isomer resulted in the formation of the other two isomers as photoproducts. These results are analogous to the experimental results from the photochemistry of dimethylpyridine vapors which was previously reported by this laboratory.[17] The phototransposition of these molecules was suggested to result from cyclization-2,6-bridging, nitrogen migration, and rearomatization. The reactivity of each isomer was found to be quite different. This was suggested to be based on the stability of their intermediates. The radical stabilization plays role in determining the rate of reaction leading to the difference in the formation of the other two isomers. In cyanopyridine, 3-cyanopyridine (**38**) is considered to be the least reactive species according to the radical stabilization in its intermediate, **BC-38**, which is extended by the cyano group attaching on the position 1 of the allylic system. This agrees well with the experimental result and the theoretical value of substituted allyl radical[38] which is applied to this azaprefulvene intermediate. 2-Cyanopyridine (**36**) is considered to be the moderate reactive species although it has the least radical stabilization. The reactivity of **36** depends on the steric hindrance of the CN group on the ring position 2 in the formation of azaprefulvene intermediate. Also, the intermediate of, **BC-36**, can result in the formation of **BC-36** during phototransposition period by one nitrogen migration, which is considered as an energy wasting process. Hence, 4-Cyanopyridine (**38**) is the most reactive isomer in this series.

Photolysis of methylpyridine vapors (**6-8**) at 254 nm was also studied resulting in the conclusion that they also undergo phototransposition via the using 2,6-bonding-nitrogen migration instead of the Dewar-pyridine or azaprismane mechanism that have been reported by other groups.[12,14] The experimental result shows that 2-methylpyridine (**6**) is the least reactive isomer. This is consistent with the suggestion that it undergoes an energy wasting process during phototransposition and that the formation of the azaprefulvene intermediate **BC-6** is hindered by the methyl group at the ring position 2. Because of the lack of steric hindrance, the reactivity of 3-methylpyridine (**7**) and 4-methylpyridine (**8**) are greater than **6**. The reactivity of these two isomers is quite similar to each other and they are consistent with the radical stabilization energy reported in the literature.[38]

Multistep syntheses of various deuterated pyridines and cyanopyridines were designed and carried out successfully. Two important deuterium labeling methods have been used in this synthesis. The H-D exchange in strong base condition was found to be useful for incorporating deuterium atom on pyridine N-oxide derivatives. Another method is deuteriumolysis/hydrogenolysis, which is a convenient way to change chlorine atoms at any position on the pyridine ring to D or H. The final products were obtained as pure compounds which were ready to use for photolytic experiments.

Using these deuterium-labeled compounds, the phototransposition mechanism could be followed. The photochemistry of a variety of deuterated pyridines in the vapor phase showed that pyridine undergoes phototransposition after photochemical excitation

canceling the long-held belief that pyridine is photo-unreactive. The mechanism that explains the observed reactions was suggested to involve electrocyclic ring closure-nitrogen migration and rearomatization which leads to all deuterated photoproducts that could be observed in NMR spectra. The same explanation is consistent with the photochemistry of all pyridine analogues, such as methylpyridines, dimethylpyridines, and cyanopyridines. In contrast, the interconverting Dewar-pyridine and azaprismane mechanisms cannot explain the capricious formations of photoproducts observed in several experiments. This shows that the 2,6-bonding-cyclization, nitrogen migration and rearomatization involving the formation of azaprefulvene intermediates is the best mechanistic pathway to explain the vapor phase photochemistry of pyridine and pyridine derivatives. These results are also consistent with reports by various research groups.[19,20,65]

REFERENCES

1. Padwa, A. *Chem. Rev.* **1977**, 77, 37-68.

2. Palmer, I. J; Ragazos, N. I.; Bernardi, F.; Olivucci, M.; Robb, M. A. *J. Am. Chem. Soc.* **1993**, 115, 673-685.

3. Scott, L. T.; Jones, M. *Chem. Rev.* **1972**, 72, 181-202.

4. Sarkar, S. K.; Ghoshal, S. K.; Kastha, G. S. *J. Chem. Phys.* **1982**, 76, 825-833.

5. Wilzbach, K. E.; Rausch, D. *J. Am. Chem. Soc.* **1970**, 92, 2178-2179.

6. van Tamelen, E. E.; Pappas, S. P. *J. Am. Chem. Soc.* **1963**, 85(20), 3297-3298.

7. Linnell R. H.; Noyes, Jr. W. A. *J. Am. Chem. Soc*., **1951**, 73, 3986-3988.

8. Mathias, E.; Heicklen, J. *Mol. Photochem*. **1972**, 4(4), 31-48.

9. Roquitte B. C. unpublished work performed at the Argonne National Laboratory

10. Noyes, Jr. W. A.; Al-ani, K. E. *Chem. Rev*. **1974**, 74, 29-43.

11. Chapman, O. L.; McIntosh, C. L.; Pacansky, J. *J. Am. Chem. Soc.* **1973**, 95, 614-617.

12. Roebke, W. *J. Phys. Chem.* **1970**, 74, 4198-4203.

13. Kebede, N. Ph.D. Thesis, Worcester Polytechnic Institute, Massachusetts, **1998**, 114-116.

14. Caplain, S.; Lablache-Combier, A. *J. Chem. Soc. Chem. Commun.* **1970**, 1247-1248.

15. Caplain, S.; Catteau, J. P.; Lablache-Combier, A. *J. Chem. Soc. Chem. Commun*. **1970**, 1475-1476.

16. Pascual, O. S. and Tuazon, L. O. *Philippines Nucl. J*. **1966**, 49-51; *Chem. Abs*.: 1967, 66, 115125b.

17. Pavlik, J. W.; Kebede, N.; Thompson, M.; Day, A. C.; Baltrop, J. A. *J. Am. Chem.*

Soc. **1999**, 121, 5666-5673.

18. Chachisvillis M.; Zewail, A. H. *J. Phys. Chem. A*. **1999**, 103, 7408-7418.
19. Zhong, D.; Diau, E. W. -G.; Bernhardt, T. M.; Feyter, S. D.; Roberts, J. D.; Zewail, A. H. *Chem. Phys. Lett.* **1998**, 298, 129-140.
20. Lobastov, V. A.; Srinivasan, R. Goodson, B. M.; Ruan, C. Y.; Feenstra, J. S.; Zewail, A. H. *J. Phys. Chem. A.* **2001**, 105(50), 11159-11164.
21. Yamasaki, I.; Sushida, K.; Baba, H. *J. Chem. Phys*. **1979**, 71(1), 381-387.
22. Noyes, Jr., W. A.; Harter, D. A. *J. Chem. Phys.* **1967**, 46, 674-680.
23. Kaplan, L.; Wilzbach, K. E. *J. Am. Chem. Soc.* **1968**, 90(12), 3291-3292.
24. Villa, E.; Amirav, A.; Lim, E. C. *J. Phys. Chem.* **1988**, 92(19), 5393-5397.
25. Bryce-Smith, D.; Gilbert, A. *Tetrahedron*, **1976**, 32, 1309-1326.
26. Srinivasan, R.; Feenstra, J. S.; Park, S. T.; Xu, S.; Zewail, A. H. *Science*, **2005**, 307, 558-563.
27. Stephenson, H. P. *J. Chem. Phys*. **1954**, 22, 1077-1082.
28. Innes, K. K.; Byrne, J. P.; and Ross, I. G. *J. Mol. Spectrosc*. **1967**, 22, 125-147.
29. Suzuki M.; Fujita, M.; akemura, T.; Baba, H. *Bull. Chem. Soc. Jpn*., **1988**, 61, 3461-3466.
30. Japar, S.; Ramsay, D. A. *J. Chem. Phys*. **1973**, 58, 5832-5833.
31. Wassam, Jr. W. A.; Lim E. C. *J. Chem. Phys*. **1978**, 68, 433-454.
32. Lim, E. C. "Excited States", Vol. 3, ed. by Lim, E. C. Academic Press, New York, 1977, p. 305.
33. Akiyama, S.; Yamauchi, S.; Hirota, N. *J. Phys. Chem*. **1993**, 97, 40-45.
34. Hoover, R. J.; Kasha, M. *J. Am. Chem. Soc*. **1969**, 91, 6508-6510.

35. Latas, K. J.; Power, R. K.; Nishimura, A. M. *Chem. Phys. Lett*. **1979**, 65, 272-277.

36. Nakashima, K.; Matsui, K.; Koyanagi, M.; Kanda, Y. *Mem. Fac. Sci., Kyushu Uniy., Ser. C.* **1979**, 11(2), 281-292.

37. Tero-Kubota, S.; Akiyama, K.; Ikoma, T.; Ikegami, Y. *J. Phys. Chem*. **1991**, 95, 766-770.

38. Lehd M.; Jensen F. *J. Org. Chem*. **1991**, 56, 884-885.

39. Carey, F. A.; Sundberg, R. J. *Advanced Organic Chemistry*, 4th ed. New York: Kluwer Academic/Plenum Publishers, **2000**, 695.

40. Kebede, N.; Pavlik, J. W. *J. Heterocyclic Chem*. **1997**, 34, 685-686.

41. Kawazoe, Y.; Ohnishi, M.; Yoshioka, Y. *Chem. Pharm. Bull.* **1964**, 12(11), 1384-1386.

42. Zoltewicz, J. A.; Kauffman, G. M. *J. Org. Chem.* **1969**, 34(5), 1405-1411.

43. Abramovitch R. A.; Saha, M.; Smith, E. M.; Coutts, R. T. *J. Am. Chem. Soc.* **1967**, 89(6), 1537-1538.

44. Sr Ann Immaculata Gallaher, I. H. M.; Lalinsky, B. A.; Cuper, C. M. *J. Org. Chem*. **1970**, 35(4), 1175-1176.

45. Matsuki, Y.; Katakuse, Y.; Katashima, M.; Matsuura, H.; Goromaru, T. *Chem. Pharm. Bull.* **1989**, 37(6), 1637-1638.

46. Buu-Hoi, Ng, Ph.; Xuong, Ng. D.; Nam, Ng. H.; Binon, F.; Royer, R. *J. Chem. Soc*. **1953**, 1358-1364

47. Stephen, C. R.; Bianco, E. J.; Pilgrim, F. J. *J. Am Chem. Soc.*, **1955**, 77, 1701-1702.

48. Kebede N. Personal discussion.

49. Vogel, A. I. Revised by Furniss, B. S.; Hannaford, A. J.; Rogers, V.; Smith, P. W. G.;

Tatchell, A. R., Thames Polytechnic. *Vogel's Textbook of Practical Organic Chemistry, Including Qualitative Organic Analysis*, 4th ed. London: Longman Group, Ltd., **1978**, 848.

50. Ochiai, E. *J. Org. Chem.* **1953**, 18, 534-550.
51. Pirkle W. H.; Dines, M. B. *J. Org. Chem.* **1969**, 34(8), 2239-2244.
52. Talukdar, S.; Hsu, J. L.; Chou, T. C.; Fang, J. M. *Tetrahedron Lett.*, **2001**, 42, 1103-1105.
53. Bosin, T. R.; Raymond, M. G.; Buckpitt, A. R. *Tetrahedron Letts.* **1973**, 47, 4699-4700.
54. Proffet, Von E.; Steinke, W. *J. Prakt. Chem.* **1961**, (4)13, 58-75.
55. Azzam, R.; Borggraeve, W. D.; Compernolle, F.; Hoornaert, G. J. *Tetrahedron Letts.* **2004**, 45, 1885-1888.
56. Molenaar-Langeveld, T. A.; Vermeulen, P. E.; Nibbering, N. M. M.; Morgan, P. D.; Brenton, A. G.; Beynon, J. H.; Sensharma, D. C.; Jennings, K. R. *Org. Mass Spectrometry*, **1979**, 14, 524-531.
57. Sojka, S. A. *J. Org. Chem*., **1979**, 44, 307-308.
58. Copéret, C.; Adolfsson, H.; Khuong, T. V.; Yudin, A. K.; Sharpless, K. B. *J. Org. Chem.* **1998**, 63, 1740-1741.
59. Zoltewicz J. A.; Kauffman, G. M. *Tetrahedron Letts.,* **1967**, 4, 337-342.
60. Zoltewicz J. A.; Smith, C. L. *J. Am. Chem. Soc.* **1966**, (88)20, 4766-4767.
61. Evans, R. F.; Brown, H. C. *J. Org. Chem.* **1962**, 27, 1329-1336.
62. Yamanaka, H.; Araki, T.; Sakamoto, T. *Chem. Pharm. Bull.* **1988**, 36(6), 2244-2247.
63. Pavlik, J. W. In: Molecular and Supramolecular Photochemistry Vol.1: Organic

Photochemistry. V. Ramamurthy, K. J. Schanze, eds. Marcel Dekker Inc. New York, 1997, 57-110.

64. Macleod, P. J.; Pincock, A. L.; Pincock, A. J.; Thompson, K. A. Unpublished results.

65. Cao, Z.; Zhang, Q.; Peyerimhoff, S. D. *Chem. Eur. J*. **2001**, 7(9), 1927-1935.

66. Vongnakorn, T. Experimental results for Master Thesis, Chulalongkorn University, **2004**.

APPENDIX

A. NMR spectra of synthetic compounds

1. Picolinic acid N-oxide-6-d (**75-6-d**)

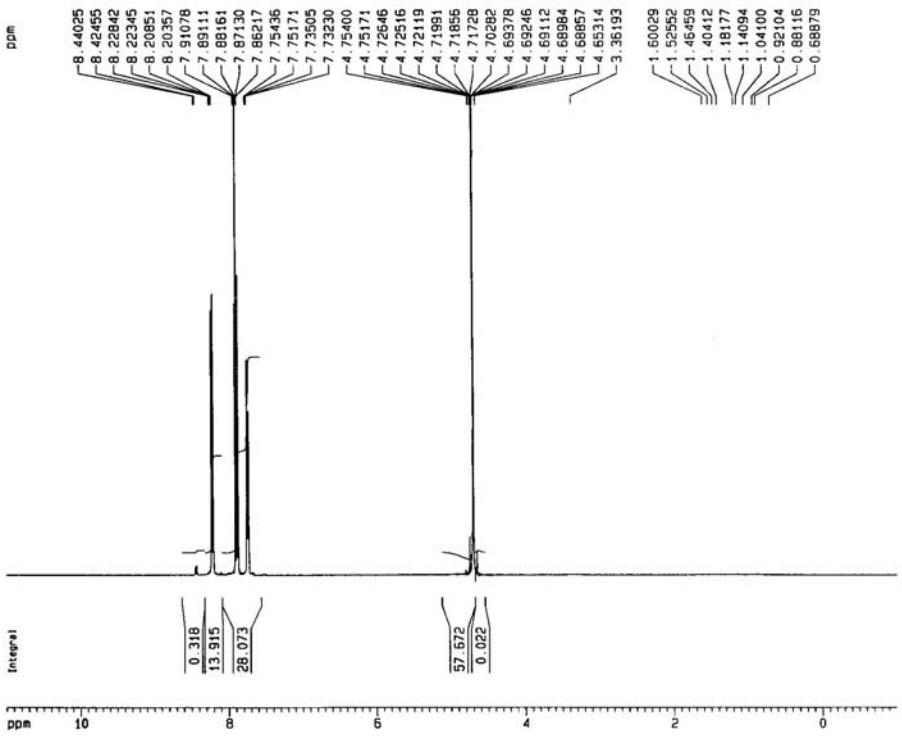

Figure A.1 ^{1}H-NMR spectrum of picolinic acid N-oxide-6-d

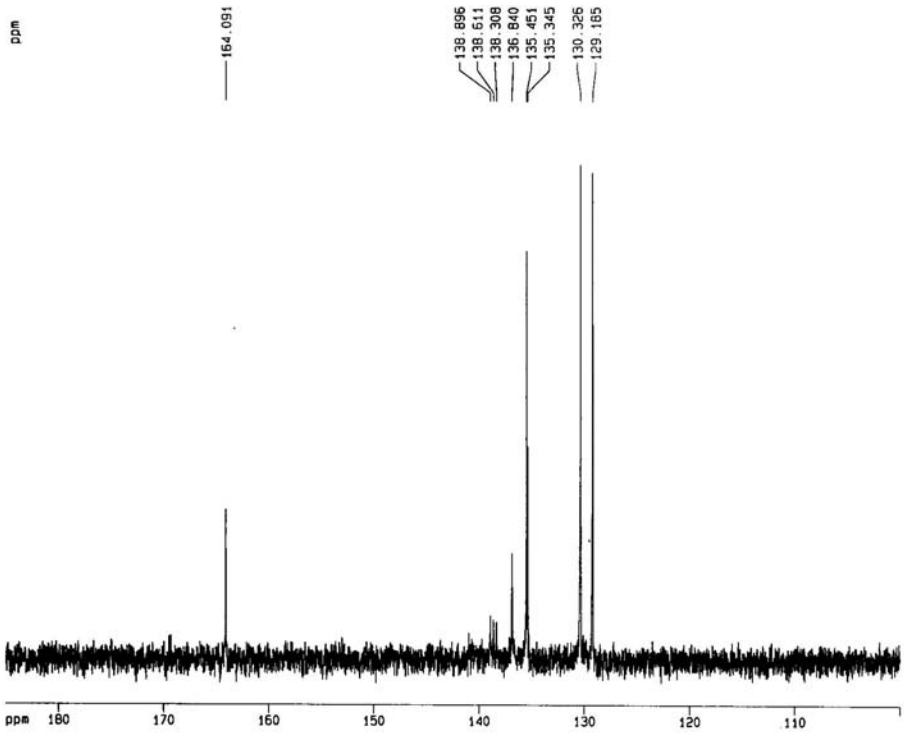

Figure A.2 ^{13}C-NMR spectrum of picolinic acid N-oxide-6-d

2. 4-Nitropicolinic acid N-oxide-6-d (**71-6-d**)

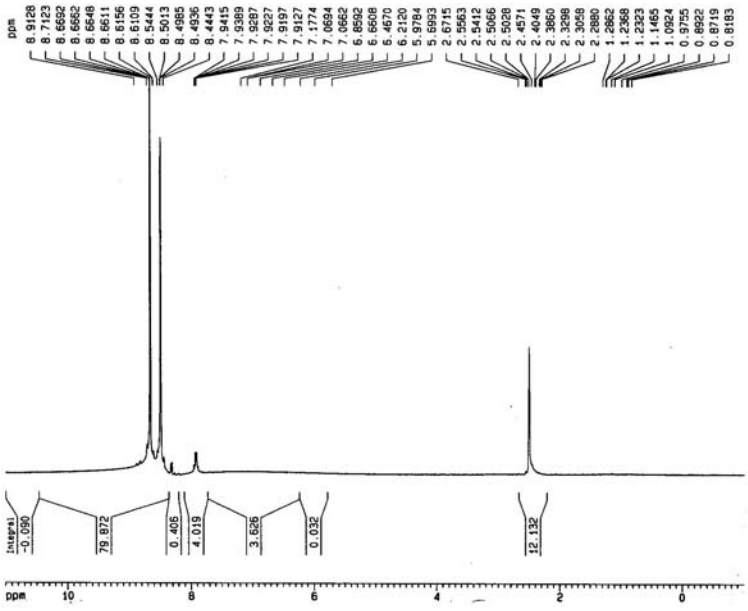

Figure A.3 ^{1}H-NMR spectrum of 4-nitropicolinic acid N-oxide-6-d

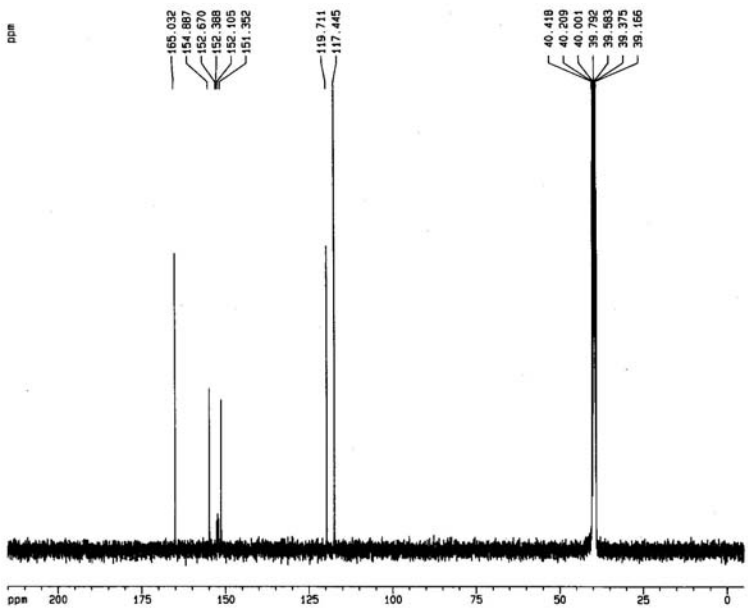

Figure A.4 ^{13}C-NMR spectrum of 4-nitropicolinic acid N-oxide-6-d

3. Methyl 4-nitropicolinate N-oxide-6-d (**76-6-d**)

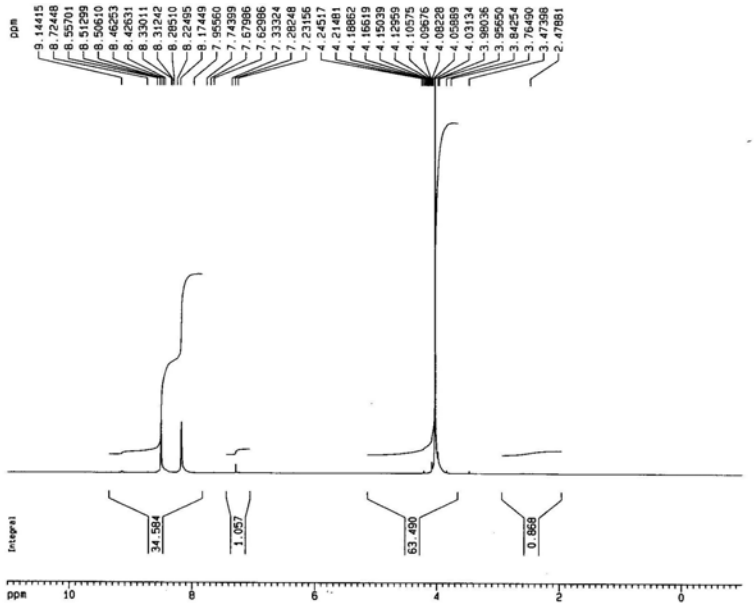

Figure A.5 ^{1}H-NMR spectrum of methyl 4-nitropicolinate N-oxide-6-d

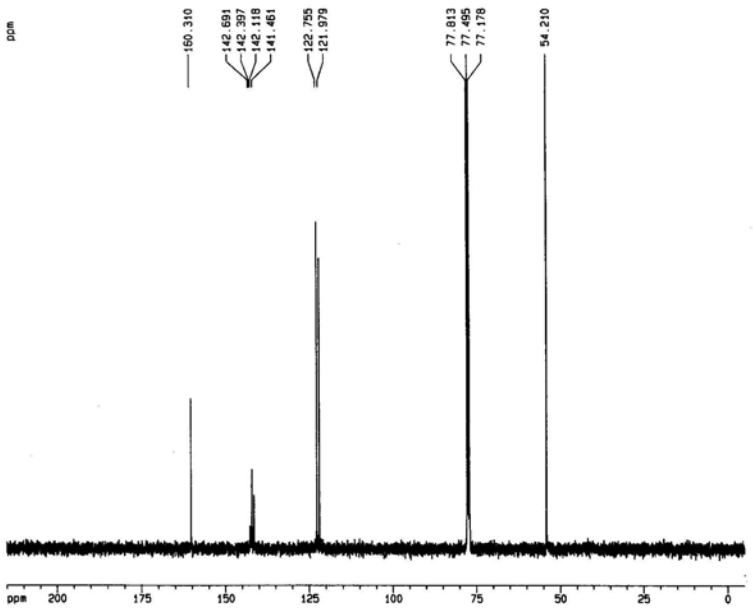

Figure A.6 ^{13}C-NMR spectrum of methyl 4-nitropicolinate N-oxide-6-**d**

4. Methyl 4-chloropicolinate N-oxide-6-d (**77-6-d**)

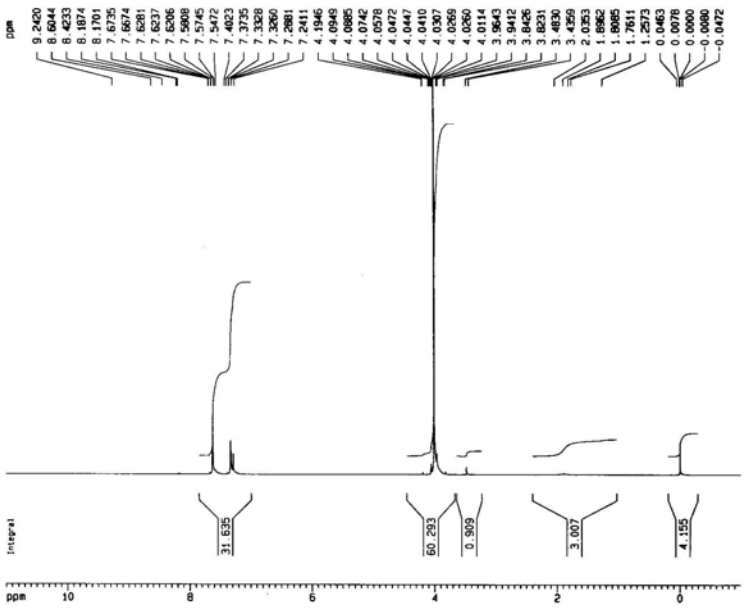

Figure A.7 ^{1}H-NMR spectrum of methyl 4-chloropicolinate N-oxide-6-d

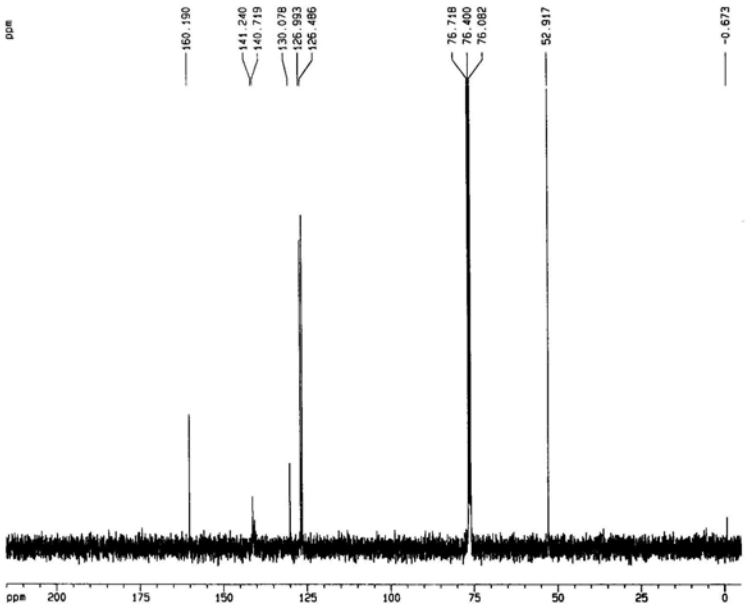

Figure A.8 ^{13}C-NMR spectrum of methyl 4-chloropicolinate N-oxide-6-d

5. Methyl 4-chloropicolinate-6-d (**78-6-d**)

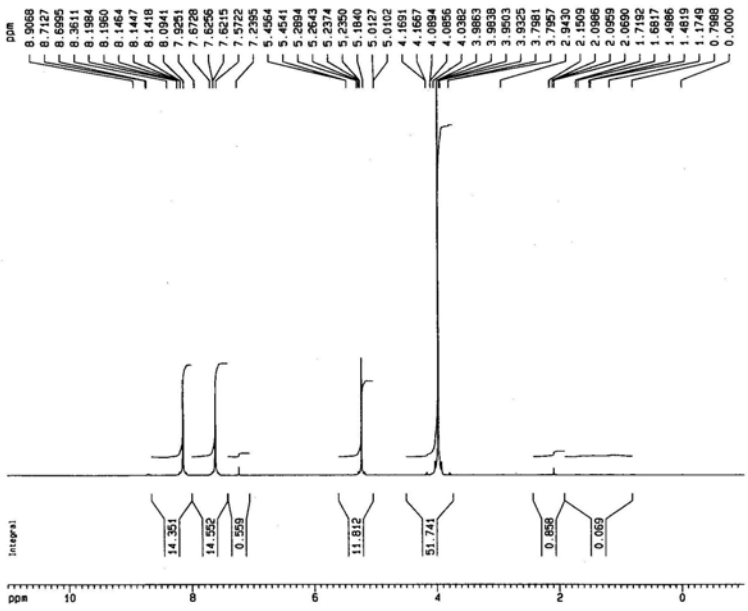

Figure A.9 ^{1}H-NMR spectrum of methyl 4-chloropicolinate-6-d

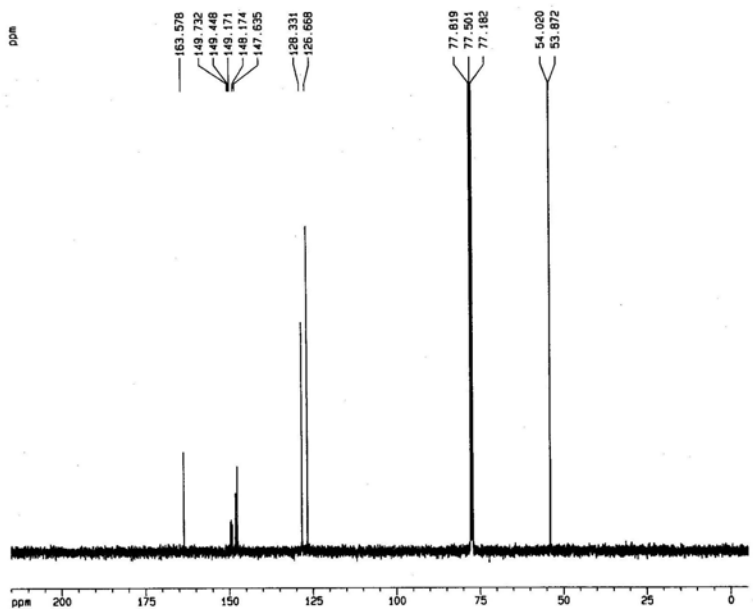

Figure A.10 ^{1}H-NMR spectrum of methyl 4-chloropicolinate-6-d

6. methyl picolinate-4,6-d_2 (**79-4,6-d_2**)

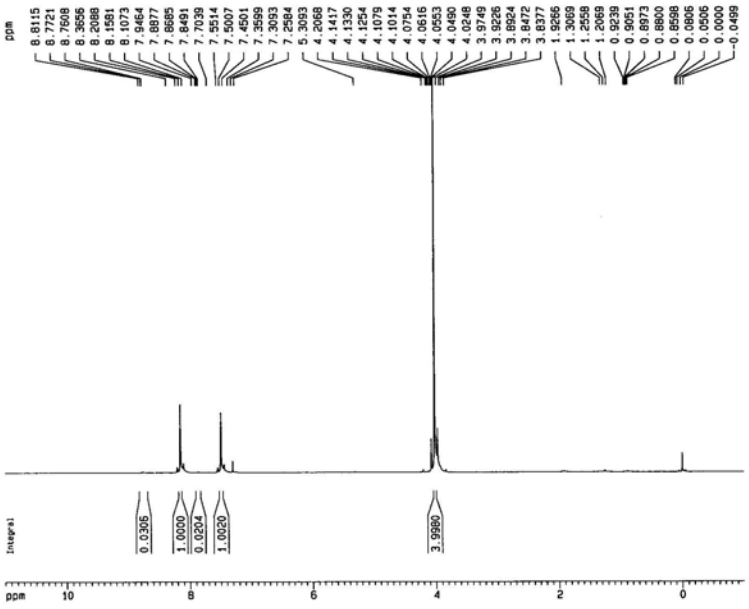

Figure A.11 ^{1}H-NMR spectrum of methyl picolinate-4,6-d_2

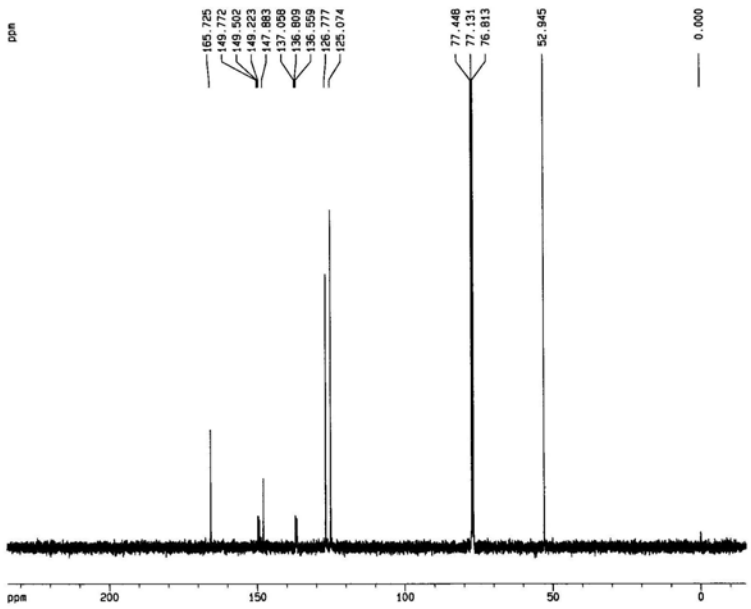

Figure A.12 ^{13}C-NMR spectrum of methyl picolinate-4,6-d_2

7. Picolinamide-4,6-d_2 (**80-4,6-d_2**)

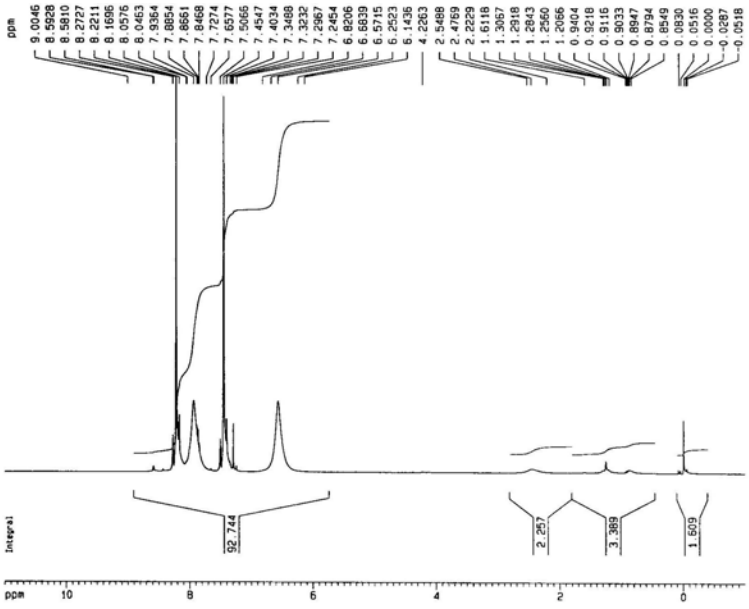

Figure A.13 ^{1}H-NMR spectrum of picolinamide-4,6-d_2

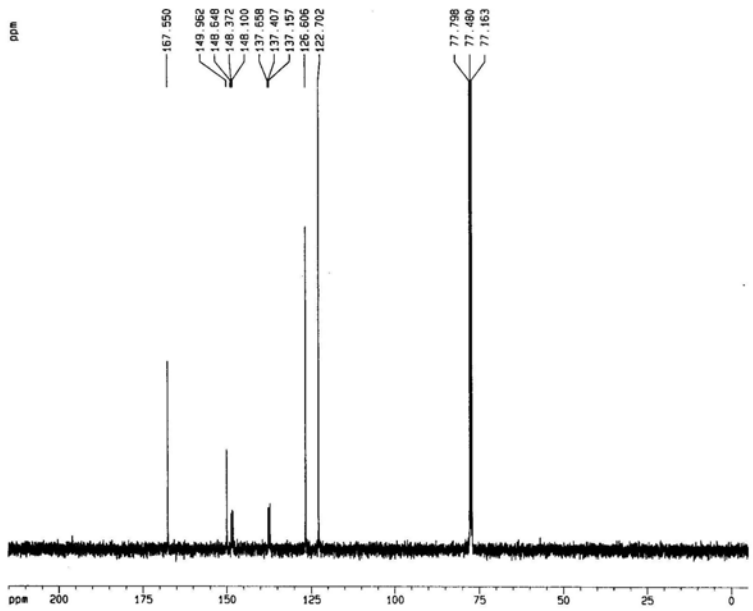

Figure A.14 ^{13}C-NMR spectrum of picolinamide-4,6-d_2

8. Nicotinic acid N-oxide-2,6-d_2 (**61-2,6-d_2**)

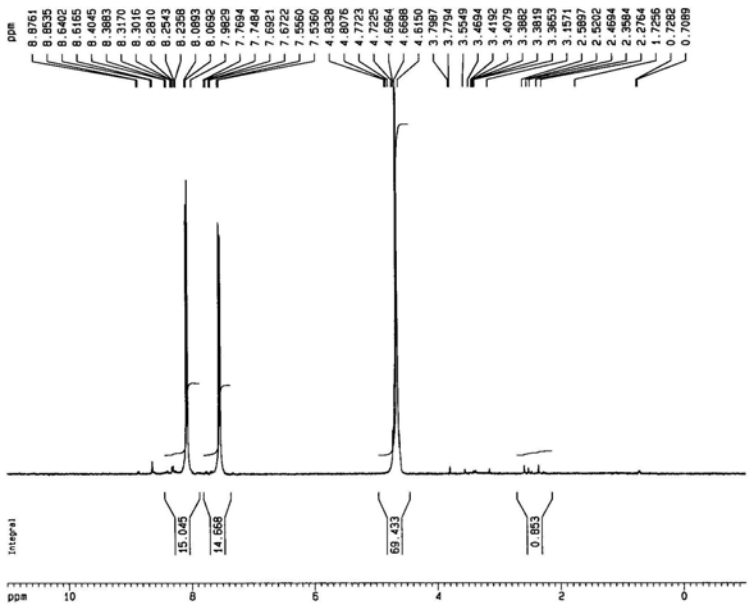

Figure A.15 ^{1}H-NMR spectrum of nicotinic acid N-oxide-2,6-d_2

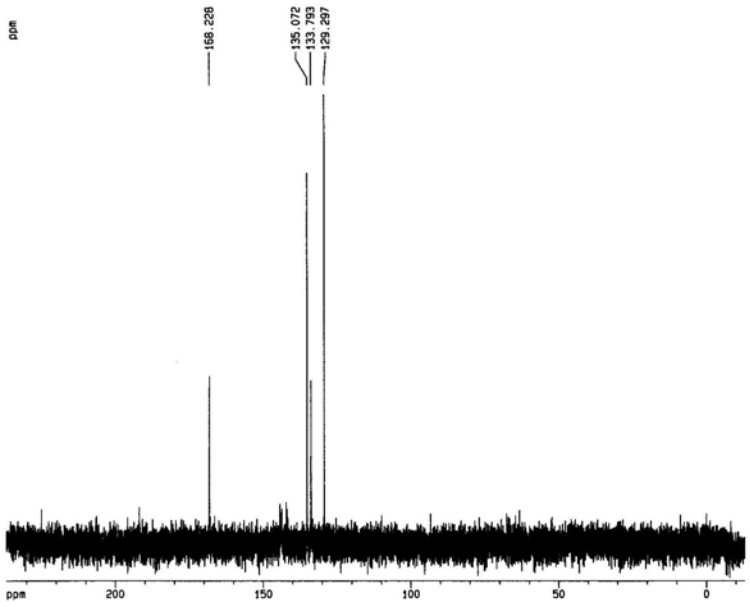

Figure A.16 ^{13}C-NMR spectrum of nicotinic acid N-oxide-2,6-d_2

9. Methyl nicotinate N-oxide-2,6-d_2 (**62-2,6-d_2**)

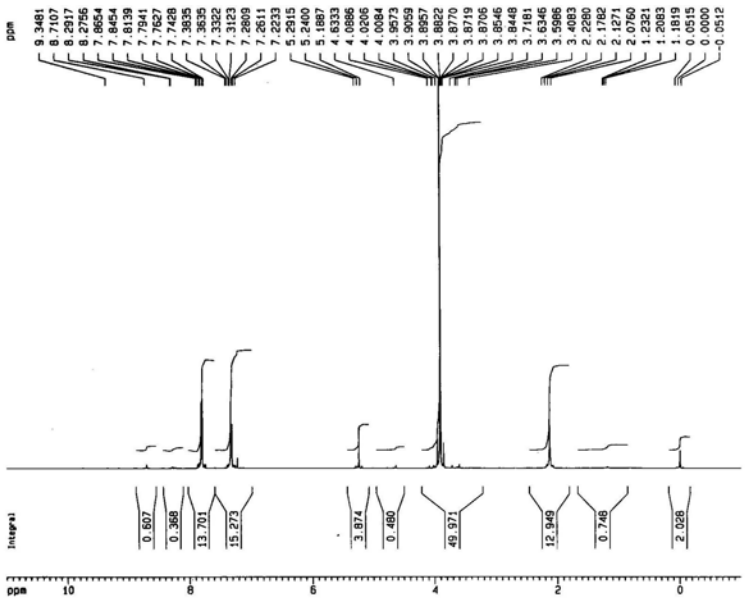

Figure A.17 ^{1}H-NMR spectrum of methyl nicotinate N-oxide-2,6-d_2

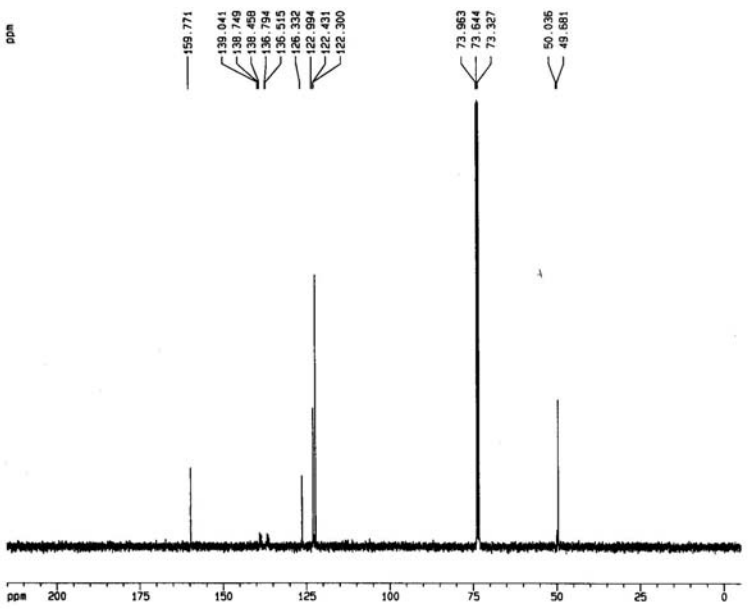

Figure A.18 ^{13}C-NMR spectrum of methyl nicotinate N-oxide-2,6-d_2

10. Methyl nicotinate-2,6-d_2 (**63-2,6-d_2**)

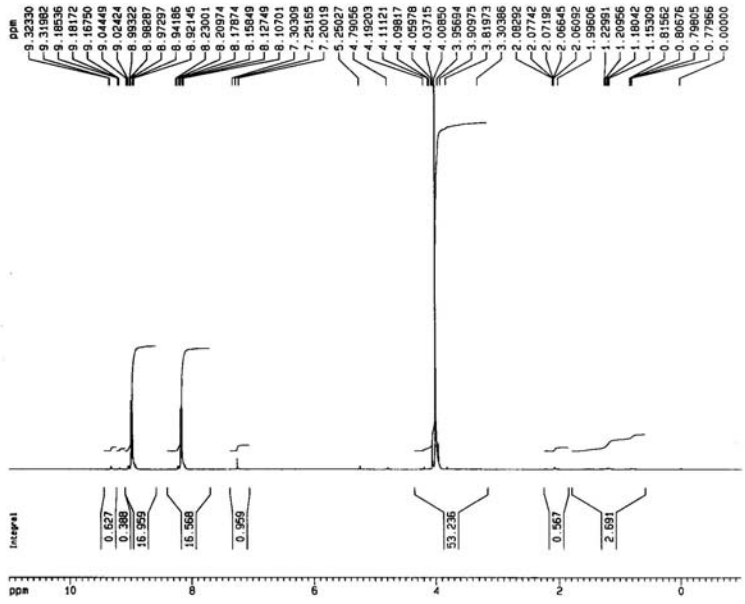

Figure A.19 ^{1}H-NMR spectrum of methyl nicotinate-2,6-d_2

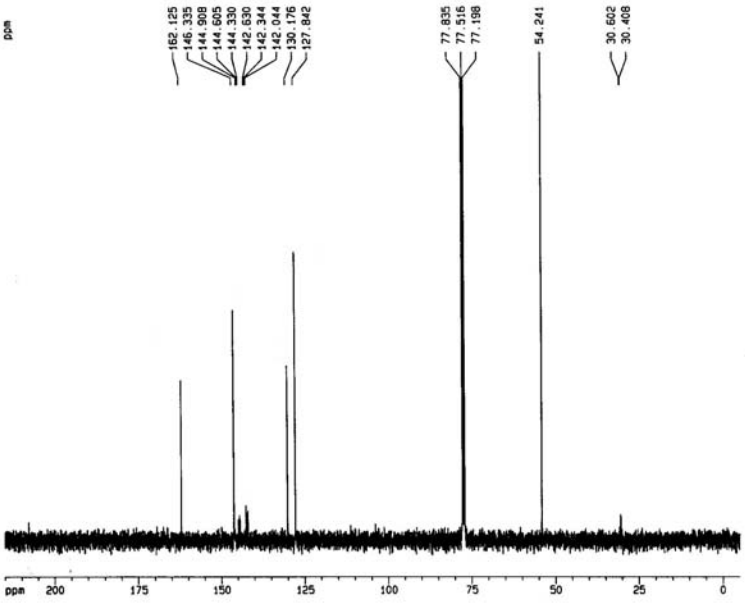

Figure A.20 ^{13}C-NMR spectrum of methyl nicotinate-2,6-d_2

11. Nicotinamide-2,6-d_2 (**64-2,6-d_2**)

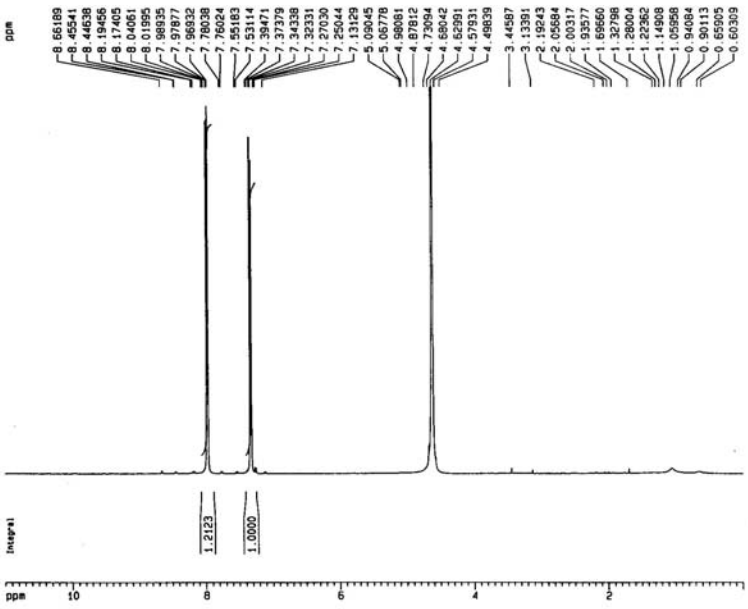

Figure A.21 ^{1}H-NMR spectrum of nicotinamide-2,6-d_2

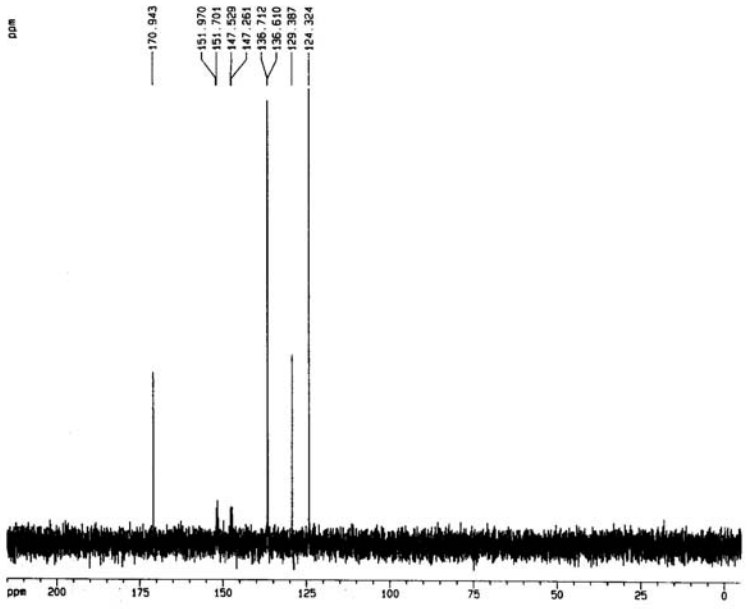

Figure A.22 ^{13}C-NMR spectrum of nicotinamide-2,6-d_2

12. Isonicotinic acid N-oxide-2,6-d_2 (**54-2,6-d_2**)

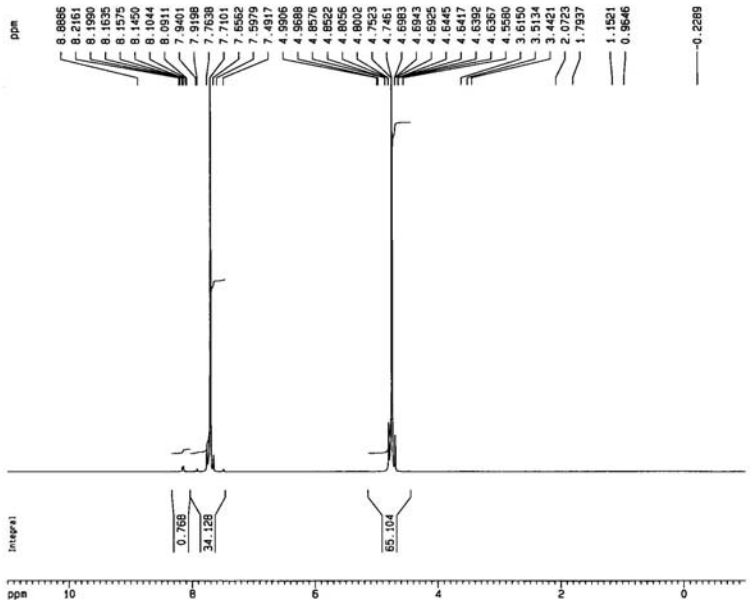

Figure A.23 ^{1}H-NMR spectrum of isonicotinic acid N-oxide-2,6-d_2

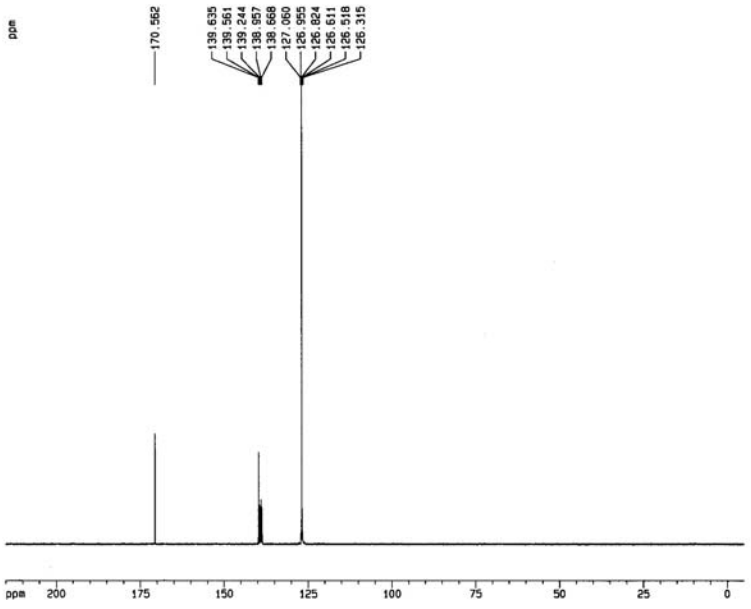

Figure A.24 ^{13}C-NMR spectrum of isonicotinic acid N-oxide-2,6-d_2

13. Methyl isonicotinate N-oxide-2,6-d_2 (**58-2,6-d_2**)

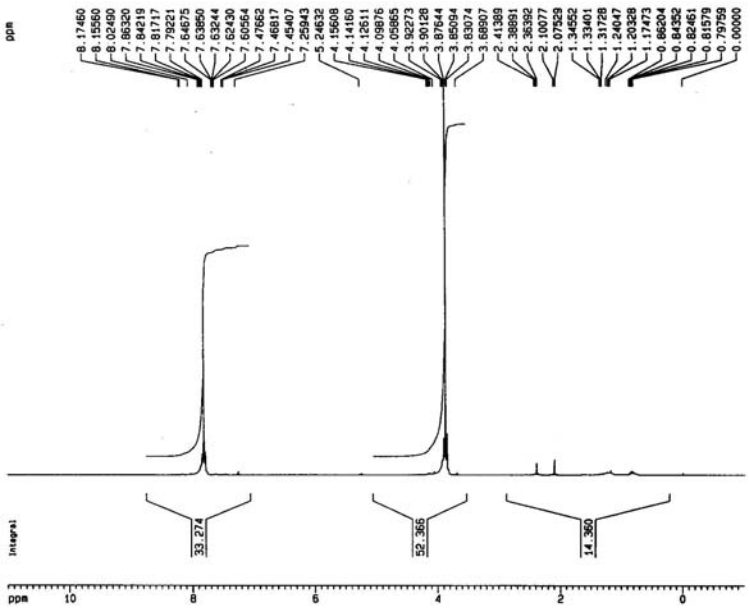

Figure A.25 ^{1}H-NMR spectrum of methyl isonicotinate N-oxide-2,6-d_2

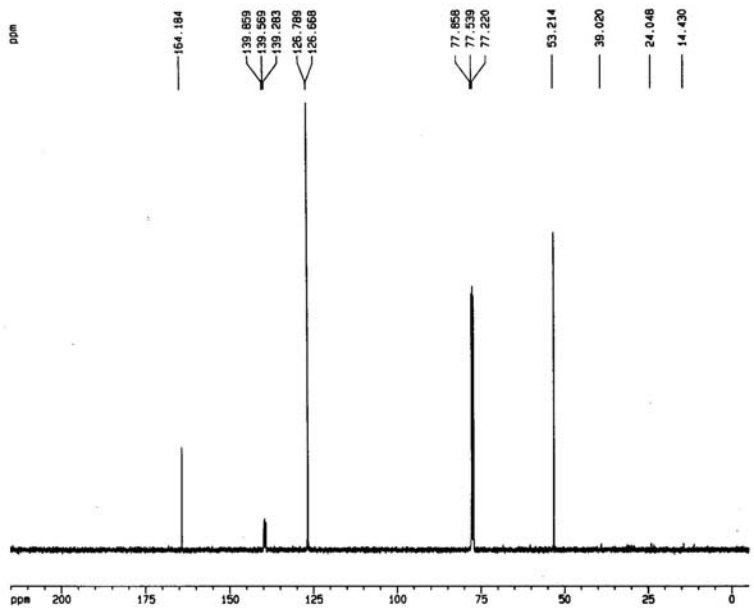

Figure A.26 ^{13}C-NMR spectrum of methyl isonicotinate N-oxide-2,6-d_2

14. Methyl isonicotinate-2,6-d_2 (**59-2,6-d_2**)

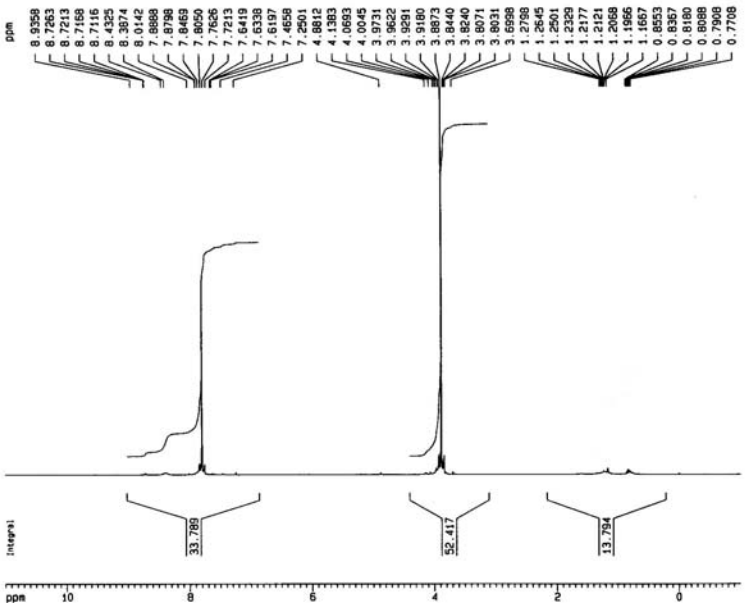

Figure A.27 ^{1}H-NMR spectrum of methyl isonicotinate-2,6-d_2

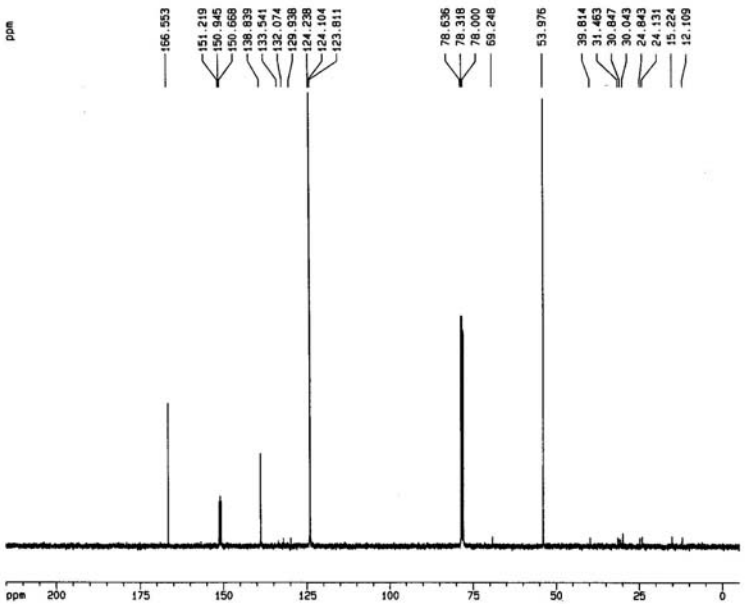

Figure A.28 ^{13}C-NMR spectrum of methyl isonicotinate-2,6-d_2

15. Pyridine N-oxide-2,6-d_2 (**53-2,6-d_2**)

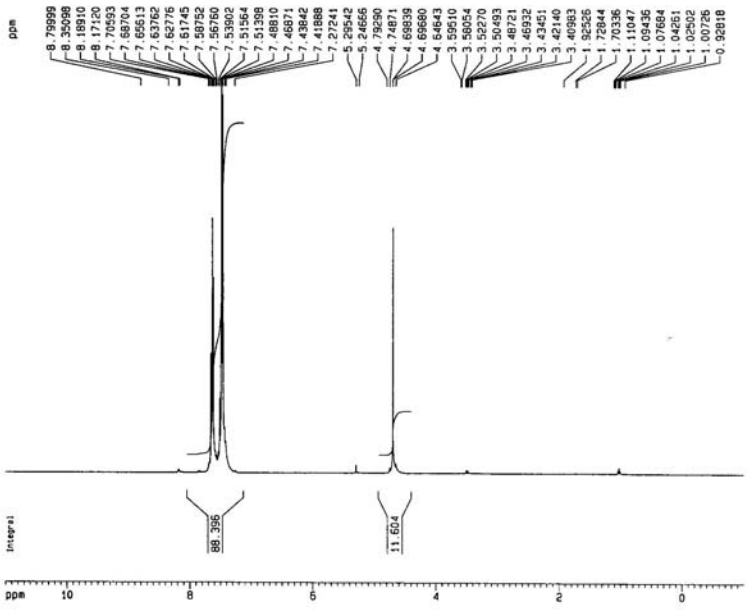

Figure A.29 ^{1}H-NMR spectrum of pyridine N-oxide-2,6-d_2

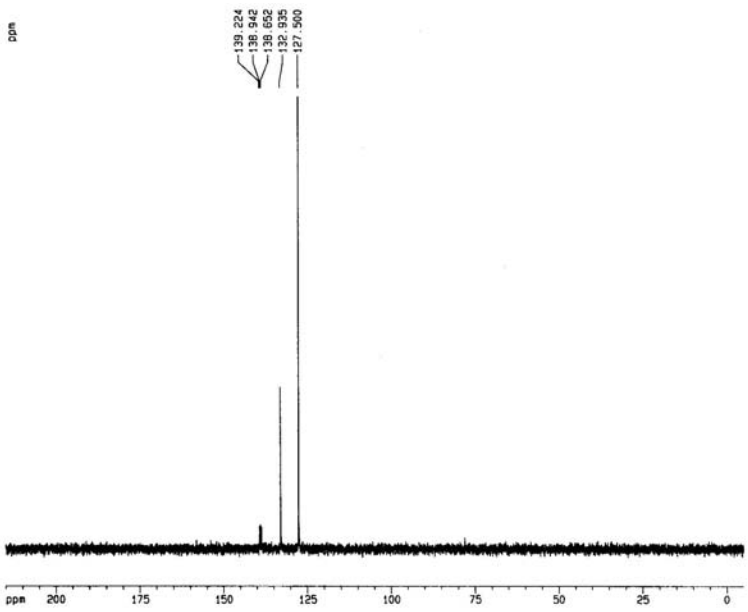

Figure A.30 ^{13}C-NMR spectrum of pyridine N-oxide-2,6-d_2

16. Pyridine N-oxide-3,4,5-d_3 (**53-3,4,5-d_3**)

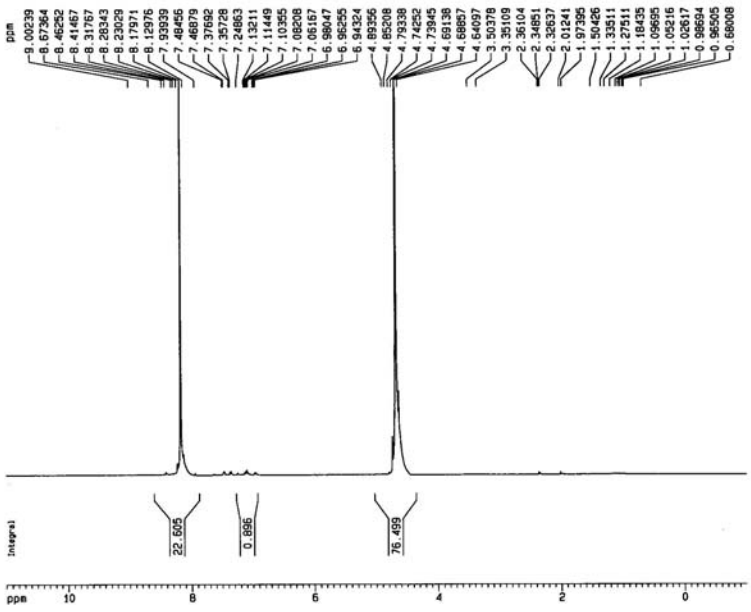

Figure A.31 ^{1}H-NMR spectrum of pyridine N-oxide-3,4,5-d_3

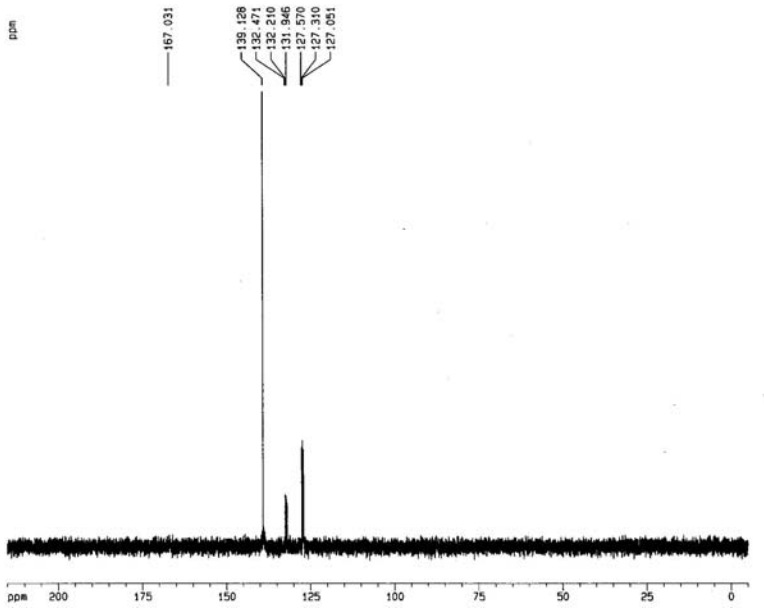

Figure A.32 ^{13}C-NMR spectrum of pyridine N-oxide-3,4,5-d_3

17. 4-Nitropyridine N-oxide-2,6-d_2 (**81-2,6-d_2**)

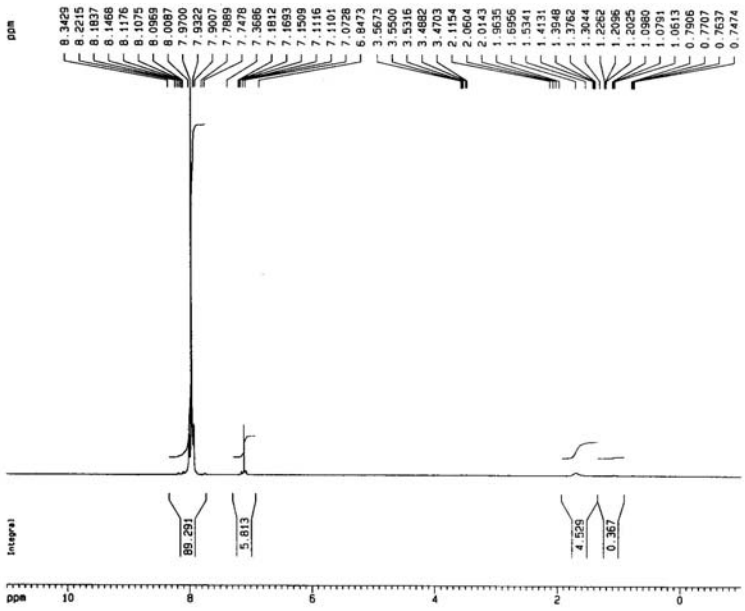

Figure A.33 ^{1}H-NMR spectrum of 4-nitropyridine N-oxide-2,6-d_2

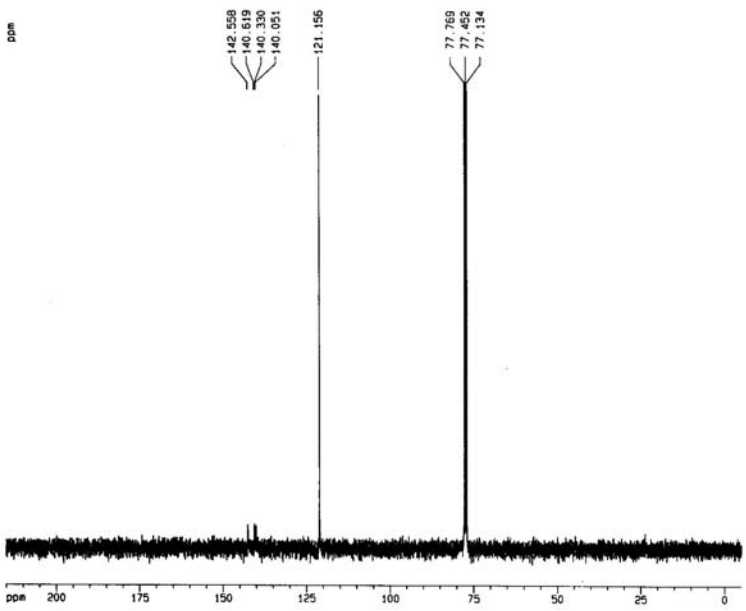

Figure A.34 ^{13}C-NMR spectrum of 4-nitropyridine N-oxide-2,6-d_2

18. 4-Chloropyridine N-oxide-2,6-d_2 (**82-2,6-d_2**)

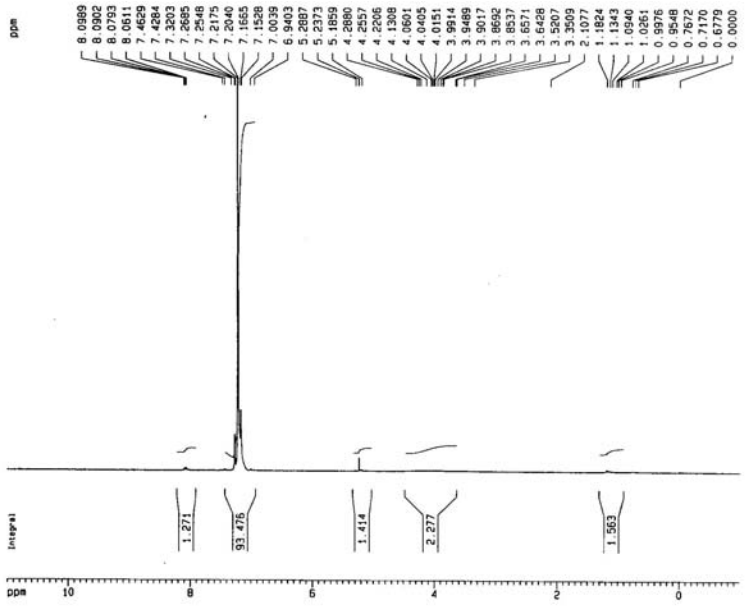

Figure A.35 ^{1}H-NMR spectrum of 4-chloropyridine N-oxide-2,6-d_2

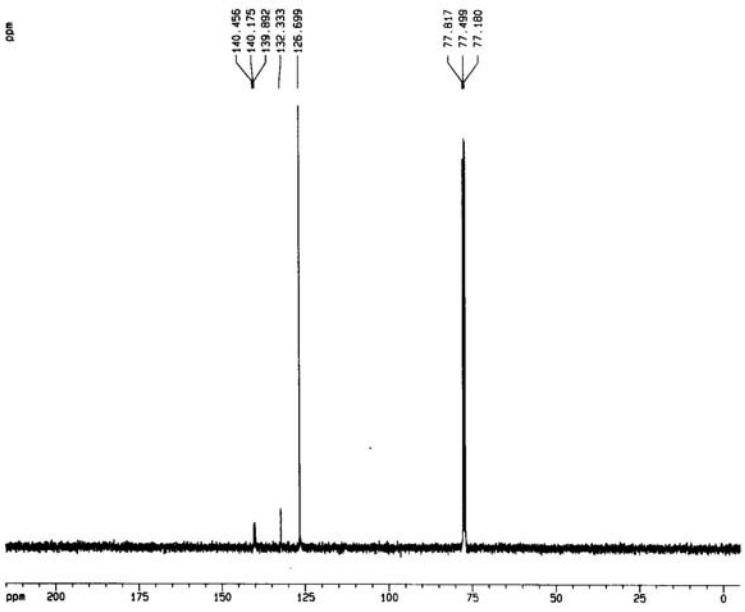

Figure A.36 ^{13}C-NMR spectrum of 4-chloropyridine N-oxide-2,6-d_2

19. 4-Chloropyridine-2,6-d_2 (**83-2,6-d_2**)

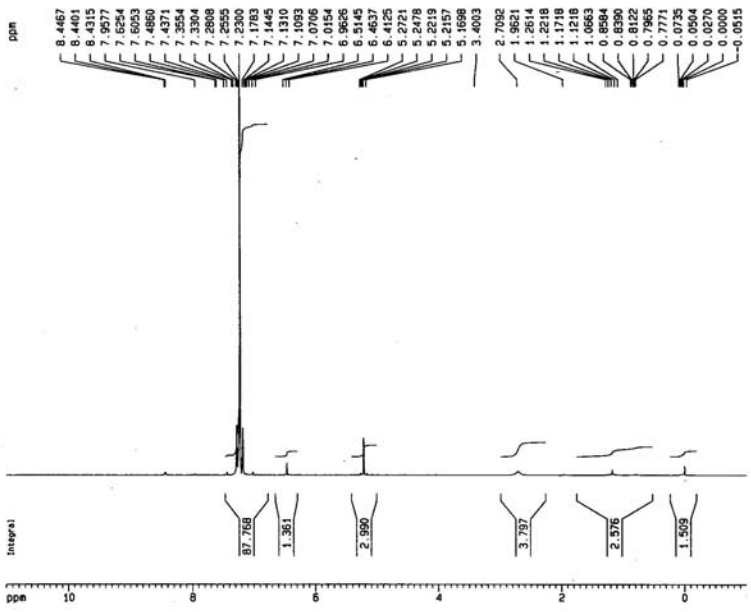

Figure A.37 ^{1}H-NMR spectrum of 4-chloropyridine-2,6-d_2

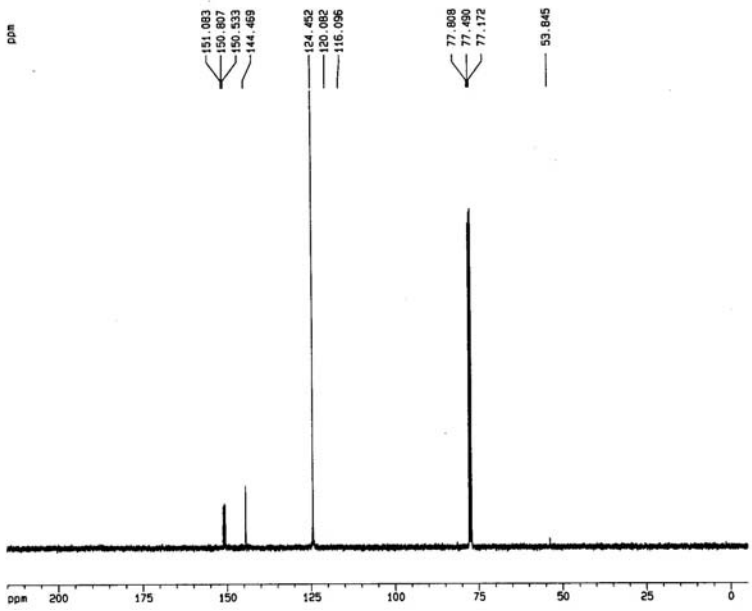

Figure A.38 ^{13}C-NMR spectrum of 4-chloropyridine-2,6-d_2

20. 3,5-Dichloropyridine N-oxide (**85**)

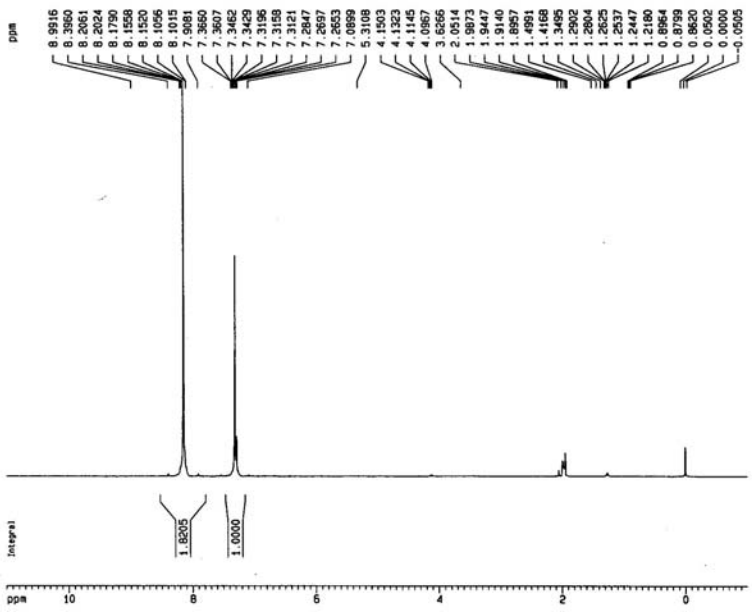

Figure A.39 ^{1}H-NMR spectrum of 3,5-dichloropyridine N-oxide

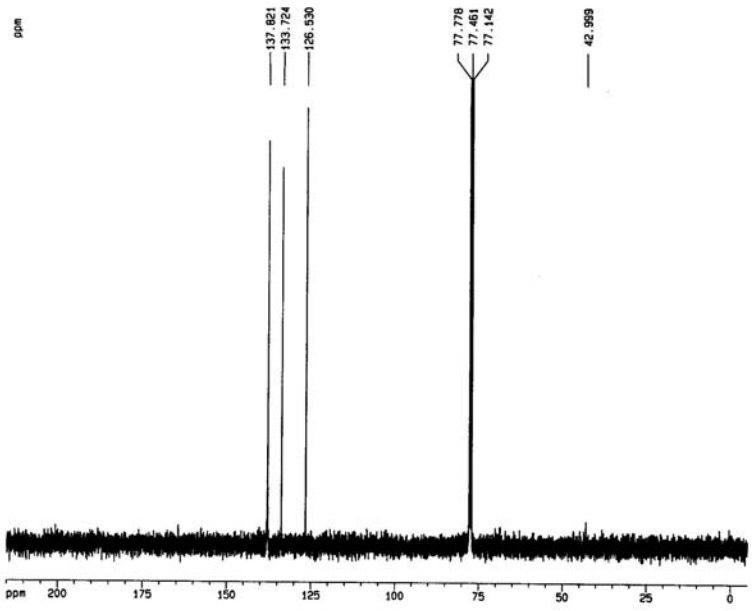

Figure A.40 ^{13}C-NMR spectrum of 3,5-dichloropyridine N-oxide

21. 3,5-Dichloropyridine N-oxide-2,4,6-d_3 (**85-2,4,6-d_3**)

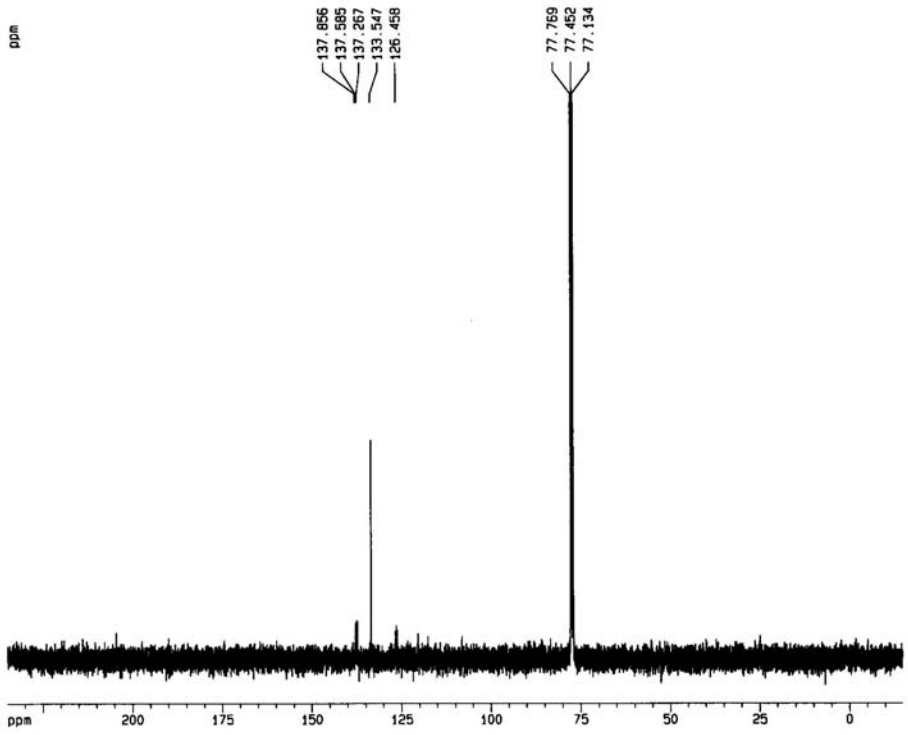

Figure A.41 ^{13}C-NMR spectrum of 3,5-dichloropyridine N-oxide-2,4,6-d_3

22. 3,5-dichloropyridine-2,4,6-d_3 (**84-2,4,6-d_3**)

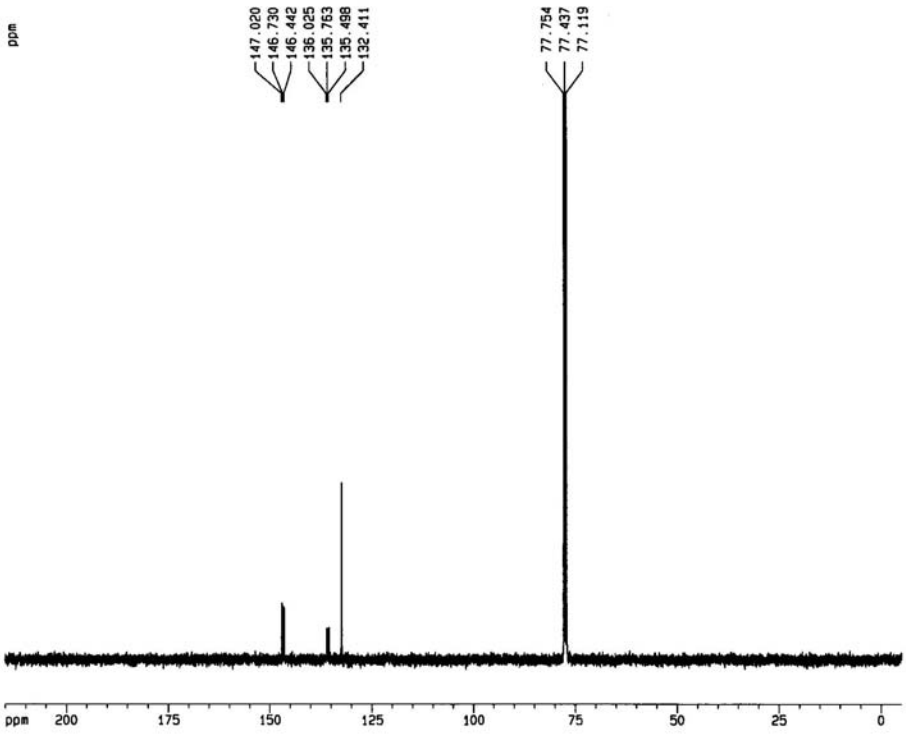

Figure A.42 ^{13}C-NMR spectrum of 3,5-dichloropyridine-2,4,6-d_3

23. 3,5-Dichloropyridine-2,6-d_2 (**84-2,6-d_2**)

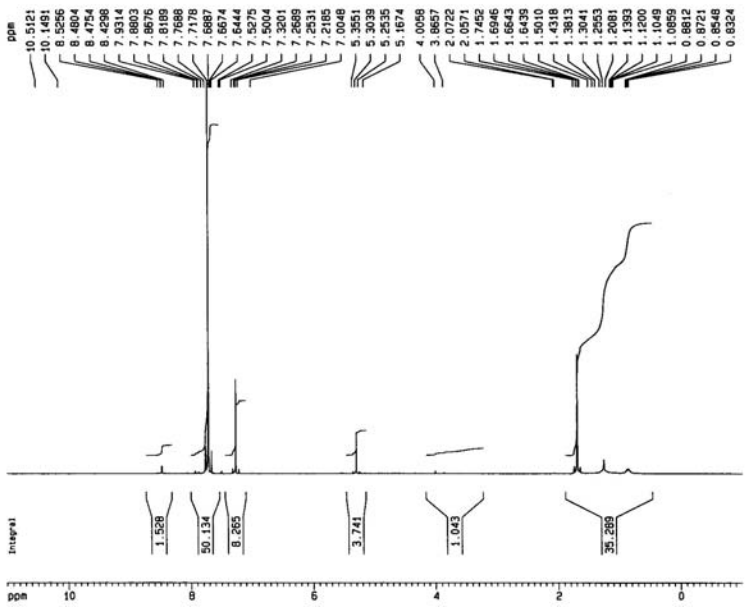

Figure A.43 ^{1}H-NMR spectrum of 3,5-dichloropyridine-2,6-d_2

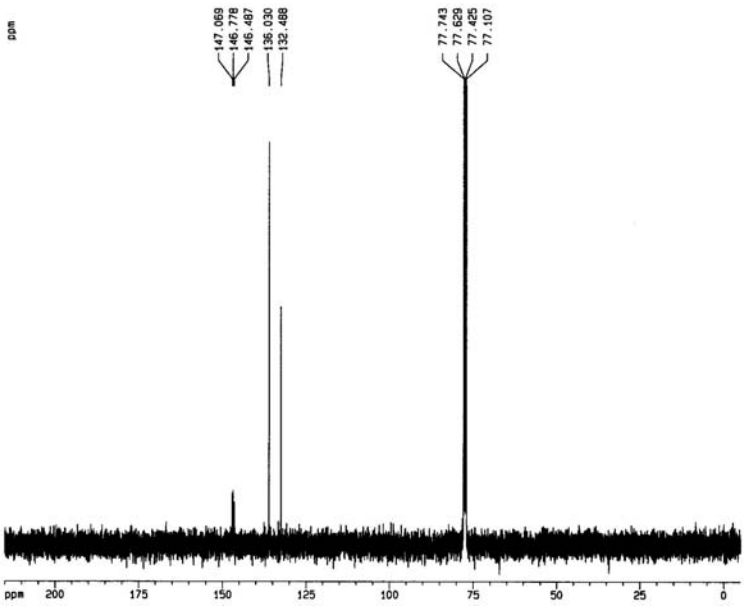

Figure A.44 ^{13}C-NMR spectrum of 3,5-dichloropyridine-2,6-d_2

24. Pyridine N-oxide-d_5 (**53-2,3,4,5,6-d_5**)

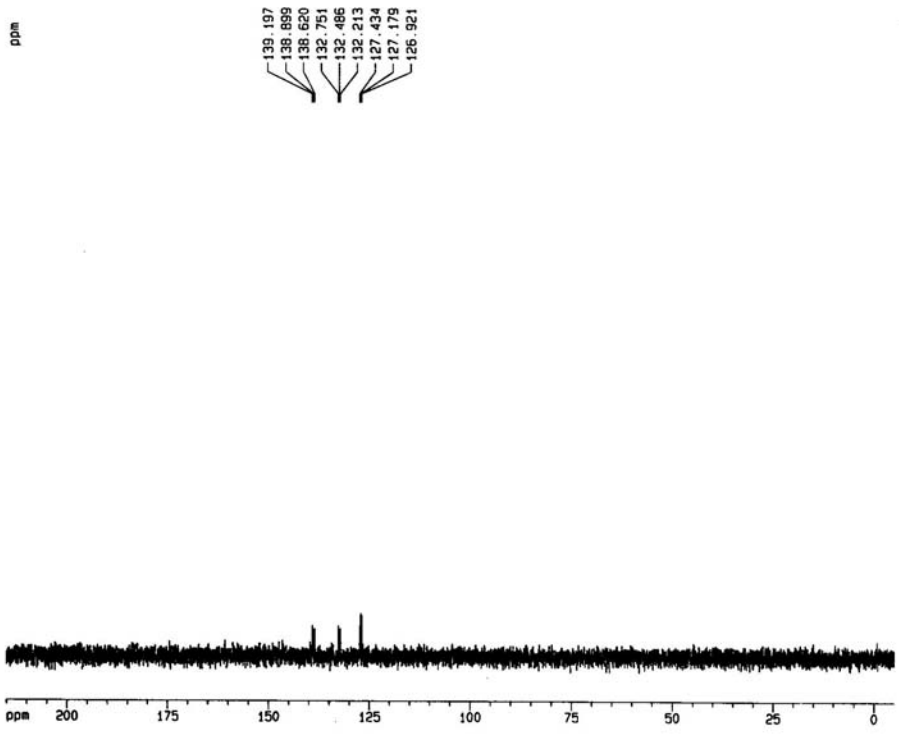

Figure A.45 ^{13}C-NMR spectrum of pyridine N-oxide-d_5

25. 3-Chloropyridine N-oxide-2,4,5,6-d_4 (**87-2,4,5,6-d_4**)

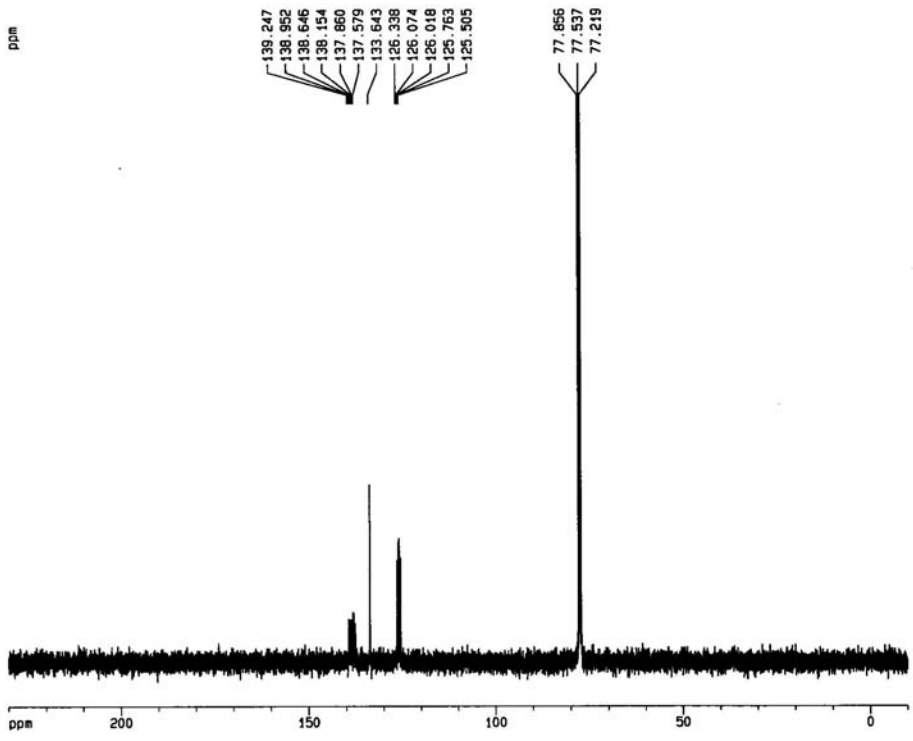

Figure A.46 ^{13}C-NMR spectrum of 3-chloropyridine N-oxide-2,4,5,6-d_4

26. 3-Chloropyridine-2,4,5,6-d_4 (**86-2,4,5,6-d_4**)

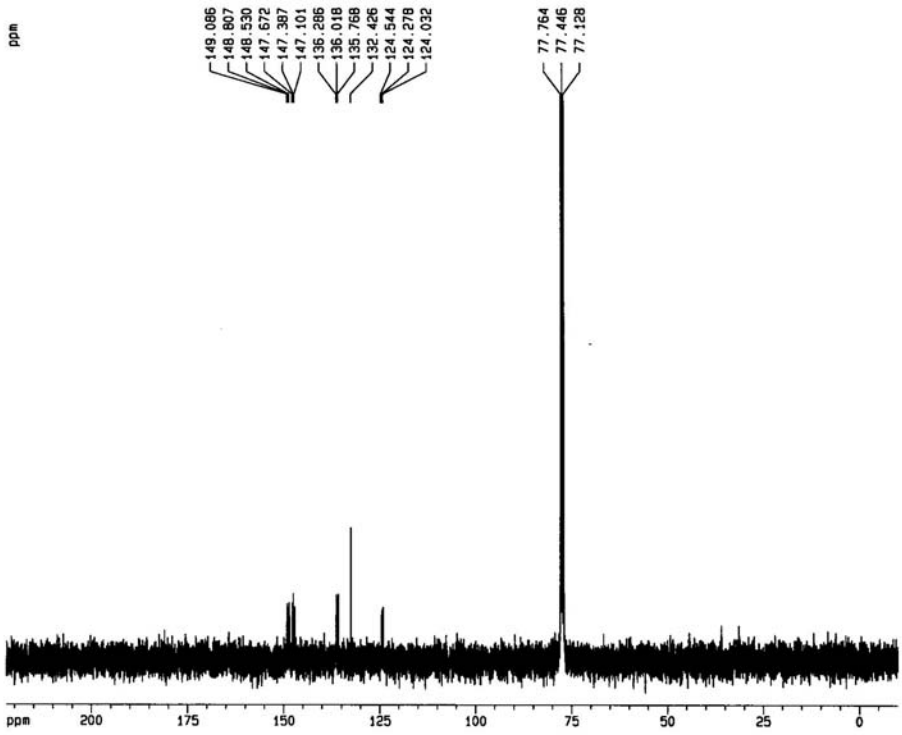

Figure A.47 ^{13}C-NMR spectrum of 3-chloropyridine-2,4,5,6-d_4

27. 2-Chloropyridine-3,4,5,6-d_4 (**88-3,4,5,6-d_4**)

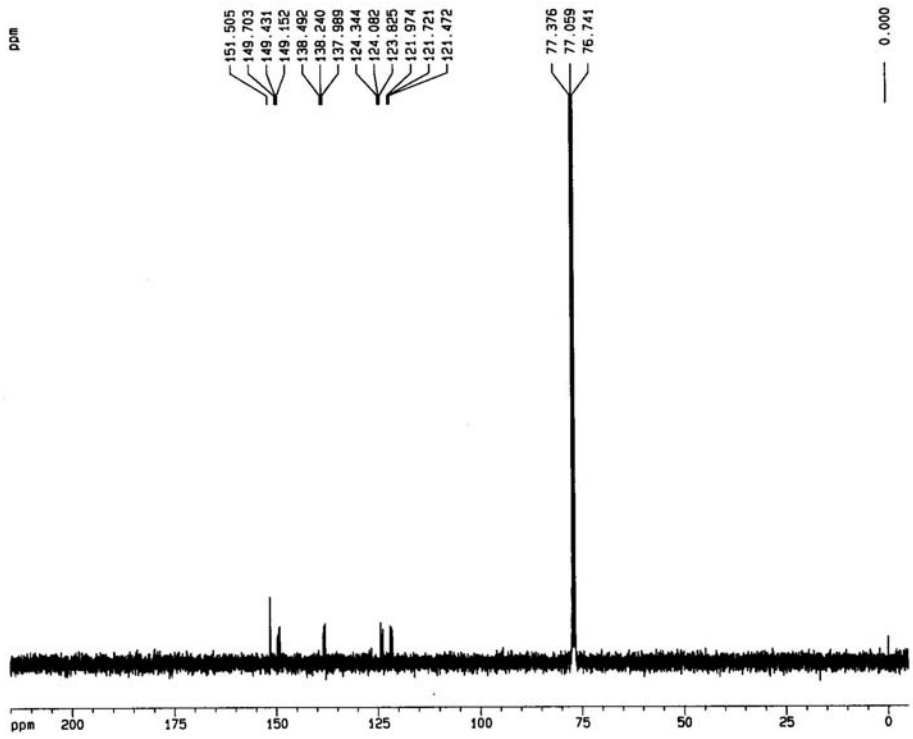

Figure A.48 ^{13}C-NMR spectrum of 2-chloropyridine-3,4,5,6-d_4

28. 2,5-Dichloropyridine-3,4,6-d_3 (**92-3,4,6-d_3**)

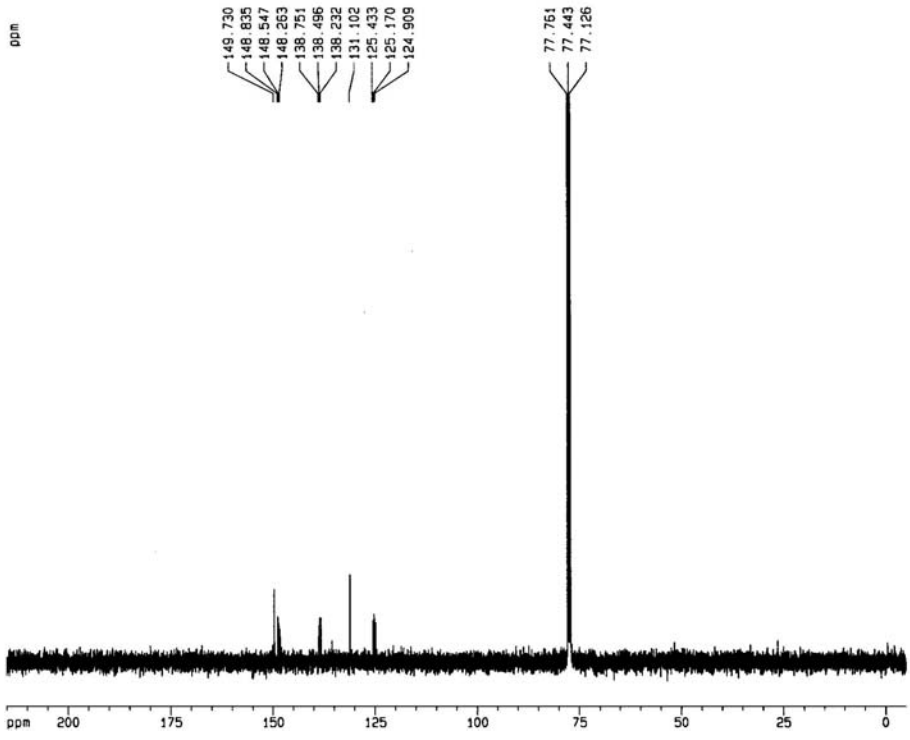

Figure A.49 ^{13}C-NMR spectrum of 2,5-dichloropyridine-3,4,6-d_3

29. 2,3-Dichloropyridine-4,5,6-d_3 (**91-4,5,6-d_3**)

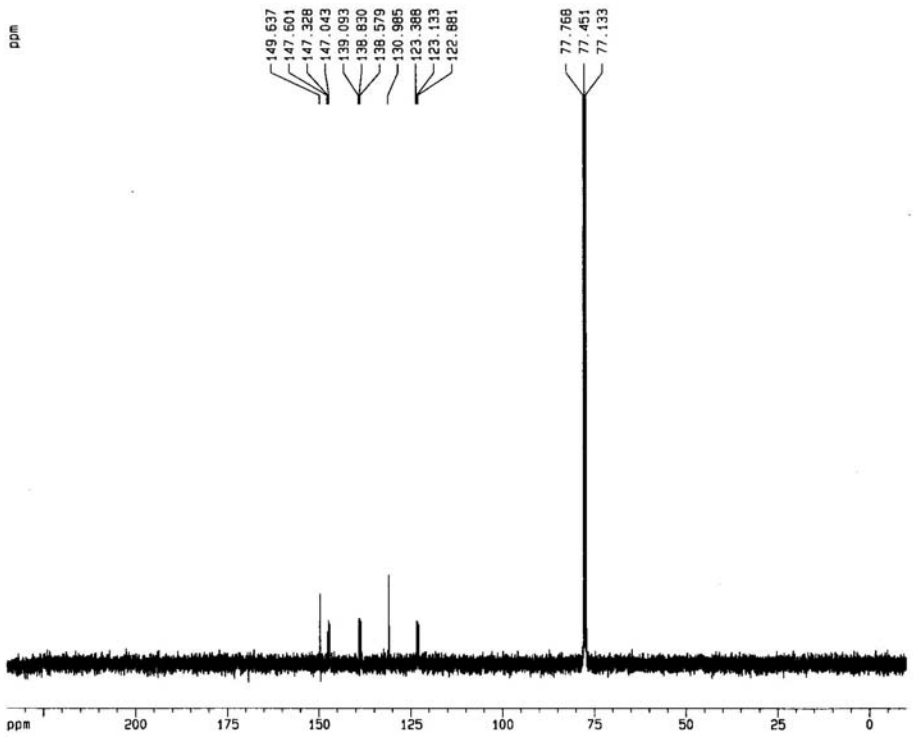

Figure A.50 ^{13}C-NMR spectrum of 2,3-dichloropyridine-4,5,6-d_3

30. 3,5-Dichloropyridine-2,4,6-d_3 (**84-2,4,6-d_3**)

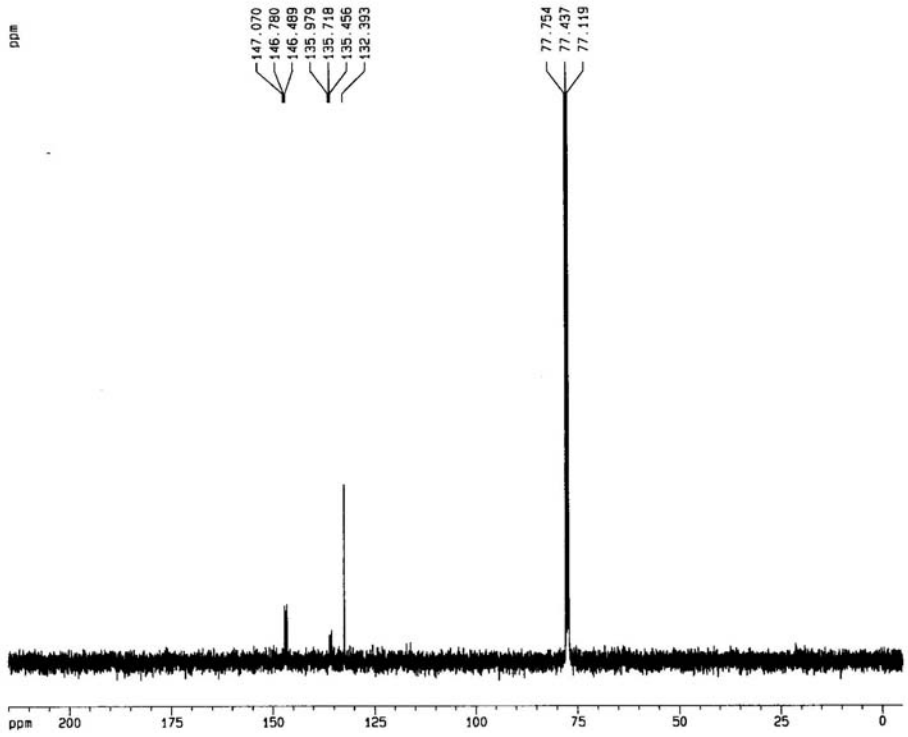

Figure A.51 ^{13}C-NMR spectrum of 3,5-dichloropyridine-2,4,6-d_3

31. 3,4-Dichloropyridine-2,5,6-d_3 (**93-2,5,6-d_3**)

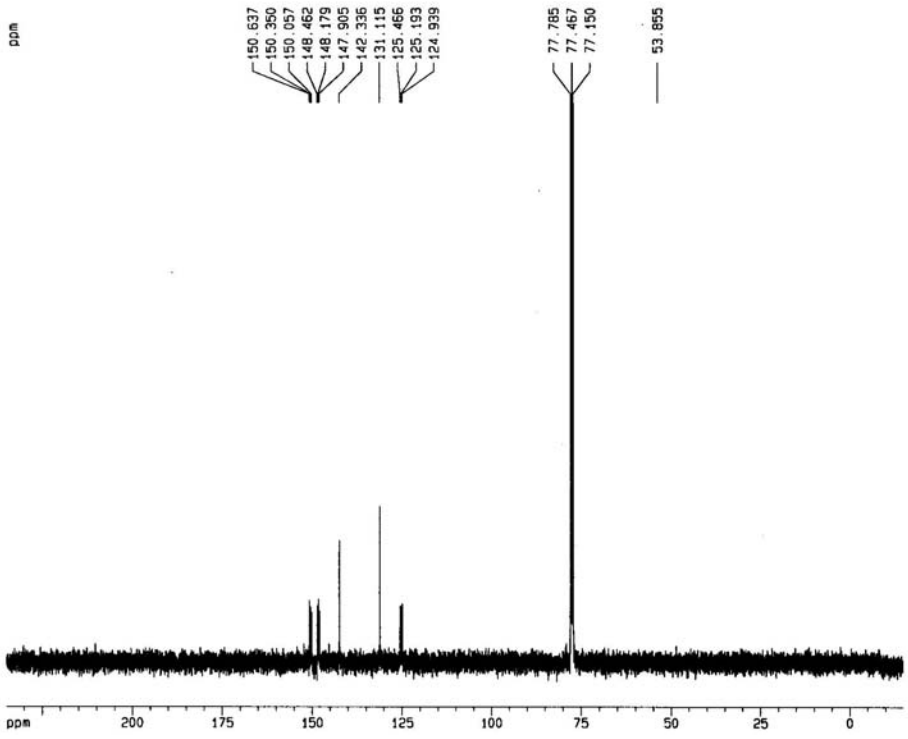

Figure A.52 ^{13}C-NMR spectrum of 3,4-dichloropyridine-2,5,6-d_3

32. 2,4-Dichloropyridine-3,5,6-d_3 (**94-3,5,6-d_3**)

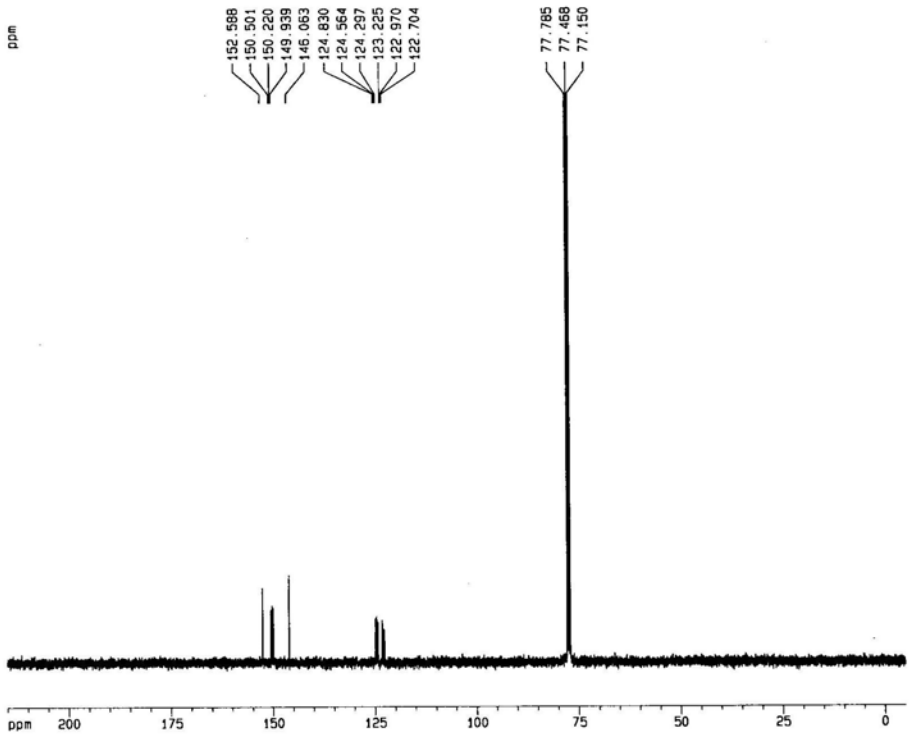

Figure A.53 ^{13}C-NMR spectrum of 2,4-dichloropyridine-3,5,6-d_3

33. 4-Nitropyridine N-oxide-2,3,5,6-d_4 (**81-2,3,5,6-d_4**)

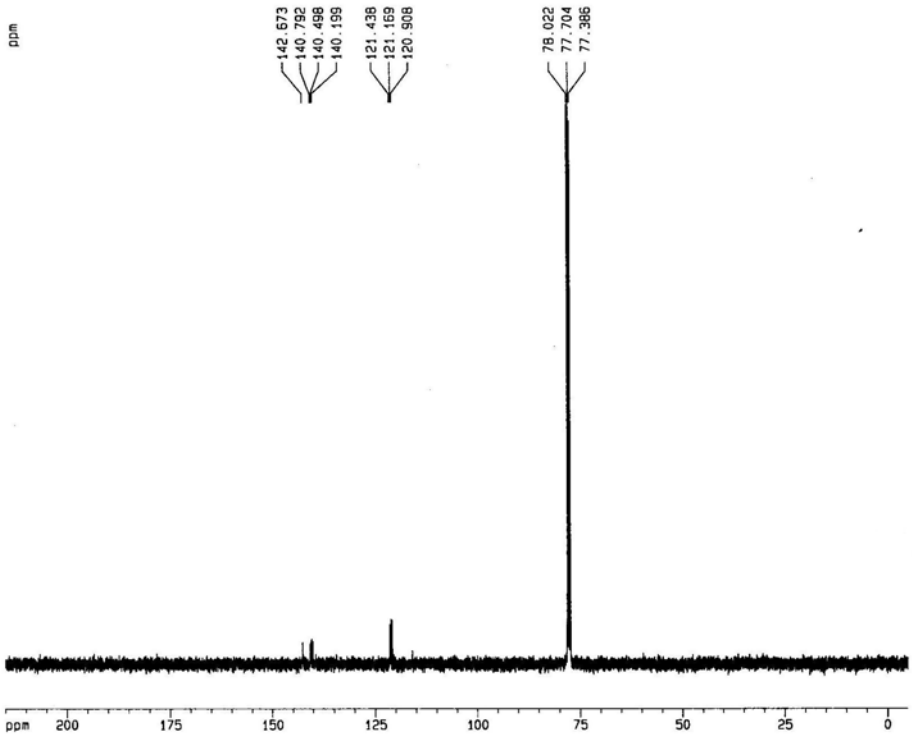

Figure A.54 ^{13}C-NMR spectrum of 4-nitropyridine N-oxide-2,3,5,6-d_4

34. 4-Chloropyridine N-oxide-2,3,5,6-d_4 (**82-2,3,5,6-d_4**)

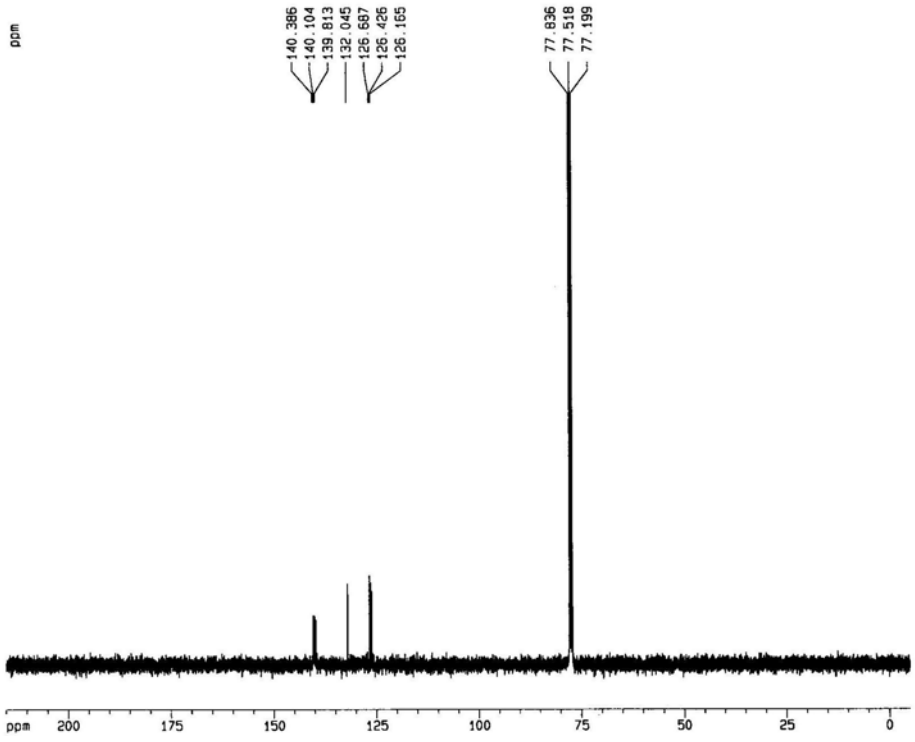

Figure A.55 ^{13}C-NMR spectrum of 4-chloropyridine N-oxide-2,3,5,6-d_4

B. Mass Spectra of synthetic compounds

1. Methyl 4-chloropicolinate N-oxide-6-d (**77-6-d**)

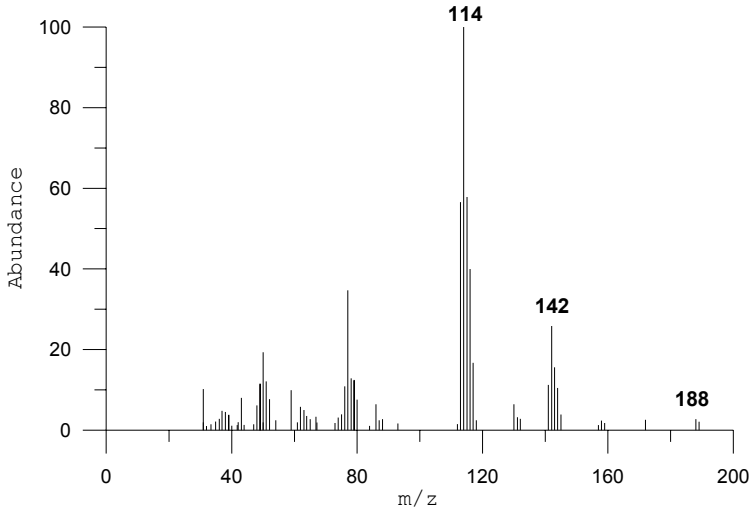

Figure B.1 MS of methyl 4-chloropicolinate N-oxide-6-d

2. Methyl 4-chloropicolinate-6-d (**78-6-d**)

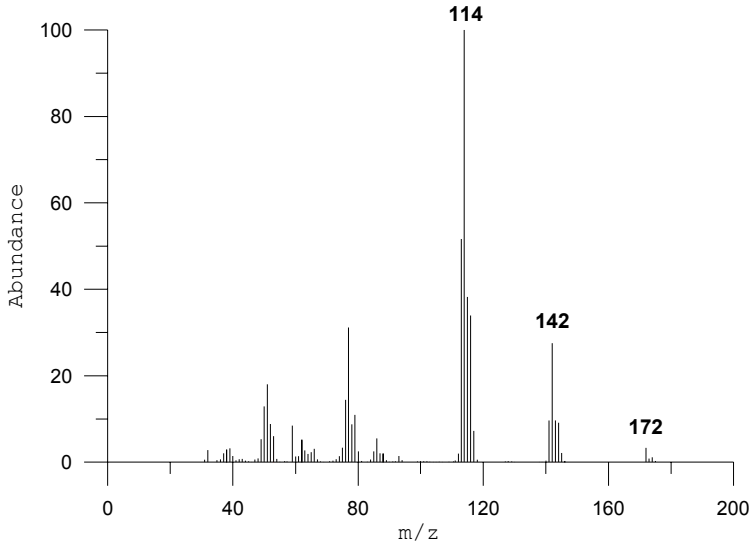

Figure B.2 MS of methyl 4-chloropicolinate-6-d

3. Picolinamide-4,6-d_2 (**80-4,6-d_2**)

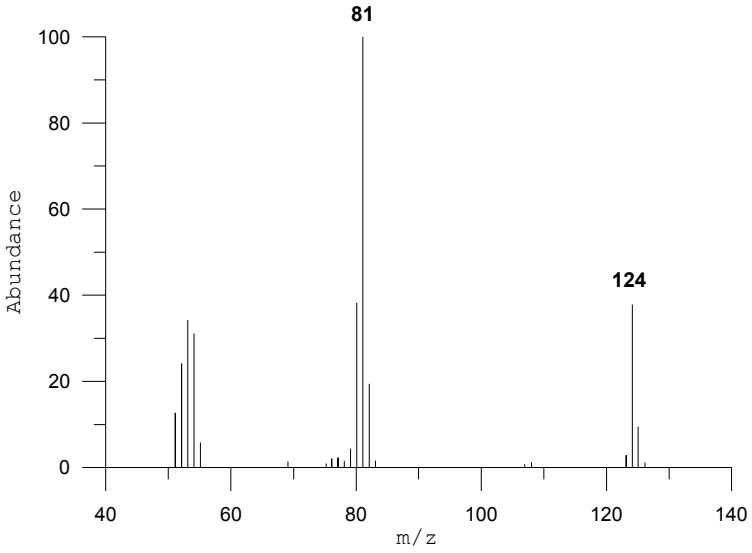

Figure B.3 MS of picolinamide-4,6-d_2

4. Nicotinamide-2,6-d_2 (**64-2,6-d_2**)

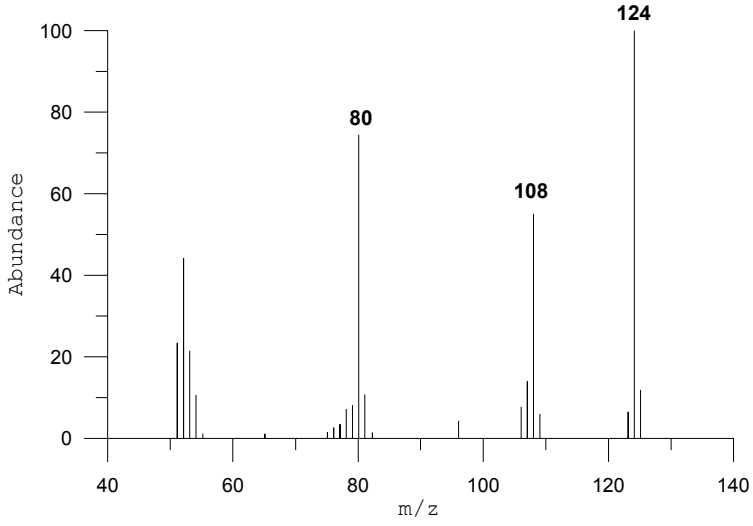

Figure B.4 MS of nicotinamide-2,6-d_2

5. Isonicotinamide-2,6-d_2 (**60-2,6-d_2**)

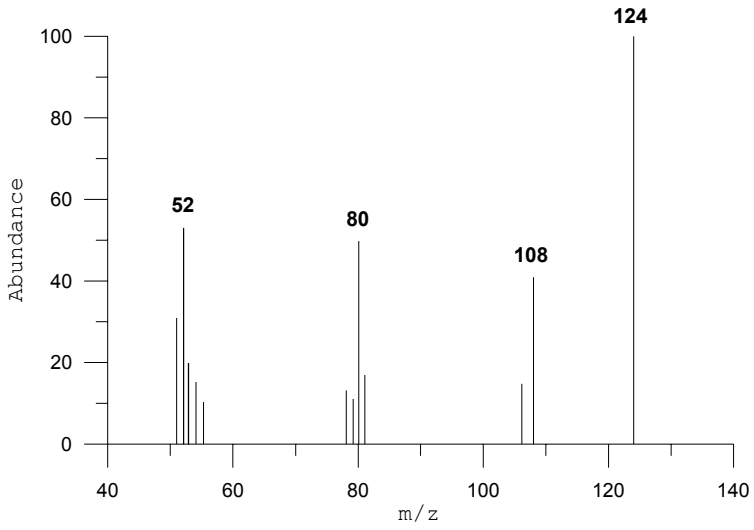

Figure B.5 MS of Isonicotinamide-2,6-d_2

6. Methyl isonicotinate N-oxide-2,6-d_2 (**58-2,6-d_2**)

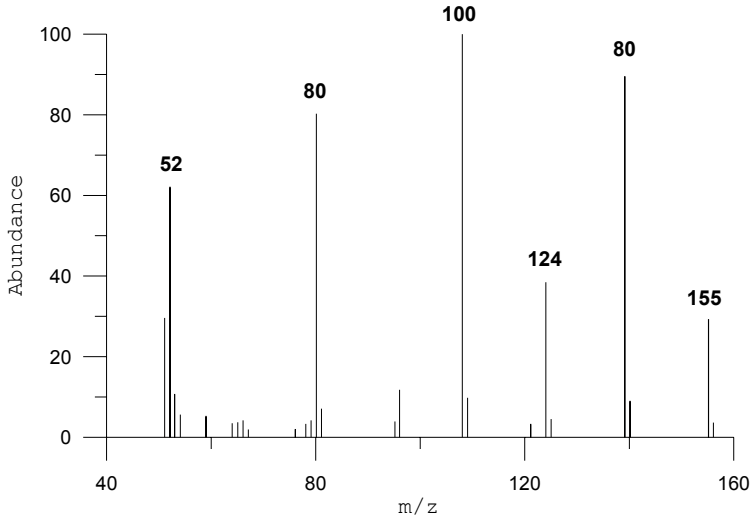

Figure B.6 MS of methyl isonicotinate N-oxide-2,6-d_2

7. Pyridine N-oxide-2,6-d_2 (**53-2,6-d_2**)

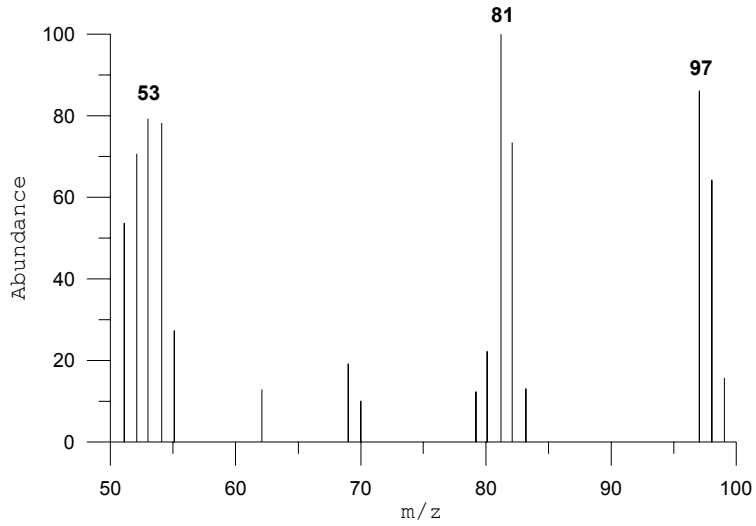

Figure B.7 MS of pyridine N-oxide-2,6-d_2

8. 4-Nitropyridine N-oxide-2,6-d_2 (**81-2,6-d_2**)

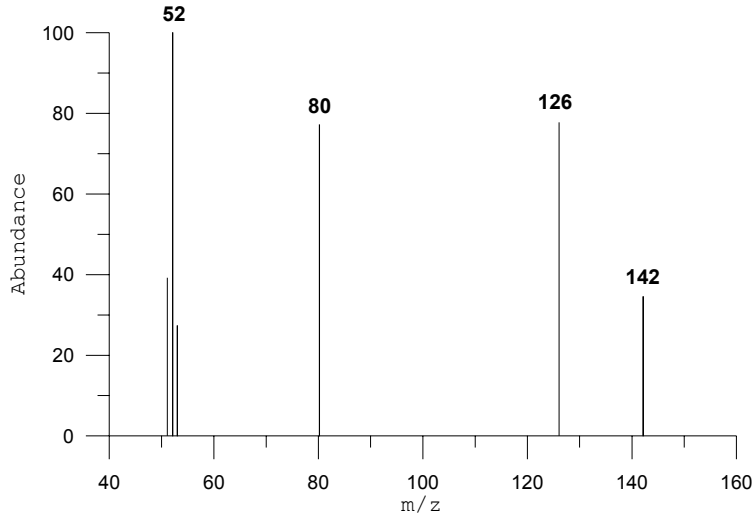

Figure B.8 MS of 4-nitropyridine N-oxide-2,6-d_2

9. 4-Chloropyridine N-oxide-2,6-d_2 (**82-2,6-d_2**)

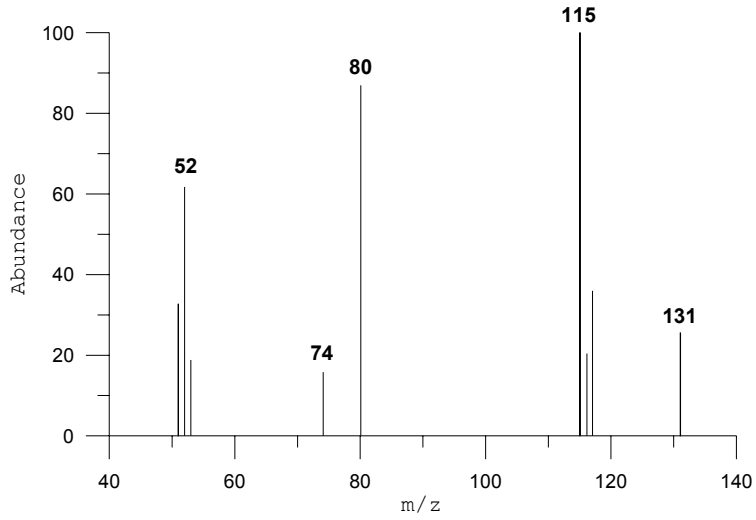

Figure B.9 MS of 4-chloropyridine N-oxide-2,6-d_2

10. 4-Chloropyridine-2,6-d_2 (**83-2,6-d_2**)

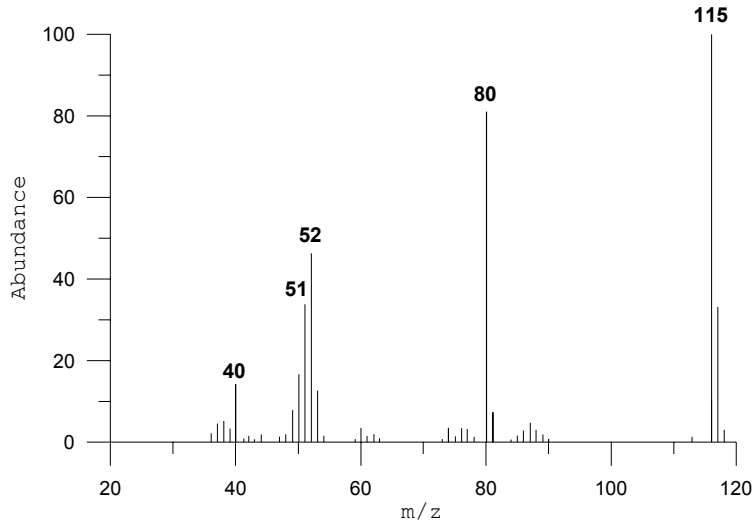

Figure B.10 MS of 4-chloropyridine-2,6-d_2

11. 3,5-dichloropyridine N-oxide (**85**)

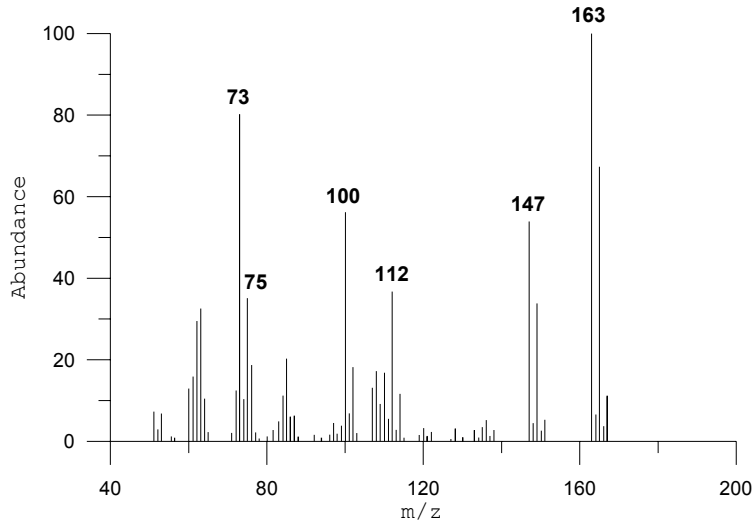

Figure B.11 MS of 3,5-dichloropyridine N-oxide

12. 3,5-dichloropyridine N-oxide-2,4,6-d_3 (**85-2,4,6-d_3**)

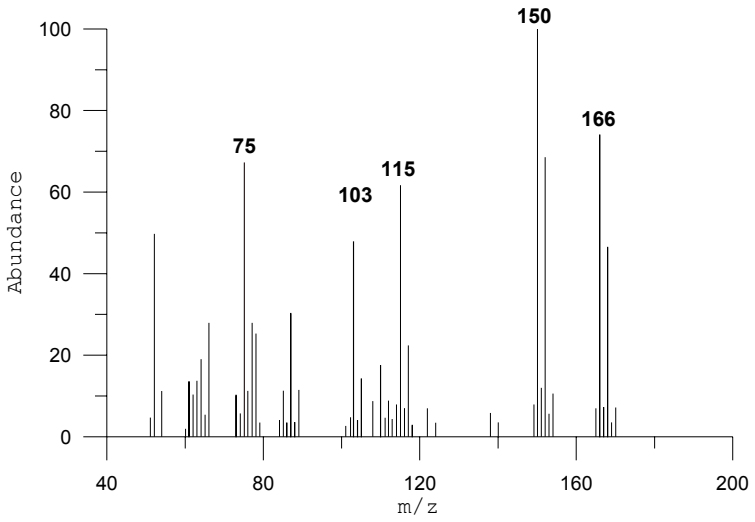

Figure B.12 MS of 3,5-dichloropyridine N-oxide-2,4,6-d_3

13. 3,5-dichloropyridine-2,4,6-d_3 (**84-2,4,6-d_3**)

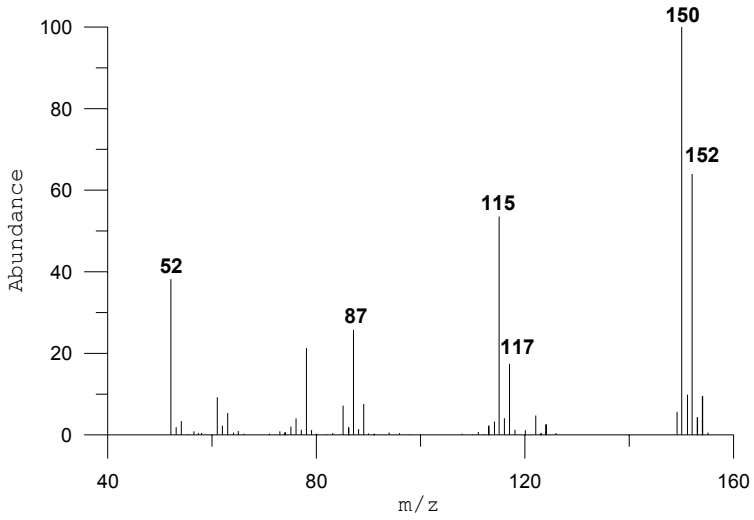

Figure B.13 MS of 3,5-dichloropyridine-2,4,6-d_3

14. 3,5-dichloropyridine-2,6-d_2 (**84-2,6-d_2**)

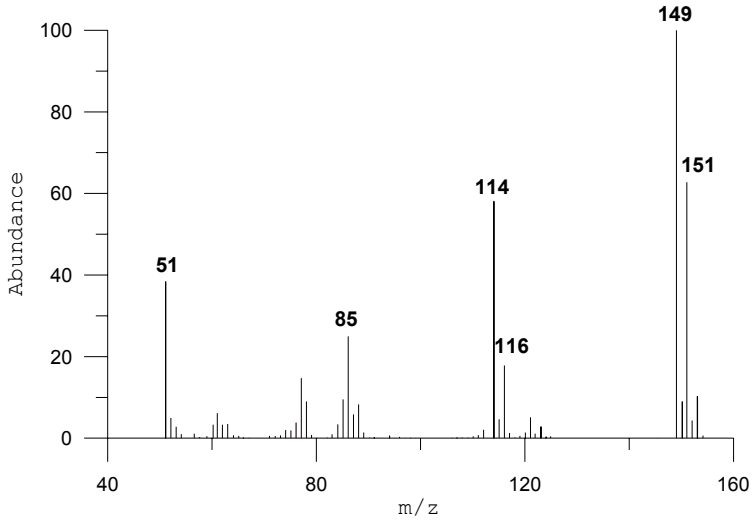

Figure B.14 MS of 3,5-dichloropyridine-2,6-d_2

15. 3-Chloropyridine-2,4,5,6-d_4 (**86-2,4,5,6-d_4**)

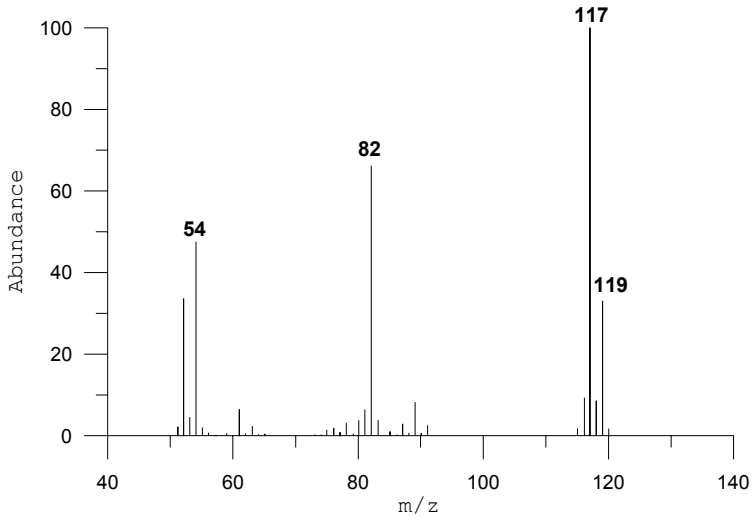

Figure B.15 MS of 3-Chloropyridine-2,4,5,6-d_4

16. 2-Chloropyridine-3,4,5,6-d_4 (**88-3,4,5,6-d_4**)

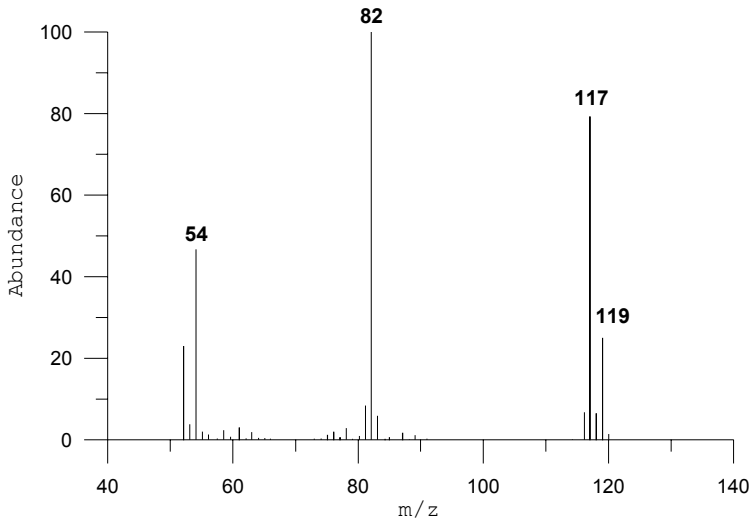

Figure B.16 MS of 2-Chloropyridine-3,4,5,6-d_4

17. 2,5-Dichloropyridine-3,4,6-d_3 (**92-3,5,6-d_3**)

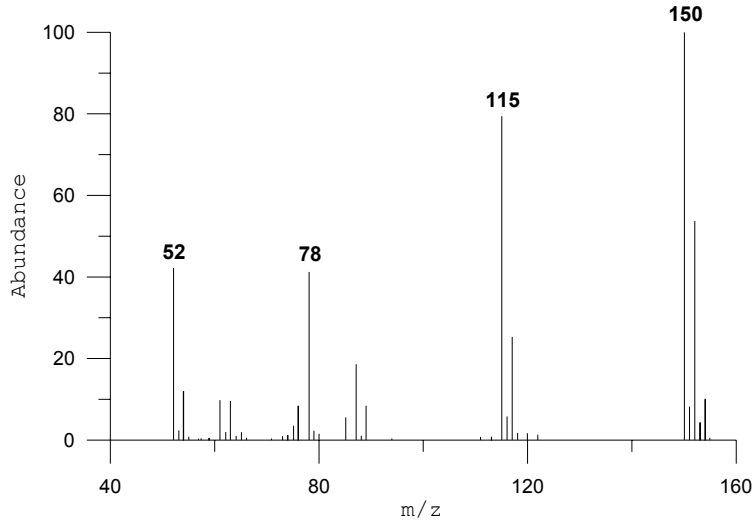

Figure B.17 MS of 2,5-dichloropyridine-3,4,6-d_3

18. 2,3-Dichloropyridine-4,5,6-d_3 (**91-4,5,6-d_3**)

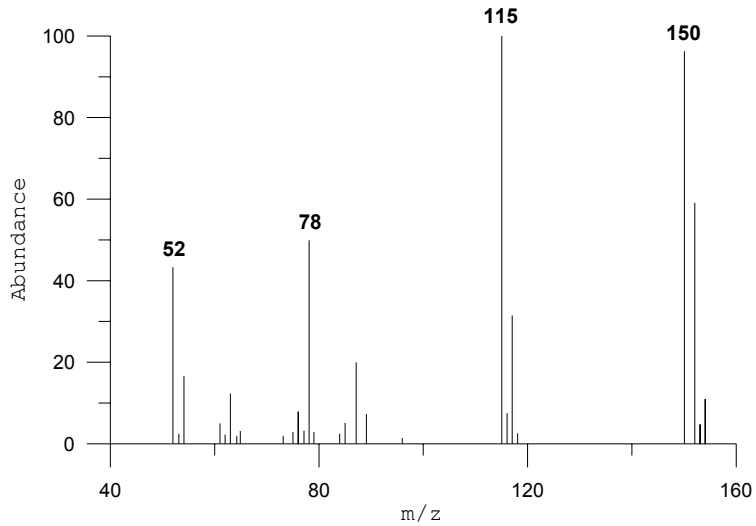

Figure B.18 MS of 2,3-dichloropyridine-4,5,6-d_3

19. 3,4-Dichloropyridine-2,5,6-d_3 (**93-2,5,6-d_3**)

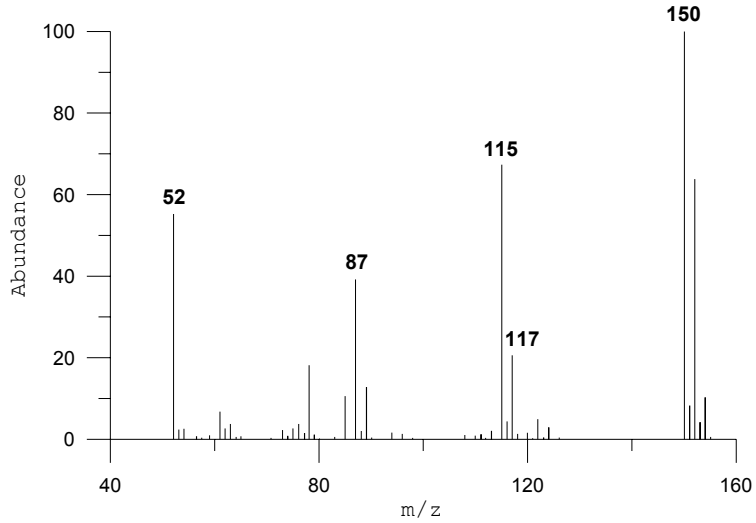

Figure B.19 MS of 3,4-dichloropyridine-2,5,6-d_3

20. 2,4-Dichloropyridine-3,5,6-d_3 (**94-3,5,6-d_3**)

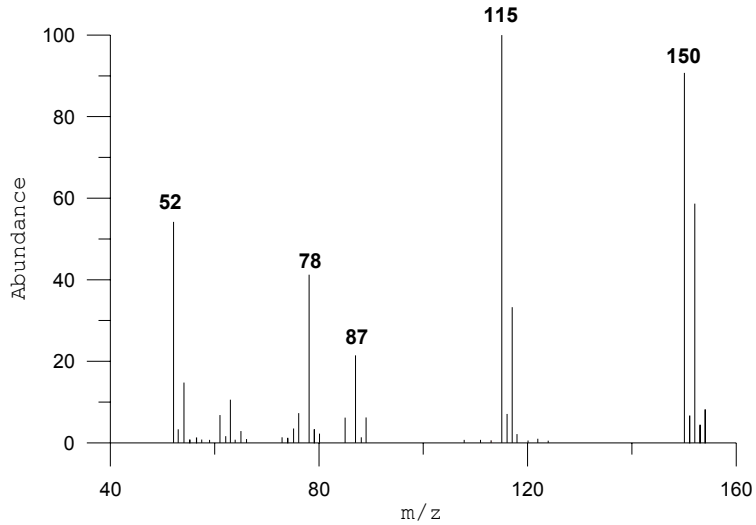

Figure B.20 MS of 2,4-dichloropyridine-3,5,6-d_3

21. 4-Nitropyridine N-oxide-2,3,5,6-d_4 (**81-2,3,5,6-d_4**)

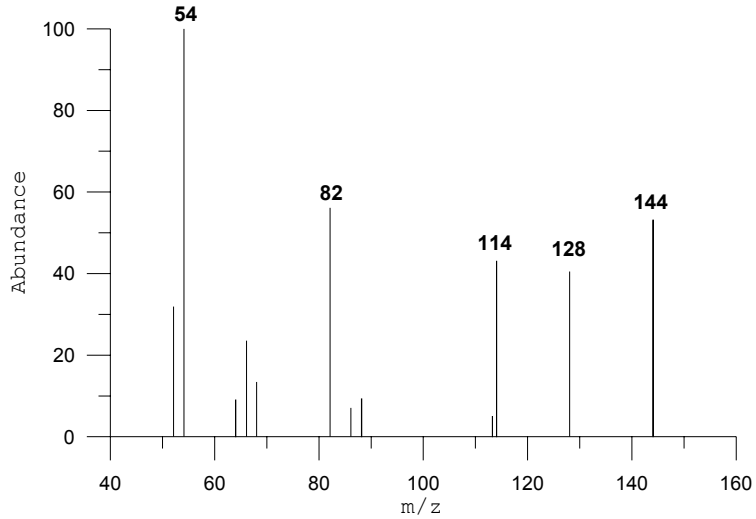

Figure B.21 MS of 4-nitropyridine N-oxide-2,3,5,6-d_4

22. 4-Chloropyridine N-oxide-2,3,5,6-d_4 (**82-2,3,5,6-d_4**)

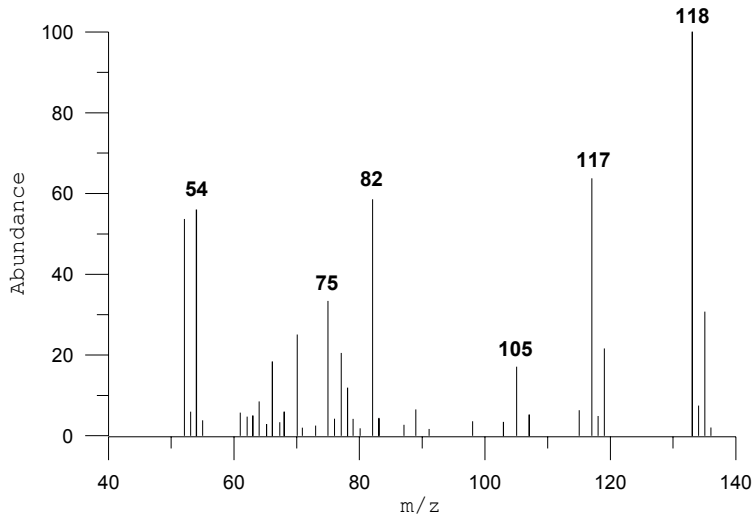

Figure B.22 MS of 4-chloropyridine N-oxide-2,3,5,6-d_4

C. UV spectra of cyanopyridines

1. 2-Cyanopyridine (**36**)

Concentration = 8×10^{-5} M

$\varepsilon_{254} = 3275$

$\varepsilon_{max} = 4325$

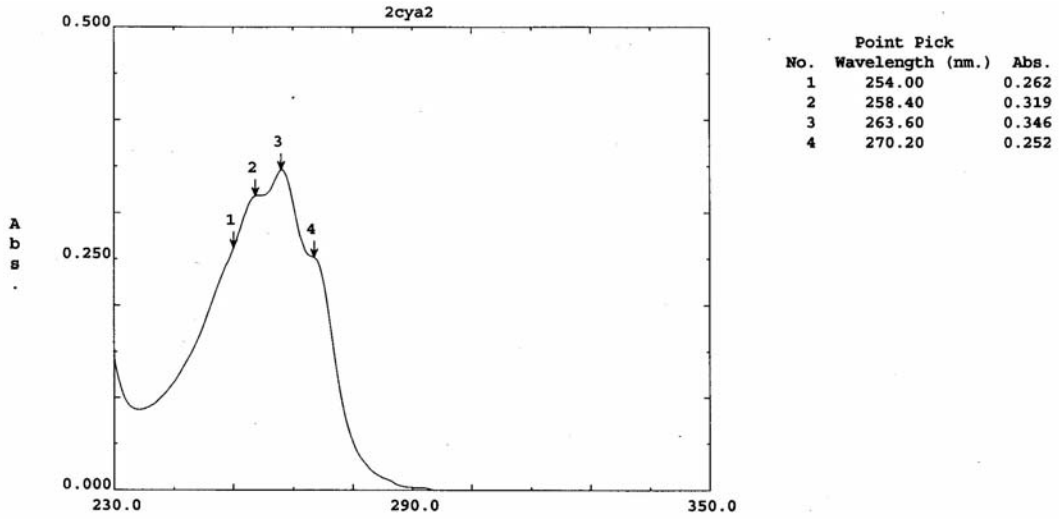

Figure C.1 Absorption spectrum of 2-cyanopyridine in 1:1 ethanol/methanol

2. 3-Cyanopyridine (**37**)

Concentration = 8×10^{-5} M

$\varepsilon_{254} = 4450$

$\varepsilon_{max} = 5450$

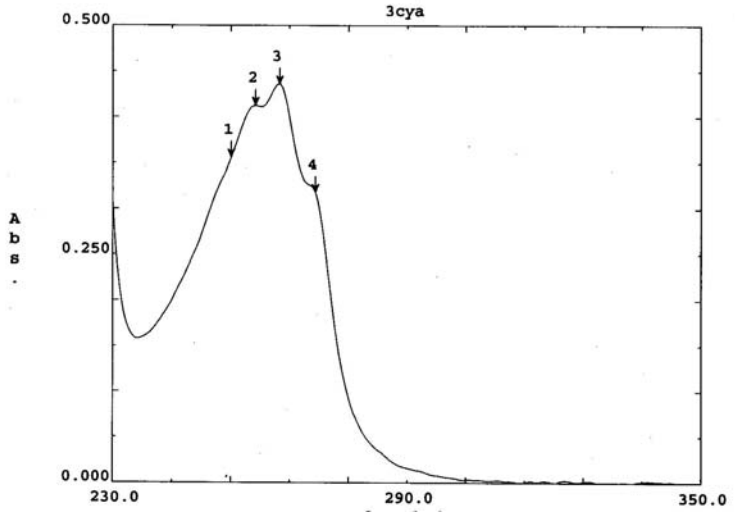

Point Pick No.	Wavelength (nm.)	Abs.
1	254.00	0.356
2	259.00	0.413
3	264.00	0.436
4	271.20	0.318

Figure C.2 Absorption spectrum of 3-cyanopyridine in 1:1 ethanol/methanol

3. 4-Cyanopyridine (**38**)

Concentration = 8×10^{-5} M

$\varepsilon_{254} = 2100$

$\varepsilon_{max} = 4512$

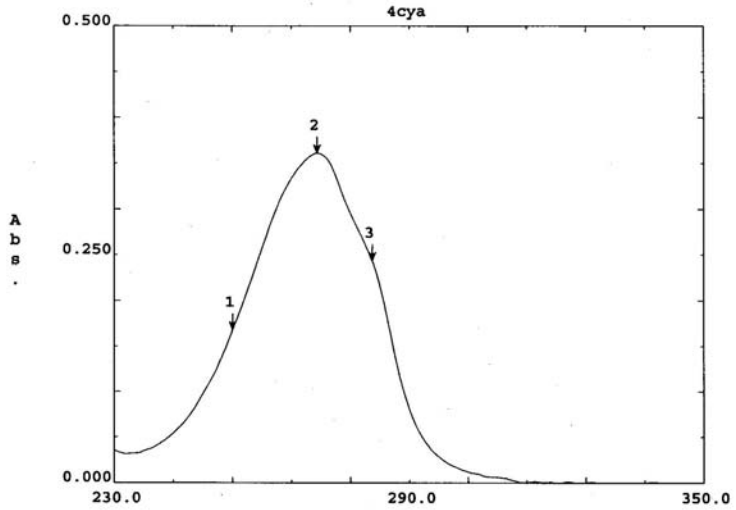

Point Pick

No.	Wavelength (nm.)	Abs.
1	254.00	0.168
2	271.20	0.361
3	282.40	0.244

Figure C.3 Absorption spectrum of 4-cyanopyridine in 1:1 ethanol/methanol

D. UV spectra of methylpyridine vapors

1. 2-Methylpyridine (vapor)

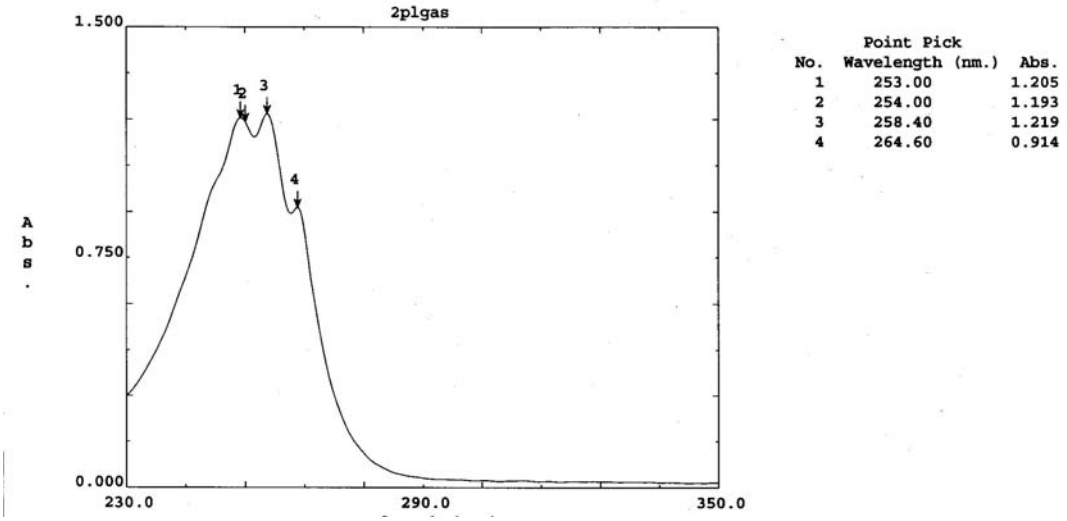

Figure D.1 Absorption spectrum of 2-methylpyridine vapor[66]

2. 3-Methylpyridine (vapor)

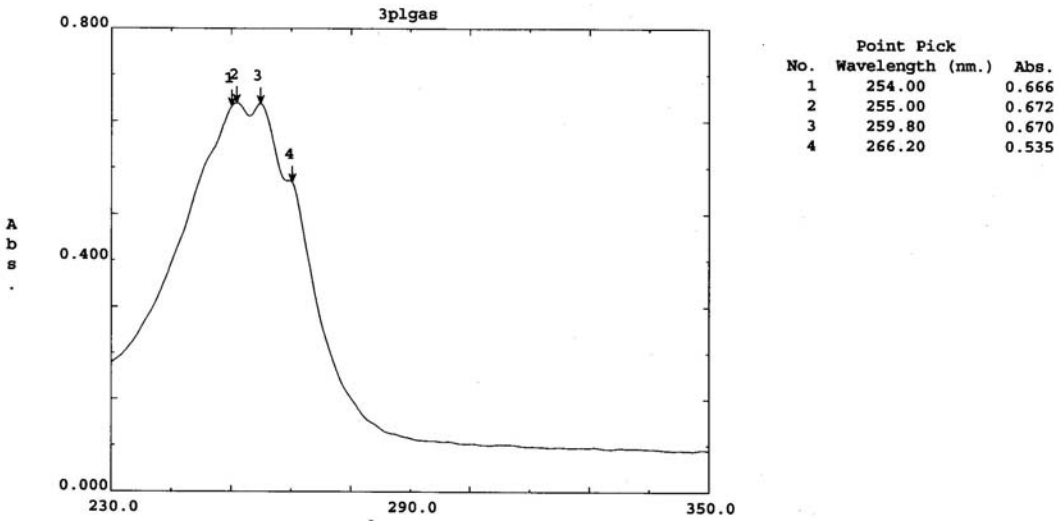

Figure D.2 Absorption spectrum of 3-methylpyridine vapor[66]

3. 4-Methylpyridine (vapor)

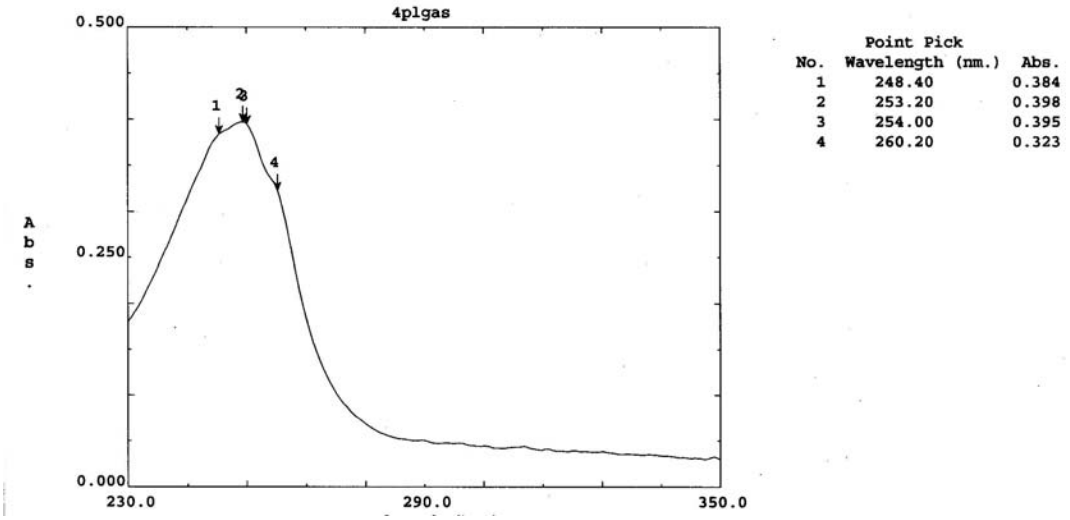

Figure D.3 Absorption spectrum of 4-methylpyridine vapor[66]